

Detection of Latent DNA using Intercalating Dyes

Alicia M. Haines

BSc (Forensic and Analytical Chemistry), BSc (Honours)

A thesis submitted for fulfilment of the degree of Doctor of Philosophy

School of Biological Sciences
Faculty of Science and Engineering
Flinders University, Adelaide, Australia

September, 2016

TABLE OF CONTENTS

TABLE OF CONTENTS	iii
ABSTRACT	vii
DECLARATION.....	ix
ACKNOWLEDGEMENTS	x
LIST OF FIGURES	xi
LIST OF TABLES	xviii
LIST OF SCHEMES	xx
LIST OF ABBREVIATIONS AND SYMBOLS	xxii
PUBLICATIONS.....	xxiv
CONFERENCE PROCEEDINGS.....	xxvi
SEMINARS AND PRESENTATIONS.....	xxviii
AWARDS	xxix
Chapter 1.....	1
1. Introduction	3
1.1 Fluorescence and Fluorophores.....	3
1.2 DNA Structure	5
1.3 DNA Binding Dyes	6
2. Applications of nucleic acid binding dyes	10
2.1 Staining in gel electrophoresis	10
2.2 DNA quantification.....	12
2.3 DNA amplification and detection (qPCR)	13
2.4 Flow Cytometry, Cell staining.....	16
2.5 Nucleic acid dyes for fluorescent microscopic investigations of forensic relevant samples	18
3. Concluding remarks	20
4. Thesis Aims	21
5. References	22
6. Supplementary Information	28
Chapter 2.....	33
2.1 Introduction.....	34
2.1.1 Nucleic acid binding dyes	34
2.2 PUBLICATION	37
2.2.1 Statement of Authorship	38
2.3 Further Methodology	43
2.3.1 Gel Electrophoresis using pre-cast staining	43

2.3.2 Saliva staining.....	43
2.3.3 Data analysis	44
2.4 Further Results and Discussion.....	45
2.4 Concluding Remarks:	63
2.5 References (<i>Supplemental to Publication</i>).....	65
2.6 Appendix A.....	66
Chapter 3.....	87
3.1 Introduction.....	88
3.1.2 Background on DNA extraction.....	89
3.1.3 Phenol/Chloroform Extraction:.....	90
3.1.4 Chelex® Extraction:.....	90
3.1.5 Solid Phase Extraction:.....	91
3.1.6 Background on STR profiling;.....	91
3.1.7 'Direct' PCR	92
3.1.8 Summary	93
3.2 PUBLICATION	94
Statement of Authorship	95
3.3 Further Results and Discussion.....	104
3.4 Chapter Summary	115
3.5 References (<i>supplemental to publication</i>).....	117
3.6 APPENDIX B.....	120
Chapter 4.....	142
4.1 Introduction.....	143
4.1.8 Forensic light sources.....	145
4.1.9 Summary	149
4.2 Methodology	150
4.2.1 Dye solution preparation	150
4.2.2 Background fluorescence.....	150
4.2.3 DNA binding dyes with DNA.....	150
4.2.4 Detection of DNA within fingerprints	150
4.2.5 Specificity of dyes.....	151
4.2.6 Detection using Polilight®	151
4.2.7 Quantification of DNA within fingerprints.....	152
4.3 Results and discussion (Gel Doc™ detection)	154
4.3.1 Background Fluorescence	154
4.3.2 DNA binding dyes with DNA.....	155
4.2.3 Detection of DNA within fingerprints	161

Statement of Authorship	164
Author Contributions.....	164
4.2.4 Specificity of the dyes	167
4.2.5 Sensitivity of DNA/dye complex, detection	174
4.4 Results and discussion (Polilight® detection)	178
4.4.1 Detection of DNA	178
4.4.2 Detection of DNA and protein within fingerprints	185
4.3.3 Detection of DNA within biological samples	192
4.3.4 Other publications	194
Statement of Authorship	195
Author Contributions.....	195
4.5 Chapter Summary	198
4.6 References (<i>supplemental to publications</i>)	199
4.7 APPENDIX C.....	201
Chapter 5.....	221
5.1 Introduction	222
5.1.1 Hairs as evidence	222
5.1.2 Hair structure	222
5.1.3 Hair as a source of DNA.....	223
5.1.4 Nuclear staining of hairs	224
5.1.5 Comparison of current methodology to potential new dyes for nuclear staining of hair follicles.	225
3.2 PUBLICATION	228
Statement of Authorship	229
5.3 Further Results and Discussion.....	236
5.5 OTHER PUBLICATIONS	261
Statement of Authorship	262
Statement of Authorship	265
5.4 Chapter Summary	268
5.6 References (Supplemental to publication)	270
5.6 APPENDIX D	273
Chapter 6.....	310
6.1 Introduction.....	311
6.1.2 UV Spectrometry.....	311
6.1.3 Fluorometry	312
6.1.4 Slot Blots	312
6.1.5 Hybridization probes for nucleic acid detection	312

6.1.6 Quantitative PCR	314
6.1.6 Summary.....	316
6.2 PUBLICATION	317
Statement of Authorship	318
1. Introduction	320
2. Materials and methods	321
3. Results and discussion	323
4. References	331
6.3 Further methodology.....	333
6.3.1 Intercalating dyes for qPCR.....	333
6.3.2 Dye combinations for qPCR.....	333
6.3.3 DD interaction with ssDNA study	334
6.4 Further results and discussion	335
6.4.3 Analysis of DD ssDNA binding	352
6.5 Chapter Summary	354
6.6 References (<i>Supplemental to publication</i>).....	355
6.7 APPENDIX E (Supporting information).....	357
Chapter 7	363
7.1 Preface	364
7.2 Concluding remarks	365
7.3 Future impact	368
7.3.2 Staining of tape-lifts	370
7.3.3 Staining of other items.....	374
7.4 Final Statement.....	377
7.5 References	378
7.6 APPENDIX F	380

ABSTRACT

This thesis outlines the use of DNA binding dyes that can target the collection of latent DNA deposited by touch at crime scenes. A range of dyes are available that bind to DNA at high specificity for laboratory-based applications but rarely applied to *in situ* detection. This work on a surface-based application of dyes for latent DNA detection has not been investigated previously.

Six common nucleic acid-binding dyes were selected due to their increase in fluorescence when in the presence of double stranded-DNA (SYBR[®] Green I, Diamond[™] Nucleic Acid Dye, GelGreen[™], GelRed[™], EvaGreen[™] and Redsafe[™]); four of the six dyes are permeable to cell membranes. The fluorescence from dye/DNA complex was detected using a high intensity light source, the Polilight[®] (PL500), an excitation wavelength of 490 nm and emission observed/recorded through interference filters centred at 530 nm or 550 nm depending on the dye emission. Some biological samples such as hair and skin were visualized under a fluorescent microscope (Nikon Optiphot) using a B2A filter cube.

Detection of DNA was observed within different biological samples such as saliva, skin, blood and hair which make it possible to select samples that are more likely to produce STR profiles after direct amplification. The properties of nucleic acid binding dyes were reviewed within Chapter 1 detailing the use of dyes in various applications along with the chemistry and common modes of interaction with DNA. Chapter 2 looks at the properties of common DNA binding dyes used in gel electrophoresis and determines their sensitivity in a gel medium. Chapter 3 outlines the effects the dyes had on DNA extraction, amplification, quantification and the amplification and detection of STRs. Diamond[™] dye (DD) was found to have the least effect of DNA extraction; GelGreen[™] (GG) had the least effect on STR detection and amplification; GelRed (GR) quenched the fluorescent signal in the quantification of DNA (Qubit[®]) and resulted in no STR amplification or detection. Chapter 4 discussed the results of the *in situ* detection of DNA within biological samples and as a surface based application. DD appeared to be the ideal dye for detection as it had a lower background signal compared with other dyes and had the highest DNA fluorescent enhancement after SYBR Green. Chapter 5 reviews DD along with other dyes for the

detection of DNA within hair follicles; DD shows the staining of nuclei with limited background fluorescence and also showed successful direct STR amplification. Chapter 6 outlines the use of DD for quantitative PCR allowing for a more cost effective alternative to SG.

The outcome of this work is a novel means to detect DNA *in situ* within biological samples and on surfaces that makes the screening of samples more efficient and successful. The investigation so far has concluded that EvaGreen™ and Diamond™ dye are the optimum dyes for this novel application based on their properties of binding and limited interactions with downstream forensic applications such as DNA extraction, amplification and STR typing. The use of these dyes as a screening methodology for tape-lifts would be a future application of this work to provide a way to selectively choose areas that have a higher DNA content for analysis.

DECLARATION

I certify that this thesis does not incorporate without acknowledgment any material previously submitted for a degree or diploma in any university; and that to the best of my knowledge and belief it does not contain any material previously published or written by another person except where due reference is made in the text.



Alicia M. Haines
August, 2016

ACKNOWLEDGEMENTS

Firstly, I would like to express my sincere gratitude to my supervisor Prof. Adrian Linacre for the continuous support of my PhD study and related research, for his patience, motivation, and immense knowledge. His guidance helped me in the research and writing of this thesis. I could not have imagined having a better supervisor and mentor for my study.

Besides my supervisor, I would like to thank the rest of my PhD thesis supervisory team: Prof. Hilton Kobus for his insightful comments and encouragement throughout the last 4 years.

I thank my fellow lab-mates Jennifer, Renée, Sherryn and all the others that came through the lab during my candidature, for the stimulating discussions, sharing our stressful moments and for all the fun we have had in the last four years. A special mention to Jennifer for being my conference buddy when we travelled to the US and of course providing unwavering support over coffee! I will miss our times together in the office.

Last but not the least, I would like to thank my family: my Mum, Marion, who has always been a shoulder of support throughout my many years at university, I would not be where I am and who I am today without her support and guidance. To my Dad, Bob, who has helped with giving me a place to live (reduced rent! Thanks Dad). To my lovely sister Catherine who always tries to listen about my research but finds catalogues more interesting. My niece Indigo, who provides a light in sometimes dark places and always happy to give her Aunty a hug, and also to my brother and his family for their support. As well as all my friends, especially those that attempted to read this thesis, and the rest of my family who have supported me throughout my PhD and writing my thesis and in my life in general.

LIST OF FIGURES

-
- Figure 1.1** (A) Example of a fluorescent spectrum of a fluorophore showing excitation in red and emission in green, stokes shift is indicated with arrows, the intensity is in arbitrary units. (B) Jablonski diagram, absorption of light resulting in excitation and fluorescence emission, adapted from [1, 2].
- Figure 1.2** Schematic representation of the DNA structure showing the phosphate group, nitrogenous bases, deoxyribose sugar molecule and the hydrogen bonding linking the two strands together.
- Figure 1.3** Schematic representation of the DNA double helix with indications of the minor and major groove of DNA and along with the various dye binding mechanisms, adapted from [4].
- Figure 1.4** Molecular structure of ethidium bromide (**left**), GelRed [2] (**Centre**) and GelGreen [2] (**right**).
- Figure 1.5** Molecular structure of SG (left) and PG (right) showing the various binding mechanisms the dyes have with DNA, adapted from [1].
- Figure 1.6** Molecular structure of DAPI (left) and Hoechst 33342 (right)
- Figure 1.7** Schematic representation of how SYBR Green (SG) molecules bind during RT-PCR and fluorescence when bound to ds-DNA, adapted from [25].
-
- Figure 2.1** Image of agarose gel 1% of varying masses of DNA (0.5-50 ng) stained pre-casting of gel with SYBR[®] Green (1X concentration) run for 30 min at 131V.
- Figure 2.2** The fluorescent signal of the bands present in Easy Ladder I (2000, 1000, 500, 250 and 100 bp) at varying mass of DNA (50, 40, 30, 20, 10, 5, 2.5, 1) and 0.5 ng of control DNA with loading dye was measured using the Bio-Rad Gel Doc EZ Imager. A, B and F used UV-transillumination (excitation at 302 nm, emission filter 535-640 nm) and C, D and E used Blue-transillumination (excitation at 460 nm, emission filter 560-700 nm) (A) ethidium bromide 0.5 µg/mL, (B) RedSafe™ 1X, 1:20,000 dilution, (C) GelRed™ 1X, (D) SYBR[®] Green I 1X, (E) Diamond™ Nucleic Acid Dye 1X and (F) GelGreen™ 1X.
- Figure 2.3** The average fluorescent signal of the bands present in Easy Ladder I (5 replicates) at varying mass of DNA (50, 40, 30, 20, 10, 5, 2.5, 1) and 0.5 ng of control DNA with loading dye and R² values showing the linearity of the dyes signal, was measured using the Bio-Rad Gel Doc EZ Imager. A, B and F used UV-transillumination (excitation at 302 nm, emission filter 535-640 nm) and C, D and E used Blue-transillumination (excitation at 460 nm, emission filter 560-700 nm) (A) ethidium bromide 0.5 µg/mL, (B) RedSafe™ 1X, 1:20,000 dilution, (C) GelRed™ 1X, (D) SYBR[®] Green I 1X, (E) Diamond™ Nucleic Acid Dye 1X and (F) GelGreen™ 1X.
- Figure 2.4** Comparison of average volume intensity of bands at different DNA mass (ng) with post electrophoresis staining with ethidium bromide (0.5 µg/mL) and staining pre electrophoresis with ethidium bromide (0.5 µg/mL). Error bars

showing 95% confidence with 5 repetitions.

Figure 2.5 Comparison of volume intensity of bands at different DNA mass (ng) with post electrophoresis staining with GelRed (1X) and staining pre electrophoresis. Error bars showing 95% confidence with 5 repetitions.

Figure 2.6 Comparison of volume intensity of bands at different DNA mass (ng) with post electrophoresis staining with RedSafe (1X) and staining pre electrophoresis. Error bars showing 95% confidence with 5 repetitions.

Figure 2.7 Comparison of volume intensity of bands at different DNA mass (ng) with post electrophoresis staining with SYBR Green (1X) and staining pre electrophoresis. Error bars showing 95% confidence with 5 repetitions.

Figure 2.8 Comparison of volume intensity of bands at different DNA mass (ng) with post electrophoresis staining with Diamond dye (1X) and staining pre electrophoresis. Error bars showing 95% confidence with 5 repetitions.

Figure 2.9 Comparison of volume intensity of bands at different DNA mass (ng) with post electrophoresis staining with GelGreen (1X) and staining pre electrophoresis. Error bars showing 95% confidence with 5 repetitions.

Figure 2.10 Showing the permeability of the binding dyes in a fresh saliva sample at 100x magnification using a 1x concentration dye solution in sterile water. A = Ethidium Bromide, B = RedSafe, C = GelRed, D = Diamond Dye, E = GelGreen and F = SYBR Green I. UV excitation for A, B and C, blue excitation was used for D, E and F.

Figure 2.11 Showing the permeability of the binding dyes in a fresh saliva sample at 40x magnification using a 1x concentration dye solution in sterile water. A = Ethidium Bromide, B = RedSafe, C = GelRed, D = Diamond Dye, E = GelGreen and F = SYBR Green I. UV excitation for A, B and C, blue excitation was used for D, E and F.

Figure 3.1 Profiler plus[™] (Life Technologies) showing the size range for the known alleles represented by box length containing locus name. Colour indicates the fluorescent label attached to the allele. The internal size standard is shown in red.

Figure 3.2 Schematic diagram showing the silica surface within a spin column during the DNA extraction process in the presence of a chaotropic salt (Na^+) and a SG molecule showing the sites for electrostatic interaction with DNA.

Figure 3.3 Comparison of average profile peak heights when binding dyes are added directly to the STR amplification process or has undergone a DNA extraction. Error bars showing within a 95% confidence.

Figure 3.4 Schematic diagram of potential spectral overlap resulting in fluorescent quenching of the Qubit signal by the GR dye molecules

Figure 3.5 Effect DNA binding dyes has on the quantification of DNA using Qubit. Error bars showing 95% confidence. Results were obtained in triplicate. All samples had the same DNA concentration (10 ng/ μL).

Figure 3.6 Agarose Gel 4% post stained with Diamond Dye (1X) showing the products from

the STR typing reaction (1) Promega 1Kb ladder, (2) Positive, (3) RS, (4) RS.2, (5) DD (6) DD.2, (7) SG, (8) SG.2, (9) EG, (10) EG.2, (11) GR, (12) GR.2.

Figure 3.7 Schematic diagram of SG binding sites to ssDNA STR fragment repeat unit (AATG) part of TH01-allele 7.

Figure 3.8 Fluorescent labels attached to the PCR products analyzed by the Genetic Analyzer 3130xl (A) ROX, red emission (B) 5-FAM, blue emission and (C) JOE, green emission. The fourth dye NED the structure is unknown, proprietary information

Figure 3.9 Schematic diagram of DD and NED excitation and emission signals showing the spectral overlap resulting in possible FRET.

Figure 3.10 Schematic diagram of 5-FAM and RS excitation and emission signals showing the spectral overlap resulting in possible FRET

Figure 4.1 Molecular structure of SYBR[®] Green I [1] (**left**), GelRed[™] [2] (**Centre**), GelGreen[™] [2] (**right**) and EvaGreen[™] (**below**) [3].

Figure 4.2 Background signal of DNA binding dyes on glass (5 µL, 20X) using Gel Doc[™] EZ imager lane band analysis tool.

Figure 4.3 Comparison of background signal of dyes (5 µL, 20X) with DNA (1 ng) and dye intensity was measured while dye/DNA was still in solution on a glass substrate.

Figure 4.4 Background signal compared with 1 ng of DNA signal on different surfaces using GG (20X, 5 µL).

Figure 4.5 Background signal compared with 1 ng of DNA signal on different surfaces using SG (20X, 5 µL).

Figure 4.6 Signal of binding dyes with varying amounts of DNA with a background control (no DNA) using the dyes at 20X concentration (5 µL) detection using Gel Doc[™] EZ Imager, lane band analysis tool.

Figure 4.7 Comparison of DNA binding dyes signal (1X concentration) within a gel medium (1% agarose) and on a surface (glass) at varying DNA amounts, undertaken in triplicate.

Figure 4.8 Fluorescent signal detected within fingerprints using GG (20X, 5 µL) after different treatments on glass substrate. The values shown are minus the negative control (dyes intrinsic fluorescence) 1 indicates pointer finger, 2 middle, 3 ring and 4 pinky.

Figure 4.9 Comparison of left and right hand fingerprints stained with SG at 40X concentration (5 µL) on a glass substrate. The values shown are minus the negative control (dyes intrinsic fluorescence) 1 indicates pointer finger, 2 middle, 3 ring and 4 pinky.

Figure 4.10 Comparison of bacterial signals (1×10^6 cells/µL) on different substrates using both GG and SG binding dyes (20X, 5 µL), signal is shown minus background (intrinsic

fluorescence of dye).

- Figure 4.11** Intensity of signals from varying amounts of bacterial DNA (cells/ μL) showing the initial signal and then the signal after 10 min incubation using SG binding dye (20X, 5 μL).
- Figure 4.12** Comparison of background intensity to BSA (2 $\mu\text{g}/\mu\text{L}$) intensity using six DNA binding dyes at 20X concentration (5 μL) on a glass substrate.
- Figure 4.13** Intensity of BSA signals (2 $\mu\text{g}/\mu\text{L}$) minus the background signal using binding dyes at 20X concentration.
- Figure 4.14** Average volume intensity of DNA binding dyes (5 μL at 20X concentration) in the presence of DNA (50 ng), protein (BSA at 50 ng) and negative control (dye/ H_2O) exposure time was at 1.2 s using Gel Doc™ lane band analysis tool. Results were undertaken in triplicate with error bars show 95% confidence.
- Figure 4.15** Average intensity enhancement of the binding dyes in the presence of DNA (50 ng) and protein (BSA at 50 ng) to the background of the dyes (intrinsic fluorescence) exposure time was at 1.2 s using Gel Doc™ lane band analysis tool. Results were undertaken in triplicate with error bars show 95% confidence.
- Figure 4.16** Average intensity enhancement of the binding dyes in the presence of DNA (50 ng) and protein (BSA at 50 ng) to the background of the dyes (intrinsic fluorescence) exposure time was at 10 s using Gel Doc™ lane band analysis tool. Results were undertaken in triplicate with error bars show 95% confidence.
- Figure 4.17** Detection parameters of the Gel Doc™ EZ Imager in relation to the excitation and emission signals of SYBR® Green when using blue transillumination. Excitation at 460 nm (green band) and emission filter from 560-700 nm (black box).
- Figure 4.18** Detection parameters of the Gel Doc™ EZ Imager in relation to the excitation and emission signals of SYBR® Green when using UV transillumination. Excitation at 302 nm (red band) and emission filter 535-640 nm (black box).
- Figure 4.19** Intrinsic fluorescence of dyes DD, GG and RS without DNA present in a 20x H_2O solution with varying exposure times using a 550 nm cut-off filter; (A) exposure time 1/10 s, (B) exposure time 1/5 s, (C) exposure time 1/2 s, (D) exposure time 1 s.
- Figure 4.20** Intrinsic fluorescence of dyes DD, GG and RS without DNA present in a 20x H_2O solution with varying exposure times using a 555 nm interference filter (A) 1/5 s, (B) 1/2 s, (C) 1 s, (D) 2 s, (E) 2.5 s.
- Figure 4.21** GelGreen (40x) varying DNA concentration with varying exposure times over a 3 min time period with a 555 nm cut-off filter (A) exposure 1.6 s at time 0, (B) exp 1.6 s (C) exp 2 s time 1 min, (D) exp 2.5 s time 1min, (E) exp 0.62 s at time 1 min, (F) exp 1.6 s at time 3 min.
- Figure 4.22** Varying amounts of DNA on a glass substrate with DNA binding dyes DD, GG, RS and GR (20X, 5 μL) at an exposure time of 1/5 s using a 550 nm cut-off filter with (A) 0.5 ng, (B) 1 ng, (C) 5 ng, (D) 10 ng.
- Figure 4.23** 1 ng of DNA with staining using DD, GG, RS and GR at 20X concentration with varying exposure times (A) 1/5 s, (B) 1/2 s, (C) 1 s, (D) 2 s.

- Figure 4.24** Varying amounts of DNA with binding dyes DD, GG, RS and GR (20X, 5 μ L) and negative control (bottom row) at an exposure of 1/5 s using 555 nm interference filter (A) 0.5 ng, (B) 1 ng, (C) 5 ng, (D) 10 ng.
- Figure 4.25** Detection of DNA within fingerprints using DD (20X in H₂O) on a glass substrate using Polilight[®] at 490 nm excitation (A) 40X magnification using Nikon Optiphot fluorescent microscope with B2A filter cube, (B) emission detection using a 535 nm interference filter and (C) emission detection using a 550 nm cut-off filter.
- Figure 4.26** Detection of protein within fingerprints using Qubit[®] Protein Reagent (20X in H₂O) on a glass substrate using Polilight at 490 nm excitation (A) 40X magnification using Nikon Optiphot fluorescent microscope with B2A filter cube, (B) emission detection using a 535 nm interference filter and (C) emission detection using a 550 nm cut-off filter.
- Figure 4.27** Comparison of BSA (1, 5 and 10 ng) signal to DNA (1, 5 and 10 ng) using DD (20X in H₂O) with excitation at 490 nm and emission through a 535 nm interference filter.
- Figure 4.28** DNA concentration within fingerprints on acetate paper quantified using Qubit[®] 2.0 Fluorometer, readings were in triplicate, raw results for each volunteer see Appendix C table C-16-18.

- Figure 5.1** Schematic diagram of fluorescence spectra of DAPI compared with SYBR Green, showing the UV/blue region and blue/green region and the comparison of the fluorescent enhancement when in the presence of DNA.
- Figure 5.2** Showing plucked hair follicle with skin sheath (A) before staining and (B) after staining with EG 20X.
- Figure 5.3** Showing plucked hair follicle with skin sheath (A) before staining and (B) after staining with DD 20X.
- Figure 5.4** Showing plucked hair follicle with skin sheath (A) before staining and (B) after staining with RS 20X.
- Figure 5.5** Comparison of average DNA quant (Qubit[®] HS ds-DNA assay) from stained plucked hairs after DNA extraction (4 replicates for each dye), error bars show 95% confidence.
- Figure 5.6** Comparison of average DNA quant (Investigator[®] qPCR kit) from stained shed hairs after DNA extraction (4 replicates for each dye), error bars show 95% confidence.
- Figure 5.7** Comparison of the average peak heights obtained from plucked hairs when amplified directly or amplified after extraction. The average is based on profile replicates (4 hairs) then an overall average of 32 (alleles) for each. Error bars show 95% confidence.
- Figure 5.8** Screened hair stained with DD (20X) viewed under a fluorescent microscope at 40X magnification with an exposure time of 1 s. NGM[™] Profile of directly amplified hair.

- Figure 5.9** Screened hair stained with DD (20X) viewed under a fluorescent microscope at 40X magnification with an exposure time of 1 s. NGM™ Profile of directly amplified hair. Hair was placed in category 1.
- Figure 5.10** Screened hair stained with DD (20X) viewed under a fluorescent microscope at 40X magnification with an exposure time of 1 s. NGM™ Profile of directly amplified hair. Hair was placed in category 1.5.
- Figure 5.11** Screened hair stained with DD (20X) viewed under a fluorescent microscope at 40X magnification with an exposure time of 1 s. NGM™ Profile of directly amplified hair. Hair was placed in category 2.
- Figure 5.12** Screened hair stained with DD (20X) viewed under a fluorescent microscope at 40X magnification with an exposure time of 1 s. NGM™ Profile of directly amplified hair. Hair was placed in category 2.5.
- Figure 5.13** Screened hair stained with DD (20X) viewed under a fluorescent microscope at 40X magnification with an exposure time of 1 s. NGM™ Profile of directly amplified hair. Hair was placed in category 3.
- Figure 5.14** Screened hair stained with DD (20X) viewed under a fluorescent microscope at 40X magnification with an exposure time of 1 s. NGM™ Profile of directly amplified hair. Hair was placed in category 3.
- Figure 5.15** Comparison of the percentage of hairs that produce full profiles and no profiles in each of the 5 categories of the number of nuclei. The line of best fit is shown for full profile and for no profile along with R^2 values showing the linearity of the results.
-
- Figure 6.1** DNA binding dyes screened for potential use in qPCR, analysis was undertaken with the Green Channel with DNA at a concentration of 28.4 ng/μL, reactions were done in quadruplicate.
- Figure 6.2** Average neat DNA analysis using DNA dye combinations, DNA concentration at 28.4 ng/μL, all reactions were done in quadruplicate.
- Figure 6.3** Average melt curve of screened dyes analysis was undertaken using the Green channel, reactions were done in quadruplicate.
- Figure 6.4** Average melt curve of screened dyes analysis was undertaken using the Diamond channel, reactions were done in quadruplicate.
- Figure 6.5** SG.DD dilution series using human fragment 2 analysis using diamond channel. All reactions were done in quadruplicate.
- Figure 6.6** Standard curve of SG.DD showing analysis using the Diamond channel and the Green channel, reactions were done in quadruplicate.
- Figure 6.7** Standard curve of SG Diamond channel of SG dilution series and Green Channel of SG dilution series, and reactions done in quadruplicate.
- Figure 6.8** Standard curve of SG and SG.DD Diamond channel analysis was used for SG.DD

and Green Channel was used for the analysis of the SG dilution series, and reactions done in quadruplicate.

Figure 6.9 Average melt curve of SG.DD (A) Diamond channel, (B) Green channel, reactions done in quadruplicate.

Figure 6.10 Average melt curve of SG (A) Diamond channel, (B) Green channel both reactions done in quadruplicate.

Figure 6.11 Comparison of neat DNA using SG and SG.DD reactions were done in duplicate using the green channel.

Figure 6.12 Average cycling curve using ALU nuclear DNA target, (B) Standard curve of ALU nuclear DNA target, using DD at 1X concentration with 1 being neat DNA at 28.4 ng/ μ L concentration.

Figure 6.13 Average fluorescent signal of DD (0.5X) binding to ssDNA primers at varying concentrations and length, down in quadruplicate.

Figure 6.14 Average melt curve analysis of DD with ss-DNA primers (red indicates primer SNPH16130 59 bases and pink indicates primer SNPH00147 51 bases).

Figure 6.15 Cycling curve of fluorescence intensity against cycle number for SG, BG, EG and DD at 28.4 ng/ μ L. Reactions were done in quadruplicate.

Figure 7.1 Demonstration of staining on tape-lifts with saliva present, staining using Diamond™ Dye (1 μ L of 20X concentration) under 100X magnification using Nikon Optiphot fluorescent microscope.

Figure 7.2 Demonstration of staining on tape-lifts with skin flakes, staining using Diamond™ Dye (1 μ L of 20X concentration) under 100X magnification using Nikon Optiphot fluorescent microscope.

LIST OF TABLES

Table 1.1	List of nucleic acid binding dyes commonly used for staining within gel electrophoresis.
Table 1.2	List of dyes used for DNA quantification and the type of DNA/RNA they detect and the sensitivity.
Table 1.3	Nucleic acid binding dyes used with quantitative PCR.
Table 1.4	Dyes used within Flow Cytometry and fluorescent microscopy for cell staining.
Table 1.5	Dyes used for fluorescent microscopy for forensic samples.
Table 2.1	Range of Cyanine Dyes available with their maximum excitation and emission wavelength.
Table 2.2	Dyes Selected for Study on Gel Electrophoresis showing the Different Properties of the Dyes.
Table 2.3	Summary of detection limits (ng) of the nucleic acid binding dyes using both precast staining and post electrophoresis staining.
Table 2.4	Molecular structures available of the nucleic acid binding dyes used in this study.
Table 3.1	Peak heights for alleles of amplified extracted samples that had DNA binding dyes present during the extraction process, in triplicate.
Table 3.2	Ranking of the dyes in three categories investigated within this Chapter with 1 being the lowest effect.
Table 4.1	Selected DNA binding dyes for investigation in their use for latent DNA detection.
Table 4.2	Polilight [®] excitation wavelengths include the size of the band-pass filter as well as available cut-off and interference filters.
Table 4.3	Filters to be used with the dyes depending on their excitation (Ex) and emission (Em) wavelengths.
Table 4.4	Linearity of the dyes fluorescent signal when staining DNA on a surface in comparison to DNA staining within agarose gel medium.
Table 4.5	Calculation of the amount of DNA present within fingerprints stained with GG (based on values in Figure 4.5) on substrates that have been treated.

Table 4.6	Calculated amount of DNA present within fingerprints (Figure 4.6 values) based on the line of best fit equation for SG (Figure 4.5).
Table 4.7	Varying amounts of DNA with dye staining at 20X concentration, optimal exposure time shown in brackets using a 535 nm interference filter.
Table 4.8	Staining of biological samples, hair, skin and saliva with DNA binding dyes.
Table 5.1	Currently used staining methods for hair follicles.
Table 5.2	Comparison of currently used fluorescent stains with dyes used within Chapter 2 and 3.
Table 5.3	Average DNA quant by RT-PCR (Investigator [®] Quantiplex kit) 3 replicates, of extracted hairs stained with DNA binding dyes (20X) with images of the hairs post staining (exposure time 1 s, 40X magnification) arrows pointing to increase magnification image and potential nuclei.
Table 5.4	Average DNA quant by Qubit [®] (3 replicates) of extracted hairs stained with DNA binding dyes (20X) with images of the hairs post staining (exposure time 1 s, 40X magnification).
Table 5.5	Average peak heights (4 replicates) of plucked hairs stained with DNA binding dyes (20X) then extracted using QIAamp and amplified using NGM [™] STR kit and optimum amount of DNA (1 ng).
Table 6.1	Primer sequences and amplicon properties used in RT-PCR [23] Alu sequences [24].
Table 6.2	Average Ct and standard deviation values of the dyes that amplified product analyzed using the Green and Diamond channel.
Table 6.3	Average Ct and standard deviation values of the combination of dyes that amplified product analyzed using the Green and Diamond channel.
Table 6.4	Dilution series using dye combination of SG.DD (DD at 0.5X concentration).
Table 6.5	SG Kapa dilution series using human fragment 2 primers.
Table 6.6	Comparison of R ² and efficiency values of SG and SG.DD dilution series using both the green and diamond channel.
Table 6.7	Difference in average Cq values for the SG.DD and SG dilution series using both Diamond and Green channels.
Table 7.1	Overall ranking of the dyes for each characteristic investigated within this thesis.

LIST OF SCHEMES

- Scheme 4.1** Schematic diagram of how cut-off (550 nm) and interference (535 nm) filters work in reference to SYBR[®] Green's excitation and emission spectra.
- Scheme 4.2** Schematic diagram of filters work for the detection of fluorescent signals (A) showing a barrier or cut-off filter, (B) showing an interference filter.
- Scheme 4.3** Schematic representation of the acetate paper where the fingerprints were deposited onto then cut-off into 1.5 mL tube.
- Scheme 4.4** Schematic representation of the excitation of SG with the Gel Doc EZ Imager settings the maximum excitation λ is at 460 nm; SG excitation is at 494 nm. The proportion of the SG excitation spectrum being excited with the Gel Doc is indicated in red.
- Scheme 4.5** Schematic representation of the detection of SG emission signal with the Gel Doc EZ Imager settings, maximum emission λ is between 560-700 nm; SG emission is at 521 nm. The proportion of the SG emission detection with the Gel Doc is indicated in red.
- Scheme 4.6** Schematic representation of the excitation of SG with the Polilight the maximum excitation λ is centered at 490 nm with a 40 nm bandwidth (excitation between 470-510 nm); SG excitation is at 494 nm. The proportion of the SG excitation spectrum being excited with the Polilight is indicated in red.
- Scheme 4.7** Schematic representation of the emission detection of SG with an interference filter, maximum excitation λ is centered at 530 nm with a 40 nm bandwidth (emission detection between 510-550 nm); SG emission is centered at 520 nm. The proportion of the SG emission spectrum being detected with the interference filter is indicated in red.
- Scheme 4.8** Schematic representation of the dye/DNA complex when in solution compared with the signal obtained once the dye/DNA complex had dried on a glass surface.
- Scheme 4.9** Schematic representation of the layers of the epidermis, adapted from [15].
-

- Scheme 5.1** Schematic representation of a hair follicle showing the three primary structures, Medulla, cortex and cuticle, as well as the root.
-

- Scheme 6.1** Schematic representation of the interaction of a molecular beacon with a target sequence adapted from [16].

- Scheme 6.2** Schematic diagram of a binary probe before and after the addition of the target adapted from [16].

- Scheme 6.3** Structure and mechanism of action of hydrolysis probes of TaqMan probe assay taken from Navarro, E et al [18].

Scheme 6.4 Schematic representation of how SYBR Green (SG) molecules bind during qPCR and fluoresce when bound to ds-DNA, adapted from [21].

Scheme 7.1 Schematic representation of how the dyes would work to find touch-DNA on evidentiary items within a forensic investigation (A) showing the item before staining where no evidentiary material cannot be seen (B) showing the item after staining and exciting with blue light which shows deposits of higher fluorescence indication DNA material.

LIST OF ABBREVIATIONS AND SYMBOLS

Å	Angstrom (10^{-10} metre)
ANZFSS	Australian and New Zealand Forensic Science Society
BSA	Bovine Serum Albumin
BG	BRYT Green®
CE	Capillary Electrophoresis
Cq	Quantitation cycle
DAPI	4',6-diamidino-2-phenylindole
DNA	Deoxyribonucleic acid
DD	Diamond Nucleic Acid Dye
DMSO	Dimethyl Sulfoxide
ds-DNA	Double-Stranded DNA
EDTA	Ethylenediaminetetraacetic acid
EG	EvaGreen™
EtBr	Ethidium Bromide
FSSA	Forensic Science South Australia
FWHM	Full Width at Half Maxima
GG	GelGreen™
GR	GelRed™
ISFG	International Society of Forensic Genetics
mtDNA	Mitochondrial DNA
nm	Nanometre
ng	Nanogram
PCR	Polymerase Chain Reaction
PG	PicoGreen®
qPCR	Quantitative PCR
RS	RedSafe™
RT-PCR	Real-Time PCR
RFU	Relative Fluorescent Units
s	Seconds
ss-DNA	Single-Stranded DNA
SG	SYBR® Green I
STR	Short Tandem Repeat
TAE	Tris-acetate-EDTA

TAPS	<i>N</i> -tris(hydroxymethyl)methyl-3-aminopropanesulfonic acid
TBE	Tris-borate-EDTA
TE	Tris-EDTA
UV	Ultraviolet
λ	Wavelength (nm)
μL	Microlitre

PUBLICATIONS

The publications originating from the work within this thesis are as follows:

Accepted Papers:

Alicia M. Haines, Shanan S. Tobe, Hilton Kobus, Adrian Linacre, Detection of DNA within fingerprints, *Forensic Sci. Int. Genetics Supplement Series* **4**, 2013, e290-e291.

Citations: **1** Impact Factor: 0.178 Journal Rank: 0.197 (SCImago Journal Rank)

Alicia M. Haines., S.S. Tobe., H.J. Kobus., A. Linacre, Properties of nucleic acid staining dyes used in gel electrophoresis, *Electrophoresis*. **36** (6), 2015, p. 941-944.

Citations: **6** Ranking of journal: **26/75** (Chemistry Analytical) IF: **2.482** (2015)

Alicia M. Haines, Shanan S. Tobe, Hilton Kobus, Adrian Linacre, The effect of nucleic acid binding dyes on DNA extraction, amplification and STR typing, *Electrophoresis*. **36** (20), 2015, p. 2561-2568.

Citations: **2** Ranking of journal: **26/75** (Chemistry Analytical) IF: **2.482** (2015)

Alicia M. Haines, Shanan S. Tobe, Hilton Kobus, Adrian Linacre, Successful Direct STR amplification of hair follicles after nuclear staining, *Forensic Sci. Int. Genetics Supplement Series* **5**, 2015, e65-66.

Citations: **1** Impact Factor: 0.178 Journal Rank: 0.197 (SCImago Journal Rank)

Alicia M. Haines, Shanan S. Tobe, Hilton Kobus, Adrian Linacre, Duration of in situ fluorescent signals within hairs follicles, *Forensic Sci. Int. Genetics Supplement Series* **5**, 2015, e175-176.

Citations: **0** Impact Factor: 0.178 Journal Rank: 0.197 (SCImago Journal Rank)

Alicia M. Haines, Shanan S. Tobe, Hilton Kobus, Adrian Linacre, Finding DNA: Using fluorescent in situ detection, *Forensic Sci. Int. Genetics Supplement Series* **5**, 2015, e501-502.

Citations: **0** Impact Factor: 0.178 Journal Rank: 0.197 (SCImago Journal Rank)

Alicia M. Haines, Adrian Linacre, A rapid screening method using DNA binding dyes to determine whether hair follicles have sufficient DNA for successful profiling, *Forensic Science International*, **262** (issue), 2016, p. 190-195.

Citations: 0 Ranking of journal: **5/15** in Medical, Legal (2015) IF: **1.950** (2015)

Alicia M. Haines, Adrian Linacre, Shanan S. Tobe, Optimization of Diamond™ nucleic acid dye for quantitative PCR, accepted July 2016, *BioTechniques*, Report, accepted July 2016

Ranking of journal **41/77** (2015) IF: **2.298** (2015)

Papers ready for submission:

For submission to Science & Justice, Forensic Science Medicine and Pathology (FSMP) or Electrophoresis

Alicia M. Haines, Adrian Linacre

Entitled: *Nucleic acid binding dyes: a review*, 2016

CONFERENCE PROCEEDINGS

(Name in bold denotes presenting author)

Alicia M. Haines, Shanan S. Tobe, Hilton Kobus, Adrian Linacre, Detection of DNA within fingerprints, Poster Presentation at the 25th *World Congress of the International Society for Forensic Genetics (ISFG)*, Melbourne, Australia, 2013

Alicia M. Haines, Shanan S. Tobe, Hilton Kobus, Adrian Linacre, *In situ* detection of latent DNA using nucleic acid staining dyes and an alternative light source. Oral Presentation at the ANZFSS 22nd *International Symposium on the Forensic Sciences*, Adelaide, SA, 2014

Alicia M. Haines, Shanan S. Tobe, Hilton Kobus, Adrian Linacre, Quantification of ds-DNA and protein present within the residue of fingerprints using the Qubit 2.0 Fluorometer. Poster Presentation at the ANZFSS 22nd *International Symposium on the Forensic Sciences*, Adelaide, SA, 2014

Alicia M. Haines, **Adrian Linacre**, Detection of latent DNA on surfaces, Invited speaker at the RACI (Royal Australian Chemical Institute) *National Congress*, Adelaide, SA, 2014

Alicia M. Haines, Shanan S. Tobe, Hilton Kobus, Adrian Linacre, *In situ* detection of latent DNA using nucleic acid staining dyes and an alternative light source. Oral Presentation at the 67th *Annual Meeting of the American Academy of Forensic Science*, Orlando, Florida, USA, 2015

Alicia M. Haines, Shanan S. Tobe, Hilton Kobus, Adrian Linacre, Successful Direct STR amplification of hair follicles after nuclear staining, Poster Presentation at the 26th *World Congress of the International Society for Forensic Genetics (ISFG)*, Krakow, Poland, 2015

Alicia M. Haines, Shanan S. Tobe, Hilton Kobus, Adrian Linacre, Duration of *in situ* fluorescent signals within hairs follicles, Poster Presentation at the 26th *World Congress of the International Society for Forensic Genetics (ISFG)*, Krakow, Poland, 2015

Alicia M. Haines, Shanan S. Tobe, Hilton Kobus, Adrian Linacre, Finding DNA: Using fluorescent *in situ* detection, Poster Presentation at the 26th *World Congress of the International Society for Forensic Genetics (ISFG)*, Krakow, Poland, 2015

Alicia M. Haines, Shanan S. Tobe, Hilton Kobus, Adrian Linacre, Finding DNA: Using *in situ* fluorescent detection. Oral Presentation at the 7th *European Academy of Forensic science conference*, Prague, Czech Republic, September, 2015

Alicia M. Haines, Finding DNA using fluorescent *in situ* detection, Oral Presentation at the *ANZFSS 23rd International Symposium on the Forensic Sciences*, Auckland, New Zealand, September, 2016

Alicia M. Haines, DNA binding dyes for nuclear staining of hair follicles, Poster Presentation at the *ANZFSS 23rd International Symposium on the Forensic Sciences*, Auckland, New Zealand, September, 2016

Alicia M. Haines, Alternative DNA binding dyes for real-time PCR, Poster Presentation at the *ANZFSS 23rd International Symposium on the Forensic Sciences*, Auckland, New Zealand, September, 2016

SEMINARS AND PRESENTATIONS

(Name in bold denotes presenting author)

Alicia M. Haines, Detection of latent DNA at crime scenes using intercalating dyes, School of Biological Sciences Post-Graduate Conference, July, 2013

Alicia M. Haines, Finding DNA using fluorescent detection, Three-minute Thesis Presentation, School of Biological Sciences, July, 2014

Alicia M. Haines, *In situ* detection of latent DNA at crime scenes using nucleic acid staining dyes, School of Biological Sciences Post-Graduate Conference, November, 2014

Alicia M. Haines, Finding DNA using fluorescent *in situ* detection, School of Biological Sciences Post-Graduate Conference, November, 2015

Alicia M. Haines, Finding DNA using fluorescent *in situ* detection, Seminar at Forensic Science South Australia, March, 2016

Alicia M. Haines, Adrian Linacre, Biology School seminar: Forensic Science, *CSI to DNA: detecting and profiling latent DNA*, Flinders University, School of Biological Sciences, March, 2016

AWARDS

Oscar Rivers Schmalzbach Foundation (ORSF) Research Fellowship through the Australian Academy of Forensic Sciences (\$15,000) **2016**

Research Higher Degree Student International Conference Travel Grant (\$500) **2016**

ANZFSS SA Branch Symposium Travel Stipend for the 23nd International Symposium on the Forensic Sciences (\$900) **2016**

ANZFSS National Executive Symposium Travel Award for the 23nd International Symposium on the Forensic Sciences (\$800) **2016**

Best poster presentation at the 26th Congress of the *International Society of Forensic Genetics* (out of over 400 posters, 500 Euro prize money) **2015**

The Australian Federation of University Women – South Australia (AFUW-SA) Inc. Trust Fund award for Travel (\$2,000) **2015**

Flinders University Research Student Conference Travel Grant (\$1890.40) **2015**

Faculty of Science and Engineering International Travel Award (\$1,500) **2015**

ANZFSS SA Branch Symposium Travel Award for the 22nd International Symposium on the Forensic Sciences (\$750) **2014**

Flinders University Research Scholarship (FURS)

(Undertake a Doctorate by research) **2013-2016**

Chapter 1

Nucleic acid binding dyes: A review

Nucleic acid binding dyes: A review

Abstract

Nucleic acid binding dyes are used in a range of techniques and cross over interdisciplinary scientific areas for the fluorescent detection of DNA. The aim of this review is to give a detailed guide to nucleic acid binding dyes and their use in different applications such as gel electrophoresis, cell staining, quantitative PCR and other scientific applications. Background on the dye chemistries of the major dyes used within laboratories will be discussed. New developments within the use of these dyes will also be discussed.

Key Words: DNA quantification, Gel electrophoresis, SYBR® Green I, quantitative PCR

Table of Contents

1. Introduction	3
1.1 Fluorescence and Fluorophores.....	3
1.2 DNA Structure.....	5
1.3 DNA Binding Dyes.....	6
1.3.1 Intercalating dyes.....	8
1.3.2 Groove binding dyes.....	9
2. Applications of nucleic acid binding dyes	9
2.1 Staining in gel electrophoresis	10
2.2 DNA quantification	12
2.3 DNA amplification and detection (qPCR)	13
2.4 Flow Cytometry, Cell staining	16
2.5 Nucleic acid dyes for fluorescent microscopic investigations of forensic relevant samples ...	18
3. Concluding remarks	20
4. Thesis Aims	21
5. References	22
6. Supplementary Information	28

1. Introduction

For those of us whose research revolves around DNA, it is a strange situation where DNA is never actually observed. Rather the presence of the DNA molecule is identified based on the binding of a dye to the DNA structure resulting in an emission of fluorescence. Nucleic acid binding dyes are used within many areas of scientific research. The most widely used application of nucleic acid binding dyes is in gel electrophoresis for the detection of DNA. Here for many years, ethidium bromide (EtBr) has long been the standard means of detecting DNA within gel. The ease of use and relatively high sensitivity compared to alternatives outweighed the known toxicity of the dye. Other areas of DNA detection that use binding dyes include the following: flow cytometry, fluorescent microscopy, fluorescent labelling, fluorescent DNA quantification, quantitative PCR and cell staining. The advent of new dyes in the last decade that are now commercially available means that there is much greater choice than ever before.

The ideal dye to detect DNA would be one that is safe to use in all applications, is inexpensive to buy, is simple to apply, binds to the DNA rapidly allowing quick detection, gives much increased enhancement, works on intact cells or if the DNA is as a free molecule, is very easy to visualize and does not require complex or expensive equipment for detection. Currently there are few dyes that meet all these criteria but some satisfy the majority; as will be discussed. The use of the most appropriate dye for the detection of DNA is dependent on whether the DNA is a free molecule or within the cell nucleus which is intact. This review aims to discuss the dyes available for each application and detail the chemistry behind how some of these dyes work.

1.1 Fluorescence and Fluorophores

Fluorescence spectroscopy is a powerful technique for the detection of organic and inorganic compounds. The first stage of fluorescence involves the absorption of electromagnetic radiation at a particular wavelength. This absorption of the radiation allows molecules to become excited to a higher energy state and at a higher vibrational level within the excited state. Molecules can only absorb limited amounts of radiation, this unit is known

as quanta, and corresponds to the difference in energy levels between the ground and the excited state [1].

There are two types of fluorophores, intrinsic and extrinsic. Intrinsic are those that occur naturally and extrinsic are those that are added to a sample to produce fluorescence. Extrinsic fluorophores are used when the molecule of interest is either non-fluorescent or the level of fluorescence is too low for detection. This is the case with the detection of DNA [1, 2]. There are many fluorophores that attach to DNA and display an enhanced emission; EtBr and SYBR[®] Green I (SG) are the most well-known fluorophores that bind to DNA.

There are both external and internal factors that can influence the detection of fluorescence. Internal factors include temperature, pH, the sample matrix, and the concentration and structure of the molecule. External factors include the instrument used and sensitivity of the method. The structure of the molecule can influence the level of the fluorescence depending on the functional groups present (for instance electron donating groups increase fluorescence e.g. OCH_3 ; electron withdrawing groups can reduce fluorescence e.g. Cl^- , NO_2). Fluorophores that have absorption in the visible spectrum have numerous conjugated double bonds (alternating between sigma (σ) and pi (π) bonds) such as aromatic rings [3]. The temperature can affect the molecule's wavelength of fluorescence and range of the spectrum. Temperature variation can affect the viscosity of the solution and can influence the number of collisions between fluorescing and solvent molecules [1, 2].

Internal scattering occurs when the solution contains small particles and some of the incident energy can be scattered rather than absorbed, and is mistakenly detected as fluorescence, hence can hinder the accurate detection of fluorescence [1, 2]. Between the absorption and emission spectra there will be some overlap. Figure 1 shows a typical spectrum showing the excitation and the emission of fluorescence of a fluorophore [1, 2]. The gap between excitation and emission maxima is known as the Stokes shift (Figure 1.1 A). It is an advantage for detection of fluorescence when the Stokes shift is sufficiently large to minimize the overlap between excitation and emission spectra. Fluorescence results in excitation from ground singlet state, S_1 , to first excited state, S_2 (see Figure 1.1 B); it results in excitation to a higher vibrational state in S_2 . De-excitation involves falling to the lowest vibrational state in S_2 followed by emission of light to fall back to S_1 . Thus excitation is to a

higher energy level than the de-excitation and this is why the emission wavelength is longer than excitation. This is detailed in the Jablonski diagram below (Figure 1.1 B) [1, 2].

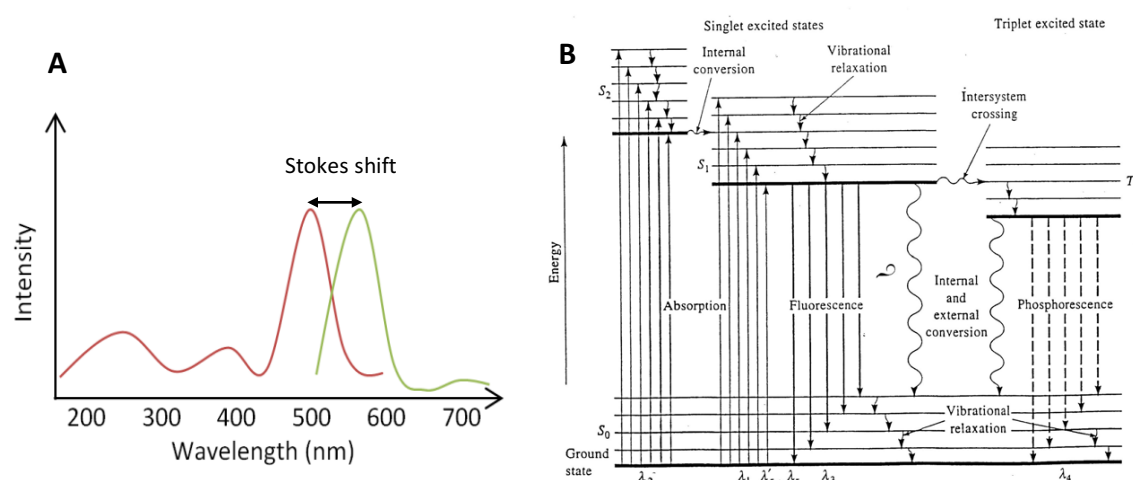


Figure 1.1: (A) Example of a fluorescent spectrum of a fluorophore showing excitation in red and emission in green, Stokes shift is indicated with arrows, and the intensity is in arbitrary units. (B) Jablonski diagram, absorption of light resulting in excitation and fluorescence emission, adapted from [1, 2].

1.2 DNA Structure

Many molecular biologists that use DNA routinely in their research might not be aware of the chemical interaction that occurs when a dye is used. Understanding the chemical interaction of dye and DNA allows the best choice of dye to be made. Firstly it is necessary to be familiar with the structure of the DNA molecule. DNA is built up of a triphosphate group, a deoxyribose sugar and one of four nitrogenous bases, adenine, thymine, cytosine and guanine. A schematic representation of DNA is shown in Figure 1.2. DNA generally exists as double-stranded molecule in a helical structure. The four bases are grouped into two types of molecules, pyrimidines (thymine and cytosine) and purines (adenine, guanine). Each base has a complementary base to which it is attracted: guanine pairs with cytosine and adenine pairs with thymine [9].

The DNA molecule can be found in three different forms termed the A, B and Z form, however, the normal state is the B-form [4]. This was first observed through x-ray diffraction [5]. The main difference between the A and B-form is that the A-helix is wider and shorter than the B-form. The Z-form is left-handed, unlike A and B which are right-handed, and the forms also differ in the number of base pairs per helical turn; A has 11 base pairs, B 10.4 and

Z has 12. Within the DNA molecule there are two grooves which arise from the base pairs not being opposed diametrically; this offset leads to a minor and major groove. The size of the major groove is 12 Å wide and 8.5 Å deep compared with the minor groove being 6 Å wide and 7.5 Å deep [4]. The major groove allows greater access to the DNA molecule than the minor groove for dye binding, however some dyes are sequence dependent resulting in preferential binding [6].

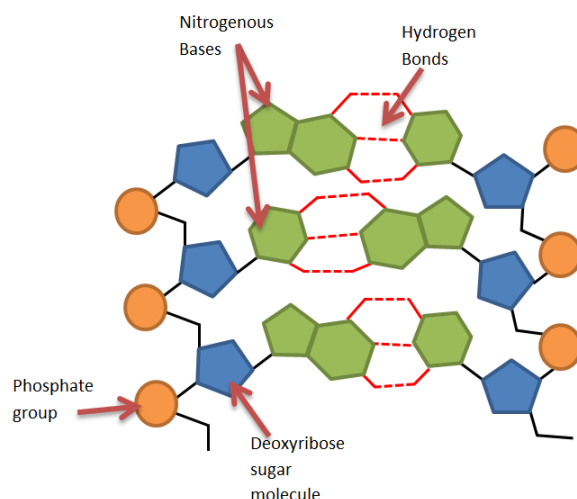


Figure 1.2: Schematic representation of the DNA structure showing the phosphate group, nitrogenous bases, deoxyribose sugar molecule and the hydrogen bonding linking the two strands together.

1.3 DNA Binding Dyes

Dyes can be separated into categories based on how they interact with DNA; intercalating dyes and groove binding dyes are the major mechanisms for DNA interactions, some dyes however do not fall into either of those mechanisms. Figure 1.3 outlines the various binding mechanisms a dye can have with DNA.

An intercalating dye is one that binds within the double strands of the DNA molecule. For this to happen effectively, the DNA molecule needs to be in its intact form and not denatured. A groove binding dye attaches to the outer backbone of the DNA when in the helical structure and can bind to single-stranded DNA. Intercalating dyes generally tend to be more specific to DNA due to the multiple binding mechanisms of the dye. Depending on the dye, each base pair offers a position of dye/DNA binding.

EtBr and SG are two of the most well-known intercalating dyes. These dyes can show up to a 1000-fold increase in fluorescent enhancement when in the presence of DNA [7]. An issue is that any dye that intercalates with the DNA molecule is potentially capable of having the same interaction with living cells, such as those of the researcher. Hence these dyes, if cell permeable, can cause mutations. Groove binding dyes can bind to the minor or major groove of the DNA, such as DAPI, a minor groove binding dye and selective for AT rich regions. These dyes can vary in enhancement but are generally much lower than their intercalating counterparts; for instance DAPI only has a 20-fold increase in enhancement [6, 8].

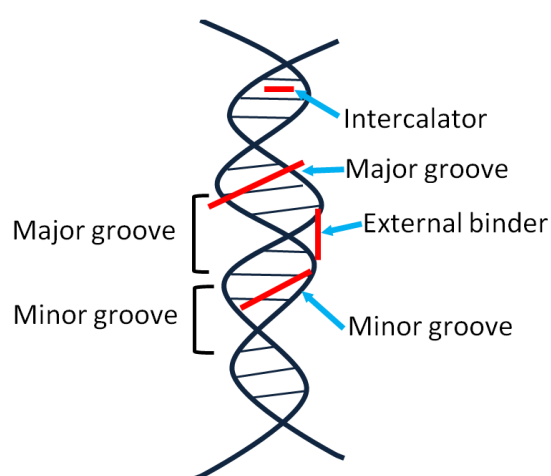


Figure 1.3: Schematic representation of the DNA double helix with indications of the minor and major groove of DNA and along with the various dye binding mechanisms, adapted from [9].

1.3.1 Intercalating dyes

Examples of intercalating dyes and their corresponding molecular structure are shown below in Figure 1.4. The molecular structure of GelRed™ (GR) is composed of two EtBr molecules with a bridging hydrocarbon chain. Due to the molecule's relatively large molecular weight (GR 1238 g/mol, GelGreen™ (GG) 1198 g/mol [10]) it cannot permeate the cell membrane. This has the benefit of making the dye less mutagenic than its single molecule counterpart, EtBr. GG is similar to GR in that it is composed of two acridine orange molecules connected with a hydrocarbon bridge; thus making the dye also impermeable to the cell membrane and therefore reducing the mutagenic potential of the dye. Both GG and GR are therefore ideal for detecting double-stranded DNA (dsDNA) as a free molecule. Both are substitutes for EtBr to detect DNA separated by gel electrophoresis.

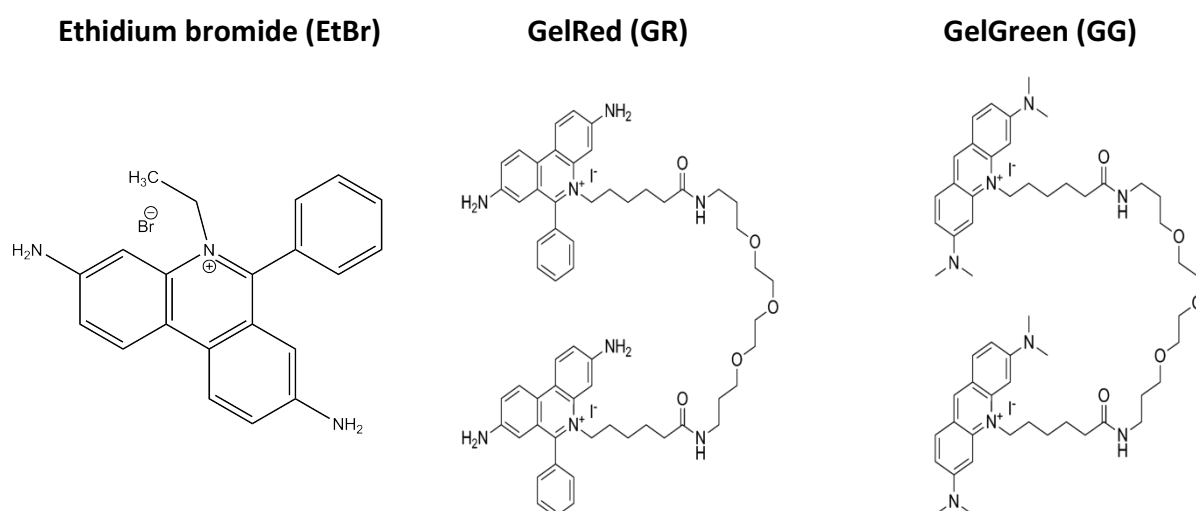


Figure 1.4: Molecular structure of ethidium bromide [7] (**left**), GelRed [10] (**Centre**) and GelGreen [10] (**right**).

PicoGreen® (PG) has been one of the most utilized dyes for DNA quantification due to its high fluorescent enhancement over 1000-fold and dsDNA specificity in comparison to other dyes like Hoechst 33258 (30-100-fold) [11, 12] and DAPI (20-fold) [6, 8]. DNA quantification with PG is very rapid with binding (96%) occurring within 10 seconds of the dye's addition to the sample [13]. The PG assay became a favoured means of quantification of DNA after DNA extraction by many forensic laboratories. PG is often favoured over dyes like DAPI and Hoechst 33258 as it is not sequence dependent (AT-selective) which affects the fluorescent intensity [14]. The molecular structure and the binding attributes of PG and SG are shown in Figure 1.5.

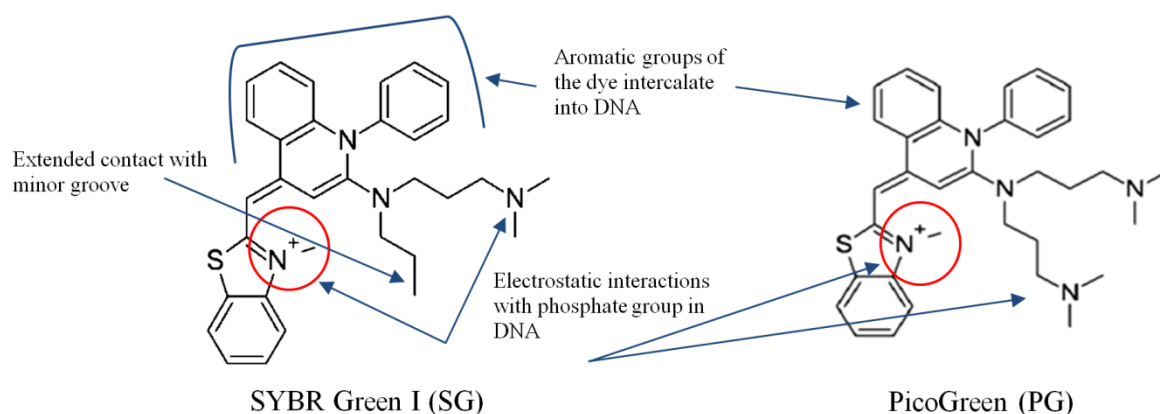


Figure 1.5: Molecular structure of SG (left) and PG (right) showing the various binding mechanisms the dyes have with DNA, adapted from [7].

1.3.2 Groove binding dyes

The most well-known DNA groove binding dyes are DAPI and the Hoechst series of dyes (33342, 33258). The structures of these dyes are shown below in Figure 1.6. In comparison to the intercalating dyes, the structures are not as complex and are much more linear than the structures for SG and GG. The aromatic rings are still present, which is a common feature of fluorophores. The linear nature of the molecules allows binding to the outer backbone of the DNA molecule. DAPI is only a 3 ring structure whereas Hoechst 33342 is a six ring structure, where both contain aromatic groups with conjugated bonds. As stated above DAPI has a 20-fold increase in fluorescence when DNA is present, whereas Hoechst 33342 has about a 30-fold increase [15].

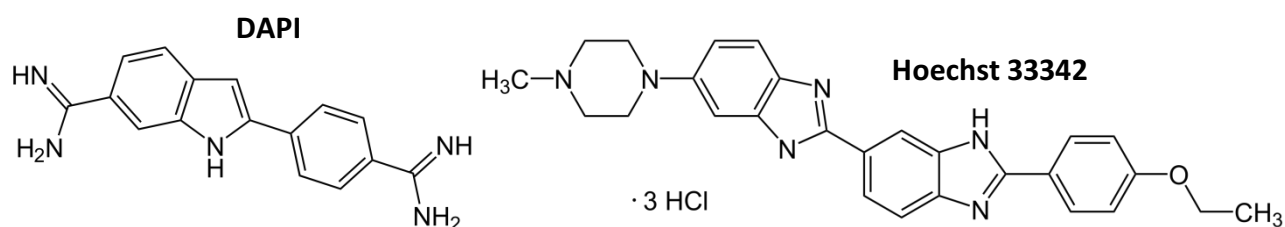


Figure 1.6: Molecular structure of DAPI (left) and Hoechst 33342 (right).

Hoechst 33258 has been used since the 1980s as a simple and rapid DNA quantification assay which was found to detect DNA down to 10 ng/mL [16]. A disadvantage of using this

dye is that it requires high salt concentration to detect dsDNA when in the presence of RNA. Further, a low salt solution is required to detect the presence of RNA [16, 17].

2. Applications of nucleic acid binding dyes

2.1 Staining in gel electrophoresis

DNA binding dyes have been used since the 1970s for the staining of nucleic acids separated within a gel matrix, when EtBr was first used [18, 19]. EtBr was one of the most widely used dyes within laboratories however was found to be mutagenic [20] and since then DNA binding dyes have been developed that are both more specific and less mutagenic than EtBr.

A number of these dyes are shown in Table 1 which also details the excitation and emission of each dye. There is now a wide variety of dyes available all of which stain DNA with similar levels of sensitivity. The availability of new engineered dyes means that mutagenic dyes like EtBr can be replaced with safer and cheaper alternatives. The dyes listed in Table 1 are also able to be added to molten agar (pre-cast staining) or added to a solution after electrophoresis (post staining).

Table 1. List of nucleic acid binding dyes commonly used for staining within gel electrophoresis.

Dye	Excitation (nm)	Emission (nm)	Mutagenic/toxicity
Ethidium bromide	300,360 [21]	590 [21]	Strong/250-500 µg [20]
SYBR Green I (Thermofisher)	494 [7]	521 [7]	Weak/33.3 µg [20]
SYBR Safe (Thermofisher)	502 ^A	530 ^A	0.5X concentration found to be non-mutagenic and non-toxic ^A
SYBR gold (Thermofisher)	495 ^A	537 ^A	Non-mutagenic [22]
GelGreen (Biotium)	500	520	Non-mutagenic [10]
GelRed (Biotium)	300, 520	600	Weak [10]
Diamond Nucleic acid dye (Promega)	494	558	Weak (at stock concentration) [10]
RedSafe (iNtRon)	309, 419, 514	537	Non-mutagenic [10]
Midori Green	300, 400, 500	540	Less mutagenic than EtBr ^B
GR Green	350	500	Less cytotoxic than SYBR Safe ^B
GelStar	493	527	No data available

^A According to the product information supplied by the manufacturer (ThermoFisher)

^B According to the product information supplied by the manufacturer (Labgene Scientific)

2.2 DNA quantification

As DNA binding dyes have been developed further, so has the technology in their applications. This is none more so than in DNA quantification. Small fluorometers can be used in conjunction with intercalating dyes to estimate the amount of DNA present within a sample, generally after a DNA extraction. Intercalating dyes that are also used for gel staining can also be used in fluorescence spectrometry for DNA quantification. Dyes such as SG [23] and PG [24] are two commonly used dyes in fluorescent quantification [25]. For both of these dyes there is a linear relationship between the fluorescent signal and the concentration of DNA, thus with more DNA being present more dye molecules can attach to the DNA and hence resulting in a higher fluorescent signal [13]. Instruments that are available for the specific use of fluorescent DNA quantification include the Qubit[®] Fluorometer (ThermoFisher) [26], AccuLite™ Mini Fluorometer (Biotium), or any instrument that measures fluorescence could be used for DNA quantification.

Table 2 details the dyes currently used for DNA quantification and their corresponding limit of detection (LOD). Hoechst 33258 can also be used for DNA quantification however the fluorescent enhancement of the dye is substantially affected by the fragmentation of the DNA sample. Here a difference of up to 70% can be observed when dealing with a highly degraded sample compared with the intact DNA [14]. The benefit of these means of DNA detection is that they are rapid to perform, requires little of the initial template and requires the use of relatively inexpensive equipment. The use of microplates allows many (96 or 384) samples to be quantified very quickly using an automated reader. These fluorometric dyes are also highly sensitive as can be seen in Table 2 and ideal in many ways as listed for research purposes. In forensic applications these methods have been superseded as they detect whole nucleic acid and do not differentiate between human and non-human DNA [17]. Forensic science laboratories have therefore adopted more human-specific methods. In particular the use of real-time PCR (or quantitative PCR, qPCR) using human specific primers which allows for greater specificity.

Table 2. List of dyes used for DNA quantification and the type of DNA/RNA they detect and the sensitivity.

Dye	Type of DNA detection	LOD	Excitation/Emission (nm)
PicoGreen	ds-DNA	25 pg/mL [11, 27]	500/523 [11]
OliGreen	ss-DNA	100 pg/mL [13]	498/518
RiboGreen	RNA	1 ng/mL [28]	500/525 [28]
AccuBlue (broad range)	ds-DNA	2 ng ^A	350/460 ^A
AccuBlue (high sensitivity)	ds-DNA	0.2 ng ^A	485/530 ^A
AccuClear	ds-DNA	30 pg total in assay ^A	468/507 ^A
AccuBlue (Next Gen)	ds-DNA	1-5 pg ^A	468/507 ^A

^A According to the product information (Biotium)

2.3 DNA amplification and detection (qPCR)

In the same field of study as fluorescent DNA quantification, quantitative-PCR (qPCR) can be used for more sensitive DNA detection. Intercalating dyes can be used in qPCR because the dye molecules can attach to the PCR amplicons, as the number of PCR amplicons increase during the reaction, a greater fluorescent signal can be observed. Thus a higher DNA concentration present correlates to a higher fluorescent signal due to more binding sites available for the dye molecules to attach. Dyes that are currently used for the quantification of DNA include EvaGreen™ (EG) [29] and SG [30, 31]. Table 3 details the list of currently used dyes for qPCR and high resolution melt (HRM) curve analysis. The binding mechanism SG molecules to PCR amplicons are shown in Figure 1.7.

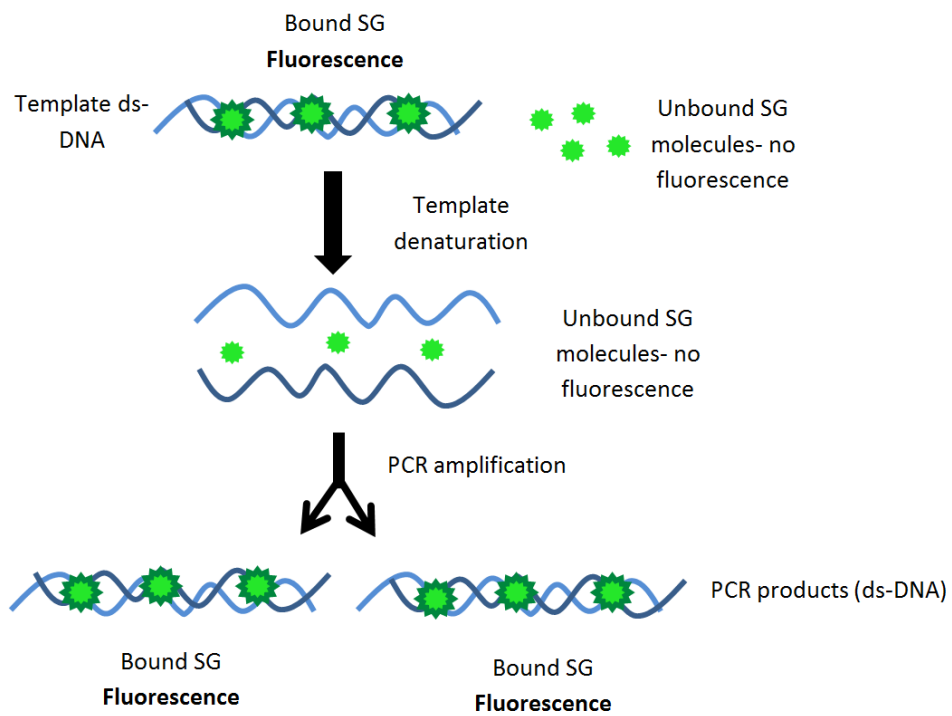


Figure 1.7: Schematic representation of how SG molecules bind during qPCR and fluoresce when bound to ds-DNA, adapted from [32].

Table 3. Nucleic acid binding dyes used with quantitative PCR

Dye	Excitation/emission	Application	Studies
SYBR Green I	494/521 [7]	qPCR	[30, 33-35]
EvaGreen	500/525	qPCR and HRM analysis	[29, 34, 35]
Diamond dye	494/558	qPCR	[See Chapter 6, Section 6.2]
LCGreen Plus	460/475	HRM	[35]
<u>SYTO Green Dyes</u>			
9	485/498	HRM analysis	[33, 36]
11	508/527	HRM analysis	[34, 35]
13	488/509	HRM / qPCR	[33-35]
14	517/549	HRM / qPCR	[35]
16	488/518	HRM / qPCR	[33-35]
21	494/517	HRM / qPCR	[34, 35]
24	490/515	HRM / qPCR	[34, 35]
25	521/556	HRM / qPCR	[35]
<u>SYTO Orange</u>			
80	531/545	qPCR	[34]
81	530/544	qPCR	[34]
82	541/560	qPCR	[33, 34]
83	543/559	qPCR	[34]
<u>SYTO Red</u>			
17	621/634	qPCR	[34]
59	622/645	qPCR	[34]
60	652/678	qPCR	[33, 34]
61	628/645	qPCR	[34]
62	652/676	qPCR	[33, 34]
63	657/673	qPCR	[34]
64	599/619	qPCR	[33, 34]
YO-PRO-1	491/509	qPCR	[33]
BEBO	468/492 [37]	qPCR	[37, 38]
BOXTO	515/552 [15, 38]	HRM analysis	[38]
ResoLight	487/503	HRM / qPCR	[35]
TO-PRO-3	642/661	qPCR	[33]
POPO-3	534/570	qPCR	[33]
BOBO-3	570/602	qPCR	[33]
SYTOX Orange	547/570	qPCR	[33]

2.4 Flow Cytometry, Cell staining

Flow cytometry is a technique that is used to measure and analyse physical characteristics of single particles, generally cells as they flow through a fluid stream and analysed by a laser. The cells when present scatters incident light from the laser source and any fluorescent molecules present on the particle/cell emits a fluorescent signal; both the scattered light and fluorescence is detected. Flow cytometry is generally used in areas like microbiology when counting bacterial cells within samples.

Flow cytometry has been used in forensic science to successfully identify and separate sperm cells [39-41]. Flow cytometry was investigated for cell sorting due to the difficulty of obtaining successful DNA typing results after an assault; due to only a small number of spermatozoa cells present compared with numerous vaginal cells recovered [41]. This technique of cell sorting was found to be superior to the preferential lysis technique when dealing with an unfavourable male to female cell ratio [41].

Another technique used for sorting forensically relevant samples is using fluorescence-assisted cell sorting, however this process uses fluorescent markers (CD45, CD227) which are attached to antibodies present within the samples [42] rather than fluorescent dyes.

Cell staining is important in histochemistry where the analysis of live and dead cells can be undertaken [43]. Dyes that are impermeable to the cell membrane are only able to stain fixed cells, where the membrane has already been broken down for the dyes to bind to the DNA. Dyes that can permeate the cell membrane can then be used to stain DNA with live cells. The most widely used dye for cellular staining is DAPI, however as DAPI excites in the UV region this can cause DNA degradation. Cyanine dyes like SYBR Green I excite in the blue region reducing potential DNA degradation.

Table 4. Dyes used within Flow Cytometry and fluorescent microscopy for cell staining.

Dye	Excitation/ emission (nm)	Application	Studies
SYBR Green I	494/521 [7]	Cell-permeable, flow cytometry and fluorescent microscopy	[44, 45]
SYTO 13	DNA 488/509 ^A RNA 491/514 ^A	Cell-permeable, live cell staining, flow cytometry	[46, 47]
Hoechst 33258	352/416 ^A	Live cell staining, Counterstain, apoptosis	[48]
Hoechst 33342	350/461 ^A	Cell-permeable, apoptosis	[49, 50]
TOPRO-3	642/661 ^A	Cell-impermeable	[48, 51, 52]
TOTO-3	642/660 ^A	Cell-impermeable, Nuclear counterstain	[48]
Propidium Iodide	535/617 ^A	Cell-impermeable, FISH, apoptosis	[50, 53]
DRAQ5	647/670 [48]	Live cell staining, flow cytometry	[48, 54]
Hexidium iodide	518/600 ^A	Cell-permeable, stains nuclei and cytoplasm	[47]
LDS 751	543/712 ^A	Cell-permeable	[52]
Nuclear Yellow	355/495 ^A	Nuclear counterstain, cell-impermeable	[9]
Ethidium homodimer-1	528/617 ^A	Dead cell stain, cell-impermeable	[55]
SYTO 9	DNA 485/498 ^A RNA 486/501 ^A	Dead cell stain, flow cytometry	[45]
DAPI	364/454 [43]	Cell-permeable, cell staining, fluorescent microscopy	[43, 49]
SYBR Gold	495/537 ^A	DNA detection in gels, cell staining, flow cytometry	[56]
Alexa Fluor 594	588/615 ^A	Fluorescent probe attached to sequences as a FISH* DNA tag	[57]
Alexa Fluor 488	493/519 ^A	Flow cytometry and fluorescence-assisted cell sorting (FACS)	[58]

*FISH stands for fluorescent *in situ* hybridization

^A According to the product information supplied by the manufacturer (ThermoFisher)

2.5 Nucleic acid dyes for fluorescent microscopic investigations of forensic relevant samples

Cell-free DNA may be present on surfaces from the breakdown of nucleated cells from sources rich in DNA and the hands act as a vector to transfer the DNA to various substrate surfaces [59-61]. Due to the presence of cell-free DNA there is the potential for the dyes to detect DNA within fingerprints; GG has been used for this application as the dye only binds to free DNA as the dye molecules cannot permeate the cell membrane [62]. For samples that have DNA enclosed within a cell membrane such as saliva or spermatozoa, dyes that are permeable to the membrane can be used for staining those forensic samples. For example SG and DAPI have been shown to stain the nuclei of forensic samples [10, 63].

The most commonly used application of DNA binding dyes in the staining of forensically relevant samples was the staining of hair follicles. The examination of hair follicles using DNA binding dyes has become important in the forensic examination process to determine if a hair sample was viable for STR analysis, depending on the number of nuclei [64, 65]. Hairs are a common type of forensic evidence found at crime scenes as human head hairs are estimated to shed around 75-150 per day [66-68]. Out of the hairs collected as forensic evidence, telogen hairs are estimated to account for 95% [69]. These hairs are generally not analyzed due to minimal nuclear DNA material as they are fully keratinized [70].

There have been many dyes used for the staining of hairs; either nuclear staining focusing on the root of the hair and attached cellular debris [64, 65, 67, 71], or studies looking at the staining the shaft of the hair [72], excluding the root bulb. Table 6 outlines the dyes used for staining forensic relevant samples.

Table 6. Dyes used for fluorescent microscopy for forensic samples.

Dye	Application
DAPI	Hair staining to determine the number of nuclei within samples [65, 67, 71, 73, 74] staining of spermatozoa nuclei [63]
RedSafe™	Hair staining, for nuclei determination [64] with successful STR amplification [75], and saliva to show ability to permeate the cell membrane [10, 76].
Diamond™ Dye	Hair staining, for nuclei determination [64] with successful STR amplification [75], saliva to show ability to permeate the cell membrane and staining of skin flakes [10, 76].
EvaGreen™	Hair staining, for nuclei determination [64] with successful STR amplification [75], and saliva to show ability to permeate the cell membrane [10, 76].
SYBR Green I	Hair staining, for nuclei determination [64] with successful STR amplification [75], saliva to show ability to permeate the cell membrane and skin flakes staining [10, 76]. Staining of DNA within fingerprints [62].
Hoechst 33258	Hair staining within the shaft of the hair [72]
TOTO-3	Hair staining [77]
Alexa Fluor 594	Determining type of biological fluids from mRNA profiling using a fluorescent probe attached to a locked nucleic acid probe for keratin (FISH) [57]
Alexa Fluor 488	Whole-blood mixtures [58]

3. Concluding remarks

Several applications of nucleic acid binding dyes have been outlined in this review along with the dyes used within those applications; including gel staining, DNA quantification, DNA detection (including flow cytometry and cell staining) and fluorescent microscopy. The main use of DNA binding dyes has been for the quantification of DNA either as a fluorescent based quantification or the use within quantitative PCR. This review has also outlined the future trends of using these dyes for the *in situ* detection of latent DNA and within forensically relevant samples. This has so far been demonstrated in the staining of hair follicles to determine their suitability for STR amplification and analysis; along with staining of fingerprints, saliva, skin fragments, spermatozoa and blood. The future of *in situ* fluorescent detection would be in the detection of touch DNA to provide a DNA-targeted approach which is currently not available. The visualization of the DNA on objects would revolutionize the collection of evidence as the DNA can be seen thus collected in a more efficient and effective approach.

4. Thesis Aims

From this review of the literature, evidence has been provided that the development of a novel method for the detection of latent DNA at crime scenes would be greatly beneficial to the forensic science discipline. If the detection of DNA with the use of fluorescent dyes is possible then they could be used in conjunction with a suitable light source for the detection of latent DNA at crime scenes. This would result in a more efficient method of DNA collection. Also if the fluorescence level can be equated to the amount of DNA present then areas that have a higher fluorescence can be swabbed as the approximate amount of DNA would be known and result in higher quality profiles.

The work reported in the thesis aimed to investigate DNA binding dyes for a surface based application for the detection of latent DNA using a DNA-targeted *in situ* fluorescent method. This thesis aims to investigate and provide the foundation of research and preliminary discoveries in this innovative approach which has currently not been undertaken. The first data Chapter examines the current literature on DNA binding dyes and further investigating their properties through gel electrophoresis and the cell permeability of the dyes. The following Chapter investigates the effects these dyes may have on downstream forensic applications such as DNA extraction, quantification, amplification, STR analysis and detection. Chapter 4 details the preliminary work on the use of these dyes for a surface-based latent DNA detection method along with staining of biological samples. Chapter 5 details the use of selected dyes for the staining of hair follicles and the ability to determine the suitability of a hair for DNA extraction based on the fluorescent signal observed. Chapter 6 details the potential use of DNA binding dyes for real-time PCR that have currently not been investigated and comparing the results to standard dyes already used. Lastly Chapter 7 provides the final thoughts and future impact this work will have in the forensic biology discipline.

Chapters of this thesis consist of published articles, short communications, reports and conference proceedings (extended abstracts and posters) along with extra data collected and overall discussion and conclusions for each of the Chapters will be presented.

5. References

- [1] J.R. Lakowicz, *Principles of Fluorescence Spectroscopy*. Third ed. 2006, New York, USA: Springer US.
- [2] J.R. Albani, *Fluorescence Spectroscopy Principles*, in *Principles and Applications of Fluorescence Spectroscopy*. 2008, Blackwell Publishing Ltd. p. 88-114.
- [3] M. Sauer., J. Hofkens., J. Enderlein, Basic principles of fluorescence spectroscopy, *Handbook of Fluorescence Spectroscopy and Imaging: From Single Molecules to Ensembles*. 2011 1-30.
- [4] J. M. Berg., J. L. Tymoczko., L. Stryer, DNA, RNA, and the Flow of Genetic Information, 2002.
- [5] J. D. Watson., F. H. Crick, Molecular structure of nucleic acids, *Nature*. 1953, **171** 737-738.
- [6] D. Banerjee., S. K. Pal, Dynamics in the DNA Recognition by DAPI: Exploration of the Various Binding Modes, *The Journal of Physical Chemistry B*. 2008, **112** 1016-1021.
- [7] A. I. Dragan., R. Pavlovic., J. B. McGivney., J. R. Casas-Finet., E. S. Bishop., R. J. Strouse., et al, SYBR Green I: Fluorescence Properties and Interaction with DNA, *Journal of Fluorescence*. 2012, **22** 1189-1199.
- [8] M. L. Barcellona., G. Cardiel., E. Gratton, Time-resolved fluorescence of DAPI in solution and bound to polydeoxynucleotides, *Biochem Biophys Res Commun*. 1990, **170** 270-280.
- [9] *Molecular Probes Handbook, A Guide to Fluorescent Probes and Labeling Technologies, 11th Edition*.
- [10] A. M. Haines., S. S. Tobe., H. J. Kobus., A. Linacre, Properties of nucleic acid staining dyes used in gel electrophoresis, *ELECTROPHORESIS*. 2015, **36** 941-944.
- [11] V. L. Singer., L. J. Jones., S. T. Yue., R. P. Haugland, Characterization of PicoGreen Reagent and Development of a Fluorescence-Based Solution Assay for Double-Stranded DNA Quantitation, *Analytical Biochemistry*. 1997, **249** 228-238.
- [12] G. Cosa., K. S. Focsaneanu., J. R. N. McLean., J. P. McNamee., J. C. Scaiano, Photophysical Properties of Fluorescent DNA-dyes Bound to Single- and Double-stranded DNA in Aqueous Buffered Solution, *Photochemistry and Photobiology*. 2001, **73** 585-599.
- [13] J. A. Nicklas., E. Buel, Quantification of DNA in forensic samples, *Analytical and Bioanalytical Chemistry*. 2003, **376** 1160-1167.
- [14] T. Sedlackova., G. Repiska., P. Celec., T. Szemes., G. Minarik, Fragmentation of DNA affects the accuracy of the DNA quantitation by the commonly used methods, *Biological Procedures Online*. 2013, **15** 1-8.
- [15] H. J. Karlsson., M. Eriksson., E. Perzon., B. Åkerman., P. Lincoln., G. Westman, Groove-binding unsymmetrical cyanine dyes for staining of DNA: syntheses and characterization of the DNA-binding, *Nucleic Acids Research*. 2003, **31** 6227-6234.
- [16] C. Labarca., K. Paigen, A simple, rapid, and sensitive DNA assay procedure, *Analytical Biochemistry*. 1980, **102** 344-352.

- [17] M. Barbisin., J.G. Shewale, Assessment of DNA extracted from forensic samples prior to genotyping, *Forensic DNA Analysis: Current Practices and Emerging Technologies*. 2013 101.
- [18] C. Aaij., P. Borst, The gel electrophoresis of DNA, *Biochimica et Biophysica Acta (BBA) - Nucleic Acids and Protein Synthesis*. 1972, **269** 192-200.
- [19] P. A. Sharp., B. Sugden., J. Sambrook, Detection of two restriction endonuclease activities in *Haemophilus parainfluenzae* using analytical agarose--ethidium bromide electrophoresis, *Biochemistry*. 1973, **12** 3055-3063.
- [20] V. L. Singer., T. E. Lawlor., S. Yue, Comparison of SYBR® Green I nucleic acid gel stain mutagenicity and ethidium bromide mutagenicity in the *Salmonella*/mammalian microsome reverse mutation assay (Ames test), *Mutation Research/Genetic Toxicology and Environmental Mutagenesis*. 1999, **439** 37-47.
- [21] R.W. Sabnis, *Handbook of biological dyes and stains: Synthesis and industrial applications*. 2010: John Wiley & Sons.
- [22] K. I. Kirsanov., E. A. Lesovaya., M. G. Yakubovskaya., G. A. Belitsky, SYBR Gold and SYBR Green II are not mutagenic in the Ames test, *Mutation Research/Genetic Toxicology and Environmental Mutagenesis*. 2010, **699** 1-4.
- [23] K. Nielsen., H. S. Mogensen., J. Hedman., H. Niederstätter., W. Parson., N. Morling, Comparison of five DNA quantification methods, *Forensic Science International: Genetics*. 2008, **2** 226-230.
- [24] Y. Chen., M. Sonnaert., S. J. Roberts., F. P. Luyten., J. Schrooten, Validation of a PicoGreen-Based DNA Quantification Integrated in an RNA Extraction Method for Two-Dimensional and Three-Dimensional Cell Cultures, *Tissue Engineering Part C: Methods*. 2011, **18** 444-452.
- [25] H. Goldshtein., M. J. Hausmann., A. Douvdevani, A rapid direct fluorescent assay for cell-free DNA quantification in biological fluids, *Annals of Clinical Biochemistry*. 2009, **46** 488-494.
- [26] M. O. Neill., J. McPartlin., K. Arthure., S. Riedel., M. Nd, Comparison of the TLDA with the Nanodrop and the reference Qubit system, *Journal of Physics: Conference Series*. 2011, **307** 012047.
- [27] S. B. Lee., B. McCord., E. Buel, Advances in forensic DNA quantification: A review, *ELECTROPHORESIS*. 2014, **35** 3044-3052.
- [28] L. J. Jones., S. T. Yue., C.-Y. Cheung., V. L. Singer, RNA Quantitation by Fluorescence-Based Solution Assay: RiboGreen Reagent Characterization, *Analytical Biochemistry*. 1998, **265** 368-374.
- [29] F. Mao., W.-Y. Leung., X. Xin, Characterization of EvaGreen and the implication of its physicochemical properties for qPCR applications, *BMC Biotechnology*. 2007, **7** 76-76.
- [30] F. Ponchel., C. Toomes., K. Bransfield., F. T. Leong., S. H. Douglas., S. L. Field., et al, Real-time PCR based on SYBR-Green I fluorescence: an alternative to the TaqMan assay for a relative quantification of gene rearrangements, gene amplifications and micro gene deletions, *BMC Biotechnology*. 2003, **3** 18.

- [31] S. Giglio., P. T. Monis., C. P. Saint, Demonstration of preferential binding of SYBR Green I to specific DNA fragments in real-time multiplex PCR, *Nucleic Acids Research*. 2003, **31** e136-e136.
- [32] C. J. Smith., A. M. Osborn, Advantages and limitations of quantitative PCR (Q-PCR)-based approaches in microbial ecology, *FEMS Microbiology Ecology*. 2009, **67** 6-20.
- [33] H. Gudnason., M. Dufva., D. D. Bang., A. Wolff, Comparison of multiple DNA dyes for real-time PCR: effects of dye concentration and sequence composition on DNA amplification and melting temperature, *Nucleic Acids Research*. 2007, **35** e127.
- [34] A.C. Eischeid, SYTO dyes and EvaGreen outperform SYBR Green in real-time PCR, *BMC Research Notes*. 2011, **4** 1-5.
- [35] J. Radvanszky., M. Surovy., E. Nagyova., G. Minarik., L. Kadasi, Comparison of different DNA binding fluorescent dyes for applications of high-resolution melting analysis, *Clinical Biochemistry*. 2015, **48** 609-616.
- [36] P. T. Monis., S. Giglio., C. P. Saint, Comparison of SYTO9 and SYBR Green I for real-time polymerase chain reaction and investigation of the effect of dye concentration on amplification and DNA melting curve analysis, *Analytical Biochemistry*. 2005, **340** 24-34.
- [37] M. Bengtsson., H. J. Karlsson., G. Westman., M. Kubista, A new minor groove binding asymmetric cyanine reporter dye for real-time PCR, *Nucleic Acids Research*. 2003, **31** e45-e45.
- [38] K. Lind., A. Stahlberg., N. Zoric., M. Kubista, Combining sequence-specific probes and DNA binding dyes in real-time PCR for specific nucleic acid quantification and melting curve analysis, *Biotechniques*. 2006, **40** 315.
- [39] N. Di Nunno., M. Melato., A. Vimercati., C. Di Nunno., F. Costantinides., C. Vecchiotti., et al, DNA Identification of Sperm Cells Collected and Sorted by Flow Cytometry, *The American Journal of Forensic Medicine and Pathology*. 2003, **24** 254-270.
- [40] N. Di Nunno., M. Melato., A. Vimercati., C. Di Nunno., F. Costantinides., C. Vecchiotti., et al, DNA Identification of Sperm Cells Collected and Sorted by Flow Cytometry, *The American Journal of Forensic Medicine and Pathology*. 2003, **24** 254-270.
- [41] W. M. J. Schoell., M. Klintschar., R. Mirhashemi., D. Strunk., A. Giuliani., G. Bogensberger., et al, Separation of sperm and vaginal cells based on ploidy, MHC class I -, CD45 -, and cytokeratin expression for enhancement of DNA typing after sexual assault, *Cytometry*. 1999, **36** 319-323.
- [42] T. J. Verdon., R. J. Mitchell., W. Chen., K. Xiao., R.A.H. Van Oorschot, FACS separation of non-compromised forensically relevant biological mixtures, *Forensic Science International: Genetics*. 2015, **14** 194-200.
- [43] T. Suzuki., K. Fujikura., T. Higashiyama., K. Takata, DNA Staining for Fluorescence and Laser Confocal Microscopy, *Journal of Histochemistry & Cytochemistry*. 1997, **45** 49-53.
- [44] F. Hammes., M. Berney., Y. Wang., M. Vital., O. Köster., T. Egli, Flow-cytometric total bacterial cell counts as a descriptive microbiological parameter for drinking water treatment processes, *Water Research*. 2008, **42** 269-277.

- [45] P. Lebaron., N. Parthuisot., P. Catala, Comparison of Blue Nucleic Acid Dyes for Flow Cytometric Enumeration of Bacteria in Aquatic Systems, *Applied and Environmental Microbiology*. 1998, **64** 1725-1730.
- [46] P.A.D. Giorgio., D.F. Bird., Y.T. Prairie., D. Planas, Flow cytometric determination of bacterial abundance in lake plankton with the green nucleic acid stain SYTO 13, *Limnology and Oceanography*. 1996, **41** 783-789.
- [47] D.J. Mason., S. Shanmuganathan., F.C. Mortimer., V.A. Gant, A fluorescent Gram stain for flow cytometry and epifluorescence microscopy, *Applied and Environmental Microbiology*. 1998, **64** 2681-2685.
- [48] R.M. Martin., H. Leonhardt., M.C. Cardoso, DNA labeling in living cells, *Cytometry Part A*. 2005, **67** 45-52.
- [49] B.C. Monger., M.R. Landry, Flow Cytometric Analysis of Marine Bacteria with Hoechst 33342, *Applied and Environmental Microbiology*. 1993, **59** 905-911.
- [50] F. Belloc., P. Dumain., M.R. Boisseau., C. Jalloustre., J. Reiffers., P. Bernard., et al, A flow cytometric method using Hoechst 33342 and propidium iodide for simultaneous cell cycle analysis and apoptosis determination in unfixed cells, *Cytometry*. 1994, **17** 59-65.
- [51] C.A. Van Hooijdonk., C.P. Glade., P.E. Van Erp, TO-PRO-3 iodide: A novel HeNe laser-excitabile DNA stain as an alternative for propidium iodide in multiparameter flow cytometry, *Cytometry*. 1994, **17** 185-189.
- [52] M.C. O'Brien., W.E. Bolton, Comparison of cell viability probes compatible with fixation and permeabilization for combined surface and intracellular staining in flow cytometry, *Cytometry*. 1995, **19** 243-255.
- [53] C. Riccardi., I. Nicoletti, Analysis of apoptosis by propidium iodide staining and flow cytometry, *Nature protocols*. 2006, **1** 1458-1461.
- [54] P.J. Smith., M. Wiltshire., S. Davies., L.H. Patterson., T. Hoy, A novel cell permeant and far red-fluorescing DNA probe, DRAQ5, for blood cell discrimination by flow cytometry, *Journal of Immunological Methods*. 1999, **229** 131-139.
- [55] M.A. King, Detection of dead cells and measurement of cell killing by flow cytometry, *Journal of Immunological Methods*. 2000, **243** 155-166.
- [56] F. Chen., J.-r. Lu., B. J. Binder., Y.-c. Liu., R.E. Hodson, Application of Digital Image Analysis and Flow Cytometry To Enumerate Marine Viruses Stained with SYBR Gold, *Applied and Environmental Microbiology*. 2001, **67** 539-545.
- [57] E. Williams., M.-H. Lin., S. Harbison., R. Fleming, The development of a method of suspension RNA-FISH for forensically relevant epithelial cells using LNA probes, *Forensic Science International: Genetics*. 2014, **9** 85-92.
- [58] L. Dean., Y.J. Kwon., M.K. Philpott., C.E. Stanciu., S.J. Seashols-Williams., T. Dawson Cruz., et al, Separation of uncompromised whole blood mixtures for single source STR profiling using fluorescently-labeled human leukocyte antigen (HLA) probes and fluorescence activated cell sorting (FACS), *Forensic Science International: Genetics*. 2015, **17** 8-16.

- [59] T. Kita., H. Yamaguchi., M. Yokoyama., T. Tanaka., N. Tanaka, Morphological study of fragmented DNA on touched objects, *Forensic Science International: Genetics*. 2008, **3** 32-36.
- [60] A. Lowe., C. Murray., J. Whitaker., G. Tully., P. Gill, The propensity of individuals to deposit DNA and secondary transfer of low level DNA from individuals to inert surfaces, *Forensic Science International*. 2002, **129** 25-34.
- [61] A. Linacre., V. Pekarek., Y.C. Swaran., S. S. Tobe, Generation of DNA profiles from fabrics without DNA extraction, *Forensic Science International: Genetics*. 2010, **4** 137-141.
- [62] A.M. Haines., S.S. Tobe., H. Kobus., A. Linacre, Detection of DNA within fingermarks, *Forensic Science International: Genetics Supplement Series*. 2013, **4** e290-e291.
- [63] A. Takamura., K. Watanabe., T. Akutsu, Development of a quantitative validation method for forensic investigation of human spermatozoa using a commercial fluorescence staining kit (SPERM HY-LITER™ Express), *International Journal of Legal Medicine*. 2016 1-9.
- [64] A.M. Haines., A. Linacre, A rapid screening method using DNA binding dyes to determine whether hair follicles have sufficient DNA for successful profiling, *Forensic Science International*. 2016, **262** 190-195.
- [65] T. Lepez., M. Vandewoestyne., D. Van Hoofstat., D. Deforce, Fast nuclear staining of head hair roots as a screening method for successful STR analysis in forensics, *Forensic Science International: Genetics*. 2014, **13** 191-194.
- [66] E.A. Graffy., D.R. Foran, *DNA / Hair Analysis A2 - Payne-James, Jason*, in *Encyclopedia of Forensic and Legal Medicine*. 2005, Elsevier: Oxford. p. 213-220.
- [67] L. Bourguignon., B. Hoste., T. Boonen., K. Vits., F. Hubrecht, A fluorescent microscopy-screening test for efficient STR-typing of telogen hair roots, *Forensic Science International: Genetics*. 2008, **3** 27-31.
- [68] C.A. Linch., D.A. Whiting., M.M. Holland, Human hair histogenesis for the mitochondrial DNA forensic scientist, *Journal of Forensic Science*. 2001, **46** 844-853.
- [69] J. Edson., E.M. Brooks., C. McLaren., J. Robertson., D. McNevin., A. Cooper., et al, A quantitative assessment of a reliable screening technique for the STR analysis of telogen hair roots, *Forensic Science International: Genetics*. 2013, **7** 180-188.
- [70] C.A. Linch, Degeneration of nuclei and mitochondria in human hairs, *Journal of Forensic Sciences*. 2009, **54** 346-349.
- [71] E.M. Brooks., M. Cullen., T. Szytdna., S.J. Walsh, Nuclear staining of telogen hair roots contributes to successful forensic nDNA analysis, *Australian Journal of Forensic Sciences*. 2010, **42** 115-122.
- [72] S. Szabo., K. Jaeger., H. Fischer., E. Tschachler., W. Parson., L. Eckhart, In situ labeling of DNA reveals interindividual variation in nuclear DNA breakdown in hair and may be useful to predict success of forensic genotyping of hair, *International Journal of Legal Medicine*. 2012, **126** 63-70.
- [73] T. Boonen., K. Vits., B. Hoste., F. Hubrecht, The visualization and quantification of cell nuclei in telogen hair roots by fluorescence microscopy, as a pre-DNA analysis

- assessment, *Forensic Science International: Genetics Supplement Series*. 2008, **1** 16-18.
- [74] M. Nilsson., S. Norlin., M. Allen, Sequencing of mtDNA in shed hairs: a retrospective analysis of material from forensic cases and a pre-screening method, *Open Forensic Sci J*. 2012, **5**.
- [75] A.M. Haines., S.S. Tobe., H. Kobus., A. Linacre, Successful direct STR amplification of hair follicles after nuclear staining, *Forensic Science International: Genetics Supplement Series*. 2015, **5** e65-e66.
- [76] A.M. Haines., S.S. Tobe., H. Kobus., A. Linacre, Finding DNA: Using fluorescent in situ detection, *Forensic Science International: Genetics Supplement Series*. 2015, **5** e501-e502.
- [77] D. McNevin., L. Wilson-Wilde., J. Robertson., J. Kyd., C. Lennard, Short tandem repeat (STR) genotyping of keratinised hair: Part 1. Review of current status and knowledge gaps, *Forensic Science International*. 2005, **153** 237-246.

6. Supplementary Information

Table S-1: Supplementary Table containing all dye information (some dyes were not included within the paper)

Nucleic acid binding dye	Excitation wavelength (nm)	Emission wavelength (nm)	Properties
SYTOX Blue	445	470	
SYTOX Green	504	523	>500 fold increase in fluorescence when bound to nucleic acids
SYTOX Orange	547	570	
SYTOX Red	640	658	
POPO-1	434	456	High affinity for nucleic acids
BOBO-1	462	481	Cell impermeable, high affinity for nucleic acids
YOYO-1	491	509	1000 fold increase in fluorescence when bound to ds-DNA, cell impermeable
TOTO-1	514	533	Cell impermeable, high affinity for nucleic acids
JOJO-1	529	545	Cell impermeable, high affinity for nucleic acids
POPO-3	534	570	
LOLO-1	565	579	
BOBO-3	570	602	
YOYO-3	612	631	
TOTO-3	642	660	
PO-PRO-1	435	455	
YO-PRO-1	491	509	
TO-PRO-1	515	531	
JO-PRO-1	530	546	
PO-PRO-3	539	567	
YO-PRO-3	612	631	
TO-PRO-3	642	661	
TO-PRO-5	747	770	

Thiazole Orange	512	~535	DNA intercalator, staining RNA in blood cells 50-2000 fold increase in quantum yield when DNA is present
Oxazole Yellow			Reporter group in probes for DNA diagnostics
PicoGreen	502	523	ds-DNA
OliGreen	498	518	ss-DNA
RiboGreen	500	525	RNA
SYBR Gold	495	537	
SYBR Green I	494	521	>1000 fold fluorescence enhancement upon DNA binding
SYBR Green II	492	513	RNA
SYBR Safe	502	530	
Acridine Orange	DNA 502 RNA 460	525 650	Powder, Cell permeable Binds to BSA
Diamond™ Nucleic acid dye (Promega)	494	558	Non-toxic/mutagenic Binds to ss-DNA, ds-DNA and RNA
CellTox™			Cytotoxicity assay dye
EvaGreen (Biotium)	~500	~525	RT-qPCR
GelGreen (Biotium)	495	520	Gel Staining Non-toxic/mutagenic
GelRed (Biotium)	300, 520	600	Gel Staining Non-toxic/mutagenic
RedSafe (iNtRON)	309, 419, 514	537	Gel staining Non-toxic/mutagenic
GelStar™ (Lonza)	493	527	Gel staining Can be mutagenic and can bind to glass, plastic and dust particulates
Fluorescein	460	515	Powder, insoluble in H ₂ O, naturally fluorescent in H ₂ O
SYTO9	DNA 485 RNA 486	DNA 498 RNA 501	Dead cell stain

SYTO11	DNA 508 RNA 510	DNA 498 RNA 501	
SYTO 12	DNA 499 RNA 500	DNA 522 RNA 519	
SYTO 13	DNA 488 RNA 491	DNA 509 RNA 514	
SYTO 14	DNA 517 RNA 521	DNA 549 RNA 547	
SYTO 16	DNA 488 RNA 494	DNA 518 RNA 525	
SYTO 18	DNA 490 RNA 493	DNA 507 RNA 527	
SYTO 21	DNA 494	DNA 517	
SYTO 24	DNA 490	DNA 515	
SYTO 25	DNA 521	DNA 566	
SYTO BC	DNA 485 DNA 487	DNA 500 RNA 504	
GR Green (Biolabo.ch \$210) (Creative Biogene \$550)	350, 500	N/A	Nucleic acid stain Cyanine dye
Midori Green Advanced (Biolabo.ch)	Minor peaks 300, 400 Major peak 500	540	Nucleic acid stain Cyanine dye
DAPI (Sigma-Aldrich)	364	454	Cell permeable
Cy2	489	506	Used for fluorescent labels for DNA and protein detection
Cy3	550	570	
Cy3B	558	572	
Cy3.5	581	594	
Cy5	650	670	
Cy5.5	675	694	
Cy7	743	767	
Hexidium iodide	518	600	cell-permeable, stains nuclei and cytoplasm

LDS 751	543	712	Cell-permeable
Nuclear Yellow	355	495	Nuclear counterstain, cell-impermeable
Ethidium homodimer-1	528	617	Dead cell stain, cell-impermeable
LCGreen Plus	440-470	470-520	HRM curve analysis, gene scanning

Chapter 2

Properties of Nucleic Acid Binding dyes

2.1 Introduction

2.1.1 *Nucleic acid binding dyes*

Nucleic acid binding dyes have been used for many years for staining DNA within gel electrophoresis; starting with the use of EtBr in the 1970's [4, 5]. Other areas that have also adapted the use of DNA fluorescent dyes are within flow cytometry, qPCR and with DNA quantification. The main groupings of dyes that have been selected based on their high fluorescent enhancement when bound to DNA are the cyanine dyes. The properties of these dyes include having a high molar absorptivity with extinction coefficients generally greater than $50,000 \text{ cm}^{-1}\text{M}^{-1}$ [6]. They have a low intrinsic fluorescence when not bound to DNA and upon binding there is generally a large fluorescence enhancement around 1000 fold increase [7]. The dyes range from moderate to high affinity to nucleic acids with little or no binding to other biopolymers. The group of cyanine dyes can be separated into different classes based on their physical characteristics such as their ability to permeate the cell membrane.

SG is a cyanine dye that has been used due to its high affinity to DNA in qPCR and other applications however the use in gel electrophoresis has diminished due to the level of mutagenicity and toxicity of the dye which is of high importance with gel electrophoresis [8]. Other dyes have now been engineered that still have a high affinity to DNA but do not permeate the cell membrane reducing the risk of binding and mutating nuclear DNA. These dyes include GG, RS, GR and DD.

When looking at dyes for their use in gel electrophoresis there are several important properties the dyes should have to make it applicable to the methodology they are:

- Reduced toxicity and mutagenicity
- High DNA affinity
- Limited effect on electrophoretic mobility and band distortion
- Easy to use
- No complicated disposal technique due to toxicity
- Stable at room temperature

- Unable to permeate cell membrane (unable to bind/mutate nuclear DNA)

A list of dyes that are currently available that bind to DNA and used for a variety of different applications were listed in Chapter 1. Six dyes, including the commonly used EtBr and SG, were investigated in this Chapter for their use in gel electrophoresis; to determine the sensitivity, permeability and most suitable methodology of staining gels for the electrophoresis of DNA.

Currently there are over 60 DNA binding dyes that could be used as a presumptive screening test for latent DNA at crime scenes. This study looks at commonly used dyes for gel electrophoresis (Table 2.2) to determine which dyes were the most sensitive for detecting DNA. The results were published in the journal *Electrophoresis* and additional supplemental material is provided in this Chapter.

Table 2.2: Dyes Selected for Study on Gel Electrophoresis showing the Different Properties of the Dyes

Dye	Pros	Cons
Ethidium Bromide	Can permeate the cell membrane	Toxic and mutagenic at low concentrations
SYBR® Green I (Sigma)	Can permeate the cell membrane (detects all DNA-including bacterial) Low background fluorescence	Toxic Mutagenic at concentrations above 33 µg Small stokes shift Unstable at room temperature
GelGreen™ (Biotium)	Non-mutagenic and non-toxic Low background fluorescence Doesn't permeate the cell membrane (detect only free DNA) Stable at room temperature	Small stokes shift
Redsafe™ (iNtRON)	Excitation in visible region Stable at room temperature for about a year	Detects RNA Large background fluorescence Natural fluorophore?/doesn't need to complex with DNA to fluoresce
GelRed™ (Biotium)	Non-mutagenic and non-toxic Large stokes shift	First excitation peak in UV-300 nm. Secondary peak in blue region much lower
Diamond™ Nucleic acid dye (Promega)	Non-mutagenic and non-toxic Stable at room temperature for 90 days Medium size stokes shift	

2.2 PUBLICATION

The results pertaining to this study on dyes used in gel electrophoresis were published in *Electrophoresis*; see article below.

A.M. Haines., S.S. Tobe., H.J. Kobus., A. Linacre, Properties of nucleic acid staining dyes used in gel electrophoresis, *ELECTROPHORESIS*. (2015), **36** 941-944.

Journal Impact Factor: **2.482**

ISI Journal Citation Reports Ranking: 2015 26/75 (Chemistry Analytical); 38/77 (BIOCHEMICAL RESEARCH METHODS)


Number of citations: **6**


2.2.1 Statement of Authorship

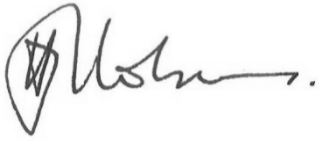
Title of Paper	Properties of nucleic acid staining dyes used in gel electrophoresis
Publication Status	Published
Publication details	Published in <i>Electrophoresis</i> 2015 36 (6) 941-944


AUTHOR CONTRIBUTIONS

By signing the Statement of Authorship, each author certified that their stated contribution to the publication is accurate and that permission is granted for the publication to be included in the candidate's thesis.

Name of Principal Author (Candidate)	Alicia M. Haines		
Contribution to the paper	Designed experimental method, performed all laboratory work and analysis, drafted the manuscript, edited manuscript and acted as corresponding author		
Signature		Date	August, 2016

Name of Co-Author	Shanan S. Tobe		
Contribution to the paper	Edited manuscript, cell permeability images		
Signature		Date	August, 2016

Name of Co-Author	Hilton J. Kobus		
Contribution to the paper	Edited manuscript		
Signature		Date	August, 2016

Name of Co-Author	Adrian Linacre		
Contribution to the paper	Helped design study and edited manuscript		
Signature		Date	August, 2016

Alicia M. Haines¹
 Shanah S. Tobe¹
 Hilton J. Kobus²
 Adrian Linacre¹

¹School of Biological Sciences,
 Flinders University, South
 Australia, Australia

²School of Chemical and Physical
 Sciences, Flinders University,
 South Australia, Australia

Received October 21, 2014

Revised December 15, 2014

Accepted December 16, 2014

Short Communication

Properties of nucleic acid staining dyes used in gel electrophoresis

Nucleic acid staining dyes are used for detecting nucleic acids in electrophoresis gels. Historically, the most common dye used for gel staining is ethidium bromide, however due to its toxicity and mutagenicity other dyes that are safer to the user and the environment are preferred. This Short Communication details the properties of dyes now available and their sensitivity for detection of DNA and their ability to permeate the cell membrane. It was found that GelRed™ was the most sensitive and safest dye to use with UV light excitation, and both GelGreen™ and Diamond™ Nucleic Acid Dye were sensitive and the safer dyes using blue light excitation.

Keywords:

Ethidium bromide / GelGreen™ / GelRed™ / RedSafe™ / SYBR® Green I
 DOI 10.1002/elps.201400496

Dyes for staining nucleic acids have been used as an indicator of fragment size along with quantity and quality of DNA based on the fluorescent signal present within the gel using originally ethidium bromide dating from 1972 [1] and 1973 [2]. More recently, a range of dyes have been developed and made available commercially that claim to be more sensitive with lower limits of detection with the added bonus of being less toxic to the user and environment. The purpose of this Short Communication is to compare a range of these dyes for their application in gel staining and comment on their salient properties in comparison to ethidium bromide.

Nucleic acid staining dyes fall into two groups being either intercalating dyes or minor groove binders. The main dyes used for nucleic acid staining are intercalating dyes, such as cyanine dyes, as they produce a large fluorescence signal when complexed with DNA. Examples of intercalating dyes are ethidium bromide, propidium iodide, and SYBR® Green I (Life Technologies). Examples of minor groove binding dyes include DAPI and Hoechst dyes [3].

Ethidium bromide intercalates with dsDNA and given this mechanism it is a well-known mutagenic compound [4]. Cyanine dyes, such as SYBR® Green I, have also been used in conjunction with nucleic acids, as probes and labels, and in applications such as flow cytometry and DNA quantification (real-time PCR as well as capillary and gel electrophoresis). As ethidium bromide is mutagenic and toxic, other dyes such as the cyanine group have been exploited for the detection of nucleic acids. Some dyes, such as ethidium bromide and SYBR® Green I, are still commonly used within laboratories despite their mutagenicity and toxicity. Ethidium bromide

has been found to be genotoxic at the concentration range typically used for gel staining (0.5 µg/mL) and cytotoxic at the highest tested dose, and classed as a strong mutagen, SYBR® Green I was found to be a weak mutagen [4, 5].

Alternative dyes for gel staining such as SYBR® Safe (Life Technologies) have been developed more recently that are promoted as being less mutagenic than ethidium bromide and SYBR® Green I. These dyes avoid issues associated with mutagenicity by interacting with the grooves of DNA instead of acting as intercalating agents. They include dyes such as Diamond™ Nucleic Acid Dye (Promega, NSW, Australia) that was reported as having a lower LOD than SYBR® Safe [6]. Alternative dyes include GelRed™ (Biotium) and GelGreen™ (Biotium) that are designed to be even less mutagenic as they do not permeate the cell membrane. Novel dyes have also been engineered for applications in DNA quantification kits that have approximately 1000-fold increase in fluorescence when DNA is present, examples of which are QuantiFluor® dsDNA System (Promega), AccuClear™ Ultra High Sensitivity dsDNA Quantitation kit (Biotium), and Qubit (Life Technologies).

This Short Communication addresses the properties including the sensitivity and permeability of four relatively new dyes that are available commercially, in comparison to ethidium bromide and SYBR® Green I.

Table 1 shows the properties of these six nucleic acid dyes including whether they are toxic, mutagenic, and cell permeable. Cell permeability is illustrated in Fig. 1, which shows that both GelRed™ and GelGreen™ did not permeate the cell membrane. The other dyes were all able to permeate the cell membrane indicating that those dyes can interact with the genomic DNA and have greater ability to cause mutations.

Correspondence: Alicia M. Haines, School of Biological Sciences, Flinders University, Bedford Park, South Australia 5042, Australia
 E-mail: alicia.haines@flinders.edu.au

Colour Online: See the article online to view Fig. 1 in colour.

Table 1. Properties of DNA-binding dyes tested in this study

Dye	Excitation (nm)	Emission (nm)	Mutagenic	Toxic	Sensitivity ^{a)} (ng)	Binding mechanism	Cell Permeable ^{b)}	Molecular weight (g/mol)
SYBR® Green I	494 [7]	520 [7]	Weak [4]	Yes [4]	0.5	Intercalator [7]	Yes	509.73 [7]
RedSafe™	309, 419, 514 [8]	537 [8]	No [8]	No [8]	5.0	Unknown	Yes	Unknown
GelGreen™	495 [9]	520 [9]	No [9]	No [9]	0.5	Intercalator [9]	No	1198.43 [12]
GelRed™	300, 250 [9]	600 [9]	Weak [9]	No [9]	0.5	Intercalator [9]	No	1239.07 [12]
Ethidium Bromide	210, 285 [11]	605	Strong [4]	0.5 µg/mL [4]	2.5	Intercalator [10]	Yes	394.31 [11]
Diamond™ Dye	494 [6]	558 [6]	Weak (only at stock concentration) [5]	Only at stock concentration (10 000×) [5]	0.5	External binder [5]	Yes	Unknown

a) See Fig. 2 showing the detection limits down to 0.5 ng (dyes may detect less than 0.5 ng of DNA but is not shown in this study).
b) See Fig. 1 showing the permeability of the DNA-binding dyes with epithelial cells.

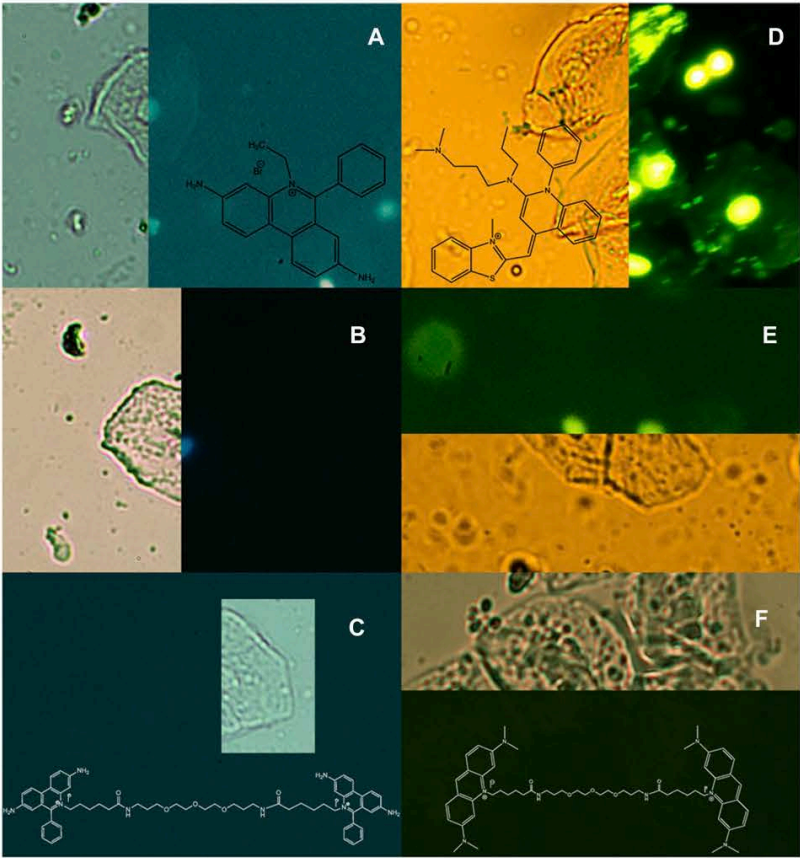


Figure 1. The permeability of the nucleic acid staining dyes in a fresh saliva sample at 100× magnification showing intact cells under white light, using a dye solution and incubated at room temperature for 30 min. (A) Ethidium bromide 0.5 µg/mL, structure shown; (B) RedSafe™ 1×, 1:20 000 dilution, structure unknown, proprietary information; (C) GelRed™ 1×, structure shown [11]; (D) SYBR® Green I 1×, structure shown [7]; (E) Diamond™ Nucleic Acid Dye 1×, structure unknown, proprietary information; (F) GelGreen™ 1×, structure shown [11]. UV excitation was used for (A)–(C); blue excitation was used for (D)–(F) using a Nikon Optiphot Microscope.

Six nucleic acid staining dyes (ethidium bromide (Sigma-Aldrich, NSW, Australia), RedSafe™ (Scientific, NSW, Australia), Diamond™ Nucleic Acid Dye (Promega), GelRed™ (Jomar Diagnostics P/L, SA, Australia), GelGreen™ (Jomar Diagnostics P/L), and SYBR® Green I (Sigma-Aldrich)) were used to stain agarose gels, based on the manufacturer's recommendations, in which DNA of known mass had been separated. A 2% agarose gel was prepared, then stained post-electrophoresis with the nucleic acid staining dyes diluted in electrophoresis buffer to make a 1:10 000 or 1:20 000 dilution

depending on the stock concentration. Ethidium bromide was diluted to a concentration of 0.5 µg/mL. A 100 bp ladder (Promega) was used at varying concentrations to determine the sensitivity of the dyes.

Each gel was prepared in2 the same way using a 100 bp ladder at varying concentrations (0.5–50 ng) by diluting the ladder to the required concentration. The varying concentrations (5 µL) were mixed with 6× loading dye (1 µL) and pipetted into the wells. The gels were run for 45 min at 129 V. The gels were then stained with the six dyes at

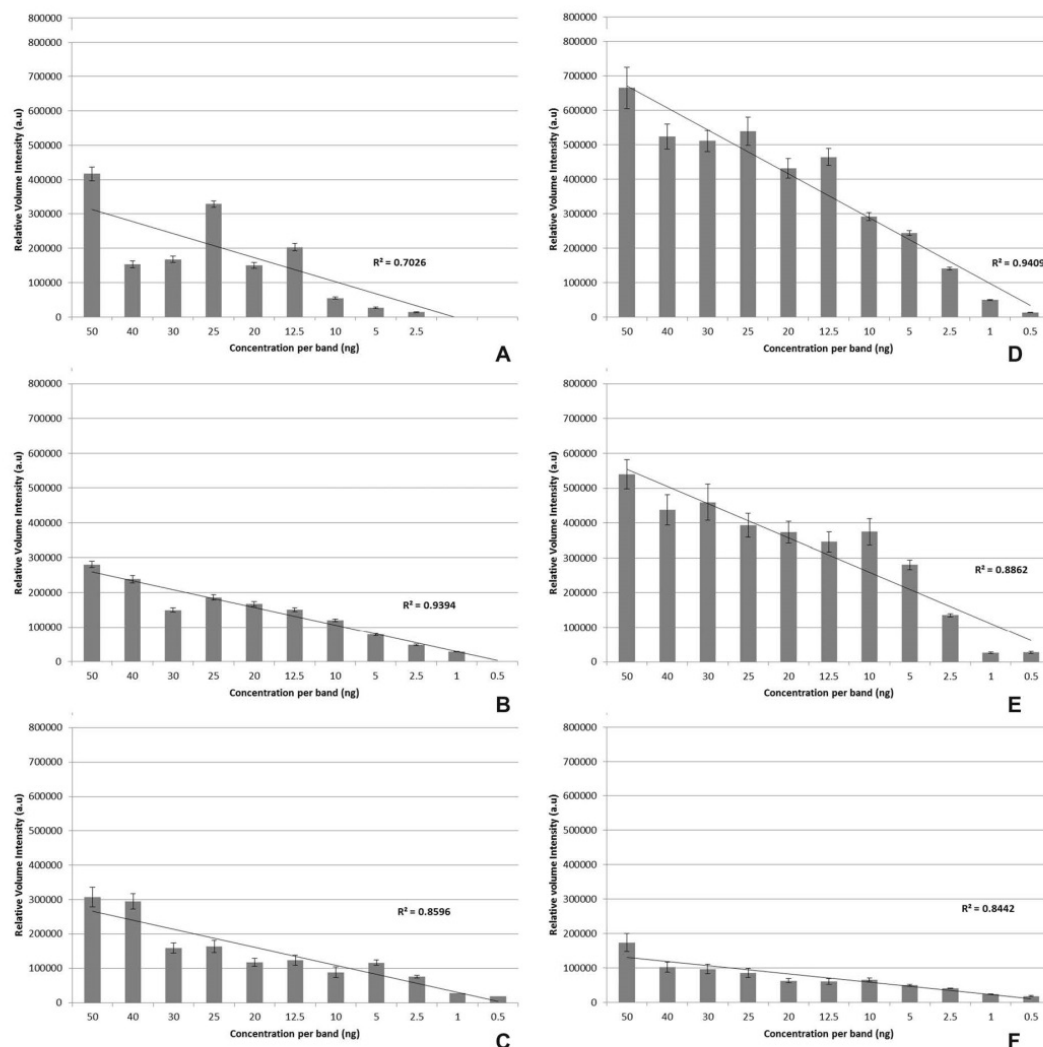


Figure 2. The average relative intensity, based on 11 replicates, at varying concentrations (0.5–50 ng) was measured using the Bio-Rad Gel Doc EZ Imager. Figure shows the linear regression and error bars with 95% confidence. (A) Ethidium bromide 0.5 μ g/mL; (B) RedSafe™ 1 \times , 1:20 000 dilution; (C) GelRed™ 1 \times ; (D) SYBR® Green I 1 \times ; (E) Diamond™ Nucleic Acid Dye 1 \times ; and (F) GelGreen™ 1 \times . (A)–(C) used UV-transillumination (excitation at 302 nm, emission filter 535–640 nm) and (D)–(F) used Blue-transillumination (excitation at 460 nm, emission filter 560–700 nm).

a concentration of 1 \times for 1 h. The stained gels were inspected using a Bio-Rad Gel Doc EZ Imager (Bio-Rad, VIC, Australia).

The relative volume intensity of each band at varying concentrations was measured using the Lane and Band Analysis program within the Image Lab™ Software Version 5.2.1 (Bio-Rad). All gels were analyzed under the same parameters with the background automatically subtracted by the software. Figure 2 shows the average relative intensity signals at varying concentrations (0.5–50 ng) for each of the nucleic acid staining dyes tested. Only four dyes could detect DNA at 0.5 ng: GelRed™, GelGreen™, SYBR® Green I, and Diamond™

Nucleic Acid Dye. RedSafe™ could detect down to 1 ng of DNA, but the intensity of the signals was quite low.

RedSafe is reported to be toxic and mutagenic than ethidium bromide by the manufacturer and from these results it is as sensitive as ethidium bromide. Based on these data, this dye is not suitable, for low-concentration DNA detection as only low signals were obtained above 1 ng. The R^2 value for RedSafe™ (0.9394) showed a linear relationship between concentration and signal intensity.

Ethidium bromide could detect concentrations down to 2.5 ng; indicating that it was the least sensitive out of the dyes tested. The general trend that should be observed is an

increase in signal intensity with an increase in DNA concentration [13]. These data obtained showed that all dyes had a linear relationship between DNA concentration and the intensity of the signals obtained. However, ethidium bromide has a low R^2 value (0.7026) in comparison to the other dyes most likely due to the lower values for 40 and 30 ng signals, which could have been due to band broadening.

SYBR® Green I detected the 0.5 ng band and followed the trend of higher intensity with an increase in DNA concentration shown by the R^2 value (0.9409). SYBR Green I had the highest intensity of all the dyes showing that this dye has a greater enhancement in signal when DNA was present.

Diamond™ Nucleic Acid Dye had the next highest intensity and could also detect down to 0.5 ng of DNA showing that it is just as sensitive as SYBR Green I and had similar signal intensities as well as an R^2 value of 0.8862 showing the linear relationship. This dye also has the advantage of being less mutagenic than SYBR Green I as stated by the manufacturer.

GelRed™ and GelGreen™ were able to detect down to 0.5 ng of DNA and both showed a linear relationship between DNA concentration and signal intensity with GelRed™ and GelGreen™ having an R^2 value of 0.8596 and 0.8442, respectively. GelGreen™ had a much lower signal intensity compared with Diamond™ Nucleic Acid Dye, which shows that the enhancement is much lower for GelGreen™ when interacting with DNA. Increasing the staining period or adding the dye before casting the gel may increase signal intensity.

Based on the results of this study, the following recommendations relating to the instrumentation are suggested: if using UV transillumination (302 or 312 nm excitation), the nucleic acid staining dye GelRed™ exhibited the greatest sensitivity compared to the other two dyes, RedSafe™ and ethidium bromide. GelRed™ has the added advantage of being less toxic than ethidium bromide as stated by the manufacturer. If using blue transillumination (460 nm excitation), the nucleic acid staining dye Diamond™ Nucleic Acid Dye followed by GelGreen™ is recommended as they both detected DNA at 0.5 ng and are claimed by the manufacturer to be less toxic and mutagenic than their counterpart SYBR® Green I [6, 10]. This study showed that Diamond™ Nucleic Acid Dye permeated the cell membrane and therefore would not be as safe as GelGreen™ but had greater signal intensity.

Recommendations for protocol: In this study, the gels were stained postelectrophoresis, which reduces the effect of electrophoretic mobility of the DNA within the gel reducing potential effects of distortion and resolution. The

manufacturer however states that GelGreen™, GelRed™, and RedSafe™ can be added to the molten gel prior to casting.

This work was supported financially by the Attorney General's Department, South Australia.

The authors have declared no conflict of interest.

References

- [1] Aaij, C., Borst, P., *Biochim. Biophys. Acta* 1972, 269, 192–200.
- [2] Sharp, P. A., Sugden, B., Sambrook, J., *Biochemical* 1973, 12, 3055–3063.
- [3] Hilal, H., Taylor, J. A., *J. Biochem. Biophys. Methods* 2008, 70, 1104–1108.
- [4] Singer, V. L., Lawlor, T. E., Yue, S., *Mutat. Res.* 1999, 439, 37–47.
- [5] Schagat, T., Hendricksen, A., [Internet] tpub. 2013, 125. Available from: <http://au.promega.com/resources/pubhub/diamond-nucleic-acid-dye-is-a-safe-and-economical-alternative-to-ethidium-bromide/> (accessed November 1, 2013).
- [6] Truman, A., Hook, B., Hendricksen, A., [Internet] tpub. 2013, 121. Available from: <http://au.promega.com/resources/pubhub/diamond-nucleic-acid-dye/> (accessed November 1, 2013).
- [7] Dragan, A. I., Pavlovic, R., McGivney, J. B., Casas-Finet, J. R., Bishop, E. S., Strouse, R. J., Schenerman, M. A., Geddes, C. D., *J. Fluoresc.* 2012, 22, 1189–1199.
- [8] RedSafe™ technical information sheet (iNtRON) [Internet] Available from: eshop.intronbio.com/product/View.asp?pldx=118 (accessed November 1, 2013).
- [9] Biotium Information sheet on GelGreen™ and GelRed™, 2012 [Internet] Available from: biotium.com/technology/gelred-gelgreen-nucleic-acid-gel-stains/ (accessed November 1, 2013).
- [10] Scaria, P. V., Shafer, R., *J. Biol. Chem.* 1991, 266, 5417–5423.
- [11] Sabins, R. W., *Handbook of Biological Dyes and Stains: Synthesis and Application*, John Wiley & Sons, NJ 2010, pp. 183.
- [12] United States Patent No. US8232050B2, *Methods of Using Dyes in Association with Nucleic Acid Staining or Detection and Associated Technology*, Biotium, Hayward, CA.
- [13] Sutherland, J. C., Lin, B., Monteleone, D. C., Mugavero, J., Sutherland, B. M., Trunk, J., *Anal. Biochem.* 1987, 163, 446–457.

2. 3 Further Methodology

2.3.1 Gel Electrophoresis using pre-cast staining

The results incorporated into the article examined only one aspect of the total study and looked at post electrophoresis staining. Additionally, staining was conducted pre-casting of the gel. The benefit of being able to add the dye to molten agar before casting means a reduction in the time of staining as gels can be examined post electrophoresis. If staining post electrophoresis this means that there is an extra period of time (~30 min) required before analyzing the gel. The major benefit of post-staining would be the reduction in the effect of electrophoretic mobility resulting in less distortion of the bands. Depending on the dye used for gel staining will result in which method to use as different dyes have different properties when used in gel staining. The manufacturer's stated protocol is assumed to be the optimal conditions for the dye. The results pertaining to this study are shown below.

A 1% agarose gel was prepared with the nucleic acid staining dyes being added before casting of the gel to make a 1:10 000 or 1:20 000 diluted gel depending on the stock concentration. The EtBr gel was diluted to a concentration of 0.5 µg/mL. Easy Ladder I (Bioline) with the following sized bands 2000, 1000, 500, 250 and 100 bp was used at varying DNA mass (50, 40, 30, 20, 10, 5, 2.5, 1 ng per band) to determine sensitivity of the dyes. Each gel was prepared in the same way: lane 1, 5 µL of Easy Ladder I; lane 2, 4 µL Easy Ladder I; lane 3, 3 µL of Easy Ladder I; lane 4, 2 µL of Easy Ladder I; lane 5, 1 µL of Easy Ladder I; lane 6, 1 in 2 dilution of Easy Ladder I; lane 7, 1 in 4 dilution of Easy Ladder I; lane 8, 1 in 10 dilution of Easy Ladder I; lane 10, 0.5 ng of control DNA stained with loading dye. The stained gels were inspected using a Bio-Rad Gel Doc™ EZ (Bio-Rad) Imager using either UV or blue transillumination depending on the dye.

2.3.2 Saliva staining

Saliva was placed onto microscope slides in a thin layer to try and obtain a single layer of epithelial cells. Before the saliva dried the DNA binding dyes (1X concentration) were applied in order to permeate intact cells. Images were taken at 40X and 100X with an exposure time of 1 s.

2.3.3 Data analysis

The relative volume intensity of the dyes at varying DNA masses was graphed and the linearity of the dyes signal was determined using a linear regression analysis. Averages of the five bands at the same DNA mass were calculated along with the standard deviation and 95% confidence interval; these values were then compared to the values obtained from post-staining.

2.4 Further Results and Discussion

Figure 2.2 shows an example of the fluorescent signal of each of the five bands detected of Easy Ladder I (2000, 1000, 500, 250 and 100 bp) at varying DNA mass 1 ng – 50 ng, and control DNA at 0.5 ng for each of the nucleic acid staining dyes used. Only four dyes could detect the control DNA at 0.5 ng (GR, GG, SG and DD).

RS was able to detect two bands at 5 ng and was only capable of detecting all bands at 50 ng. RS appears to be a naturally fluorescing dye due to the background signal present within the gel. Hence RS can only be used with higher concentrations of DNA compared to the other dyes used in this study. Based on these data, this dye is not suitable for low concentration DNA detection (below 1 ng) as might be encountered on items where DNA is deposited by touch alone. It is estimated that 1 ng of DNA would be equivalent to 167 cells [9] that would be required on a surface for RS to produce a discernable fluorescent signal.

EtBr produced similar results to RS but could detect all bands of the ladder down to 2.5 ng; indicating that it is more sensitive than RS. The general trend that should be observed is an increase in fluorescent signal with an increase in DNA mass; this was not seen with the results of EtBr. At 30 ng the signal appears to be higher than the signal for both 40 and 50 ng. For 2.5 and 5 ng it appears to show the same level of signal (figure 2.2 part A). One reason this may have occurred would be due to EtBr not having a significant increase in signal when in the presence of DNA unlike other DNA binding dyes, hence lower concentrations of DNA would be more difficult to differentiate between.

SG could detect the 0.5 ng band and followed the trend of a higher fluorescent signal with an increase in DNA mass. The 250 bp bands were not detected for 50, 40, 30 and 20 ng and most likely merged with 100 bp bands hence the large fluorescent signal produced by the 100 bp bands. Most likely this was the effect of adding the dye to precast gels instead of post-staining as this can affect the electrophoretic mobility of the DNA. This effect can also result in warping of the DNA bands within the gel (figure 2.1).

GR detected the 0.5 ng band but could only detect down to 2.5 ng/band of the Easy Ladder 1. All band sizes followed the trend of increasing the DNA mass led to the expected higher fluorescent signal. GG detected down to 0.5 ng. This study did not look at DNA masses below 0.5 ng as above 0.5-50 ng would be the typical DNA concentration range of samples being separated by gel electrophoresis.

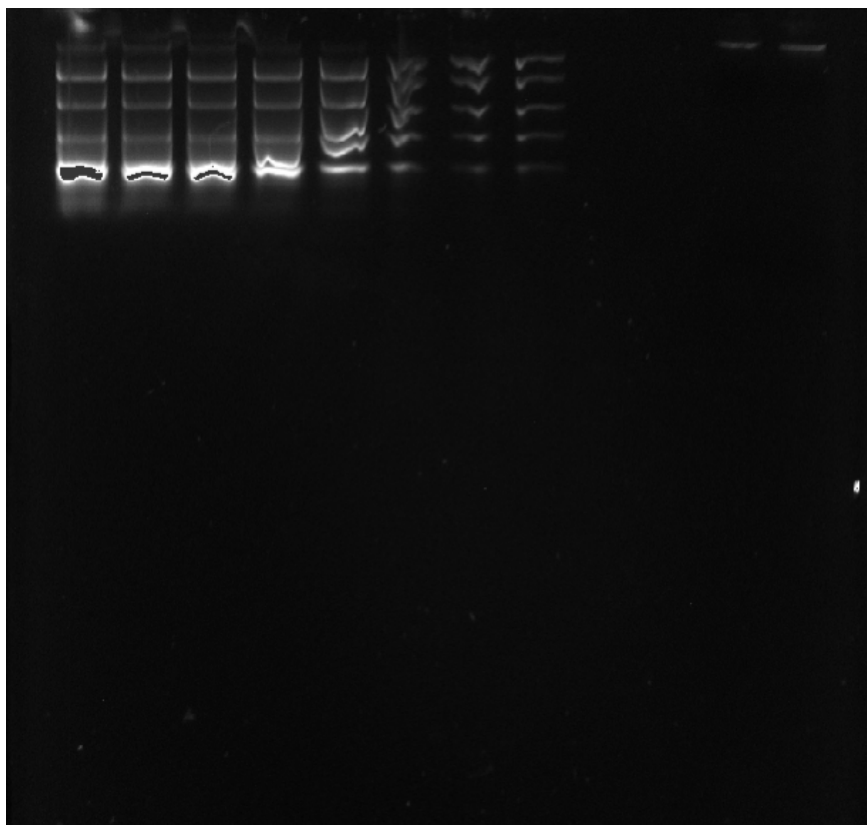


Figure 2.1: Image of agarose gel 1% of varying masses of DNA (0.5-50 ng) stained pre-casting of gel with SYBR[®] Green (1X concentration) run for 30 min at 131V

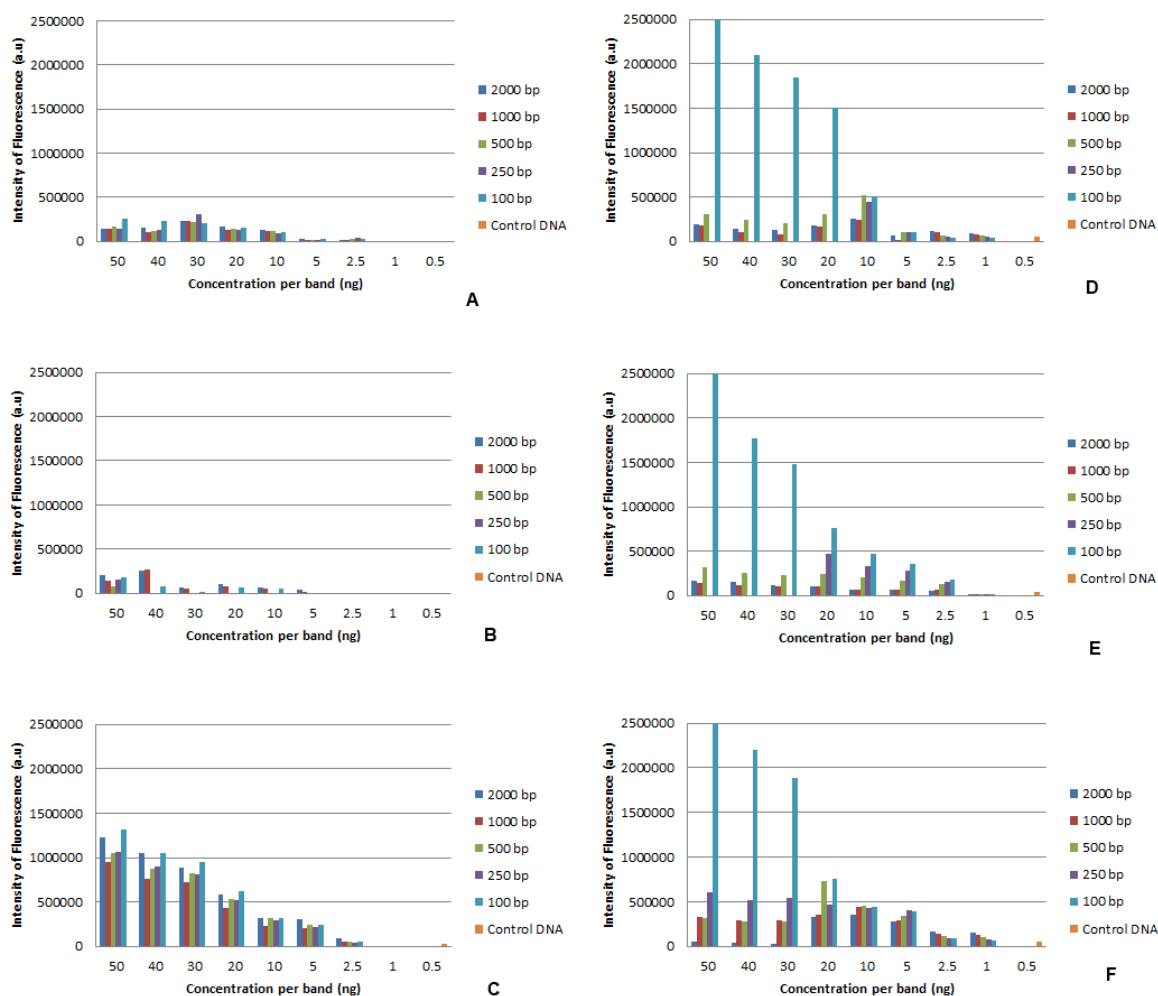


Figure 2.2: The fluorescent signal of the bands present in Easy Ladder I (2000, 1000, 500, 250 and 100 bp) at varying mass of DNA (50, 40, 30, 20, 10, 5, 2.5, 1) and 0.5 ng of control DNA with loading dye was measured using the Bio-Rad Gel Doc™ EZ Imager. A, B and F used UV-transillumination (excitation at 302 nm, emission filter 535-640 nm) and C, D and E used Blue-transillumination (excitation at 460 nm, emission filter 560-700 nm) (A) ethidium bromide 0.5 µg/mL, (B) RedSafe™ 1X, 1:20,000 dilution, (C) GelRed™ 1X, (D) SYBR® Green I 1X, (E) Diamond™ Nucleic Acid Dye 1X and (F) GelGreen™ 1X.

Averages of the bands that were detected for pre-staining are shown below in Figure 2.3 with the linear regression showing the R^2 values. DD had the highest R^2 value (0.9764) showing the direct correlation of the relative volume intensity to the amount of DNA that was present. All the dyes using blue transillumination (GG, DD and SG) had much higher signals when compared with the dyes that use UV transillumination (RS and EtBr), except for GR however this dye could not detect DNA at 1 ng. This would be due to the level of interactions of the dyes with DNA allowing for a higher fluorescent enhancement when in the presence of DNA.

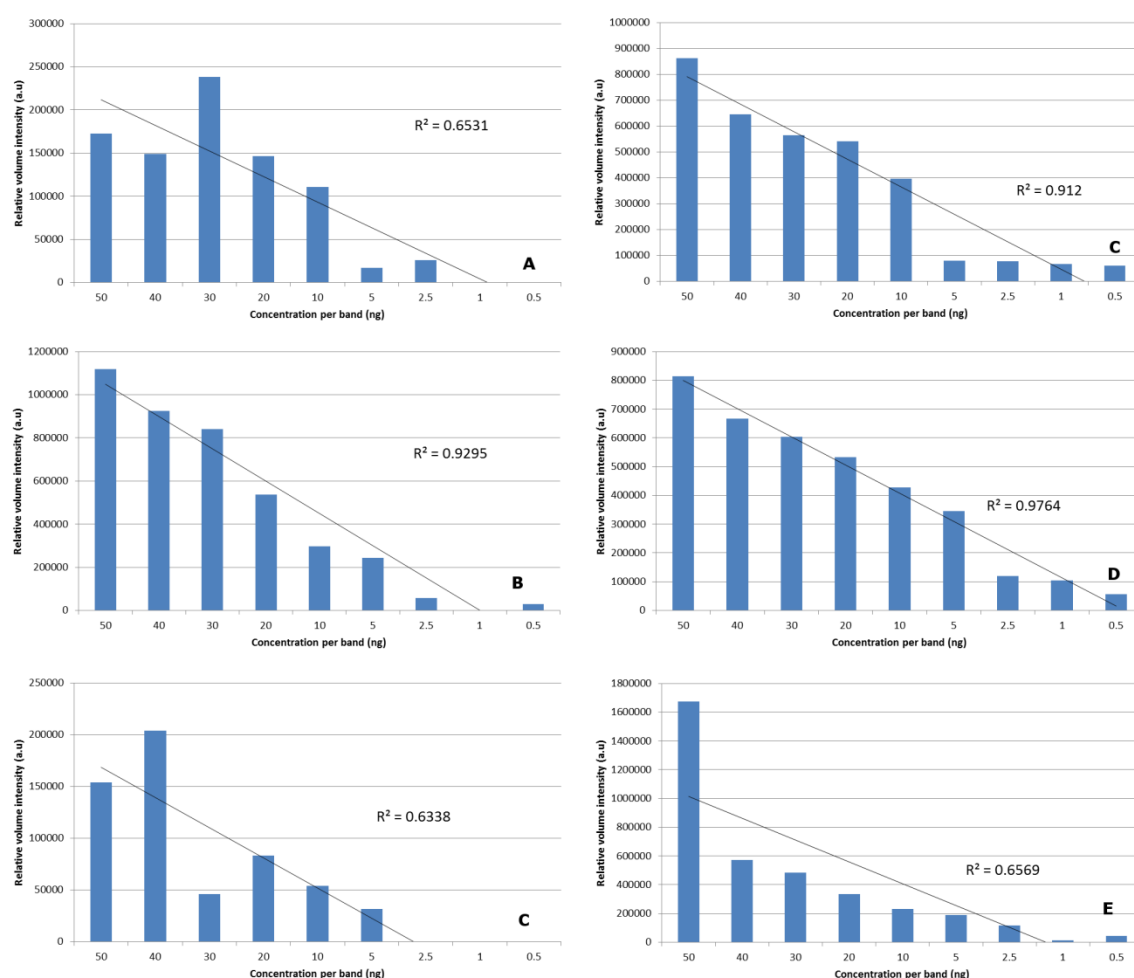


Figure 2.3: The average fluorescent signal of the bands present in Easy Ladder I (5 replicates) at varying mass of DNA (50, 40, 30, 20, 10, 5, 2.5, 1) and 0.5 ng of control DNA with loading dye and R^2 values showing the linearity of the dyes signal, was measured using the Bio-Rad Gel DocTM EZ Imager. A, B and F used UV-transillumination (excitation at 302 nm, emission filter 535-640 nm) and C, D and E used Blue-transillumination (excitation at 460 nm, emission filter 560-700 nm) (A) ethidium bromide 0.5 $\mu\text{g/mL}$, (B) GelRedTM 1X (C) RedSafeTM 1X, 1:20,000 dilution, (D) SYBR[®] Green I 1X, (E) DiamondTM Nucleic Acid Dye 1X and (F) GelGreenTM 1X.

The comparison of averages of the relative volume intensity of both pre and post-staining for each dye can be seen in the figures below (Figure 2.4-2.9). When staining with EtBr it can be seen that it doesn't matter what mode of staining was used, both methods resulted in staining of DNA mass of above 2.5 ng (figure 2.4). Below 2.5 ng there were no signals from the bands due to the poor sensitivity of the dye. The most noticeable variations between the two methodologies were with the highest DNA mass at 50 ng, where the post-staining signal was 2.4 folds higher than the signal for pre-staining. The other variation was with 30 ng signal where the pre-staining signal was 1.4 folds higher than the signal for post-staining. Due to the other masses showing little variation and both methodologies providing the same level of sensitivity it can be concluded that either method is suitable for use with higher levels of DNA mass.

The comparison of post- and pre-staining using GR can be seen in figure 2.5 showing that there was a significant increase in the intensity when using pre-staining. When specifically looking at the 50 ng signals, pre-staining had a 3.6 fold increase in signal when compared with post electrophoresis staining. The only other noticeable difference was that post-staining resulted in detection at 1 ng of DNA whereas the pre-staining did not. However due to the more significant signals using pre-staining it would be the more preferable method of choice when using GR.

Figure 2.6 shows the comparison of the two methodologies for RS. Pre-staining could only detect down to 5 ng whereas post-staining could detect down to 1 ng making it the most sensitive of the methods. Overall post-staining had higher intensity signals and when looking at 50 ng post-staining had a 1.8 fold increase in the signal compared with pre-staining. The biggest difference however was seen at 30 ng where post-staining had a 3.3 fold increase in signal. From these data the more sensitive method when using RS as the dye was post-staining after electrophoresis.

Using SG as the staining dye showed that both methods exhibited similar sensitivity as they could both detect down to 0.5 ng (Figure 2.7). Pre-staining had slightly higher intensity signals when compared with post-staining except at 2.5 and 5 ng. Due to the high variation seen at 95% confidence there was no significant difference between the two methods, however due to the warping of the bands and distortion to the electrophoretic mobility post-staining is the superior method choice when using SG.

Figure 2.8 shows the comparison of the two staining methods when using DD which shows that both methods could detect down to 0.5 ng. Most of the signals were higher when using pre-staining, however due to the large variation shown at 95% confidence there was no significant difference between the two methodologies using DD.

The comparison of the intensity of the band signals for GG when staining occurred before electrophoresis and post electrophoresis is shown in Figure 2.9. There appears to be an increase in the signal when using pre electrophoresis staining, however when looking at the 95% confidence there is quite a significant variation suggesting that there wasn't a significant increase in the signals of pre-staining to post-staining.

The comparison of the two methods using GG dye is shown in Figure 2.9 showing that the two methods had similar sensitivity as they both detected down to 0.5 ng. The pre-staining method showed slightly higher signals however, statistically there was no difference between the two methods due to the high variation between replicates (see appendix A for all gel images and tabulated data).

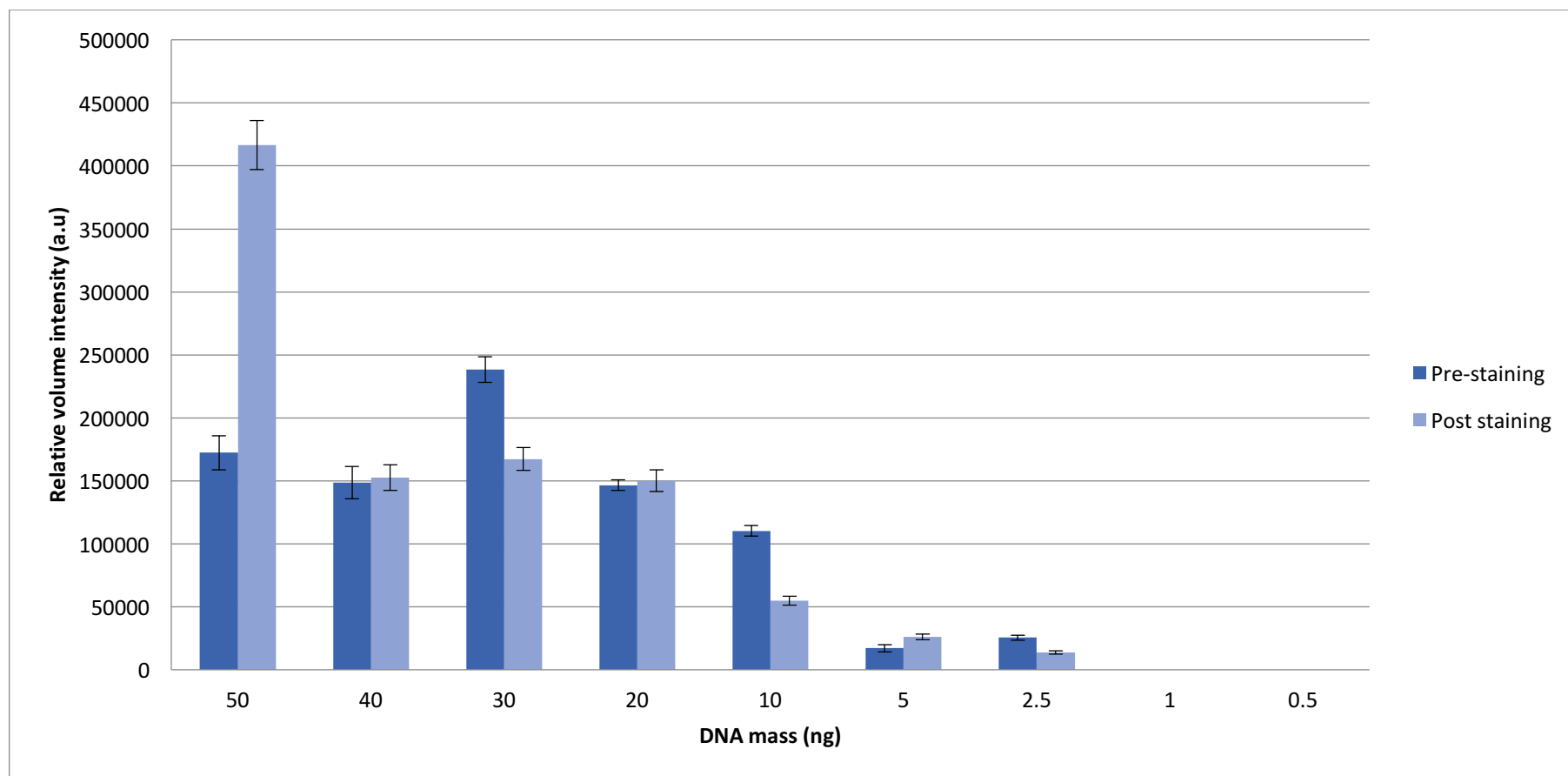


Figure 2.4: Comparison of average volume intensity of bands at different DNA mass (ng) with post electrophoresis staining with ethidium bromide (0.5 $\mu\text{g/mL}$) and staining pre electrophoresis with ethidium bromide (0.5 $\mu\text{g/mL}$). Error bars showing 95% confidence with 5 repetitions.

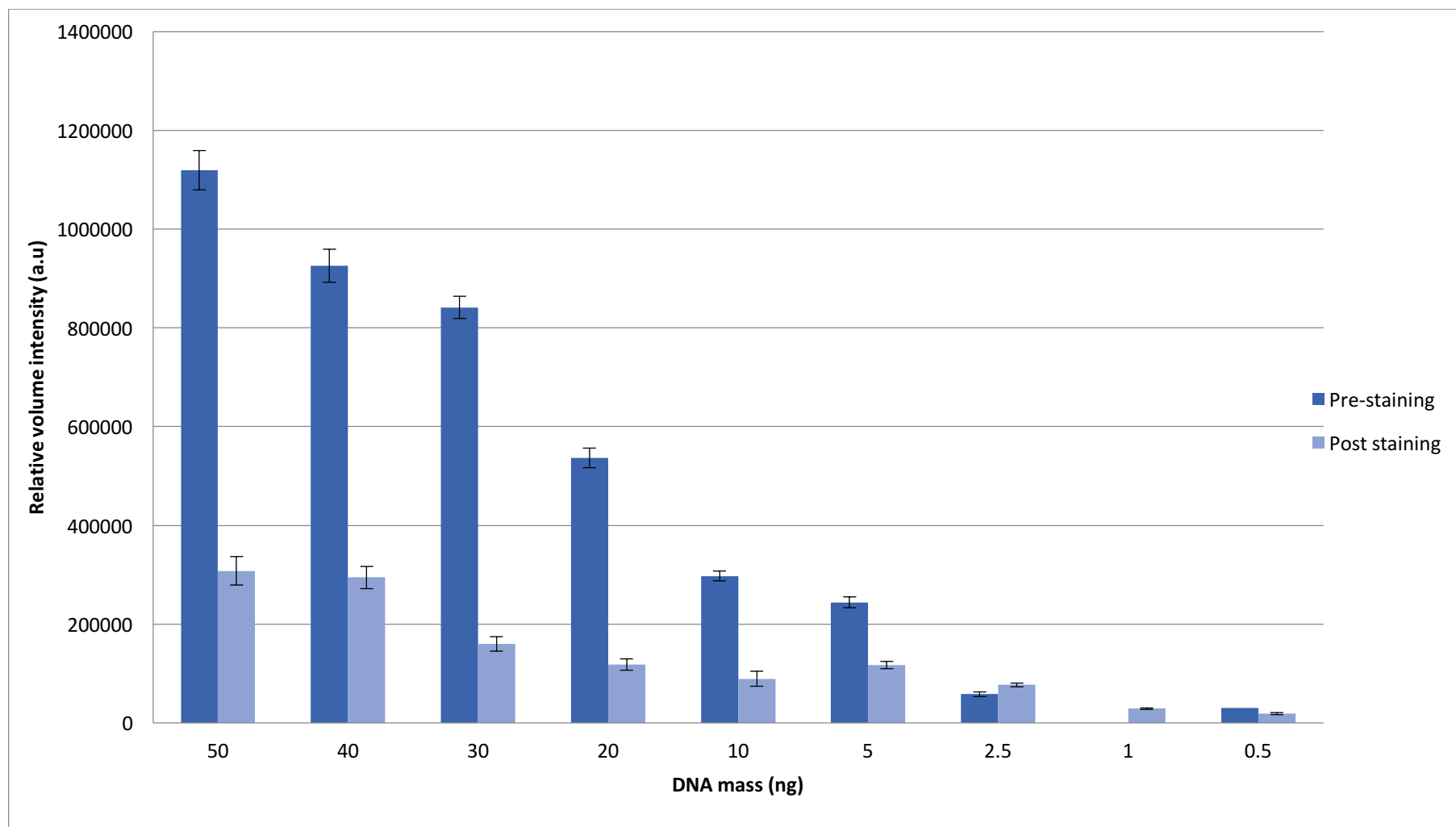


Figure 2.5: Comparison of volume intensity of bands at different DNA mass (ng) with post electrophoresis staining with GelRed (1X) and staining pre electrophoresis. Error bars showing 95% confidence with 5 repetitions.

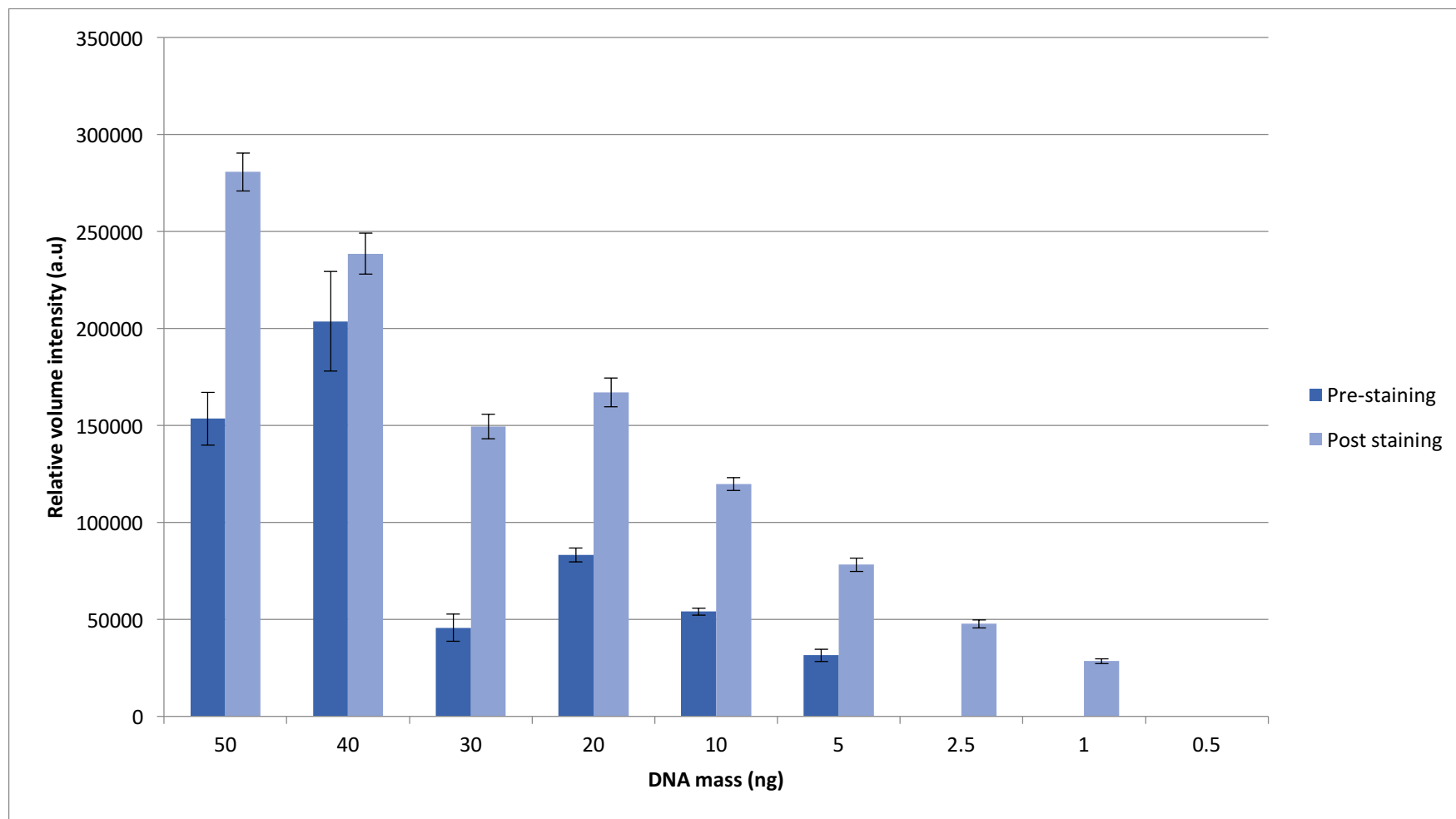


Figure 2.6: Comparison of volume intensity of bands at different DNA mass (ng) with post electrophoresis staining with RedSafe (1X) and staining pre electrophoresis. Error bars showing 95% confidence with 5 repetitions.

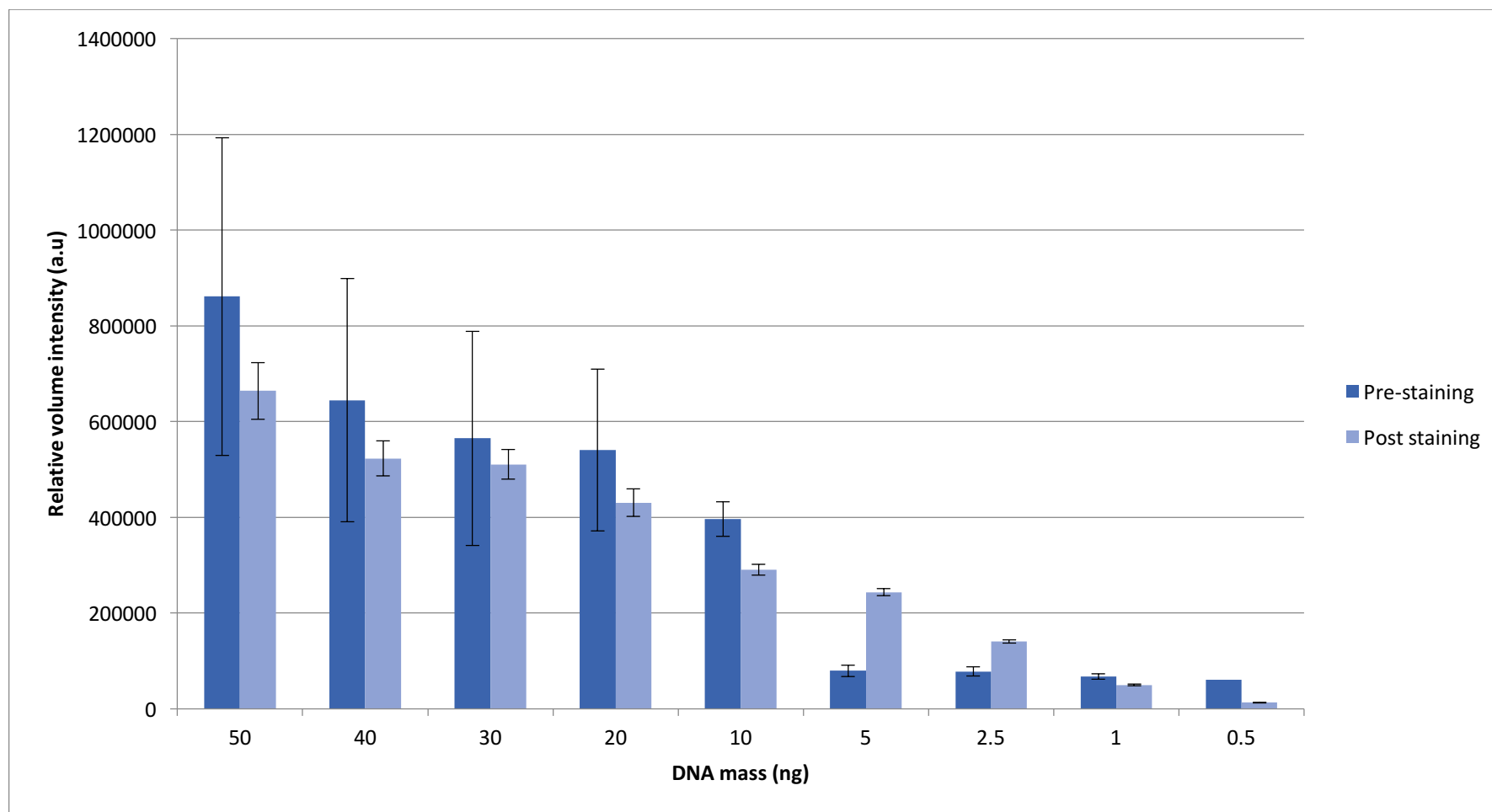


Figure 2.7: Comparison of volume intensity of bands at different DNA mass (ng) with post electrophoresis staining with SYBR Green (1X) and staining pre electrophoresis. Error bars showing 95% confidence with 5 repetitions.

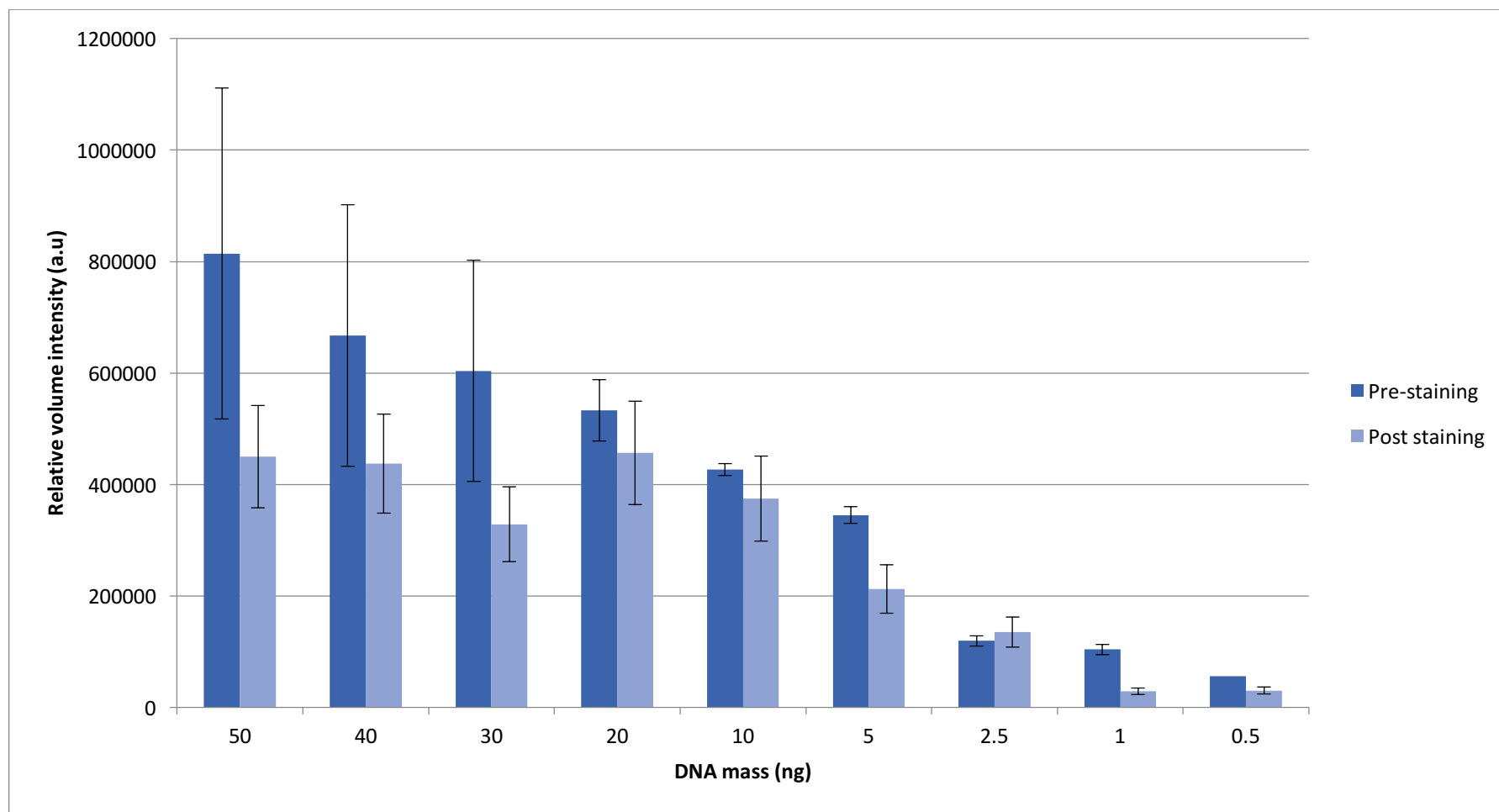


Figure 2.8: Comparison of volume intensity of bands at different DNA mass (ng) with post electrophoresis staining with Diamond dye (1X) and staining pre electrophoresis. Error bars showing 95% confidence with 5 repetitions.

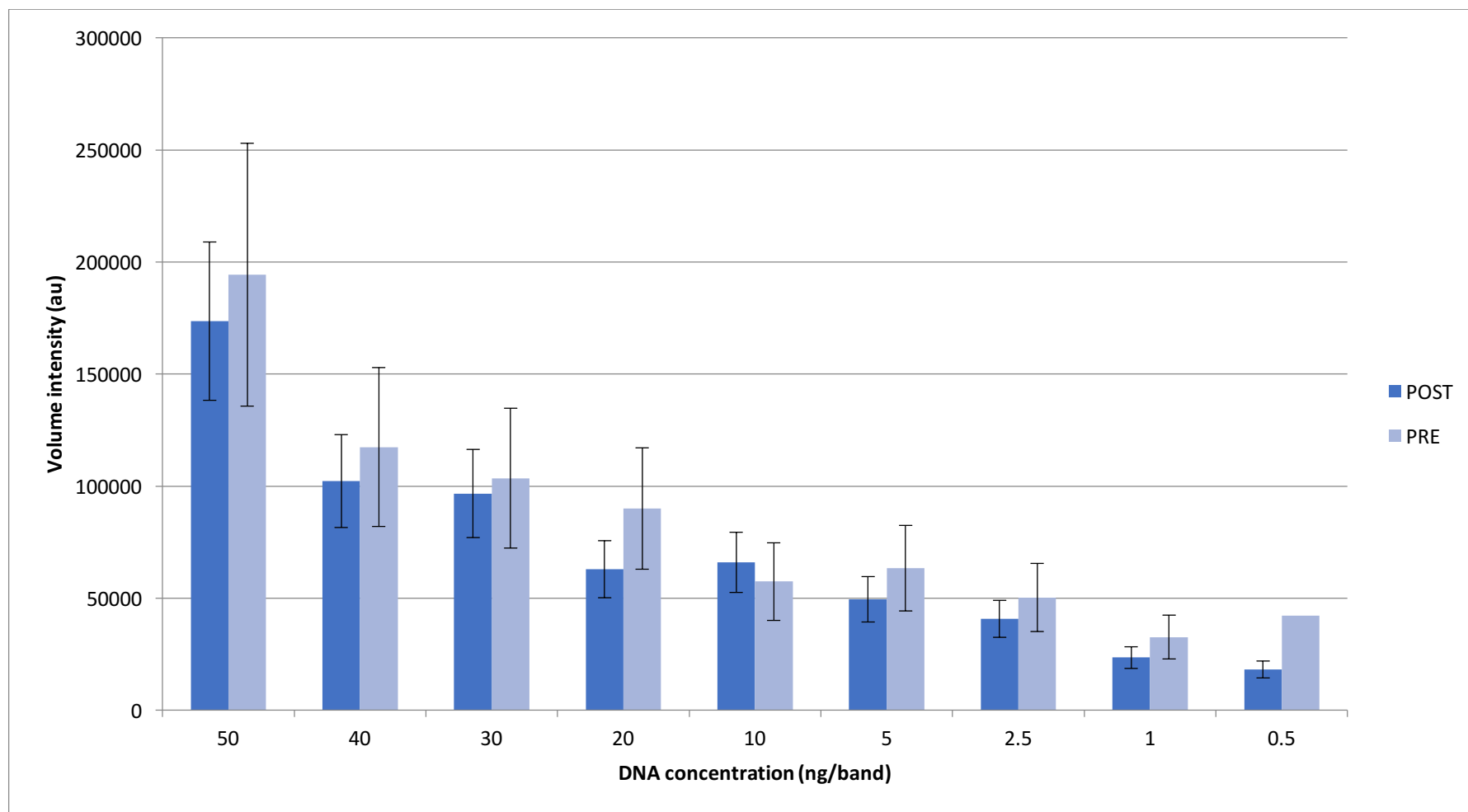


Figure 2.9: Comparison of volume intensity of bands at different DNA mass (ng) with post electrophoresis staining with GelGreen (1X) and staining pre electrophoresis. Error bars showing 95% confidence with 5 repetitions.

Table 2.3 below shows the summary of both methodologies of dye staining for gel electrophoresis with the limits of detection and the linearity of the dyes signal. When looking at the sensitivity, all dyes using blue transillumination had detection down to 0.5 ng using both staining methods. For the dyes using UV transillumination there was more variation in the DNA detection. RS could only detect down to 5 ng using pre-cast staining but 1 ng using post electrophoresis staining. When looking at the linearity of the reaction however there was a vast difference with post-staining having a much more linear relationship with an R^2 value about 0.9, in contrast to pre-staining which was down at 0.6. There was no difference between the sensitivity when using EtBr but post-staining had a slightly higher R^2 value.

Table 2.3 Summary of detection limits (ng) of the nucleic acid binding dyes using both precast staining and post electrophoresis staining.

	SG	GG	DD	RS	GR	EtBr
LOD precast	0.5	0.5	0.5	5	0.5 control 2.5 Ladder	2.5
R^2 value	0.9120	0.6569	0.9764	0.6338	0.9295	0.6531
LOD post-staining	0.5	0.5	0.5	1	0.5	2.5
R^2 value	0.9409	0.8442	0.8862	0.9394	0.8596	0.7026
Limits of detection (LOD) of the DNA binding dyes using two modes of staining, if 0.5 ng is stated for precast detection then control DNA was detected and all the bands were detected in the DNA ladder from 1 ng.						

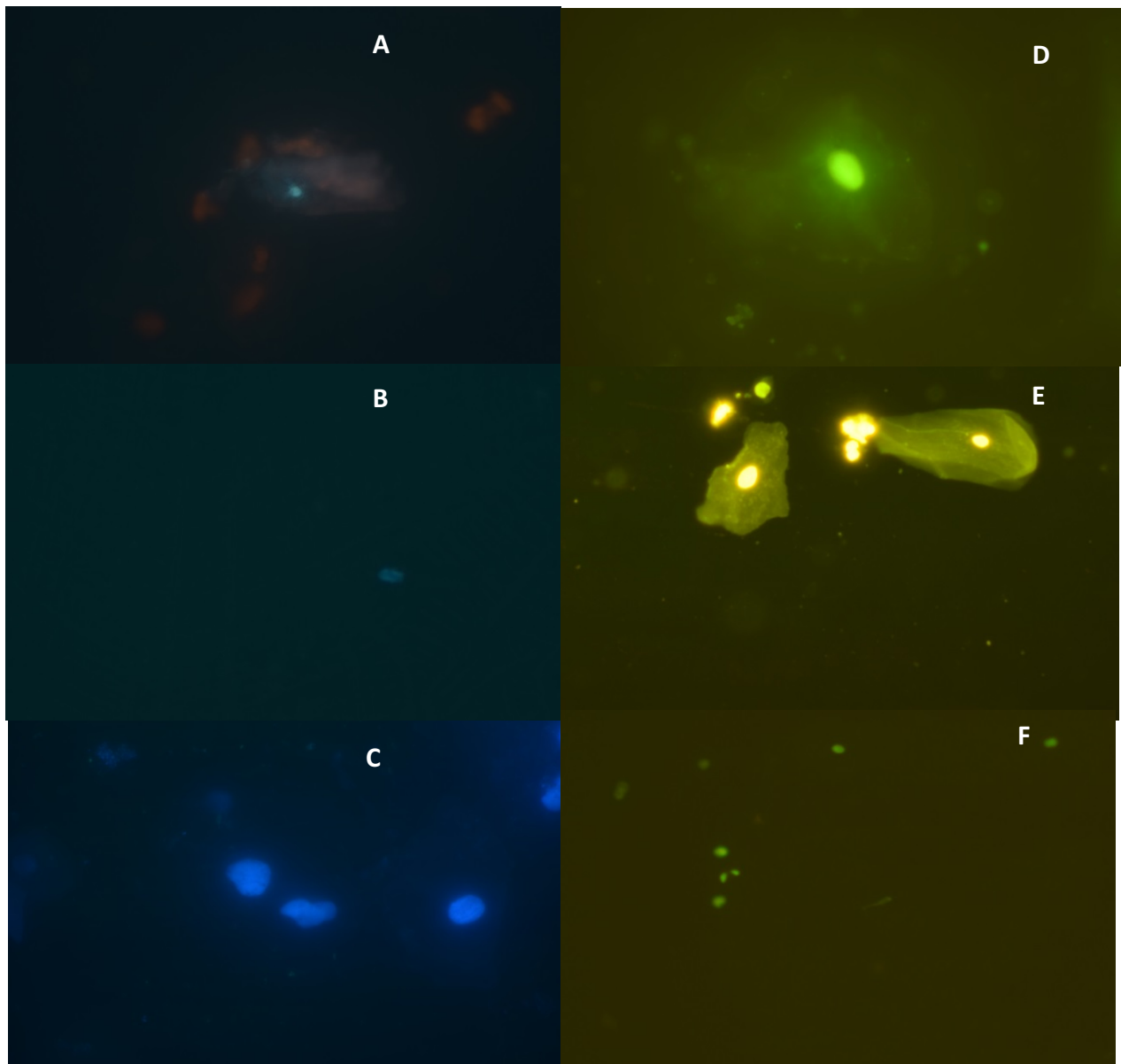


Figure 2.10: Showing the permeability of the binding dyes in a fresh saliva sample at 100x magnification using a 1x concentration dye solution in sterile water. A = Ethidium Bromide, B = RedSafe, C = GelRed, D = SYBR Green I, E = Diamond Dye and F = GelGreen I. UV excitation for A, B and C, blue excitation was used for D, E and F.

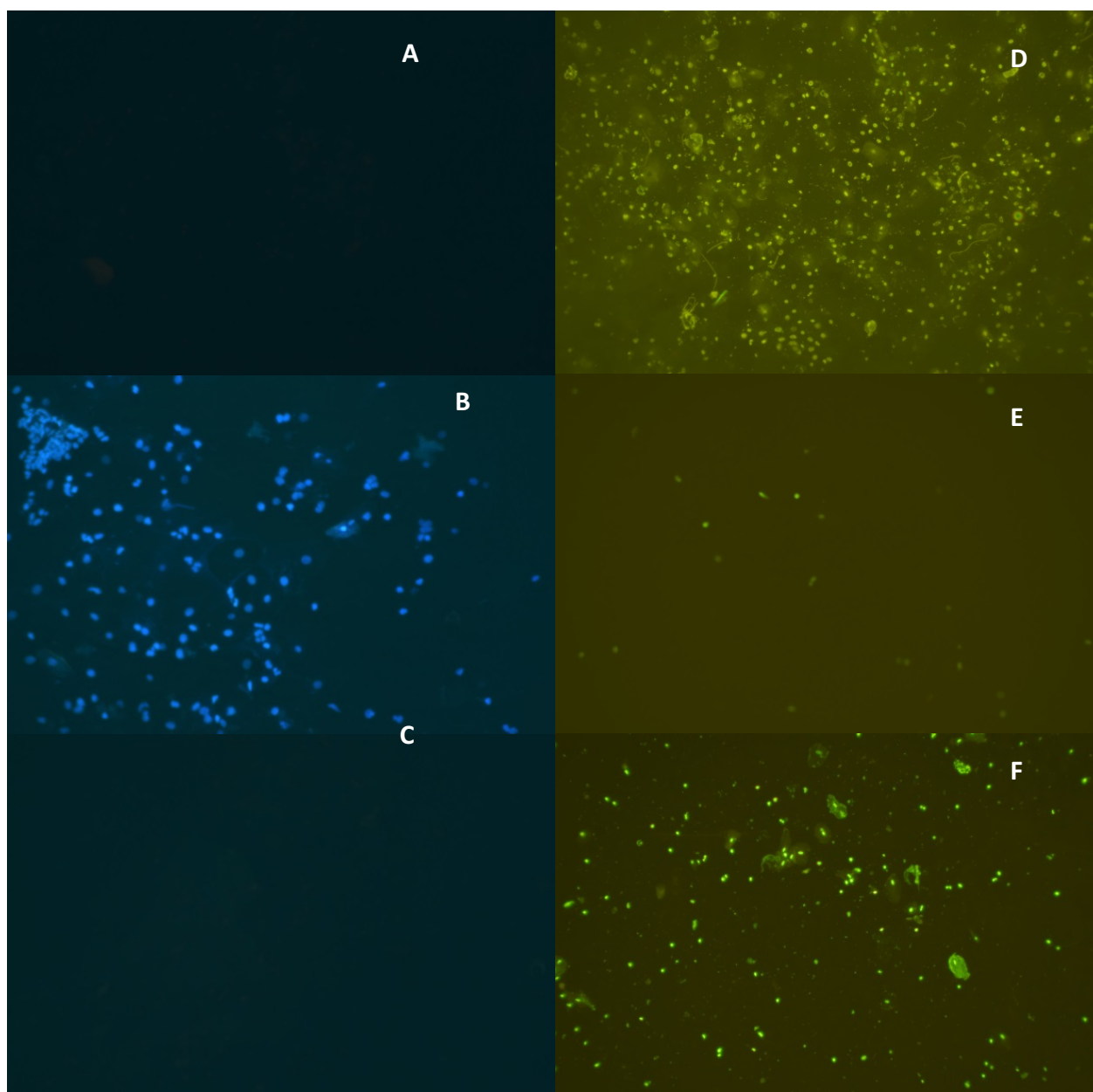


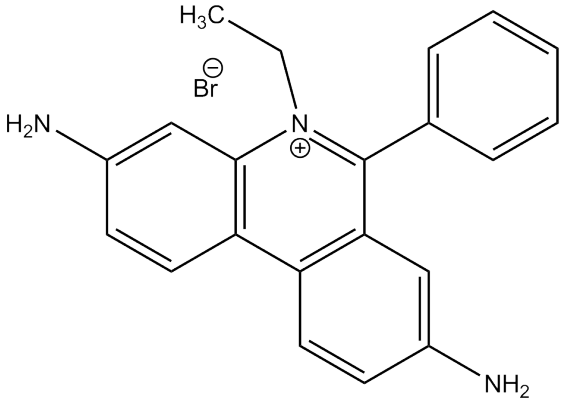
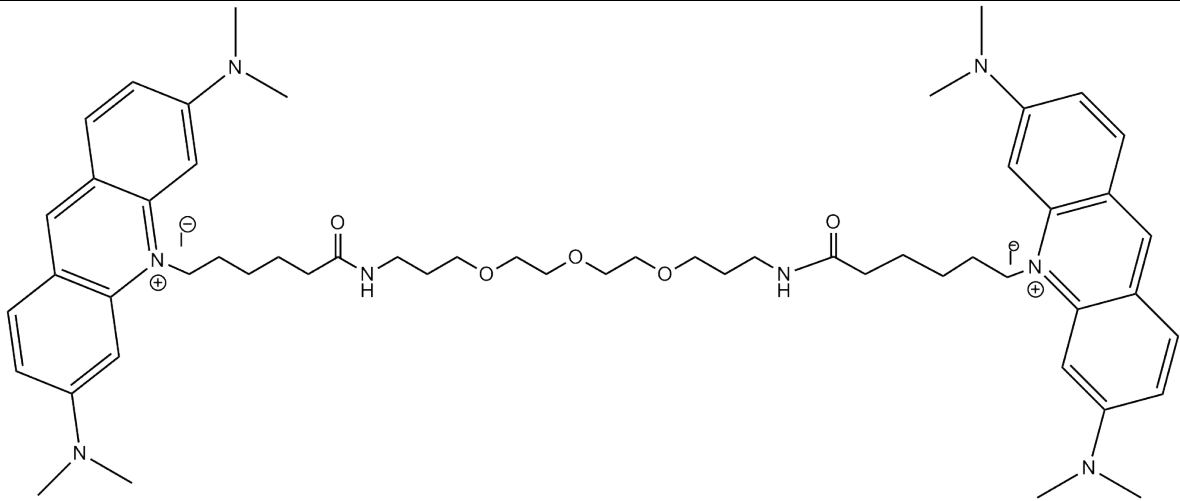
Figure 2.11: Showing the permeability of the binding dyes in a fresh saliva sample at 40x magnification using a 1x concentration dye solution in sterile water. A = Ethidium Bromide, B = RedSafe, C = GelRed, D = Diamond Dye, E = GelGreen and F = SYBR Green I. UV excitation for A, B and C, blue excitation was used for D, E and F.

When looking at the permeability of the dyes to the epithelial cells, the main contributor as to whether they would be able to permeate the membrane is the size of the dye molecules, i.e. their molecular weight and structure. Table 2.4 shows the molecular structure and the weight of the dye molecules; however RedSafe and Diamond Dye have their molecular structures covered by patents and remain unknown. Looking at the structures it can be seen that GelGreen is two molecules of the dye acridine orange with a carbon chain bridge attaching the two dye molecules together. This means that with a higher molecular weight it is much more difficult for the dye to transfer through the phospholipid bilayer of the membrane. Thus the dye cannot bind to DNA that is still retained within the cell nucleus.

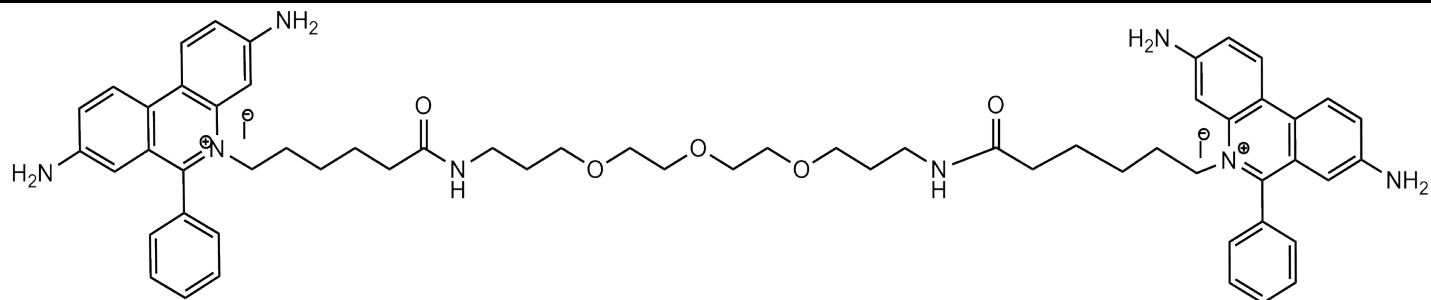
This is the same with the GelRed structure (Table 2.4) where it is two dye molecules of ethidium bromide attached by a hydrocarbon chain. As both ethidium bromide and SYBR Green dye molecules are much smaller they can permeate the cell membrane and interact with nuclear DNA which means the potential to cause mutations is increased and their toxicity is also increased. Based on analysis within this study Diamond Dye and RedSafe appeared to be permeable to the cell membrane (Figure 2.10) which suggests that the dye molecules are similar sizes to that of ethidium bromide and SYBR Green. As they can permeate the cell membrane they have the ability to interact with nuclear DNA, thus could be more mutagenic and toxic than GelGreen and GelRed; however no studies have been undertaken to determine this.

Studies have been conducted that compared the toxicity of Diamond Dye with EtBr and showed that Diamond Dye was less toxic [10] this may be due to the different binding mechanism of the dye. Diamond dye binds to DNA externally [11] unlike ethidium bromide and SYBR Green which intercalate between the base pairs of DNA [1].

Table 2.4: Molecular structures available of the nucleic acid binding dyes used in this study.

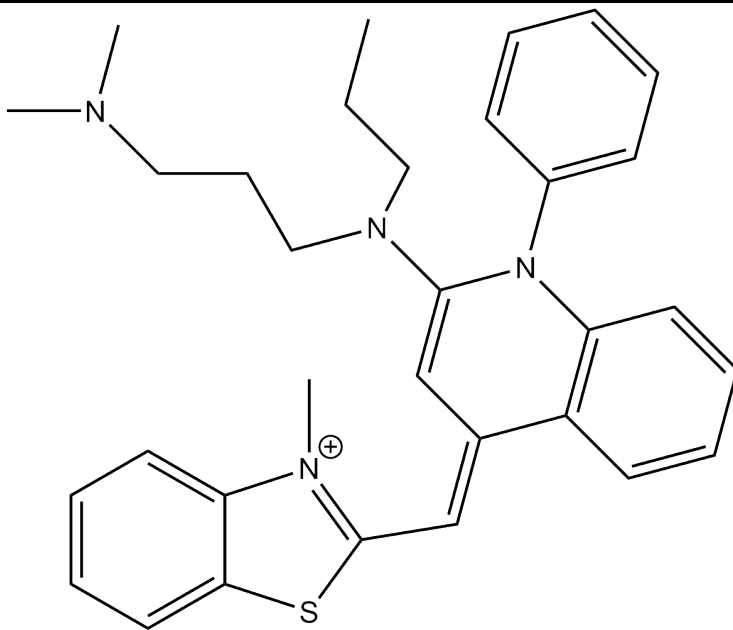
Dye	Molecular Structure	Molecular weight (g/mol)
Ethidium bromide		394.31 [10]
GelGreen™		1198.43 [11]

GelRed™



1238.37 [11]

SYBR® Green



509.73 [1]

2.4 Concluding Remarks:

Investigating the properties of the nucleic acid binding dyes in gel electrophoresis, both modes of staining was undertaken; post cast staining and adding dye to molten gel. It was found that there was less band distortion from electrophoretic mobility of the dyes when staining post electrophoresis. This was due to the dye molecules binding after the DNA bands had been separated resulting in less warping of the bands instead of being bound to the DNA while the fragments moves through the gel medium. GG appears to be more sensitive when adding dye to the molten gel rather than staining post electrophoresis due to the higher intensity values of the DNA bands.

RS and EtBr were poor staining dyes for electrophoresis as they could not detect low amounts of DNA (5 and 2.5 ng respectively); however RS did appear to be more sensitive than EtBr when staining post electrophoresis detecting down to 1 ng. Both RS and EtBr showed nuclei staining hence were membrane permeable. GR was the most sensitive of the six dyes using UV transillumination which was seen both as a pre-cast stain and post electrophoresis staining. GR showed no staining of the nuclei hence was not membrane permeable and hence would be safer than both RS and EtBr.

Dyes that could permeate the cell membrane such as SG, DD and RS could potentially be used as a biological sample stain to determine if samples would be viable for DNA analysis. This would include staining of hair shafts to determine if the hairs have DNA present to result in a DNA profile along with other sample types. The other dyes would not work as well as a biological stain if they do not permeate the cell membrane as only DNA present outside of the cell would fluoresce so the signal obtained would not be a true indicator of the DNA present for DNA analysis.

The results from this Chapter will aid in identifying and selecting potential dyes that could be used for the detection of latent DNA on either surfaces or within biological samples as a presumptive reagent to determine if a sample would be viable for STR typing.

The properties that the viable dyes would have in regards to this novel application would be the following;

- Excitation wavelength higher than UV
- Non-toxic or mutagenic
- Reasonable Stokes shift
- Sensitive and specific
- Doesn't inhibit downstream applications
- Stable and doesn't break down at room temperature

2.5 References (*Supplemental to Publication*)

- [1] C. Aaij., P. Borst, The gel electrophoresis of DNA, *Biochimica et Biophysica Acta (BBA) - Nucleic Acids and Protein Synthesis*. (1972), **269** 192-200.
- [2] P.A. Sharp., B. Sugden., J. Sambrook, Detection of two restriction endonuclease activities in Haemophilus parainfluenzae using analytical agarose--ethidium bromide electrophoresis, *Biochemistry*. (1973), **12** 3055-3063.
- [3] *Molecular Probes Handbook, A Guide to Fluorescent Probes and Labeling Technologies, 11th Edition*.
- [4] H. Hilal., J.A. Taylor, Cyanine dyes for the detection of double stranded DNA, *Journal of Biochemical and Biophysical Methods*. (2008), **70** 1104-1108.
- [5] D.T. Griffiths., S.Y. Ling, Effects of UV light on DNA chain growth and replicon initiation in human cells, *Mutation Research/DNA Repair*. (1989), **218** 87-94.
- [6] J.M. Butler, *Chapter 3 - DNA Quantitation, in Advanced Topics in Forensic DNA Typing*, Butler, J. M., Editor. 2012, Academic Press: San Diego. p. 49-67.
- [7] T.A.H. Schagat, A., Diamond™ Nucleic Acid Dye is a Safe and Economical Alternative to Ethidium Bromide. , *tpub*. (2013), **125**.
- [8] A. Truman.,B. Hook., A. Hendricksen, Diamond™ Nucleic Acid Dye: A Sensitive Alternative to SYBR® Dyes, *tpub*. (2013), **121**.
- [9] A.I. Dragan., R. Pavlovic., J.B. McGivney., J.R. Casas-Finet., E.S. Bishop., R.J. Strouse., M.A. Schenerman., C.D. Geddes, SYBR Green I: Fluorescence Properties and Interaction with DNA, *Journal of Fluorescence*. (2012), **22** 1189-1199.
- [10] R.W. Sabnis, *Handbook of biological dyes and stains: Synthesis and industrial applications*. 2010: John Wiley & Sons.
- [11] United States Patent No. US8232050B2, *Methods of Using Dyes in Association with Nucleic Acid Staining or Detection and Associated Technology*, Biotium, Hayward, CA.

2.6 Appendix A

An example of the gels used within this study for the paper and Chapter are shown below along with the relative volume intensity values for the gels each stained with different nucleic acid binding dyes.

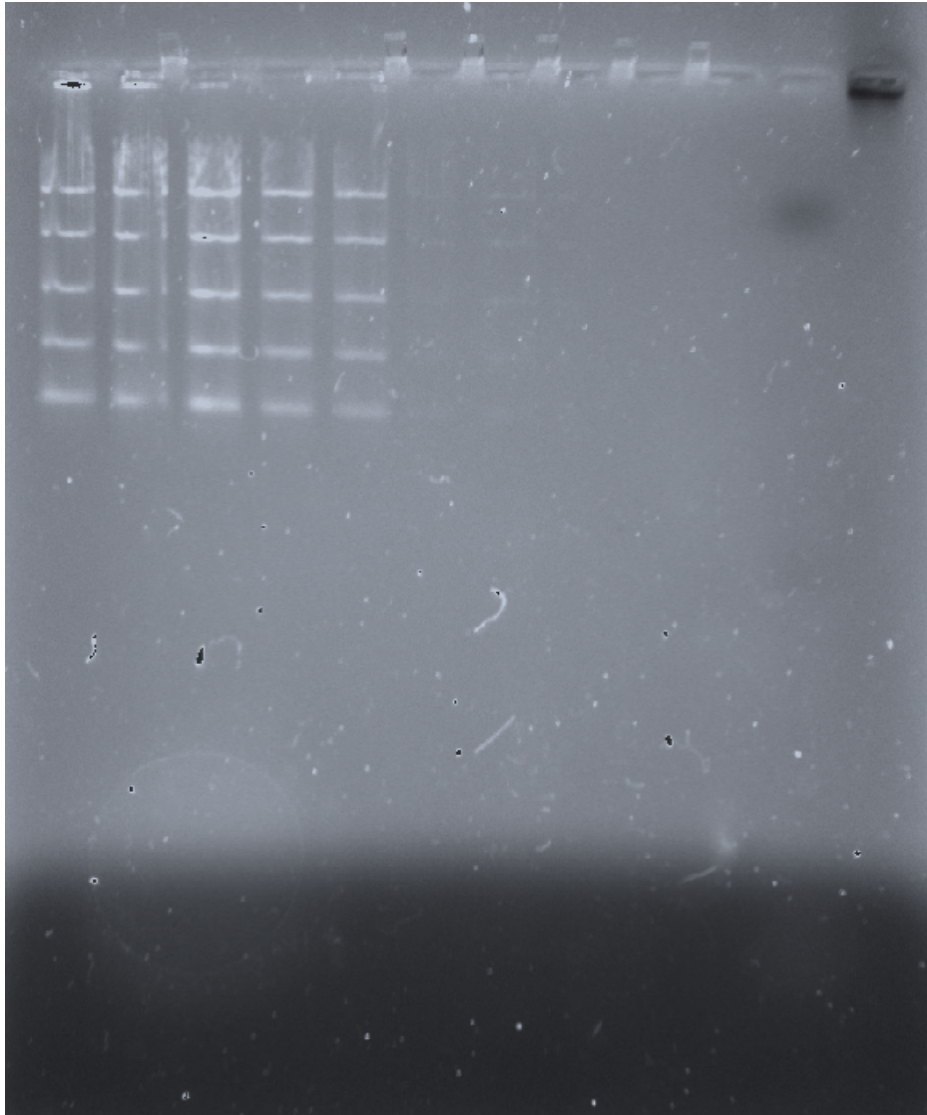


Figure A-1. Image of agarose gel 1% of varying masses of DNA (0.5-50 ng) stained pre-casting of gel with ethidium bromide (0.5 $\mu\text{g}/\text{mL}$ concentration) run for 30 min at 131V.



Figure A-2. Image of agarose gel 1% of varying masses of DNA (0.5-50 ng) stained pre-casting of gel with GelRed (1X concentration) run for 30 min at 131V.

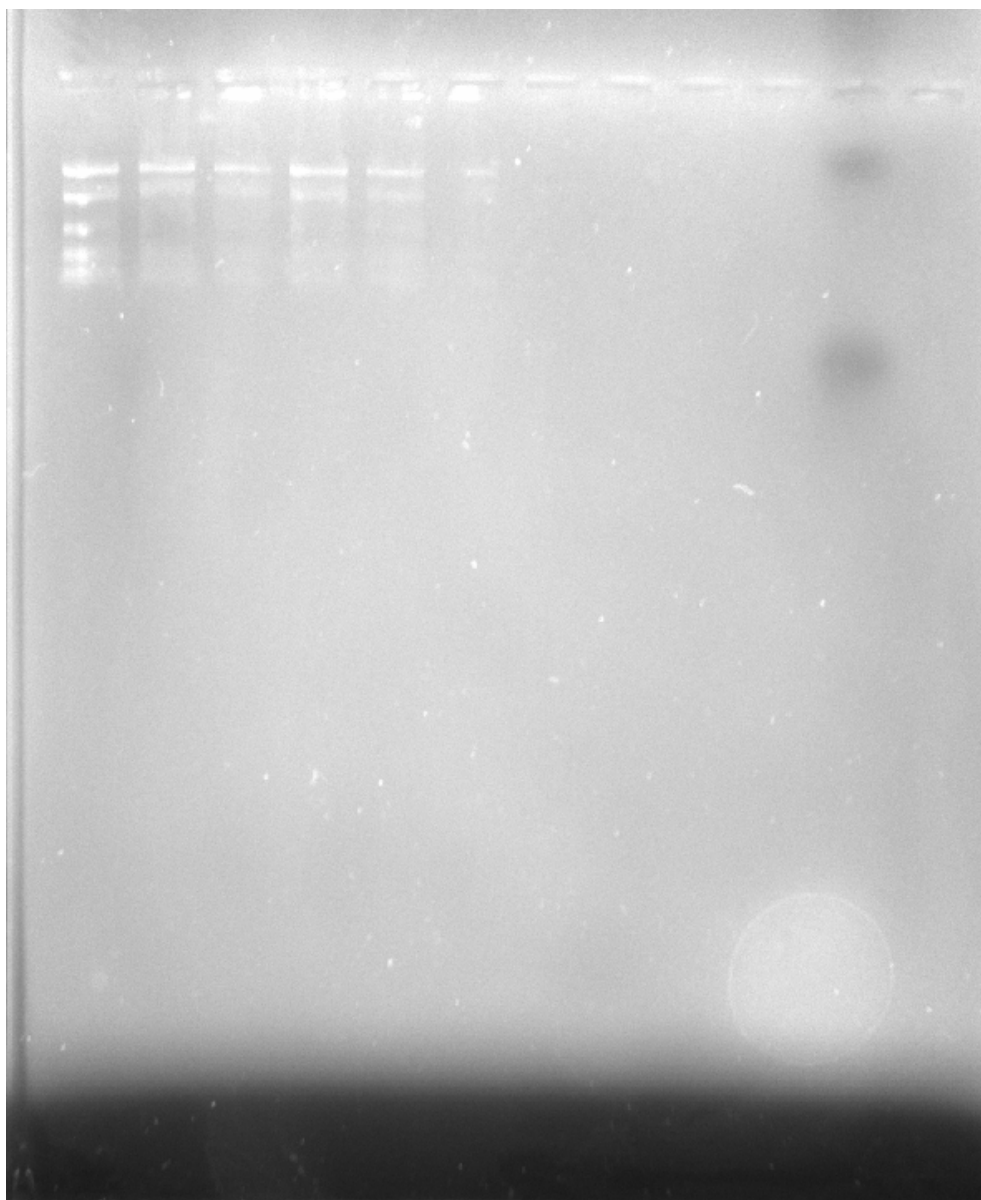


Figure A-3. Image of agarose gel 1% of varying masses of DNA (0.5-50 ng) stained pre-casting of gel with RedSafe (1X concentration) run for 30 min at 131V.

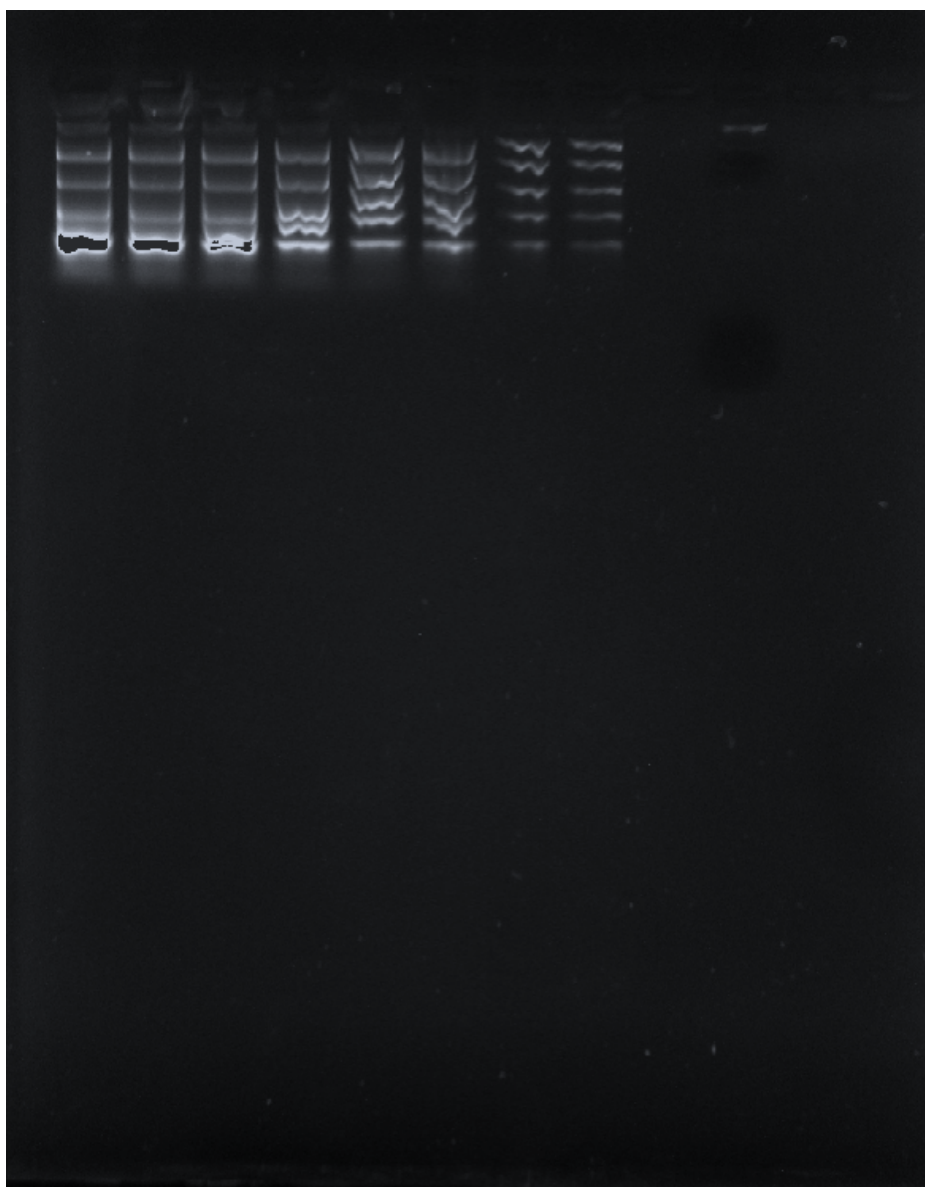


Figure A-4. Image of agarose gel 1% of varying masses of DNA (0.5-50 ng) stained pre-casting of gel with Diamond dye (1X concentration) run for 30 min at 131V.

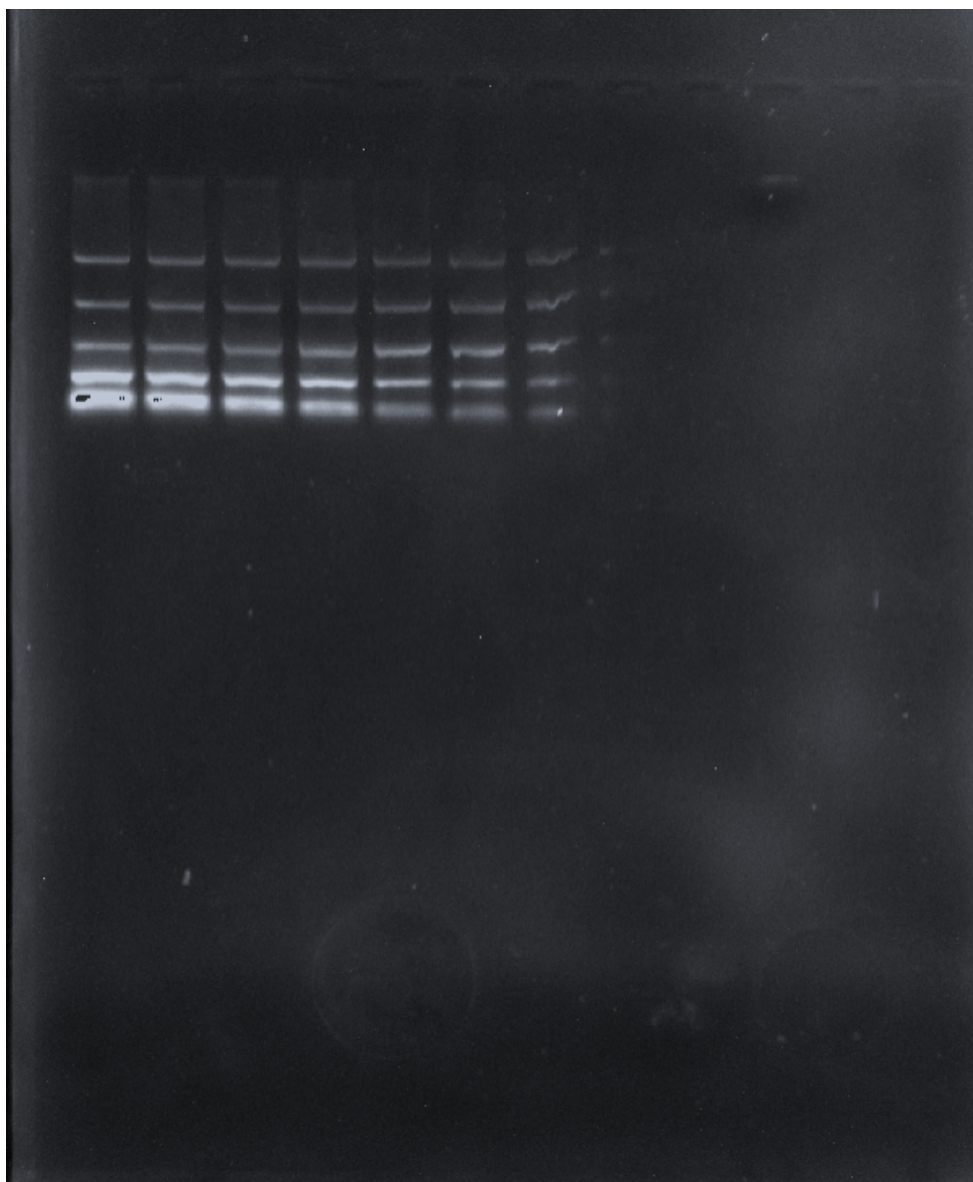


Figure A-5. Image of agarose gel 1% of varying masses of DNA (0.5-50 ng) stained pre-casting of gel with GelGreen (1X concentration) run for 30 min at 131V.

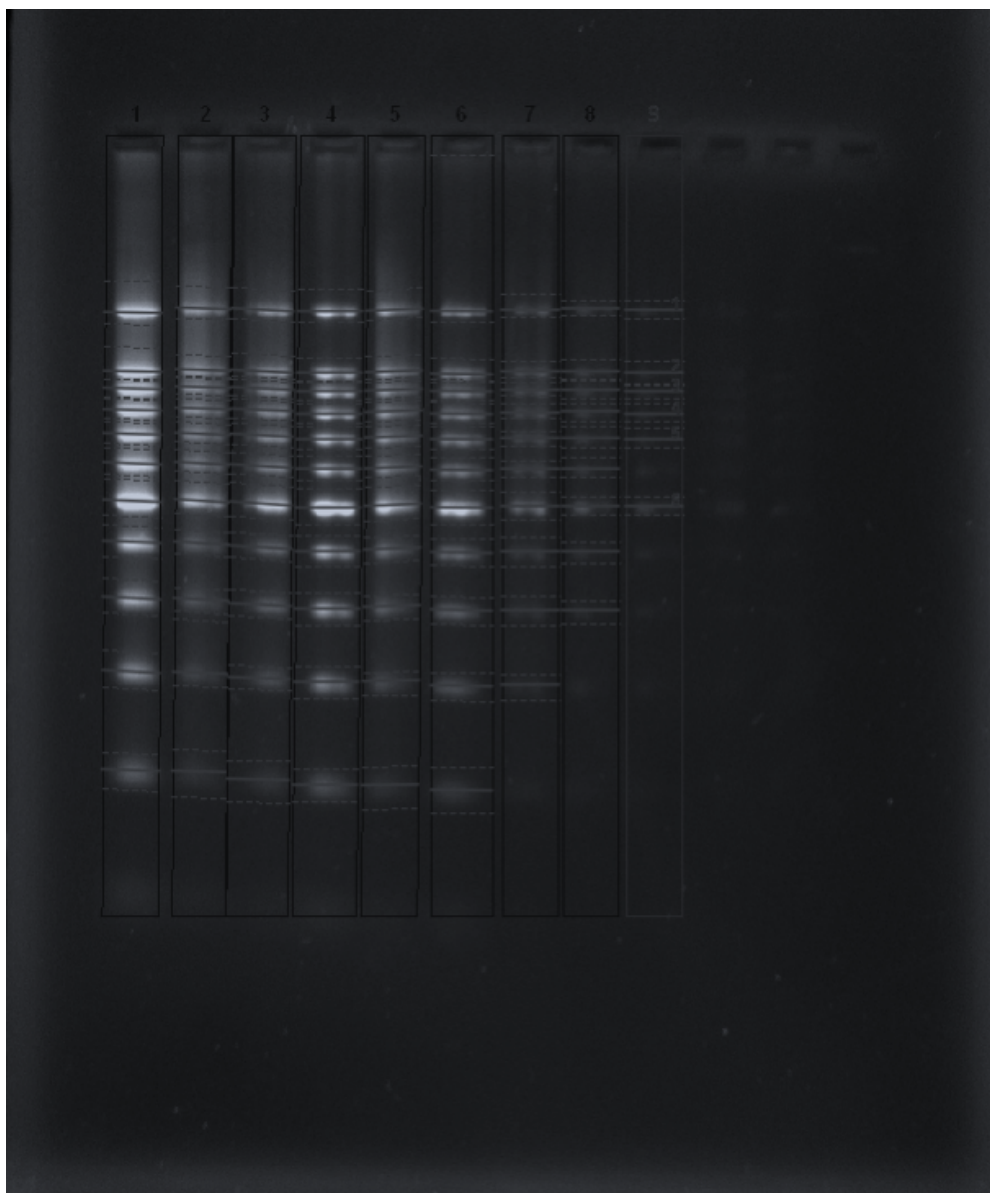


Figure A-6: Image of agarose gel 1% of varying masses of DNA (0.5-50 ng) stained post electrophoresis for 30 min with ethidium bromide (0.5 $\mu\text{g}/\text{mL}$ concentration) run for 30 min at 131V.

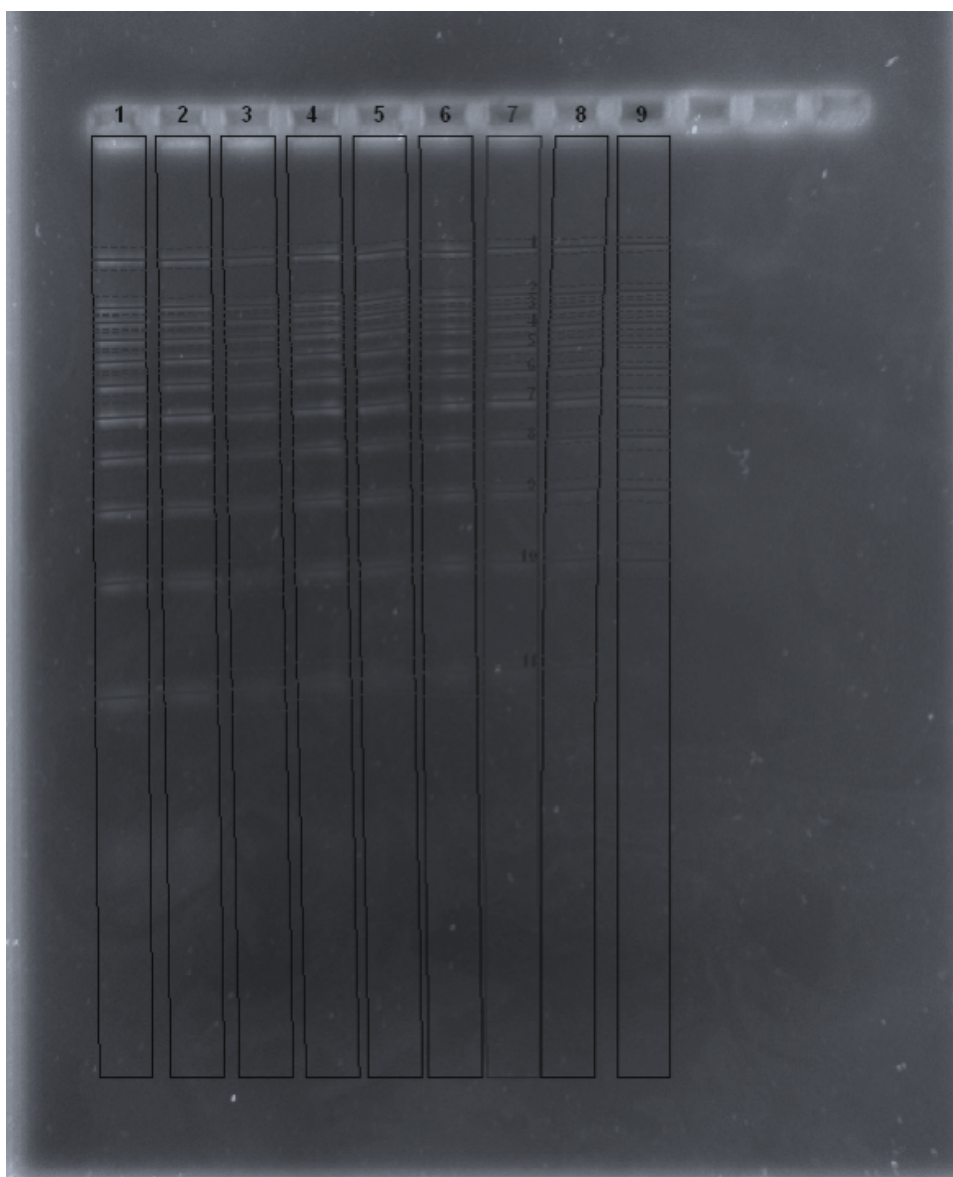


Figure A-7: Image of agarose gel 1% of varying masses of DNA (0.5-50 ng) stained post electrophoresis for 30 min with RedSafe (1X concentration) run for 30 min at 131V.

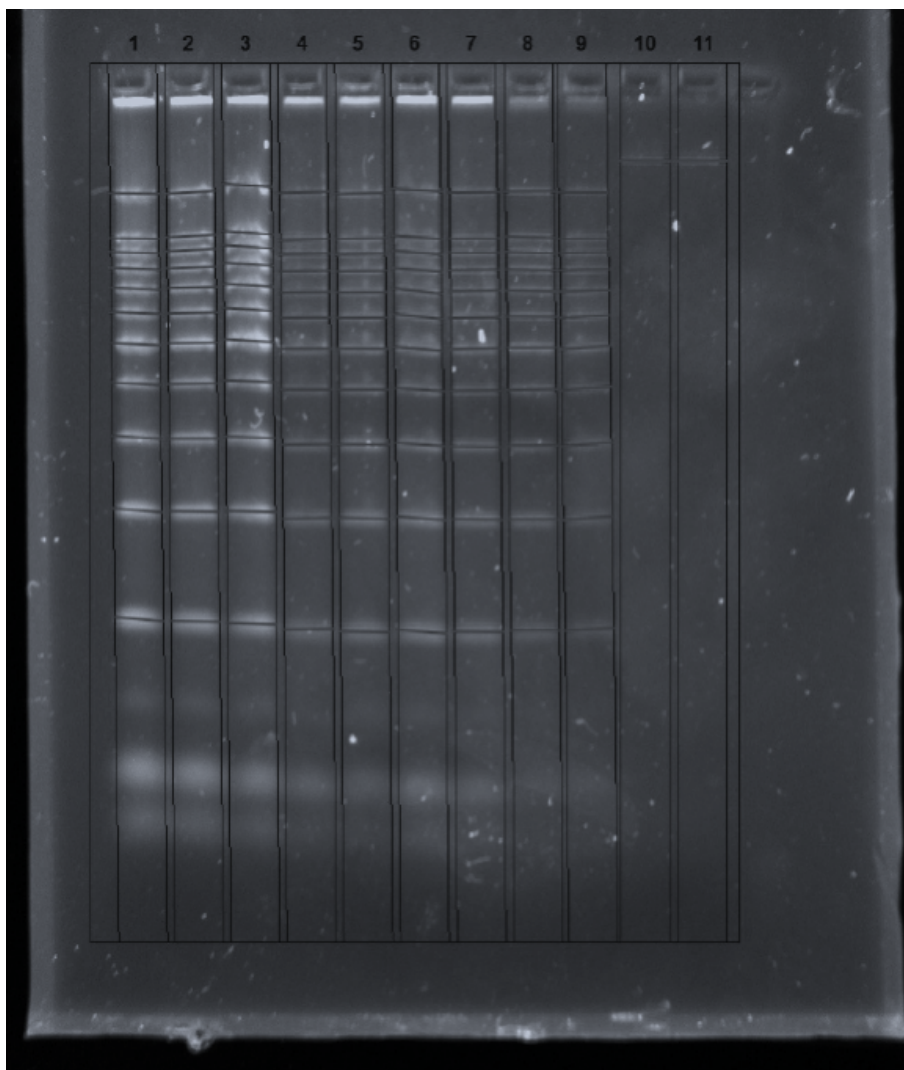


Figure A-8: Image of agarose gel 1% of varying masses of DNA (0.5-50 ng) stained post electrophoresis for 30 min with GelRed (1X concentration) run for 30 min at 131V.

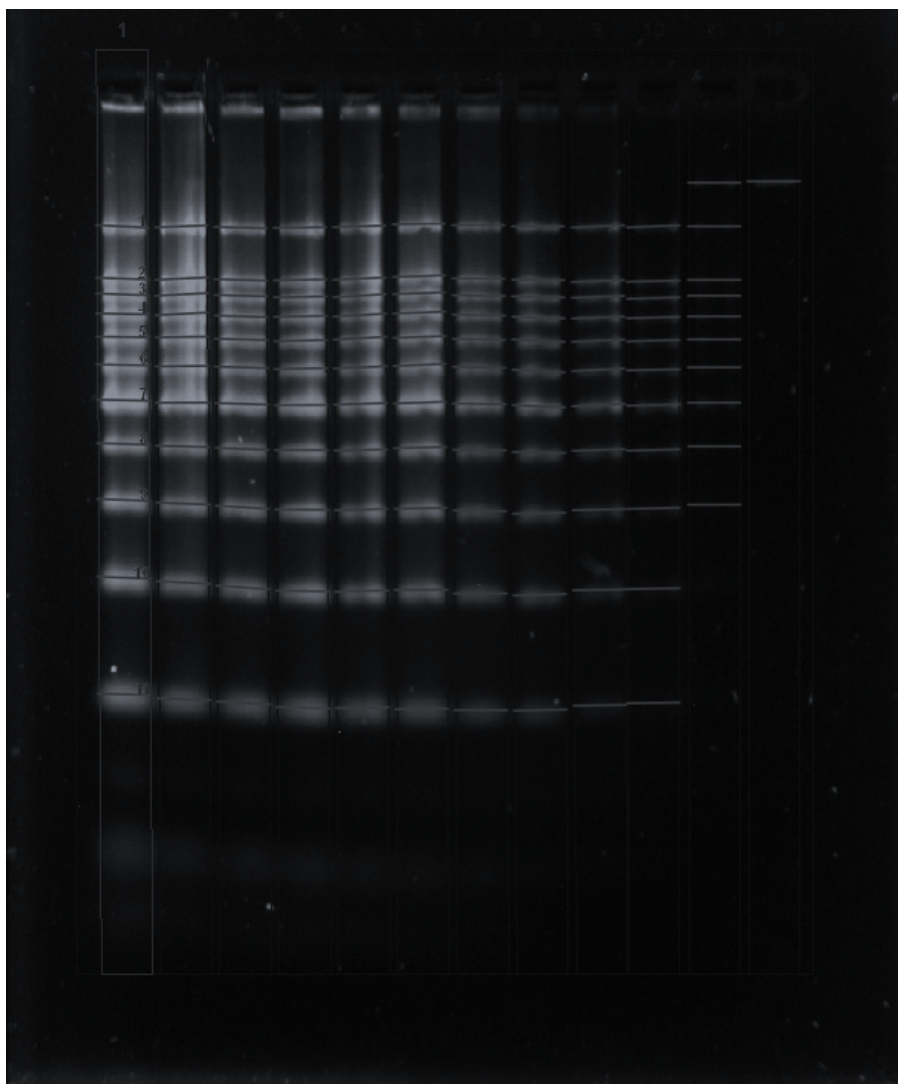


Figure A-9: Image of agarose gel 1% of varying masses of DNA (0.5-50 ng) stained post electrophoresis for 30 min with SYBR Green (1X concentration) run for 30 min at 131V.

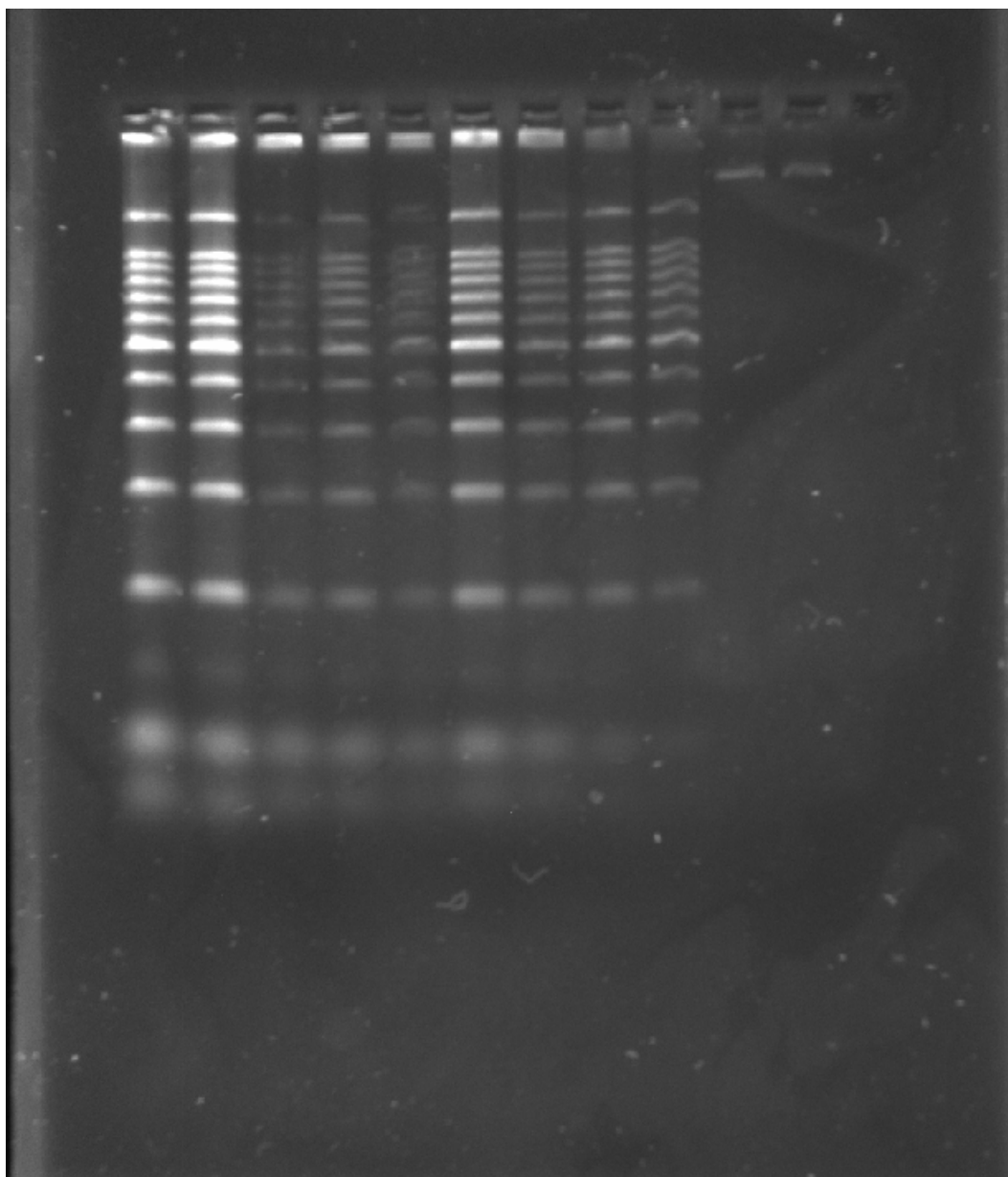


Figure A-10: Image of agarose gel 1% of varying masses of DNA (0.5-50 ng) stained post electrophoresis for 30 min with GelGreen (1X concentration) run for 30 min at 131V.

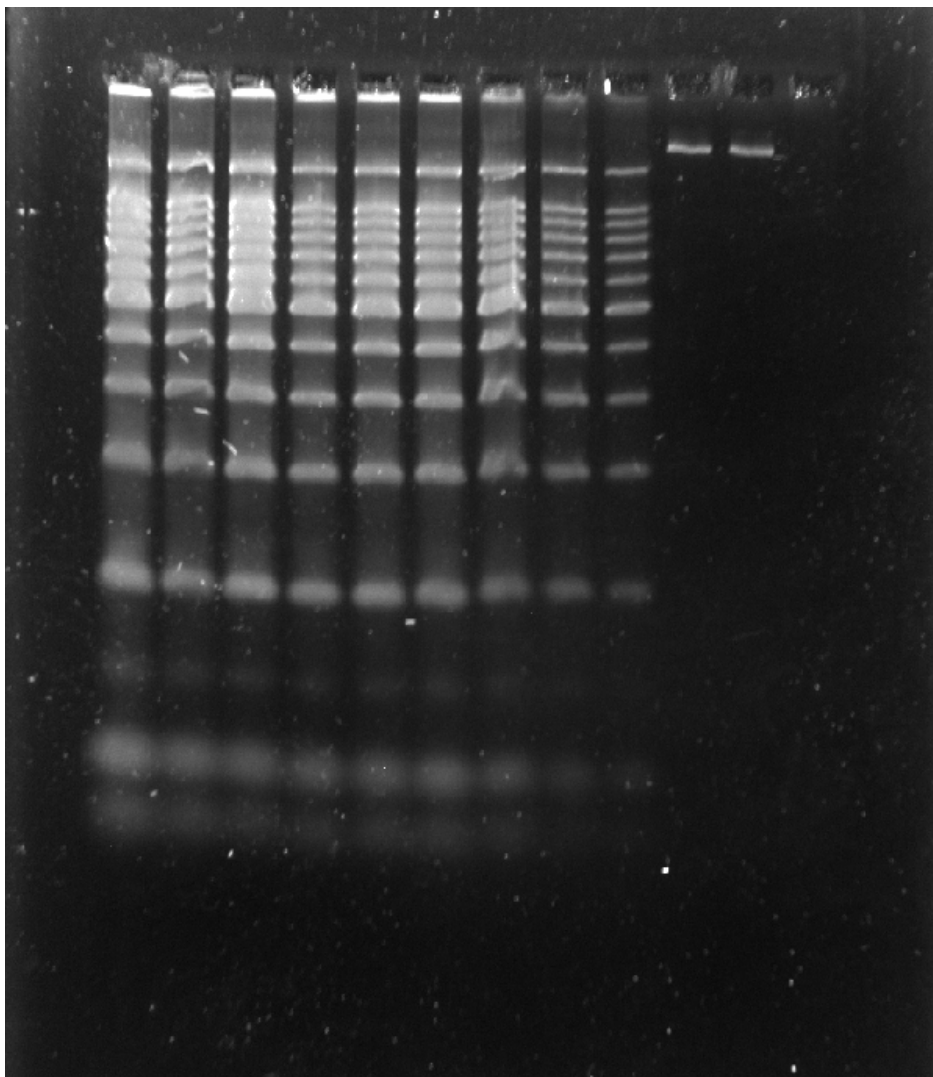


Figure A-11: Image of agarose gel 1% of varying masses of DNA (0.5-50 ng) stained post electrophoresis for 30 min with Diamond dye (1X concentration) run for 30 min at 131V.

Table A-1: Relative volume intensity (a.u) of bands at varying DNA mass of gel (Figure A-1) stained pre-casting of gel with ethidium bromide (0.5 µg/mL).

DNA Mass (ng)/ Band length (bp)	50	40	30	20	10	5	2.5	1	0.5 (control DNA 1 band)
2000 bp	145390	161001	230882	166026	131186	27470	17621	-	-
1000 bp	144050	103783	227703	130985	112828	12194	19296	-	-
500 bp	163882	124486	221703	140432	116647	6030	26666	-	-
250 bp	148204	127300	303979	137283	90115	11122	36582	-	-
100 bp	260965	226527	207298	158522	101170	29145	27872	-	-
Average	172498.2	148619.4	238313	146649.6	110389.2	17192.2	25607.4	0	-
Standard deviation	44799.5	43058.42	33816.08	13327.94	13954.58	9326.593	6786.859	0	-
95% confidence	13513.37	12988.19	10200.32	4020.254	4209.273	2813.283	2047.195	0	-

Table A-2: Relative volume intensity (a.u) of bands at varying DNA mass of gel (Figure A-2) stained pre-casting of gel with GelRed (1X concentration).

DNA Mass (ng)/ Band length (bp)	50	40	30	20	10	5	2.5	1	0.5 (control DNA 1 band)
2000 bp	1225490	1045845	891759	585051	323605	311466	86681	-	
1000 bp	945683	759206	723460	429135	233813	201788	52216	-	
500 bp	1045357	871568	829905	529785	313540	248087	56730	-	
250 bp	1066402	899445	815448	519964	296216	220393	46482	-	
100 bp	1314428	1050359	945561	621102	320982	239547	48800	-	
0.5 ng								-	30073
Average	1119472	925284.6	841226.6	537007.4	297631.2	244256.2	58181.8	0	
Standard deviation	132483.8	110737.2	74967.83	65359.29	33309.92	37220.99	14661.56	0	
95% confidence	39962.53	33402.89	22613.37	19715.04	10047.64	11227.38	4422.527	0	

Table A-3: Relative volume intensity (a.u) of bands at varying DNA mass of gel (Figure A-3) stained pre-casting of gel with RedSafe (1X concentration).

DNA Mass (ng)/ Band length (bp)	50	40	30	20	10	5	2.5	1	0.5 (control DNA 1 band)
2000 bp	212382	253746	67014	100224	62640	41958	-	-	-
1000 bp	139806	273996	56700	77112	49950	21276	-	-	-
500 bp	78948	-	-	-	-	-	-	-	-
250 bp	153252	-	-	-	-	-	-	-	-
100 bp	183762	83592	13716	72954	49950	-	-	-	-
Average	153630	203778	45810	83430	54180	31617	0	0	0
Standard deviation	45007.51	85385.48	23081.21	11995.86	5982.123	10341	0	0	0
95% confidence	13576.11	25755.76	6962.238	3618.444	1804.454	3119.269	0	0	0

Table A-4: Relative volume intensity (a.u) of bands at varying DNA mass of gel (Figure 2.1) stained pre-casting of gel with SYBR Green (1X concentration).

DNA Mass (ng)/ Band length (bp)	50	40	30	20	10	5	2.5	1	0.5 (control DNA 1 band)
2000 bp	198016	136640	131376	176680	261744	70224	123816	96712	
1000 bp	179872	99064	77280	167384	244896	4648	99904	78904	
500 bp	304248	244832	205800	312760	515928	106904	73080	64064	
250 bp	-	-	-	-	449736	107184	55384	52248	
100 bp	2762816	2098432	1847216	1506960	508592	108584	38360	46536	
0.5 ng									60760
Average	861238	644742	565418	540946	396179.2	79508.8	78108.8	67692.8	
Standard deviation	1098904	840992.7	741451.7	560689.3	118999.3	40130.11	30613.24	18259.93	
95% confidence	198016	136640	131376	176680	261744	70224	123816	96712	

Table A-5: Relative volume intensity (a.u) of bands at varying DNA mass of gel (Figure A-4) stained pre-casting of gel with Diamond dye (1X concentration).

DNA Mass (ng)/ Band length (bp)	50	40	30	20	10	5	2.5	1	0.5 (control DNA 1 band)
2000 bp	57528	47328	32487	335172	359244	286416	167076	149277	
1000 bp	334050	298707	288813	359295	440691	292485	138210	126786	
500 bp	321912	279072	277236	732921	459663	349044	115617	98532	
250 bp	605013	514845	538254	474147	425544	403971	91341	75990	
100 bp	2751960	2194581	1882512	762705	448749	392904	85680	68748	
0.5 ng									55743
Average	814092.6	666906.6	603860.4	532848	426778.2	344964	119584.8	103866.6	
Standard deviation	984288.3	778045.8	659038.7	181937.2	35553.01	48946.15	30216.89	30418.03	
95% confidence	296901.7	234690.5	198793.1	54879.71	10724.25	14764.17	9114.654	9175.324	

Table A-6: Relative volume intensity (a.u) of bands at varying DNA mass of gel (Figure A-5) stained pre-casting of gel with GelGreen (1X concentration).

DNA Mass (ng)/ Band length (bp)	50	40	30	20	10	5	2.5	1	0.5 (control DNA 1 band)
2000 bp	167678	151380	114318	106952	70180	63220	52084	19198	
1000 bp	142564	113622	103530	99702	71398	71282	63162	13572	
500 bp	324626	256418	236408	237742	206306	173884	128760	17052	
250 bp	-	-	-	475832	337502	281648	154512	4988	
100 bp	6066714	1767144	1479058	760438	468582	356004	175798	4118	
0.5 ng									42166
Average	1675396	572141	483328.5	336133.2	230793.6	189207.6	114863.2	11785.6	
Standard deviation	2536289	691916.3	577248.3	252053.5	154747.1	115221.9	49178.13	6178.5	
95% confidence	765048.6	208710.3	174121.8	76029.67	46678.07	34755.64	14834.14	1863.689	

Table A-7: Relative volume intensity (a.u) of bands at varying DNA mass of gel (Figure A-6) stained post electrophoresis with ethidium bromide (0.5 µg/mL).

DNA Mass (ng)/ Band length (bp)	50	40	30	25	20	12.5	10	5	2.5	1	0.5
1500	629305	268673	251436	386208	230958	341918	84667	37582	24037	-	-
1000	555577	222630	233036	366000	218148	235566	79292	43774	17845	-	-
900	408414	167239	187542	323088	164808	203090	64328	35260	12040	-	-
800	401104	157809	178572	336288	163338	207460	63382	29369	15265	-	-
700	354363	131692	158194	323904	141330	194350	49450	24940	18404	-	-
600	381496	106272	136528	297696	116466	168774	43387	22188	-	-	-
500	347210.7	131610	155480	318672	142604	188308.7	55427	26445	17028	-	-
400	396546	120417	158148	360288	140616	195132	53535	27090	16254	-	-
300	420626	123615	155434	359040	127218	192096	48117	25714	6149	-	-
200	403770	139523	131284	318960	110166	170338	33712	7740	5547	-	-
100	284531	109388	95220	221904	95046	130870	27563	6764	3956	-	-
Average	416631.2	152624.4	167352.2	328368	150063.5	202536.6	54805.45	26078.73	13652.5	0	0
Standard Deviation	96338.45	50553.67	44523.75	43920.04	42501.35	53187.14	17459.73	11259.05	6560.636	0	0
95 Confidence interval	19591.99	10280.91	9054.631	8931.857	8643.343	10816.47	3550.721	2289.711	1334.212	0	0

Table A-8: Relative volume intensity (a.u) of bands at varying DNA mass of gel (Figure A-8) stained post electrophoresis with GelRed (1X concentration).

DNA Mass (ng)/ Band length (bp)	50	40	30	25	20	12.5	10	5	2.5	1	0.5
1500	297603	286853	145082	118379	123711	106253	43430	113950	80195	21371	12685
1000	235683	248024	123281	109865	81055	81743	94170	98857	70950	26746	9331
900	215086	226653	96664	98685	63855	74519	29369	92536	54051	24144	9116
800	225449	238005	105006	109091	65704	79206	33540	85785	58351	28294	12556
700	220891	234479	180661	127280	68585	95503	33798	97868	76368	24295	18963
600	233619	228975	105350	123539	79163	86430	122034	96965	88107	24596	19006
500	159272	152349	149984	86258	156090	43817	61404	68828.67	43301	35475	20898
400	294507	282381	125861	161336	100876	107543	63425	143233	73659	29799	17845
300	377110	363737	178794	231899	130763	170581	88021	150027	92235	30014	24166
200	510969	467754	200896	316093	185158	252711	119497	191307	102684	45494	22747
100	617093	512474	348816	330756	247723	264364	295324	150586	107199	27950	44920
Average	307934.7	294698.5	160035.9	164834.6	118425.7	123879.1	89455.64	117267.5	77009.09	28925.27	19293.91
Standard Deviation	140612.6	109811.7	71388.43	87676.53	58529.9	73428.48	76018.08	36642.82	19988.88	6675.17	9945.597
95 Confidence interval	28595.87	22332.01	14518	17830.45	11903.01	14932.88	15459.52	7451.915	4065.065	1357.505	2022.599

Table A-9: Relative volume intensity (a.u) of bands at varying DNA mass of gel (Figure A-7) stained post electrophoresis with RedSafe (1X concentration).

DNA Mass (ng)/ Band length (bp)	50	40	30	25	20	12.5	10	5	2.5	1	0.5
1500	315928	274648	217624	265012	244376	193468	139788	115192	63360	37708	-
1000	292422	222948	138732	191488	177540	154000	122144	67480	51568	28248	-
900	220892	173184	132616	147092	123948	132440	103576	68596	50732	30228	-
800	246790	204424	136136	163636	151800	141504	114884	75944	61776	34672	-
700	277426	252164	149160	186516	159016	154176	131340	94996	44660	31944	-
600	285752	233332	149336	186868	179080	149556	131868	79024	37092	24288	-
500	177483.3	141210.7	87046.67	124813.3	113901.3	101068	84612	61438.67	38940	18729.33	-
400	316940	273548	167288	221628	187220	184800	117964	68200	43296	25520	-
300	325818	314820	160160	213312	186032	162932	128084	88792	52052	25828	-
200	333868	296076	148632	202752	182248	162008	124036	63052	34848	-	-
100	295182	238524	158092	143880	132352	114180	-	-	-	-	-
Average	280772.8	238625.3	149529.3	186090.7	167046.7	150012	119829.6	78271.47	47832.4	28573.93	0
Standard Deviation	48146.34	51983.12	31025.27	40126.99	36627.61	27392.55	15983.79	16950.85	9828.34	5776.776	0
95 Confidence interval	9791.344	10571.62	6309.494	8160.479	7448.822	5570.722	3250.564	3447.231	1998.753	1174.802	0

Table A-10: Relative volume intensity (a.u) of bands at varying DNA mass of gel (Figure A-9) stained post electrophoresis with SYBR Green (1X concentration).

DNA Mass (ng)/ Band length (bp)	50	40	30	25	20	12.5	10	5	2.5	1	0.5
1500	646360	630608	535700	554709	475772	541068	317856	261140	159456	64856	16984
1000	641080	592900	531124	522148	429572	520872	315876	265848	158356	52976	14564
900	448360	400312	398156	418132	319880	381480	259160	230956	137192	41184	10296
800	446776	405724	414524	447304	334620	394944	272316	243320	145200	44132	11924
700	421740	348040	394724	433620	309936	360052	250580	232056	142384	52448	13948
600	401236	319176	372152	420772	302060	334708	237996	223432	133760	49588	14652
500	334928	274750.7	274780	137446.7	239917.3	269206.7	184213.3	166144	110205.3	51582.67	14725.33
400	751828	582208	595100	672232	505648	559724	324676	278564	153296	52492	13376
300	990880	707696	699952	770264	593032	613580	354464	286880	153384	48092	13992
200	1159840	779988	733832	817784	645656	609752	369864	284548	142384	53768	6336
100	1063832	712756	668272	735548	583352	520124	314380	209044	112420	34848	-
Average	664260	523105.3	510756	539087.2	430858.7	464137.3	291034.7	243812	140730.7	49633.33	13079.73
Standard Deviation	291690.4	178528.1	151267.6	199364.3	138763.4	119226.2	55206.36	36698.8	16730.6	7762.296	2960.163
95 Confidence interval	59320.01	36306.59	30762.73	40543.98	28219.8	24246.59	11227.11	7463.3	3402.44	1578.59	601.9974

Table A-11: Relative volume intensity (a.u) of bands at varying DNA mass of gel (Figure A-10) stained post electrophoresis with GelGreen (1X concentration).

DNA Mass (ng)/ Band length (bp)	50	40	30	25	20	12.5	10	5	2.5	1	0.5
1500	261008	98120	116776	37312	76208	25828	81532	62436	48356	29216	20724
1000	190784	83820	127688	19756	72028	76076	81752	54076	42152	19712	16192
900	80696	57376	49808	18348	52184	78716	61512	51216	36608	15840	14828
800	72556	51612	48356	87164	53768	-	67188	43516	34892	17996	16236
700	64460	46640	34364	-	49324	-	57992	37092	40920	22528	19272
600	56056	38632	26928	-	50380	7788	48664	35376	39688	20812	15796
500	53518.67	41330.67	34760		34730.67	16544	28776	27324	28292	18788	13214.67
400	144496	105336	108548	55792	57508	47168	47652	48092	50424	35728	26972
300	226468	135828	132440	99572	44176	63932	56848	54164	39556	28424	24640
200	310684	187616	145068	167684	66924	85800	84788	66176	45408	27764	17996
100	448888	278036	238964	194832	134772	142384	108592	65648	42284	21912	14608
Average	173601.3	102213.3	96700	85057.5	62909.33	60470.67	65936	49556	40780	23520	18225.33
Standard Deviation	128507.5	74236.48	65181.29	66486.55	26748.19	41865.65	22019.64	12785.94	6218.519	6006.938	4344.777
95 Confidence interval	26134.09	15097.2	13255.68	13521.13	5439.681	8514.062	4478.052	2600.228	1264.637	1221.609	883.5813

Table A-12: Relative volume intensity (a.u) of bands at varying DNA mass of gel (Figure A-11) stained post electrophoresis with Diamond dye (1X concentration).

DNA Mass (ng)/ Band length (bp)	50	40	30	25	20	12.5	10	5	2.5	1	0.5
1500	429089	449370	353910	410644	664456	398658	622388	301236	166868	47472	40752
1000	398638	412500	341130	321386	428662	344448	366808	284700	176306	22224	22800
900	286824	277650	274200	243412	221130	260780	219700	210470	134602	20064	25872
800	321160	317160	317610	258154	238342	275028	220974	205530	142272	23616	26784
700	312502	291030	304650	233428	199472	253058	202774	191126	136760	26736	20400
600	278055	266430	291990	264264	242918	235196	165776	162422	125190	31152	23184
500	192881	194950	202800	187156.7	237908.7	170230.7	165732.7	136092.7	106149.3	38496	43632
400	409627	425550	358410	354484	519662	415636	446680	222820	135226	26976	56496
300	610648	570300	377490	402142	743704	466700	572754	220870	136162	20112	36000
200	726458	687420	399930	417144	822536	509366	621062	220558	130130	20784	24528
100	981684	917190	392850	295386	706186	517894	515840	179140	96928	38256	12960
Average	449778.7	437231.8	328633.6	307963.7	456816.1	349726.8	374589.9	212269.5	135144.8	28717.09	30309.82
Standard Deviation	233973.6	214636.6	58405.62	79084.22	242749.9	119325.7	187340.5	48266.09	22761.49	9117.501	12556.13
95 Confidence interval	47582.35	43649.86	11877.73	16083.07	49367.16	24266.83	38098.74	9815.696	4628.92	1854.193	2553.494

Chapter 3

Effects of DNA binding dyes on forensic procedures

3.1 Introduction

DNA binding dyes as discussed in chapters 1 and 2 have a range of applications within gel electrophoresis, flow cytometry and as fluorescent probes. One area that has not been greatly investigated is whether these binding dyes have any effect on downstream applications such as DNA extraction, PCR amplification and STR typing typically used procedures in forensic analysis of swabbed items. If DNA binding dyes could be used for a surface-based fluorescent detection method then it would be necessary to determine the effects these dyes might have on other forensic procedures commonly undertaken within the laboratory. If these dyes were used on a surface for DNA detection the areas would then be swabbed for DNA collection, these swabs would firstly undergo a DNA extraction followed by quantification and STR amplification and detection. These DNA binding dyes may chemically alter these processes resulting in no STR profile. If this was the case for the dyes then this novel application would not be applicable for forensic practice, highlighting the need to evaluate the effects these dyes have on forensic procedures.

Previous research has been undertaken on whether SG has an effect on PCR amplification and it was found that at certain concentrations that SG did inhibit the amplification reaction [1]. However qPCR has become a standard means of DNA quantification. Generally within the qPCR reaction the concentration of the SG present is at 1X [2]. Given that 1X concentration is specified by suppliers of qPCR reagents it is a reasonable assumption that the reaction is not inhibited at 1X and if other dyes are used at this concentration they shouldn't affect the STR amplification and hence the typing of the STR loci.

The aims of these experiments are to determine whether six commonly used dyes for gel electrophoresis effect downstream forensic applications when used at a concentration of 1X. The effect on DNA extraction, quantification, amplification and detection of STR fragments will be determined within this Chapter.

3.1.2 Background on DNA extraction

DNA extraction is performed on forensic samples to isolate the DNA that may be present into a pure form for subsequent analysis such as DNA quantified and STR typing. There are several different methodologies for DNA extraction:

- Phenol/Chloroform extraction
- Chelex extraction
- Solid phase silica gel column extraction

The method that is more widely used for DNA extraction of forensic samples is using the solid phase silica column methodology [3]. There are now many commercial kits available for specific samples. The most commonly used within forensic laboratories in Australia are:

- QIAamp Qiagen Micro/Mini Extraction kit [4]
- Promega DNA IQ kit [5, 6]
- PrepFiler™ [7]

Biological samples that may be collected from crime scenes that could be in the form of blood, semen, saliva, tissue or touched samples contains other cellular material besides from DNA. Proteins that package DNA in the cell to prevent degradation can inhibit downstream applications of DNA analysis; thus cellular material needs to be removed before analysis of the DNA. The extraction process ideally removes the inhibitors that are present that may prevent amplification by PCR. The extraction process is typically undertaken in three steps [3];

1. Lyse cells to release DNA
2. Separate DNA from cellular material
3. Isolate and purify the DNA ready for downstream applications

3.1.3 Phenol/Chloroform Extraction:

Organic extractions using phenol-chloroform is the method that has been used for the longest time to isolate DNA and widely used for many years [3], however due to the use of toxic chemicals, other methods have since been developed for use [3]. This method involves the addition of chemicals to lyse the cells; first sodium dodecylsulphate (SDS) and Proteinase K. These chemicals breakdown the cell membrane and proteins that protect the chromosomal DNA present. The phenol/chloroform mixture is then added to isolate the proteins from the DNA. The DNA is more soluble in the aqueous phase and the proteins/cellular debris is present in the organic phase. As the organic phase is denser than the aqueous, they will naturally form two layers with the organic at the bottom. Once centrifuged the DNA present in the aqueous phase can be removed and concentrated for later analysis. This method is only suitable when dealing with DNA with high molecular weights and extraction of DNA from bone sources [3, 8, 9].

3.1.4 Chelex[®] Extraction:

The Chelex[®] extraction method uses a suspension containing a chelating-resin that can be added directly to samples and was first introduced in the early 90s to the forensic community [10]. Chelex[®]-100 is an ion-exchange resin and this extraction reaction is more rapid than phenol/chloroform extraction, requires fewer steps, and can be undertaken in a single tube. Chelex[®] is made up of styrene divinylbenzene copolymers which contain paired iminodiacetate ions which act as a chelating agent to polyvalent metal ions, such as magnesium (Mg^{2+} , Ca^{2+} , and Fe^{2+}). The resin chelates with the metal ions removing the Mg^{2+} from the reaction which inhibits the nuclease enzymes that can destroy DNA; thus minimizes DNA degradation. Generally a 5% Chelex[®] suspension is used for samples and is heated to high temperatures (100 °C) to denature the cell membrane and release the DNA. However due to the high temperature the DNA also denatures thus only single-stranded DNA is yielded from this reaction. When the tube has been spun down the supernatant can be removed which contains the purified DNA and the cell debris remains at the bottom of the tube. Once supernatant is removed it can be quantified and added directly to the PCR [3].

3.1.5 Solid Phase Extraction:

Solid-phase extraction involves DNA selectively binding to a silica substrate (beads or column) and releases the DNA in a purified form. The most widely used kits for DNA extraction include:

- QIAamp mini columns (QIAGEN)
- DNA IQ (Promega)
- PrepFiler (Applied Biosystems)

For QIAGEN extraction kits QIAamp Spin columns are used, in this approach the DNA selectively adsorbs on to the silica surface in the presence of chaotropic salts at high concentrations. The chaotropic salts disrupt the hydrogen bonding in water, thus making the denatured proteins and DNA more thermodynamically stable [11, 12]. When in more acidic conditions (above 7.5 pH) the DNA adsorbs onto the silica surface; unwanted material can then be washed through and discarded. Under more alkaline conditions and at low salt concentration the DNA will no longer be adsorbed onto the silica surface and is efficiently eluted. Silica column extraction results in much more pure DNA than Chelex[®] but is more costly and requires more tube changes which can result in a loss of DNA. This methodology lends itself to a high-through put automation using a 96 well plate format [3, 9, 12]. DNA IQ and PrepFiler differs from QIAamp kits by using magnetic silica beads which results in less wash steps and tube changes reducing the loss of DNA as the reaction takes place in one tube [3, 5-7]. Both kits are amenable to automation.

3.1.6 Background on STR profiling;

DNA regions within the non-coding region of the human genome contain repeat units referred to as short tandem repeats (STRs) ranging in size from 2-7 bp in length [13]. These STRs have become essential in forensic science for identification purposes, due to their high variability among individuals [13]. Commercial STR kits used for identification in either paternity or criminal cases have been available since the late 90s [14]. The STR kit used within the research of this Chapter was Profiler Plus[™] which contains 9 STR loci plus amelogenin as the sex identification locus. The STR loci and the fluorescent dyes attached to the fragments are detailed in Figure 3.1. The three fluorescent dyes primarily used within STR kits to aid in detection are 5-FAM, JOE and NED, ROX is used as an internal size

standard. The alleles are set out in a manner where the fragments that have the same dye don't overlap; the fragments that do overlap however have different dyes attached in order for them all to be easily distinguished [13].

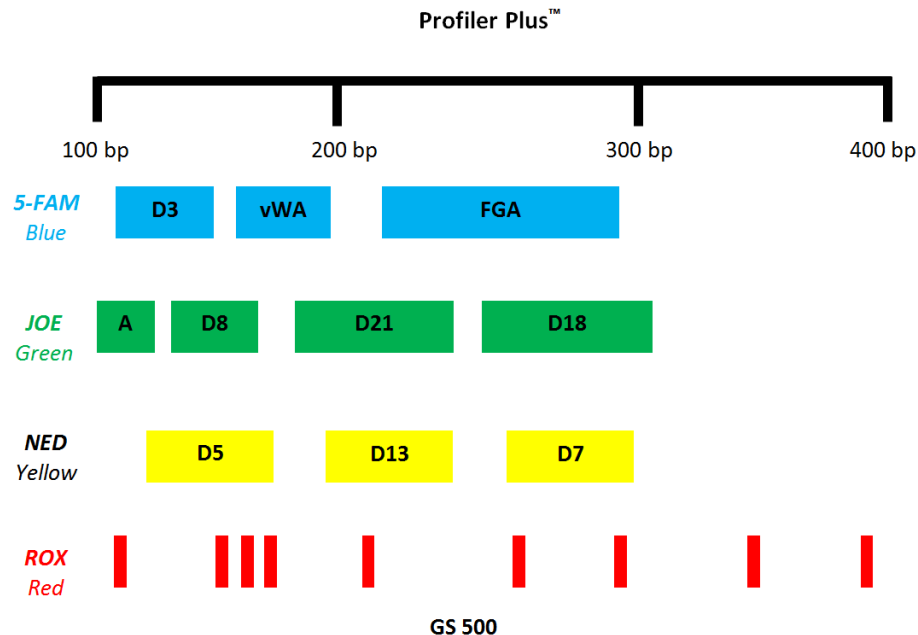


Figure 3.1: Profiler plus™ (Life Technologies) showing the size range for the known alleles represented by box length containing locus name. Colour indicates the fluorescent label attached to the allele. The internal size standard is shown in red. Adapted from [15].

The excitation of the fluorescent labels attached to the STR fragments differ with 5-FAM excited at 492 nm, JOE at 520 nm and NED at 546 nm. Their maximum emission signals are at 518, 548 and 575 nm respectively [16].

3.1.7 'Direct' PCR

A more recent development involves bypassing the extraction step and adding the sample directly to the PCR amplification. Direct amplification has been used in other areas such as microbiology since the 90's [17], however has only been utilized in forensic science since 08 [18]. This has shown to be effective for samples that might have very low amounts of DNA present, for example touched items that otherwise would result in no profile due to the substantial loss of DNA during the extraction process. Direct PCR has been undertaken of whole blood and saliva samples of FTA® card [18, 19] on human hair roots [20, 21], human

fingernails [22, 23], fibre and fabrics [24], latent DNA on various surfaces [17] and from fingerprints [25, 26].

A study by Ottens, R., *et. al* [27] shows that when using certain DNA extraction methodologies there can be around an 85% loss of DNA. When dealing with low template samples of highly degraded samples this more often results in no DNA profile with only a success rate of less than 10% (as stated by Forensic Science SA) [27].

3.1.8 Summary

This Chapter aims to determine whether specific DNA binding dyes have an effect on downstream forensic applications if they were to be used for latent DNA detection. The effects of six binding dyes on DNA extraction, quantification, amplification, direct amplification and STR fragment detection were all investigated. The summary of this Chapter will show which dye had the least effect on these processes to aid in determining the most suitable dye for a surface based fluorescent DNA detection method.

3.2 PUBLICATION

Alicia M. Haines, Shanan S. Tobe, Hilton J. Kobus, Adrian Linacre, **Effect of nucleic acid binding dyes on DNA extraction, amplification and STR typing**, *ELECTROPHORESIS*, **36** (2015) p. 2561-2568, DOI: 10.1002/elps.201500170

Supplementary information relating to this article will appear after or in the appendix of this Chapter.

Journal Impact Factor: **2.482**

ISI Journal Citation Reports Ranking: 2015 26/75 (Chemistry Analytical); 38/77 (BIOCHEMICAL RESEARCH METHODS)


Number of citations: **2**


Statement of Authorship

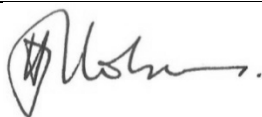
Title of Paper	Effect of nucleic acid binding dyes on DNA extraction, amplification, and STR typing
Publication Status	Published
Publication details	Published in <i>Electrophoresis</i> 2015 36 (20) 2561-2568

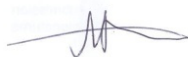
AUTHOR CONTRIBUTIONS

By signing the Statement of Authorship, each author certified that their stated contribution to the publication is accurate and that permission is granted for the publication to be included in the candidate's thesis.

Name of Principal Author (Candidate)	Alicia M. Haines		
Contribution to the paper	Designed experimental method, performed all laboratory work and analysis, drafted the manuscript, edited manuscript and acted as corresponding author		
Signature		Date	August, 2016

Name of Co-Author	Shanan S. Tobe		
Contribution to the paper	Edited manuscript		
Signature		Date	August, 2016

Name of Co-Author	Hilton J. Kobus		
Contribution to the paper	Edited manuscript, helped with fluorescence theory		
Signature		Date	August, 2016

Name of Co-Author	Adrian Linacre		
Contribution to the paper	Helped design study and edited manuscript		
Signature		Date	August, 2016

Alicia M. Haines¹
 Shanan S. Tobe¹
 Hilton J. Kobus²
 Adrian Linacre¹

¹School of Biological Sciences,
 Flinders University, Adelaide,
 South Australia

²School of Chemical and Physical
 Sciences, Flinders University,
 Adelaide, South Australia

Received March 31, 2015

Revised June 28, 2015

Accepted July 13, 2015

Research Article

Effect of nucleic acid binding dyes on DNA extraction, amplification, and STR typing

We report on the effects of six dyes used in the detection of DNA on the process of DNA extraction, amplification, and detection of STR loci. While dyes can be used to detect the presence of DNA, their use is restricted if they adversely affect subsequent DNA typing processes. DiamondTM Nucleic Acid Dye, GelGreenTM, GelRedTM, RedSafeTM, SYBR[®] Green I, and EvaGreenTM were evaluated in this study. The percentage of dye removed during the extraction process was determined to be: 70.3% for SYBR[®] Green I; 99.6% for RedSafeTM; 99.4% for EvaGreenTM; 52.7% for DiamondTM Dye; 50.6% for GelRedTM, and; could not be determined for GelGreenTM. It was then assumed that the amount of dye in the fluorescent quantification assay had no effect on the DNA signal. The presence of all six dyes was then reviewed for their effect on DNA extraction. The *t*-test showed no significant difference between the dyes and the control. These extracts were then STR profiled and all dyes and control produced full DNA profiles. STR loci in the presence of GelGreenTM at 1X concentration showed increased amplification products in comparison to the control samples. Full STR profiles were detected in the presence of EvaGreenTM (1X), although with reduced amplification products. RedSafeTM (1X), DiamondTM Dye (1X), and SYBR[®] Green I (1X) all exhibited varying degrees of locus drop-out with GelRedTM generating no loci at all. We provide recommendations for the best dye to visualize the presence of DNA profile as a biological stain and its subsequent amplification and detection.

Keywords:

DiamondTM Nucleic Acid Dye / EvaGreenTM / GelGreenTM / RedSafeTM / SYBR[®] Green I
 DOI 10.1002/elps.201500170



Additional supporting information may be found in the online version of this article at the publisher's web-site

1 Introduction

We report on an investigation into whether commonly used dyes affect the DNA extraction process or the amplification of STR loci and their detection on a CE column. The main binding dyes that are used within laboratories are SYBR[®] Green I (SG) and ethidium bromide. More recently developed dyes include EvaGreenTM (EG), GelGreenTM (GG), GelRedTM (GR), RedSafeTM (RS), and DiamondTM Nucleic Acid Dye (DD). These dyes have been engineered to be less mutagenic than the more commonly used dye SG [1]. The major application of these dyes in forensic science is for visualization of

amplified products on gels or after elution from capillary electrophoresis columns. More recently however dyes have been used to visualize latent DNA such as within fingerprints on surfaces [2] and nuclei within hair follicles [3] and epithelial cells [1]. In this context, dyes would be present when DNA is extracted and subsequently amplified and therefore their effect on these processes is important.

Nucleic acid binding dyes can be separated into two main classes of dyes: intercalating dyes such as SG and ethidium bromide, and groove binding dyes such as DAPI. SG intercalates between the base pairs of DNA, and due to electrostatic and extended groove interactions, has approximately a 1000-fold increase in fluorescence signal when complexed with DNA [4]. DAPI, which is selective to AT rich regions, has approximately a 20-fold increase in fluorescent signal when complexed with DNA [5, 6].

DNA binding dyes have also been used in real-time PCR (RT-PCR), where SG is the most widely used dye for this process [7]. As SG intercalates with double-stranded DNA

Correspondence: Alicia M. Haines, School of Biological Sciences, Flinders University, Bedford Park 5042, South Australia.
 E-mail: alicia.haines@flinders.edu.au

Abbreviations: DD, DiamondTM Nucleic Acid Dye; EG, EvaGreenTM; GG, GelGreenTM; GR, GelRedTM; RS, RedSafeTM; RET, resonance energy transfer; RFU, relative fluorescence unit; SG, SYBR[®] Green I; SPE, solid phase extraction

Colour Online: See the article online to view Fig. 1 in colour.

when used in a RT-PCR assay, the increase in PCR products results in a higher number of dye molecules that can attach to the product, resulting in a higher fluorescent signal [8, 9]. SG assays generally use a concentration of 1X for this type of reaction so it is assumed that as the RT-PCR is not inhibited the STR typing process would also likely not be inhibited if using the same concentration of dye.

Fluorescent dyes such as DAPI have been used previously to stain hair roots to visualize the nuclei present within the hair follicle. These hairs were then washed and the DNA was extracted and STR typing subsequently conducted [3, 10]. A previous study conducted on epithelial cells within saliva showed that staining of nuclei was dependent on the dye [1] where SG, RS, DD, and ethidium bromide permeated the cell membrane and stained the nuclei.

The main purpose of DNA extraction is to first remove the nucleic acids from the cellular material and secondly to purify the sample so cell debris and enzymes are removed as they may affect downstream applications. SPE is used commonly in forensic practice where the DNA binds to a silica gel surface at optimal salt molarities and pH [11]. Recently, there have been studies that bypass the DNA extraction process and place the biological sample directly into a PCR tube for amplification, known as “Direct PCR” [12]. This includes obtaining STR profiles from whole blood samples [13], saliva samples [14], anagen hair follicles [15], fabrics [16], blood stains [17], fingerprints [18], fingernails [19], and other types of biological samples. With optimization of the buffer system used in the STR profiling kits, inhibitors were able to be overcome to produce profiles from samples that otherwise would not produce a profile after DNA extraction due to the substantial loss of DNA.

The potential of this novel approach is that SG, EG, RS, GG, GR, and DD can be used for staining biological samples to visualize the DNA present within a sample at a scene. If latent DNA can be identified *in situ* then a targeted approach can be used to collect the biological material, increasing success rates for volume crime samples and streamlining the process of DNA collection in forensic science. Downstream processes such as DNA extraction and STR typing could then be conducted as normal, but with an improved chance of success due to targeted sampling. This study looks at the effect these six dyes has on the DNA extraction process and in downstream applications such as PCR and STR profiling.

2 Materials and methods

2.1 Quantification and extraction of dyes

The six nucleic acid binding dyes (20X, 10 μ L) were added to the Standard 2 (5 μ L of 10 ng/ μ L) Qubit[®] assay that had a final volume of 200 μ L using the Qubit[®] dsDNA HS Assay Kit (Life Technologies, Vic, Australia). The DNA concentration was recorded and compared to the control without dye present. Extractions were also undertaken with only the nucleic acid binding dyes present (20 μ L, 20X) with no DNA,

processed using the QIAamp[®] DNA Micro Kit (Qiagen, Vic, Australia). The manufacturer's protocol for tissue extraction was followed with exception that the first incubation time was reduced to 10 min as there was no DNA present. The samples were eluted into 30 μ L of elution buffer and then quantified using the Qubit[®] 2.0 Fluorometer using the Qubit[®] dsDNA HS Assay Kit following the manufacturer's protocol using 20 μ L of the sample. The extractions were undertaken in triplicate. The nucleic acid binding dyes (20 μ L, 20X) were also quantified using the Qubit[®] without DNA present for dye signal determination before extraction, also undertaken in triplicate.

2.2 DNA extraction

DNA extraction was undertaken both with and without the various dyes present. An initial amount of DNA 5 ng (1 ng/ μ L) with the dyes (5 μ L of 20X dye solution) was added to a 1.5 mL tube and then processed using the QIAamp[®] DNA Micro Kit. The manufacturer's protocol for tissue extraction was followed with exception that the first incubation time was reduced to 10 min as the DNA was already in a purified form. The DNA was eluted into 30 μ L of elution buffer and then quantified using the Qubit[®] 2.0 Fluorometer using the Qubit[®] dsDNA HS Assay Kit following the manufacturer's protocol. The extractions were undertaken in triplicate.

2.2.1 PCR amplification and conditions

STR profiling was undertaken both with the various dyes and without using the AmpFLSTR[®] ProfilerPlus[®] (Life Technologies) kit. STR amplification reactions were prepared as per manufacturer's protocol with a final PCR volume of 50 μ L. All reactions had 1 ng of control DNA supplied by kit. All dyes were diluted to a working solution of 20X, 2.5 μ L was added to the PCR to give a final concentration of 1X in the STR amplification. The remaining volume was made up with sterile H₂O. The reactions were undertaken in triplicate.

The control and DNA/dye extracted samples were also amplified following the above protocol using an optimal DNA concentration of 1 ng based on Qubit[®] quantification. The remaining volume was made up with sterile H₂O.

The amplification was conducted in a GeneAmp[®] System 9600 thermal cycler (Life Technologies) following the manufacturer's cycling conditions, using the standard 28 cycles.

2.2.2 Capillary electrophoresis

CE was performed on an ABI 3130xl Genetic Analyser (Life Technologies) using POP-4 polymer (Life Technologies). PCR sample (2 μ L) was added to a solution of 0.3 μ L of ABI GeneScan-400 ROX Size Standard (Life Technologies) and 9.5 μ L of Hi-Di[™] Formamide (Life Technologies). Samples were then denatured at 95°C for 3 min. Electrophoresis was

conducted at 3 kV with a 10 s injection. The data were analyzed using Gene mapper v3.2. The detection threshold was set at 30 relative fluorescence units (RFU).

2.2.3 Data analysis

The data were analyzed and the variation was assessed using a paired two sample means *t*-test using both one and two tailed tests for the binding dyes effect on extraction and one tailed test for STR amplification.

3 Results and discussion

3.1 Effect of binding dyes on DNA quantification and extraction

The effect of the dyes on the extraction and Qubit® quantification system was investigated by first showing the amount of dye lost through the extraction process and secondly the direct effect of the dyes when present in the Qubit reaction on the DNA signal at a standard stock concentration (1X). Table 1 shows the Qubit readings of the binding dyes before and after extraction. The overall percentage loss of the binding dyes after extraction was calculated based on the Qubit readings that resulted in SG having a loss of 70.3%, RS a loss of 99.6%, EG a loss of 99.4%, DD a loss of 52.7%, GR a loss of 50.6%, and the dye loss for GG could not be calculated as the Qubit® readings of the dye was too low. Shown in Table 1 are the Qubit® readings for Standard 2 assay with binding dyes. This shows that SG, RS, EG, and GG all increase the DNA signal when present in the assay. GR quenches the signal as there was a high reduction in the DNA signal when GR was present in the assay. DD had no effect on the DNA signal. As more than 50% of the dye was removed during the extraction process it was assumed there was minimal dye present in the extract and even less of the dye in the Qubit® assay, hence the effect on the Qubit® readings would be minimal.

Table 2 shows the average percentage of DNA loss when binding dyes were present that were compared with the control. Based on the average the greatest loss of DNA was seen when the dye RS was present followed by SG, GR, EG, GG, and the dye that had the lowest effect on the loss of DNA was DD. The variation of the percentage loss of DNA when dyes were present was analyzed using a paired *t*-test (Table 3) that shows the means were not significantly different due to replicate three that showed a much higher loss than the other replicates thus increasing the variance.

When looking at the average percentage loss of DNA the dyes that had a higher effect have an intercalating-based mechanism of interaction with DNA (shown in the column on the right of Table 2). It could be assumed from these data (Table 2) that the intercalating dyes disrupt the DNA binding mechanism to the silica gel as the chaotropic salts would have limited binding sites with the DNA, resulting in a higher loss.

The dye that had the least effect on the percentage loss (DD) has a different mechanism of interaction; DD is an external groove binding dye [20] and with limited or no electrostatic interactions that may affect the binding mechanism of DNA to the silica gel column. However based on the *t*-test (Table 3) the means showed no significant difference indicating the dyes may not affect the extraction procedure. SPE is based on the weak interaction of the DNA molecule with the silica phase. If however the nucleic acid binding dye, such as SG, was bound to the DNA fragment it reduces the number of interactions that the DNA can form with the silica surface. As the binding mechanism for RS was not disclosed by the supplier, it was not possible to make assumptions as to why this dye molecule would cause the greatest loss of DNA in comparison to the control sample. It is likely that the dye has electrostatic interactions with DNA that would prevent the dye/DNA complex from binding to the silica column surface and hence the DNA would be lost through the wash stages.

3.2 Effect of binding dyes on STR amplification and detection

All six extracted DNA/dye samples along with the control produced full DNA profiles (See Supporting Information) showing that the dye present in the extract did not affect the STR amplification. Although the dyes were used in the PCR at a final concentration of 1X (manufacturer's recommended working concentration), it would be expected that the relative concentration of the dyes carried through from extraction would be less, as the data (this study) demonstrate that at least 50.6% of dye was removed for GR and up to 99.6% for RS, therefore the concentration of dye present in the extract would be substantially lower than 1X.

Table 4 shows the peak heights obtained from the nine STR loci and amelogenin when in the presence of DNA binding dyes and in the absence of any dye. Control DNA was used from the kit with no dye present to provide a reference to STR typing with each of the six dyes and the data presented are in RFU.

When a dye was added to the amplification reactions, a full DNA profile with all correct 18 STR alleles and amelogenin was only recorded when GG and EG were present. An average of the triplicate reaction indicates an increase in reaction product at all alleles when GG was present compared to the control samples. A decrease in the RFU values for all of the STR alleles was noted within the full DNA profiles when EG was present. RS failed to amplify six alleles in all of the triplicate reactions and resulted in lower peak heights compared with the control. RS however had a lower effect on STR typing when compared with DD, SG, and GR.

A similar number of alleles were recorded for DD although the average RFU values were very low and either typical of low level DNA typing results or the presence of an inhibitor to PCR. Only four alleles were recorded in the presence of SG and GR resulted in no signal for any of the alleles or amelogenin in any of the replicates.

Table 1. Average Qubit® quantification readings of binding dyes (20 µL, 20X) before and after extraction showing the percentage of dye removed through extraction with the average quantification readings of Qubit® Standard 2 (5 µL, 10 ng/µL) with binding dyes (10 µL, 20X, 1X final concentration in reaction) standard deviation shown in brackets

	SG	RS	EG	DD	GR	GG
Average dye only (ng/µL)	0.0168 (0.01)	1.85 (0.2)	0.974 (0.02)	0.0175 (0.001)	0.0122 (0.01)	NR
Average extract dye (ng/µL)	0.005 (0.004)	0.00613 (0.002)	0.00579 (0.001)	0.00830 (0.003)	0.00601 (0.002)	NR
Dye removed (%)	70.3	99.6	99.4	52.7	50.6	NR
Average DNA standard reading (10 ng) with dye (1X)	15.4 (0.1)	14.1 (0.1)	13.2 (0.1)	10.0 (0.1)	0.123 (0.001)	10.5 (0.06)

NR: No result, Qubit® signal too low.

Table 2. Percentage of DNA loss from extraction process using control DNA (5 ng) also in the presence of nucleic acid binding dyes (5 µL, 20 x H₂O) using QIAamp® DNA Micro kit (Qiagen)

	Percentage of DNA loss			Average percentage loss	Percentage loss compared with control	Binding mechanism to DNA
	Replicate 1	Replicate 2	Replicate 3			
Control	49.2	49.6	89.9	62.9	–	–
DD	66.4	56.1	88.8	70.4	7.5	External binder [20]
SG	66.7	75.3	92.4	78.1	15.2	Intercalator, electrostatic, and extended groove interactions [4]
GG	50.1	82.9	81.6	71.5	8.6	Intercalator [1]
GR	81.8	72.8	85.8	80.1	17.2	Intercalator [1]
RS	90.5	69.4	100	86.6	23.7	Unknown
EG	66.3	81.2	68.6	72.0	9.1	Release on demand mechanism [24]

Table 3. *t*-test comparisons of the DNA percentage loss through extraction with and without DNA binding dyes *t*-critical was calculated to be 2.91 for a one-tailed test and 4.30 for a two-tailed test when values fall below *t* critical results in H₀ (means are not different) being accepted

	POS	GG	RS	EG	DD	SG	GR
POS							
GG	–0.684						
RS	–2.57	–0.965					
EG	–0.578	–0.0588	1.09				
DD	–1.42	–0.0838	–4.05	–0.122			
SG	–2.24	0.905	–0.990	0.675	–1.32		
GR	–1.56	–0.701	–1.25	0.980	–1.52	–0.300	

Figure 1 shows an electropherogram of the blue channel (5-FAM) when each of the six dyes was present compared to the positive control (no dye). This shows that there was at least one allele amplified when the dyes were present for all dyes except GR. The EG sample showed smaller peaks in comparison to the positive control and there was distortion of the peak's morphology.

A *t*-test was undertaken to determine if the dyes added to the STR amplification resulted in a significant difference compared to the peak heights of the control. Table 5 shows the *t*-values obtained when comparing the overall peak height from the STR profile of the control samples and when each of the six dyes were present. The *t*-critical value was used to determine whether the null hypothesis was rejected. When comparing the average peak area it shown that there was no statistical difference between the control and GG and the null hypothesis ($H_0 = \mu_1 = \mu_2$) was not rejected. All other dyes were statistically different to the control. The only other comparison that resulted in the H_0 not being rejected was

between EG and RS, they were shown to be statistically the same.

Reasons why the STR fragments were not detected could have been due to one or a combination of the following: (1) STR fragments were not amplified due to dye inhibition during PCR amplification; (2) samples were not injected due to bound dye molecules that resulted in the dye/DNA complex having a neutral charge; (3) fluorescent quenching of STR fragments signal by the dye molecules; or (4) fluorescent energy transference from the STR fragments to free dye molecules.

3.3 Effect of dyes on PCR amplification

To determine whether no alleles were amplified for some of the loci or whether alleles were not injected into the column, the PCR products were separated on an agarose gel

Table 4. Average peak height (three replicates) of control DNA (1 ng) without dye present (positive control) and when the nucleic acid binding dyes (1X final concentration) were present in the STR amplification

Locus	Allele	Average peak height (RFU)						
		Positive control	GelGreen	RedSafe	EvaGreen	Diamond dye	SYBR green I	GelRed
D3S1358	14	631	930	632	449	125	NR	NR
	15	659	940	568	439	105	28.3	NR
vWA	17	857	1566	607	648	72	NR	NR
	18	809	1271	605	571	61	NR	NR
FGA	23	654	1007	145	671	NR	NR	NR
	24	647	1009	173	503	NR	NR	NR
Amelogenin	X	669	821	426	492	169	97.5	NR
	X	669	410	213	246	84.3	48.8	NR
D8S1179	13	700	1146	401	457	62.2	11.5	NR
	13	700	1146	401	457	62.2	11.5	NR
D21S11	30	626	963	NR	491	10.5	NR	NR
	30	626	963	NR	491	10.5	NR	NR
D18S51	15	636	1061	149	242	NR	NR	NR
	19	579	1020	131	235	NR	NR	NR
D5S818	11	533	589	340	371	174	NR	NR
	11	533	589	340	371	174	NR	NR
D13S317	11	511	705	424	416	39.7	NR	NR
	11	511	705	424	416	39.7	NR	NR
D7S820	10	382	528	NR	294	NR	NR	NR
	11	404	566	NR	237	NR	NR	NR
Number of alleles	18	20	20	12.7	17.7	6	3	0
Profile %		100	100	63.3	88.3	30	8.3	0
Average peak height (RFU) of profile		616.72	896.68	299.02	424.86	59.39	9.879	0

NR: = no result.

Table 5. *t*-test comparisons for average peak height and number of alleles amplified of the nucleic acid binding dyes used in this study

<i>t</i> -test for average peak height of profile (<i>t</i> critical = 1.72)								
	POS	GG	RS	EG	DD	SG	GR	
<i>t</i> -test for number of alleles amplified (<i>t</i> critical = 2.91)	POS	-6.31	7.72	8.14	20.31	23.81	23.7	
	GG	—	9.36	9.32	12.36	13.66	14.07	
	RS	11	11	-2.77	5.75	6.03	6.148	
	EG	1	1	-2.40	11.83	14.14	14.77	
	DD	3.36	3.36	1.524	3.94	4.061	4.312	
	SG	11	11	5.28	4	0.789	1.826	
	GR	—	—	19	7.57	1.44	1	

The values obtained from the *t*-test were compared to that of the *t*-critical value to determine if the null hypothesis was rejected. Figures in bold indicate the null hypothesis that the compared averages were the same at 95% confidence was accepted.

(data not shown). There were no bands present for the GR amplification indicating that this dye inhibited the PCR. A few extremely faint bands could be seen for the amplification products in the presence of SG. Products were seen from both RS reactions but only from one DD reaction.

At least one allele was amplified and detected in the presence of GG, RS, EG, DD, and SG, and therefore complete inhibition had not occurred. SG is one of the more common dyes used in RT-PCR, however it was previously shown to inhibit PCR when using gel stained samples [21]. The dye was used at a concentration of 1X in both RT-PCR and in these PCR amplifications; hence inhibition of the PCR was thought unlikely.

3.4 Effect of dyes on CE injection

Capillary electrophoresis used for STR profiling uses electrokinetic injection as the mode of introducing the samples to the capillary. This type of injection is selective toward negative ions [22]. If the dye molecules are bound to the DNA fragment, for instance SG, which has electrostatic interactions with the DNA molecule, the fragments would be neutrally charged and not injected into the capillary. As two STR alleles plus amelogenin were detected when SG was present, although with very low peak heights, the implication is that a portion of fragments unbound to SG molecules were injected into the capillary. The size of the DNA product

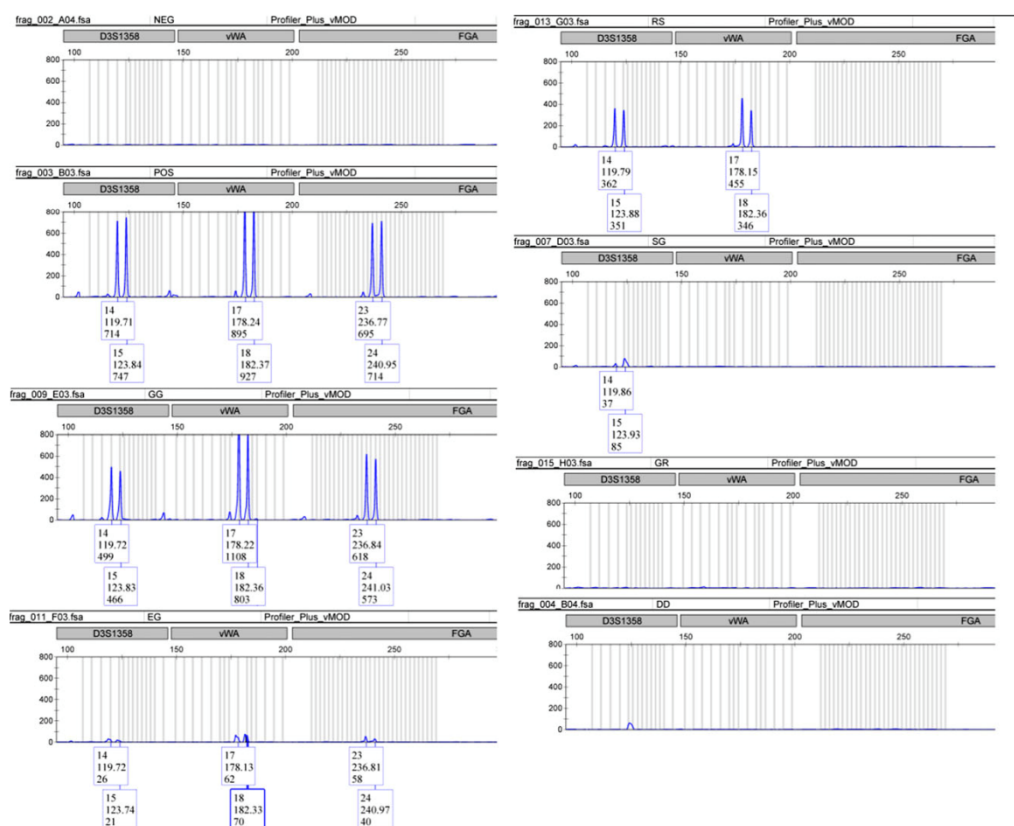


Figure 1. Electropherogram showing blue channel only (5-FAM) when each of the six dyes were present in the amplification of STR loci, without dyes (POS) and both without DNA and dyes (NEG). The loci shown are D3S1358, vWA, and FGA from left (smallest) to right (largest). The scale at the right is the RFU values.

will affect the ability of SG molecules to attach due to the selectivity of the dye molecule; hence a smaller fragment size will have less binding sites available. Amelogenin has the smallest fragment size (106 bp, X chromosome) and D7S317 locus amplifies short STR alleles that results in less binding sites for SG molecules to bind, allowing for injection into the capillary.

3.4.1 Fluorescent quenching

Quenching of fluorescence occurs due to different mechanisms. Collisional quenching can occur when the excited state fluorophore is deactivated upon contact with another molecule present in the solution; the deactivating molecule must have a molecular structure that will accept the transferred energy [23]. In this mechanism of quenching the fluorophore is returned to the ground state during an encounter with another molecule (collisional impact); neither of which

are chemically changed in this process [23]. This could occur within the capillary when the fluorophores attached to the STR fragments, excited from the argon laser, are returned to their ground state due to collisional quenching from the free dye molecules. This would result in no fluorescent signal; hence no STR peaks would be detected.

3.4.2 Fluorescent resonance energy transfer

Resonance energy transfer (RET) occurs when the emission spectrum of a fluorophore (donor) overlaps with the absorption spectrum of another molecule (acceptor). RET does not involve the emission of light from the donor as the absorption of energy is not from the fluorescent emission of the donor, rather a dipole–dipole interaction occurs between the donor and acceptor [23]. This type of energy transfer offers another explanation as to the cause of some STR fragments not producing a signal. The fluorophore attached to the STR

Table 6. Fluorophores excitation and emission wavelengths of the dyes used in this study

Dye	Excitation (nm)	Emission (nm)
5-FAM	492	518
JOE	520	548
NED	546	575
SG	494	520
DD	494	558
RS	300, 419, 514	537
EG	500	525
GG	495	520
GR	300, 520	600

Table showing the six dyes used in this study and the four dyes attached to one of the primers by Life Technologies in the STR amplification.

fragment could act as a donor to the dye molecules present or vice versa. This would result in a transfer of energy but without the emission resulting in a loss of signal from the fluorophore attached to the STR fragment. The excitation and emission wavelengths for the fluorophores that are attached to the STR fragments are shown in Table 6. The dyes that consistently resulted in only a few STR fragments being detected were DD, SG, and RS. If the dyes were acting as the donor or as the acceptor then those interactions with the STR fluorophores may have occurred, resulting in no fluorescent signal for those STR fragments. Based on the spectral data (Table 6), SG could be the donor and 5-FAM could be the acceptor as there is overlap between the dyes fluorescent spectra. This would also be the case for DD being the donor and NED being the acceptor; RS (donor) and NED/JOE (acceptor); 5-FAM (donor) and RS (acceptor); JOE/5-FAM (donor) and SG (acceptor) and finally 5-FAM (donor) and DD (acceptor).

4 Concluding remarks

The percentage of dye removed during the extraction process was determined to be: 70.3% for SG; 99.6% for RS; 99.4% for EG; 52.7% for DD; 50.6% for GR, and; could not be determined for GG. From these data it was assumed that the amount of dye present in the extract and then in the Qubit assay would be low and have a minimal effect of the quantification readings. These extracts were then amplified and all reactions produced full DNA profiles showing that the dye present in the extract had no effect on the STR amplification process. The analysis of the average percentage loss of DNA using a paired *t*-test showed no significant difference when dyes were present in the extraction and when compared with the control.

From the data collected in this study when having dyes at a concentration of 1X present in the STR reaction showed that the GR dye most likely inhibits the PCR amplification process as no STR peaks were detected in any of the replicates. The GG dye had no effect on STR typing. The EG dye amplified all STR fragments but had a lower peak height when compared with the positive control. STR alleles were consistently not de-

tected in the presence of RS. This was the same for DD and SG; however the effect of the presence of SG was that on average one allele and the amelogenin allele were recorded. The reason why some of the STR alleles were not detected could be due to a number of reasons such as: collisional quenching, FRET, no amplification or no injection of fragments. If staining a sample for the presence of latent DNA and subsequent extraction and STR profiling was undertaken, it is recommended that GelGreen™ be used as it had the least effect on both DNA extraction and STR amplification.

This work was supported financially by the Attorney General's Office, South Australia.

The authors have declared no conflict of interest.

5 References

- [1] Haines, A. M., Tobe, S. S., Kobus, H. J., Linacre, A., *Electrophoresis*. 2015, 36, 941–944.
- [2] Haines, A. M., Tobe, S. S., Kobus, H. J., Linacre, A., *Forensic Sci. Int. Genet.* 2013, 4, e290–e291.
- [3] Lopez, T., Vandewoestyne, M., Van Hoofstat, D., Deforce, D., *Forensic Sci. Int. Genet.* 2014, 13, 191–194.
- [4] Dragan, A. I., Pavlovic, R., McGivney, J. B., Casas-Finet, J. R., Bishop, E. S., Strouse, R. J., Schenerman, M. A., Geddes, C. D., *J. Fluoresc.* 2012, 22, 1189–1199.
- [5] Barcellona, M. L., Cardiel, G., Gratton, E., *Biochem. Biophys. Res. Commun.* 1990, 170, 270–280.
- [6] Banerjee, D., Pal, S. K., *J. Phys. Chem. B* 2008, 112, 1016–1021.
- [7] Higuchi, R., Fockler, C., Dollinger, G., Watson, R., *Biotechnology* 1993, 11, 1026–1030.
- [8] Nielsen, K., Mogensen, H. S., Hedman, J., Niederstätter, H., Parson, W., Morling, N., *Forensic Sci. Int. Genet.* 2008, 2, 226–230.
- [9] Pfaffl, M. W., *Nucleic Acids Res.* 2001, 29, e45.
- [10] Brooks, E. M., Cullen, M., Szytydna, T., Walsh, S. J., *Aust. J. Forensic Sci.* 2010, 42, 115–122.
- [11] Goodwin, W. D., Linacre, A., Hadi, S., *An Introduction to Forensic Genetics*, Wiley-Blackwell, Oxford 2011.
- [12] Verheij, S., Harteveld, J., Sijen, T., *Forensic Sci. Int. Genet.* 2012, 6, 167–175.
- [13] Ohhara, M., Kurosu, Y., Esumi, M., *Biotechniques* 1994, 17, 726, 728.
- [14] Park, S. J., Kim, J. Y., Yang, Y. G., Lee, S. H., *J. Forensic Sci.* 2008, 53, 335–341.
- [15] Ottens, R., Taylor, D., Abarno, D., Linacre, A., *Forensic Sci. Med. Pathol.* 2013, 9, 238–243.
- [16] Linacre, A., Pekarek, V., Swaran, Y. C., Tobe, S. S., *Forensic Sci. Int. Genet.* 2010, 4, 137–141.
- [17] Swaran, Y. C., Welch, L., *Forensic Sci. Int. Genet.* 2012, 6, 407–412.
- [18] Templeton, J. E., Linacre, A., *Biotechniques* 2014, 57, 259–266.
- [19] Tie, J., Uchigasaki, S., *Electrophoresis* 2014, 35, 3188–3192.

- [20] Truman, A., Hook, B., Hendricksen, A., [Internet] *tpub*. 2013, 121. Available from: <http://au.promega.com/resources/pubhub/diamond-nucleic-acid-dye/> (accessed January 1, 2015).
- [21] Nath, K., Sarosy, J. W., Hahn, J. C., Di Como, J., J. *Biochem. Biophys. Methods* 2000, 42, 15–29.
- [22] Krivácsy, Z., Gelencsér, A., Hlavay, J., Kiss, G., Sárvári, Z., *J. Chromatogr. A* 1999, 834, 21–44.
- [23] Lakowicz, J. R., *Principles of Fluorescence Spectroscopy*. 3rd edition. Springer US, New York 2006.
- [24] Mao, F., Leung, W.-Y., Xin, X., *BMC Biotechnol.* 2007, 7, 76–76.

3.3 Further Results and Discussion

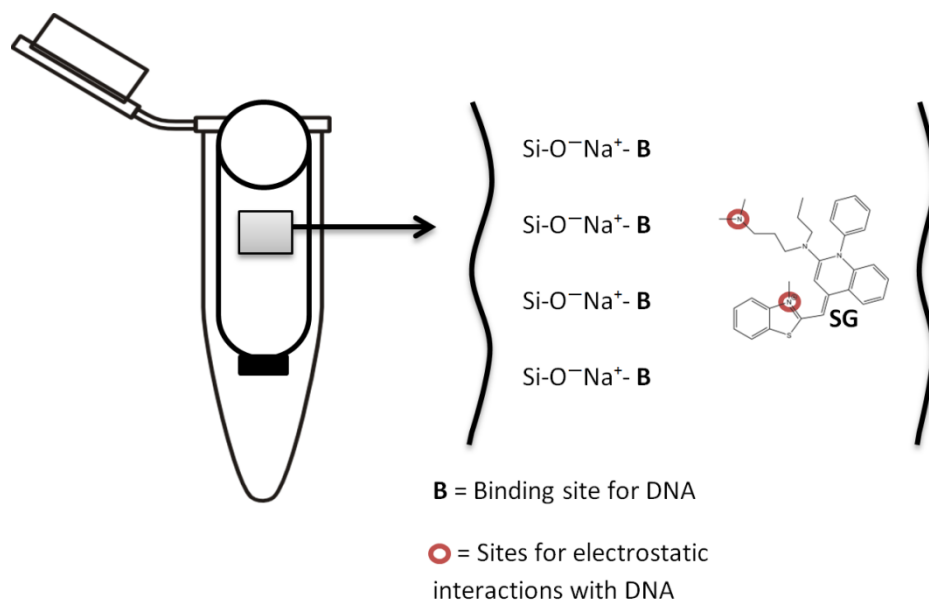


Figure 3.2: Schematic diagram showing the silica surface within a spin column during the DNA extraction process in the presence of a chaotropic salt (Na^+) and a SG molecule showing the sites for electrostatic interaction with DNA.

Figure 3.2 shows a diagram of the silica gel column used within a typical DNA extraction. The binding sites are shown that would potentially bind with DNA in the presence of a chaotropic agent. DNA would bind electrostatically to the silica surface as DNA is negatively charged (phosphate groups in the DNA backbone). If however the nucleic acid binding dye, such as SG, was bound to the DNA fragment it could reduce the number of interactions the DNA could form with the silica surface as SG also has electrostatic interactions with DNA, shown above (Figure 3.2). As the binding mechanism for RS is unknown, it is hard to make assumptions as to why this dye molecule would cause a greater increase in the loss of DNA. It would be likely that the dye has electrostatic interactions with DNA that would prevent the dye/DNA complex from binding to the silica column surface and hence lost through the wash stages.

DNA samples that were extracted with DNA binding dyes present were amplified and the peak heights of the alleles are shown in Table 3.1. All samples produced full STR profiles (18 alleles) including GR that previously had no amplification when amplified directly. There was variation between the control and the samples that had dyes present however this is likely due to the variation in the DNA concentration rather than the dye being present and

effecting the detection of the STR fragments. Figure 3.3 shows the comparison of the average peak height of profile when the dyes were added directly to the amplification reaction or when the sample has been put through an extraction process. The most noticeable difference in the results is with GR as there was no amplification when the dye was added directly to the amplification reaction, which suggests the dye completely inhibits the reaction. However when an extraction was undertaken the majority of the dye has been removed and hence amplification can proceed. This was similar for SG and RS in which the reaction was inhibited when added directly but had a significant increase in the peak height when an extraction was undertaken to remove the dye.

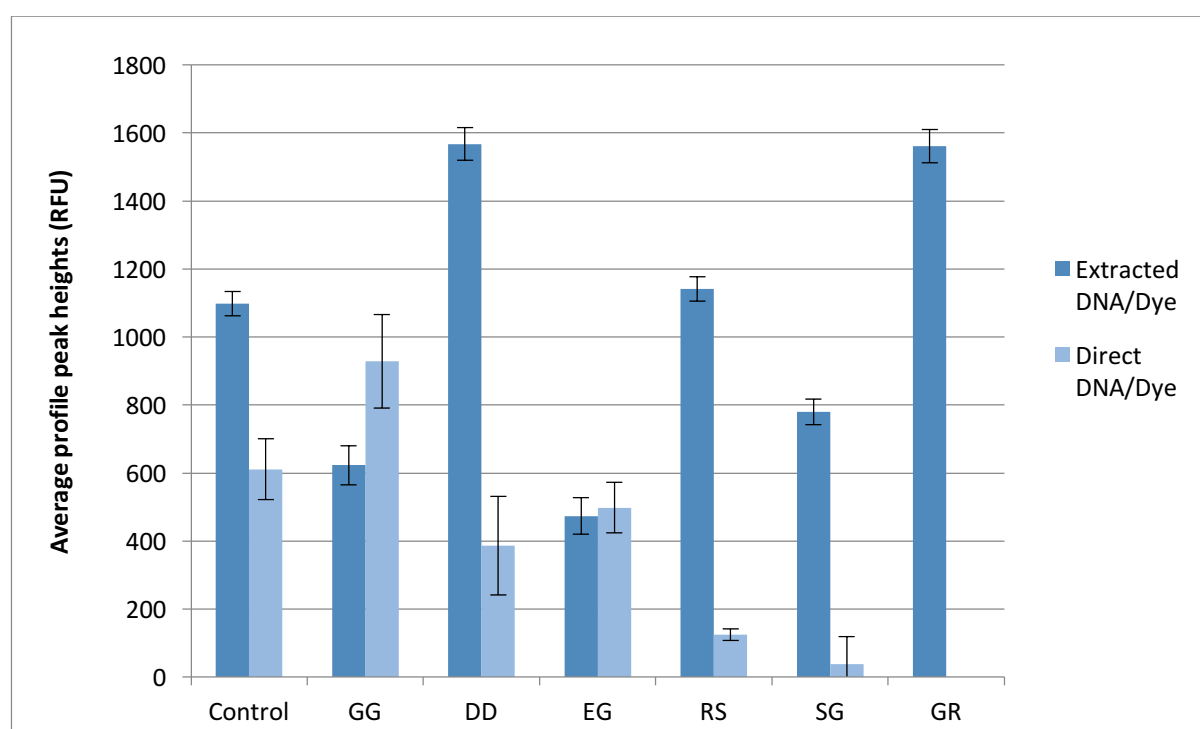


Figure 3.3: Comparison of average profile peak heights when binding dyes are added directly to the STR amplification process or has undergone a DNA extraction. Error bars showing within a 95% confidence.

Table 3.1: Peak heights for alleles of amplified extracted samples that had DNA binding dyes present during the extraction process, in triplicate.

Locus	Allele	Control	GG	DD	EG	RS	SG	GR
D3S1358	15	1374	549	1798	372	1136	739	1561
	16	1186	451	1406	300	950	726	1534
	14	1455	1407	2070	1238	1510	1261	2166
vWA	19	1156	1120	1912	894	1543	1113	1858
	20	1390	522	1581	325	1199	968	1813
FGA	24	1146	403	1920	256	1334	816	1828
	X	1191	887	1491	669	1160	808	1412
Amelogenin	X	1191	887	1491	669	1160	808	1412
	13	1246	1226	1836	1111	1431	1169	1821
D8S1179	14	1168	1075	1948	1025	1409	969	1953
	29	1256	744	1934	443	1097	959	1773
D21S11	30	1233	631	1700	397	1372	843	1753
	12	1009	239	1657	258	963	691	1569
D18S51	18	1046	165	1415	149	960	583	1590
	10	907	516	1293	309	1041	646	1370
D5S818	13	963	513	1092	377	961	642	1225
	8	998	465	1296	262	987	644	1329
D13S317	9	787	467	1273	295	1097	503	1373
	7	637	103	1231	68.0	832	399	1068
D7S820	11	612	83.0	1013	56.0	672	300	825
Average Peak Height (RFU) of profile		1097	622.6	1568	473.6	1141	779.3	1561
Variance		53176	140494	98384	119362	54461	61190	103232
Standard Deviation		230.6	374.8	313.6	345.5	233.3	247.3	321.3
95% confidence interval		35.45	57.63	48.23	53.12	35.88	38.03	49.40

Figure 3.5 shows the effect the binding dyes have on the quantification of the DNA when using the Qubit[®] detection system. Known concentrations of DNA (10 ng/ μ L) in the presence of the binding dyes was quantified and compared with the control. GR quenched the signal as a DNA quant value of 0.123 ng/ μ L was obtained. Figure 3.4 shows the excitation and emission spectra of both GR and PG as it is commonly used for DNA quantification [28] and it is assumed that the dye reagent used in Qubit[®] would be similar if not PG itself. PG is the fluorescent dye used in the Quant-iT[™] system which is similar to the Qubit[®]. GR has a secondary excitation peak around 520 nm which overlaps with the emission signal of PG which would suggest why there was a fluorescent quenching effect when GR dye molecules were present in the Qubit[®] reaction. Based on the quant value for GR, the signal was reduced by 98.8%, as the signal was quenched by such a large amount there may have been other factors resulting in the quenching of the Qubit signal. This could be collisional energy transfer between the dye molecules or fluorescent resonance energy transfer (FRET).

DD had the least effect as there was only a slight decrease in the signal (0.43 ng/ μ L) the other dyes had an increase in the signal as the dyes could also bind to the DNA resulting in an increase in the signal as the dyes probably have a similar excitation and emission as the Qubit[®] reagent. SG had the highest enhancement of the signal which may be due to the dye being more selective for DNA than the other dyes.

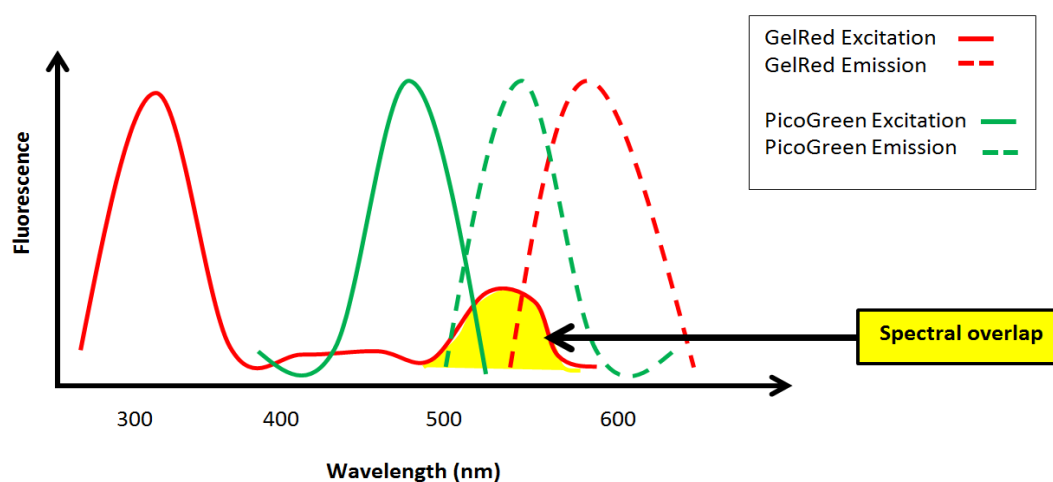


Figure 3.4: Schematic diagram of potential spectral overlap resulting in fluorescent quenching of the Qubit[®] signal by the GR dye molecules

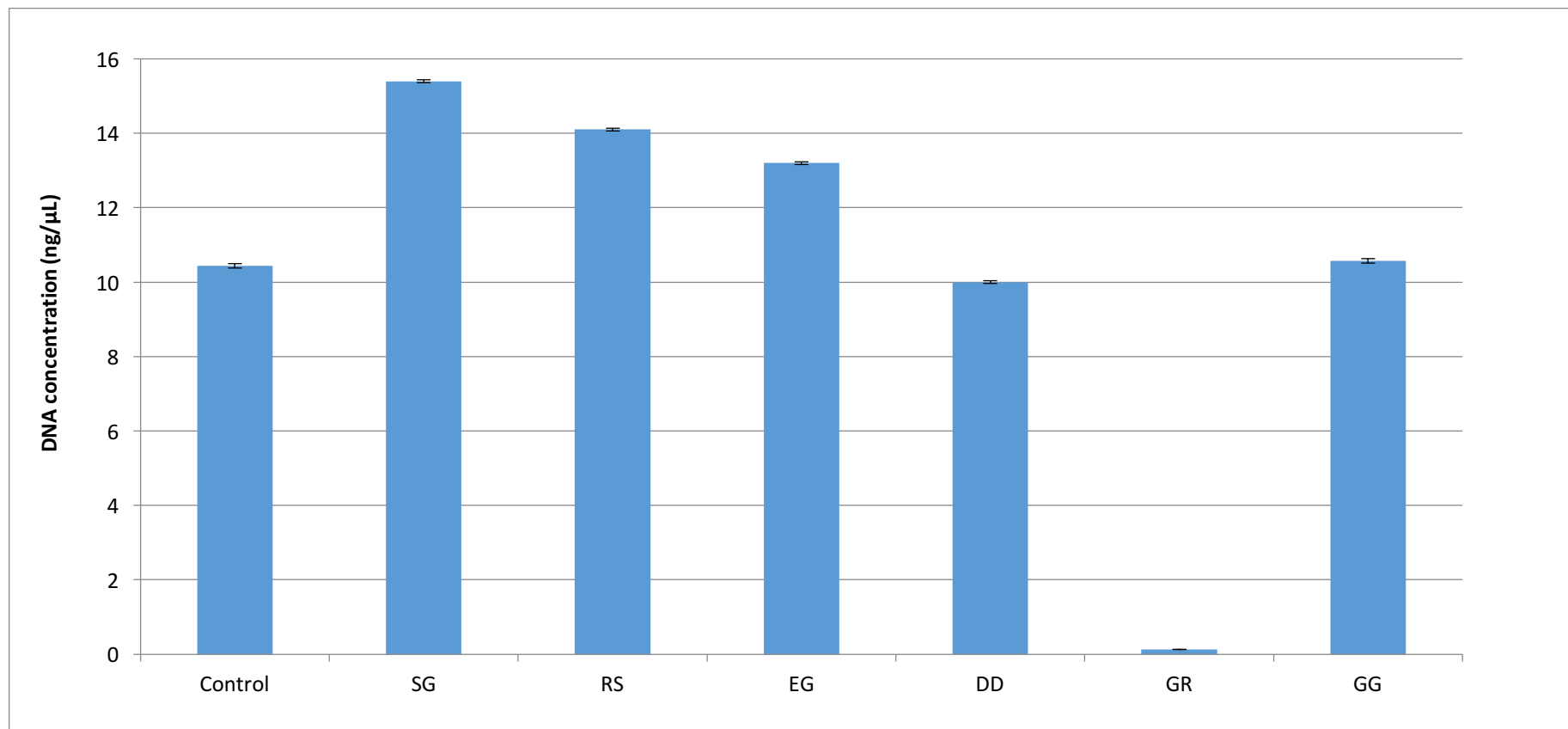


Figure 3.5: Effect DNA binding dyes has on the quantification of DNA using Qubit. Error bars showing 95% confidence. Results were obtained in triplicate. All samples had the same DNA concentration (10 ng/μL).

A few reasons as to why the STR fragments were not detected could have been due to one or a combination of the following, which were discussed partly in the publication;

1. STR fragments were not amplified due to dye inhibition during PCR amplification
2. Samples were not injected due to bound dye molecules which resulted in the dye/DNA complex to have a neutral charge (electro-kinetic injection)
3. Fluorescent quenching of STR fragments signal from the dye molecules that could be present or attached to the fragment.
4. Fluorescent energy transference: energy from the STR fragments fluorophore was being transferred to free dye molecules that might be present via dipole-dipole interactions.
5. Internal conversion in which fluorescence was emitted and those photons of energy are re-absorbed by surrounding dye molecules resulting in no signals from the STR fragments fluorophores.
6. Intersystem crossing another energy loss pathway resulting in phosphorescence.

As no peaks were detected when the GR dye was present it would be most likely due to the dye inhibiting the PCR amplification process. An agarose gel was run (Figure 3.6) so see if PCR products were present that were not detected by the 3130xL. There were no peaks present for the GR reaction which is further support that GR inhibited the reaction. No products could be seen for the SG reactions, most likely due to inhibition as well. Products were seen within both RS reactions but only within one DD reaction.

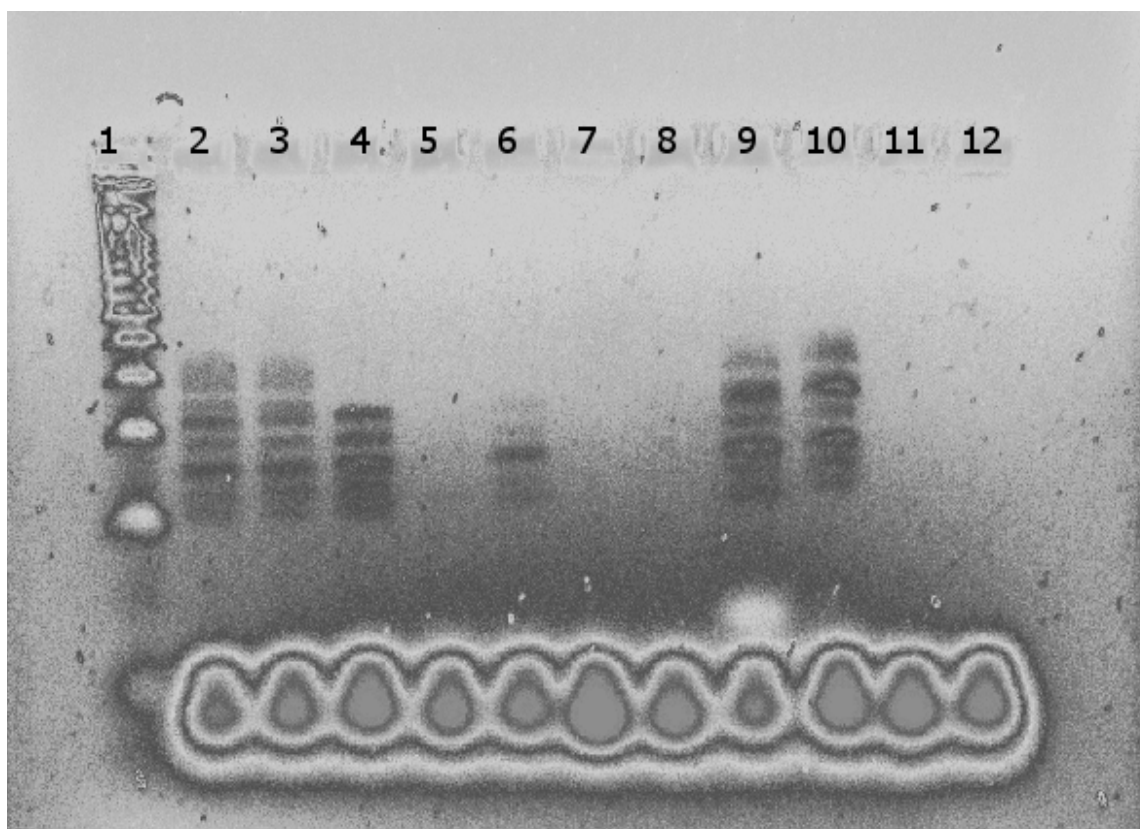


Figure 3.6 Agarose Gel 4% post stained with Diamond Dye (1X) showing the products from the STR typing reaction (1) Promega 1Kb ladder, (2) Positive, (3) RS, (4) RS.2, (5) DD (6) DD.2, (7) SG, (8) SG.2, (9) EG, (10) EG.2, (11) GR, (12) GR.2.

As the dyes other than GR exhibited amplification of at least one locus it shows that amplification of some of the STR fragments was successful, therefore the dyes did not completely inhibit the reaction, or mildly inhibited, as many loci were not amplified. SG is one of the more common dyes used in qPCR for DNA quantification and a multitude of other applications. SG however was previously shown to inhibit PCR when using gel stained samples. In the reaction for real-time (or qPCR) the dye is at a concentration of 1X which was the same concentration used in this reaction. It would have been assumed that as SG does not inhibit the qPCR at that concentration it wouldn't inhibit the STR amplification at the same concentration. It could then be assumed that the SG dye didn't inhibit or only slightly inhibited the reaction, therefore another reason outlined above might have been the cause of the limited detection. This would be the same for the EG dye as this dye's main application is in qPCR. More loci were amplified however when EG was present in comparison to when SG was present. The other dyes have not been used in real-time PCR and so it is unknown whether the dyes were acting as inhibitors in the reaction.

Capillary electrophoresis used for STR profiling uses electrokinetic injection as the mode of introducing the samples to the capillary. The driving force behind this type of injection is the electric field which was produced by the injection voltage applied to the electrode present in the sample solution. This type of injection is selective towards negative ions. This would imply that the injection process was selective towards the charged molecules present within the sample which would include the single-stranded STR fragments. If the dye molecules happened to have been bound to the DNA fragment, for instance SG, which has electrostatic interactions with DNA (phosphate group in the backbone of DNA) this could result in the fragment being neutrally charged, hence would prevent that molecule from being injected into the capillary. As some alleles plus Amelogenin were detected when SG was present, but with very low peak heights, this could mean that there were a portion of those selected fragments in which the SG molecules were not attached and allowed for the injection as they still retained a charge. One reason that may have resulted in the fragments having less SG molecules attached could have been due to the size of those fragments. As Amelogenin has a small fragment size (106 bp, X chromosome) it may reduce the ability of SG to find a binding site due to the selectivity of the dye molecule which intercalates between the base pairs of DNA within the minor groove and the extended propyl chains play a role in establishing the length of SG's binding site, approximately 4 bp in length [29].

The binding sites available to SG are shown in Figure 3.7 of an AATG repeat unit that would be found within TH01 STR fragment. Although as stated the length of SG binding site is 4 bp so only one SG molecule may bind to the repeat unit shown. Even though only one SG molecule may bind to an AATG repeat unit the loss of the negative charges across the fragment may have reduced the ability of the fragment being injected onto the capillary, thus resulting in the fragment not being detected.

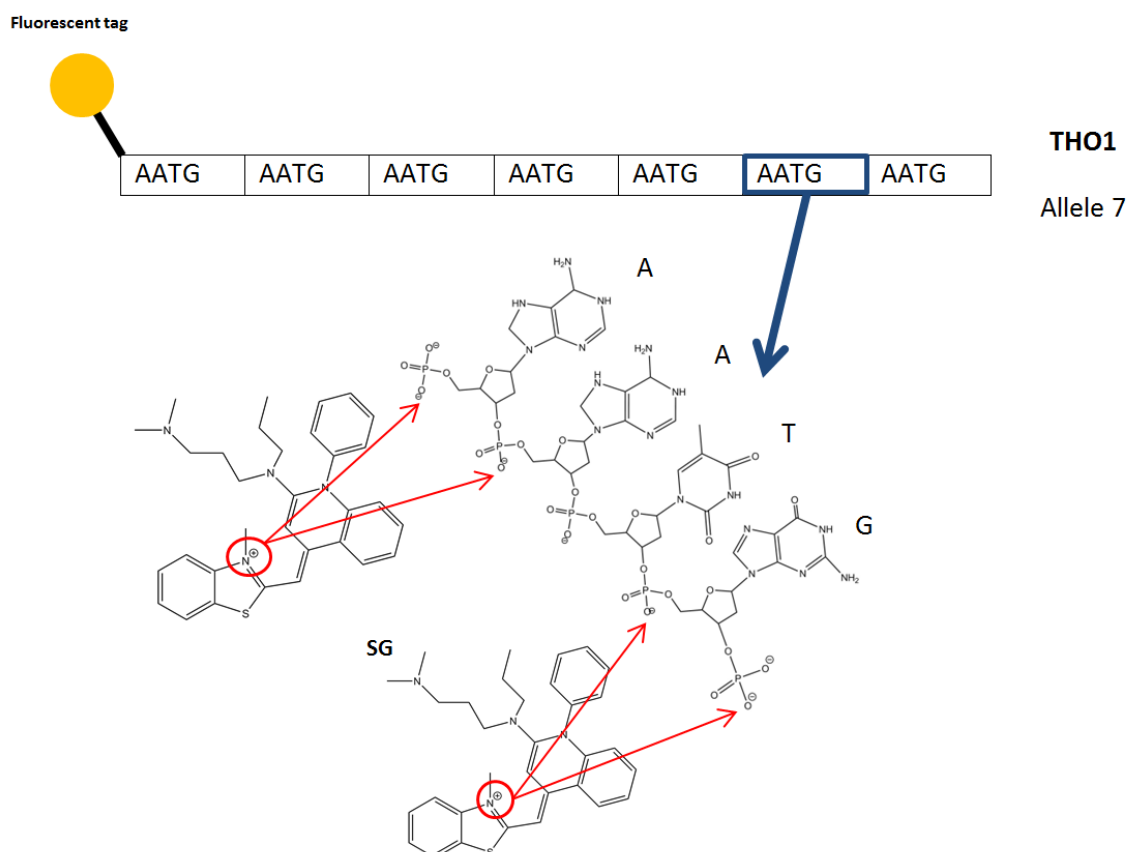


Figure 3.7: Schematic diagram of SG binding sites to ssDNA STR fragment repeat unit (AATG) part of TH01-allele 7

The other possible reason for the fragments not being detected could be due to possible FRET between the dye molecules themselves and with the fluorescent fluorophores attached to the STR fragments. Figure 3.8 below shows the structure of the fluorescent tags attached to the STR fragments used in the NGM™ kit. The excitation and emission spectra of the dyes used as the fluorescent labels of the PCR products and the binding dyes used in the study were compared (see article).

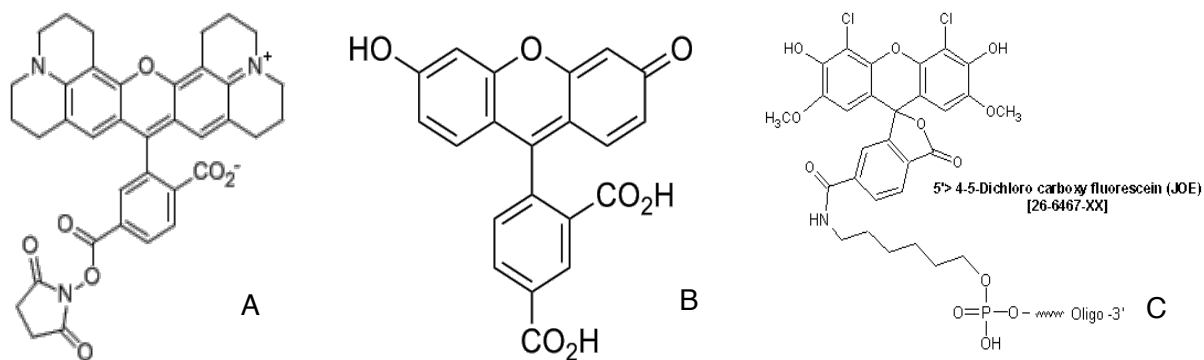


Figure 3.8: Fluorescent labels attached to the PCR products analyzed by the Genetic Analyzer 3130xl (A) ROX, red emission (B) 5-FAM, blue emission and (C) JOE, green emission. The fourth dye NED the structure is unknown, proprietary information

The dyes that could have potential FRET are indicated below, as the dyes can act as both a donor and an acceptor of energy. The only DNA binding dyes that would result in either the donation or acceptance of the energy were SG, DD and RS. These dyes were the ones that had the least amount of alleles detected, which may suggest that FRET was taking place and resulted in the fragments not being detected. Figure 3.9 below shows an example of this donor → acceptor relationship between DD and NED. This shows the spectral overlap in which DD's emission signal overlaps with NED's excitation wavelength causing the DD emission to be absorbed by NED. Figure 3.10 shows how the fluorescent label 5-FAM attached to the STR fragments emission signal can overlap with the RS dye molecules excitation wavelength meaning that if the two dye molecules for dipole-dipole interactions then FRET can occur resulting in fluorescence from the acceptor molecule [30].

Donor → Acceptor

- SG → 5-FAM
- DD → NED
- RS → NED, JOE
- JOE, 5-FAM → SG
- 5-FAM → DD
- 5-FAM → RS

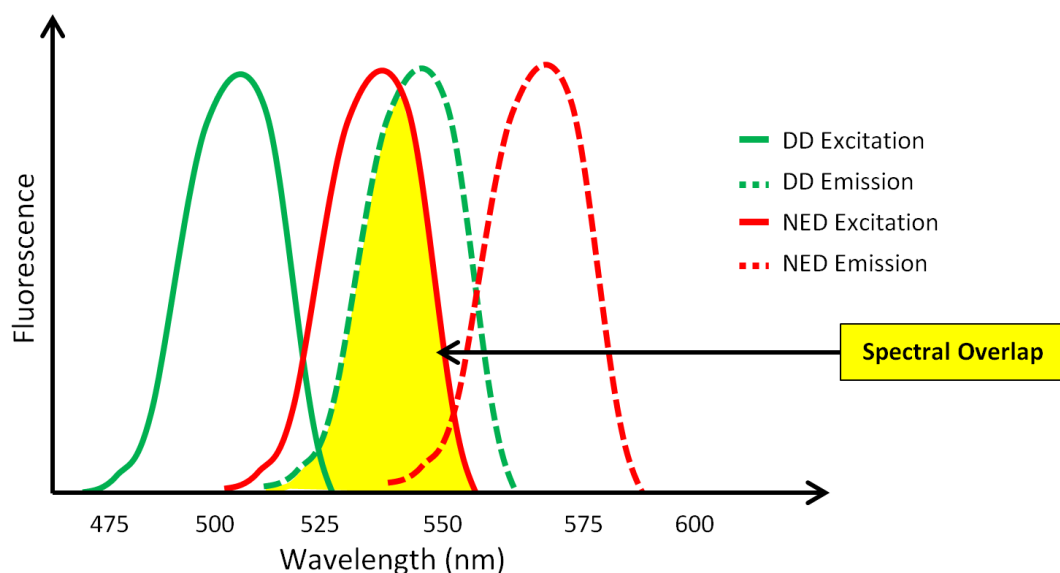


Figure 3.9: Schematic diagram of DD and NED excitation and emission signals showing the spectral overlap resulting in possible FRET.

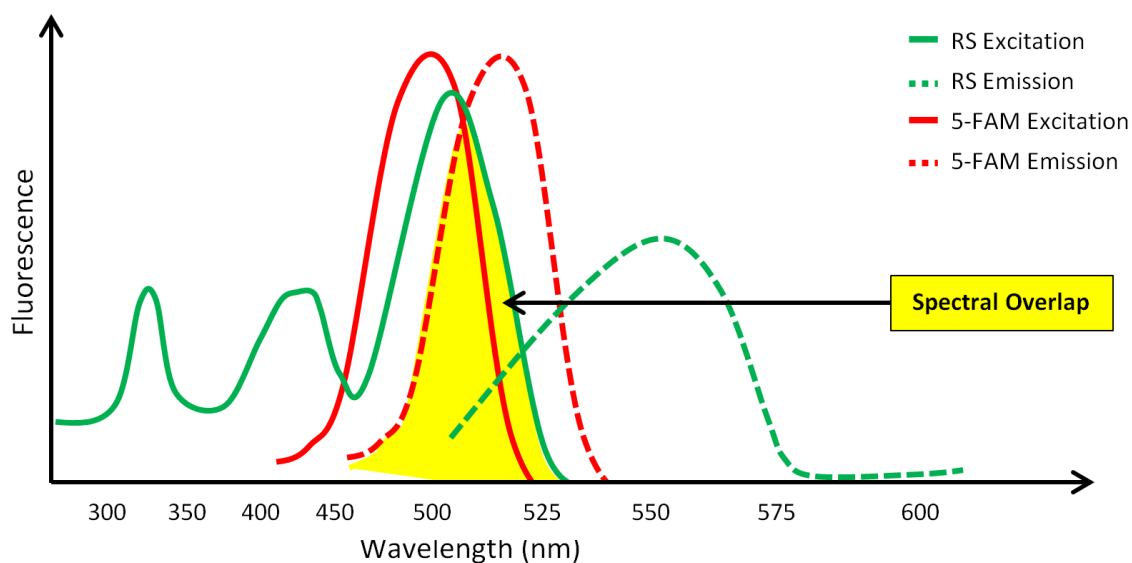


Figure 3.10: Schematic diagram of 5-FAM and RS excitation and emission signals showing the spectral overlap resulting in possible FRET

The energy from the emission of 5-FAM dye molecules could potentially be used by RS dye molecules that may have been present in the sample resulting in no fluorescent signal from those STR fragments with 5-FAM attached this is known as internal conversion.

3.4 Chapter Summary

It was found in this study the dye that had the least effect on DNA extraction was DD, followed by GG, EG, SG, and GR with RS having the highest effect. The dye that had the least effect on STR amplification and detection was GG followed by EG, RS, DD, SG and GR had no allele amplification including Amelogenin. GR likely quenches the fluorescent signal as this was found to occur when adding the dye to the quantification reaction or completely inhibits the PCR amplification.

The impact these results has on the future work using DNA binding dyes for the detection of latent DNA is high as the dye that has the least effect on DNA extraction, quantification and STR typing would be the dye mostly likely chosen for the novel application of using fluorescent *in situ* detection for finding DNA. The dye that had the least effect in general was EG.

Table 3.2: Ranking of the dyes in three categories investigated within this Chapter with 1 being the lowest effect

Ranking	Effect on DNA Extraction (DNA loss)	% of dye removed after extraction	Effect on DNA quantification	Effect on direct STR Typing
1	DD	RS	DD	GG
2	GG	EG	GG	EG
3	EG	SG	EG	RS

From the above ranking in Table 3.2 it can clearly be seen that EG was ranked in the top three for the six dyes tested in the three categories. Statistical analysis can be undertaken to determine the significance behind the results to ascertain the best dye based on properties investigated.

Another property that was investigated within in previous Chapters was the ability for the dye to permeate the cell membrane and interact with genomic DNA. Although it would be assumed that having this property would increase the mutagenicity of the binding dye at

particular concentrations it would be ideal for this novel application as it would be preferred for the dye to interact with as much DNA material present resulting in a higher fluorescent signal. It was also stated in the previous studies that both DD and EG have much lower mutagenicity levels than SG which is known to be a strong mutagen.

3.5 References *(supplemental to publication)*

- [1] K. Nath., J. W. Sarosy., J. Hahn., C. J. Di Como, Effects of ethidium bromide and SYBR® Green I on different polymerase chain reaction systems, *Journal of Biochemical and Biophysical Methods*. 2000, **42** 15-29.
- [2] F. Ponchel., C. Toomes., K. Bransfield., F. T. Leong., S. H. Douglas., S. L. Field, et al, Real-time PCR based on SYBR-Green I fluorescence: an alternative to the TaqMan assay for a relative quantification of gene rearrangements, gene amplifications and micro gene deletions, *BMC Biotechnology*. 2003, **3** 18.
- [3] J. M. Butler, *Chapter 2 - DNA Extraction Methods*, in *Advanced Topics in Forensic DNA Typing*, Butler, J. M., Editor. 2012, Academic Press: San Diego. p. 29-47.
- [4] V. Castella., N. Dima-Simonin., C. Brandt-Casadevall., P. Mangin, Forensic evaluation of the QIAshredder/QIAamp DNA extraction procedure, *Forensic Science International*. 2006, **156** 70-73.
- [5] DNA IQ™ System-Database protocol. Technical Bulletin No. 297. Promega Corporation, Inc., June 2002; revised 11/13.
- [6] A. Bowden., R. Fleming., S. Harbison, A method for DNA and RNA co-extraction for use on forensic samples using the Promega DNA IQ™ system, *Forensic Science International: Genetics*. 2011, **5** 64-68.
- [7] M. G. Brevnov., H. S. Pawar., J. Mundt., L. M. Calandro., M. R. Furtado., J. G. Shewale, Developmental Validation of the PrepFiler™ Forensic DNA Extraction Kit for Extraction of Genomic DNA from Biological Samples*, *Journal of Forensic Sciences*. 2009, **54** 599-607.
- [8] M. R. Green., J. Sambrook, *Molecular cloning: a laboratory manual*. Vol. 1. 2012: Cold Spring Harbor Laboratory Press New York.
- [9] W. D. Goodwin, *An introduction to forensic genetics / William Goodwin, Adrian Linacre, Sibte Hadi*. Essentials of forensic science., ed. Linacre, A. and Hadi, S. 2011, Oxford: Wiley-Blackwell.
- [10] P. S. Walsh., D. A. Metzger., R. Higuchi, Chelex 100 as a medium for simple extraction of DNA for PCR-based typing from forensic material, *Biotechniques*. 1991, **10** 506-513.
- [11] B. Vogelstein., D. Gillespie, Preparative and analytical purification of DNA from agarose, *Proceedings of the National Academy of Sciences*. 1979, **76** 615-619.
- [12] R. Boom., C. Sol., M. Salimans., C. Jansen., P. Wertheim-van Dillen., J. Van der Noordaa, Rapid and simple method for purification of nucleic acids, *Journal of Clinical Microbiology*. 1990, **28** 495-503.
- [13] J. M. Butler, *Chapter 5 - Short Tandem Repeat (STR) Loci and Kits*, in *Advanced Topics in Forensic DNA Typing*, Butler, J. M., Editor. 2012, Academic Press: San Diego. p. 99-139.

- [14] H. A. Hammond., L. Jin., Y. Zhong., C. T. Caskey., R. Chakraborty, Evaluation of 13 short tandem repeat loci for use in personal identification applications, *American journal of human genetics*. 1994, **55** 175.
- [15] C. M. Ruitberg., D. J. Reeder., J. M. Butler, STRBase: a short tandem repeat DNA database for the human identity testing community, *Nucleic Acids Research*. 2001, **29** 320-322.
- [16] *Molecular Probes Handbook, A Guide to Fluorescent Probes and Labeling Technologies, 11th Edition*.
- [17] Y. C. Swaran., L. Welch, A comparison between direct PCR and extraction to generate DNA profiles from samples retrieved from various substrates, *Forensic Science International: Genetics*. 2012, **6** 407-412.
- [18] S. J. Park., J. Y. Kim., Y. G. Yang., S. H. Lee, Direct STR Amplification from Whole Blood and Blood- or Saliva-Spotted FTA® without DNA Purification*, *Journal of Forensic Sciences*. 2008, **53** 335-341.
- [19] D. Y. Wang., C.-W. Chang., N. J. Oldroyd., L. K. Hennessy, Direct amplification of STRs from blood or buccal cell samples, *Forensic Science International: Genetics Supplement Series*. 2009, **2** 113-114.
- [20] M. Hayashida., K. Iwao-Koizumi., S. Murata., K. Kinoshita, Single-Tube Genotyping from a Human Hair Root by Direct PCR, *Analytical Sciences*. 2009, **25** 1487-1489.
- [21] R. Ottens., D. Taylor., D. Abarno., A. Linacre, Successful direct amplification of nuclear markers from a single hair follicle, *Forensic Science, Medicine, and Pathology*. 2013, **9** 238-243.
- [22] R. Ottens., D. Taylor., A. Linacre, DNA profiles from fingernails using direct PCR, *Forensic Science, Medicine, and Pathology*. 2014.
- [23] J. Tie., S. Uchigasaki, Detection of short tandem repeat polymorphisms from human nails using direct polymerase chain reaction method, *ELECTROPHORESIS*. 2014, **35** 3188-3192.
- [24] A. Linacre., V. Pekarek., Y. C. Swaran., S. S. Tobe, Generation of DNA profiles from fabrics without DNA extraction, *Forensic Science International: Genetics*. 2010, **4** 137-141.
- [25] J. E. Templeton.A. Linacre,DNA profiles from fingermarks, *Biotechniques*. 2014, **57** 259-266.
- [26] J. E. L. Templeton., D. Taylor., O. Handt., P. Skuza., A. Linacre, Direct PCR Improves the Recovery of DNA from Various Substrates, *Journal of Forensic Sciences*. 2015, **60** 1558-1562.
- [27] R. Ottens., J. Templeton., V. Paradiso., D. Taylor., D. Abarno., A. Linacre, Application of direct PCR in forensic casework, *Forensic Science International: Genetics Supplement Series*. 2013, **4** e47-e48.
- [28] S. J. Ahn., J. Costa., J. Rettig Emanuel, PicoGreen Quantitation of DNA: Effective Evaluation of Samples Pre-or Post-PCR, *Nucleic Acids Research*. 1996, **24** 2623-2625.

- [29] A. I. Dragan., R. Pavlovic., J. B. McGivney., J. R. Casas-Finet., E. S. Bishop., R. J. Strouse, et al, SYBR Green I: Fluorescence Properties and Interaction with DNA, *Journal of Fluorescence*. 2012, **22** 1189-1199.
- [30] A. Gust., A. Zander., A. Gietl., P. Holzmeister., S. Schulz., B. Lalkens, et al, A starting point for fluorescence-based single-molecule measurements in biomolecular research, *Molecules*. 2014, **19** 15824-15865.

3.6 APPENDIX B

B.1 Profiles obtained showing the effect of the dyes on peak heights and allele amplification with the dyes added directly to the reaction

Profile example for each dye and control (POS, NEG) 8 all together

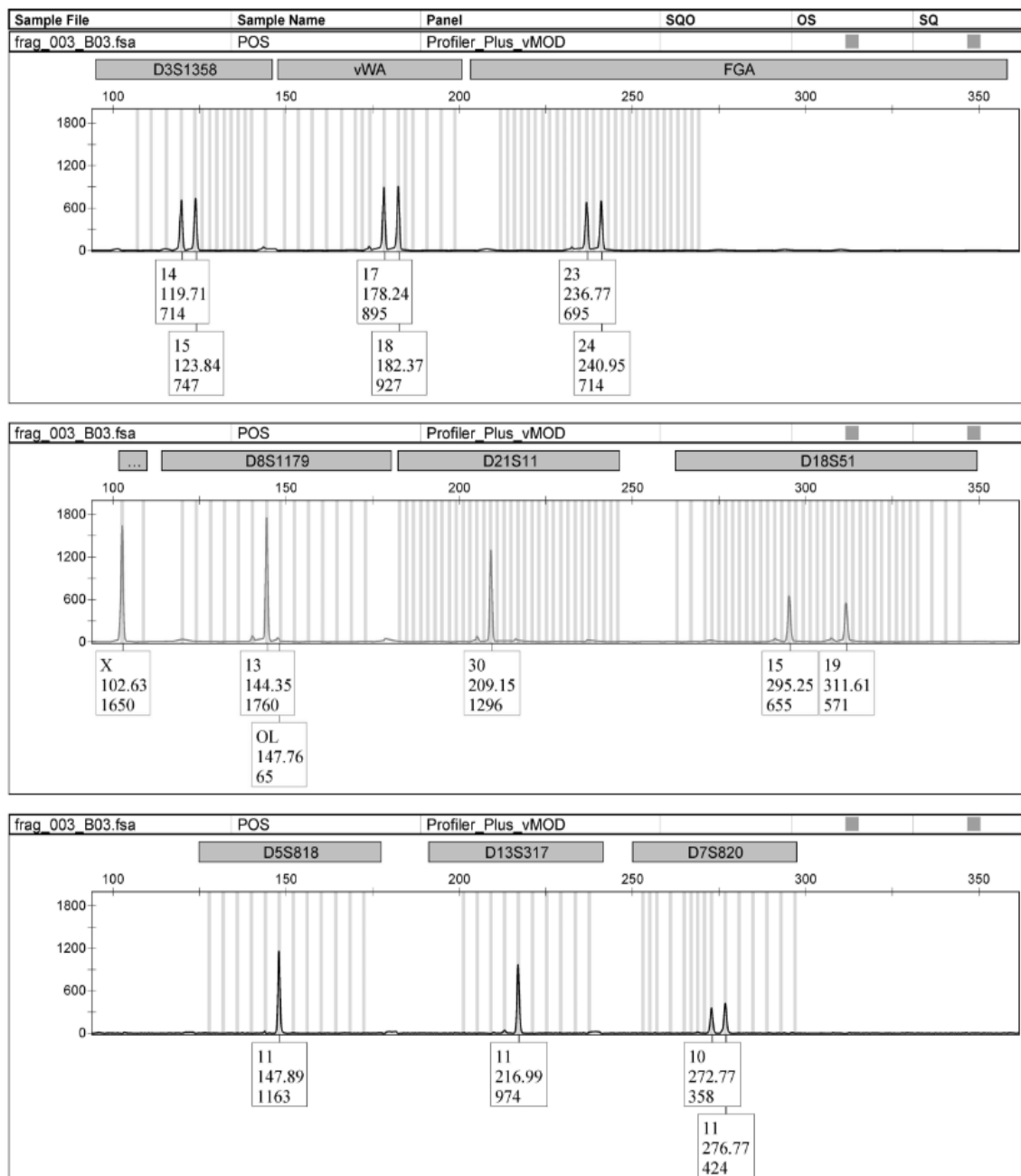


Figure B1: Positive control (1 ng control 9978 DNA) with no dye added to the reaction.

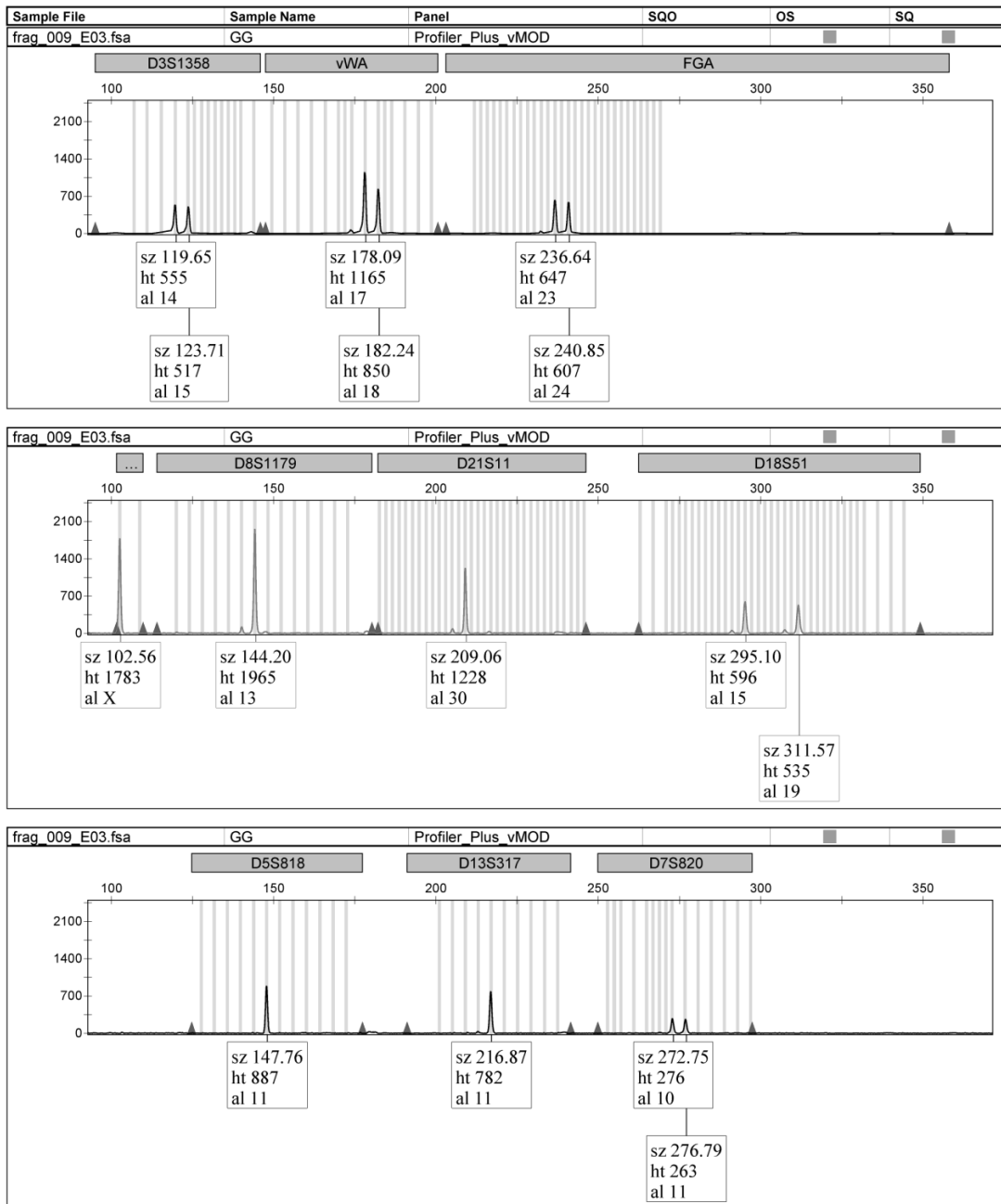


Figure B2: 1 ng of control DNA with GG (1X) using ProfilerPlus kit (which amplifies 18 alleles and amelogenin) 29 cycles.

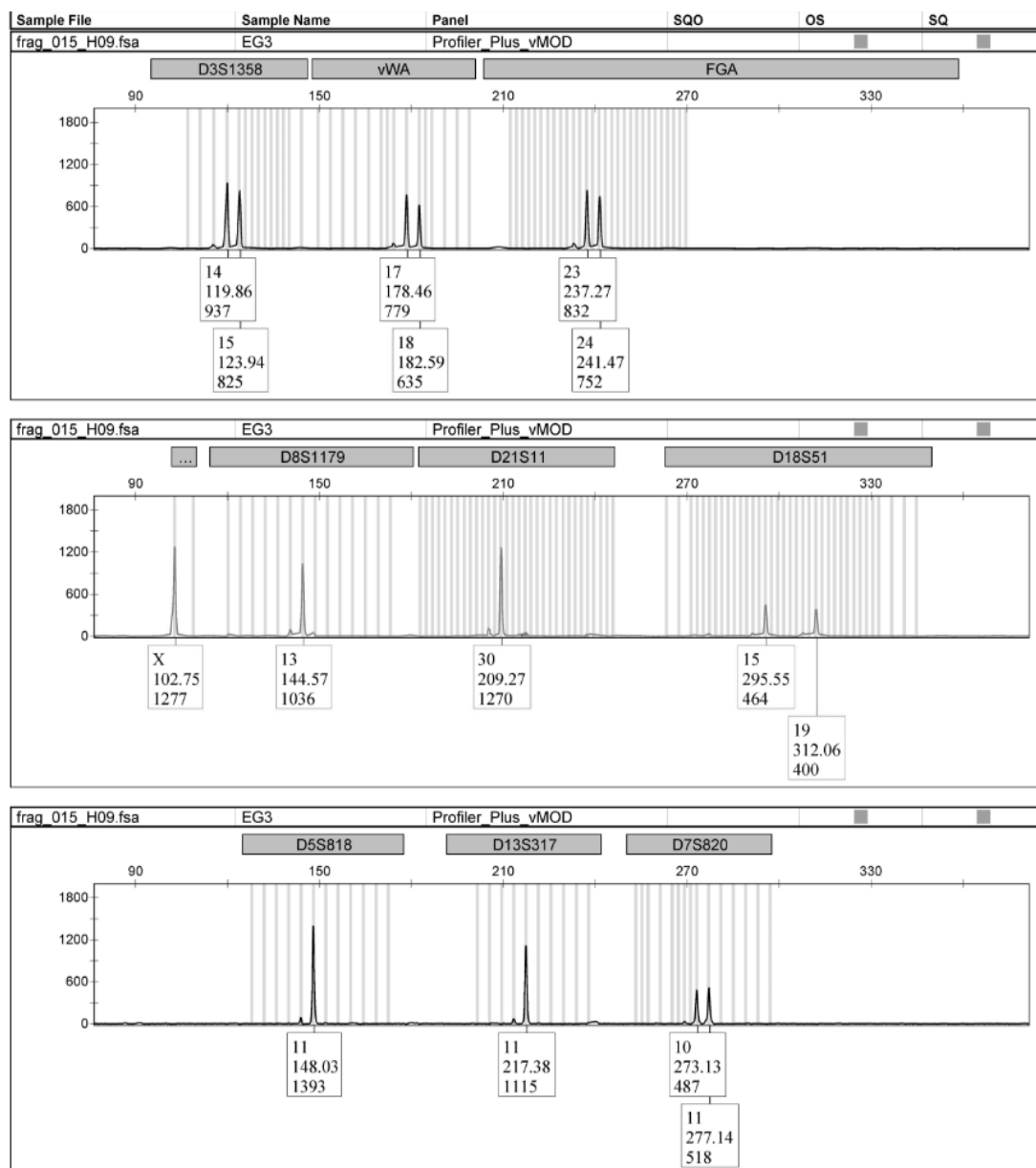


Figure B3: 1 ng of control DNA with EG (1X) using ProfilerPlus kit (which amplifies 18 alleles and amelogenin) 29 cycles.

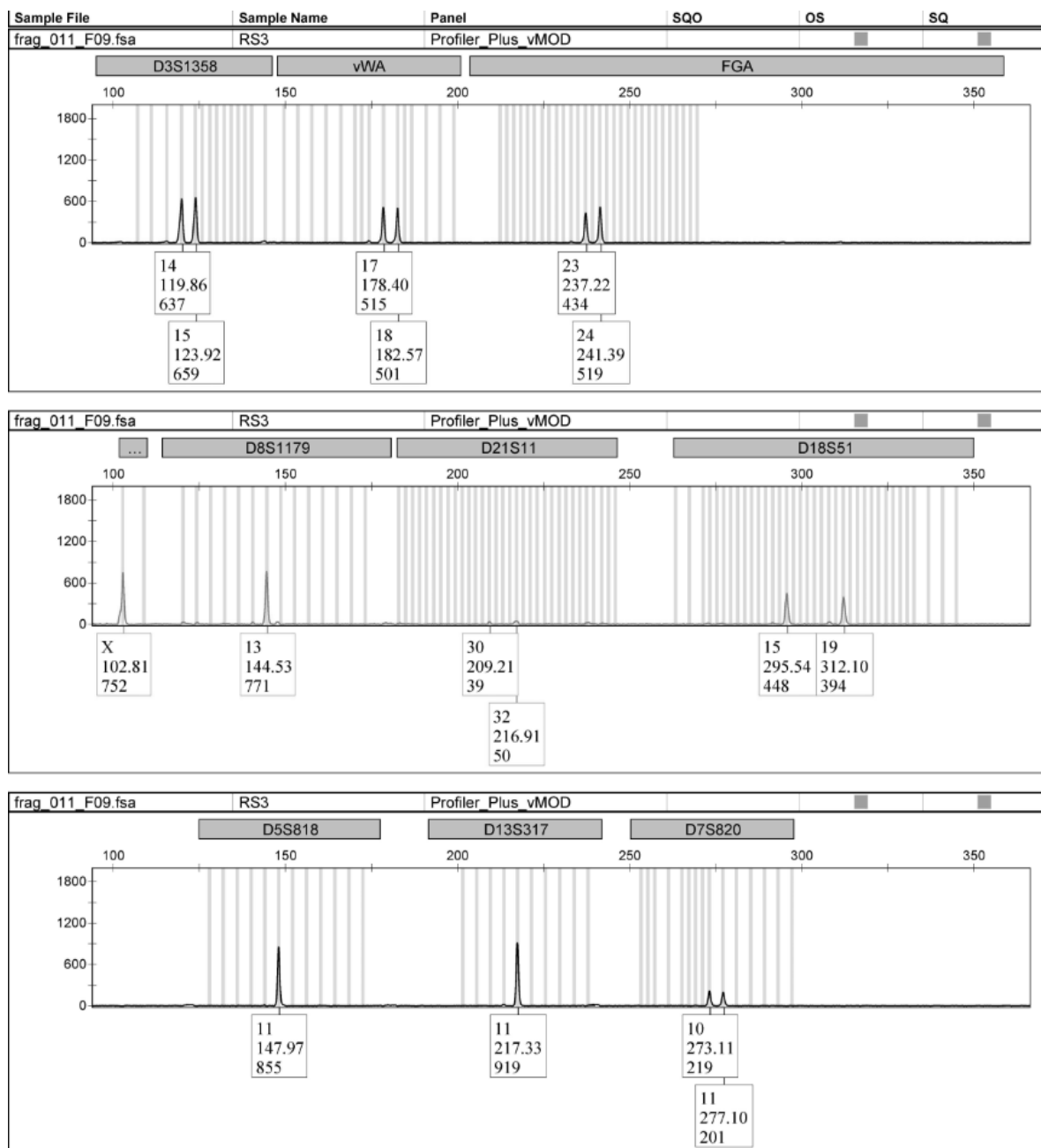


Figure B4: 1 ng of control DNA with RS (1X) using ProfilerPlus kit (which amplifies 18 alleles and amelogenin) 29 cycles.

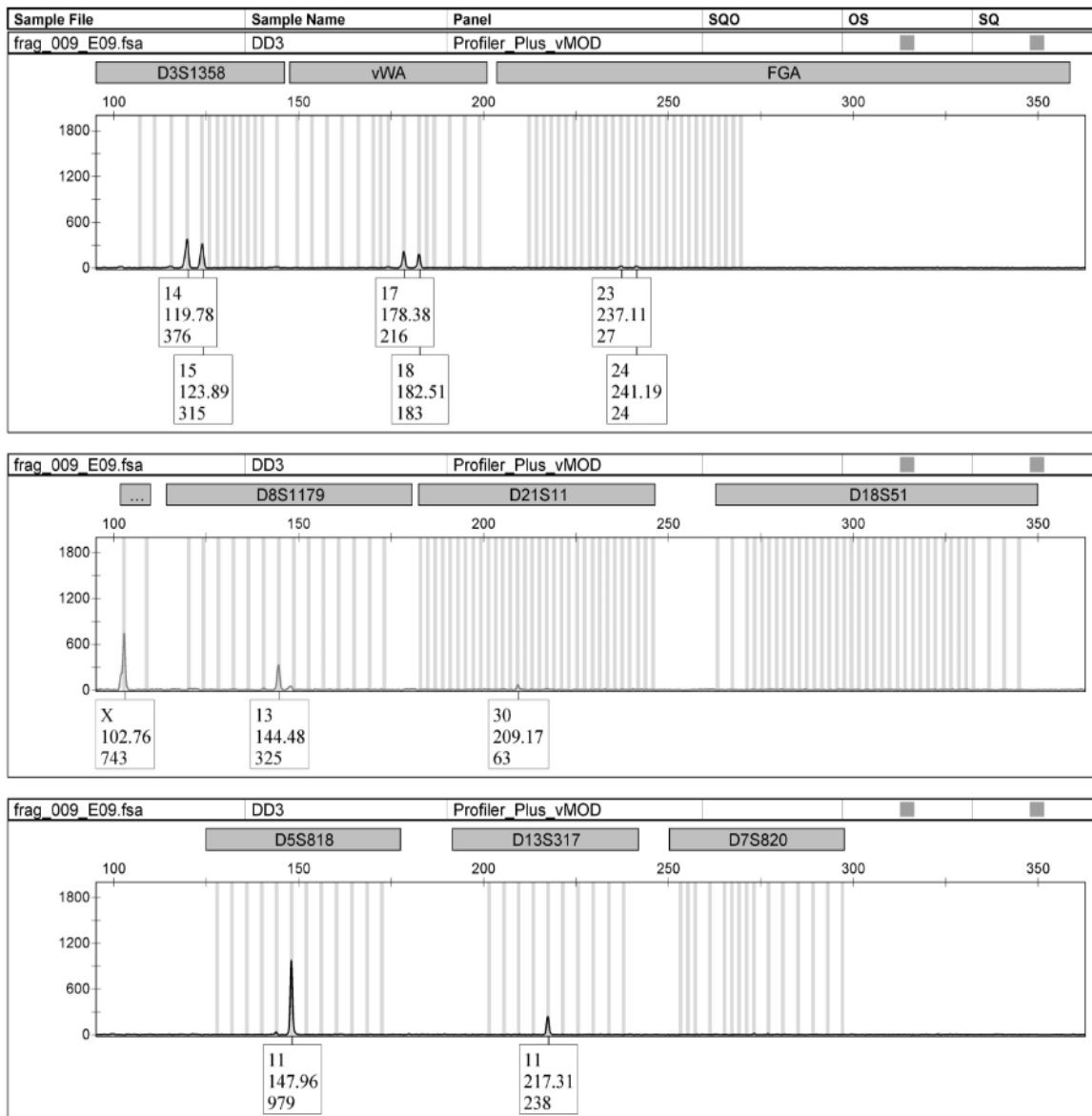


Figure B5: 1 ng of control DNA with DD (1X) using ProfilerPlus kit (which amplifies 18 alleles and amelogenin) 29 cycles.

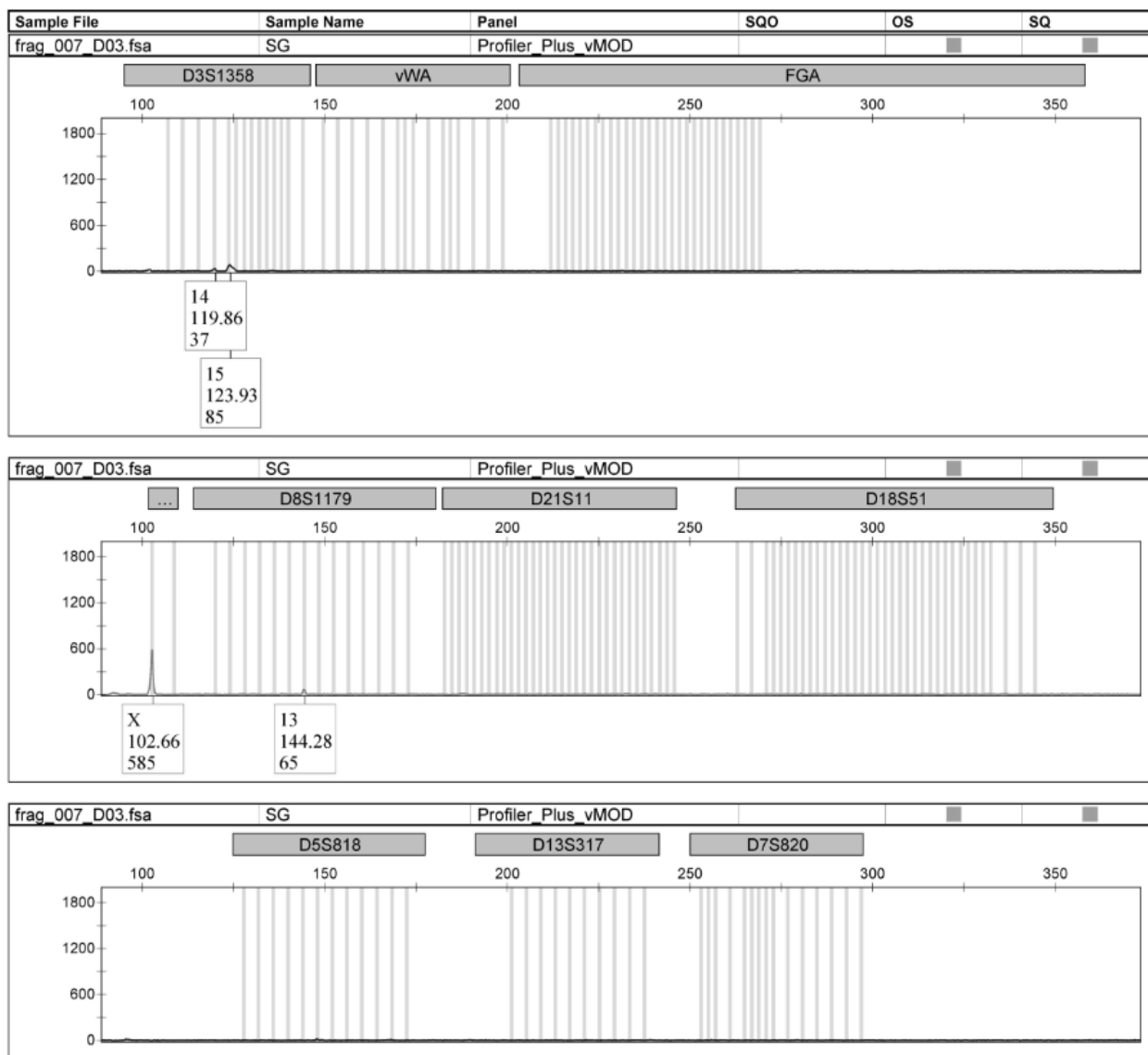


Figure B6: 1 ng of control DNA with SG (1X) using ProfilerPlus kit (which amplifies 18 alleles and amelogenin) 29 cycles.

Table B1: Triplicate results of positive control with no dye added to the reaction

		1	2	3	Average
5-FAM	14	714	659	519	630
	15	747	725	506	659
	17	895	1056	619	856
	18	927	842	657	808
	23	695	706	561	654
	24	714	675	553	647
	x	825	722.5	459.5	669
	X	825	722.5	459.5	669
JOE	13	880	697	523.5	700
	13	880	697	523.5	700
	30	648	753.5	475	625
	30	648	753.5	475	625
	15	655	768	485	636
	19	571	720	448	579
	11	581.5	516	501.5	533
	11	581.5	516	501.5	533
NED	11	487	633	412	510
	11	487	633	412	510
	10	358	488	299	381
	11	424	443	344	403
Profile %		100	100	100	100
	Average peak height				617
	Variance				12860

Table B2: Triplicate results of GelGreen dye added to the reaction

		1	2	3	Average
5-FAM	14	499	1086	1206	930
	15	466	1151	1204	940
	17	1108	1785	1805	1566
	18	803	1391	1620	1271
	23	618	1184	1218	1006
	24	573	1223	1230	1008
	x	790	795.5	876.5	820
	X	790	795.5	876.5	410
JOE	13	899	1089.5	1449	1145
	13	899	1089.5	1449	1145
	30	598	1182	1108.5	962
	30	598	1182	1108.5	962
	15	582	1428	1174	1061
	19	526	1362	1172	1020
	11	413	611.5	741	588
	11	413	611.5	741	588
NED	11	376.5	913	825.5	705
	11	376.5	913	825.5	705
	10	262	759	563	528
	11	250	732	715	565
Profile %		100	100	100	100
	Average peak height				896
	Variance				77124

Table B3: Triplicate results of RedSafe dye added to the reaction

		1	2	3	Average
5-FAM	14	362	637	898	632
	15	351	659	694	568
	17	455	515	851	607
	18	346	501	968	605
	23	0	434	0	144
	24	0	519	0	173
	x	373.5	376	528	425
	X	373.5	376	528	213
JOE	13	245.5	385.5	572	401
	13	245.5	385.5	572	401
	30	0	0	0	0
	30	0	0	0	0
	15	0	448	0	149
	19	0	394	0	131
	11	259	427.5	334.5	340
	11	259	427.5	334.5	340
NED	11	252	459.5	561	424
	11	252	459.5	561	424
	10	0	219	0	0
	11	0	201	0	0
		12	14	12	12.6
		60	70	60	63.3
Number of alleles (20)					
Profile %					
Average peak height					299
Variance					44941.92

Table B4: Triplicate results of EvaGreen dye added to the reaction

		1	2	3	Average
5-FAM	14	0	715	632	449
	15	0	678	641	439
	17	62	896	987	648
	18	70	763	879	570
	23	58	1000	956	671
	24	0	787	721	502
	x	154	661	661.5	492
	X	154	661	661.5	246
JOE	13	47	596.5	727	456
	13	47	596.5	727	456
	30	78.5	666.5	728.5	491
	30	78.5	666.5	728.5	491
	15	0	465	262	242
	19	0	450	255	235
	11	33	552.5	526	370
	11	33	552.5	526	370
NED	11	34.5	679	535	416
	11	34.5	679	535	416
	10	0	513	368	293
	11	0	343	368	237
Number of alleles (20)		13	20	20	17.6
Profile %		65	100	100	88.3
Average peak height					425
Variance					15382

Table B5: Triplicate results of Diamond dye added to the reaction

		1	2	3	Average
5-FAM	14	0	0	376	125
	15	0	0	315	105
	17	0	0	216	72.0
	18	0	0	183	61.0
	23	0	0	0	0
	24	0	0	0	0
	x	27.5	106.5	371.5	168
	X	27.5	106.5	371.5	84.3
JOE	13	0	24	162.5	62.2
	13	0	24	162.5	62.2
	30	0	0	31.5	10.5
	30	0	0	31.5	10.5
	15	0	0		0
	19	0	0		0
	11	0	31	489.5	174
	11	0	31	489.5	174
NED	11	0	0	119	39.7
	11	0	0	119	39.7
	10	0	0	0	0
	11	0	0	0	0
Number of alleles (20)		0	4	14	6
Profile %		0	20	70	30
Average peak height					59.4
Variance					3594

Table B6: Triplicate results of SYBR Green dye added to the reaction

		1	2	3	Average
5-FAM	14	0	0	0	0
	15	85.0	0	0	28.3
	17	0	0	0	0
	18	0	0	0	0
	23	0	0	0	0
	24	0	0	0	0
	x	292	0	0	97.5
	X	292	0	0	48.8
JOE	13	34.5	0	0	11.5
	13	34.5	0	0	11.5
	30	0	0	0	0
	30	0	0	0	0
	15	0	0	0	0
	19	0	0	0	0
	11	0	0	0	0
	11	0	0	0	0
NED	11	0	0	0	0
	11	0	0	0	0
	10	0	0	0	0
	11	0	0	0	0
Number of alleles (20)		5	0	0	3
Profile %		25	0	0	8.33
Average peak height					9.87
Variance					51.1

Table B7: Triplicate results of GelRed dye added to the reaction

		GelRed			Average
		1	2	3	
5-FAM	14	0	0	0	0
	15	0	0	0	0
	17	0	0	0	0
	18	0	0	0	0
	23	0	0	0	0
	24	0	0	0	0
	x	0	0	0	0
	X	0	0	0	0
JOE	13	0	0	0	0
	13	0	0	0	0
	30	0	0	0	0
	30	0	0	0	0
	15	0	0	0	0
	19	0	0	0	0
NED	11	0	0	0	0
	11	0	0	0	0
	11	0	0	0	0
	11	0	0	0	0
	10	0	0	0	0
	11	0	0	0	0
Number of alleles (20)		0	0	0	0
Profile %		0	0	0	0
Average Peak Height				0	0
Variance					0

B.2 Examples of profiles obtained showing the effect of the dyes on peak heights and allele amplification after DNA extraction to remove the DNA binding dyes

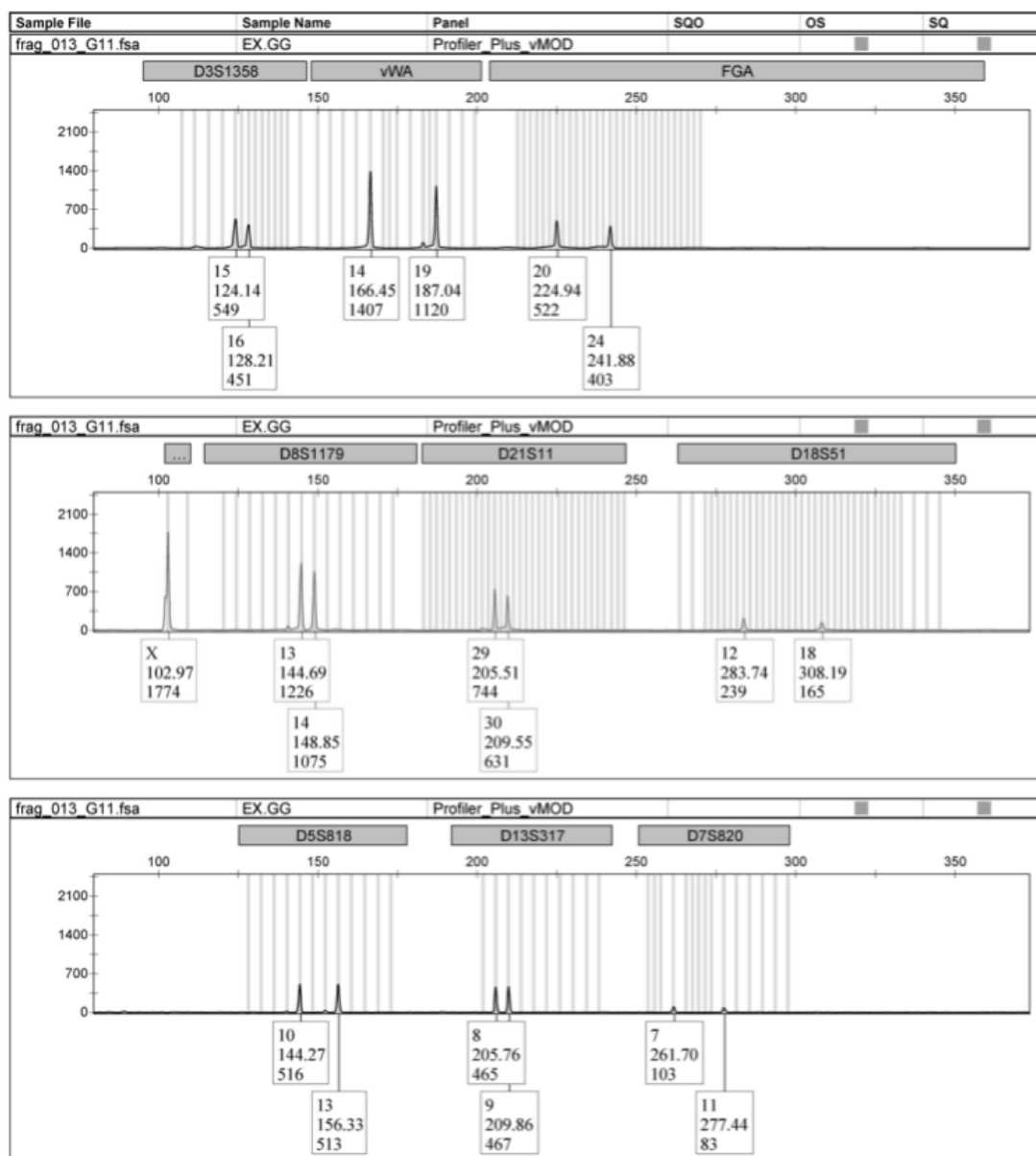


Figure B8: Control DNA with GG extract using ProfilerPlus kit (which amplifies 18 alleles and amelogenin) 29 cycles.

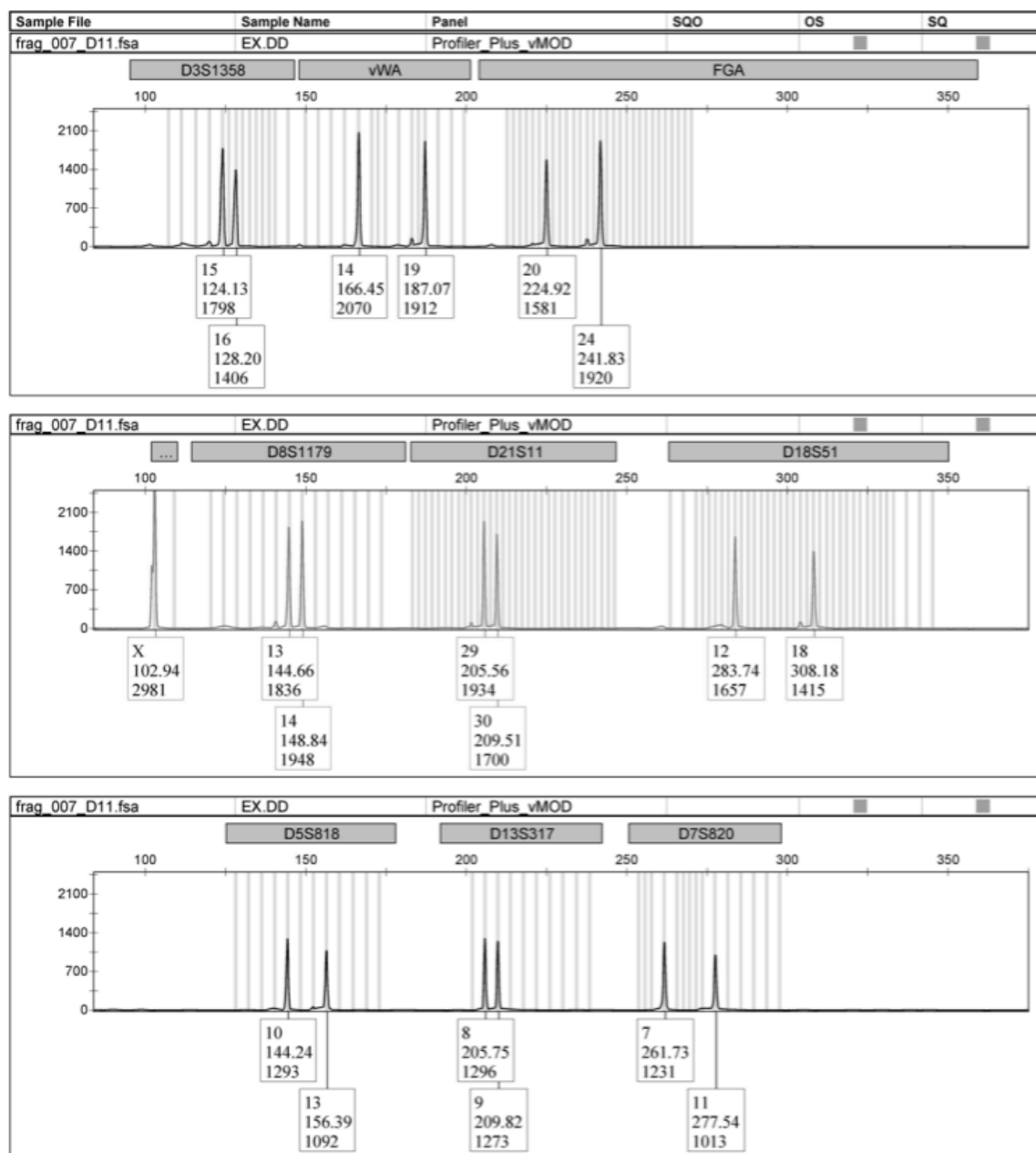


Figure B9: Control DNA with DD extract using ProfilerPlus kit (which amplifies 18 alleles and amelogenin) 29 cycles.

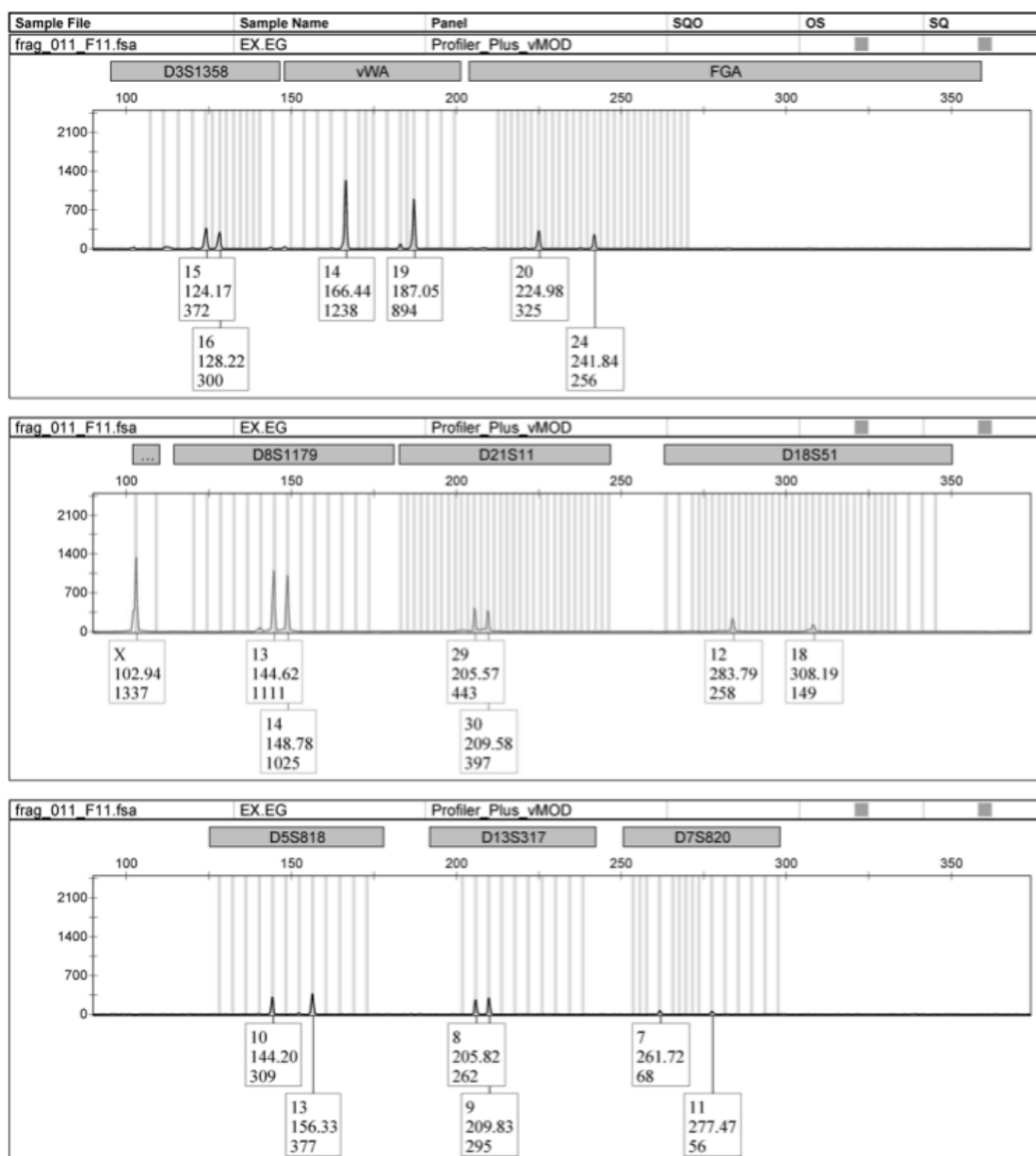


Figure B10: Control DNA with EG extract using ProfilerPlus kit (which amplifies 18 alleles and amelogenin) 29 cycles.

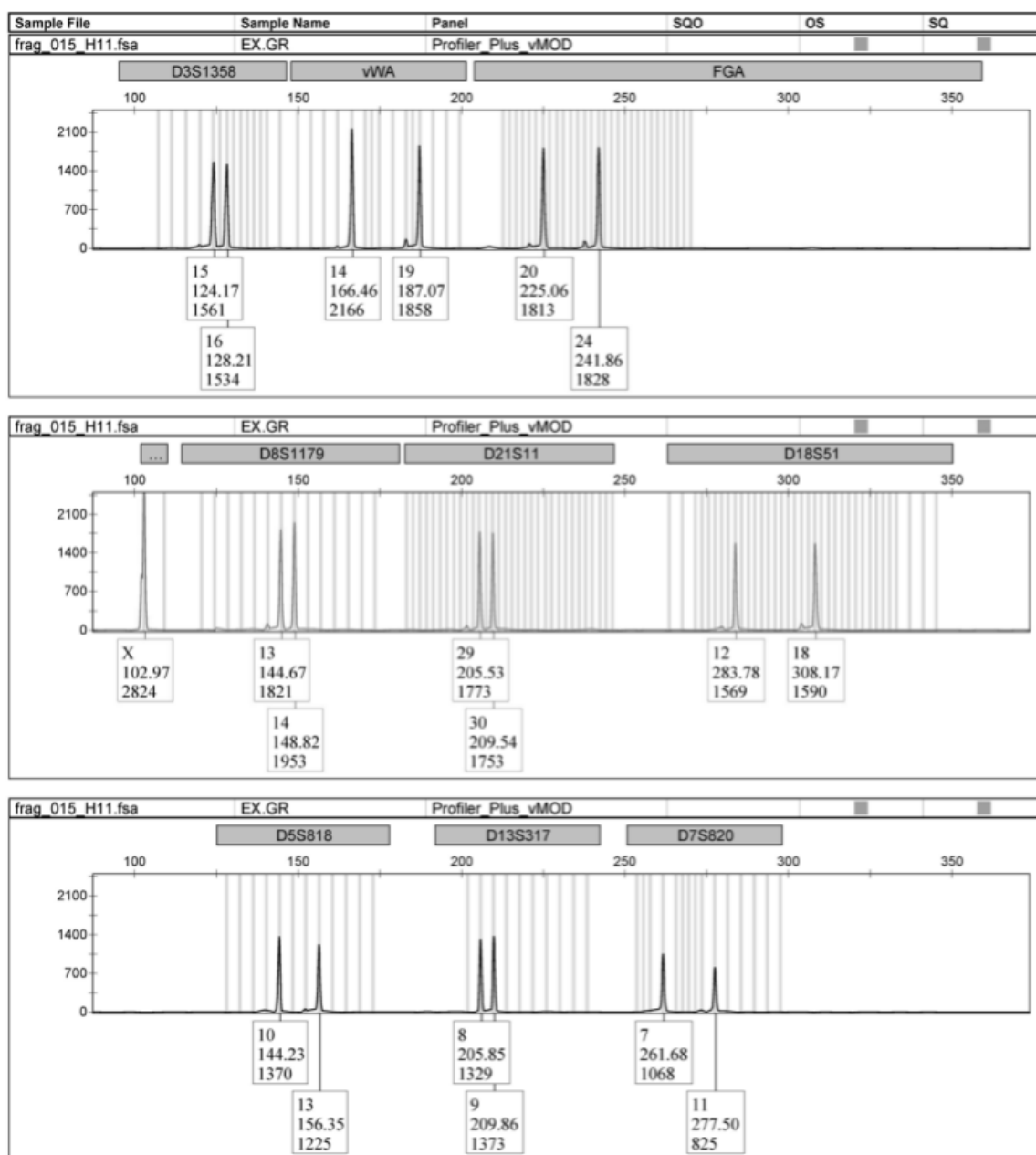


Figure B11: Control DNA with GR extract using ProfilerPlus kit (which amplifies 18 alleles and amelinogenin) 29 cycles.

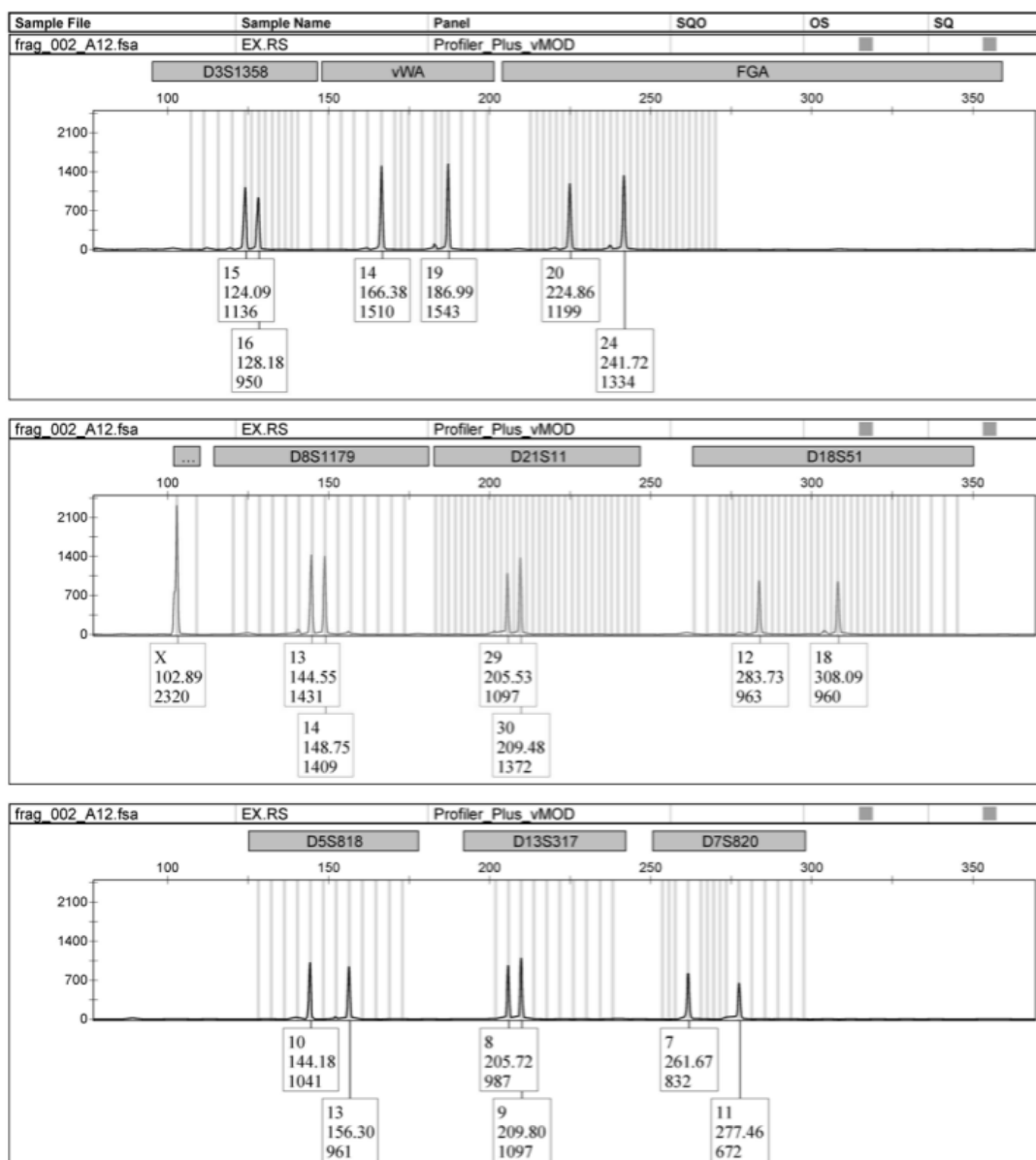


Figure B12: Control DNA with RS extract using ProfilerPlus kit (which amplifies 18 alleles and amelogenin) 29 cycles.

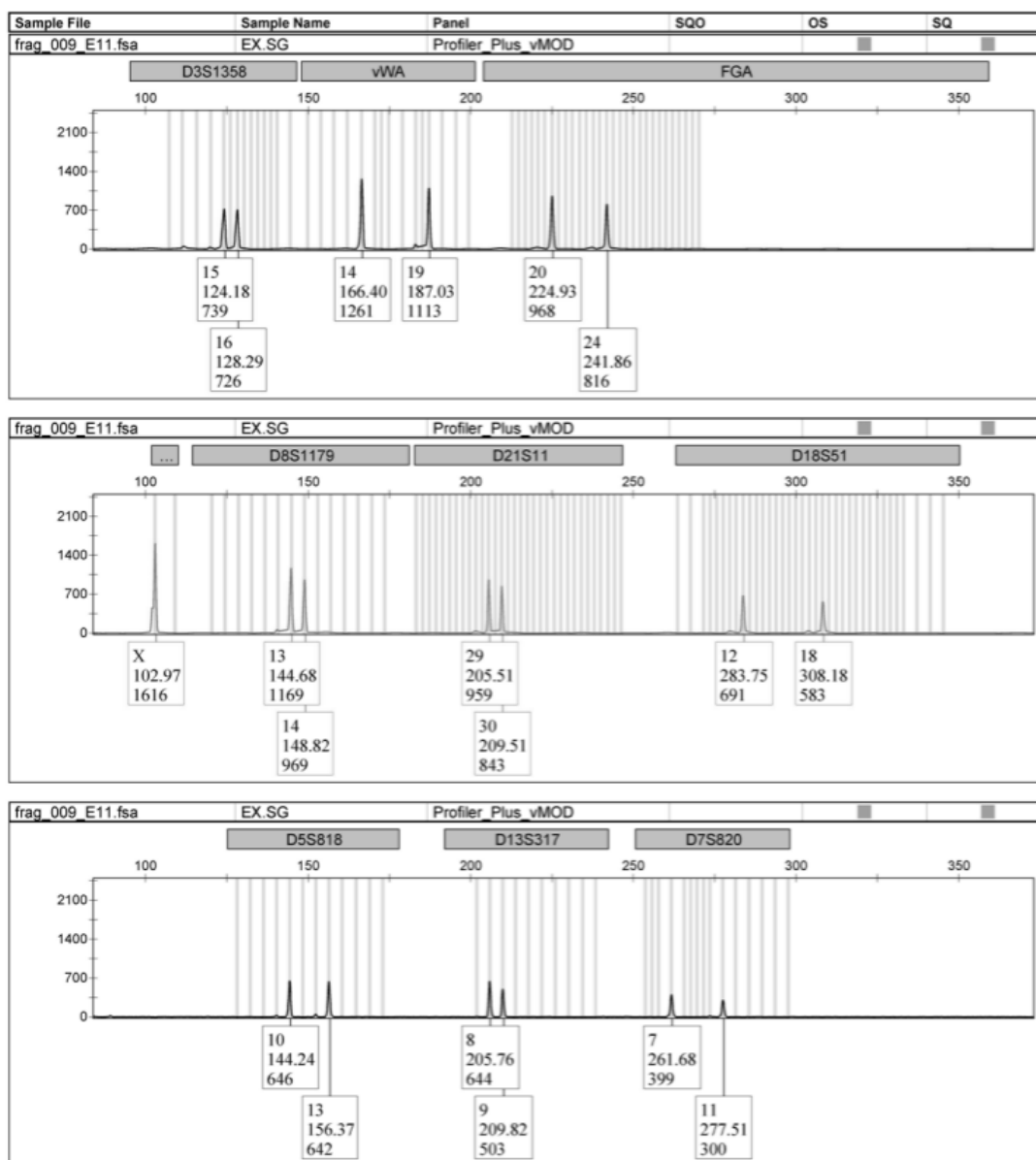


Figure B13: Control DNA with SG extract using ProfilerPlus kit (which amplifies 18 alleles and amelogenin) 29 cycles.

Table B8: Percentage of DNA loss after solid phase extraction with and without binding dyes present and the overall increase in the loss when compared with the control.

	Percentage Loss			Average Percentage Loss	Standard Deviation	95% Confidence Interval	Standard Error	T-Test or p value	Means are not the same	Increase in loss %
	1	2	3							
Control	49.2	49.6	89.9	62.9	23.3	9.10	13.5			
DD	66.4	56.1	88.8	70.4	16.7	6.51	9.65	0.675	Yes	7.5
SG	66.7	75.3	92.4	78.1	13.1	5.09	7.55	0.197	Yes	8.6
GG	50.1	82.9	81.6	71.5	18.5	7.23	10.7	0.322	Yes	9.1
GR	81.8	72.8	85.8	80.1	6.65	2.59	3.84	0.164	Yes	15.2
RS	90.5	69.4	100	86.6	15.6	6.09	9.04	0.113	Yes	17.2
EG	66.3	81.2	68.6	72.0	8.02	3.12	4.63	0.288	Yes	23.7

B1.3 Effects on Qubit quantification

Table B-9: Effects of the dyes on Qubit DNA quantification with the addition of each dye to the quantification reaction (1X total concentration).

	Control	SG	RS	EG	DD	GR	GG
Average Control DNA (10 ng/μL)	10.4	15.4	14.1	13.3	10.0	0.123	10.7
Average Dye Only (ng/μL)	-	0.0104	1.85	0.974	0.0175	0.0120	TL*
Average Extract Dye (ng/μL)	-	0.00500	0.00840	0.00737	0.0111	0.00800	-
Difference (ng/μL)	-	0.00536	1.84	0.966	0.00644	0.00404	-
Dye percentage loss	-	51.7	99.5	99.2	36.7	33.6	-

Table B10: The effects of the dyes on Qubit quantification before and after the dyes were submitted to an extraction process without DNA present to determine about of dye lost through this process.

	ng/ μ L					
	1	2	3	Average	Difference	%
SG 20x	0.0125	0.0125	0.0125	0.0125		
SG 20x EXTRACT	0.0052	0.0051	0.005	0.0051	0.0074	59.2*
EG 20x	0.0968	0.0971	0.0971	0.097		
EG 20x EXTRACT	TL	TL	TL	TL		
RS 20x	0.0189	0.0188	0.0188	0.018833		
RS 20x EXTRACT	TL	TL	TL	TL		

Chapter 4

DNA binding dyes for new application

4.1 Introduction

Nucleic acid binding dyes are generally used to visualize bands following gel electrophoresis which has been investigated in Chapter 2. The effect the dyes had on extraction, amplification and STR typing was investigated in Chapter 3. This Chapter looks at the use of these dyes with previous studies in mind to determine if any of the chosen dyes would be suitable for a surface based *in situ* detection method for DNA. A list of properties the dye should have for this new surface based application was compiled to aid in finding applicable dyes, listed below;

- Excitation wavelength longer than UV (>350 nm) to reduce the chance of DNA degradation
- Non-toxic or mutagenic
- Reasonable separation of excitation and emission bands to allow for interference filters to optimize results (reasonable Stokes shift)
- Cheap
- Minimal inherent fluorescence of the molecule, resulting in a higher fold enhancement when in the presence of DNA
- Applicable to crime scenes (potentially as a spray)
- Doesn't stain objects present at crime scenes
- Have a high sensitivity and specificity for DNA and not interact with the substrate and produce background fluorescence.
- Does not inhibit downstream applications such as PCR and STR profiling
- Stable dye at room temperature

The properties of these dyes were then used to narrow down the 64 dyes stated in Chapter 1 and 2 to six dyes based on their DNA binding properties. Table 4.1 below lists the selected dyes along with their spectral properties.

Table 4.1: Selected DNA binding dyes for investigation in their use for latent DNA detection.

Dye	Acronym	Main Function	Excitation (nm)	Emission (nm)
SYBR [®] Green I	SG	qPCR, Flow Cytometry	494	520
Diamond [™] Nucleic Acid Dye	DD	Gel staining	494	558
EvaGreen [™]	EG	qPCR	500	530
GelGreen [™]	GG	Gel staining	495	520
GelRed [™]	GR	Gel staining	300, 250	600
RedSafe [™]	RS	Gel staining	309, 419, 514	537

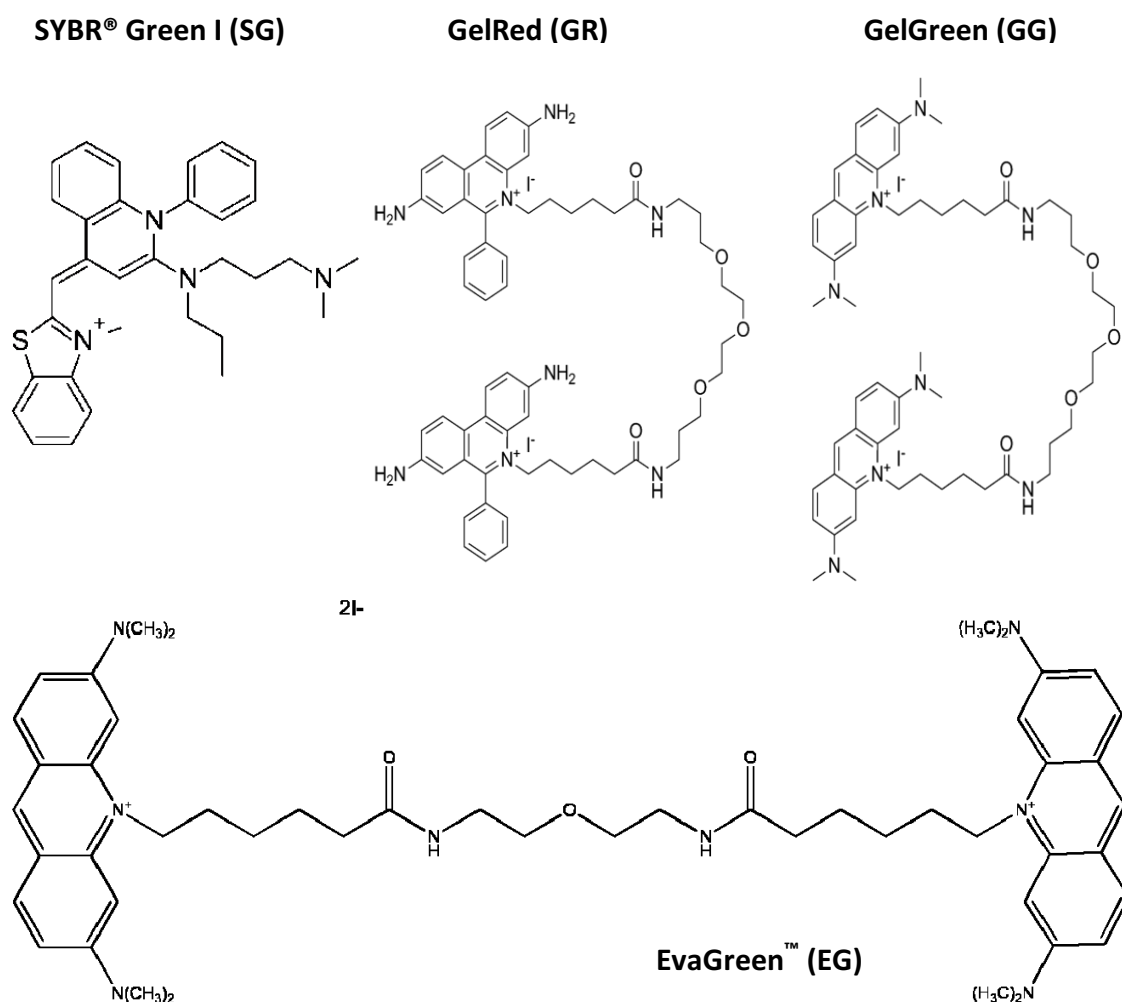


Figure 4.1: Molecular structure of SYBR[®] Green I [1] (**left**), GelRed[™] [2] (**Centre**), GelGreen[™] [2] (**right**) and EvaGreen[™] (**below**) [3]

The majority of the dyes chosen were based on their low mutagenicity and toxicity except for SG. SG has been shown to be mutagenic above 33.3 µg/µL [4] but was chosen for this study as a control due to the high sensitivity and specificity to DNA, as SG has around a 1000-1500 fold in fluorescent enhancement [1, 5]. Figure 4.1 shows the chemical structure of some of the dyes, EG's structure is not provided by the manufacturer but is thought to be a bridge with a homo-monomer attached either side [3]. EG's assumed structure is very similar to that of GG and GR which are two homo-monomers attached with a linkage bridge, GG is two acridine monomers and GR is two EtBr monomers. This increase in structure compared with SG results in the dye being impermeable to the cell membrane, thus reducing the risk of the dyes interacting with genomic DNA and causing mutations. DD and RS structures are unknown and proprietary information.

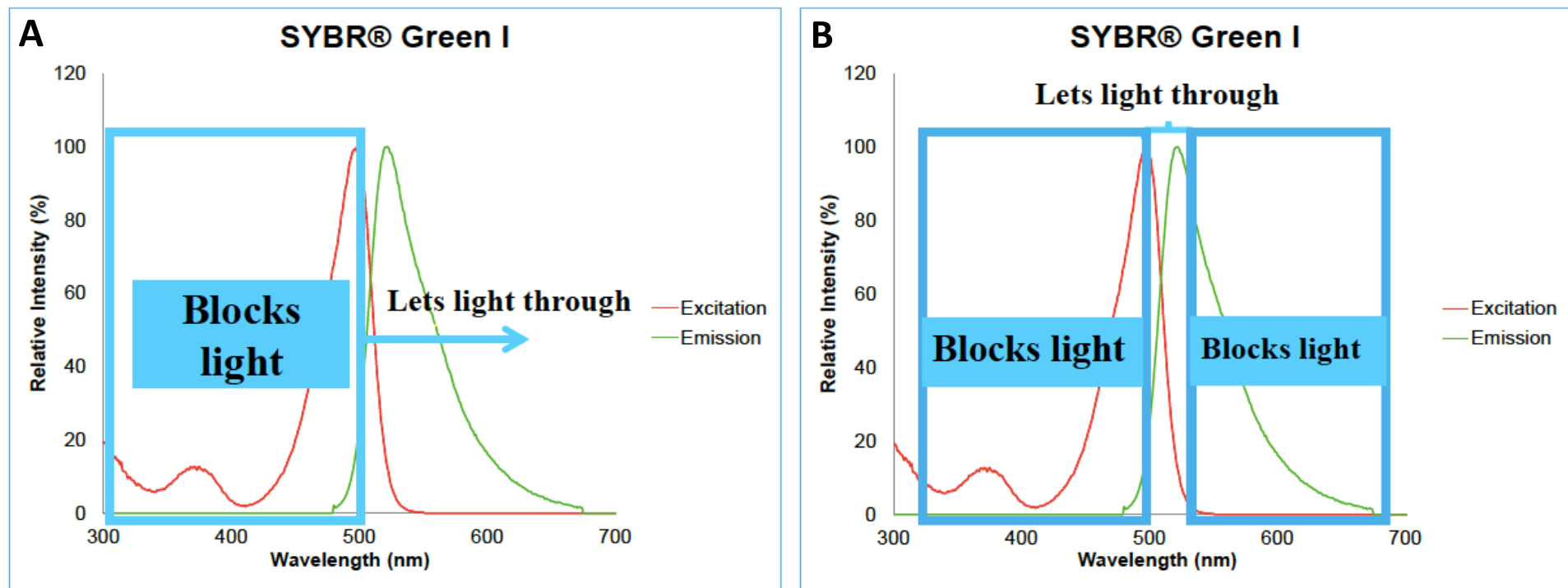
4.1.8 Forensic light sources

Forensic light sources have been used for decades to search for material at crime scenes that can range from dried blood stains, fingerprints in blood and textile fibres where different wavelengths can be used for visualization [6-8]. There are multiple different types of light sources such as CRIME-LITE [9], OPTIMAX Multi-lite, SUPERLITE 400 (Lumatec) [10, 11], CrimeScope® (SPEX forensics) [12, 13], Polilight® and Poliray™ (Rofin) [6, 14] light sources are just to name a few. These light sources can use LED or xenon light sources and filters to obtain wavelengths necessary for detection of material. Table 4.2 outlines the different wavelengths available for the Polilight® along with available filters.

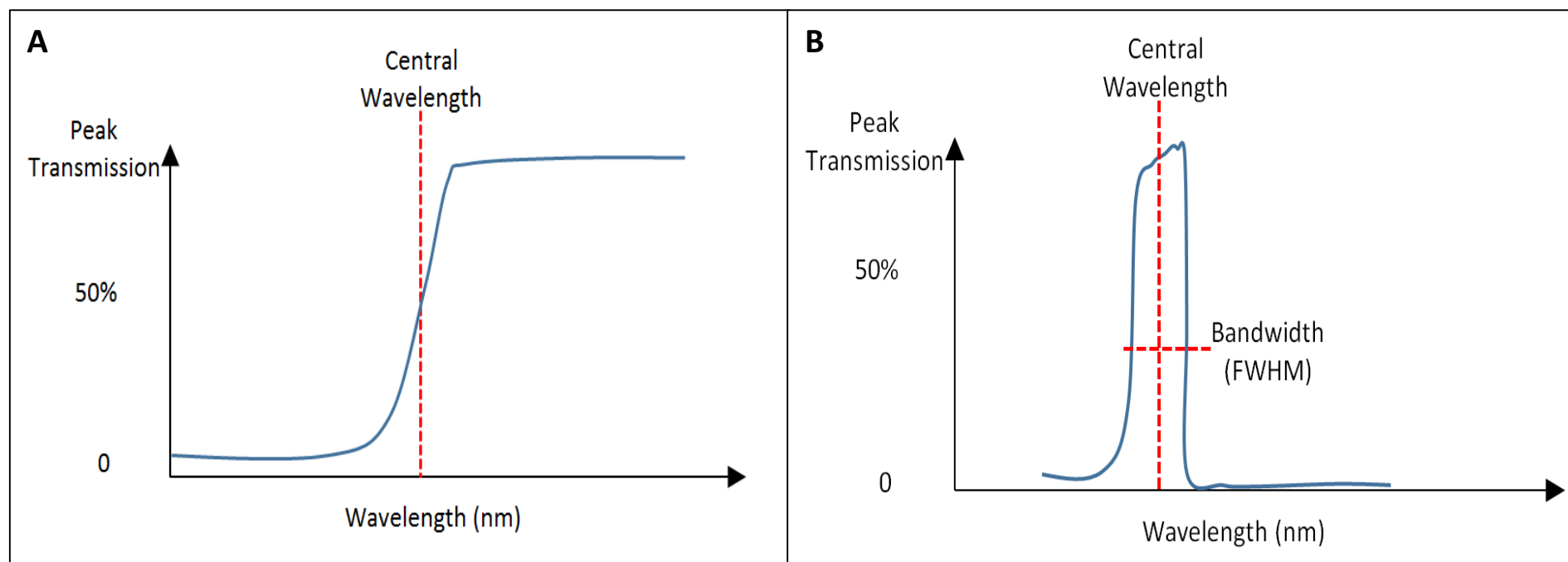
Filters:

- Cut-off/barrier filters
- Interference filters

Scheme 4.1 shows how cut-off and interference filters work in reference to SG's excitation and emission spectrum, showing that cut-off filters allow more light through whereas interference filters only allow a certain bandwidth of light through depending on band-pass of the filter (eg. 40 nm). Scheme 4.2 shows how the light is transmitted through the two different filter types.



Scheme 4.1: Schematic diagram of how (A) cut-off (550 nm) and (B) interference (535 nm) filters work in reference to SYBR® Green's excitation and emission spectra.



Scheme 4.2: Schematic diagram of filters work for the detection of fluorescent signals (A) showing a barrier or cut-off filter, (B) showing an interference filter.

Table 4.2: Polilight[®] excitation wavelengths include the size of the band-pass filter as well as available cut-off and interference filters.

Polilight wavelengths	Cut-off filters	Interference filters
White (280 nm BP)	495 nm (B+W)	350 nm
350 nm (80 nm BP)	550 nm (B+W)	415 nm
415 nm (40 nm BP)	570 nm (B+W)	450 nm
450 nm (100 nm BP)	475 nm (Polilight-high pass)	505 nm (degraded)
470 nm (40 nm BP)	515 nm (Polilight-high pass)	530 nm (40 nm bandpass)
*490 nm (40 nm BP)	550 nm (Polilight-high pass)	555 nm (degraded)
505 nm (40 nm BP)	590 nm (Polilight-high pass)	610 nm
530 nm (40 nm BP)		650 nm
555 nm (27 nm BP)		700 nm
590 nm (40 nm BP)		750 nm
620 nm (40 nm BP)		
650 nm (40 nm BP)		
IR 700-1100 nm		
* Shaded wavelengths indicates suitability for use with DNA binding dyes chosen for analysis		

4.1.9 Summary

Within this Chapter DNA binding dyes will be investigated for their use as a surface based *in situ* detection method for DNA. Their ability to detect down to low levels of DNA will be investigated along with the use of these dyes for the detection of DNA with fingerprints. The specificity of the dyes will be investigated by looking at the intensity of signals from the dyes in the presence of proteins and with bacterial DNA. This Chapter has been separated into two sections based on the mode of detection. The first section is all on detection using the Gel Doc™ EZ Imager and the second section using the Polilight® for a more specific excitation wavelength and filters for a more specific detection system than the parameters used with the Gel Doc™.

4.2 Methodology

4.2.1 Dye solution preparation

GelGreen™ (GG), GelRed™ (GR), SYBR® Green (SG) and Diamond™ dye (DD) all come in stock concentrations of 10,000X in either DMSO or H₂O these dyes were diluted to differing concentrations 40X (1 µL in 250 µL, H₂O) and 20X (1 µL in 500 µL H₂O). RedSafe (RS) comes in a stock concentration of 20,000X and was diluted in H₂O to obtained 40X (1 µL in 500 µL) and 20X concentrations (1 µL in 1 mL). EvaGreen™ was obtained in a 20X concentrated solution in H₂O.

4.2.2 Background fluorescence

The fluorescence of the dyes without DNA was tested by placing 5 µL of the dye solution (20X, in H₂O) onto a glass slide and recorded the volume intensity using gel band analysis tool with the Gel Doc™ EZ Imager (Bio-Rad) using blue transillumination for all the dyes except GR which used UV transillumination.

4.2.3 DNA binding dyes with DNA

The intensity of the dyes with varying amounts of DNA was investigated. DNA at 1 ng, 10 ng and 50 ng was placed onto glass slides and allowed to dry. DNA binding dyes were then applied to the surface where the DNA was placed (5 µL, 20X) and as a control (no DNA). The volume intensity was recorded using gel band analysis tool with the Gel Doc™ EZ Imager using blue transillumination for SG, GG, EG, DD and RS. A histogram was created using excel with the line of best fit showing equation and R² value was recorded. GR was not analyzed as it uses a different mode of transillumination.

4.2.4 Detection of DNA within fingerprints

The volume of intensity of fingerprints was investigated using SG and GG. Fingerprints were deposited onto a plastic surface (Parafilm®) 1 hr after hand washing for a 10 s period. Dyes diluted in H₂O were then applied to the surface where the fingerprint had been deposited, along with a negative control (dye/H₂O only). The results were analysed using Excel and the

amount of DNA present was calculated using the line of best fit from the calibration curve (4.2.3).

4.2.5 Specificity of dyes

DNA binding dyes signal in the presence of bacteria was measured using 1 μL of bacterial DNA (1×10^6 cells/ μL) in the presence of SG and GG (5 μL at 20X concentration) on different surfaces (plastic, glass and Parafilm) with detection using the Gel Doc™ EZ Imager (blue tray). Varying amounts of bacterial DNA (100,000 – 1,000,000 cells/ μL) was then placed in the presence of SG (5 μL at 20X concentration) on a glass surface. Signals were detected using Gel Doc™ EZ Imager (blue tray) at initial staining and then after 10 min incubation at room temperature.

DNA binding dyes signal at 20X concentration (5 μL) in the presence of BSA was measured using 1 μL of BSA (2 $\mu\text{g}/\mu\text{L}$) compared with background (5 μL of dye at 20X) on a glass surface and detected using Gel Doc™ EZ Imager (blue tray except GR used UV tray). The enhancement in the presence of DNA and protein was investigated using 50 ng of DNA and 50 ng of protein in the presence of the binding dyes (5 μL at 20X concentration) on a glass surface with detection using the Gel Doc™ EZ Imager lane band analysis tool (blue tray, except for GR using UV tray). Exposure times at 1.2 s and at 10 s were used.

4.2.6 Detection using Polilight®

The sensitivity and specificity of the dyes used the Polilight® set at 490 nm. The background signal of dyes (5 μL at 20X concentration) on a glass substrate was detected using various filters and exposure times. The excitation wavelength and filters that were used with each of the binding dyes is shown in Table 4.3. GG (5 μL at 40X concentration) in the presence of DNA (1, 10, 20 and 50 ng of DNA) was detected through a 550 nm cut-off filter. The DNA binding dyes RS, DD, GR and GG (5 μL at 20X concentration) in the presence of DNA (0.5-10 ng) on a glass surface was detected through 550 nm cut-off filter and 535 nm interference filter.

Fingermarks stained with the DNA binding dye, DD (5 μ L at 20X concentration), was detected through both 550 nm cut-off filter and 535 nm interference filter. Fingermarks were then stained with a protein dye (Qubit[®] protein assay dye, 5 μ L at 20X concentration) on glass surfaces and detected with both filters.

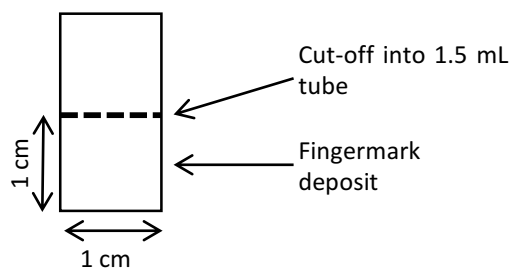
Enhancement of DD in the presence of DNA and BSA protein at 1-10 ng was detected on glass surfaces using a 535 nm interference filter. Detection of DNA within various biological samples such as, hair, skin flakes, blood and saliva, used the DNA binding dyes at a 20X concentration (1 μ L of the dye was added to the biological sample). Samples were viewed under a Nikon Optiphot fluorescent microscope using a B2A filter cube and images were captured using an exposure time of 1 s under 400X magnification.

Table 4.3: Filters to be used with the dyes depending on their excitation (Ex) and emission (Em) wavelengths.

Dye	Ex λ_{\max} (nm)	Polilight [®] setting (nm)	Em λ_{\max} (nm)	Interference filter (nm)	Cut-off filter (nm)
SG	494	490 (40 nm)*	520	530	515
DD	494	490 (40 nm)	558	555	550
GG	495	490 (40 nm)	520	530	515
GR	300, 250	350 (80 nm)	600	610	590
EG	500	490/505 (40 nm)	530	530	515
RS	309, 419, 514	415/505 (40 nm)	537	530	515
*The bandwidth (full width at half maxima, FWHM) of the filter settings for the Polilight wavelengths is shown in brackets.					

4.2.7 Quantification of DNA within fingermarks

Clear acetate paper was treated with 0.5% bleach and UV (10 min each side) using Spectrolinker™. Fingermarks were placed onto individual pieces of treated acetate paper for 10 s, hands were washed 1 hr before deposit (see Scheme 4.3). The deposits were then placed into a 1.5 mL tube with 240 μ L of TE 1X buffer with 10 μ L of ethanol. The tube was mixed (vortex for 10 s) then heated at 80 °C for 15 min followed by another vortex (10 s). 10 μ L was then removed for DNA quantification using Qubit[®] following the manufacturer's recommended protocol.



Scheme 4.3: Schematic representation of the acetate paper where the fingerprints were deposited onto then cut-off into 1.5 mL tube.

4.3 Results and discussion (Gel Doc™ detection)

4.3.1 Background Fluorescence

Figure 4.2 shows the background signal of the dyes, SG dye has the lowest background fluorescence on glass compared with both GG and RS. The background fluorescence of RS is approximately 18 times greater than GG and 38 times greater than SG.

Reasons for background fluorescence:

1. Bacterial DNA present even though slides were placed under UV light
2. The dyes are interacting with the substrate itself even though the dyes are specific for DNA
3. There is reflection off the surface from the excitation light that is being captured along with the fluorescence emission from the dye at 520 nm.
4. The dyes are naturally fluorescent

Even though there is high background fluorescence these cyanine dyes particularly SG should have a 1000 fold increase in fluorescence when DNA is present [1]. In theory this background fluorescence should be negligible.

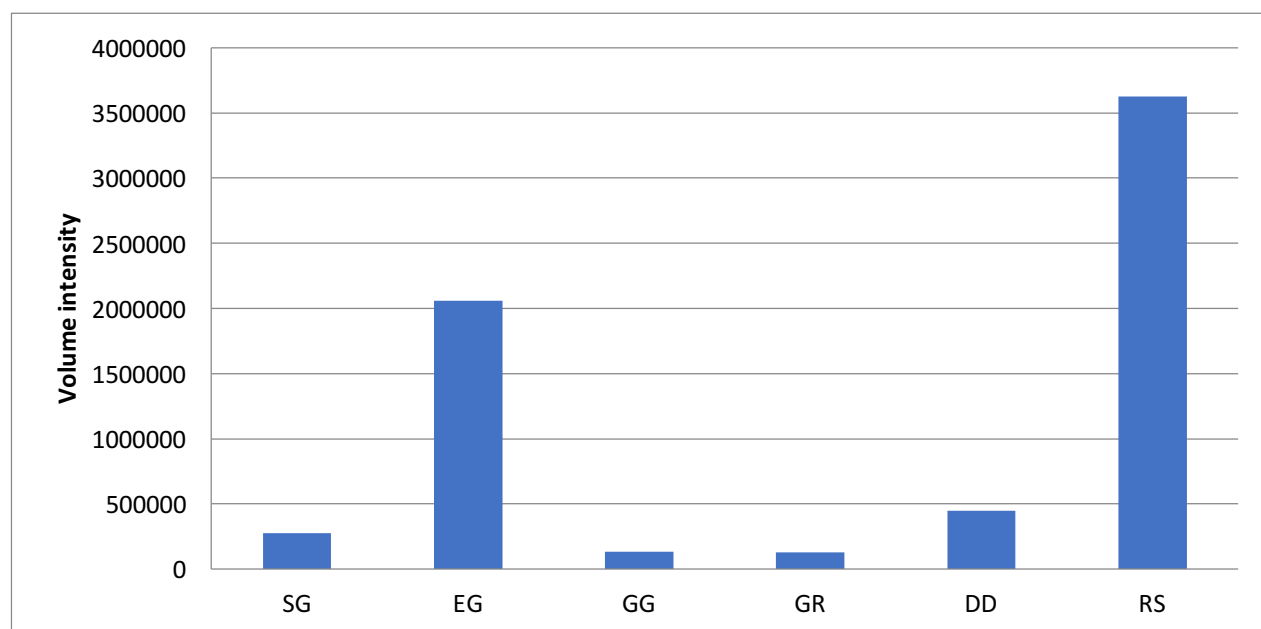


Figure 4.2: Background signal of DNA binding dyes on glass (5 μ L, 20X) using Gel Doc™ EZ imager lane band analysis tool.

4.3.2 DNA binding dyes with DNA

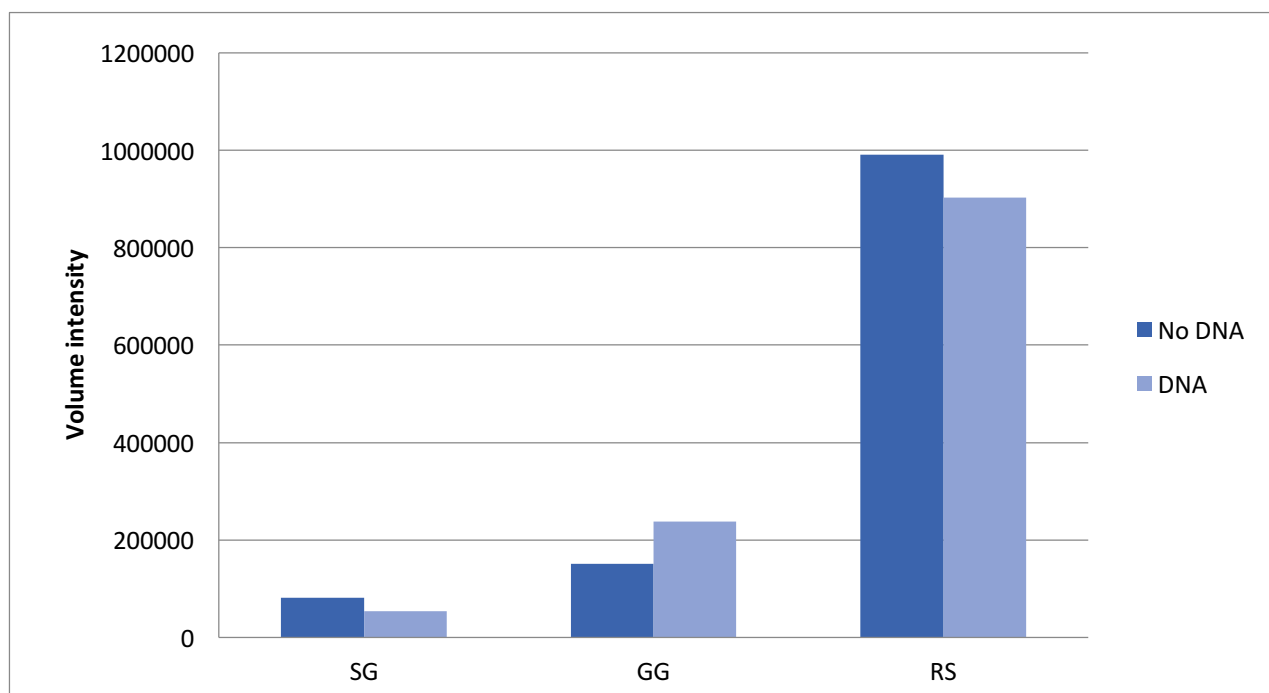


Figure 4.3: Comparison of background signal of dyes (5 μ L, 20X) with DNA (1 ng) and dye intensity was measured while dye/DNA was still in solution on a glass substrate.

DNA (1 ng) was pipetted onto the glass surface and allowed to dry and then the dyes were added onto the DNA and the fluorescence was measured in solution. Figure 4.3 shows the background signal of the dye on the glass substrate compared with the dye/DNA complex. SG and RS the background signal when no DNA was present was higher than when DNA was present. With GG there was a slight increase in the dye/DNA signal. As SG has such a high fluorescent enhancement when DNA is present around 1000-1500 fold increase [1, 5], it is unusual for there to be a decrease in the signal for the dye/DNA complex. This may have been due to the type of substrate if there was any reflection of the glass surface interfering with the intensity signal. Another reason may be due to the sensitivity of the detection. As the Gel Doc™ was used with the blue tray the detection parameters do not excite SG at the maximum excitation or detect at the highest emission wavelength.

Figure 4.4 and 4.5 show the different intensity signals of the dyes' fluorescence on various substrate surfaces for GG and SG respectively. The signals are compared against the

dye/DNA complex to determine if certain surfaces results in a higher fluorescent enhancement. For GG there was a higher fluorescent enhancement on the glass surface (3.7) compared with Parafilm (2.0) and plastic (1.5). When looking at the enhancement of SG on different surfaces glass had the highest enhancement at 24, much higher than GG. On the other substrates SG had an enhancement level of 1.2 for Parafilm and 5.1 for plastic. Both glass and plastic substrates for SG had a higher enhancement in comparison to GG. Parafilm was the only substrate where the enhancement was higher for GG than SG.

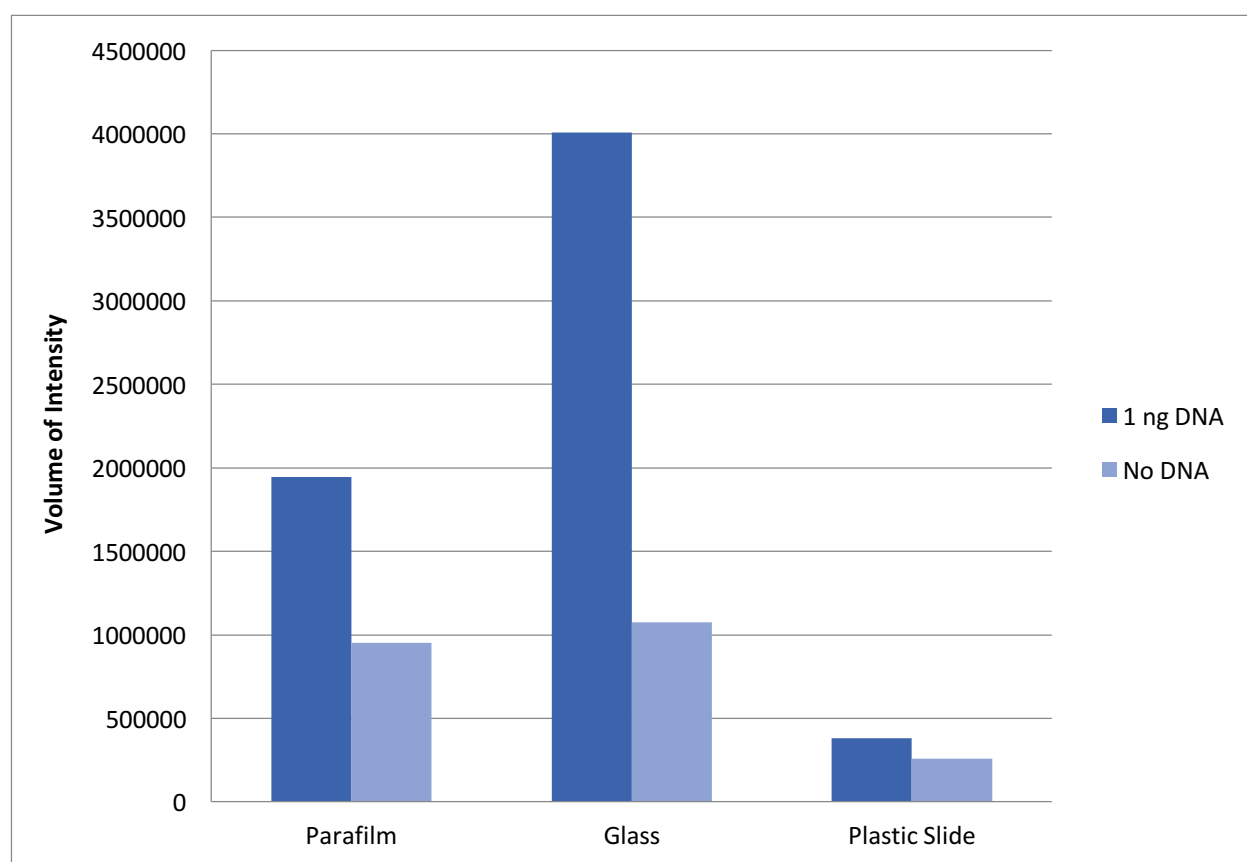


Figure 4.4: Background signal compared with 1 ng of DNA signal on different surfaces using GG (20X, 5 μ L).

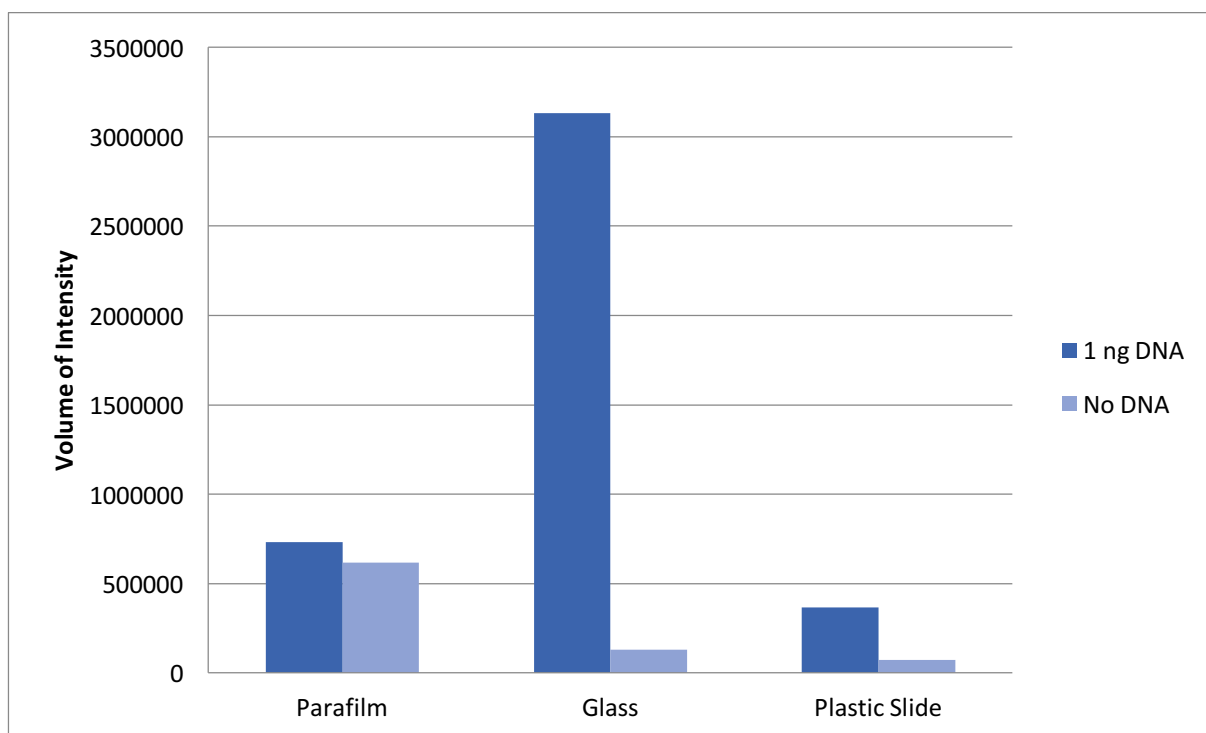


Figure 4.5: Background signal compared with 1 ng of DNA signal on different surfaces using SG (20X, 5 μ L).

As SG and GG showed the highest enhancement on a glass substrate, they were used to test with other DNA binding dyes with varying amounts of DNA. Figure 4.5 shows the signal of different dyes binding with varying amounts of DNA along with the line of best fit for signal versus concentration for each dye. The R^2 values obtained from the line of best fit are presented in Table 4.4 showing the linearity of the dyes fluorescent signal. The R^2 values for surface based detection was compared with the R^2 values obtained within the previous Chapters for within gel based detection.

Table 4.4: Linearity of the dyes fluorescent signal when staining DNA on a surface in comparison to DNA staining within agarose gel medium.

Dye	R^2 (surface)	R^2 (post-gel staining)*	R^2 (Pre-gel staining)*
SG	0.8697	0.9409	0.9334
RS	0.3337	0.9394	0.6338
EG	0.721	N/A	N/A
DD	0.7264	0.8862	0.9748
GG	0.7433	0.8442	0.6791
*denotes results obtained from previous work within Chapter 2. EG was not assessed as a dye used for gel staining hence no results for the linearity of EG within a gel medium			

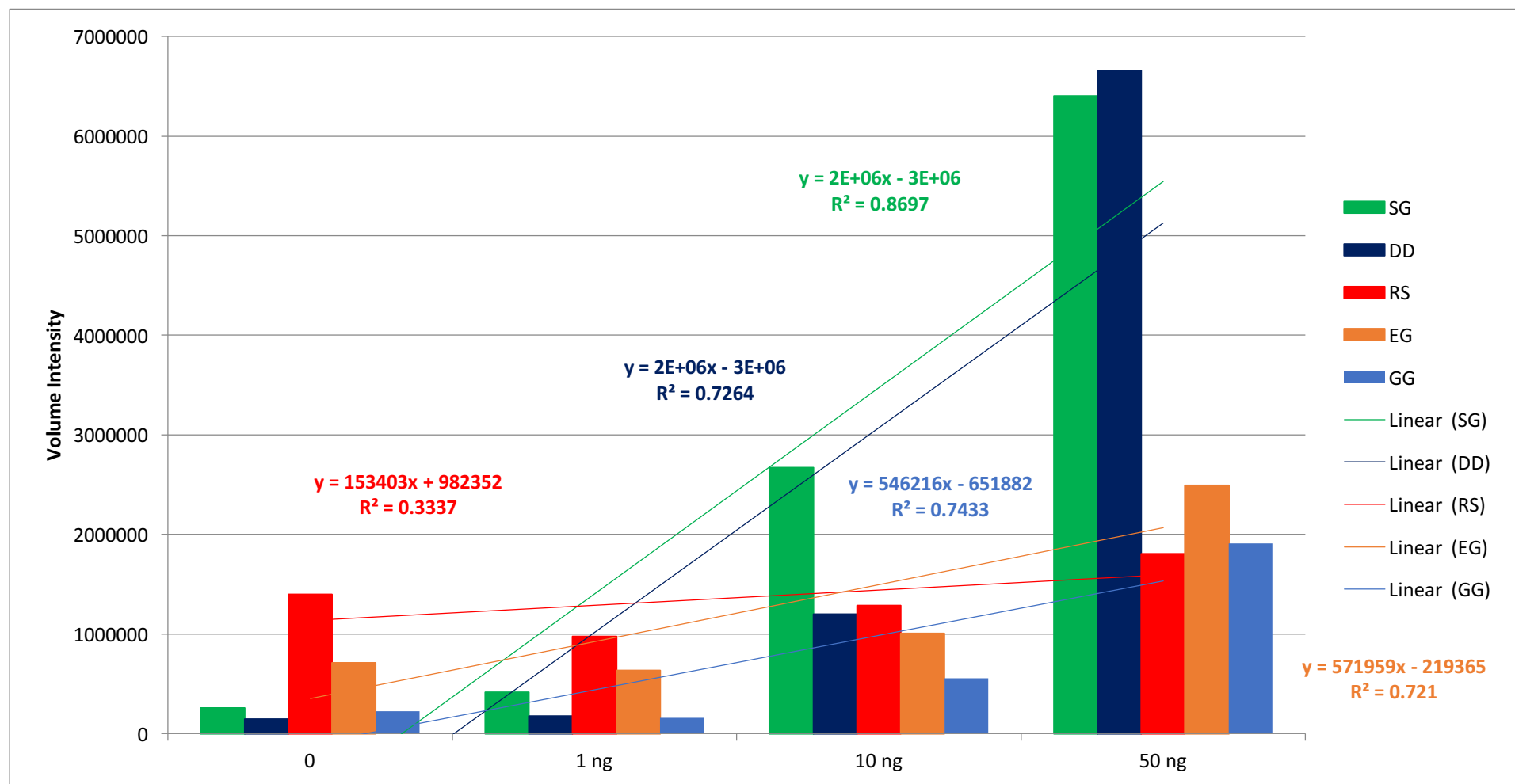


Figure 4.6: Signal of binding dyes with varying amounts of DNA with a background control (no DNA) using the dyes at 20X concentration (5 μ L) detection using Gel Doc™ EZ Imager, lane band analysis tool.

SG and DD had the highest signals at 50 ng of DNA compared with RS, GG and EG. RS showed little variation between the different amounts of DNA and the background signal of the dye itself. The assumption could then be made that the dye was naturally fluorescent with the intrinsic fluorescence being so high. This was also supported with the R^2 value of RS being 0.33, showing that there was not a linear relationship between the amounts of DNA and the intensity of the DNA/dye signal. This value was substantially different when comparing it to the R^2 value obtained in Chapter 2 for DNA/gel detection which was 0.63 and 0.93 for the different gel staining methods.

All other dyes had R^2 values above 0.7 showing a weak linearity of the dyes. The values however were lower when compared with the R^2 values obtained with gel staining which were all above 0.8 for post staining. One reason for the lower R^2 values obtained could have been due to there being no DNA amounts between 10 and 50 ng unlike in the gel staining study there were more amounts of DNA investigated.

Figure 4.7 shows the comparison of the DNA signals in a gel medium compared with on a surface (glass) for detection using the Gel Doc™ EZ Imager. The background signal was much higher on the surface compared with the gel. DD had the highest signal on the surface detection compared with the other dyes tested. GG had a much higher signal in the gel compared with surface detection at 50 ng and 10 ng; the signal at 1 ng was higher for the surface compared with the gel.

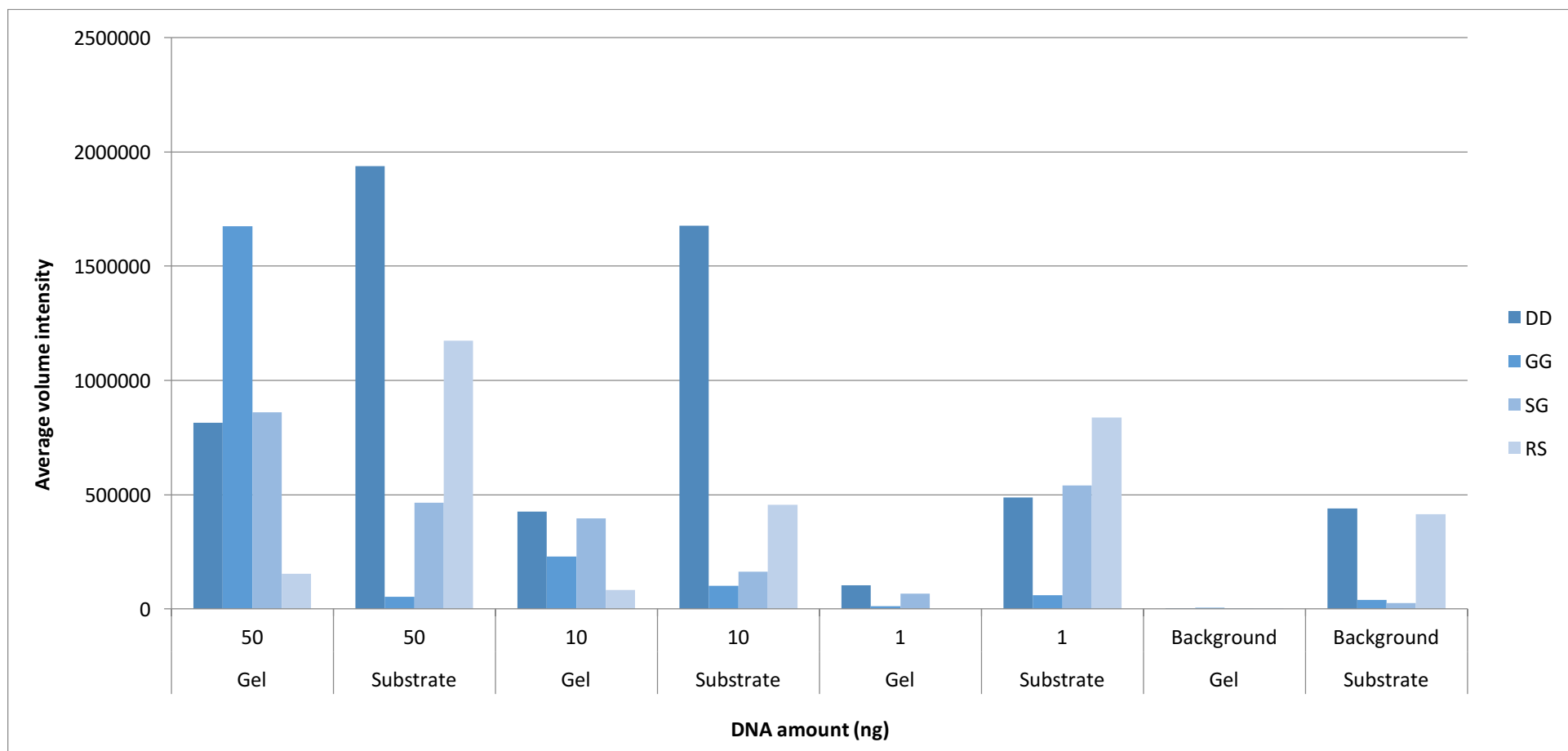


Figure 4.7: Comparison of DNA binding dyes signal (1X concentration) within a gel medium (1% agarose) and on a surface (glass) at varying DNA amounts, undertaken in triplicate.

4.2.3 Detection of DNA within fingerprints

The aim of this section was to try and determine the amount of DNA within fingerprints and whether DNA can become visible using the DNA binding dyes, not as a method of enhancement.

The amount of DNA within fingerprints was investigated using the fluorescent DNA binding dyes SG and GG. A negative control was used in order to determine what percentage of the signal was from the background and what was from the fingerprint itself. Figure 4.8 shows the fingerprint signals on surfaces that have been pre-treated to reduce the amount of background fluorescence due to bacterial DNA present on the surface. The results show a higher signal for those fingerprints deposited onto a surface that had been washed and UV treated compared with washing only. These two treatments were then compared with a non-treated surface in which the dye was allowed to dry over the fingerprint before detection of fluorescence. Most of the fingerprints had lower signals for the dried marks compared with the two treatments. The amount of DNA was then calculated based on the equation of the line of best fit (Figure 4.6) shown in Table 4.5. The values range from 1.38-1.76 ng across the different treatments.

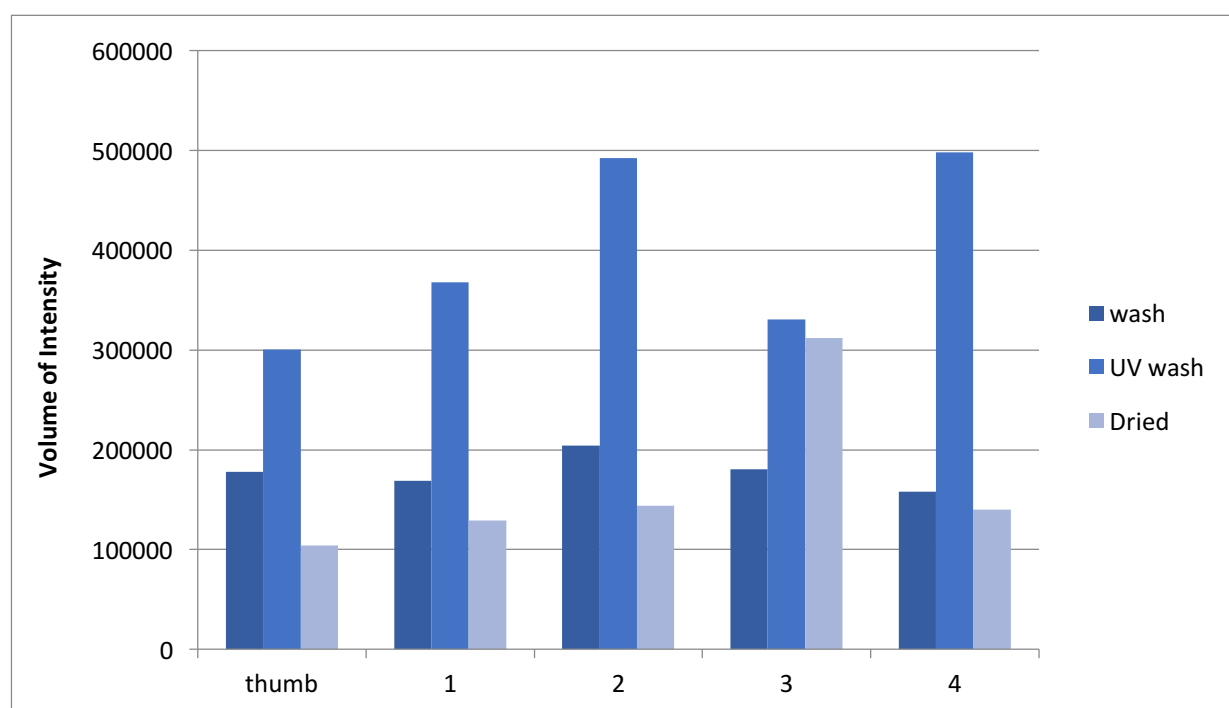


Figure 4.8: Volume intensity signal detected within fingerprints using GG (20X, 5 μ L) after different treatments on glass substrate. The values shown are minus the negative control (dyes intrinsic fluorescence) 1 indicates index finger, 2 middle, 3 ring and 4 pinky.

Table 4.5: Calculation of the amount of DNA present within fingermarks stained with GG (based on values in Figure 4.5) on substrates that have been treated

Sample	Wash	UV wash	Dried
Thumb	1.52	1.38	1.38
Finger 1	1.50	1.43	1.43
Finger 2	1.57	1.46	1.46
Finger 3	1.52	1.76	1.76
Finger 4	1.48	1.45	1.45
Equation used for calculation of DNA amount, $y = 546,216x - 651,882$, from Figure 4.5, fingerprint intensities minus the negative control was used in these calculations			

Figure 4.9 compares the fluorescent signal of fingermarks from the left and right hand using GG as the binding dye. A negative control was taken to determine the level of intrinsic fluorescence of the dye itself and of the background signal (potential bacterial DNA). The fingerprint that had the highest signal was from the 4th finger on the left hand (pinky) which has the smallest surface area in comparison to the other fingers and thumb. The amount of DNA that was present was then determined based on the equation of line of best fit (Figure 4.6) for GG values are shown in Table 4.6. The values range from 1.5-1.9 ng of DNA. The values seemed to vary between fingers and between left and right hand with no clear distinctions.

Table 4.6: Calculated amount of DNA present within fingermarks (Figure 4.6 values) based on the line of best fit equation for SG (Figure 4.5).

Sample	Left hand (ng)	Right hand (ng)
Thumb	1.67	1.59
Finger 1	1.64	1.57
Finger 2	1.50	1.58
Finger 3	1.52	1.58
Finger 4	1.93	1.65
Equation used for calculation of DNA amount $y = 2 \times 10^6 x - 3 \times 10^6$, fingerprint intensities minus the negative control was used in these calculations.		

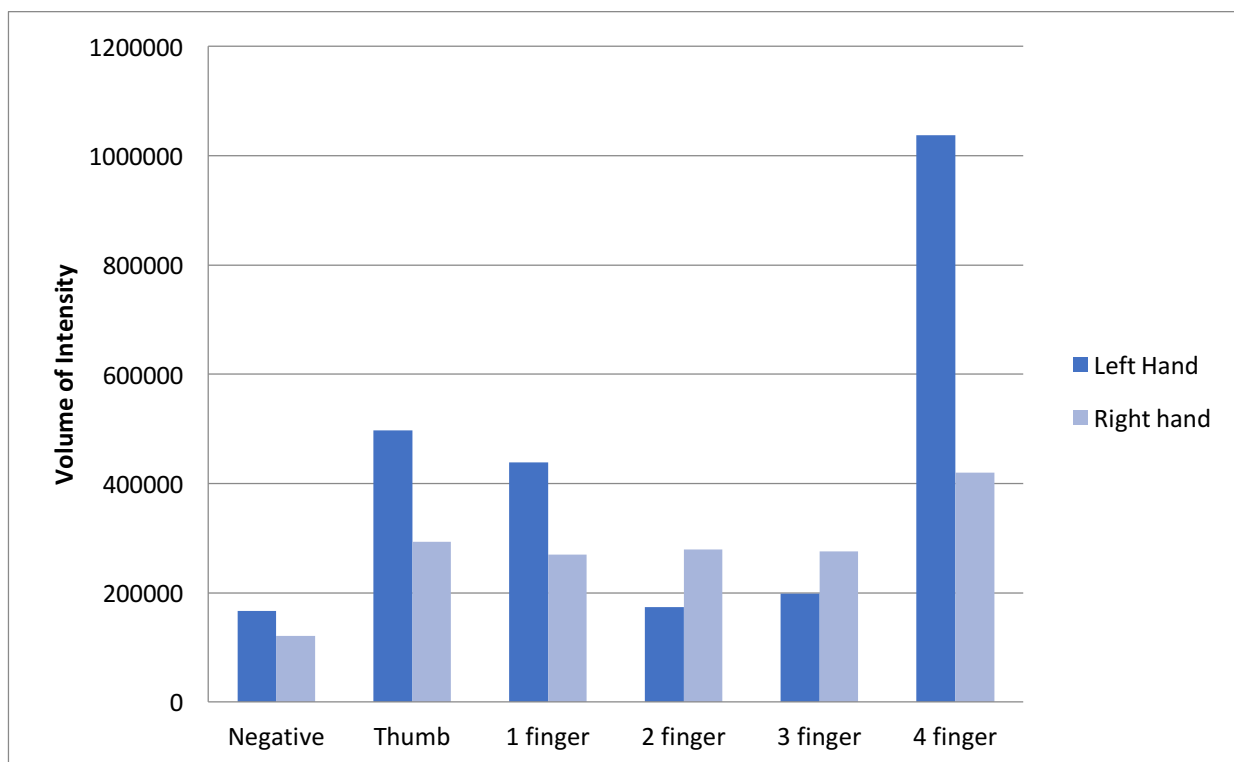


Figure 4.9: Comparison of left and right hand fingerprints stained with SG at 40X concentration (5 μ L) on a glass substrate. The values shown are minus the negative control (dyes intrinsic fluorescence) 1 indicates pointer finger, 2 middle, 3 ring and 4 pinky.

Other results related to the detection of DNA within fingerprints using fluorescent dyes was presented at the 25th *International Society of Forensic Genetics* (see Appendix C, Figure C-24, for poster presentation), conference proceedings was also published. Details of the paper are listed below and the article itself appears on the following pages.

Alicia M. Haines, Shanan S. Tobe, Hilton J. Kobus, Adrian Linacre, **Detection of DNA within fingerprints**, *Forensic Science International: Genetics Supplement Series*, **4** (2013), e65-e66


Citations: **1**


Statement of Authorship

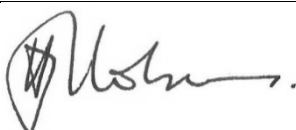
Title of Paper	Detection of DNA within fingerprints
Publication Status	Published 2013
Publication details	Published in <i>Forensic Science International: Genetics Supplement Series</i>


Author Contributions

By signing the Statement of Authorship, each author certified that their stated contribution to the publication is accurate and that permission is granted for the publication to be included in the candidate's thesis.

Name of Principal Author (Candidate)	Alicia M. Haines		
Contribution to the paper	Designed experimental method, performed all laboratory work and analysis, drafted the manuscript, edited manuscript and acted as corresponding author		
Signature		Date	August, 2016

Name of Co-Author	Shanan S. Tobe		
Contribution to the paper	Limited editing on manuscript		
Signature		Date	August, 2016

Name of Co-Author	Hilton J. Kobus		
Contribution to the paper	Edited manuscript		
Signature		Date	August, 2016

Name of Co-Author	Adrian Linacre		
Contribution to the paper	Helped design study and edited manuscript		
Signature		Date	August, 2016



Detection of DNA within fingerprints



Alicia M. Haines^{a,*}, Shanan S. Tobe^a, Hilton Kobus^b, Adrian Linacre^a

^a School of Biological Sciences, Flinders University, Adelaide, Australia

^b School of Chemical and Physical Sciences, Flinders University, Adelaide, Australia

ARTICLE INFO

Article history:

Received 23 August 2013

Accepted 2 October 2013

Keywords:

Fingerprint detection

Fluorescence

GelGreen

Latent DNA

SYBR Green I

ABSTRACT

DNA is deposited onto a surface by touch yet few means have been developed for its *in situ* detection. A range of dyes are available that bind to DNA at high specificity and here we report on the use of two of these dyes to detect latent DNA. SYBR[®] Green I and GelGreen were used to detect DNA within fingerprints after fingers and thumbs were pressed onto a range of substrates such as Parafilm[®]. A solution of dye was then pipetted onto the mark and allowed to dry briefly. There was a high level of fluorescence where the fingerprint was present indicating the dye had bound to DNA however a low level of fluorescence was present in the negative controls. To determine whether this background fluorescence was due to bacteria present on the substrates the dyes were pipetted onto a bacterial culture and the level of fluorescence was observed. It was found that SYBR[®] Green I had a higher level of fluorescence compared with GelGreen[™] and that both dyes fluoresce when in the presence of bacterial cells. By altering the volume and concentration of dye, ridge detail within the fingerprint may be observed allowing for the possibility of not only detecting latent DNA but also using this method for human identification and fingerprint comparison.

© 2013 Elsevier Ireland Ltd. All rights reserved.

1. Introduction

Latent DNA at crime scenes is collected by swabbing areas that have a high potential for the presence of DNA; substrates include door handles, phones and objects that have been used in an assault. These swabs are then submitted to a laboratory for DNA extraction and profiling. An issue with this process is that the majority of swabs produce no profile as the amount of DNA present is too low; one reason being that most of the DNA is lost during the extraction process [1]. To be able to visualize latent DNA at crime scenes, specifically touch DNA, would result in a targeted approach for the collection of DNA samples and a more efficient method. Bright [2] suggests that epithelial cells are sloughed off the skin surface and transferred onto various substrates by touch and that these cells are keratinised and lack nuclei; the DNA present on the surface is either present as a free molecule (cell free DNA), or within a cell membrane [3,4]. Currently there are techniques that can detect certain types of biological fluids such as semen using different wavelengths of light which can cause fluorescence. Chemical reagents such as luminol can be used for blood detection and amylase tests for saliva, these methods however do not detect DNA [5]. For the detection of latent fingerprints there are many

techniques available such as powder dusting and cyanoacrylate fuming on non-porous substrates and reagents such as DFO and ninhydrin that react with the amino acids on porous substrates [6]. There are currently no methods that enhance fingerprints by detecting the DNA present. SYBR Green I (SG) is a dye used in gel electrophoresis for the detection of DNA as it intercalates between the base pairs of DNA. When SG is in the presence of DNA there is approximately a 1000 fold increase in the emission of fluorescence. SG has a maximum excitation wavelength of 494 nm and a maximum emission wavelength at 520 nm and can also permeate the cell membrane [7,8]. The aim of this study was to determine whether dyes such as SG can detect DNA within fingerprints.

2. Methodology

2.1. Dye preparation

SYBR[®] Green I (Invitrogen) and GelGreen[™] (Biotium) were diluted to varying working solution concentrations in sterile water.

2.2. Substrate preparation

Plastic slides, glass slides and Parafilm[®] were placed under UV before use. Dye solution (5 μ L) was pipetted onto the surface of the substrate and fluorescence was measured either in solution, after the dye had dried or after the dye was washed off the surface with H₂O.

* Corresponding author at: Flinders University, GPO Box 2100, School of Biological Sciences, Adelaide, SA 5001, Australia. Tel.: +61 8201 5003.
E-mail address: alicia.haines@flinders.edu.au (A.M. Haines).

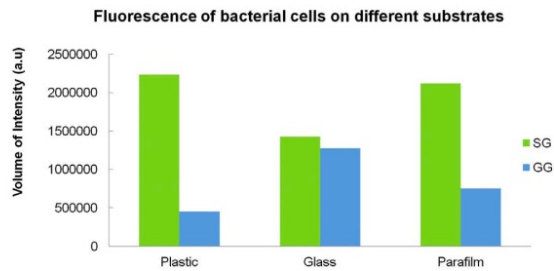


Fig. 1. Volume of intensity of SYBR Green 1 (SG) and GelGreen (GG) (5 μ L of $20\times$ solution in H_2O) in the presence of *E. coli* DH5 α in PBS solution (1 μ L $\sim 10^6$ cells) with fluorescence measured with dye in solution on substrate.

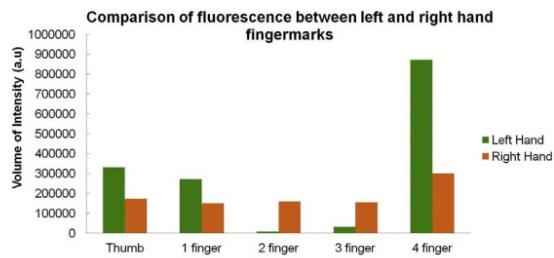


Fig. 2. Volume of intensity of fingerprints on Parafilm[®] where the dye GG (5 μ L of $40\times$ solution in H_2O) was pipetted onto the surface and allowed to air dry.

2.3. Visualization

The intensity of fluorescence was measured using the Bio-Rad Gel Doc EZ Imager. Fluorescence of the negative controls was subtracted from the samples fluorescence.

3. Results and discussion

Fig. 1 shows that both dyes produce a high intensity of fluorescence when in the presence of bacterial cells (a potential cause of background fluorescence). It is shown that SG has a higher intensity than GelGreen as the dye can permeate the cell membrane [8]. Fig. 2 shows that there is fluorescence when a

fingerprint was present on the substrate and that there was a high variability between the marks created by different fingers. It is known that many factors may be involved in the deposition of DNA onto a surface such as substrate type, nature of contact, environmental factors and the individual depositing the DNA.

4. Concluding remarks

This study has found that DNA within fingerprints can be detected using the intercalating dyes SYBR[®] Green I and GelGreen[™] however it is unknown if the DNA detected is human or bacterial. It was also found that there was variability between the fluorescence when comparing fingerprints from left and right hands due to the individual depositing DNA, the duration and type of contact and the substrate surface.

Role of funding

Funding was provided by the Department of Justice, South Australia.

Conflict of interest

None.

References

- [1] F. Alessandrini, M. Cecati, M. Pesaresi, et al., Fingerprints as evidence for a genetic profile: morphological study on fingerprints and analysis of exogenous and individual factors affecting DNA typing, *J. Forensic Sci.* 48 (2003) 1–7.
- [2] J. Bright, S.F. Petricevic, Recovery of trace DNA and its application to DNA profiling of shoe insoles, *Forensic Sci. Int.* 145 (2004) 7–12.
- [3] A.R. Wickenheiser, Trace DNA: a review, discussion of theory, and application of the transfer of trace quantities of DNA through skin contact, *J. Forensic Sci.* 47 (2002) 442–450.
- [4] A. Linacre, V. Pekarek, Y. Swaran, et al., Generation of DNA profiles from fabrics without DNA extraction, *Forensic Sci. Int. Genet.* 4 (2010) 137–141.
- [5] N. Vandenberg, R.A.H. van Oorschot, The use of Piliight[®] in the detection of seminal fluid, saliva, and bloodstains and comparison with conventional chemical-based screening tests, *J. Forensic Sci.* 51 (2006) 361–370.
- [6] C. Lennard, Forensic sciences | fingerprint techniques, in: P.T. Alan, P. Colin (Eds.), *Encyclopedia of Analytical Science*, second ed., Elsevier, Oxford, 2005, pp. 414–423.
- [7] A.I. Dragan, R. Pavlovic, J.B. McGivney, et al., SYBR Green I: fluorescence properties and interaction with DNA, *J. Fluoresc.* 22 (2012) 1189–1199.
- [8] T. Ohta, S. Tokishita, H. Yamagata, Ethidium bromide and SYBR Green I enhance the genotoxicity of UV-irradiation and chemical mutagens in *E. coli*, *Mutat. Res.* 492 (2001) 91–97.

4.2.4 Specificity of the dyes

DNA binding dyes SG and GG were chosen to view their interaction with bacterial cells to mimic the background fluorescence before latent evidence (fingerprint etc.) has been deposited. Glass, plastic and parafilm were used as substrates. Figure 4.10 shows the signals of the dye/bacterial DNA complex on different substrate surfaces. SG had higher signals than GG on all three surfaces with the highest signal produced on the plastic surface. GG had the highest signal produced on the glass surface.

Different concentrations of bacterial DNA (cells/ μL) were placed onto a glass surface to see the difference in intensity at different DNA concentrations (Figure 4.11). The R^2 values show that there was a more linear relationship after the 10 min incubation (0.63) compared with the initial intensity signals (0.51). The intensity of the signals after the incubation period also resulted in higher fluorescence compared with the initial detection. This was likely due to there being more time for the dye molecules to bind to the bacterial DNA present on the surface.

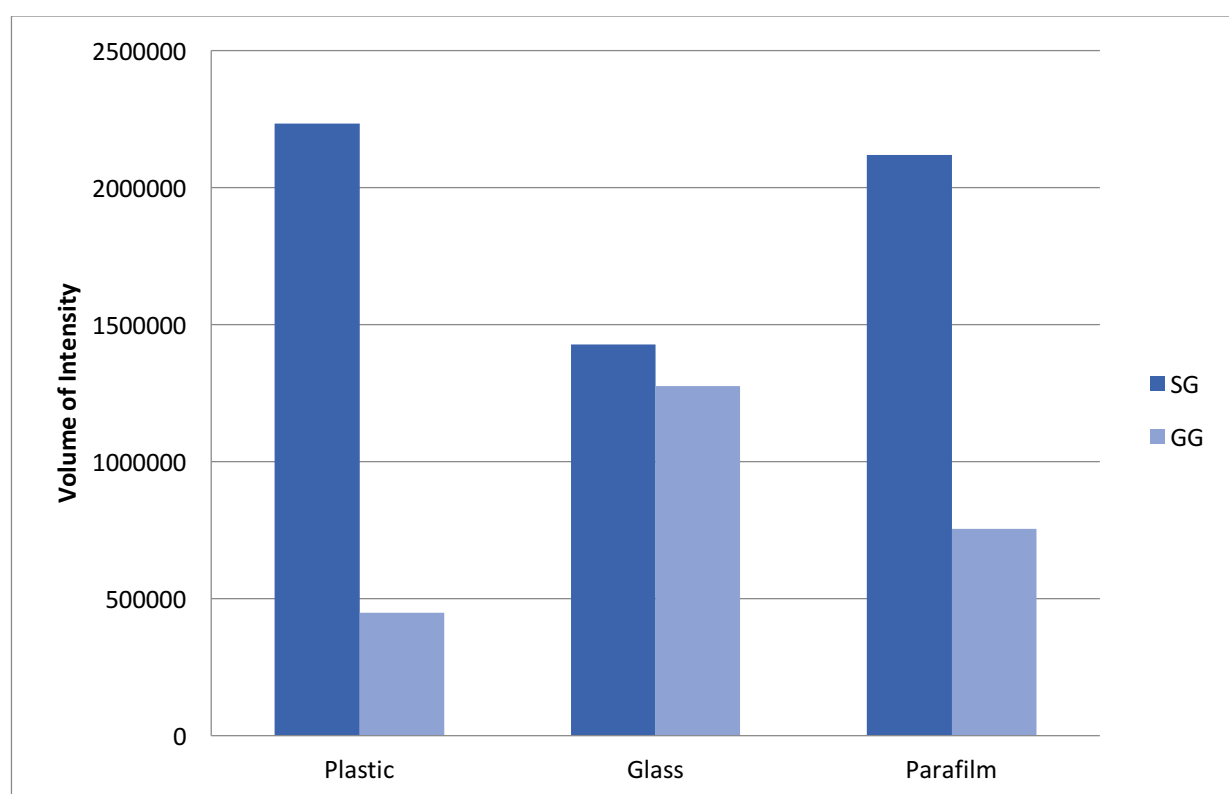


Figure 4.10: Comparison of bacterial signals (1×10^6 cells/ μL) on different substrates using both GG and SG binding dyes (20X, 5 μL), signal is shown minus background (intrinsic fluorescence of dye).

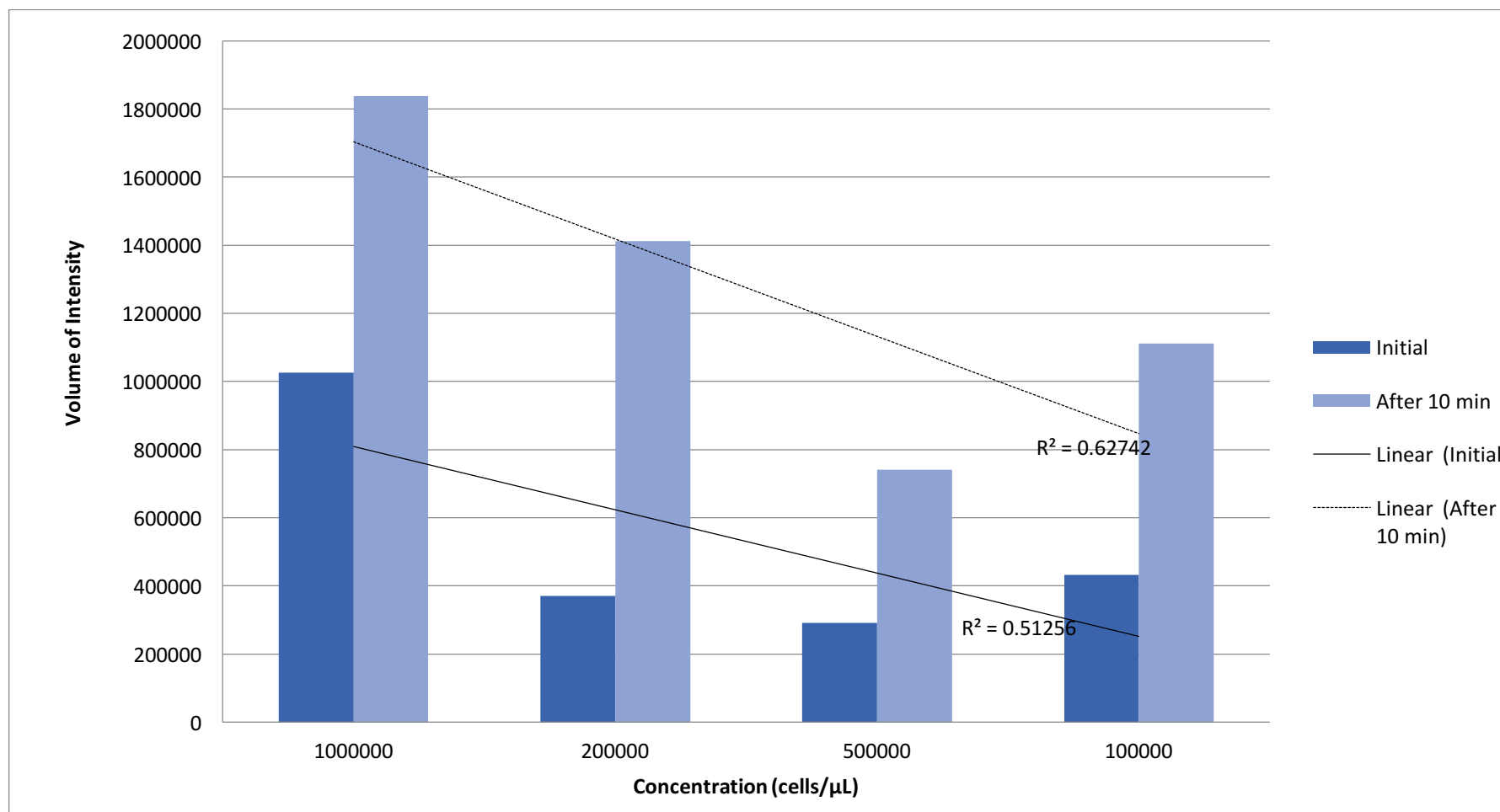


Figure 4.11: Intensity of signals from varying amounts of bacterial DNA (cells/μL) showing the initial signal and then the signal after 10 min incubation using SG binding dye (20X, 5 μL).

The specificity of the DNA binding dyes was also investigated by looking at the signals obtained when in the presence of proteins rather than DNA; minimizing other types of contaminants that could potentially be present on a surface before latent evidence is deposited. The binding intensity of the dyes with BSA is shown in Figure 4.12 compared with the background signal of the dye itself (intrinsic fluorescence). Figure 4.13 shows the signal for BSA only (BSA/dye signal minus background). In Figure 4.13 it can be seen that RS signal was quenched in the presence of BSA as the signal was lower for BSA/dye than for dye alone. All other dyes show an increase in the intensity when in the presence of BSA. DD had the highest signal in the presence of BSA followed by EG and then SG. BSA is a complex protein which might be why there are potential binding sites for the dyes (EG, SG, DD). This was also a relatively high concentration of protein and it would be unlikely to have this level of concentration on surfaces.

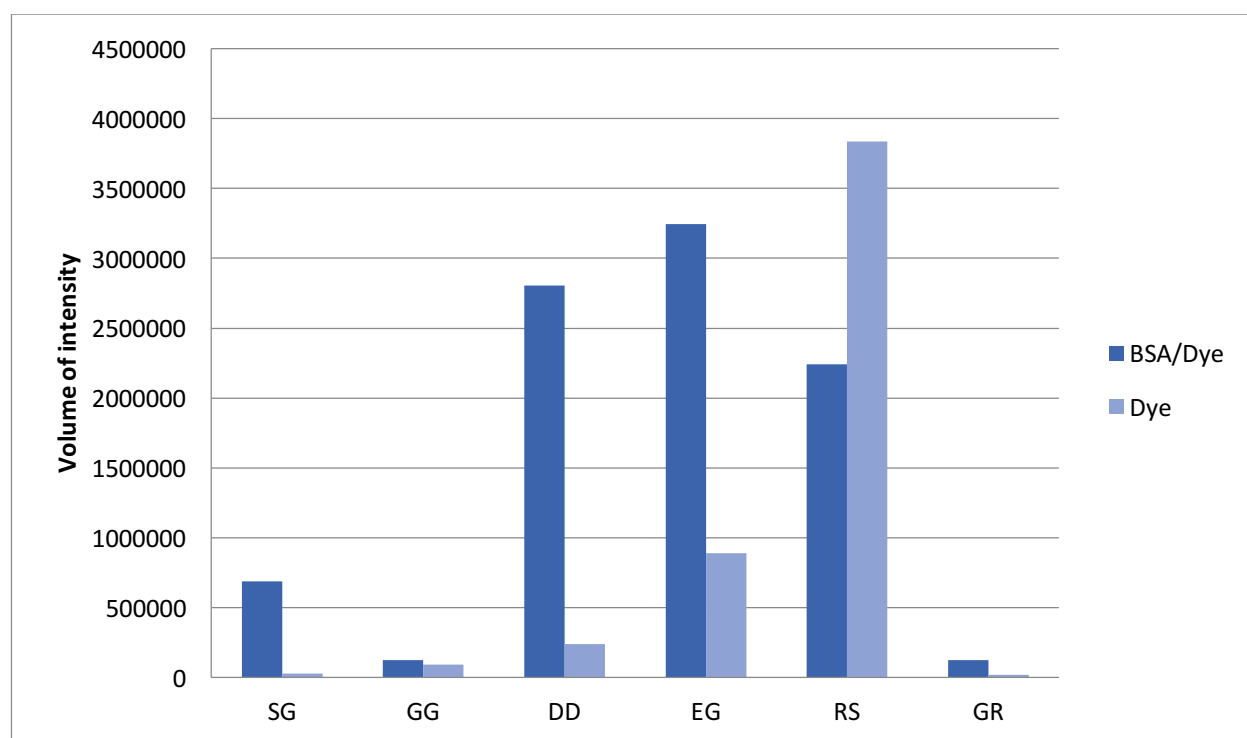


Figure 4.12: Comparison of background intensity to BSA (2 $\mu\text{g}/\mu\text{L}$) intensity using six DNA binding dyes at 20X concentration (5 μL) on a glass substrate.

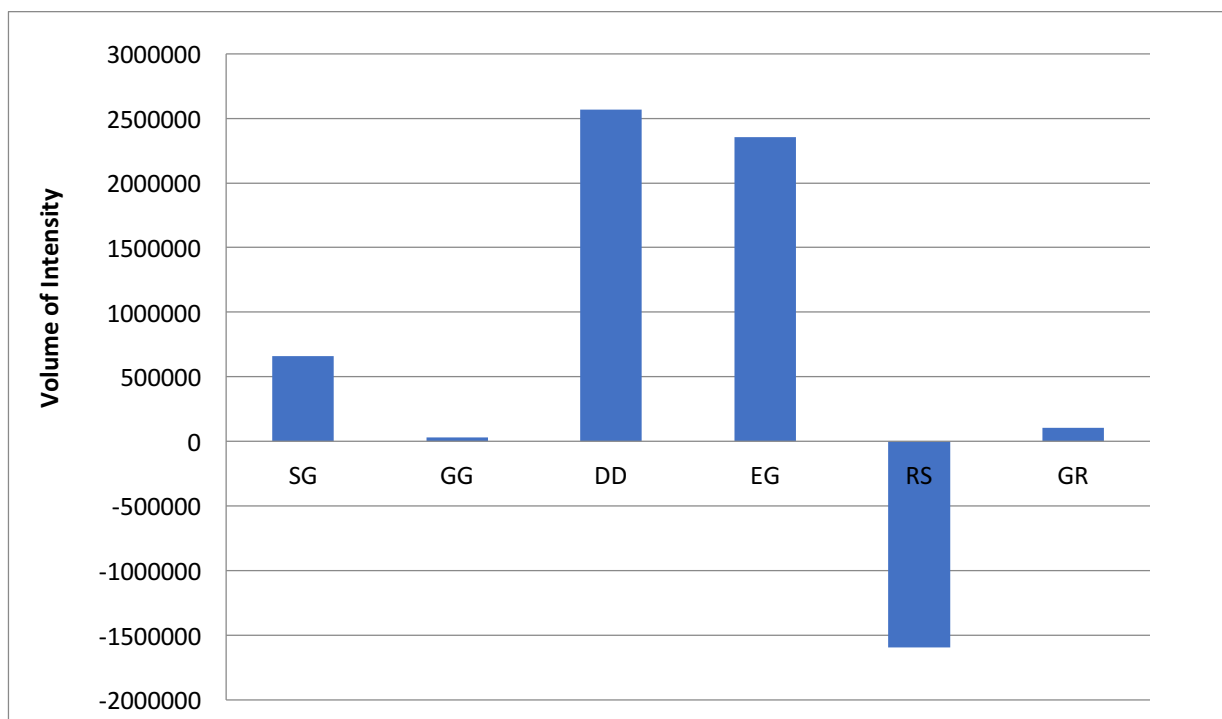


Figure 4.13: Intensity of BSA signals (2 $\mu\text{g}/\mu\text{L}$) minus the background signal using binding dyes at 20X concentration.

Figure 4.14 looks at the average volume intensity of the binding dyes in the presence of DNA and protein, both at 50 ng, and the intrinsic fluorescence of the dyes. RS had the highest background signal which was expected based on previous results, most likely due to the dye being naturally fluorescent. GG and GR had the lowest background signal. DD had the highest signal for DNA and RS had the highest signal with protein (due to the natural fluorescence of the dye). To determine which dyes had the highest intensity in the presence of DNA in comparison to the background signal, the enhancement of the dyes was calculated and shown in Figure 4.15. SG had the highest enhancement for DNA at 46 fold increase compared with the background signal, followed by DD at 16 and EG at 12. For protein, SG had 2.3 fold increase in signal intensity compared with DD at 1.2 and EG at 0.3. So the DNA binding dyes have interactions with protein but only minimal in comparison to their enhancement when in the presence of DNA. Figure 4.16 shows the enhancement of the dyes using a longer exposure time (10 s) which resulted in lower enhancement values for SG and DD but higher values for GG (from 4.2 to 6.5) and GR (2.1 to 3.6).

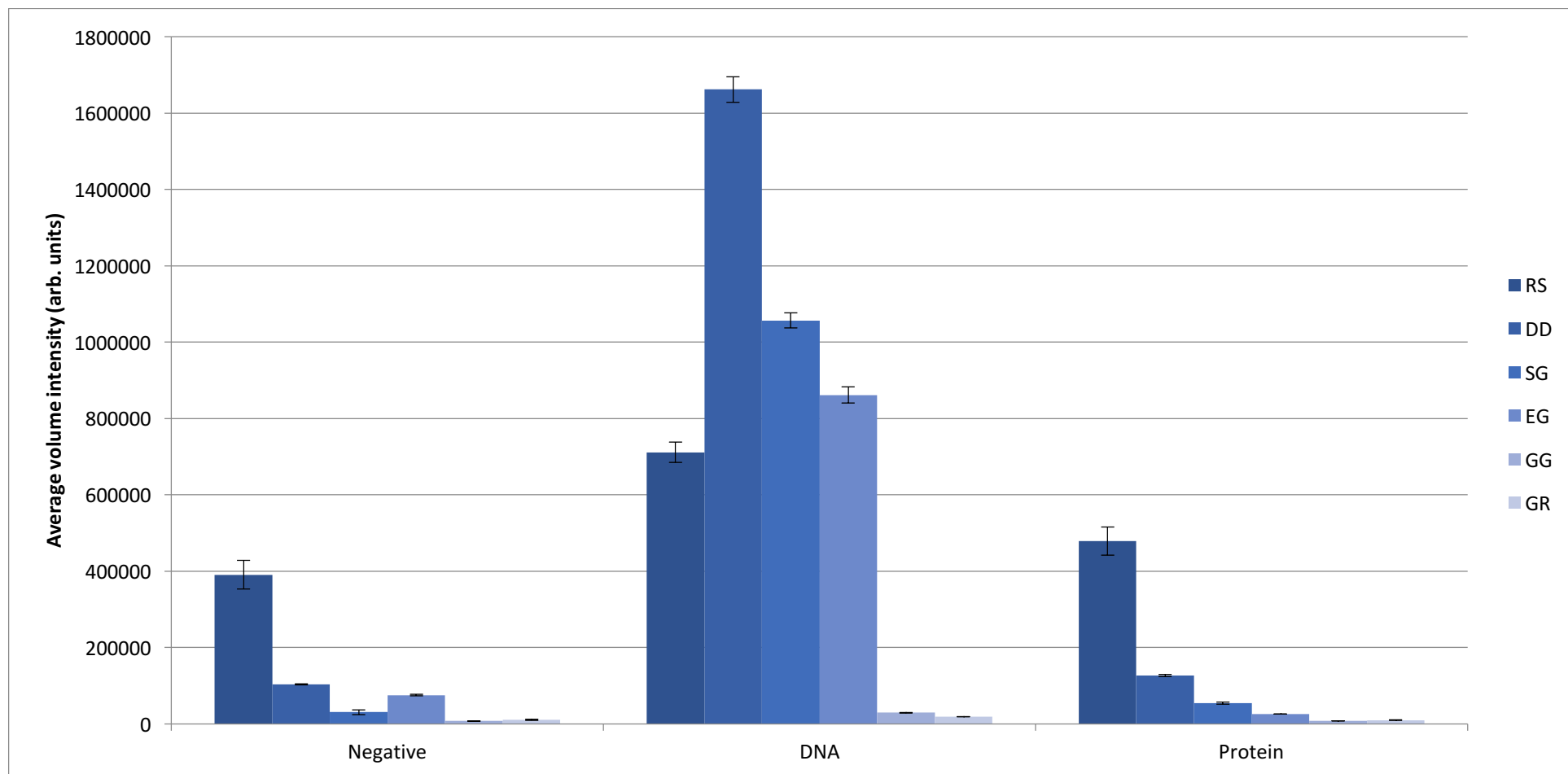


Figure 4.14: Average volume intensity of DNA binding dyes (5 μ L at 20X concentration) in the presence of DNA (50 ng), protein (BSA at 50 ng) and negative control (dye/H₂O) exposure time was at 1.2 s using Gel Doc™ lane band analysis tool. Results were undertaken in triplicate with error bars show 95% confidence.

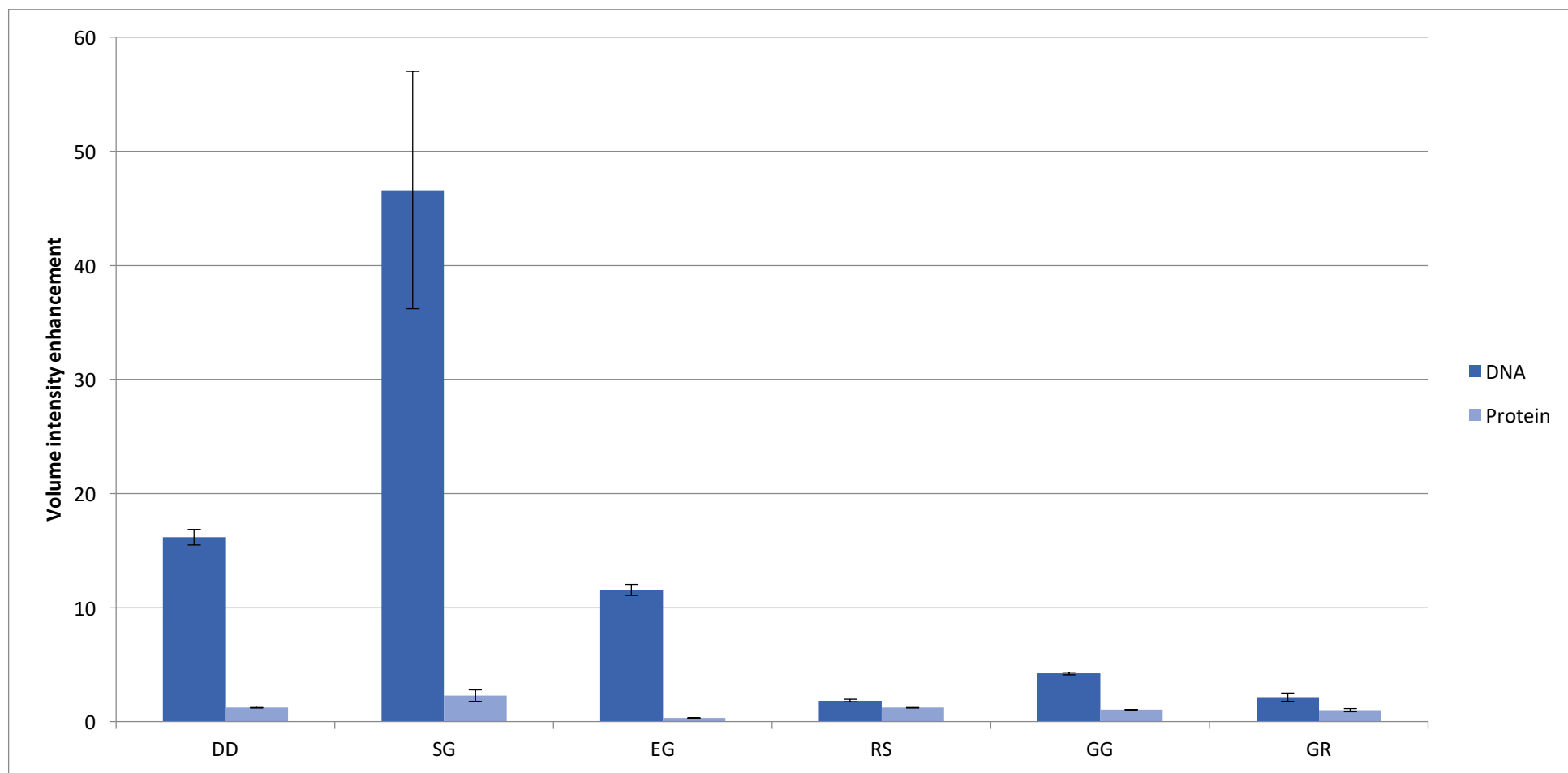


Figure 4.15: Average intensity enhancement of the binding dyes in the presence of DNA (50 ng) and protein (BSA at 50 ng) to the background of the dyes (intrinsic fluorescence) exposure time was at 1.2 s using Gel Doc™ lane band analysis tool. Results were undertaken in triplicate with error bars show 95% confidence.

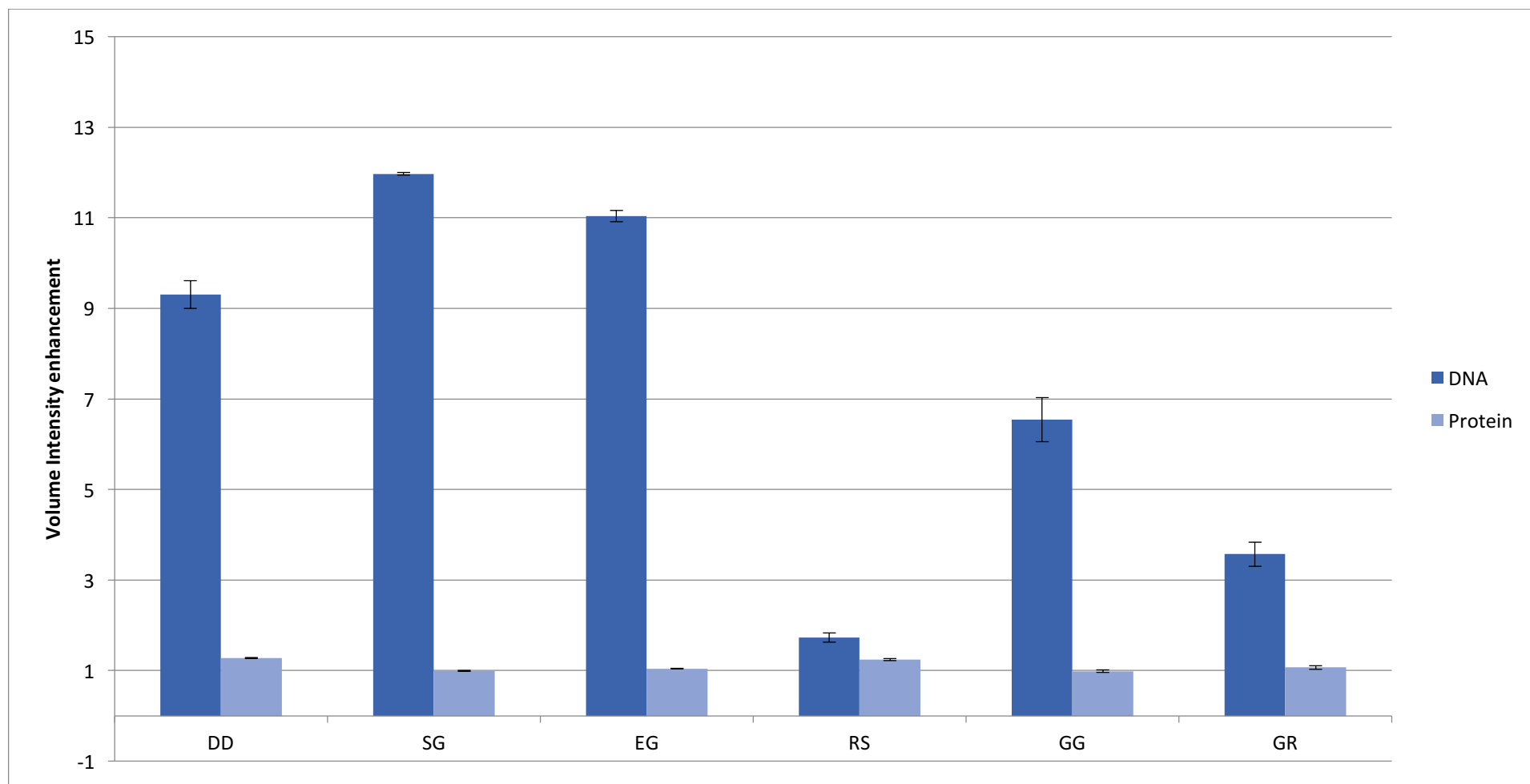


Figure 4.16: Average intensity enhancement of the binding dyes in the presence of DNA (50 ng) and protein (BSA at 50 ng) to the background of the dyes (intrinsic fluorescence) exposure time was at 10 s using Gel Doc™ lane band analysis tool. Results were undertaken in triplicate with error bars show 95% confidence.

4.2.5 Sensitivity of DNA/dye complex, detection

Due to the excitation and emission settings of the Bio-Rad Gel Doc™ EZ Imager, shown in Figure 4.17 A (blue transillumination) and Figure 4.17 B (UV transillumination), the SYBR Green molecules when intercalated with ds-DNA are not being excited at the maximum excitation wavelength (494 nm) and the emission is being detected after the maximum emission wavelength (521 nm). This is a plausible reason why the presence of DNA on the slides did not result in a 1000-fold increase in the level of fluorescence, as stated in the literature [1]. This could also account for the background fluorescence being so high.

For a more sensitive detection method a light source that can provide wavelength detection so that excitation is close to the maximum wavelength of the dye is required; the Polilight® provides broad spectrum white light with waveband selection using a range of interference filters. Interference filters provide a sharp cut-off and minimize overlap. To maximize contrast reflected excitation light must be excluded from the signal detection. Observation/measurement can therefore be made through cut-off or barrier filters. Scheme 4.4 shows schematically the excitation using the Gel Doc™ EZ Imager with a maximum excitation at 460 nm. The bandwidth of the excitation is unknown. Scheme 4.5 shows the detection using the Gel Doc™. Both these settings for excitation and emission are not centered to capture the dyes maximum fluorescent signal. Scheme 4.5 shows schematically the excitation using the Polilight® 490 nm waveband selection. The proportion of spectrum being excited is much greater compared with the Gel Doc™ settings. The Polilight® can also be used in conjunction with barrier filters and interference filters to detect the fluorescent signal of the dye/DNA complex at its maximum wavelength (Scheme 4.7).

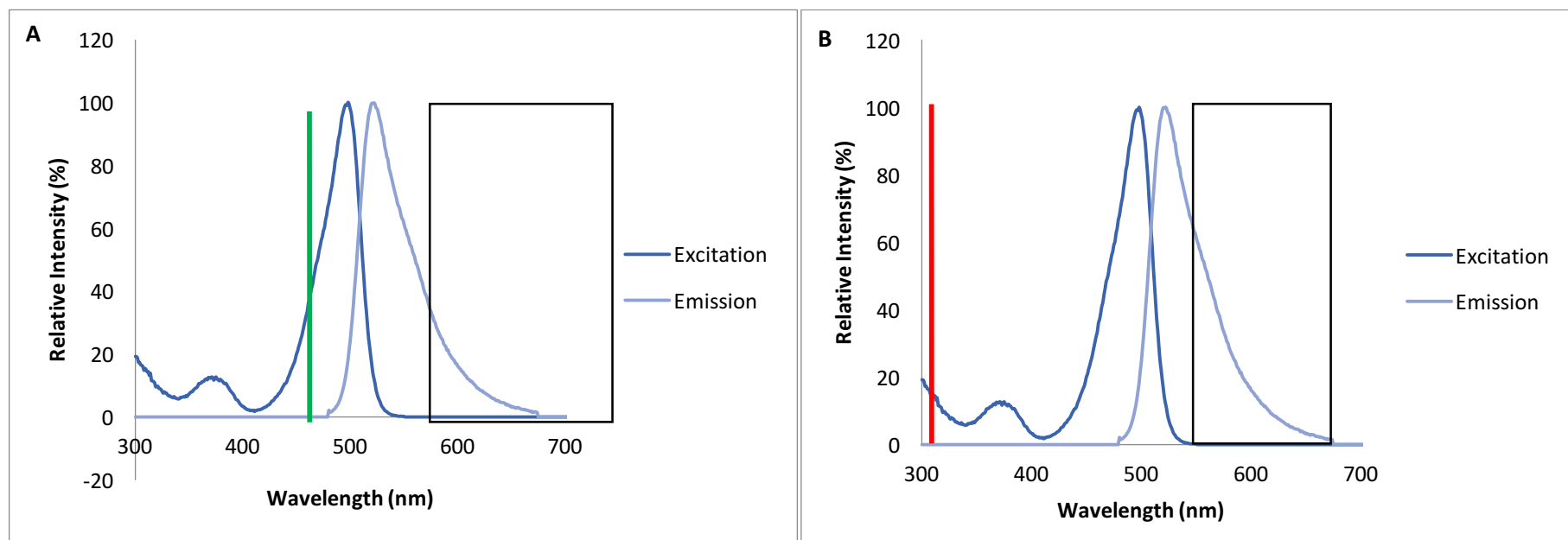
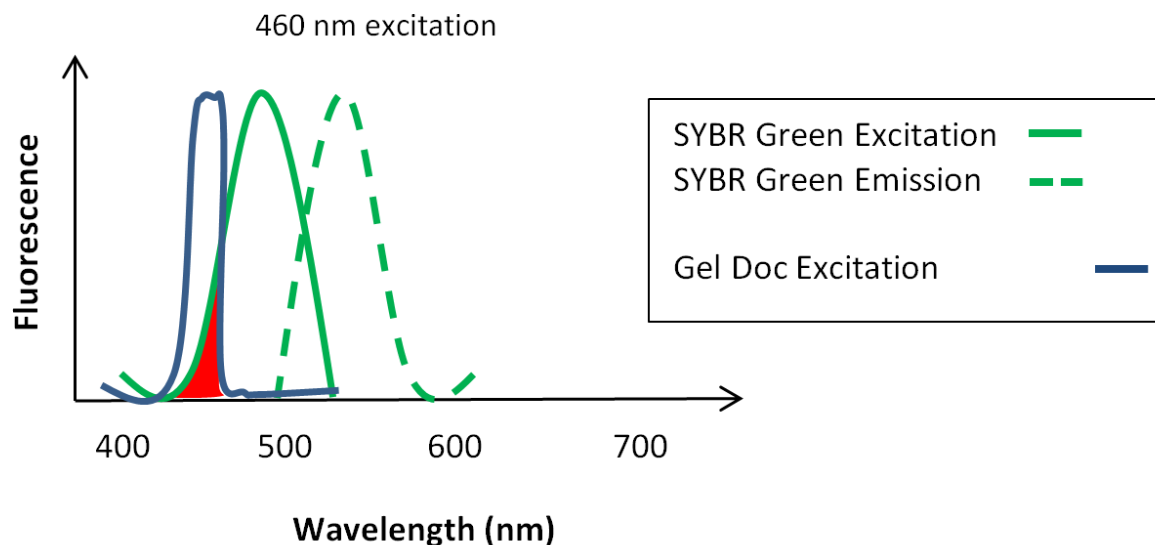
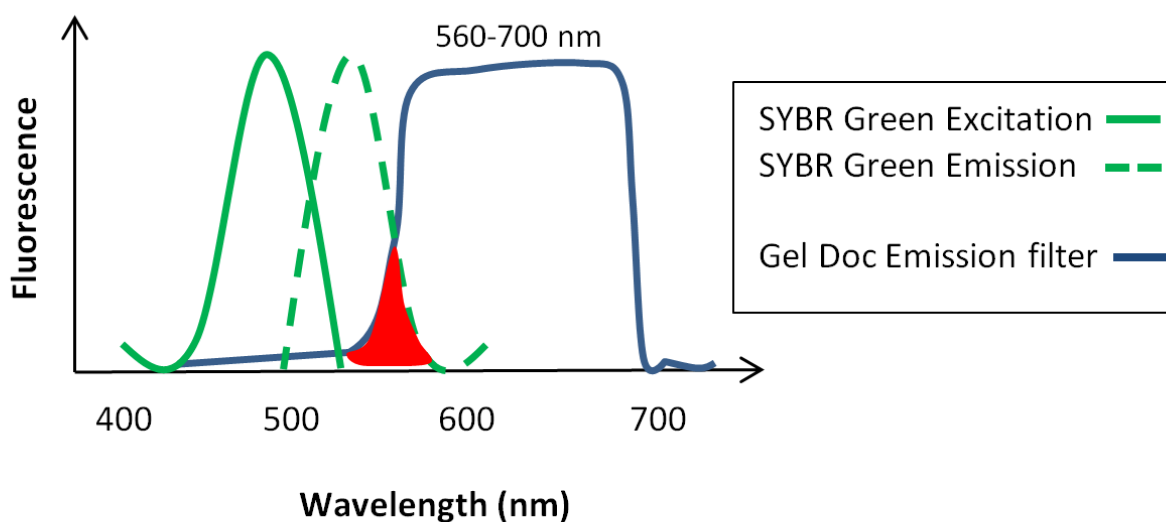


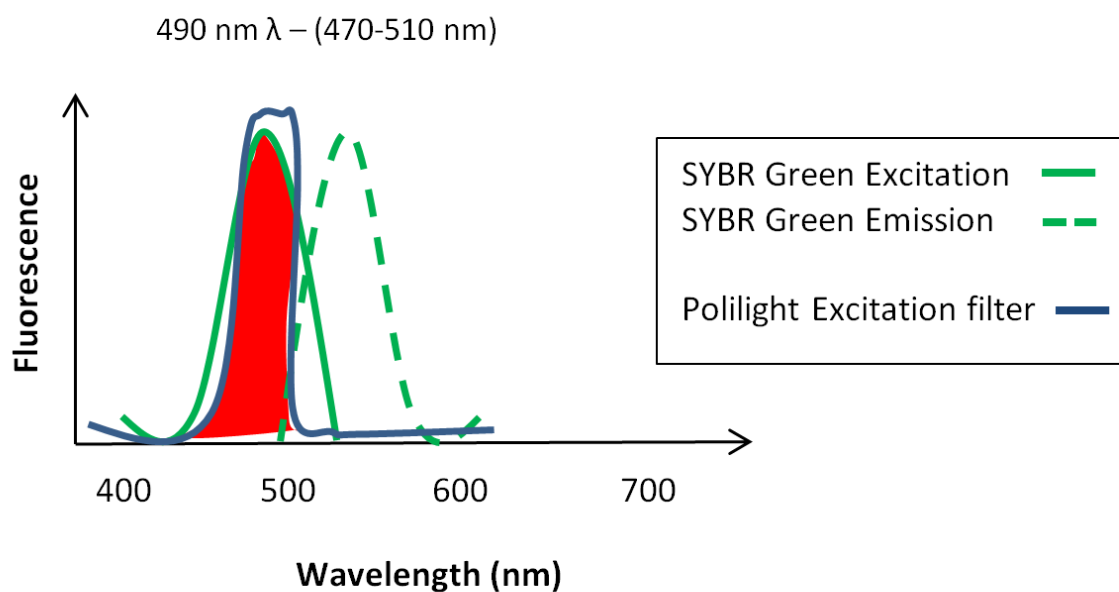
Figure 4.17: (A) Detection parameters of the Gel Doc™ EZ Imager in relation to the excitation and emission signals of SYBR® Green when using blue transillumination. Excitation at 460 nm (green band) and emission filter from 560-700 nm (black box). (B) Detection parameters of the Gel Doc™ EZ Imager in relation to the excitation and emission signals of SYBR® Green when using UV transillumination. Excitation at 302 nm (red band) and emission filter 535-640 nm (black box).



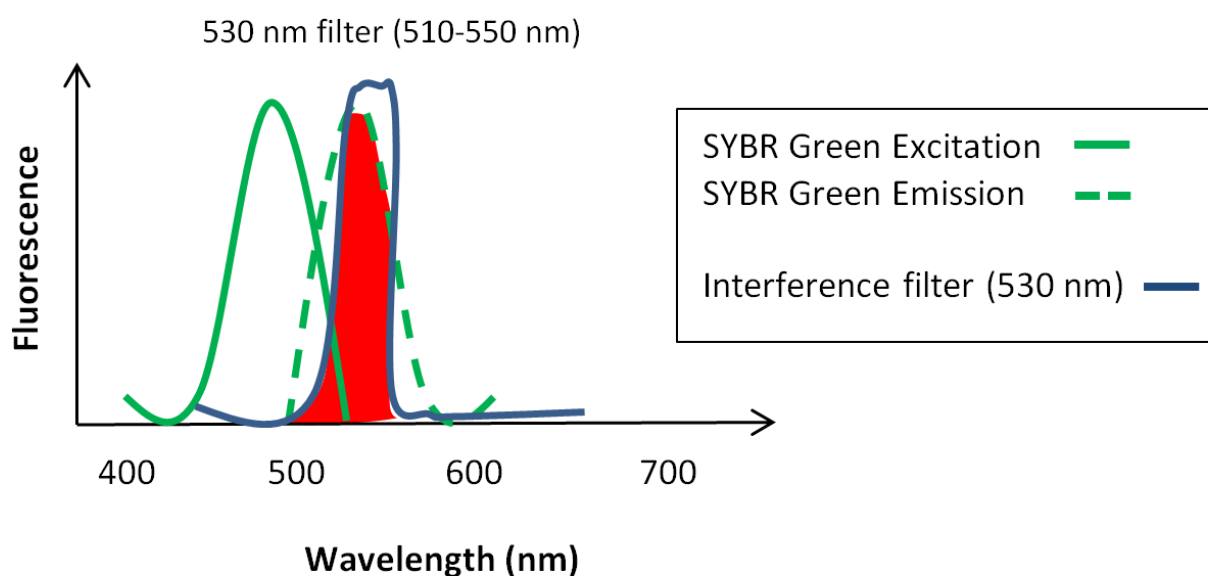
Scheme 4.4: Schematic representation of the excitation of SG with the Gel Doc™ EZ Imager settings the maximum excitation λ is at 460 nm; SG excitation is at 494 nm. The proportion of the SG excitation spectrum being excited with the Gel Doc™ is indicated in red.



Scheme 4.5: Schematic representation of the detection of SG emission signal with the Gel Doc™ EZ Imager settings, maximum emission λ is between 560-700 nm; SG emission is at 521 nm. The proportion of the SG emission detection with the Gel Doc™ is indicated in red.



Scheme 4.6: Schematic representation of the excitation of SG with the Polilight® the maximum excitation λ is centered at 490 nm with a 40 nm bandwidth (excitation between 470-510 nm); SG excitation is at 494 nm. The proportion of the SG excitation spectrum being excited with the Polilight® is indicated in red.



Scheme 4.7: Schematic representation of the emission detection of SG with an interference filter, maximum excitation λ is centered at 530 nm with a 40 nm bandwidth (emission detection between 510-550 nm); SG emission is centered at 520 nm. The proportion of the SG emission spectrum being detected with the interference filter is indicated in red.

4.4 Results and discussion (Polilight® detection)

4.4.1 Detection of DNA

To increase the sensitivity of excitation and detection of the dye/DNA complex the Polilight® in combination with associated filters (outlined in section 4.2.5) replaced the Gel Doc™. The intrinsic fluorescence of the dyes was then investigated using the Polilight® and detection using a SLR Nikon camera with cut-off filters (Figure 4.19) and interference filters (Figure 4.20) with varying exposure times.

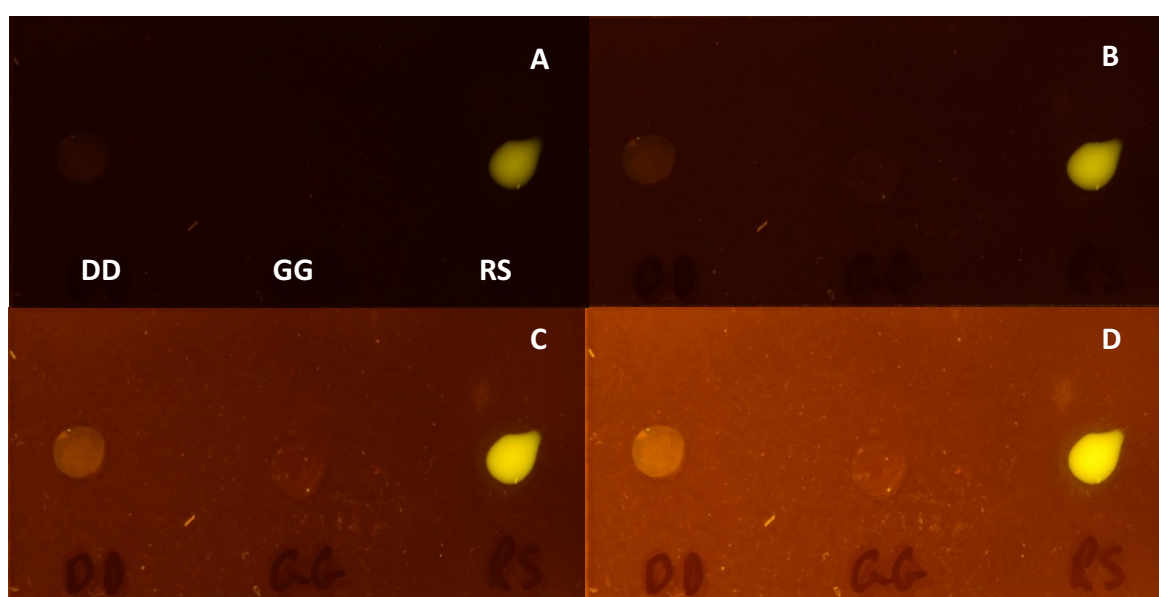


Figure 4.19: Intrinsic fluorescence of dyes DD, GG and RS without DNA present in a 20x H₂O solution with varying exposure times using a 550 nm cut-off filter; (A) exposure time 1/10 s, (B) exposure time 1/5 s, (C) exposure time 1/2 s, (D) exposure time 1 s.

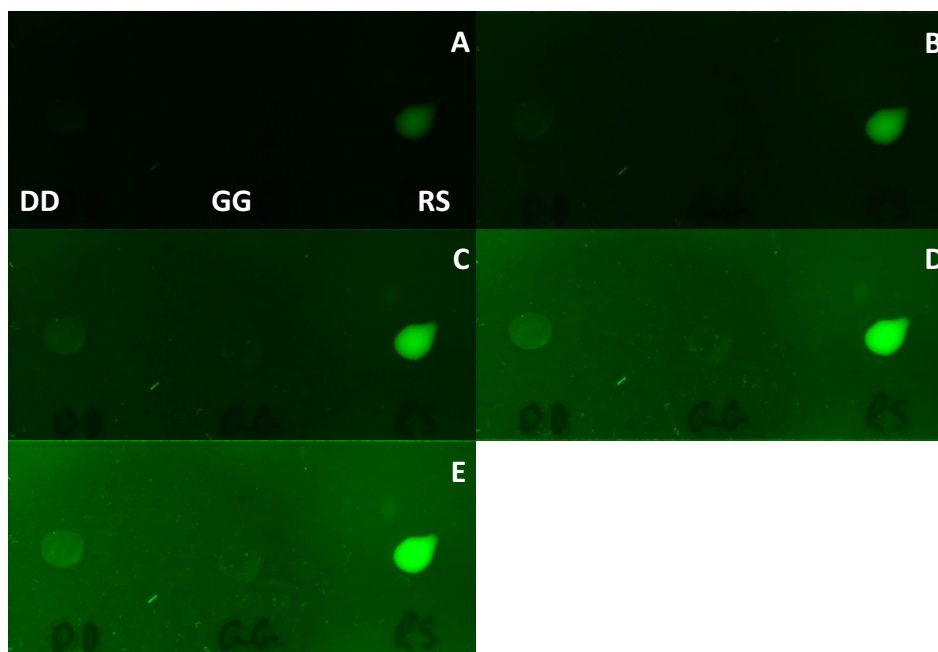
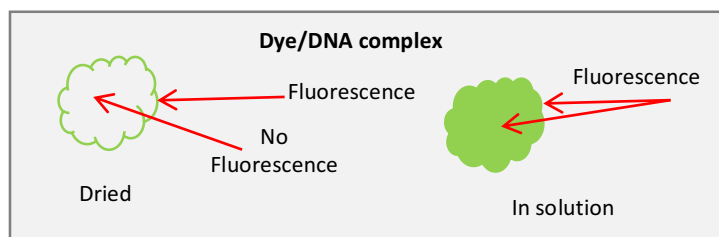


Figure 4.20: Intrinsic fluorescence of dyes DD, GG and RS without DNA present in a 20x H₂O solution with varying exposure times using a 555 nm interference filter (A) 1/5 s, (B) ½ s, (C) 1 s, (D) 2 s, (E) 2.5 s.

Figure 4.21 shows the signals of varying amounts of DNA using GG at a concentration of 40X which shows signals down at the 1 ng of DNA. At this mass of DNA the signal was clearer at an exposure time of 2 s after 1 min of the initial staining period than the other exposure times tested. However when using a concentration of 20X of GG DNA was only detected at 5 ng (Figure 4.21, 4.22)

Figures 4.22, 4.23 and 4.24 show the detection of DNA at different amounts with staining using GG, RS and DD with both cut-off and interference filters and varying exposure times. Both images show that RS was a naturally fluorescent dye based on the high background signal obtained with both filters. DD was the only dye that had a signal down at 0.5 ng, which shows the potential use of this dye for further investigation.

Clear detectable fluorescence was noted when the dye was placed on top of the dried DNA, when the dye droplet was still in solution, but when dried the fluorescence could only be seen at the boundary of the stain not throughout the stain (see Scheme 4.8). The background fluorescent signal increased when the concentration of dye was increased. This was still low for SG and GG. DD did have a higher background signal when the concentration was increased but when in the presence of DNA the signal was very high.



Scheme 4.8: Schematic representation of the dye/DNA complex when in solution compared with the signal obtained once the dye/DNA complex had dried on a glass surface.

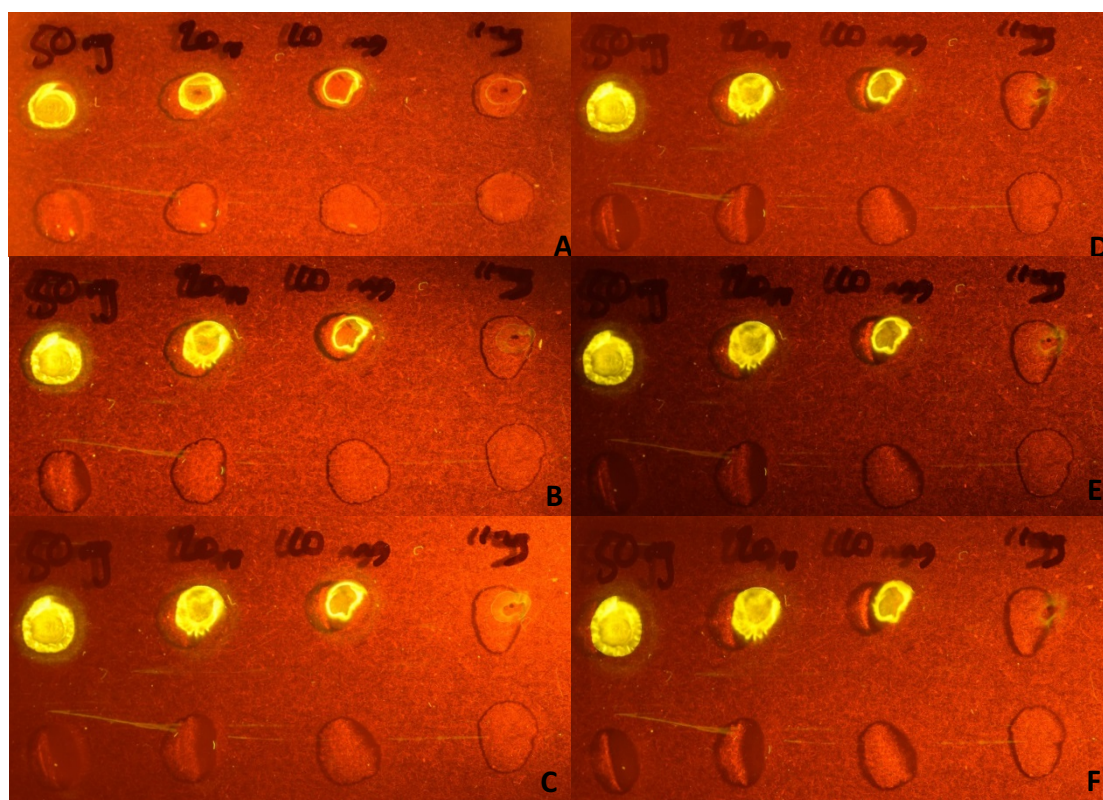


Figure 4.21: GelGreen (40x) varying DNA concentration with varying exposure times over a 3 min time period with a 555 nm cut-off filter (A) exposure 1.6 s at time 0, (B) exp 1.6 s (C) exp 2 s time 1 min, (D) exp 2.5 s time 1min, (E) exp 0.62 s at time 1 min, (F) exp 1.6 s at time 3 min.

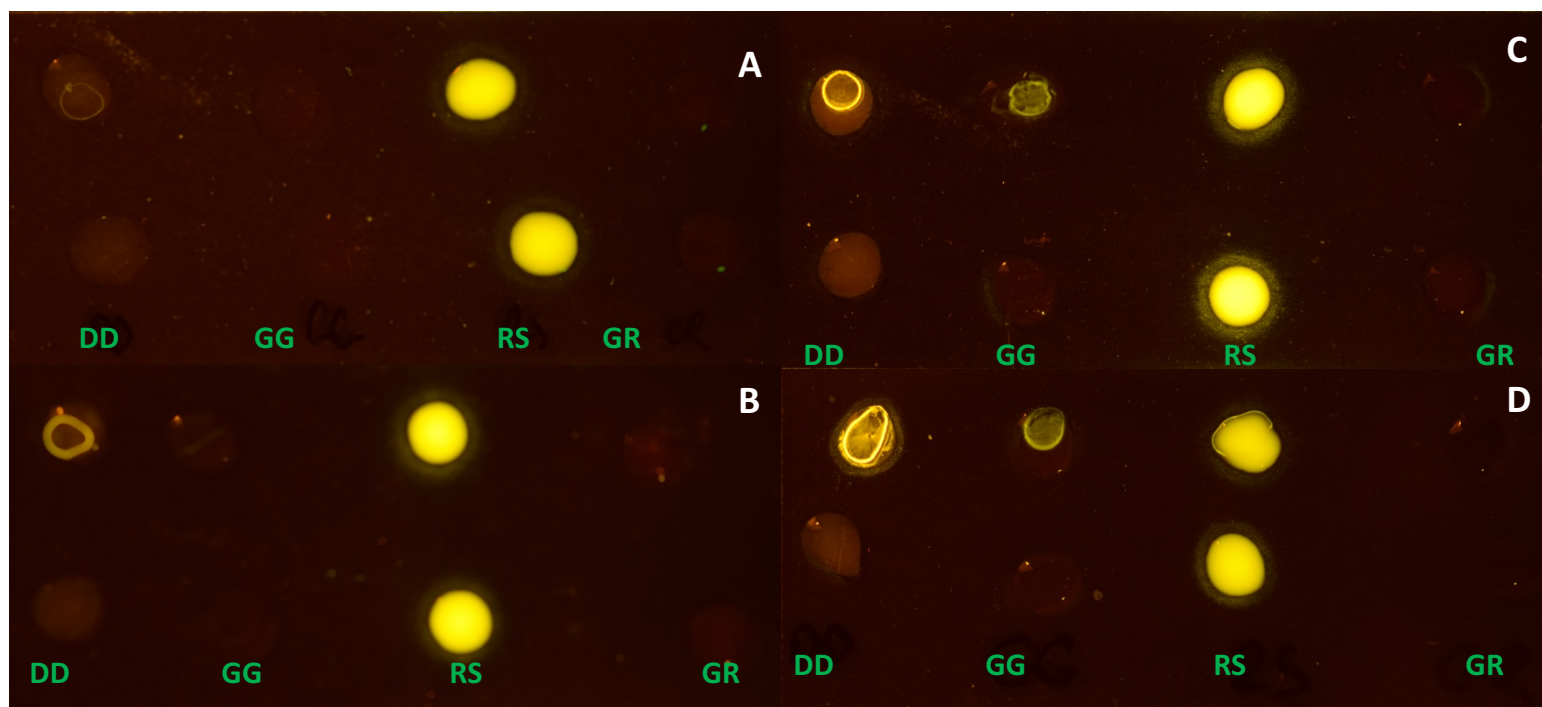


Figure 4.22: Varying amounts of DNA on a glass substrate with DNA binding dyes DD, GG, RS and GR (20X, 5 μ L) at an exposure time of 1/5 s using a 550 nm cut-off filter with (A) 0.5 ng, (B) 1 ng, (C) 5 ng, (D) 10 ng.

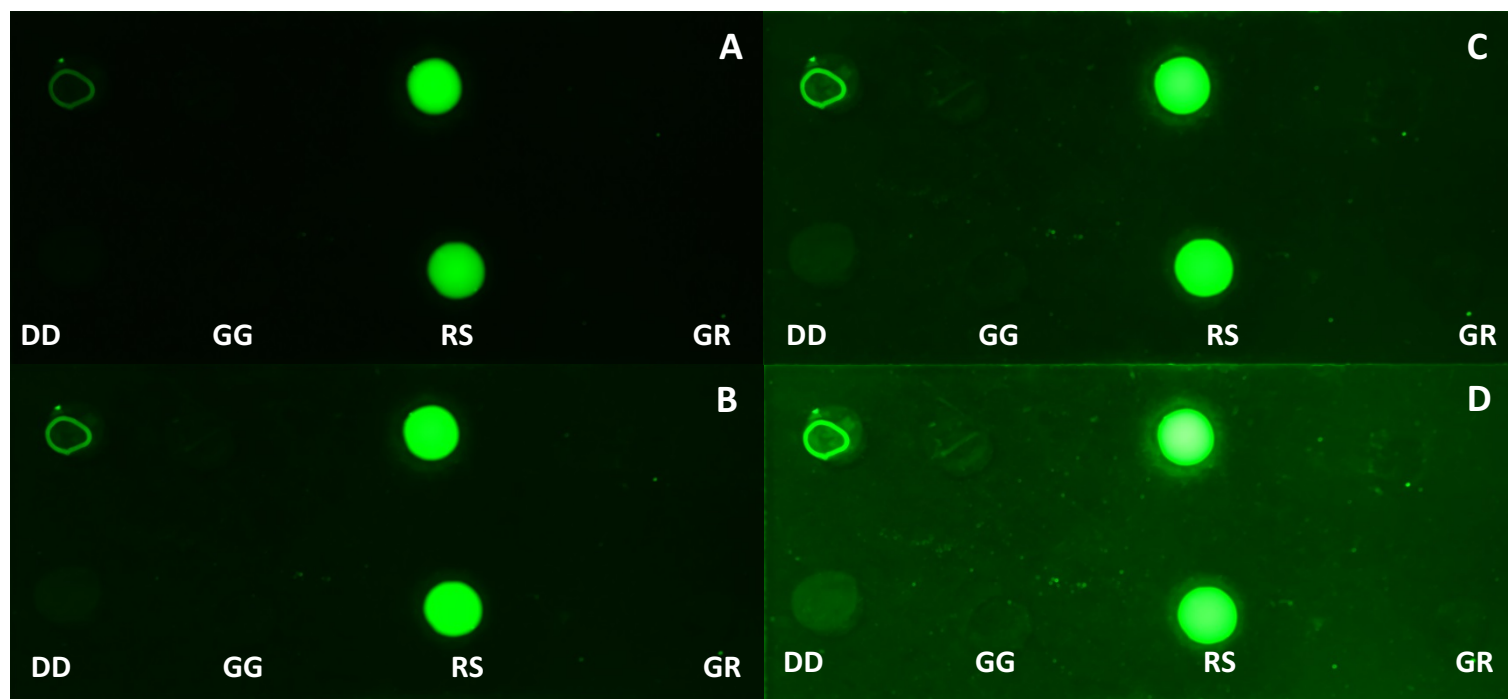


Figure 4.23: 1 ng of DNA with staining using DD, GG, RS and GR at 20X concentration with varying exposure times (A) 1/5 s, (B) 1/2 s, (C) 1 s, (D) 2 s. (alter 1/2 to be the same size as all other text)

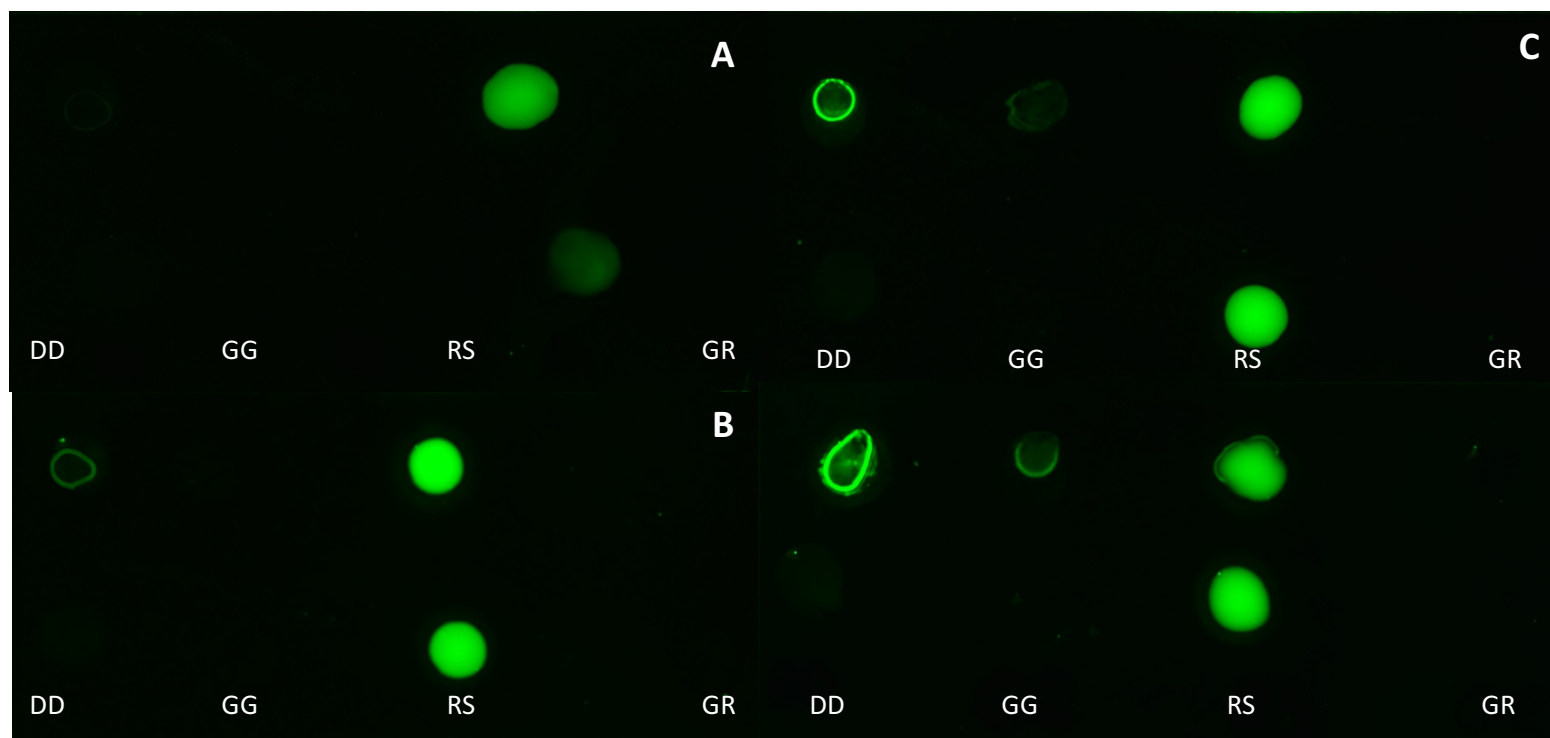


Figure 4.24: Varying amounts of DNA with binding dyes DD, GG, RS and GR (20X, 5 μ L) and negative control (bottom row) at an exposure of 1/5 s using 555 nm interference filter (A) 0.5 ng, (B) 1 ng, (C) 5 ng, (D) 10 ng.

Table 4.7: Varying amounts of DNA with dye staining at 20X concentration, optimal exposure time shown in brackets using a 535 nm interference filter.

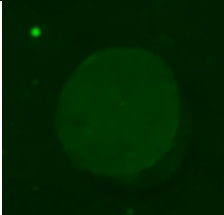
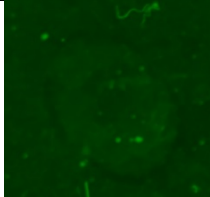
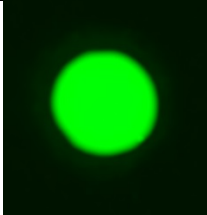
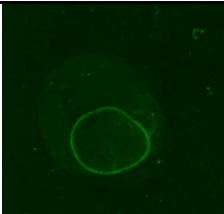
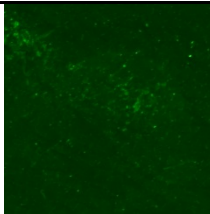
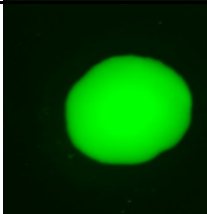

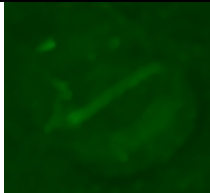
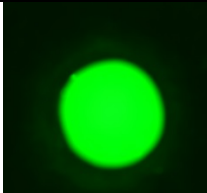
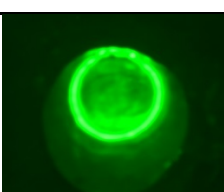
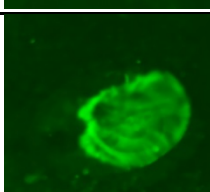
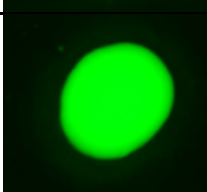
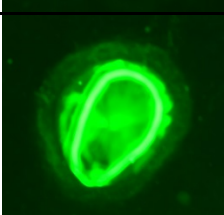
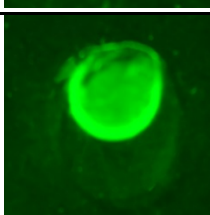
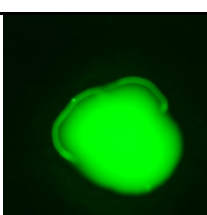
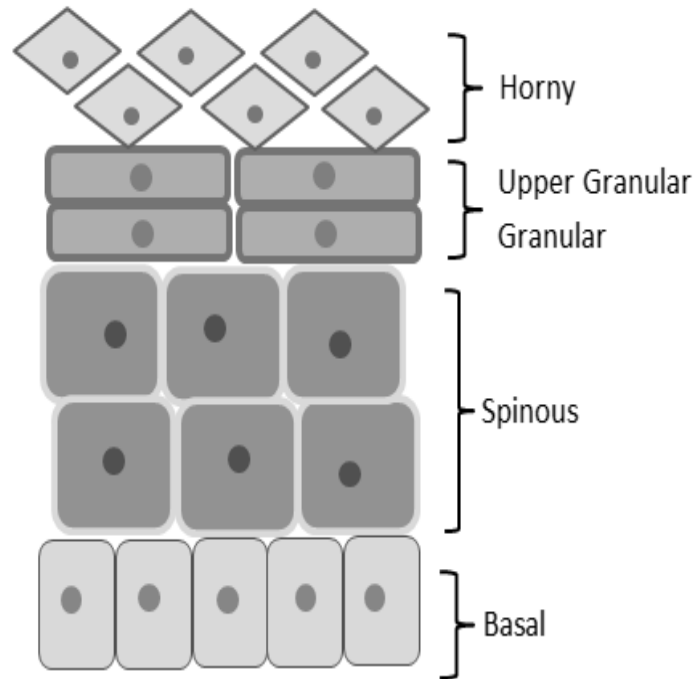
DNA (ng/ μ L)	DD (1 s)	Detected DNA	GG (2 s)	Detected DNA	RS (1/2 s)	Detected DNA
Negative						
0.5 ng		✓		x		x
1 ng		✓		x		x
5 ng		✓		✓		x
10 ng		✓		✓		✓

Table 4.7 shows the signal from varying amounts of DNA stained with various DNA binding dyes with their optimal exposure times for the dye. DD had an optimal exposure time of 1 s, GG was at 2 s and RS at $\frac{1}{2}$ s, GR had no staining of DNA and therefore did not have an optimal exposure time. Based on Table 4.7, DD had the highest sensitivity with detection down at 0.5 ng.

4.4.2 Detection of DNA and protein within fingermarks

The outermost layer of skin is known as the epidermis and the bottom layer of skin is called the dermis. The epidermis is made up of tightly compacted cells, epithelium, which is divided into distinct layers, horny, upper granular, granular, spinous and basal, depicted below, Scheme 4.9. The horny layer is the outermost layer composed of dead cells and acts as a protective barrier against the exposure of underlying tissue to infections, chemicals and dehydration. These dead cells are regularly removed through the process of desquamation required for skin renewal. Through this process the dead cells are transferred to the substrate surface when creating a fingermark. Throughout this process of skin renewal, cells migrate towards the surface from the basal layer through the epidermis in around 30 days [15]. Proteins are produced during this period and could be transferred to the fingermark residue during substrate interaction, it has been estimated that the amount of protein present in residues was 384 µg [16]. Covering the horny layer is a hydrolipidic film comprised of glycerides and fatty acids, cholesterol and sterol esters. These constituents are produced in the granular layer by keratinocytes but are also found in the sebum. These compounds could also be present in fingermark residues as this film comes in contact with the substrate [15-18].

The dermis layer contains around five million secretory glands including eccrine, apocrine and sebaceous glands, the secretions reach the surface via the epidermal pores. The major component of a fingermark is sebum, secreted by the sebaceous glands, which are present all over the body except hands and feet. Hence, the sebum is transferred to the fingertips after contact has been made with other parts of the body. Sebum has been found to contain wax esters, phospholipids and triglycerides; due to the hydrolipidic film the following compounds are found, cholesterol, glycerides and free fatty acids. Secretions from eccrine glands, which are present all over the body, consist of mostly water but inorganic and organic compounds have been identified [15]. The most abundant compound present in the secretions are proteins and polypeptides, lactic acids has also been detected within fingermark residue [18]. Fingermark residues can also have contaminants present from sources such as food and bacterial spores [15]. A list of fingermark residues is listed in Table 4.8.



Scheme 4.9: Schematic representation of the layers of the epidermis, adapted from [15].

There are two stages that lead to the composition of fingerprints; the first stage involves the transfer and creation of the fingerprint and the second stage involves the elapsed time between transfers resulting in the aged composition of the fingerprint stage.

The factors that influence the first stage of composition are the following [19];

- Factors involved in the deposition such as pressure and duration of contact
- Donor characteristics
- Substrate surface; porous, semi-porous and non-porous

The factors that influence the second stage of composition are the following;

- Environmental factors such as humidity, temperature, light exposure, etc.
- Substrate surface
- Enhancement methodology

Table 4.8: Summary of compounds present within the residue of a fingerprint

Proteins	Sebum <ul style="list-style-type: none">• Wax esters• Phospholipids and triglycerides
Dead cells	Eccrine secretions <ul style="list-style-type: none">• Water• Inorganic and organic compounds• Proteins and polypeptides• Lactic acid
Glycerides	Contaminants <ul style="list-style-type: none">• Food• Bacterial spores• Chemicals found in makeup
Fatty acids	
Cholesterol	
Sterol esters	

The detection of DNA fluorescence in fingerprints was investigated earlier in this chapter using the Gel Doc™ EZ Imager as the means of detection. This section reports on the detection of DNA and protein fluorescence within fingerprints using the Polilight® for excitation when applying different filters for emission detection. The fingerprints were also viewed under a fluorescent microscope to visualise any cell debris. Figure 4.25 shows a fingerprint stained with DD and Figure 4.26 shows a fingerprint stained with a protein dye. From visual analysis it can be seen that there was more protein within the fingerprint and ridge patterns could be seen under 40X magnification but not visible when using a DNA binding dye. Although no studies have directly compared the amount of protein to the amount of DNA within fingerprints it is an assumption that fingerprints would contain more protein than DNA. As previously stated the estimate of protein within fingerprint residue was 384 µg, it is unlikely to obtain this amount of DNA within a fingerprint.

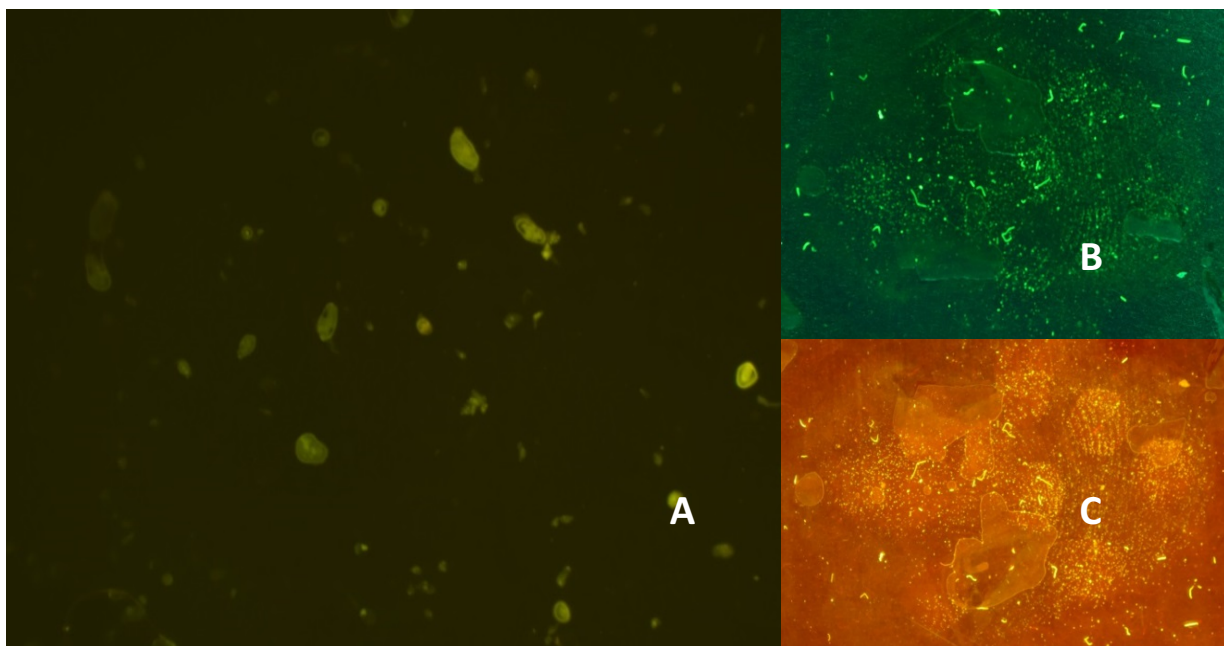


Figure 4.25: Detection of DNA within fingerprints using DD (20X in H₂O) on a glass substrate using Polilight® at 490 nm excitation (A) 40X magnification using Nikon Optiphot fluorescent microscope with B2A filter cube, (B) emission detection using a 535 nm interference filter and (C) emission detection using a 550 nm cut-off filter.

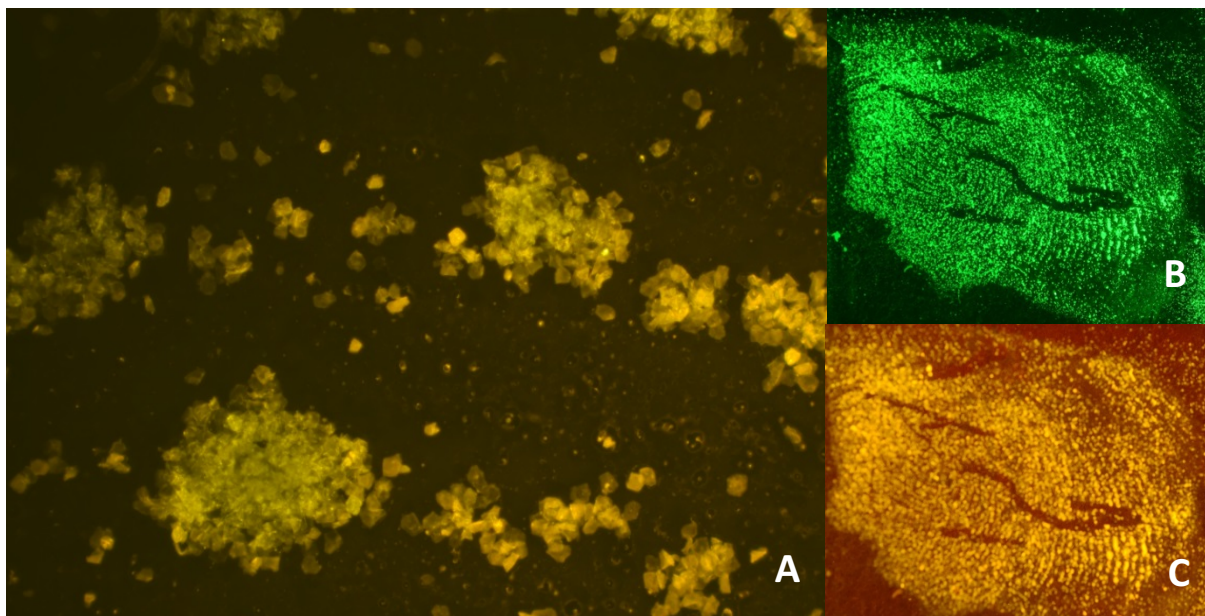


Figure 4.26: Detection of protein within fingerprints using Qubit® Protein Reagent (20X in H₂O) on a glass substrate using Polilight® at 490 nm excitation (A) 40X magnification using Nikon Optiphot fluorescent microscope with B2A filter cube, (B) emission detection using a 535 nm interference filter and (C) emission detection using a 550 nm cut-off filter.

The comparison between the fluorescent signal from DNA and protein was evaluated under Polilight[®] excitation (centered at 490 nm) and emission detection through a 530 nm interference filter (Figure 4.27). There was a visible fluorescent signal down to 1 ng of DNA using DD staining but there was only a very weak signal from the protein. No increase in the visible fluorescent signal from protein was observed with increasing concentration; whereas the emission from DNA showed increasing intensity with increasing concentration.

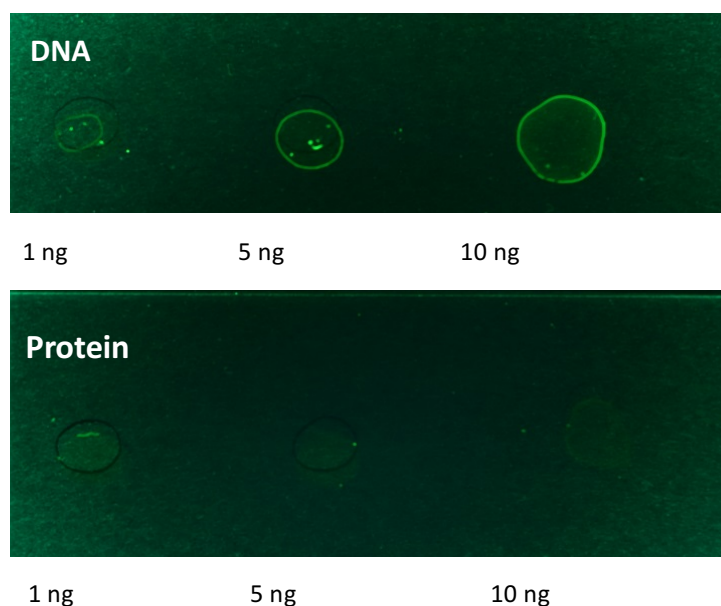


Figure 4.27: Comparison of BSA (1, 5 and 10 ng) signal to DNA (1, 5 and 10 ng) using DD (20X in H₂O) with excitation at 490 nm and emission through a 535 nm interference filter.

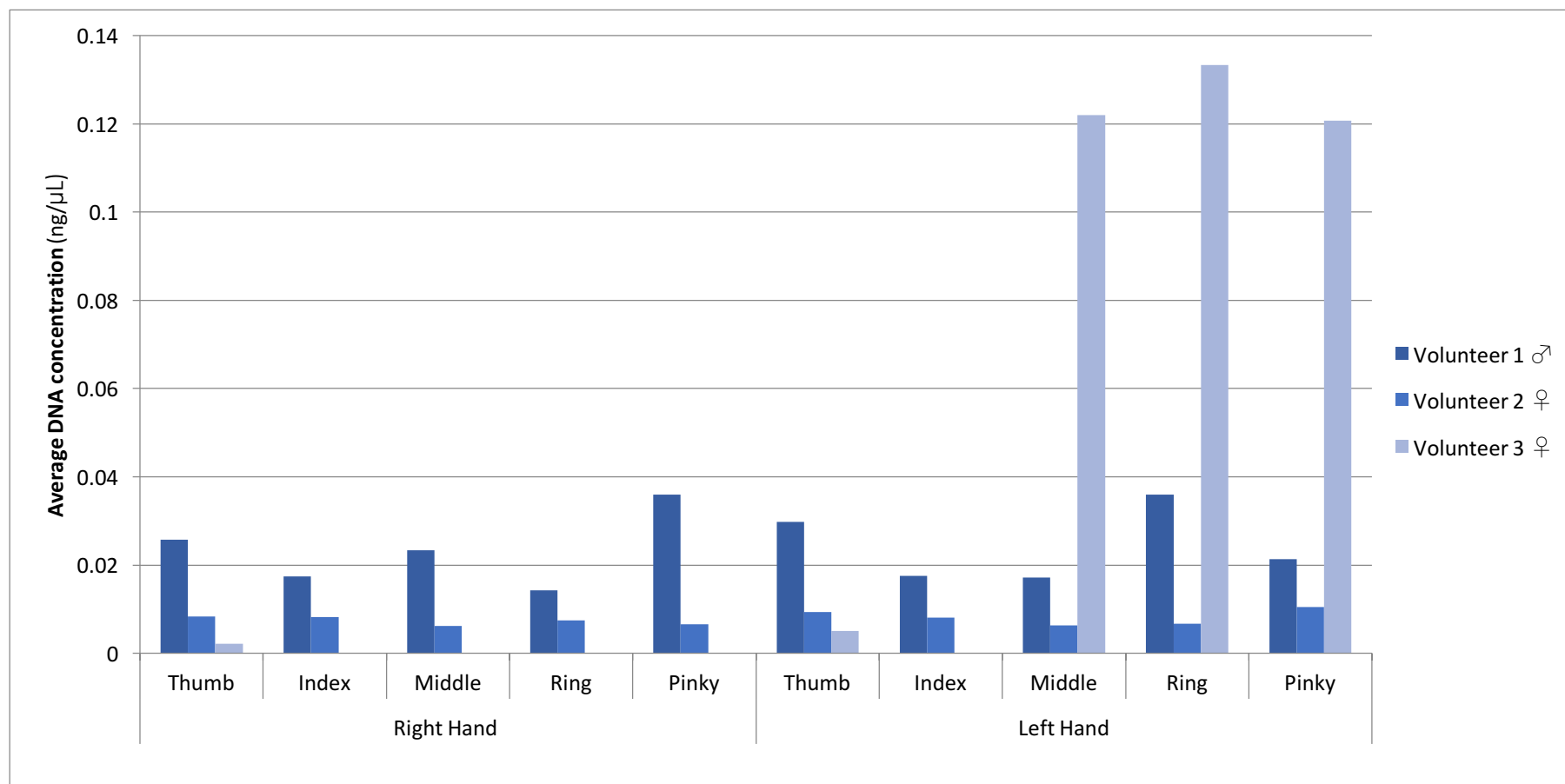


Figure 4.28: DNA concentration within fingermarks on acetate paper quantified using Qubit® 2.0 Fluorometer, readings were in triplicate, raw results for each volunteer see Appendix C table C-16-18.

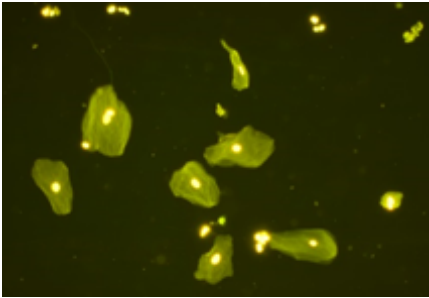
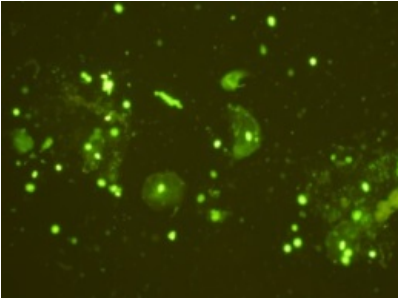
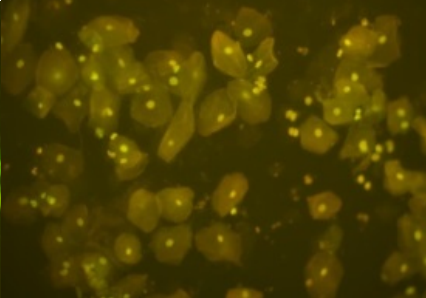
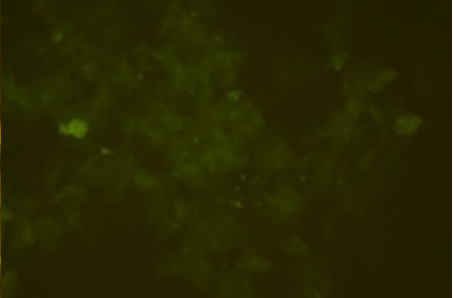
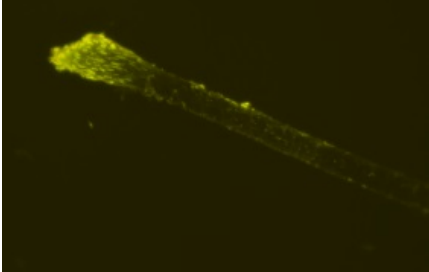
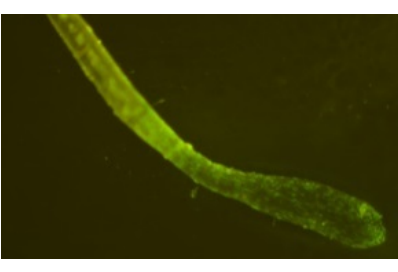
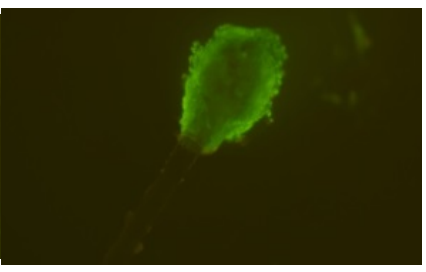
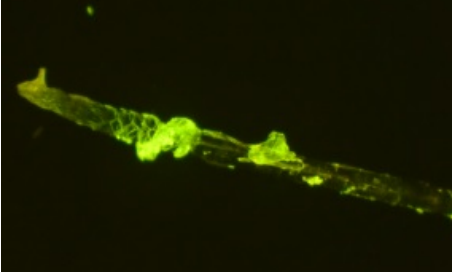
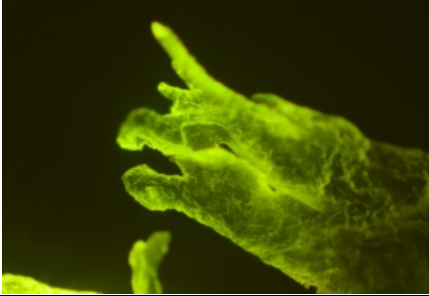
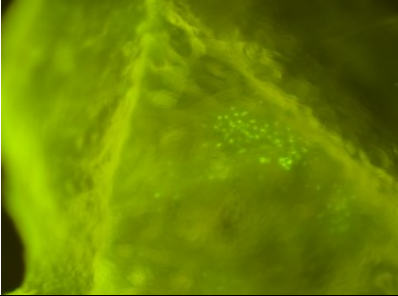
Figure 4.28 shows the amount of DNA that was quantified within fingerprints deposited on acetate paper. The paper was placed in a TE buffer solution without using an extraction kit or wash steps to try and reduce loss of DNA. It has been estimated that around 85% of DNA can be lost during an extraction process [20]. This was also demonstrated in Chapter 3, where around 63% of DNA was lost through a solid phase extraction. The quantification of DNA was undertaken using the buffer that had the sample present.

Volunteer 3 had the highest readings for their left hand middle, ring and pinky fingerprints all other prints from the right hand and from the other two volunteers had similar readings around 0.02 ng/μL. From previous work within this Chapter, looking at the fluorescent signal from the dyes on average had quantification values around 1.39-1.9 ng/μL, which was much higher than those values obtained from the acetate paper.

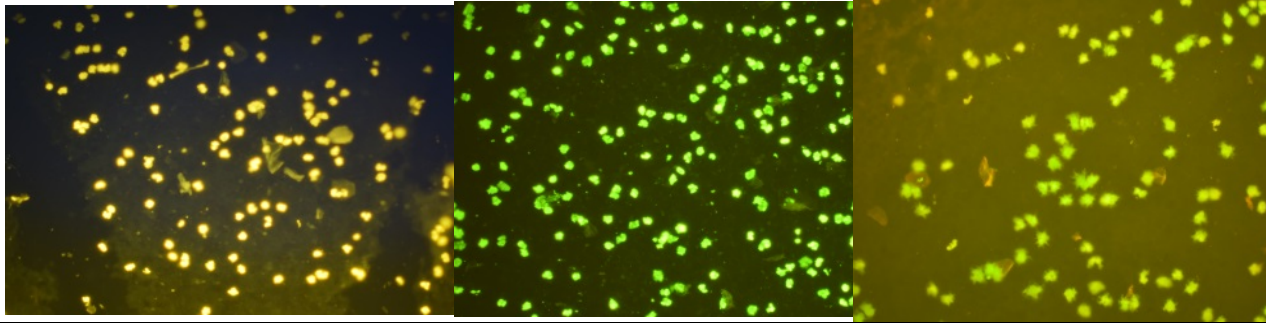
The amount of protein present within the fingermark was also investigated using the sample solution that was quantified for DNA but using a Qubit[®] Protein assay kit. The assay can detect protein between the concentrations of 12.5 μg/mL and 5 mg/mL. Most of the samples resulted in undetectable readings, only two samples out of all that were tested produced a result (0.48 μg, see Appendix, Figure C-24).

4.3.3 Detection of DNA within biological samples

Table 4.8: Staining of biological samples, hair, skin and saliva with DNA binding dyes.

Biological Sample	DD	SG	EG	RS
Saliva				
Hair				
Skin			N/A	N/A

Blood



Staining of biological samples (plucked hairs, dead skin and saliva) with DNA binding dyes used at a concentration of 20X with 5 μ L applied to the sample. Samples were viewed under a Nikon Optiphot fluorescent microscope using a B2A filter cube and images were captured using an exposure time of 1 s under 400X magnification. Nuclei can be seen within the saliva and hair samples.

Table 4.8 above shows the staining of various biological samples with DNA binding dyes RS, EG, DD and SG. GG and GR were not used as they do not permeate the cell membrane staining would not be as sensitive compared with the other dyes that do permeate a membrane. The manufacture states that EG does not permeate the cell membrane however, from the results shown in Table 4.8 nuclei staining is clearly seen within saliva and hair follicles.

Nuclei could be seen within the saliva samples for all dyes but difficult to see with RS due to the high background signal and low sensitivity of the dye. Most of the fluorescence from the skin samples may be the auto-fluorescence of the skin itself but there are fluorescent clusters. A fair assumption is that these are extra-cellular DNA. Staining of the hair follicles shows nuclei present which will be further investigated in the following Chapter.

4.3.4 Other publications

Other results related to the detection of latent DNA using fluorescent dyes was presented at the 26th *International Society of Forensic Genetics* (see Appendix C for poster presentation), conference proceedings was also published. Details of the paper are listed below and the article itself appears on the following pages.


Alicia M. Haines, Shanan S. Tobe, Hilton J. Kobus, Adrian Linacre, **Finding DNA: Using fluorescent in situ detection**, *Forensic Science International: Genetics Supplement Series*, **5** (2015), e501-502


Statement of Authorship

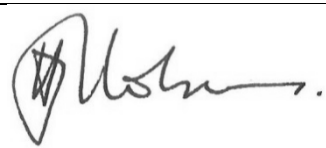
Title of Paper	Finding DNA: Using fluorescent in situ detection
Publication Status	Published 2015
Publication details	Published in <i>Forensic Science International: Genetics Supplement Series</i>


Author Contributions

By signing the Statement of Authorship, each author certified that their stated contribution to the publication is accurate and that permission is granted for the publication to be included in the candidate's thesis.

Name of Principal Author (Candidate)	Alicia M. Haines		
Contribution to the paper	Designed experimental method, performed all laboratory work and analysis, drafted the manuscript, edited manuscript and acted as corresponding author		
Signature		Date	August, 2016

Name of Co-Author	Shanan S. Tobe		
Contribution to the paper	Gave limited guidance		
Signature		Date	August, 2016

Name of Co-Author	Hilton J. Kobus		
Contribution to the paper	Edited manuscript		
Signature		Date	August, 2016

Name of Co-Author	Adrian Linacre		
Contribution to the paper	Helped design study and edited manuscript		
Signature		Date	August, 2016



Contents lists available at ScienceDirect

Forensic Science International: Genetics Supplement Series

journal homepage: www.elsevier.com/locate/FSIGSS



Finding DNA: Using fluorescent *in situ* detection

Alicia M. Haines^{a,*}, Shanan S. Tobe^a, Hilton Kobus^b, Adrian Linacre^a

^a School of Biological Sciences, Flinders University, Adelaide, Australia

^b School of Chemical and Physical Sciences, Flinders University, Adelaide, Australia

ARTICLE INFO

Article history:

Received 17 August 2015

Accepted 19 September 2015

Available online xxx

Keywords:

DiamondTM dye

Fluorescence

Latent DNA

SYBR[®] Green I

ABSTRACT

It is known that DNA can be deposited onto a surface by touch yet few means have been developed for its *in situ* detection. Collecting touch-DNA samples can be difficult as likely locations rather than the DNA is targeted leading to many samples that are submitted to a forensic laboratory containing little or no DNA. A range of dyes are available that bind to DNA at high specificity for application within the laboratory and here we report on the use of these dyes to detect latent DNA on various substrates and within biological samples. Six common nucleic acid-binding dyes were selected due to their increase in fluorescence when in the presence of double stranded-DNA; four of the six dyes are permeable to cell membranes. The fluorescence from dye/DNA complex was detected using a high intensity light source, the Polilight[®] (PL500), an excitation wavelength of 490 nm and emission observed/recorded through interference filters centred at 530 nm or 550 nm depending on the dye emission. The samples were visualised under a fluorescent microscope (Nikon Optiphot) using a B2A filter cube. The detection limit of DNA was determined for the selected dyes along with the optimal conditions, such as buffer composition and dye concentration for a range of surfaces. The ability for the dyes to detect DNA within biological samples such as saliva, hair, skin, fingerprints, and hair follicles was also determined.

© 2015 Published by Elsevier Ireland Ltd.

1. Introduction

Finding latent DNA at crime scenes will aid greatly in the collection of DNA and biological material by directing the examiner to locations where touch DNA may be present using a targeted approach. Nucleic acid binding dyes in forensic practice are used for the detection of DNA within gel electrophoresis and in quantification techniques. Ethidium bromide was first used in the early 70s for staining gels [1], since this development other dyes that are more sensitive and specific have been engineered for use. Such dyes include SYBR[®] Green and PicoGreen[®] which have been used in analysis methodologies either by fluorescent quantification or by real-time PCR [2].

Two main modes of interaction of dyes with DNA include intercalating and groove binding mechanisms. SYBR Green and ethidium bromide are examples of intercalating dyes that bind between the base pairs of DNA [3]. DAPI is an example of a groove binding dye that binds to AT rich regions of DNA. The binding mechanism affects the sensitivity and specificity of the dye with DNA. SYBR Green which, has both electrostatic and extended

groove contact, has an increased sensitivity of a 1000-fold when bound to DNA [3]; compared to DAPI which only has a 20 fold increase in fluorescent enhancement [4].

Fluorescence microscopy is an area of forensic science that has utilized DNA binding dyes to stain biological samples to view the fluorescent signal such as within saliva [2] and hairs [5]. The number of nuclei revealed by this process can then be used to determine the viability for obtaining a DNA profile from these samples. DAPI has been used as a fast nuclear stain for hair samples and could be used as a screening technique to profile samples with high number of nuclei present [5,6]. The effects these dyes have on the extraction and amplification processes was recently investigated which shows that GelGreenTM, EvaGreenTM and RedSafeTM had the least effect on DNA amplification and DiamondTM dye had the least effect of DNA extraction [7].

This study looks at the use of more sensitive dyes for the detection of latent DNA either on surfaces or within biological samples that might be present as forensic evidence such as hairs to provide a targeted approach to sample collection. The use of six nucleic acid binding dyes for this approach was investigated to determine the suitability in this novel approach. The dyes investigated were SYBR Green I (SG), Diamond Nucleic Acid Dye (DD), GelGreen (GG), GelRed (GR), EvaGreen (EG) and RedSafe (RS).

* Corresponding author at: Flinders University GPO Box 2100, School of Biological Sciences, Adelaide, SA 5001, Australia.

E-mail address: alicia.haines@flinders.edu.au (A.M. Haines).

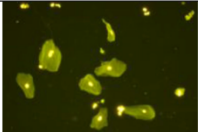
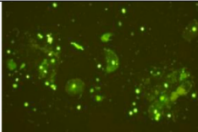
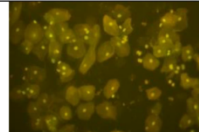
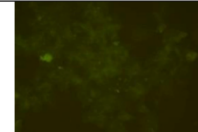
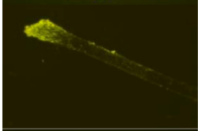
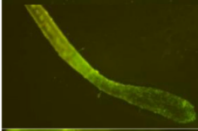
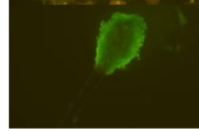
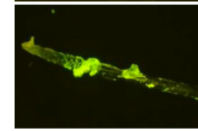
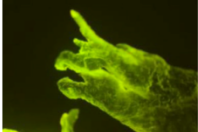
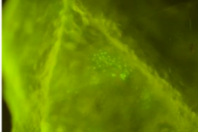
<http://dx.doi.org/10.1016/j.fsigs.2015.09.198>

1875–1768/© 2015 Published by Elsevier Ireland Ltd.

Please cite this article in press as: A.M. Haines, et al., Finding DNA: Using fluorescent *in situ* detection, Forensic Sci. Int. Gene. Suppl. (2015), <http://dx.doi.org/10.1016/j.fsigs.2015.09.198>

Table 1

Staining of biological samples, hair, skin and saliva with DNA binding dyes.

Biological Sample	DD	SG	EG	RS
Saliva				
Hair				
Skin			<p>Staining of biological samples (plucked hairs, dead skin and saliva) with DNA binding dyes used at a concentration of 20X with 5 µL applied to the sample. Samples were viewed under a Nikon Optiphot fluorescent microscope using a B2A filter cube and images were captured using an exposure time of 1 s under 400X magnification. Nuclei can be seen within the saliva and hair samples.</p>	

2. Methodology

2.1. Staining

Biological samples were stained with the six DNA binding dyes at a concentration of 20X. The samples stained comprised shed, plucked hairs, saliva, dead skin, fingerprints and diluted extracted DNA (0.5–50 ng).

2.2. Fluorescent detection

Samples were viewed using a Nikon Optiphot fluorescent microscope using a B2A filter cube. Images were taken using an exposure time of 1 s. Samples that were on a glass surface (fingerprints and extracted DNA) were placed under a Nikon camera with filters attached (cut-off at 530 nm, interference at 555 and 530 nm) and excited using a Polilight (490 nm).

3. Results and discussion

Table 1 below shows the use of four DNA binding dyes for the staining of biological samples such as saliva and hairs to view the nuclei present. The dyes have also been shown in the use for staining latent DNA samples such as fingerprints and extracted DNA. DNA down to 0.5 ng was able to be detected using DD and SG. When staining skin fragments the signal would most likely be auto fluorescence from the skin itself however there are regions of fluorescent clusters which could be either bacterial or intracellular DNA. GG and GR were not suitable dyes for detecting DNA within samples due to the dyes not being able to permeate the cell membrane.

4. Concluding remarks

The use of DNA binding dyes has been investigated for staining biological samples to view nuclei present. Latent DNA can be detected using these dyes allowing for a targeted approach when collecting material at a scene. Recommended dyes include SG, EG and DD. GR and GG were not ideal for staining. Samples that have a high fluorescent signal can then correspond to the STR profile that could be produced after amplification.

Conflict of interest

None.

Role of funding

Funding was provided by Forensic Science South Australia and the Attorney General's Department, South Australia.

References

- [1] C. Aaij, P. Borst, The gel electrophoresis of DNA, *Biochim. Biophys. Acta (BBA)–Nucleic Acids Protein Synth.* 269 (1972) 192–200.
- [2] A.M. Haines, S.S. Tobe, H.J. Kobus, A. Linacre, Properties of nucleic acid staining dyes used in gel electrophoresis, *Electrophoresis* 36 (2015) 941–944.
- [3] A.I. Dragan, et al., SYBR Green I: fluorescence properties and interaction with DNA, *J. Fluoresc.* 22 (2012) 1189–1199.
- [4] M.L. Barcellona, G. Cardiel, E. Gratton, Time-resolved fluorescence of DAPI in solution and bound to polydeoxynucleotides, *Biochem. Biophys. Res. Commun.* 170 (1990) 270–280.
- [5] L. Bourguignon, B. Hoste, T. Boonen, K. Vits, F. Hubrecht, A fluorescent microscopy-screening test for efficient STR-typing of telogen hair roots, *Forensic Sci. Int. Genet.* 3 (2008) 27–31.
- [6] T. Lopez, M. Vandewoestyne, D. Van Hoofstat, D. Deforce, Fast nuclear staining of head hair roots as a screening method for successful STR analysis in forensics, *Forensic Sci. Int. Genet.* 13 (2014) 191–194.
- [7] A.M. Haines, S.S. Tobe, H.J. Kobus, A. Linacre, The effect of nucleic acid binding dyes on DNA extraction, amplification and STR typing, *Electrophoresis* (2015), doi:<http://dx.doi.org/10.1002/elps.201500170>.

Please cite this article in press as: A.M. Haines, et al., Finding DNA: Using fluorescent *in situ* detection, *Forensic Sci. Int. Gene. Suppl.* (2015), <http://dx.doi.org/10.1016/j.fsigs.2015.09.198>

4.5 Chapter Summary

This Chapter looked at the use of DNA binding dyes for a surface-based detection application, primarily focusing on glass as the initial substrate, in which the background of the dyes was investigated and then in the presence of DNA. The first section looked at the detection using Gel Doc™ detection and analysis but, due to the wide detection limits of this instrumentation the detection was not specific for the dye/DNA complex, a more specific mode of detection was investigated. Using the Gel Doc™ the amount of DNA within a fingerprint was investigated using the lane band analysis tool as a way of quantifying the signal. The values obtained for the fingerprints was compared to the standard curve produced of varying DNA concentrations

The Polilight® was used to supply a more specific excitation wavelength at 490 nm and interference and cut-off filters were used for the detection of the dye/DNA complex; this varied depending on the dye used. From the initial results of this work it was found that RS was not a suitable dye as a surface-based detection method due to the dye being naturally fluorescent. Detection of DNA was only possible at 10 ng of DNA, however for this method to be applicable for latent DNA more sensitive detection is required. DD showed detection of the DNA at 0.5 ng which is promising for latent DNA detection. DD was shown to have optimal detection at an exposure of 1 s, GG had an optimal exposure time of 2 s and RS due to the high background had an optimal exposure time of 1/5 s. DD optimal concentration was at 20X however GG had optimal detection with a concentration at 40X. GG does not permeate the cell membrane so does not pose the same health risks as other dyes (SG, DD) but may also not be the most beneficial if there are intact cells deposited on surfaces for detection.

These dyes were also evaluated for their use for staining biological samples such as hair follicles, saliva, blood and skin samples to see the types of signals obtained from these samples, locating regions that have high fluorescence indicating potential sources of DNA for further analysis. The use of these dyes for hair follicle staining will be investigated within the following Chapter to determine the usefulness and whether the predictability of the hair's STR profile relates to the fluorescent signal (number of visible nuclei).

4.6 References (supplemental to publications)

- [1] A.I. Dragan., R. Pavlovic., J.B. McGivney., J.R. Casas-Finet., E.S. Bishop., R.J. Strouse, et al., SYBR Green I: Fluorescence Properties and Interaction with DNA, *Journal of Fluorescence*. 2012, **22** 1189-1199.
- [2] A.M. Haines., S.S. Tobe., H.J. Kobus., A. Linacre, Properties of nucleic acid staining dyes used in gel electrophoresis, *ELECTROPHORESIS*. 2015, **36** 941-944.
- [3] I. Kavanagh., D. Leake.G. Ball, *Dye blends*, 2013, Google Patents.
- [4] V.L. Singer., T.E. Lawlor., S. Yue, Comparison of SYBR® Green I nucleic acid gel stain mutagenicity and ethidium bromide mutagenicity in the Salmonella/mammalian microsome reverse mutation assay (Ames test), *Mutation Research/Genetic Toxicology and Environmental Mutagenesis*. 1999, **439** 37-47.
- [5] G. Cosa., K.S. Focsaneanu., J.R.N. McLean., J.P. McNamee., J.C. Scaiano, Photophysical Properties of Fluorescent DNA-dyes Bound to Single- and Double-stranded DNA in Aqueous Buffered Solution, *Photochemistry and Photobiology*. 2001, **73** 585-599.
- [6] C. Lennard., M. Stoilovic, Application of forensic light sources at the crime scene, *The Practice of Crime Scene Investigation*. 2004 97-124.
- [7] N. Vandenberg., R.A. Oorschot, The Use of Polilight® in the Detection of Seminal Fluid, Saliva, and Bloodstains and Comparison with Conventional Chemical-Based Screening Tests, *Journal of Forensic Sciences*. 2006, **51** 361-370.
- [8] H.J. Kobus., E. Silenieks., J. Scharnberg, Improving the effectiveness of fluorescence for the detection of semen stains on fabrics, *Journal of Forensic Sciences*. 2002, **47** 819-823.
- [9] S.A.G. Lambrechts., A. van Dam., J. de Vos., A. van Weert., T. Sijen., M.C.G. Aalders, On the autofluorescence of fingerprints, *Forensic Science International*. 2012, **222** 89-93.
- [10] A. Fiedler., J. Rehdorf., F. Hilbers., L. Johrdan., C. Stribl., M. Benecke, Detection of Semen(Human and Boar) and Saliva on Fabrics by a Very High Powered UV-/VIS-Light Source, *Open Forensic Science Journal*. 2008, **1** 12-15.
- [11] S. Seidl., R. Hausmann., P. Betz, Comparison of laser and mercury-arc lamp for the detection of body fluids on different substrates, *International Journal of Legal Medicine*. 2007, **122** 241-244.
- [12] M. Pizzamiglio., A. Mameli., G. Maugeri., L. Garofano, Identifying the culprit from LCN DNA obtained from saliva and sweat traces linked to two different robberies and use of a database, *International Congress Series*. 2004, **1261** 443-445.
- [13] M.M. Schulz., F. Wehner., H.-D. Wehner, The Use of a Tunable Light Source (Mini-Crimescope MCS-400, SPEX Forensics) in Dissecting Microscopic Detection of Cryptic Epithelial Particles, *Journal of Forensic Sciences*. 2007, **52** 879-883.
- [14] J. Wawryk., M. Odell, Fluorescent identification of biological and other stains on skin by the use of alternative light sources, *Journal of Clinical Forensic Medicine*. 2005, **12** 296-301.

- [15] S.M. Thomasma., D.R. Foran, The influence of swabbing solutions on DNA recovery from touch samples, *Journal of Forensic Sciences*. 2013, **58** 465-469.
- [16] A. Girod., R. Ramotowski., C. Weyermann, Composition of fingermark residue: a qualitative and quantitative review, *Forensic Science International*. 2012, **223** 10-24.
- [17] V. Drapel., A. Becue., C. Champod., P. Margot, Identification of promising antigenic components in latent fingermark residues, *Forensic Science International*. 2009, **184** 47-53.
- [18] E. Candi., R. Schmidt., G. Melino, The cornified envelope: a model of cell death in the skin, *Nature reviews Molecular cell biology*. 2005, **6** 328-340.
- [19] R.S. Ramotowski, Composition of latent print residue, *Advances in Fingerprint Technology*. 2001, **20016363**.
- [20] R. Ottens., J. Templeton., V. Paradiso., D. Taylor., D. Abarno., A. Linacre, Application of direct PCR in forensic casework, *Forensic Science International: Genetics Supplement Series*. 2013, **4** e47-e48.

4.7 APPENDIX C

Table C-1: Maximum absorbance wavelength (λ_{\max}) of the cyanine dyes at a 20X stock solution in sterile water

Dye	λ_{\max} (nm)
GelGreen™	474, 497
RedSafe™	492
SYBR® Green I	495

Cyanine dyes have molar extinction coefficients above $50,000 \text{ cm}^{-1}\text{M}^{-1}$ however the exact extinction coefficients in water for GelGreen and RedSafe is unknown and various values exist for SYBR Green I. So for approximate values of concentration in nanomolar (nM) an extinction coefficient of $50,000 \text{ cm}^{-1}\text{M}^{-1}$ will be used.

Table C-2: GelGreen at 474 nm

	1	2	3	Average	Concentration (M)	C (mM)	C(μM)	C(nM)
1X	0.0044	0.0046	0.0047	0.0045	9.133E-08	9.13E-05	0.091	91.3
10X	0.0977	0.0976	0.0974	0.097	1.951E-06	0.00195	1.951	1951
20X	0.209	0.2093	0.2092	0.209	4.183E-06	0.00418	4.183	4183
40X	0.3604	0.3602	0.3603	0.3603	7.206E-05	0.007206	7.206	7206

Table C-3: RedSafe at 492 nm

	1	2	3	Average	Concentration (M)	C (mM)	C(μM)	C(nM)
1X	0.0087	0.0083	0.0082	0.0084	1.68E-06	0.000168	0.168	168
10X	0.12	0.1166	0.1167	0.1166	2.33E-06	0.002332	2.332	2332
20X	0.45	0.4523	0.4526	0.4521	9.04E-06	0.009042	9.042	9042
40X	1.10	1.1017	1.1018	1.1017	2.20E-04	0.022034	22.034	22034

Table C-4: SYBR Green I at 495 nm

	1	2	3	Average	Concentration (M)	C (mM)	C(μM)	C(nM)
1X	0.0001	0.0002	0.0001	0.00013	2.6E-09	2.67E-06	0.0026	2.66
10X	0.0965	0.0966	0.0965	0.0965	1.9E-06	0.00193	1.930	1930.6
20X	0.2876	0.283	0.2861	0.2855	5.7E-06	0.00571	5.711	5711.3
40X	0.5393	0.5394	0.5397	0.5394	1.1E-05	0.01078	10.78	10789

Dye	Extinction Coefficient ($M^{-1}cm^{-1}$)
GelGreen	130,000 in Methanol
RedSafe	unknown
SYBR Green I	75,000

Table C-5: Mutagenicity of dyes at a concentration that results in no colonies in the Ames test

Dye	nmol
SYBR Green I	65
SYBR Green II	75
SYBR Gold	40
Ethidium Bromide	2000

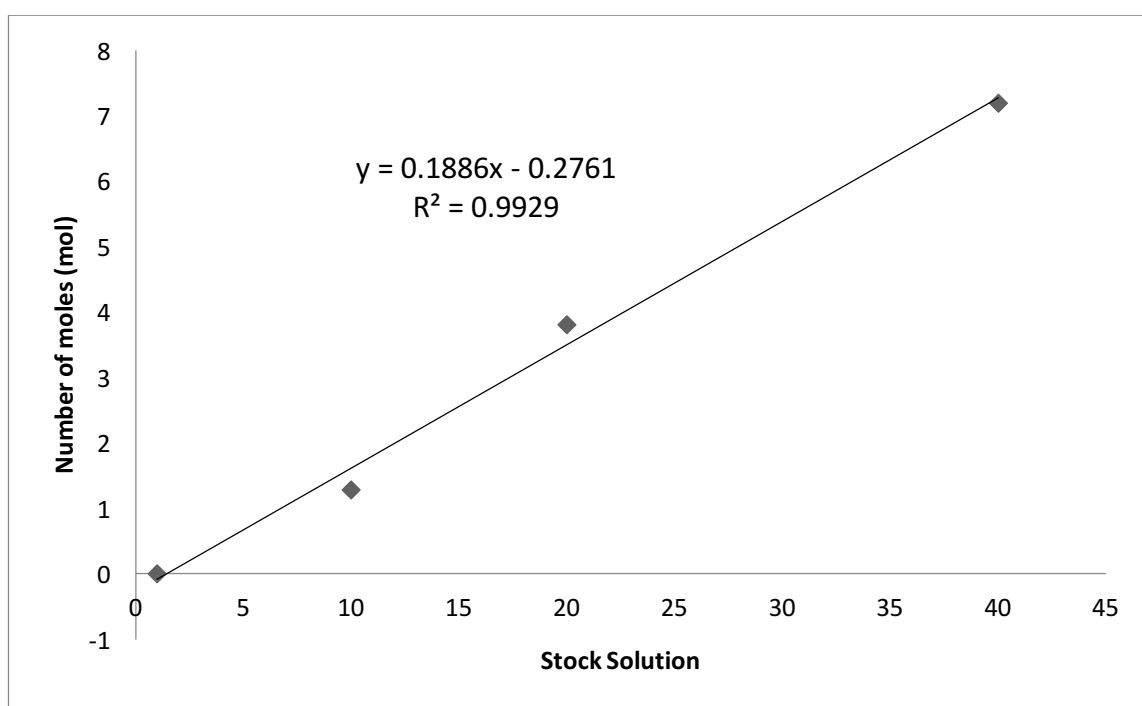


Figure C-1: Standard curve of stock concentration against number of moles showing line of best fit and equation

Using the equation of line of best fit the approximate stock solution concentration can be determined. SYBR Green I at a concentration of 65 nmol results in no colonies so can be classed as toxic and mutagenic at this level. 65 nmol is approximately a 230X stock solution. As the studies undertaken so far only use a 20X stock solution has been used which means there is a low level of mutagenicity and low toxicity however as the dye can permeate the cell membrane caution is still advised at any concentration.

UV/Vis spectra of dyes in other mediums

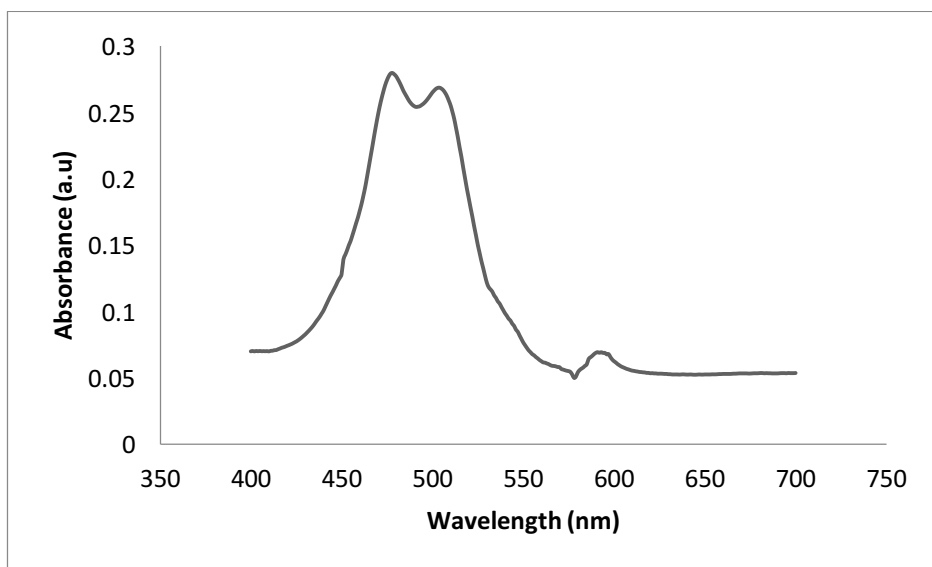


Figure C-2: UV/Vis spectrum of GG in H₂O at 20X concentration

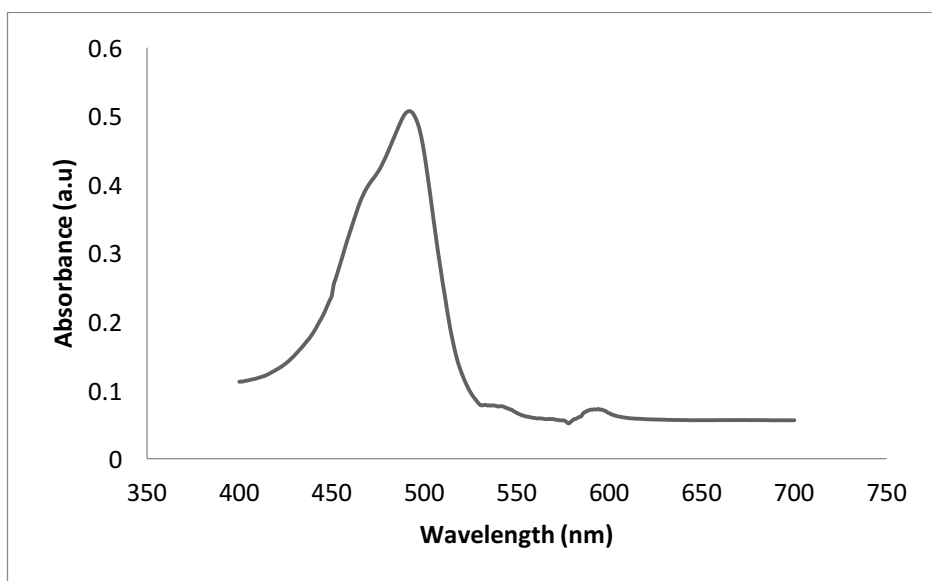


Figure C-3: UV/Vis spectrum of RS in H₂O at 20X concentration

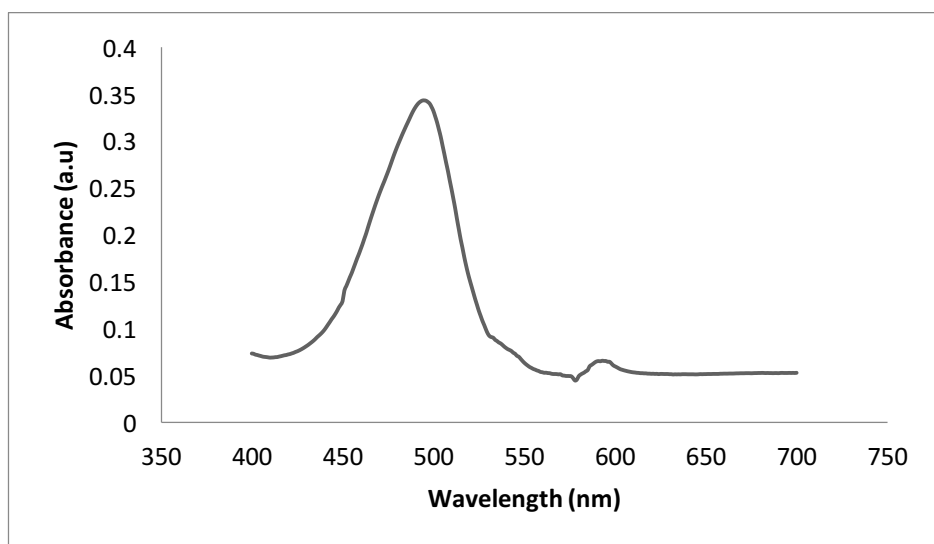


Figure C-4: UV/Vis spectrum of SG in H₂O at 20X concentration

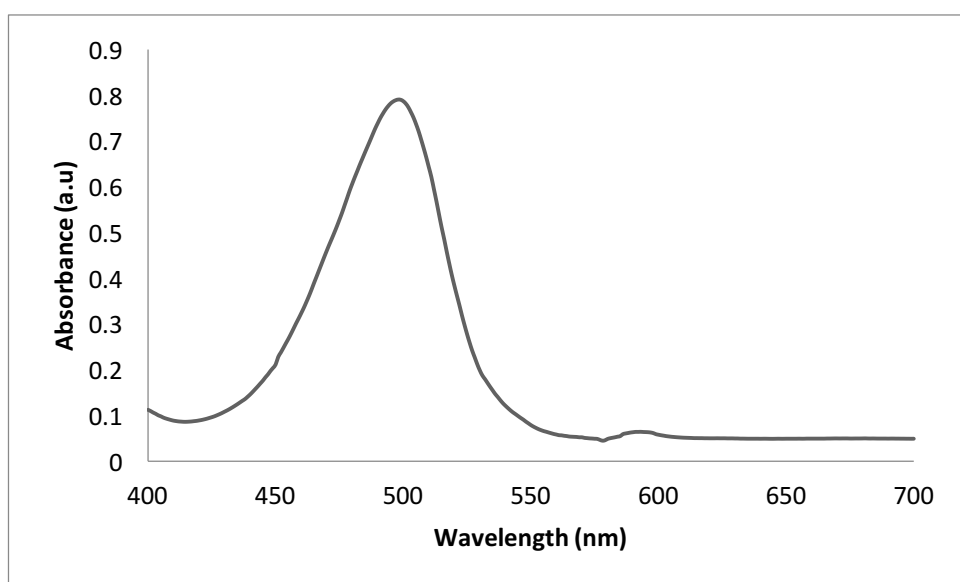


Figure C-5: UV/Vis spectrum of SG in DMSO at 20X concentration

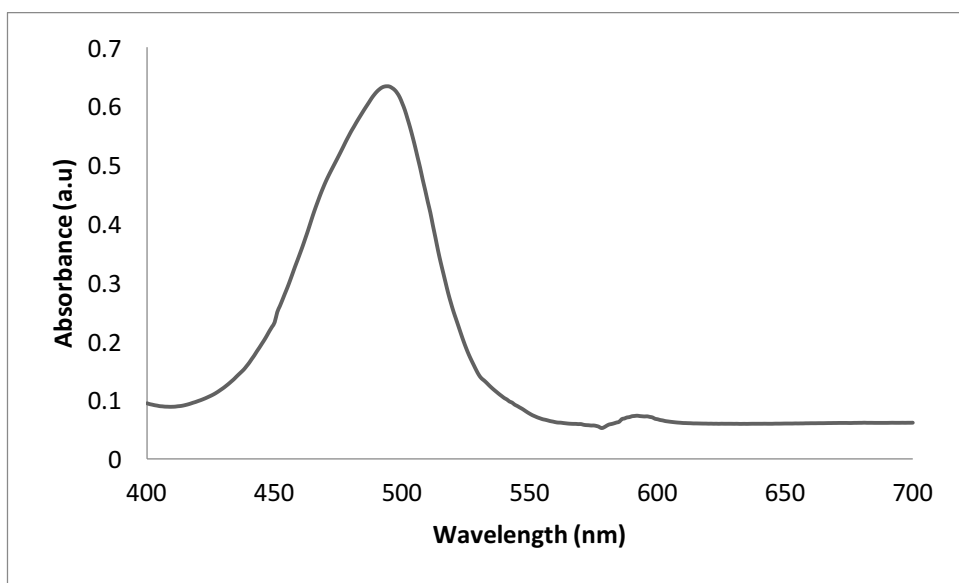


Figure C-6: UV/Vis spectrum of SG in TBE at 20X concentration

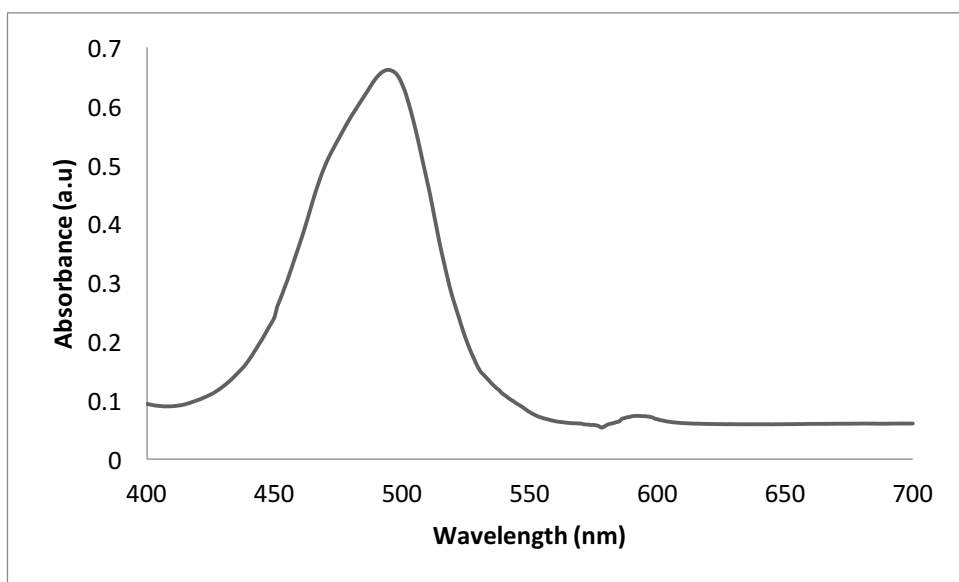


Figure C-7: UV/Vis spectrum of SG in PBS at 20X concentration

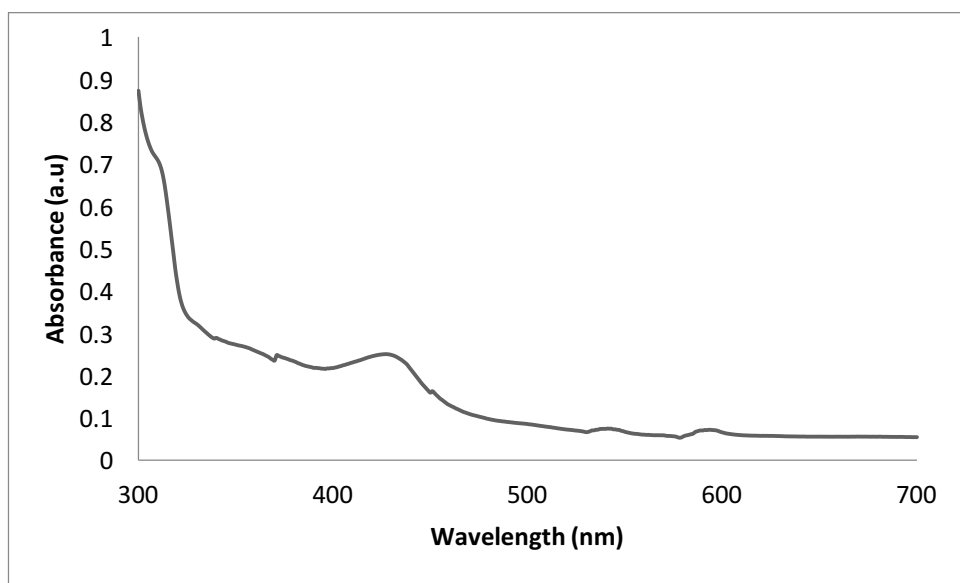


Figure C-8: UV/Vis spectrum of RS in DMSO at 20X concentration

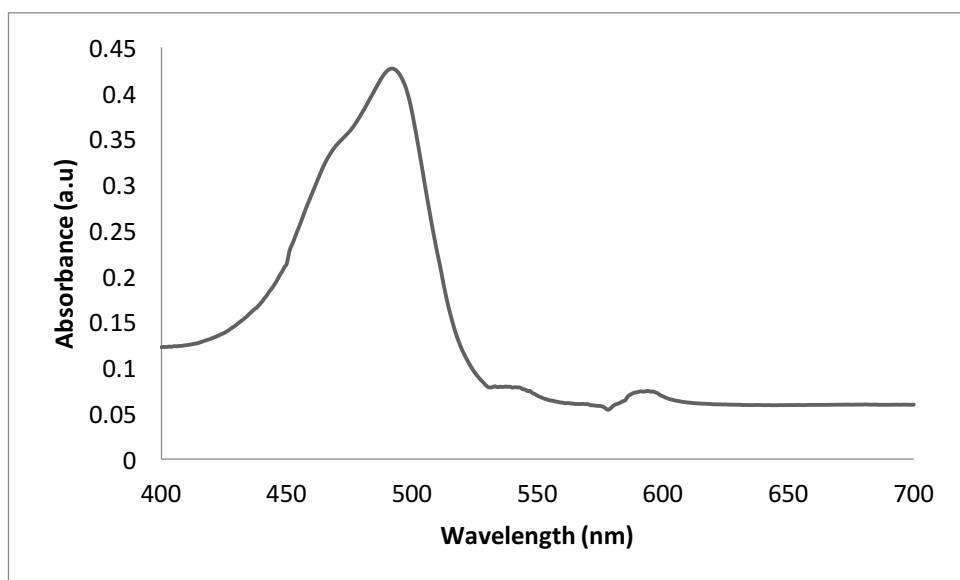


Figure C-9: UV/Vis spectrum of RS in TBE at 20X concentration

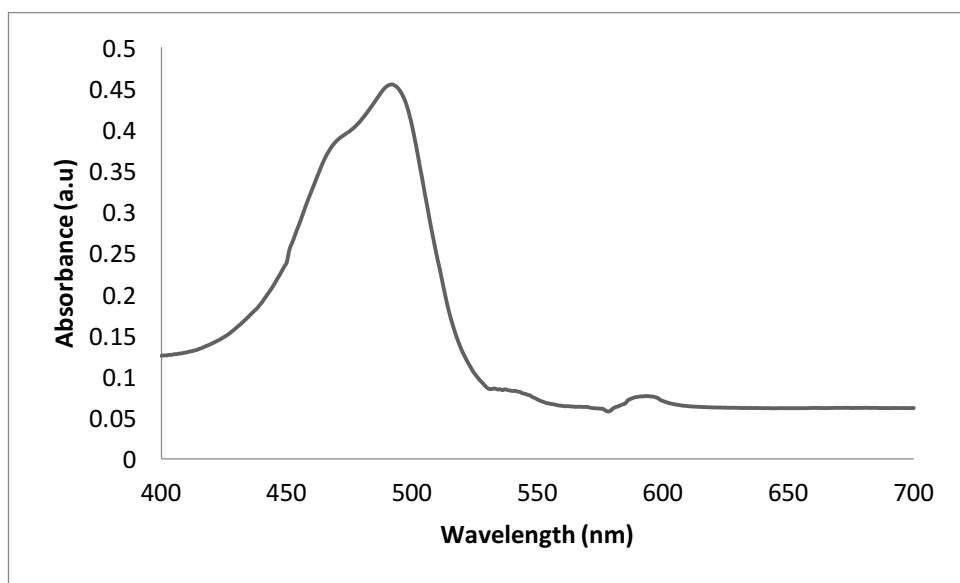


Figure C-10: UV/Vis spectrum of RS in PBS at 20X concentration

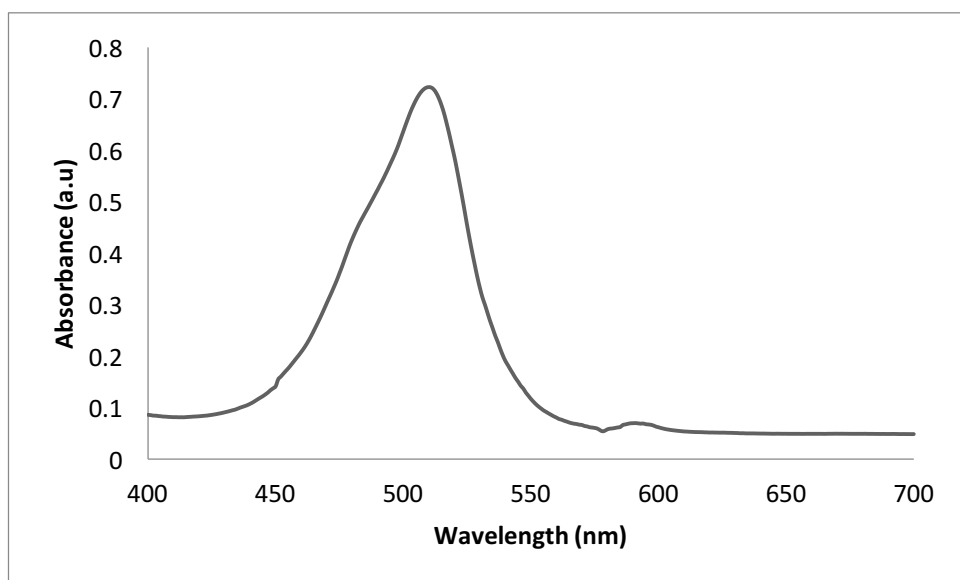


Figure C-11: UV/Vis spectrum of GG in DMSO at 20X concentration

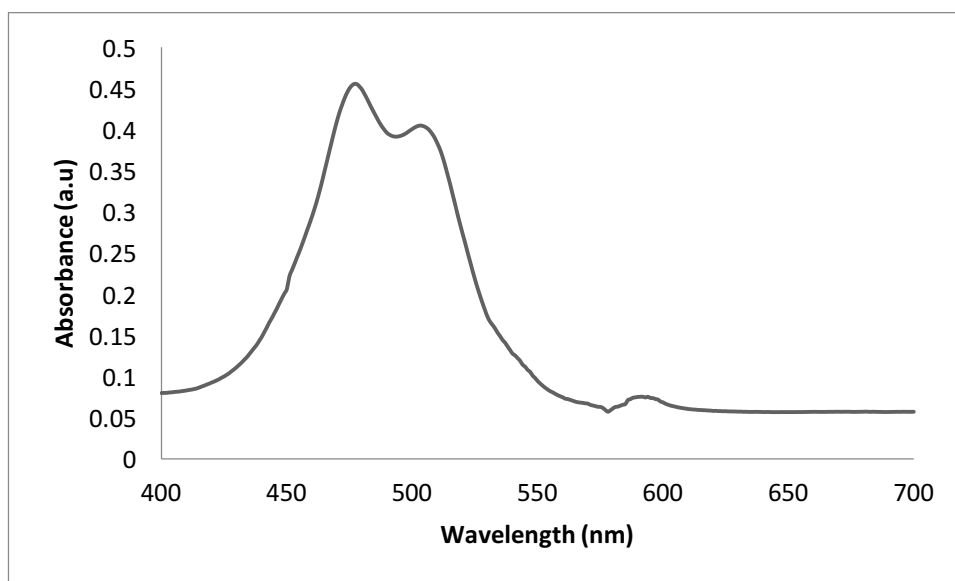


Figure C-12: UV/Vis spectrum of GG in PBS at 20X concentration

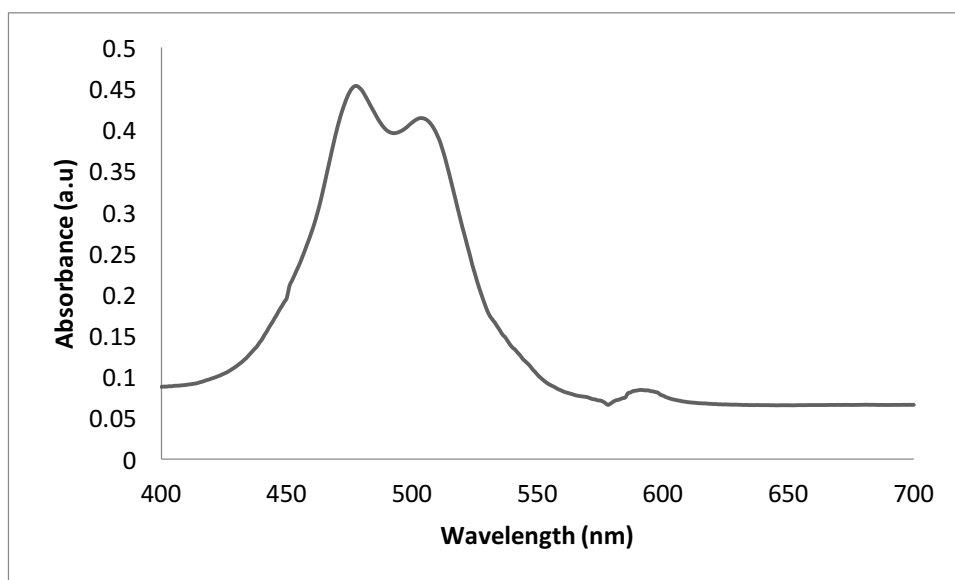


Figure C-13: UV/Vis spectrum of GG in TBE buffer at 20X concentration

Table C-6: Maximum wavelength of absorption of SYBR® Green I in various buffer solutions

Buffer	λ_{max} (nm)	Absorbance (a.u)
TBE	494	0.6267
PBS	495	0.6625
DMSO	498	0.7907
H ₂ O	495	0.2856

Table C-7: Maximum wavelength of absorption of RedSafe™ in various buffer solutions

	λ_{max} (nm)	Absorbance (a.u)
TBE	492	0.4208
PBS	492	0.4517
DMSO	427	0.2501
H ₂ O	492	0.4521

Table C-8: Maximum wavelength of absorption of GelGreen™ in various buffer solutions

Buffer	$\lambda_{\text{max 1}}$	Absorbance (a.u)	$\lambda_{\text{max 2}}$	Absorbance (a.u)
TBE	478	0.4496	503	0.4135
PBS	477	0.4472	503	0.4083
DMSO	510	0.7214		
H ₂ O	474	0.2092	497	0.2046

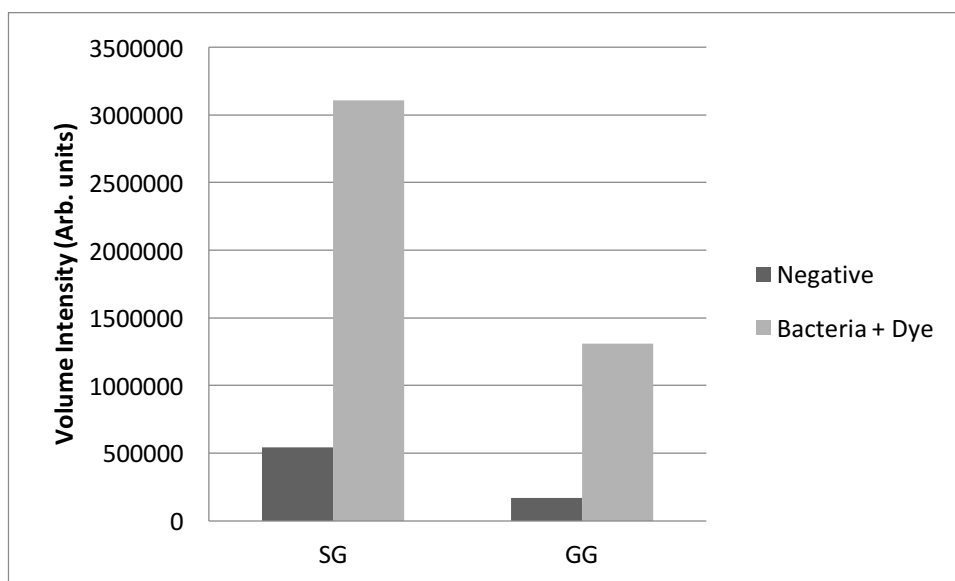


Figure C-14: Comparison of background signal and in the presence of bacteria for SG and GG once dye had dried on glass surface

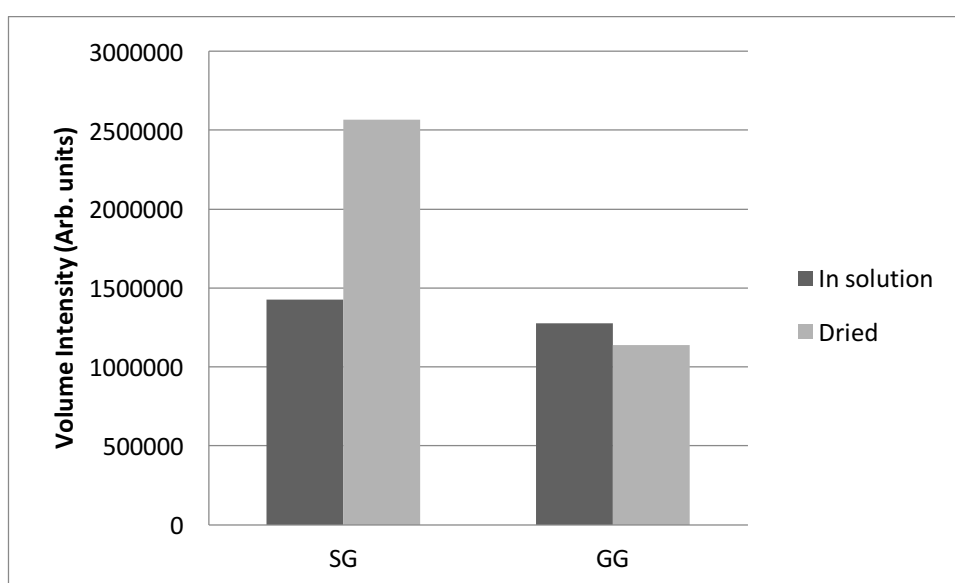


Figure C-15: Comparison of background signal and in the presence of bacteria for SG and GG with dye in solution on a glass substrate

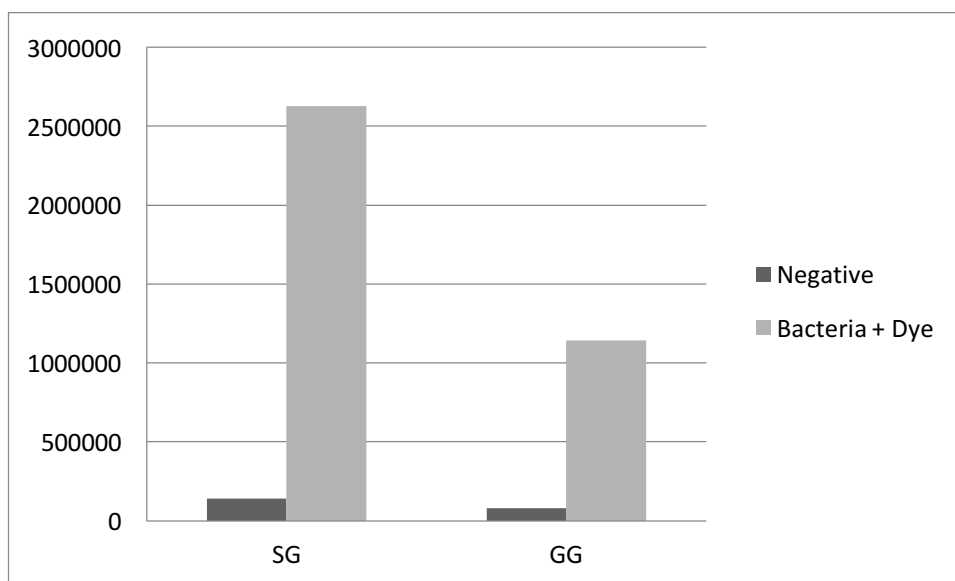


Figure C-16: Comparison of background signal and in the presence of bacteria for SG and GG once dye had dried on a plastic surface

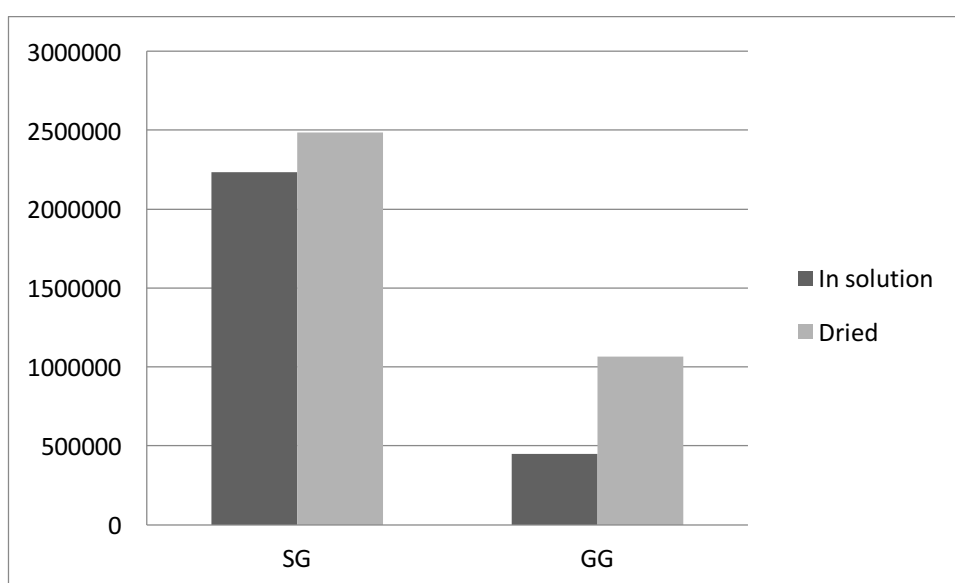


Figure C-17: Comparison of background signal and in the presence of bacteria for SG and GG with dye in solution on a glass substrate

Table C-9: Volume intensity data for RS (20X) 1.12 s exposure

	Negative	DNA	Protein	DNA enhancement	Protein enhancement
1	499473	789984	588159	1.581635	1.177559
2	347913	673767	428796	1.936596	1.232481
3	324012	668980	419740	2.064677	1.295446
Average	390466	710910.3	478898.3	1.860969	1.235162
st dev	95156.23	68521.62	94730.79	0.250244	0.058989
95%	37055.44	26683.47	36889.77	0.097449	0.022971

Table C-10: Volume intensity data for DD (20X) 1.12 s exposure

	Negative	DNA	Protein	DNA enhancement	Protein enhancement
1	108878	1588570	128744	14.59037	1.182461
2	99190	1783210	134290	17.97772	1.353866
3	101178	1615446	117180	15.96638	1.158157
Average	103082	1662409	126738	16.17815	1.231495
st dev	4177.978	86121.24	7127.695	1.703578	0.106671
95%	1626.975	33537.06	2775.644	0.663402	0.04154

Table C-11: Volume intensity data for SG (20X) 1.12 s exposure

	Negative	DNA	Protein	DNA enhancement	Protein enhancement
1	22211	1102969	43890	49.65868	1.976048
2	15096	1081336	55624	71.63063	3.684685
3	53235	986193	62712	18.52527	1.178022
Average	30180.67	1056833	54075.33	46.60486	2.279585
st dev	16558.63	50724.54	7761.688	26.68406	1.280602
95%	6448.211	19752.99	3022.532	10.39122	0.498688

Table C-12: Volume intensity data for EG (20X) 1.12 s exposure

	Negative	DNA	Protein	DNA enhancement	Protein enhancement
1	73491	785607	24628	10.68984	0.335116
2	69720	906500	26740	13.00201	0.383534
3	81302	891844	25488	10.96952	0.313498
Average	74837.67	861317	25618.67	11.55379	0.344049
st dev	4823.264	53868.37	867.1568	1.261966	0.035863
95%	1878.26	20977.25	337.6855	0.491431	0.013965

Table C-13: Volume intensity data for GG (20X) 1.12 s exposure

	Negative	DNA	Protein	DNA enhancement	Protein enhancement
1	7620	17780	8255	2.333333	1.083333
2	16560	18120	11280	1.094203	0.681159
3	6105	18537	7881	3.036364	1.290909
Average	10095	18145.67	9138.667	2.154633	1.018467
st dev	4613.095	309.5764	1521.83	0.983335	0.310007
95%	1796.417	120.5543	592.6263	0.382927	0.120722

Table C-14: Volume intensity data for GR (20X) 1.12 s exposure

	Negative	DNA	Protein	DNA enhancement	Protein enhancement
1	5980	27370	6555	4.576923	1.096154
2	7434	29736	7788	4	1.047619
3	7316	30326	7552	4.145161	1.032258
Average	6910	29144	7298.333	4.240695	1.058677
st dev	659.3714	1277.323	534.3734	0.300092	0.033352
95%	256.7703	497.4112	208.094	0.116861	0.012988

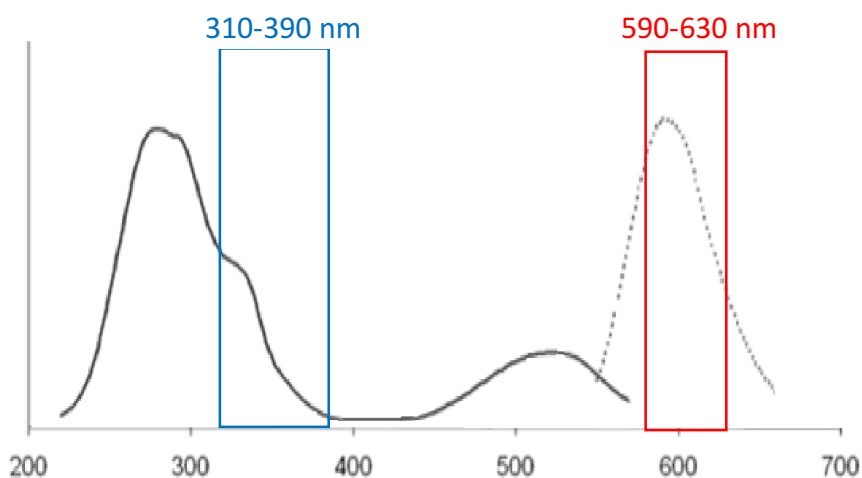


Figure C-18: Spectrum of GelRed showing the excitation and emission and the settings of the filters to be used mentioned in table 1.

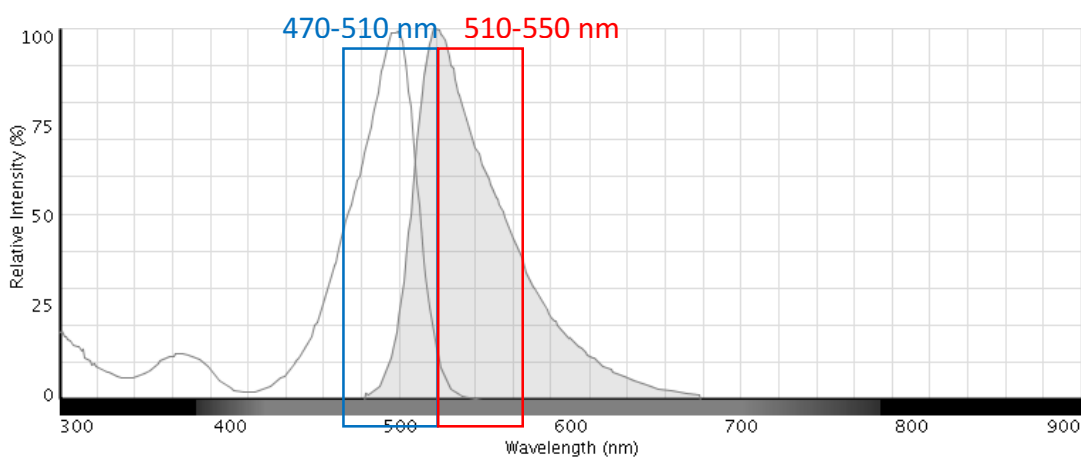


Figure C-19: spectrum of SYBR Green I showing the excitation and emission and the settings of the filters to be used mentioned in table 1.

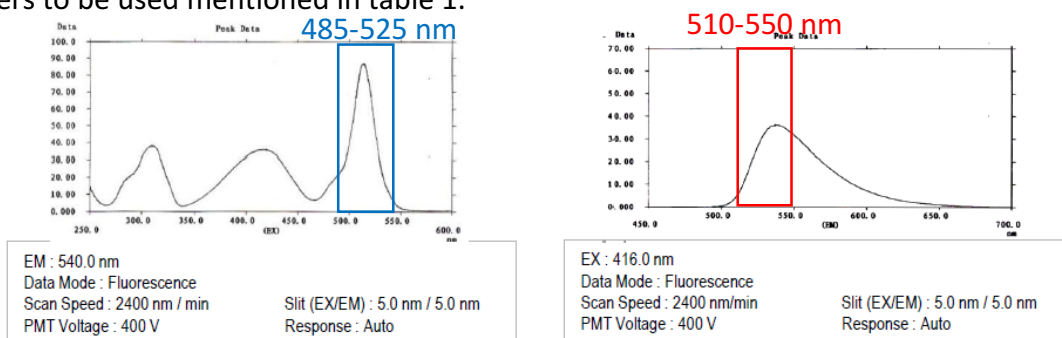


Figure C-20: Spectrum of RedSafe showing excitation and emission and the settings of the filters to be used mentioned in table 1.

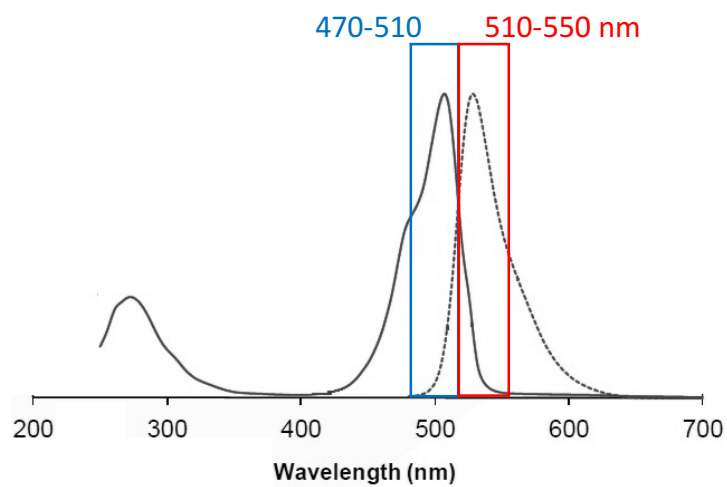


Figure C-21: Spectrum of GelGreen showing excitation and emission and the settings of the filters to be used mentioned in table 1.

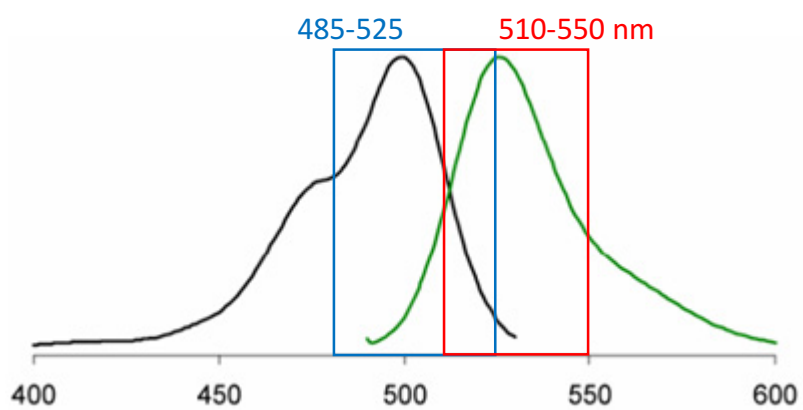


Figure C-22: Spectrum of EvaGreen showing excitation and emission and the settings of the filters to be used mentioned in table 1.

Table C-16: Volunteer 1 quantification of each fingerprint on acetate paper using Qubit

♂	1 (ng/μL)	2(ng/μL)	3(ng/μL)	Average(ng/μL)
R T	0.026	0.0259	0.0255	0.0258
R I	0.018	0.0167	0.0176	0.017433
R M	0.0235	0.0233	0.0232	0.023333
R R	0.0143	0.0142	0.0142	0.014233
R P	0.0362	0.036	0.0358	0.036
L T	0.0299	0.0297	0.0296	0.029733
L I	0.0176	0.0175	0.0174	0.0175
L M	0.0173	0.0172	0.0171	0.0172
L R	0.0361	0.0361	0.0358	0.036
L P	0.0214	0.0213	0.0212	0.0213

Table C-17: Volunteer 2 quantification of each fingerprint on acetate paper using Qubit

♀	1(ng/μL)	2(ng/μL)	3(ng/μL)	Average(ng/μL)
Negative	0.007	0.0071	0.0072	0.0071
R T	0.0083	0.0083	0.0083	0.0083
R I	0.008	0.0082	0.0084	0.0082
R M	0.0061	0.0062	0.0062	0.006167
R R	0.0072	0.0075	0.0075	0.0074
R P	0.0065	0.0066	0.0067	0.0066
L T	0.0094	0.0094	0.0094	0.0094
L I	0.0079	0.0081	0.0082	0.008067
L M	0.0063	0.0063	0.0062	0.006267
L R	0.0066	0.0068	0.0068	0.006733
L P	0.0102	0.0105	0.0108	0.0105

Table C-18: Volunteer 3 quantification of each fingerprint on acetate paper using Qubit

♀	1(ng/μL)	2(ng/μL)	3(ng/μL)	Average(ng/μL)
Negative	0.122	0.12	0.119	0.120333
R T	0.0066	0	0	0.0022
R I	0	0	0	0
R M	0	0	0	0
R R	0	0	0	0
R P	0	0	0	0
L T	0.0051	0.005	0.005	0.005033
L I	0	0	0	0
L M	0.125	0.121	0.12	0.122
L R	0.137	0.132	0.131	0.133333
L P	0.123	0.119	0.12	0.120667

Detection of DNA within Fingermarks



Alicia M. Haines¹, Shanan S. Tobe¹, Hilton Kobus², Adrian Linacre¹

¹School of Biological Sciences, Flinders University, Adelaide, Australia

²School of Chemical and Physical Sciences, Flinders University, Adelaide, Australia



Presented at the 2013 ISFG Conference Melbourne, Australia

Funding was provided by the Department of Justice, South Australia

Introduction

We report on a process to detect latent DNA associated with fingermarks. While there are many techniques available for the enhancement of fingermarks that involve amino acid interactions, there are no techniques for fingermark enhancement that involve interactions with DNA.

Latent DNA at crime scenes is collected by swabbing areas that have a high potential for the presence of DNA; substrates include door handles, phones and objects that have been used in an assault. These swabs are then submitted to a laboratory for DNA extraction and profiling. An issue with this process is that the majority of swabs produce no profile as the amount of DNA present is too low; one reason being that most of the DNA is lost during the extraction process [1]. To be able to visualize latent DNA at crime scenes, specifically touch DNA, would result in a targeted approach for the collection of DNA samples and a more efficient method.

Bright [2] suggests that epithelial cells are sloughed off the skin surface and transferred onto various substrates by touch and that these cells are keratinised and lack nuclei; the DNA present on the surface is either present as a free molecule (cell free DNA), or within a cell membrane [3-4].

Currently there are techniques that can detect certain types of biological fluids such as semen using different wavelengths of light which can cause fluorescence. Chemical reagents such as luminol is used for blood stain detection and amylase tests for saliva, these methods however do not detect DNA [5]. For the detection of latent fingermarks there are many techniques available such as powder dusting and cyanoacrylate fuming on non-porous substrates and reagents such as DFO and ninhydrin that react with the amino acids on porous substrates [6].

SYBR® Green 1 and GelGreen™ are nucleic acid staining dyes used in gel electrophoresis. They have a maximum excitation wavelength at 494 nm and emission at 520 nm [7]. The fluorescence and absorption spectra of SYBR Green I is shown in Fig. 1. A and B below.

This study investigated whether the intercalating dyes SYBR® Green I and GelGreen™ could detect DNA within fingermarks on various substrate surfaces. If DNA at crime scenes could be visualized then more DNA could be targeted resulting in more swabs producing high quality profiles.

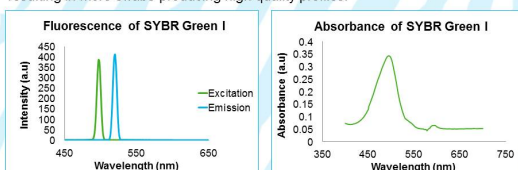


Fig 1. A. Fluorescence spectrum of SYBR Green I 20X solution in H₂O, emission at 494 nm and excitation at 520 nm. Fig 1. B. Absorbance spectrum of SYBR Green I 20X solution diluted with H₂O, maximum absorption at 495 nm.

Method

Dye Preparation: SYBR® Green I (Invitrogen) and GelGreen™ (Biotium) were diluted to varying working solution concentrations in sterile H₂O.

Substrate Preparation: Plastic slides, glass slides and Parafilm® were placed under UV before use.

Dye Application: 5 µL of dye was pipetted onto the surface of the substrate and fluorescence was measured either in solution, after the dye had dried or after the dye was washed off using H₂O.

Visualization: The intensity of fluorescence was measured using the Bio-Rad Gel Doc EZ Imager. Fluorescence of the negative controls was subtracted from the samples' fluorescence.

Results

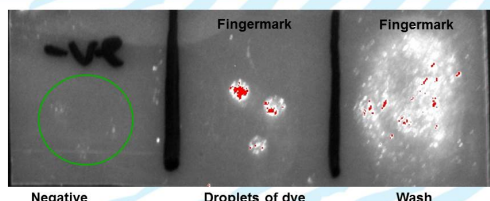


Fig 2. Fluorescence when SG 100x solution is pipetted onto Parafilm® where no fingermark was present and where a 30 s fingermark was made

Correspondence: Alicia M. Haines, Flinders University, South Australia, Ph. (08) 8201 5003, alicia.haines@flinders.edu.au

Bacterial Background Study

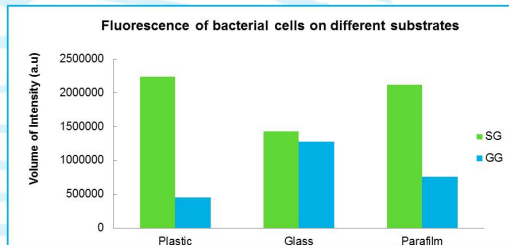


Fig 3. Volume of intensity of SYBR Green 1 (SG) and GelGreen (GG) (5 µL of 20x solution in H₂O) in the presence of *E. coli* DH5α in PBS solution (1 µL ~10⁶ cells) with fluorescence measured with dye in solution on different substrates

Fingermark Study

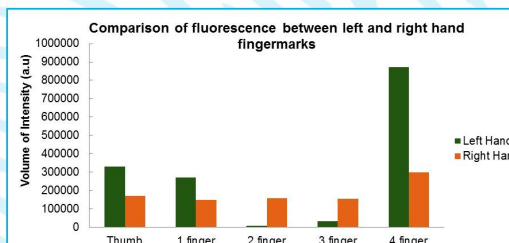


Fig 4. Volume of intensity of 5 s fingermarks on Parafilm® where the dye GG (5 µL of 40x solution in H₂O) was pipetted onto the surface and allowed to air dry

Discussion

Fig. 1 shows that fluorescence on Parafilm® was greatly increased when a fingermark was present. Background fluorescence in the negative control is low compared with the intensity when a fingermark was present.

Fig 2 shows that both dyes produce a high intensity of fluorescence when in the presence of bacterial cells. SG has a higher intensity as the dye can permeate the cell and bind with cellular DNA [8].

Fig 3 illustrates the variability in fluorescence between left and right hands and different fingers. Many factors are involved in the deposition of DNA onto a surface which may include; substrate surface, nature of contact, environmental factors and the individual depositing the DNA.

One issue with using SG is that it can permeate the cell membrane and thus can be mutagenic at high concentrations (33 µg) [8] which means the dye might not be viable for this novel method if a high concentration is required for DNA detection.

Another issue present with using these dyes for DNA detection was that fluorescence was present when no fingermark was present. So this means that either there was bacterial DNA present on the surface, the dyes were interacting with the surface or due to the light reflecting off the surface. For the improvement of this novel method the background fluorescence will need to be reduced.

Concluding Remarks

This study has found that DNA within fingermarks can be detected using the intercalating dyes SYBR® Green I and GelGreen™ however it is unknown if the DNA detected is human or bacterial as both dyes have a high interaction with bacterial DNA.

References

- [1] F. Alessandrini, M. Cecati, M. Pesaresi, et al. Fingerprints as Evidence for a Genetic Profile: Morphological Study on Fingerprints and Analysis of Exogenous and Individual Factors Affecting DNA Typing. *J. Forensic Sci.* 48 (2003) 1-7.
- [2] J. Bright, S.F. Petricic, Recovery of trace DNA and its application to DNA profiling of shoe insoles. *Forensic Sci. Int.* 145 (2004) 7-12.
- [3] R.A. Wickens, Trace DNA: A review, Discussion of Theory, and Application of the Transfer of Trace Quantities of DNA Through Skin Contact. *J. Forensic Sci.* 47 (2002) 442-450.
- [4] A. Linacre, V. Pekarek, Y. Swaran, et al. Generation of DNA profiles from fabrics without DNA extraction. *Forensic Sci. Int. Genet.* 4 (2010) 137-141.
- [5] N. Vandenberg, R.A.H. van Oorschot, The Use of Poilight® in the Detection of Seminal Fluid, Saliva, and Bloodstains and Comparison with Conventional Chemical-Based Screening Tests. *J. Forensic Sci.* 51 (2006) 361-370.
- [6] C. Lennard, Forensic Sciences | Fingerprint Techniques, in: P.T. Alan, P. Colin, Encyclopedia of Analytical Science, second ed, Elsevier, Oxford, 2005, pp. 414-423.
- [7] A. Dragan, R. Pavlovic, J.B. McGinley, et al. SYBR Green I: Fluorescence properties and Interaction with DNA. *J. Fluorescence* 22 (2012) 1189-1199.
- [8] T. Ohta, S. Tokishita, H. Yamagata, Ethidium bromide and SYBR Green I enhance the genotoxicity of UV-irradiation and chemical mutagens in *E. coli*. *Mut. Res.* 492 (2001) 91-97.

Figure C-23: Poster presentation entitled “Detection of DNA within fingermarks” at the 25th Congress of the international society of Forensic Genetics, Melbourne, 2013

Quantification of ds-DNA and protein present within the residue of fingermarks using the Qubit 2.0 Fluorometer

Alicia. M. Haines¹, Jennifer Templeton¹, Shanan. S. Tobe¹, Hilton Kobus², Adrian Linacre¹

¹ School of Biological Sciences, Flinders University, South Australia

² School of Chemical and Physical Science, Flinders University, South Australia

Introduction

DNA can be recovered from fingermarks present on various substrates using an extraction process or direct PCR methodology. STR profiles have been obtained from touched samples but the actual total DNA (bacterial and human) within the residue of a fingermark is ambiguous. As the DNA within fingermarks can be highly variable due to many factors such as temperature, surface type and shedding ability, it is difficult to determine a specific value but a range can be obtained to give an approximation as to how much DNA is present that can aid in enhancement methodologies.

A study by Daly *et al.* showed that from 300 participants the mean amount of DNA recovered from hands touching an object for 60 seconds using the Quantifiler kit with prior extraction was 5.85 ng for wood, 1.23 ng for fabric and 0.52 ng for glass. The estimated range of total DNA obtained was 0-169 ng for wood, 0-14.8 ng for fabric and 0-5.2 ng for glass [1]. However the study did not look at plastic as a surface.

This study aims to determine the total DNA (bacterial and human DNA) and protein present within a fingermark without doing a typical extraction and quantifying the DNA using the Qubit 2.0 Fluorometer (Life Technologies, AUS) from a plastic surface (plastic bag).

Method

• Sample Collection

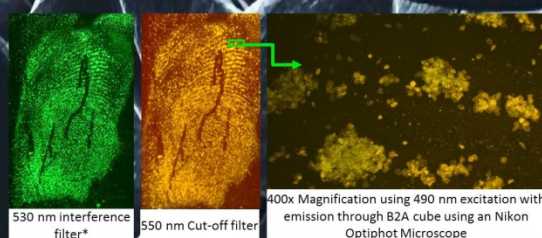
Fingermarks were deposited onto a 1 cm x 1 cm plastic surface that had been cleaned with bleach, isopropyl alcohol and placed under UV for 20 min prior to fingermark deposit. Participants were asked to wash their hands and then deposit a fingermark on the plastic 1 hour after hand-washing. The plastic square was then placed into a microcentrifuge tube and buffer (10 µL of Ethanol 100%, 240 µL 1X TE buffer) was added to the sample then vortexed (30 s) and centrifuged (1 min at 13,000 rpm). An aliquot of the sample (20 µL) was removed for protein analysis, then the sample was heated at 85°C for 20 min. Aliquots of the sample was then removed for DNA quantification.

• Quantification using Qubit 2.0 Fluorometer

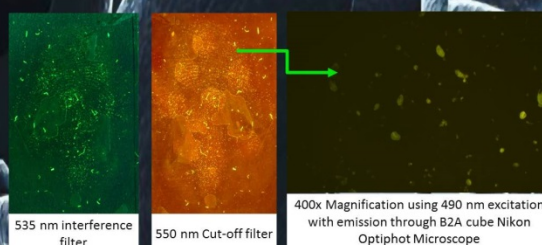
Quantification of ds-DNA and protein was carried out according to the manufacturer's protocol by using 20 µL of the sample.



Fingermarks-Protein Dye



Fingermarks-DNA Dye



The fingermarks above show that there appears to be more protein present than DNA within a fingermark which was also shown in the quantification results. Under the microscope the ridge patterning of the protein fingermark can be seen but the DNA fingermark the ridge patterning could not be identified.

*Note: the grooves present in the fingermark was from the pipette tip spreading the dye across the mark not an artefact of the fingermark itself.

Results

Table 1: Mean DNA concentration quantified by the Qubit 2.0 Fluorometer and the total DNA present within a fingermark

Source of DNA*	Average reading (ng/µL)	Sample - Negative control (ng/µL)	Total DNA** (ng)
Negative Control	0.0071		
R T	0.0083	0.00120	0.30
R I	0.0082	0.00110	0.28
R M	0.0062	-0.00093	0
R R	0.0074	0.00030	0.075
R P	0.0066	-0.00050	0
L T	0.0094	0.00230	0.58
L I	0.0081	0.00097	0.24
L M	0.0063	-0.00083	0
L R	0.0067	-0.00037	0
L P	0.0105	0.00340	0.85
Average Total DNA			0.23

* R denotes right hand L = Left hand, T=thumb, I=index, M=middle, R=ring, P=pinky

** Total DNA refers to the total amount in the 250 µL buffer that was used to remove the fingermark from the plastic surface, so Total DNA= (Sample-Negative control) X 250 µL

Table 2: Mean concentration of protein quantified by the Qubit 2.0 Fluorometer and the total protein content present within a fingermark

Source of protein*	Average reading (ng/µL)**	Sample - Negative control (ng/µL)	Total Protein*** (µg)
Negative Control	<10	0.0	0.0
R T	<10	0.0	0.0
R I	<10	0.0	0.0
R M	10.0	10.0	2.5
R R	<10	0.0	0.0
R P	<10	0.0	0.0
L T	<10	0.0	0.0
L I	<10	0.0	0.0
L M	11.0	11.0	2.8
L R	<10	0.0	0.0
L P	<10	0.0	0.0
Average Total Protein			0.48

* R denotes right hand L = Left hand, T=thumb, I=index, M=middle, R=ring, P=pinky

** If the signal was below 10 ng/µL then it would only give a reading of <10 ng/µL

*** Total Protein refers to the total amount in the 250 µL buffer that was used to remove the fingermark from the plastic surface, so Total Protein= (Sample-Negative control) X 250 µL

Conclusion

From the results the average total amount of DNA present within a fingermark (1 cm²) was 0.23 ng and the average total protein content was determined to be 0.48 µg on a plastic surface (cut up plastic bag). There was about a 2000 fold increase in the protein content compared with the DNA signal. Persistent signals in the negative controls will be investigated in further studies.

References

[1] Daly, D.J., Murphy, C. & McDermott, S.D. The transfer of touch DNA from hands to glass, fabric and wood. *Forensic Sci. Int. Genet.* 6 (2012) 41-46.

Funding was provided by the Attorney General's Office, South Australia

Correspondence: alicia.haines@flinders.edu.au



Figure C-24: Poster presentation entitled "Quantification of ds-DNA and protein present within the residue of fingermarks using the Qubit 2.0 Fluorometer" at the ANZFS symposium, Adelaide, 2015

Finding DNA; using fluorescent *in situ* detection



Alicia M. Haines¹, Shanan S. Tobe¹, Hilton Kobus², Adrian Linacre¹

¹School of Biological Sciences, Flinders University, Adelaide, Australia

²School of Chemical and Physical Sciences, Flinders University, Adelaide, Australia



Presented at the 26th Congress of the ISFG (2015) Krakow, Poland

Funding was provided by the Attorney General's Department, South Australia

Introduction

Finding latent DNA at crime scenes will aid greatly in targeting and collection of samples by directing the examiner to locations where touch DNA may be present. Detecting DNA has been performed in the laboratory using nucleic acid binding dyes within gel electrophoresis and in quantification techniques. Ethidium bromide was first used in the early 70's for staining gels [1] and more recently dyes such as SYBR[®] Green and PicoGreen[®] have been used in DNA quantification [2].

Two main modes of interaction of dyes with DNA include intercalating and groove binding mechanisms. SYBR[®] Green and ethidium bromide are intercalating dyes that bind between the base pairs of DNA [3] and DAPI binds to AT rich regions of DNA [4]. The binding mechanism of the dye with DNA affects the sensitivity and specificity e.g. SYBR[®] Green has both electrostatic and extended groove contact with a fluorescent enhancement of 1000 fold [3].

This study looks at the application of recently available dyes for the detection of latent DNA encountered during a forensic examination. Six nucleic acid binding dyes was investigated to determine their sensitivity and specificity. The dyes investigated were SYBR[®] Green I (SG), Diamond[™] Nucleic acid dye (DD), GelGreen[™] (GG), GelRed[™] (GR), EvaGreen[™] (EG) and RedSafe[™] (RS). The properties of these DNA binding dyes are shown in Table 1.

Table 1: Properties of the selected nucleic acid binding dyes

Binding Dye	Main Function	Excitation (nm)	Emission (nm)	Binding Mechanism	Fluorescent Enhancement (DNA)
SYBR [®] Green I (SG)	qPCR, Flow cytometry, Gel Staining	494	520	Intercalator	1000
Diamond [™] Dye (DD)	Gel Staining	494	558	External binder	N/A
GelGreen [™] (GG)	Gel Staining	495	520	Intercalator	N/A
GelRed [™] (GR)	Gel Staining	300, 250	600	Intercalator	N/A
EvaGreen [™] (EG)	qPCR, DNA gel stain, isothermal amplification	500	530	Release on demand mechanism	70
RedSafe [™] (RS)	Gel Staining	309, 419, 514	537	N/A	N/A

N/A= information not available

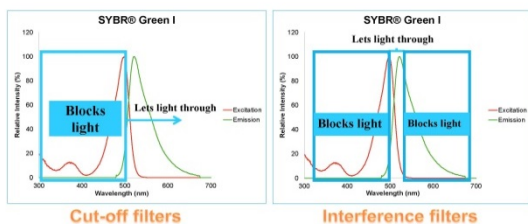
Method

2.1 Staining

Biological samples were stained with the six DNA binding dyes at a concentration of 20X. The samples stained comprised shed, plucked hairs, saliva, dead skin, fingerprints and diluted extracted DNA (0.5 ng up to 50 ng)

2.2 Fluorescent detection

Samples were viewed using a Nikon Optiphot fluorescent microscope using a B2A filter cube. Images were taken using an exposure time of 1 s. Samples on a glass surface (fingerprints and extracted DNA) were placed under a Nikon camera with filters attached (cut-off at 530 nm, interference at 555 and 530 nm) and excited using a Polilight (490 nm). The differences between cut-off and interference filters are shown below. Interference filters are more specific to a target emission signal.



Correspondence: Alicia M. Haines, Flinders University, South Australia
Email: alicia.haines@flinders.edu.au

Results

Table 2: Saliva stained with DNA binding dyes at a concentration of 20X showing cell permeability

Dye	Saliva Samples
Diamond [™] Dye	
EvaGreen [™]	
SYBR [®] Green I	
RedSafe [™]	
GelGreen [™]	

Table 3: Biological samples stained with SG (20X concentration)

Biological Sample	Image
Hair	
Skin	
Blood	

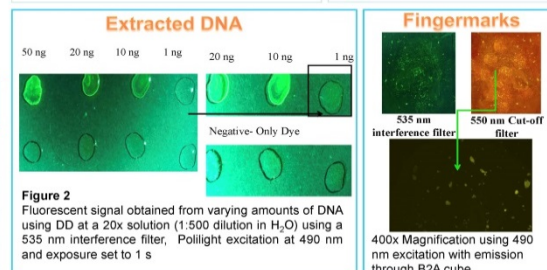


Figure 2: Fluorescent signal obtained from varying amounts of DNA using DD at a 20x solution (1:500 dilution in H₂O) using a 535 nm interference filter. Polilight excitation at 490 nm and exposure set to 1 s

Table 4: Plucked hair samples staining with DNA binding dyes at 20X concentration

Biological Sample	DD	GG	EG	RS
Hair				

Discussion

Tables 2, 3 and 4 depict the staining of individual nuclei using selected DNA binding dyes applied to samples such as saliva and hairs. The dyes can effectively stain latent DNA within fingerprints. DNA could be detected down to 1 ng using DD and SG. When staining skin fragments the signal would most likely be auto fluorescence from the skin itself, however regions of fluorescent clusters could be either bacterial or intracellular DNA. GG does not permeate the cell membrane (table 4) resulting in no nuclei being stained within the hair.

Concluding Remarks

- Latent DNA can be detected using selected dyes allowing a targeted approach when collecting material at a scene.
- Recommended dyes include SG, EG and DD. GR and GG were not ideal for staining.
- Samples that have a high fluorescent signal are those most likely to provide an STR profile.

References

- [1] Aaij C., Borst P. The gel electrophoresis of DNA. *Biochimica et Biophysica Acta (BBA)* 1972; 269(2): p 192-200.
- [2] Haines, A.M., et al., Properties of nucleic acid staining dyes used in gel electrophoresis. *Electrophoresis*, 2015; 36(6): p. 941-944.
- [3] Origen, A.I., et al., SYBR Green I: Fluorescence Properties and Interaction with DNA. *Journal of Fluorescence*, 2012; 22(4): p. 1189-1199.
- [4] Barcellona, M.L., et al., Time-resolved fluorescence of DAPI in solution and bound to polydeoxynucleotides. *Biochem Biophys Res Commun*, 1990; 176(1): p. 270-80.

Figure C-25: Poster presentation presented at the 26th congress of the ISFG, Krakow, Poland, 2015.

Chapter 5

DNA binding dyes for nuclear hist staining

5.1 Introduction

5.1.1 Hairs as evidence

Humans shed around 75-150 hairs per day and therefore can provide potential forensic evidence at crime scenes [1, 2]. The primary technique for hair examination is through comparative microscopy [3]. Multiple hairs can be evaluated for similarities of known and unknown samples. Through microscopy the origin of the hair can be identified (human or animal) along with the hair growth type (essential for further analysis). Once identified as human, microscopic analysis can determine the ethnic origin (Caucasian, Asian or African) and body area from which the hair came from [4]. Other features of the hairs that microscopy can examine is the shape of the hair tip, colour, pigment pattern and if any potential damage had occurred that relates to the hair as evidence [5]. The issue with microscopy however is the lack of ability of assigning a probability to those features as it is highly challenging, resulting in the analysis being considered as a qualitative assessment and not an objective classification. Due to the qualitative nature, microscopic comparisons of hairs may not be sufficient to eliminate an individual as the donor of a hair [3, 5-7]. Although microscopic examination is an important aspect of hair analysis as forensic evidence there are limits to the level of discrimination that this technique can offer.

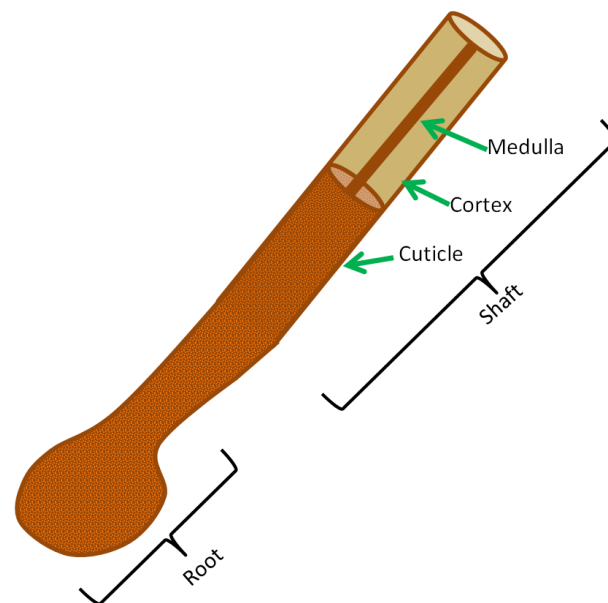
Different types of microscopy along with comparison microscopy can be used for the analysis of hair follicles such as the following:

- Scanning electron microscope [8]
- Fluorescent microscopy [9, 10]
- Confocal microscopy [11]

5.1.2 Hair structure

There are three primary structures that form the foundations of a hair follicle these are the medulla, the cortex and the cuticle. The medulla is the central shaft shown in Scheme 5.1 which consists of mostly air. Surrounding the medulla is the cortex which is mostly made up of the protein keratin and it is here that the pigment melanin is found. The cuticle is the

outermost layer of the hair shaft (Scheme 5.1) [1]. There are three phases of hair growth: (1) anagen, (2) catagen and (3) telogen. Anagen hairs are the active growth phase described as the formation of new hair follicle and lengthening of the hair shaft. If hairs within this stage are forcibly removed, this often results in the removal of follicular material adhering to the root often containing intact nuclear DNA. Catagen hairs are the least likely of hairs to be found at a crime scene as this stage is short-lived and involves the termination of cell division. The telogen phase is known as the resting stage before the hair is shed naturally and contributes to about 95 % of hairs collected as forensic evidence [5].



Scheme 5.1: Schematic representation of a hair follicle showing the three primary structures, Medulla, cortex and cuticle, as well as the root.

5.1.3 Hair as a source of DNA

Hairs as forensic evidence can be an important source of DNA; however they contain minute amounts of DNA unlike other evidence such as a large blood stain or saliva swab. The main section of the hair follicle that contains the most DNA is within the hair root. The shaft of the hair has minimal nuclear DNA but does still contain mitochondrial DNA (mtDNA) which is often analyzed to aid in forensic investigations [12].

DNA typing of hairs is the most accurate method of matching a sample hair with an individual, although during the keratinization of the hair shaft DNA is lost. There is however still nucleated cells attached to the root of the hair during the anagen phase [1].

Phenol extraction of telogen hairs yielded a quantity of 550 pg or less of nuclear DNA per hair and showed to be degraded using real-time PCR of ALU fragments [13] (this is a nuclear-based marker). As the amount of DNA that can be extracted from telogen hairs is minimal and highly degraded, obtaining full DNA profiles are shown to be rare. This has led to the use of mtDNA analysis [13].

Extractions of DNA results in substantial amount of loss due to the many tube changes and wash steps; this loss has been estimated to be around 84% for Promega IQ and 72% for QIAGEN Micro kit [17]. It was also shown previously (Chapter 3) that there was around 63% loss of DNA using the QIAGEN Micro kit [18]. Inhibitors to the PCR process co-extract with many DNA extraction processes. Melanin is an example of an inhibitor; however some of the inhibitory effects of this pigment can be reduced with the addition of extra *Taq* DNA polymerase and Bovine Serum Albumin (BSA) [14]. Studies have been undertaken that looked at amplifying the hair follicles directly with the addition of extra *Taq* which resulted in partial and full profiles using NGM™ Select [15]. Single-tube genotyping of hairs has also been undertaken omitting the extraction step using direct amplification [16].

5.1.4 Nuclear staining of hairs

As a means of trying to determine a hair's viability for STR typing, staining methods were employed to give an approximation of the number of nuclei present and thereby indicating the chances of obtaining an STR profile. Such staining methods have been established using fluorescent dyes such as DAPI [2, 9, 10, 19], TOTO-3 [20] and Hoechst 33258 [21]; however DAPI, being the more researched dye, has been implemented within forensic laboratories. Other stains that are not fluorescent consist of visible stains such as haematoxylin [5, 22]. The fluorescent dyes and stains are detailed below in Table 5.1 showing the properties and main functions of the dyes.

Table 5.1: Currently used staining methods for hair follicles

Staining method		Excitation (nm)	Emission (nm)	Cell permeable	Main Function
Fluorescent dyes	DAPI [2, 9, 19]	358	461	Cell impermeant at low concentrations	Nuclear and chromosome counterstain
	TOTO-3[20]	640	660	Cell impermeant	Nuclear counterstain
	Hoechst 33258[21]	352	461	Cell permeant	Counterstain, apoptosis
Visible dyes	Haematoxylin [5, 22]				Histological staining

5.1.5 Comparison of current methodology to potential new dyes for nuclear staining of hair follicles.

Table 5.2 shows the properties of the current dyes used within laboratories for hair follicle staining as listed in Table 5.1. The nucleic acid binding dyes that were investigated in previously (Chapters 1-4) are also included. The comparisons show the difference in the excitation and emission signals as well as the comparison of fluorescent enhancement of the known dyes. For instance DAPI which has a 20 fold increase in fluorescence signal when DNA is present is compared to SYBR Green which has around 1000-1500 fold increase in fluorescence signal when DNA is present.

Table 5.2: Comparison of currently used fluorescent stains with dyes used within Chapter 2 and 3

Fluorescent Stain		Excitation (nm)	Emission (nm)	Fluorescence Enhancement	Cell permeable
Hair stain	DAPI	358	461	~20 [23, 24]	Permeable at high concentrations
	TOTO-3	640	660		Impermeable
	Hoechst 33258	352	461	~30 [25]	Permeable
Gel electrophoresis/real-time PCR	SYBR Green	494	520	~1000-1500 [25, 26]	Permeable
	EvaGreen	500	525	~70 [27]	Impermeable (as stated by manufacturer)
	Diamond Dye	494	558	Unknown	Permeable
	GelGreen	495	520	Unknown	Impermeable
	RedSafe	300, 419, 514	537	Unknown	Permeable

Figure 5.1 below shows a schematic diagram of the excitation and emission spectra of DAPI in comparison to SG with the relative fluorescent enhancement when in the presence of DNA. This shows that SG is more sensitive for the detection of DNA than DAPI producing a much higher signal, which would suggest this dye be much more efficient at staining hair nuclei than DAPI.

The results in Chapter 2 showed that the fluorescence response to DNA using DD and GG was similar to that of SG and therefore the assumption is that they have a similar enhancement level. Another benefit of using these dyes instead of DAPI is that they have an excitation wavelength longer than UV which means the hairs do not need to be exposed to UV light thus preventing any risk of DNA degradation. As the amount of DNA present on the hair follicle is minimal the optimal method should not involve the exposure to UV light.

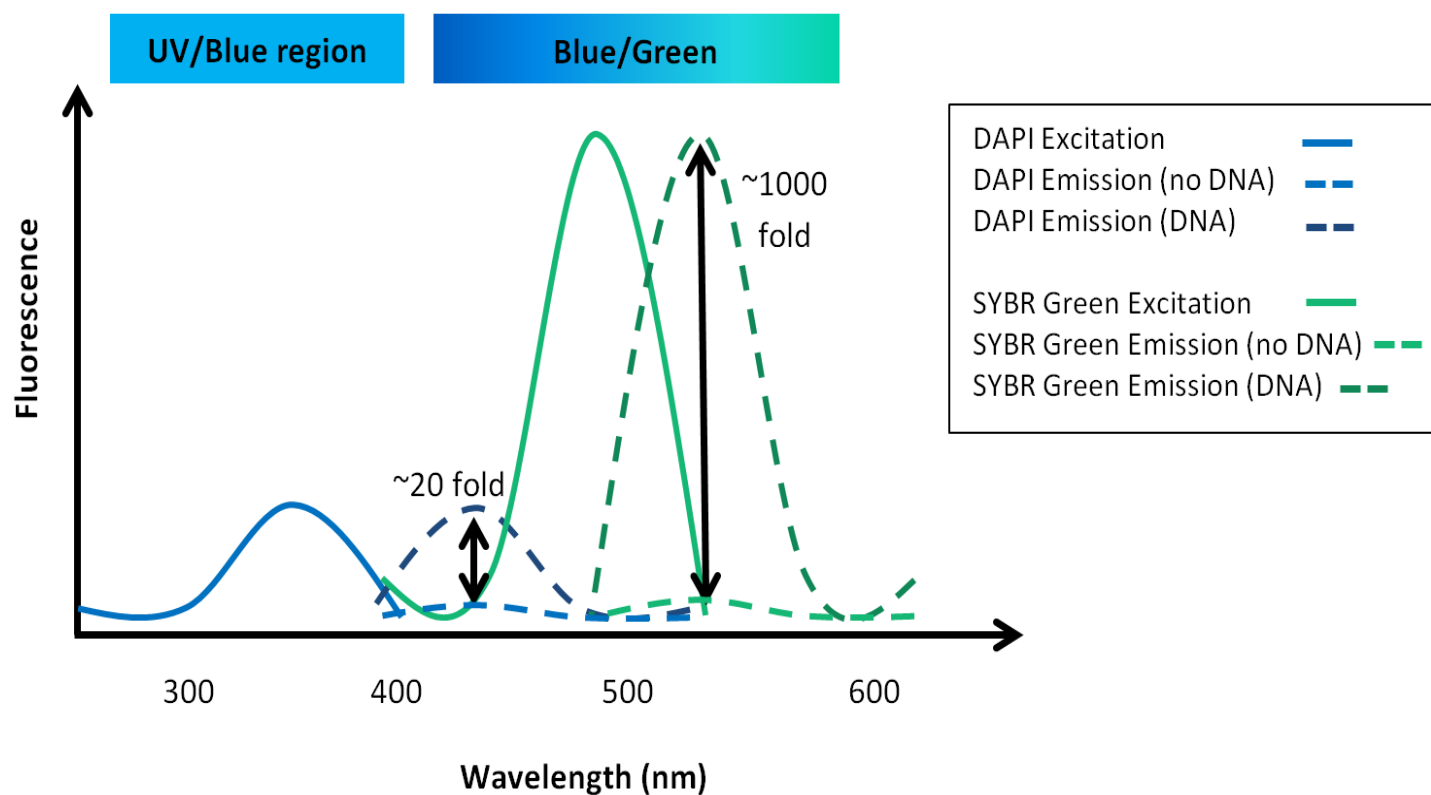


Figure 5.1: Schematic diagram of fluorescence spectra of DAPI compared with SYBR Green, showing the UV/blue region and blue/green region and the comparison of the fluorescent enhancement when in the presence of DNA.

5.2 PUBLICATION

The results pertaining to this study on dyes used for nuclear staining of hair follicles were submitted for publication in *Forensic Science International*; see article below.

Alicia M. Haines & Adrian Linacre, **A rapid screening method using DNA binding dyes to determine whether hair follicles have sufficient DNA for successful profiling.** *Forensic Science International*, **262** (2016) 190-195.

Impact factor of Journal: 2.345 (5 year), **1.950** (2015) published by Thomson Reuters


Ranking of Journal: **5/16** in Medical, Legal, (2015) published by Thomson Reuters

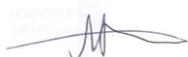
Statement of Authorship

Title of Paper	A rapid screening method using DNA binding dyes to determine whether hair follicles have sufficient DNA for successful profiling		
Publication Status	Accepted 2016		
Publication details	<i>Forensic Science International</i>		

AUTHOR CONTRIBUTIONS

By signing the Statement of Authorship, each author certified that their stated contribution to the publication is accurate and that permission is granted for the publication to be included in the candidate's thesis.

Name of Principal Author (Candidate)	Alicia M. Haines		
Contribution to the paper	Designed experimental method, performed all laboratory work and analysis, drafted the manuscript, edited manuscript and acted as corresponding author		
Signature		Date	August, 2016

Name of Co-Author	Adrian Linacre		
Contribution to the paper	Helped design study and edited manuscript		
Signature		Date	August, 2016



A rapid screening method using DNA binding dyes to determine whether hair follicles have sufficient DNA for successful profiling



Alicia M. Haines*, Adrian Linacre

School of Biological Sciences, Flinders University, Adelaide, Australia

ARTICLE INFO

Article history:

Received 10 December 2015
Received in revised form 16 February 2016
Accepted 12 March 2016
Available online 19 March 2016

Keywords:

Diamond™ Nucleic Acid Dye
Fluorescence microscopy
Forensic evidence recovery
Hair follicles
STR analysis

ABSTRACT

We report a simple screening method to assess the viability of successful DNA profiling from single hair follicles. A total of 48 hair samples (shed and plucked) were collected from male and female donors and the root tips (0.5 cm) were stained using one of three DNA binding dyes (EvaGreen™, Diamond™ Nucleic Acid Dye and RedSafe™) at 20× concentration. The hairs were subsequently viewed under a Nikon Optiphot fluorescent microscope to count the approximate number of nuclei in one plane of view. The hairs were then processed using either (1) a DNA extraction kit (QIAmp® Mini Kit) and then amplified using the AmpFLSTR® NGM™ kit, which amplifies 15 short tandem repeat (STR) loci plus the gender marker amelogenin, or (2) by direct PCR amplification using the same DNA profiling kit. Diamond™ dye had the lowest background signal and plucked hairs treated with this dye produced full DNA profiles when amplified directly and was chosen to screen a further 150 mixed hair samples. These hairs were separated into one of five categories (1, >100 nuclei; 1.5, 50–99 nuclei; 2, 1–49 nuclei; 2.5, no nuclei but high fluorescent signal; 3, no nuclei and very low fluorescent signal) from which 60 of the hairs were chosen to undergo direct amplification using the NGM™ kit. It was found that there was a direct correlation to the category designation and the ability to obtain a DNA profile up-loadable to the Australian DNA Database. Approximately 91% of category 1 hairs resulted in either a full or high partial (12–29 alleles) profile by direct PCR whereas about 78% of category 3 hairs exhibited no amplification. The results show that this method can be used to predict successful STR amplification from single hair follicles. It is a rapid, sensitive, cheap, non-destructive and easy to perform methodology applicable for screening multiple hairs in order to aid forensic investigators in predicting hairs that will yield DNA results.

© 2016 Elsevier Ireland Ltd. All rights reserved.

1. Introduction

Hairs are encountered frequently during a forensic investigation with telogen hairs the most commonly found as many humans shed approximately 75–100 hairs per day [1]. It has been estimated that 95% of hairs collected at a crime scene are identified as telogen hairs [2], typically lacking a follicular tag, as opposed to anagen hairs which are in the active growth stage, requiring force to be removed from the scalp and hence often contain cellular material [3]. Microscopy is the primary technique used for determining whether cellular material suitable for DNA profiling is adhering to the hairs. Recent studies have reported the usefulness of staining hairs with various dyes to visualize the nuclei within the hair root. These dyes include haematoxylin as this binds to chromatin

present within DNA and histone complexes and stains the nuclei a dark violet [2,4]. DAPI is a minor groove binding dye that has also been used to stain hairs so as to visualize the number of nuclei present to determine viability for STR profiling [5,6]. DAPI has a relatively low binding specificity to DNA, as it has a positive signal when in the presence of detergents and other compounds. DAPI only has approximately a 20-fold increase in fluorescent signal when in the presence of DNA [7,8]. Hoechst 33258 dye has also been used to label the DNA within hair follicles *in situ*. However this method is time consuming requiring overnight staining with the DNA dye and the whole process takes several days [9].

Nucleic acid binding dyes have been used for a range of purposes such as flow cytometry, gel electrophoresis and DNA quantification. There are a range of different types of binding dyes that have various mechanisms which affects their level of fluorescence enhancement; SYBR Green I (SG), which is an intercalating dye as well as having electrostatic and extended groove interactions, has an approximate 1000-fold fluorescent enhancement when in the presence of DNA [10]. This compares

* Corresponding author at: School of Biological Sciences, Flinders University, GPO Box 2100, Adelaide, SA 5001, Australia. Tel.: +61 8201 5003.
E-mail address: alicia.haines@flinders.edu.au (A.M. Haines).

<http://dx.doi.org/10.1016/j.forsciint.2016.03.026>
0379-0738/© 2016 Elsevier Ireland Ltd. All rights reserved.

with ethidium bromide, another well-known intercalating dye, which only has a 20–100-fold increase in fluorescent enhancement [11]. Recently available dyes with reported high fluorescence in the presence of DNA have been engineered to be less toxic and mutagenic than both SG and ethidium bromide such as Gel-GreenTM and DiamondTM Nucleic Acid Dye.

EvaGreenTM (EG) is a DNA binding dye which has been manufactured for its use in real-time PCR. The dye has also been used for DNA quantification, quantitative PCR and high resolution melt curve analysis [12]. The dye was found to have approximately a 70 times increase in fluorescent enhancement when in the presence of DNA [12], which is much lower than SG, however, another study stated it had similar DNA detection limits to SG [13]. This compares with a recent study [14] reporting that EG had a fluorescent enhancement of 602% compared with SG at 2544% [14]. It was found that EG was stable with its use in real-time PCR and has a relatively low PCR inhibition [12]. The manufacturer states that this dye is impermeable to cell membranes making it an unlikely stain for nuclei within hair follicles, which will be reviewed in this study.

RedSafeTM (RS) is a DNA binding dye used in gel electrophoresis primarily to replace ethidium bromide due to its toxic and mutagenic nature. This dye was found to detect down to 1 ng of DNA and be capable of permeating the cell membrane [15]; such capability makes the stain suitable for biological samples such as hair shafts.

DiamondTM Nucleic Acid Dye's (DD) mechanism for DNA interaction is as an external binder. This dye has been found to be less toxic and mutagenic than ethidium bromide [16,17]. Due to a different mechanism of interaction compared with SYBR Green I it may have a decrease in intensity when in the presence of DNA. However it was found that the dye was as sensitive as SYBR[®] Green down to 0.5 ng of DNA in gel electrophoresis [15]. It was also found to permeate the cell membrane, allowing an interaction with genomic DNA. Due to the dye's cell permeability it may be a useful dye in staining biological samples for nuclei visualization.

Successful direct amplification of human hair roots has previously been undertaken to amplify single nucleotide polymorphisms (SNPs) [18] and the amplification of short tandem repeats (STRs) [19]. The application of direct PCR aims to reduce contamination and loss of DNA that can be experienced when undergoing DNA extraction [20]. Using direct PCR has shown to generate higher profile peak heights and less allele drop-out compared to using a DNA extraction process [21]. A study has previously shown that there was around a 60% loss of DNA during the extraction process with a minor increase when DNA binding dyes were present [22]. The amount of DNA that was lost when DNA binding dyes were present depended on the binding mechanism of the dye [22]. STR profiles have been generated directly after nuclear staining of the hair follicles with DNA binding dyes, RS, EG, DD and SG and showed that only SG had allele drop-out [23].

This study aims to review the use of three DNA binding dyes RS, EG and DD that are more sensitive than dyes used previously for nuclear staining of hair follicles using fluorescent microscopy and undertaking both DNA extraction and direct amplification. One dye, DiamondTM dye, was selected to screen 150 mixed hair samples and determine their viability for direct STR amplification.

2. Materials and method

2.1. Hair sample collection

Shed and plucked hairs were collected (48 in total) from both male and female donors varying in colour and age. Shed hairs (150 in total) were then collected from both male and female donor participants that varied in age and colour.

2.2. Nucleic acid binding dyes preparation

EvaGreenTM (Jomar Diagnostics P/L, SA, AUS) and DiamondTM Nucleic Acid Dye (Promega, NSW, AUS) were diluted to a working solution of 20× (1 in 500 dilution) in sterile water. RedSafeTM (Scientific, NSW, AUS) was diluted to a working concentration of 20× (1 in 1000 dilution) in sterile water.

2.3. Fluorescence microscopy and nuclear hair staining

The hair roots were removed (0.5 cm) from the shaft and placed onto glass slides. The dyes (1 µL of 20×) were then applied to the roots and a coverslip was placed on top to reduce contamination and aid in visualization of the nuclei.

Once the selected dye was applied to the hair root it was visualized under a microscope (Nikon Optiphot) using a B2A emission cube. The hair root image was then captured using a Nikon camera set at an exposure time of 1/20 s or 1/50 s at 40× or 100× magnification. The number of nuclei that were present in the image was recorded. As a hair root is three-dimensional and the image was only taken of one plane of view it would be expected to have a higher number of nuclei than visualized, however to attain standardization only one focal plane across the hair root was captured and nuclei recorded. Images were taken before and after staining to determine the level of auto-fluorescence.

Plucked and shed hairs were stained individually with DNA binding dyes and subjected to either DNA extraction then amplification, or were amplified directly. Four hairs for plucked and shed hairs were analyzed for all three dyes for both extraction and direct PCR. A total of 48 hairs were analyzed.

2.4. Extraction and PCR amplification

Selected stained hair roots that showed good fluorescent signal were placed into a 1.5 mL tube and extraction of the DNA was undertaken following the QIAmp[®] Mini Kit protocol (QIAGEN Vic, AUS) that used both dithiothreitol (DTT) and proteinase K in the digestion process of the hair, with an incubation time of 1 h at 56 °C. The DNA was eluted into 50 µL of AE buffer. After extraction the samples were quantified using the Qubit[®] 2.0 Fluorometer using the Qubit[®] dsDNA HS Assay Kit in triplicate (ThermoFisher Scientific, Vic, AUS) following the manufacturer's protocol. If the sample was quantified below 0.5 ng/µL the sample was submitted for real-time PCR (RT-PCR) analysis using the Investigator[®] Quantiplex RT-PCR kit (QIAGEN Vic, AUS) in triplicate following the manufacturer's protocol. The samples were then amplified using 10 µL of the sample (diluted to 1 ng/µL if required) which was placed into a 0.2 mL thin walled tube containing 10 µL of PCR master mix from the AmpF[®] STR NGMTM kit (Life Technologies) along with 5 µL of primer mix to make up a final volume of 25 µL. The amplification was conducted using GeneAmp[®] System 9600 (Life Technologies) thermal cycler following the manufacturer's protocol. A standard cycle number of 29 was used throughout the study. The NGMTM kit amplifies 15 STR loci plus the amelogenin locus.

2.5. Direct PCR amplification and conditions

The stained root fragment was placed into a 0.2 mL thin walled tube containing 10 µL of PCR master mix from the NGMTM kit along with 5 µL of primer mix and 1 µL of AmpliTaq Gold[®] DNA polymerase (Life Technologies). A further 9 µL of sterile water was added to make up a final volume of 25 µL. The amplification was conducted using GeneAmp[®] System 9600 thermal cycler using the manufacturer's protocol. A standard cycle number of 29 was used throughout the study.

2.6. Application of screening method

The screening method was applied to 150 hairs; they were separated into five categories based on their fluorescent signal from: 1, >100 nuclei; 1.5, 50–99 nuclei; 2, 1–49 nuclei; 2.5, no nuclei but high fluorescent signal; 3, no nuclei and very low fluorescent signal. Out of 150 hairs stained with DD, 60 representative hairs were selected for direct amplification using NGM™ kit with an increased final extension time at 60 °C of 45 min to reduce split peaks.

2.7. Capillary electrophoresis

Capillary electrophoresis was performed on an ABI 3130XL Genetic Analyser (Life Technologies) using POP-4™ polymer (Life Technologies). An aliquot of 2 µL of the amplified samples was added to a solution containing 0.3 µL of GeneScan-500 LIZ® Size Standard and 9.5 µL of Hi-Di™ Formamide. Samples were denatured at 95 °C for 3 min. Electrophoresis was conducted at 3 kV with a 10 s injection. The data were analyzed using GeneMapper® v3.2. The detection threshold was set at 30 RFU (relative fluorescence units).

2.8. Data analysis

The data were tabulated based on the number and percentage of alleles generated from the 15 STR loci amplified by the NGM™ kit and the average peak height of the profile (15 STR loci plus amelogenin).

3. Results

3.1. Extraction of hair follicles stained with DD, RS and EG

A total of 48 hairs were analyzed after staining with three DNA binding dyes, DD, RS and EG (8 plucked, 8 shed per dye). A total of 24 hairs (4 shed, 4 plucked per dye) underwent DNA extraction and amplification using NGM™ with the results shown in Tables 1 (plucked hairs) and Table 2 (shed hairs). Examples of shed and plucked hairs stained with the three DNA binding dyes are shown below (Fig. 1). Images of the hairs before and after staining were undertaken to determine the level of auto-fluorescence, which was negligible as the nuclei were not visible unless stained with DNA binding dyes (data not shown).

Table 1

Extracted plucked hairs stained with nucleic acid binding dyes (>100 nuclei), DNA concentration quantified with Qubit® in triplicate, profile percentage (30 alleles) and average peak height of each profile.

Plucked hairs			
Sample	DNA concentration (ng/µL)	Profile %	Average peak height (RFU)
EG 1	2.71	100	1303.1
EG 2	2.92	100	1441.5
EG 3	1.51	100	951.65
EG 4	3.38	100	1226.1
DD 1	0.145 (0.247)	100	1448.8
DD 2	0.0901 (0.149)	0	NR
DD 3	0.101 (0.193)	100	1064.6
DD 4	0.0161 (0.0277)	0	NR
RS 1	1.83	100	1304.8
RS 2	3.91	100	1344.0
RS 3	2.04	100	1213.5
RS 4	0.308 (0.593)	100	1484.2

NR= No result.

Samples quantified with Qubit® below 0.5 ng/µL were then quantified with Investigator® Quantiplex RT-PCR kit in triplicate shown in brackets.

Table 2

Extracted shed hairs stained with nucleic acid binding dyes showing the number of nuclei, DNA concentration (quantified with Investigator® Quantiplex RT-PCR Kit in triplicate), profile percentage (30 alleles) and average peak height (RFU) of each profile.

Shed hairs				
Sample	No. nuclei	DNA concentration (pg/µL)	Profile %	Average peak height (RFU)
EG 1	0	0.31	0	NR
EG 2	0	2.08	0	NR
EG 3	0	0.46	0	NR
EG 4	0	4.23	0	NR
DD 1	0	4.87	21.9	125
DD 2	0	4.77	12.5	75.6
DD 3	~20	29.5	12.5	70.0
DD 4	~20	11.18	3.10	55.0
RS 1	0	4.83	12.5	67.6
RS 2	0	3.34	0	NR
RS 3	0	4.93	15.6	70.7
RS 4	0	NR	0	NR

NR= No result.

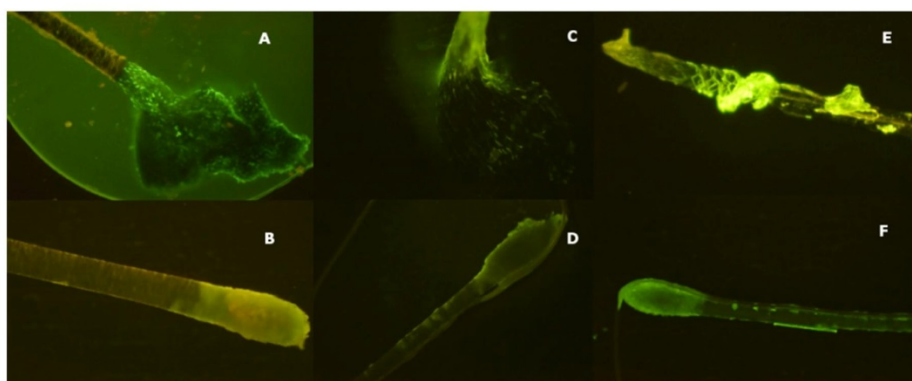


Fig. 1. Fluorescent signals of plucked and shed hairs stained with EG, DD and RS (A) EG plucked, (B) EG shed, (C) DD plucked, (D) DD shed, (E) RS plucked, (F) RS shed with an exposure time of 1/50 s using a Nikon Optiphot Fluorescent microscope using a B2A filter cube at 100× magnification.

All extracted plucked hairs stained with the three binding dyes were quantified which resulted in DNA concentrations between 0.016 and 3.9 ng/ μ L. All hairs produced STR profiles except for two DD stained hairs that had the lowest DNA quant values (Table 1). The shed hairs were also quantified (RT-PCR) and resulted in DNA quant values between 0.31 and 29.5 pg/ μ L however DNA typing of six hairs resulted in partial profiles (see Table 2).

3.2. Directly amplified hairs stained with DD, RS and EG

Direct amplification of stained plucked hairs resulted in full DNA profiles (30 alleles) for all hairs stained with DD, RS and EG. EG had an overall peak height average of 2517 RFU, DD had 2062 RFU and RS had the highest peak height average at 2777 RFU (Table 3).

Table 3

Average peak heights (RFU) of alleles amplified from plucked hair follicles (4 replicates per dye) stained with DNA binding dyes (1 μ L of 20 \times dye) and directly amplified using NGM™ kit.

Locus	EG	DD	RS
D10S1248	2465.5	1890.8	2385.8
	2058.8	1539.3	2031.5
vWA	4151.6	4065.5	3710.1
	4151.6	4065.5	3710.1
D16S539	1811.3	940.75	2744.0
	1473.8	798.50	2376.3
D2S1338	1153.3	751.75	2251.3
	660.50	393.75	1678.3
Amelogenin	2827.0	2190.0	3493.8
	5640.0	4389.0	5269.8
D8S1179	8112.5	7218.0	7051.5
	7214.5	6380.5	6601.5
D21S11	224.00	117.75	356.00
	218.75	110.75	348.00
D18S51	926.25	441.75	1754.0
	754.75	356.25	1546.8
D22S1045	5749.3	5373.5	5694.3
	5967.8	5531.8	5842.5
D19S433	1609.8	1123.3	1896.5
	1398.3	969.75	1756.5
TH01	1425.4	890.75	1910.0
	1425.4	884.00	1910.0
FGA	1524.0	1009.5	2202.3
	1084.0	694.25	1724.8
D2S441	6274.8	5768.8	5120.8
	4616.5	3596.5	3717.5
D3S1358	1638.5	1343.5	2501.8
	1154.5	1047.8	2084.8
D1S1656	743.50	548.75	1297.8
	827.00	617.75	1440.8
D12S391	691.00	514.75	1326.3
	554.75	420.75	1120.5
Average peak height of profile (RFU)	2516.5	2062.0	2776.7

RFU = relative fluorescent units.

Table 4

Number of alleles (out of 30), profile percentage and average peak height of each profile, from shed hair follicles stained with DNA binding dyes, DD, RS and EG (1 μ L of 20 \times dye) and directly amplified using NGM™ STR kit (Life Technologies).

	No of Alleles	Profile %	Average peak height (RFU)
DD 1	0	0	0
DD 2	2	6.7	56
DD 3	3	10	49
DD 4	0	0	0
EG 1	0	0	0
EG 2	12	40	48
EG 3	0	0	0
EG 4	0	0	0
RS 1	2	6.7	40
RS 2	0	0	0
RS 3	0	0	0
RS 4	0	0	0

However after statistical analysis using an ANOVA single factor test it showed that the mean values were statistically the same (F value 0.998 and F_{crit}^{***} value 3.09).

Direct amplification of shed hairs stained with DNA binding dyes resulted in only a few alleles being amplified (2–12 alleles) with reduced peak heights (Table 4). Two hairs stained with DD had more than 2 alleles being amplified and EG had one hair that had 12 alleles being amplified.

From the data based on 48 hairs that were analyzed, and due to the low background signal of the dye compared with EG and RS, DD was selected to screen a further 150 hairs for the presence of DNA. DD also had no allele drop-out when amplified directly and due to the substantial loss that can occur during DNA extraction [20,22] it was decided to amplify the hairs directly to increase the chances of obtaining alleles and up-loadable profiles where a minimum of 12 alleles are required for the Australian National DNA Database.

3.3. Application of screening method

Five categories were established for the screening of hair samples with the five categories and a corresponding hair for each is shown in Fig. 2. The ideal amount of template DNA for STR amplification is around 0.5–1 ng of DNA, and assuming there is around 6 pg of DNA per somatic cell nucleus [24], 83–167 nuclei would be required to give a DNA profile. This evaluation aided in the category designations with category 1 being above 100 nuclei; category 1.5, 50–99 nuclei; category 2, 1–49 nuclei; category 2.5, no nuclei but high fluorescent signal and category 3, no nuclei with low fluorescent signal.

From 150 hairs that were stained with DD, 60 representative hairs were chosen for STR direct amplification. Out of the 60 hairs, 18 were identified as category 3 (exhibiting very low fluorescence) in which only 1 hair resulted in a full profile, with about 78% of the category 3 hairs resulting in no amplification (Table 5). Of the category 1 hairs 91% generated either a full profile or high partial profile. Approximately 55% of category 1.5 hairs and 43% of category 2 hairs resulted in a high partial profile; showing a correlation between the designated hair category and the number of alleles amplified. The results show that the lower the hair category designation for the screened hairs, the higher the chance of obtaining an up-loadable profile onto Australian National DNA Database (more than 12 alleles).

A high partial profile obtained from a category 3 hair is shown in Fig. 3, exhibiting peaks that were relatively small (~50 RFU) but there were no nuclei seen or skin attached placing the hair into category 3. However 16 alleles were amplified using this method showing the sensitivity.

4. Discussion

Initially 48 hairs were analyzed to establish a screening method for hair follicles using three DNA binding dyes RS, EG and DD. Out of these 48, 24 hairs underwent DNA extraction after staining and 24 were amplified directly. DD was then chosen to screen 150 hairs due to the low background signal when analyzing the hair roots under fluorescent microscopy. Direct amplification was chosen to reduce the amount of DNA that could be potentially lost during extraction especially when dealing with shed hairs that have minute amounts of DNA present.

This study screened 150 hairs with the DNA binding dye DD and 60 were chosen for direct STR amplification. From these 60, 18 hairs were designated category 3 and resulted in approximately 80% with no amplification. A total of 14 hairs were category 2.5 where about 64% resulted in no amplification. Category 2 had a total of 7 hairs that gave 43% with high partial profiles; category 1.5 had 50% with high partial profiles (10 total hairs). Of the category

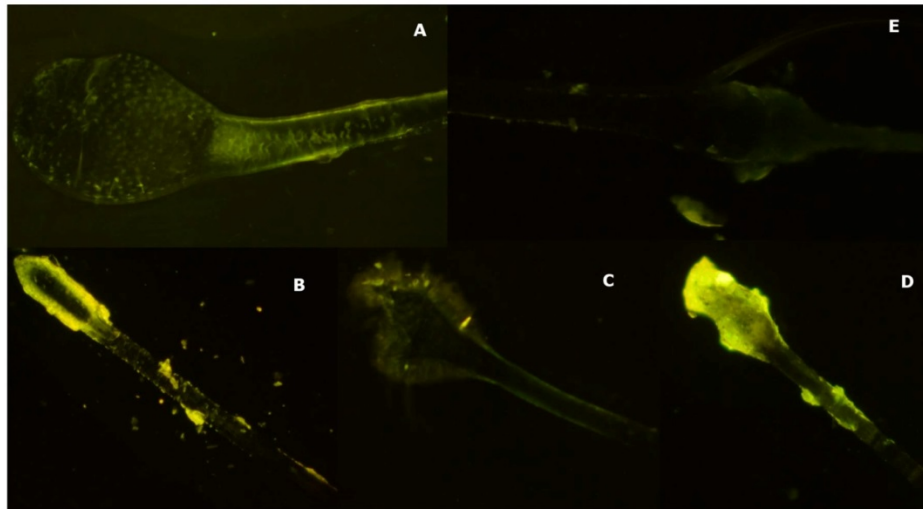


Fig. 2. Screened hair samples from 5 different categories based on fluorescent signal, (A) category 1, >100 nuclei, (B) category 1.5, 50–99 nuclei, (C) category 2, 1–49 nuclei, (D) category 2.5, no nuclei/high signal, (E) category 3, no nuclei/very low signal. Exposure time of 1/20 s using a Nikon Optiphot Fluorescent microscope using a B2A filter cube at 40× magnification.

1 hairs 55% produced full DNA profiles (30 alleles) from a total of 11 hairs. This study has shown that there was a direct correlation between the category designation and the ability to obtain an uploaded STR profile onto the Australian National DNA Database.

The results shown are in agreement with other studies undertaken in which hairs that appear to have no nuclei or a low number of nuclei are unlikely to produce STR profiles [2,5,6]. However all previous studies undertook different DNA extraction methods before amplification which may have resulted in a

substantial loss of DNA. Brooks et al. [6] when using DAPI staining only had around a 30% success rate of obtaining DNA profiles (18 alleles) from hairs that had over 30 nuclei. The results generated from this study show about a 72% success rate of obtaining either a full or high partial profile (over 12 alleles) from hairs in category 2 (1–49 nuclei). The higher success rate obtained within this study was most likely the result of directly amplifying the stained hairs in order to reduce the amount of DNA lost during the extraction step. The other factor would be that the NGM™ STR kit may have a

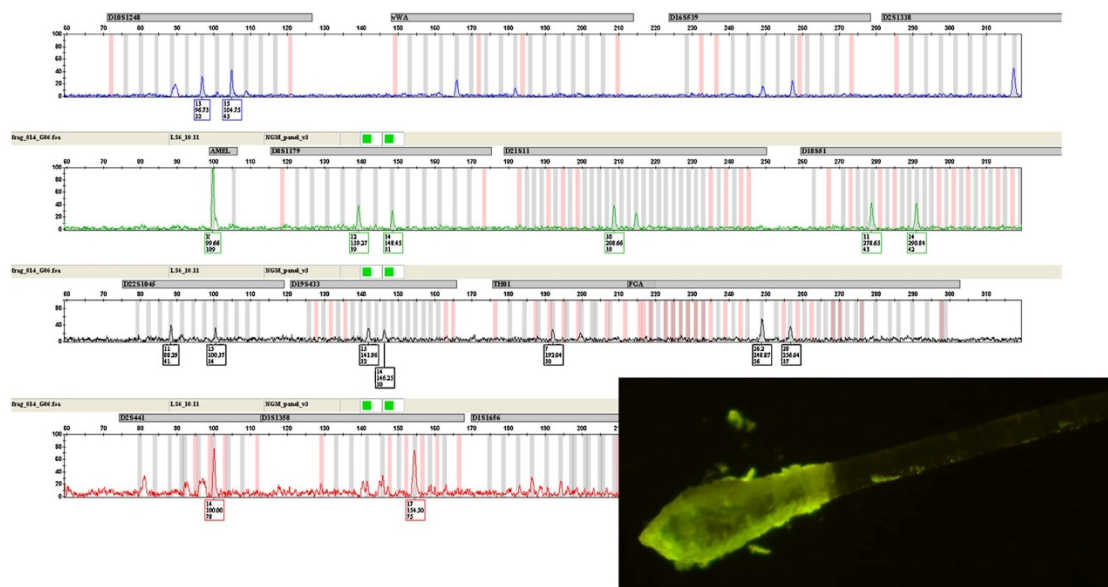


Fig. 3. Electropherogram of DNA from a screened hair, category 3 designation showing amplification of 16 alleles plus amelogenin (NGM™ STR kit). Scale at the right shows RFU values.

Table 5

Percentage of hairs that produce full, high partial, low partial and no profile for each hair staining category with total number of hairs amplified using NGM™ STR kit.

Category	Full profile (30 alleles)	High partial profile (12–29 alleles) ^a	Low partial profile (1–11 alleles)	No profile	Total number of hairs
1	54.5	36.4	9.09	0	11
1.5	20.0	50.0	30.0	0	10
2	28.6	42.9	0	28.6	7
2.5	7.14	14.3	14.3	64.3	14
3	5.55	5.56	11.1	77.8	18

^a Minimum of 12 alleles required to be uploaded onto the Australian National DNA Database.

higher sensitivity than kits used in previous studies (ProfilerPlus™). Looking at results of a previous study using haematoxylin there was still only a 75% success rate in obtaining alleles (11 ± 3 alleles) from hairs that had 81–100 nuclei [2]. This study using DNA binding dyes was shown to be highly sensitive where there was a 91% success rate of obtaining alleles (12–30 alleles) with hairs from category 1 (>100 nuclei).

5. Conclusion

The results from this study after staining 150 hairs with DD have been shown to be more sensitive than DAPI and haematoxylin staining previously undertaken possibly due to the use of direct amplification which bypasses the extraction stage where a substantial amount of DNA can be lost. This screening methodology is sensitive, cheap, fast and easy to perform on multiple hairs to aid in finding viable hair roots for STR amplification. The process is also non-destructive which means the hairs can be used for other non-DNA analysis; the dyes used in the studied are also stated by the manufacturer to be non-toxic and non-mutagenic.

Role of funding

Funding was provided by the Attorney General's Department, South Australia.

Conflict of interest

Conflict of interest: none.

Acknowledgements

We thank Dr. Shanan Tobe for the use of the Nikon Optiphot fluorescent microscope used within this study as well as Emeritus Professor Hilton Kobus and their ongoing support during this study.

References

- [1] L. Bourguignon, B. Hoste, T. Boonen, K. Vits, F. Hubrecht, A fluorescent microscopy-screening test for efficient STR-typing of telogen hair roots, *Forensic Sci. Int.: Genet.* 3 (2008) 27–31.
- [2] J. Edson, E.M. Brooks, C. McLaren, J. Robertson, D. McNevin, A. Cooper, J.J. Austin, A quantitative assessment of a reliable screening technique for the STR analysis of telogen hair roots, *Forensic Sci. Int.: Genet.* 7 (2013) 180–188.
- [3] D. McNevin, L. Wilson-Wilde, J. Robertson, J. Kyd, C. Lennard, Short tandem repeat (STR) genotyping of keratinised hair: part 1. Review of current status and knowledge gaps, *Forensic Sci. Int.* 153 (2005) 237–246.
- [4] A.H. Fischer, K.A. Jacobson, J. Rose, R. Zeller, Hematoxylin and eosin staining of tissue and cell section/stile case, Cold Spring Harb. Protocols/retain, 2008 pdb-prot4986.
- [5] T. Lepez, M. Vandewoestyne, D. Van Hoofstat, D. Deforce, Fast nuclear staining of head hair roots as a screening method for successful STR analysis in forensics, *Forensic Sci. Int.: Genet.* 13 (2014) 191–194.
- [6] E.M. Brooks, M. Cullen, T. Szydna, S.J. Walsh, Nuclear staining of telogen hair roots contributes to successful forensic nDNA analysis, *Aust. J. Forensic Sci.* 42 (2010) 115–122.
- [7] M.L. Barcellona, G. Cardiel, E. Gratton, Time-resolved fluorescence of DAPI in solution and bound to polydeoxynucleotides, *Biochem. Biophys. Res. Commun.* 170 (1990) 270–280.
- [8] D. Banerjee, S.K. Pal, Dynamics in the DNA recognition by DAPI: exploration of the various binding modes, *J. Phys. Chem. B* 112 (2008) 1016–1021.
- [9] S. Szabo, K. Jaeger, H. Fischer, E. Tschachler, W. Parson, L. Eckhart, In situ labeling of DNA reveals interindividual variation in nuclear DNA breakdown in hair and may be useful to predict success of forensic genotyping of hair, *Int. J. Legal Med.* 126 (2012) 63–70.
- [10] A.I. Dragan, R. Pavlovic, J.B. McGivney, J.R. Casas-Finet, E.S. Bishop, R.J. Strouse, M.A. Schenerman, C.D. Geddes, SYBR green I: fluorescence properties and interaction with DNA, *J. Fluoresc.* 22 (2012) 1189–1199.
- [11] K.G. Strothkamp, R.E. Stothkamp, Fluorescence measurements of ethidium binding to DNA, *J. Chem. Educ.* 71 (1994) 77.
- [12] F. Mao, W.-Y. Leung, X. Xin, Characterization of EvaGreen and the implication of its physicochemical properties for qPCR applications, *BMC Biotechnol.* 7 (2007), 76–76.
- [13] F. Sang, J. Ren, Capillary electrophoresis of double-stranded DNA fragments using a new fluorescence intercalating dye EvaGreen, *J. Sep. Sci.* 29 (2006) 1275–1280.
- [14] J. Radvansky, M. Surovy, E. Nagyova, G. Minarik, L. Kadasi, Comparison of different DNA binding fluorescent dyes for applications of high-resolution melting analysis, *Clin. Biochem.* 48 (2015) 609–616.
- [15] A.M. Haines, S.S. Tobe, H.J. Kobus, A. Linacre, Properties of nucleic acid staining dyes used in gel electrophoresis, *Electrophoresis* 36 (2015) 941–944.
- [16] T. Schagat, A. Hendricksen, Diamond™ Nucleic Acid Dye is a safe and economical alternative to ethidium bromide [Internet], tpub 125 (2013), available from: <http://au.promega.com/resources/pubhub/diamond-nucleic-acid-dye-is-a-safe-and-economical-alternative-to-ethidium-bromide/> (date visited 01.06.15).
- [17] A. Truman, B. Hook, A. Hendricksen, Diamond™ Nucleic Acid Dye: a sensitive alternative to SYBR® Dyes [Internet], tpub 121 (2013), available from: <http://au.promega.com/resources/pubhub/diamond-nucleic-acid-dye/> (date visited 01.06.15).
- [18] M. Hayashida, K. Iwao-Koizumi, S. Murata, K. Kinoshita, Single-tube genotyping from a human hair root by direct PCR, *Anal. Sci.* 25 (2009) 1487–1489.
- [19] R. Ottens, D. Taylor, D. Abarno, A. Linacre, Successful direct amplification of nuclear markers from a single hair follicle, *Forensic Sci. Med. Pathol.* 9 (2013) 238–243.
- [20] R. Ottens, J. Templeton, V. Paradiso, D. Taylor, D. Abarno, A. Linacre, Application of direct PCR in forensic casework, *Forensic Sci. Int.: Genet. Suppl. Ser.* 4 (2013) e47–e48.
- [21] Y.C. Swaran, L. Welch, A comparison between direct PCR and extraction to generate DNA profiles from samples retrieved from various substrates, *Forensic Sci. Int.: Genet.* 6 (2012) 407–412.
- [22] A.M. Haines, S.S. Tobe, H.J. Kobus, A. Linacre, Effect of nucleic acid binding dyes on DNA extraction, amplification, and STR typing, *Electrophoresis* 36 (2015) 2561–2568.
- [23] A.M. Haines, S.S. Tobe, H. Kobus, A. Linacre, Successful direct STR amplification of hair follicles after nuclear staining, *Forensic Sci. Int.: Genet. Suppl. Ser.* (2015), <http://dx.doi.org/10.1016/j.fsigss.2015.09.026>.
- [24] J.M. Butler, DNA quantitation, in: *Advanced Topics in Forensic DNA Typing: Methodology*, Academic Press/Elsevier, San Diego, 2011, pp. 49–67 (Chapter 3).

5.3 Further Results and Discussion

In order to determine the level of auto fluorescence of the hairs, images were taken of the hair before staining with the DNA binding dyes and after staining. This was done for multiple hairs for each dye, Figures 5.1-5.3 shows examples of three plucked hairs stained with EvaGreen™ (EG), RedSafe™ (RS) and Diamond™ Dye (DD).

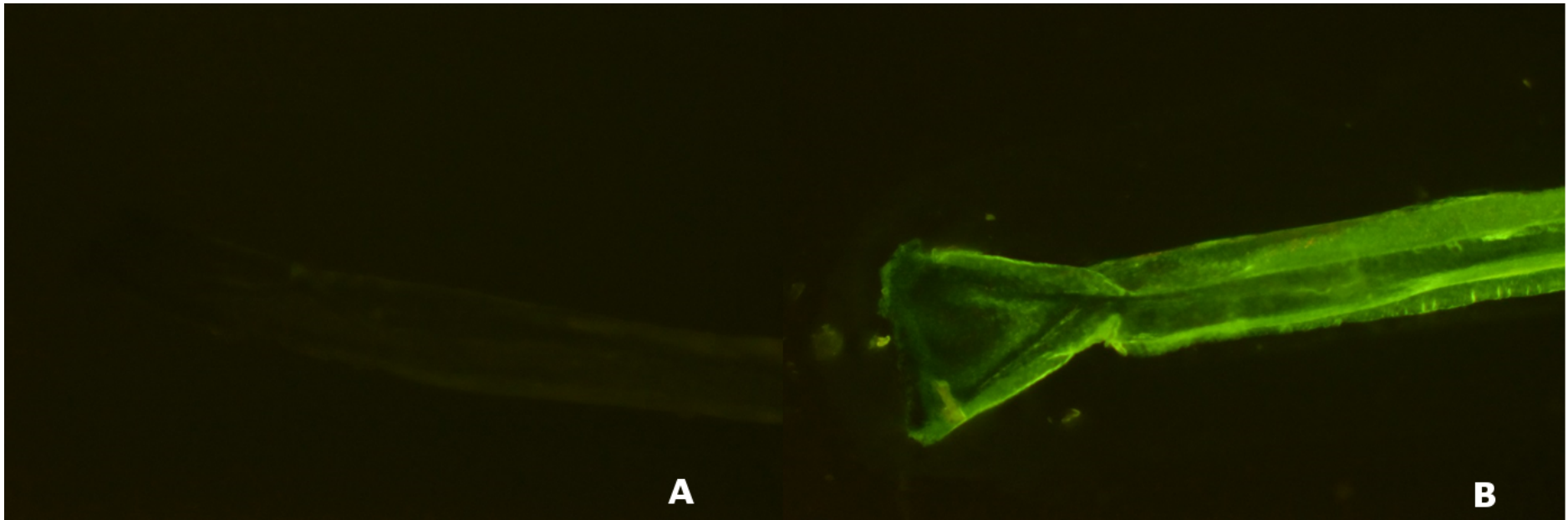


Figure 5.2: Showing plucked hair follicle with skin sheath (A) before staining and (B) after staining with EG 20X.

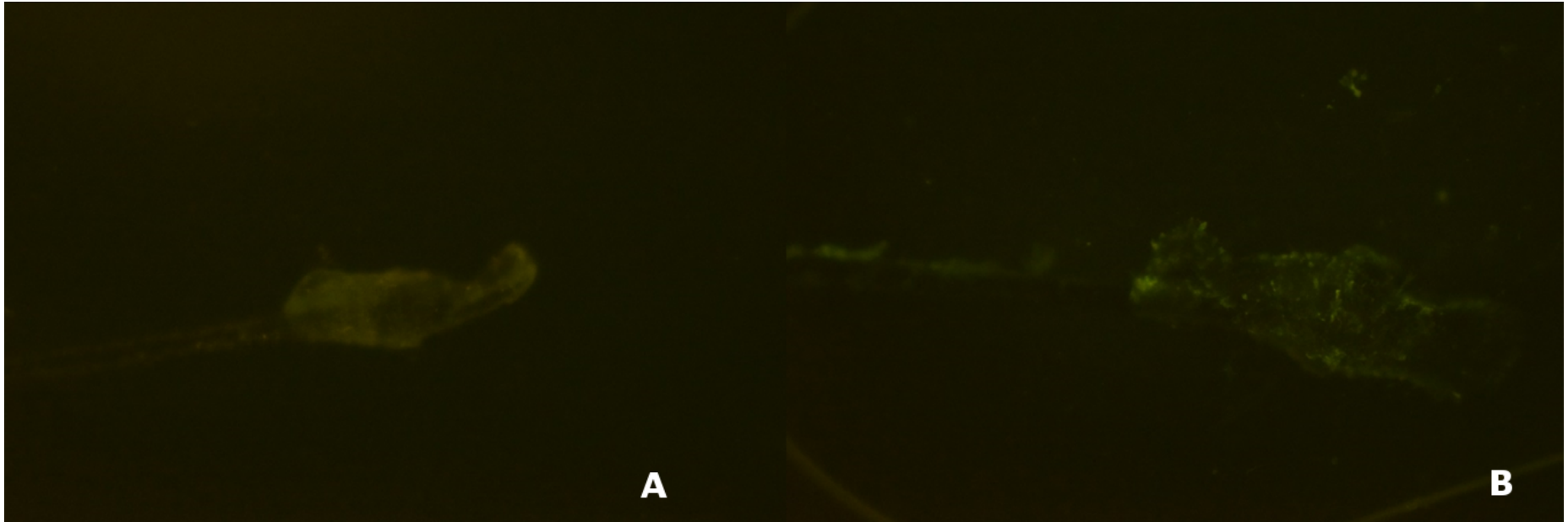


Figure 5.3: Showing plucked hair follicle with skin sheath (A) before staining and (B) after staining with DD 20X.

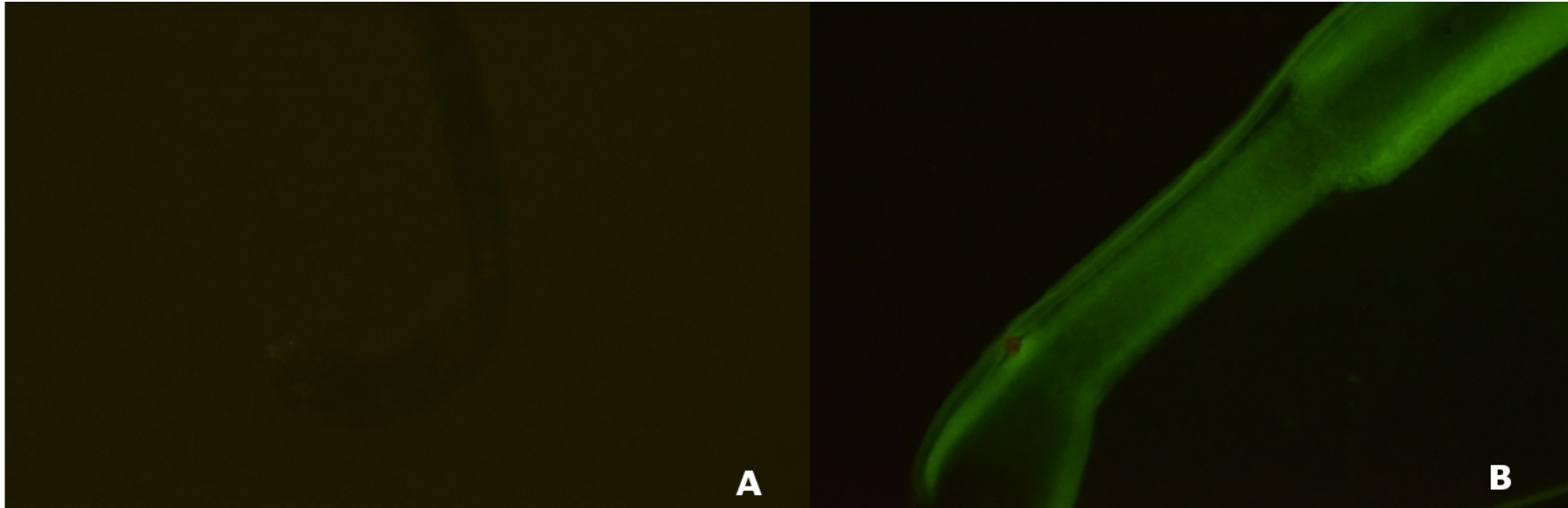
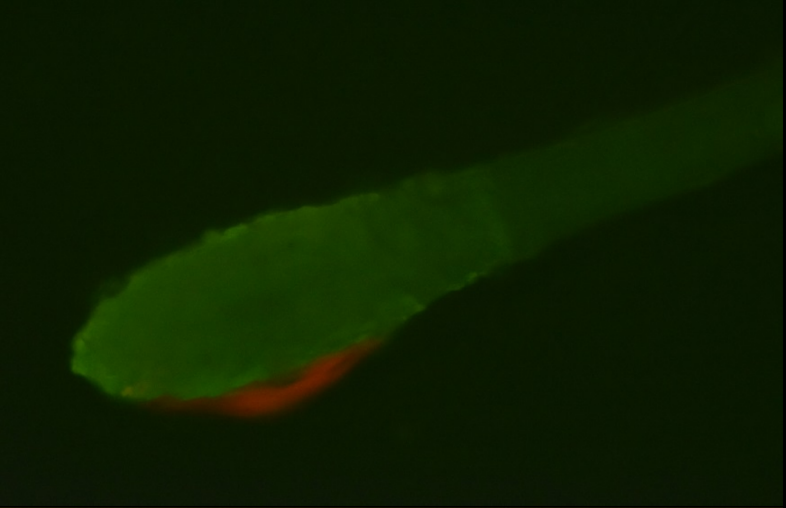
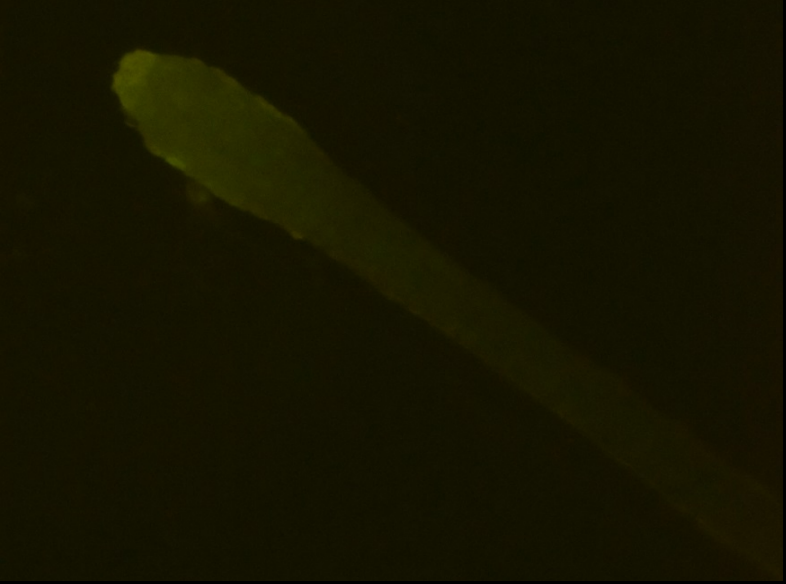
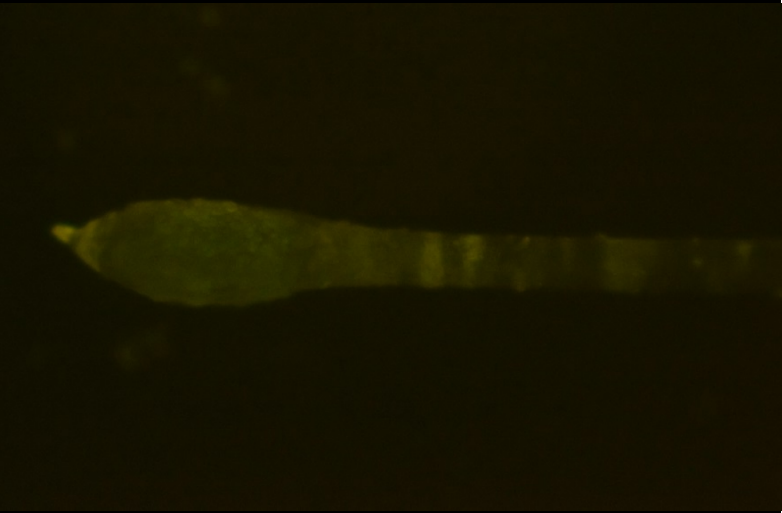
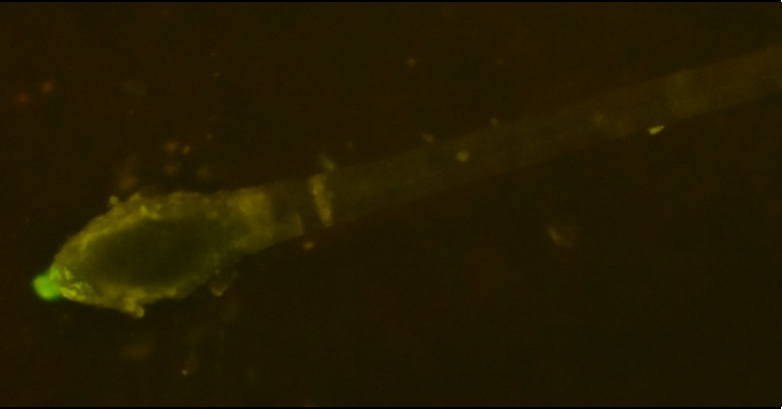



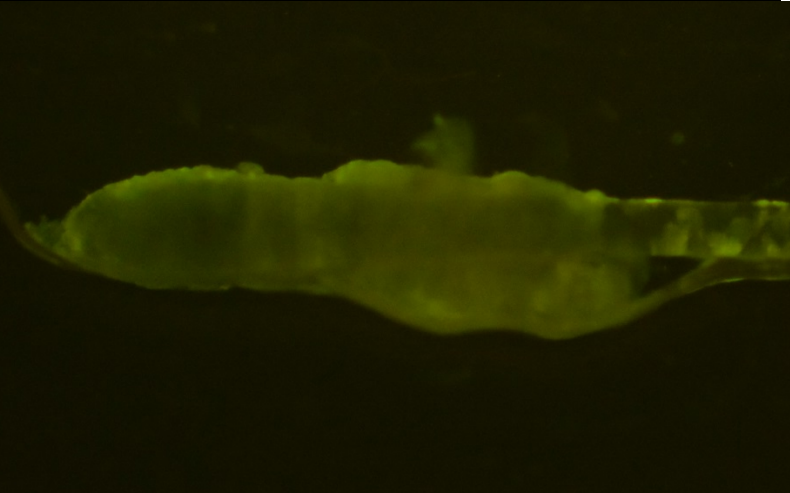
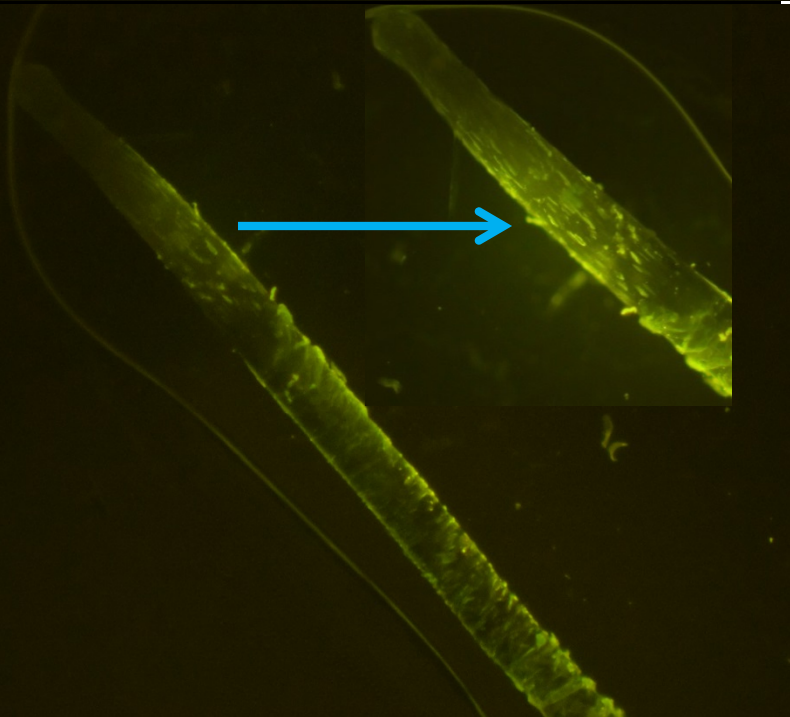

Figure 5.4: Showing plucked hair follicle with skin sheath (A) before staining and (B) after staining with RS 20X.

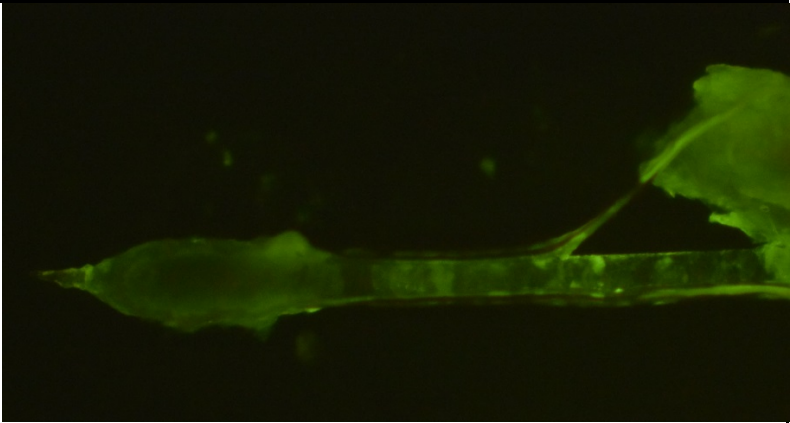
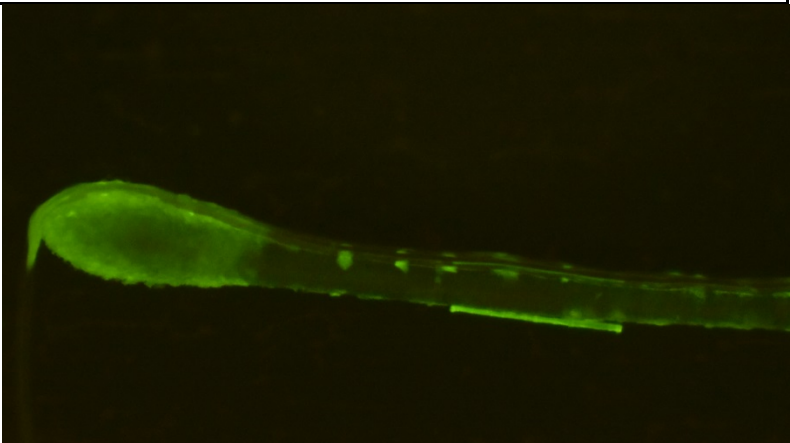
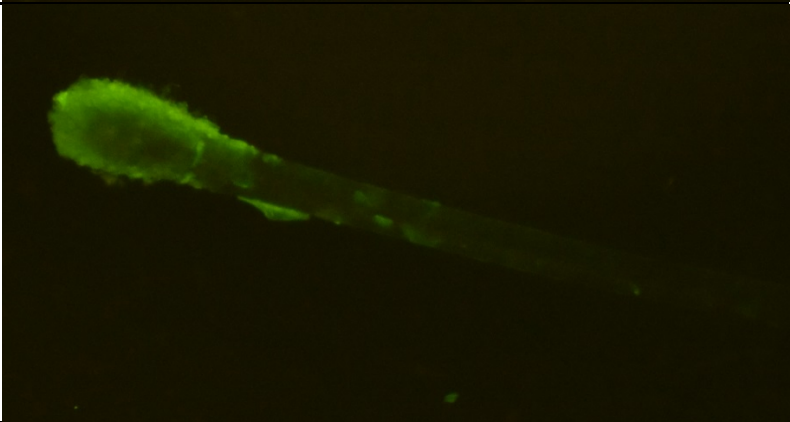
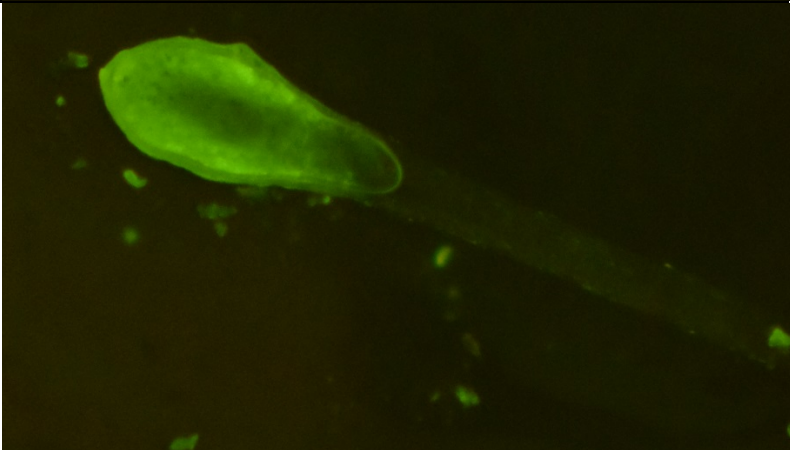
Table 5.3 below shows the stained shed hairs before they had undergone DNA extraction. The DNA quantifications obtained from RT-PCR are also shown in Table 5.3 in order to show that when there appears to be a higher fluorescent signal that corresponds to a higher DNA quantification value. DD had staining of two shed hairs that had nuclei present; these hairs (DD 3, DD4) had the highest quantification values which were expected due to more genetic material being present. On average the shed hairs had quantification values ranging from 0.31-29.5 pg/ μ L with most hairs having DNA quantifications around 4 pg/ μ L.

Table 5.3: Average DNA quantification by RT-PCR (Investigator[®] Quantiplex kit) 3 replicates, of extracted hairs stained with DNA binding dyes (20X) with images of the hairs post staining (exposure time 1 s, 40X magnification) arrows pointing to increase magnification image and potential nuclei.

Sample	Average DNA Quantification (pg/ μ L)	Image of Hair follicle
EG 1	0.31	
EG 2	2.08	

<p>EG 3</p> <p>0.460</p>	
<p>EG 4</p> <p>4.23</p>	
<p>DD 1</p> <p>4.87</p>	

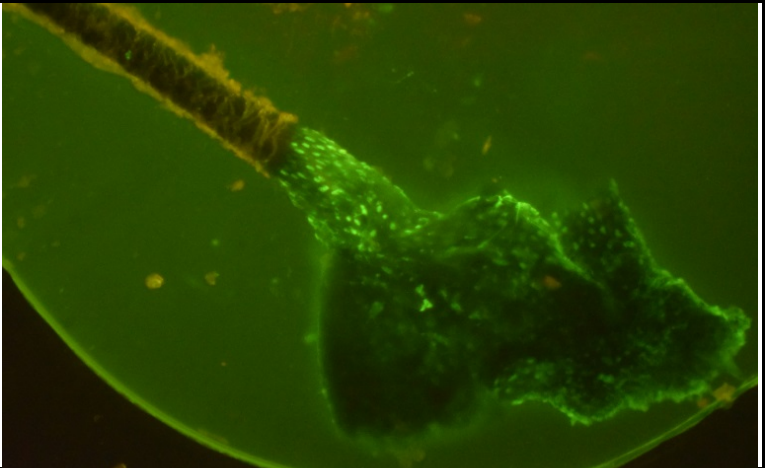
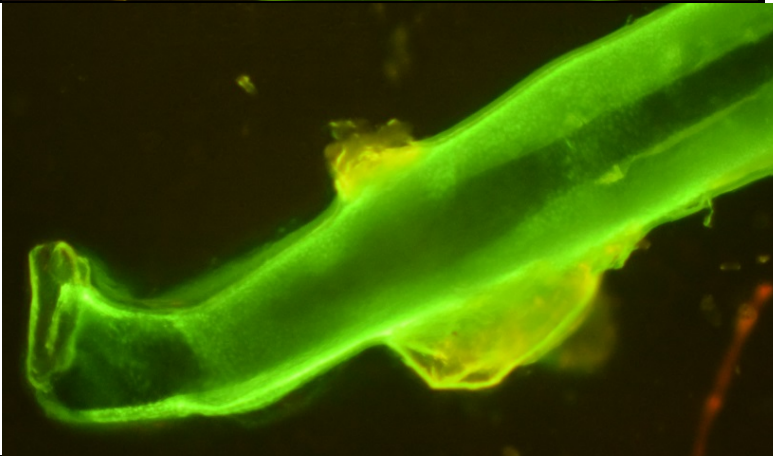
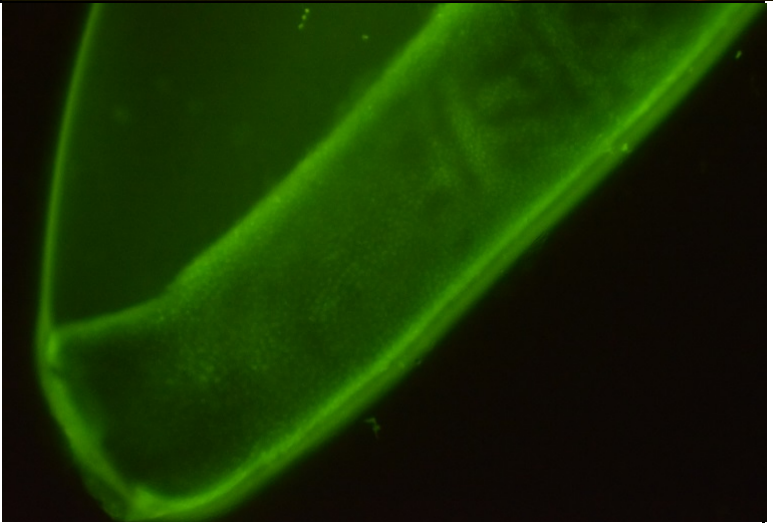
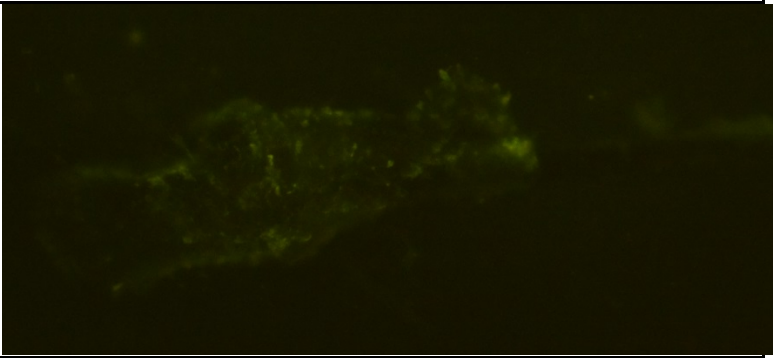
<p>DD 2</p> <p>4.77</p>	
<p>DD 3</p> <p>29.5</p>	
<p>DD 4</p> <p>11.2</p>	

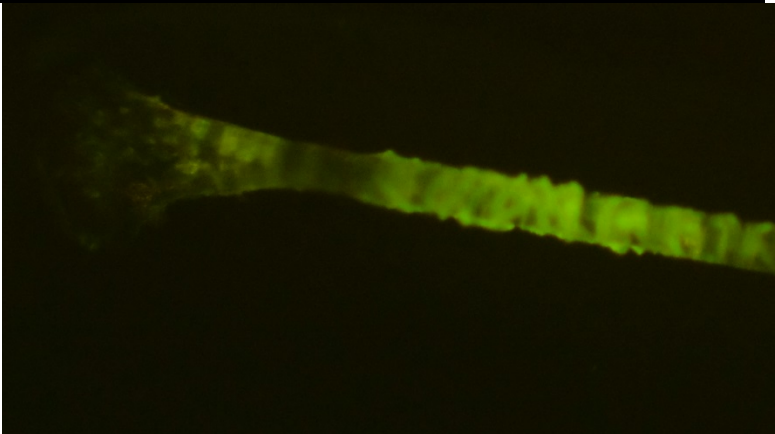
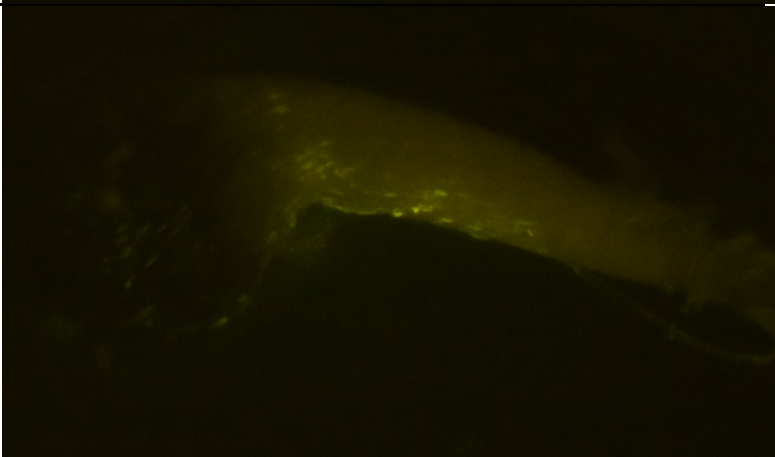
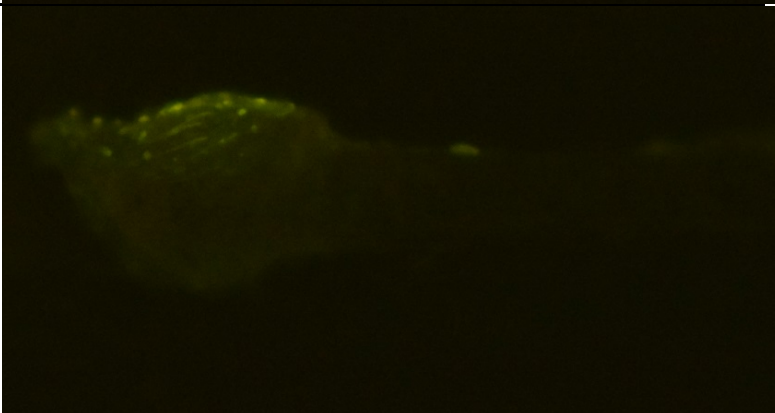
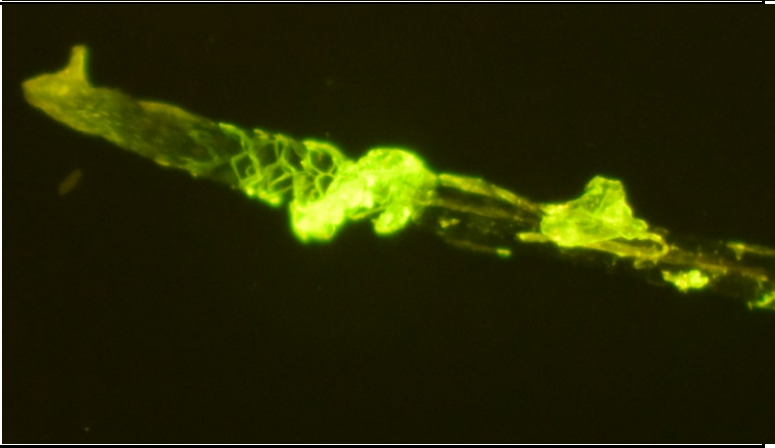
<p>RS 1</p> <p>4.83</p>	
<p>RS 2</p> <p>3.34</p>	
<p>RS 3</p> <p>4.93</p>	
<p>RS 4</p> <p>NR</p>	

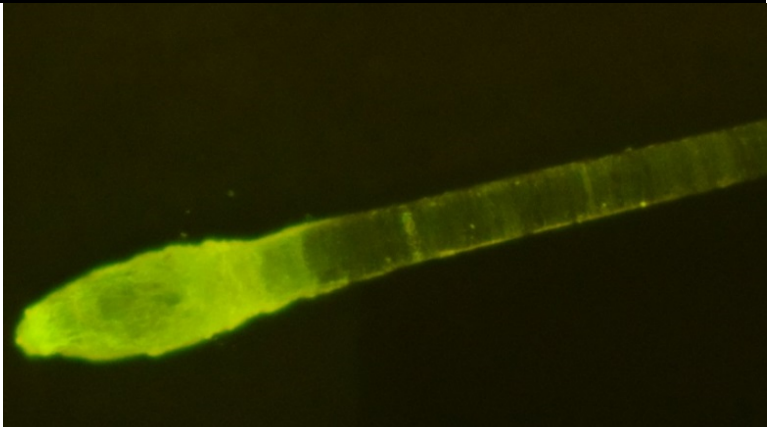
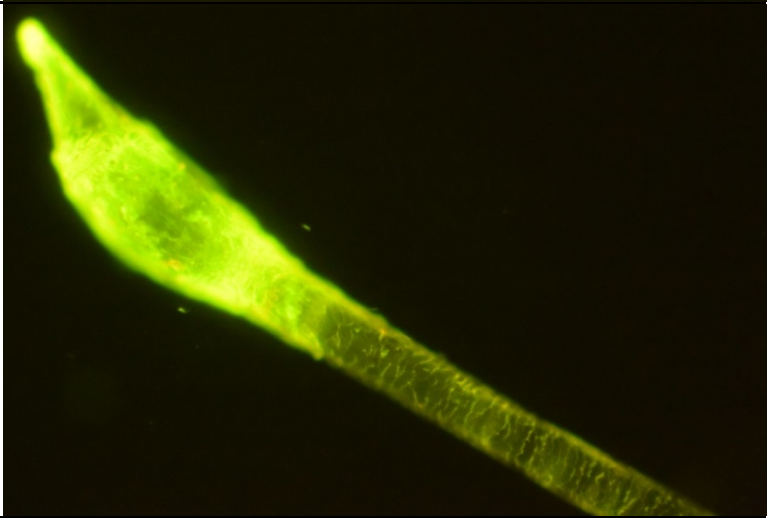
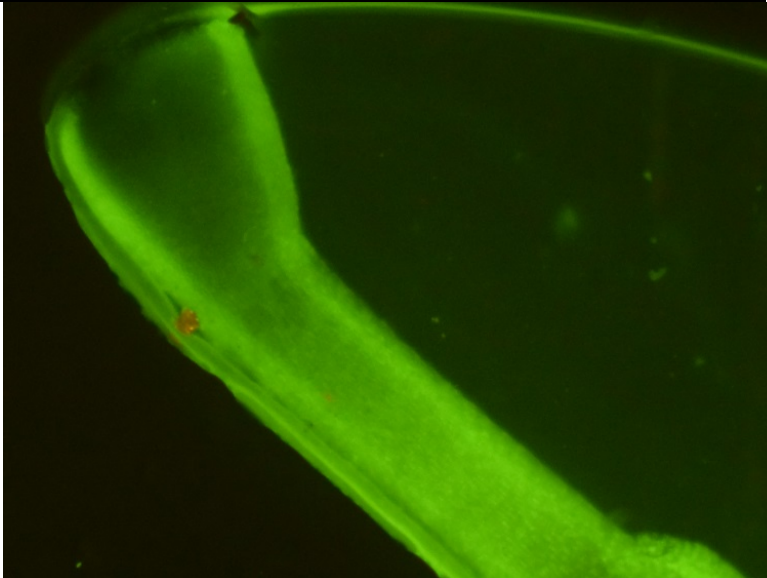
A sample of 12 plucked hairs was obtained which were then stained with the three binding dyes (4 hairs per dye; RS, DD and EG). Images of the stained hairs are shown below (Table 5.4) along with the DNA quantification values obtained after extraction (QIAamp) using the DNA HS Qubit[®] assay. It can be seen that when there were a large number of nuclei present higher DNA quantification values were obtained. The DNA concentration values were not as high as expected with the number of nuclei that appear to be present in the hair follicle and hair skin sheath attached (EG1, Table 5.4) where the quantification value obtained was 2.71 ng/μL, which would be equivalent to 452 cells (6 pg/cell [28]). It has been estimated that plucked hairs with roots present can obtain DNA quantifications from 1 ng up to 750 ng per root [29]. As there is a skin sheath around the hair follicle there are hundreds maybe thousands of small fluorescent dots indicating the location of nuclei. As this image is only captured in one focal plane it would be expected there would be a lot more nuclei present than is seen in the image. One reason why there were lower quantification values than expected may be due to the substantial loss of DNA that can be experienced during an extraction as there are multiple tube changes and washes, resulting in many opportunities for there to be a loss of DNA [17, 18].

Table 5.4: Average DNA quantifications by Qubit[®] (3 replicates) of extracted hairs stained with DNA binding dyes (20X) with images of the hairs post staining (exposure time 1 s, 40X magnification).

Sample	Average DNA Quantification (ng/μL)	Image of hair
EG 1	2.71	

EG 2 2.92	
EG 3 1.51	
EG 4 3.38	
DD 1 0.145	

DD 2 0.0901	
DD 3 0.101	
DD 4 0.0161	
RS 1 1.83	

<p>RS 2 3.91</p>	
<p>RS 3 2.04</p>	
<p>RS 4 0.308</p>	

The average DNA quantification values obtained after DNA extraction of the hair follicles stained with the three dyes are shown in Figure 5.5. The hairs stained with DD had the lowest quantification values with an average around 0.09 ng/ μ L compared with EG at 2.6 ng/ μ L and RS at 2.0 ng/ μ L. The hairs stained with EG gave quantification values around 30 times higher than the quantifications obtained when using DD. The error bars showing the confidence at 95% indicates that there was a significant difference between DD and EG, DD and RS but RS and EG showed no significant difference as indicated by the overlap of the error bars. As the effects of these dyes were already established previously (Chapter 4) it was determined that DD had the lowest effect on the extraction process. RS was shown to have the highest effect [18]. The main cause of this substantial decrease would be likely due to the hairs not having the same amount of genetic material. The images in Table 5.4 show that most of the hairs stained with EG and RS had a skin sheath attached to the follicular tag and hence would contain more genetic material than hairs with just a root.

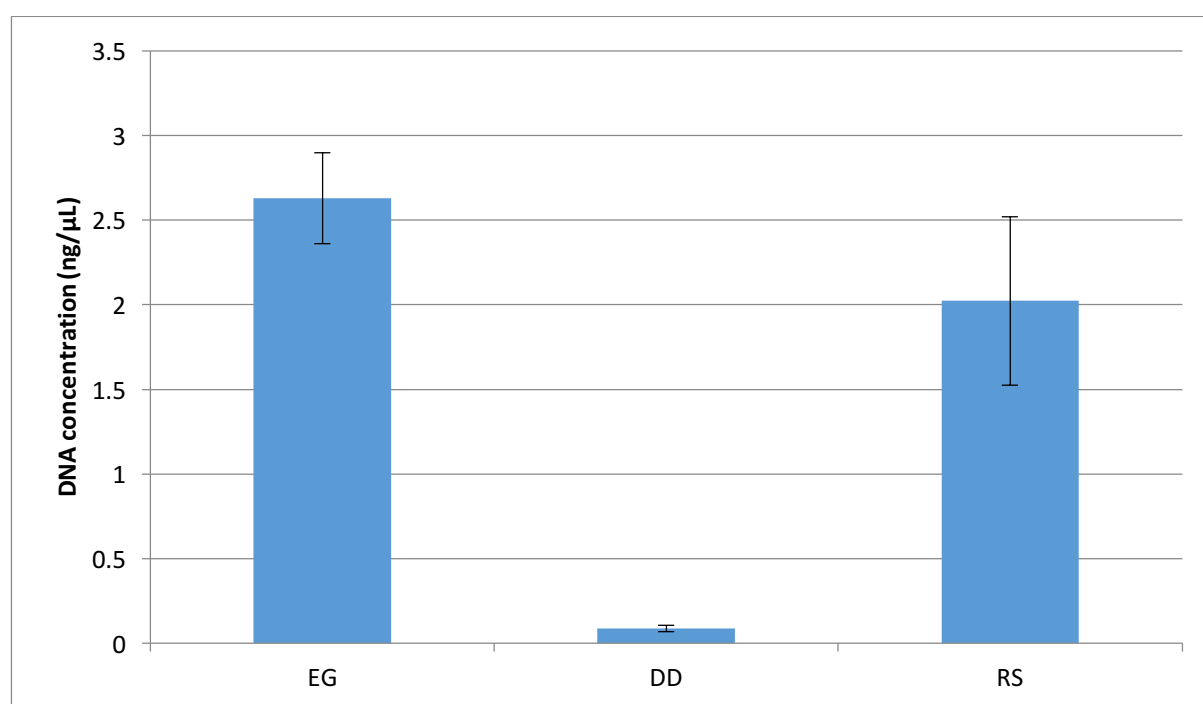


Figure 5.5: Comparison of average DNA quantification (Qubit[®] HS ds-DNA assay) from stained plucked hairs after DNA extraction (4 replicates for each dye), error bars show 95% confidence.

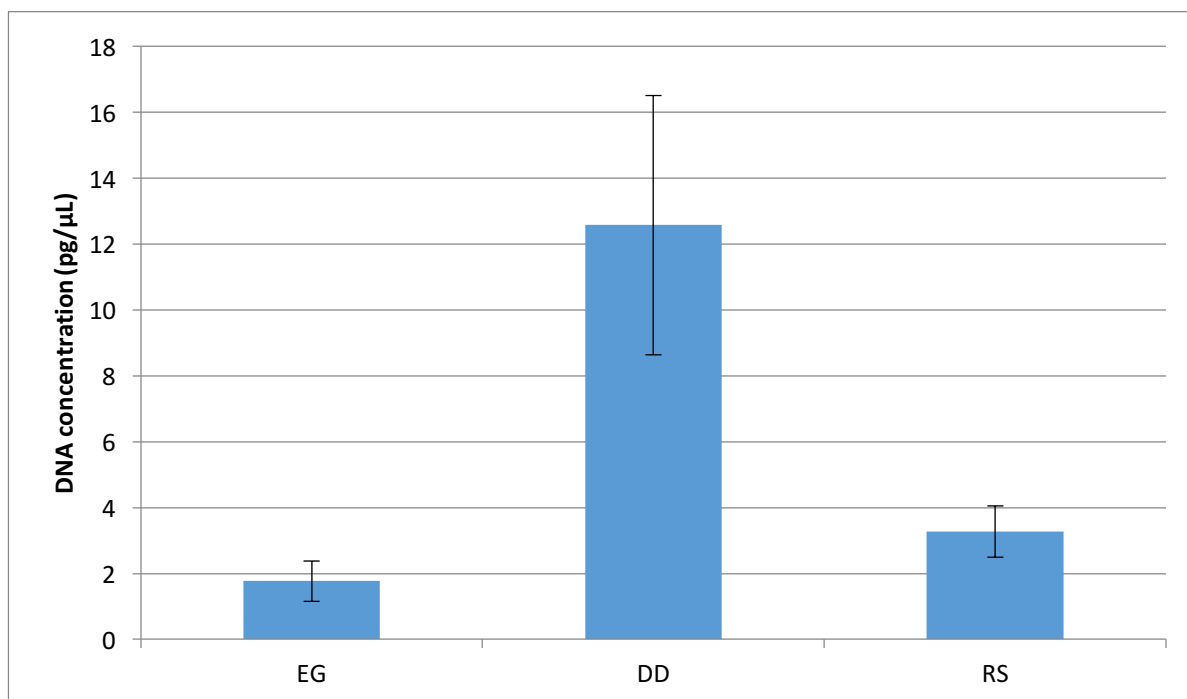


Figure 5.6: Comparison of average DNA quantification (Investigator® qPCR kit) from stained shed hairs after DNA extraction (4 replicates for each dye), error bars show 95% confidence.

Table 5.5 below shows the average alleles obtained after STR amplification using the NGM™ kit of the extracted stained hairs. All hairs produced full DNA profiles except for two hair samples stained with DD. No amplification product was obtained and the samples were re-amplified with the same result. The most reasonable assumption would be that the reaction did not have enough DNA template to amplify any detectable product. DNA quantification values for these two hairs were 90 pg/μL and 16.1 pg/ μL for DD 1 and DD 2 respectively using Qubit®. The quantification values obtained when using RT-PCR, which is a more sensitive method, were 149 pg/ μL and 27.7 pg/ μL respectively. As only 10 μL can be added to the STR amplification reaction the amount of DNA material within the reaction would have been between 0.9-1.5 ng for DD 1 and 0.16-0.28 ng for DD 2. DD 1 is within the optimal range of DNA for STR amplification but DD 2 would have been too low for amplification.

Figure 5.6 shows the average DNA quantification values obtained from the stained shed hairs after extraction. The extracts were quantified by Qubit but only two hairs stained with DD had results (both with visible nuclei: DD3, 26.33 pg/μL; DD4, 12.66 pg/μL). All shed hairs were then quantified by QIAamp DNA Investigator kit (Qiagen). DD stained hairs had a

substantially higher average DNA quantification value due to the two hairs with visible nuclei. There was not a significant difference between the average DNA quantification values for the EG and RS stained hairs.

Figure 5.7 shows the average peak heights of profiles obtained from hairs stained with each dye using both an extraction method and direct amplification method. The peak heights were shown to be statistically the same for all three dyes when samples were extracted, as would be as expected as the amount of starting material was optimized for around 1 ng. For direct amplification the starting material cannot be adjusted hence the variability of the peak heights. All three dyes had an increase in average peak height when using direct amplification most likely due to more DNA material being present for amplification.

Table 5.5: Average peak heights (4 replicates) of plucked hairs stained with DNA binding dyes (20X) then extracted using QIAamp and amplified using NGM™ STR kit and optimum amount of DNA (1 ng)

Locus	Extracted		
	EG	DD	RS
D10S1248	1523.5	1468.5	1543.8
	1334.5	1231.0	1418.3
vWA	1289.4	1639.0	1408.5
	1289.4	1443.0	1408.5
D16S539	1133.8	1192.3	1094.5
	949.75	1192.3	973.25
D2S1338	755.25	1010.0	828.50
	745.00	817.50	669.00
Amelogenin	2441.0	1570.3	2753.8
	2120.8	1570.3	2372.5
D8S1179	2260.8	1931.0	2311.8
	2028.0	1887.0	2246.5
D21S11	1695.5	1525.0	1789.5
	1523.3	1498.5	1531.0
D18S51	1334.5	1179.0	1457.5
	1202.5	973.50	1222.8
D22S1045	1711.0	2029.0	1995.8
	1606.5	1783.5	1881.5
D19S433	1522.5	1138.8	1749.0
	1360.5	1138.8	1601.5
TH01	1412.5	1106.5	1506.1
	1412.5	1197.5	1506.1
FGA	1118.0	1117.0	1267.3
	1034.0	1133.5	1185.8
D2S441	725.25	1114.5	751.00
	686.00	990.00	792.00
D3S1358	663.50	939.50	671.75
	563.75	984.00	637.50
D1S1656	494.00	974.50	620.50
	550.50	928.00	654.00
D12S391	487.25	762.50	498.00
	403.50	748.00	424.50
Average Peak Height (RFU)	1230.6	1256.7	1336.6
standard deviation	540.99	344.23	601.77
95% confidence	62.579	39.818	69.609

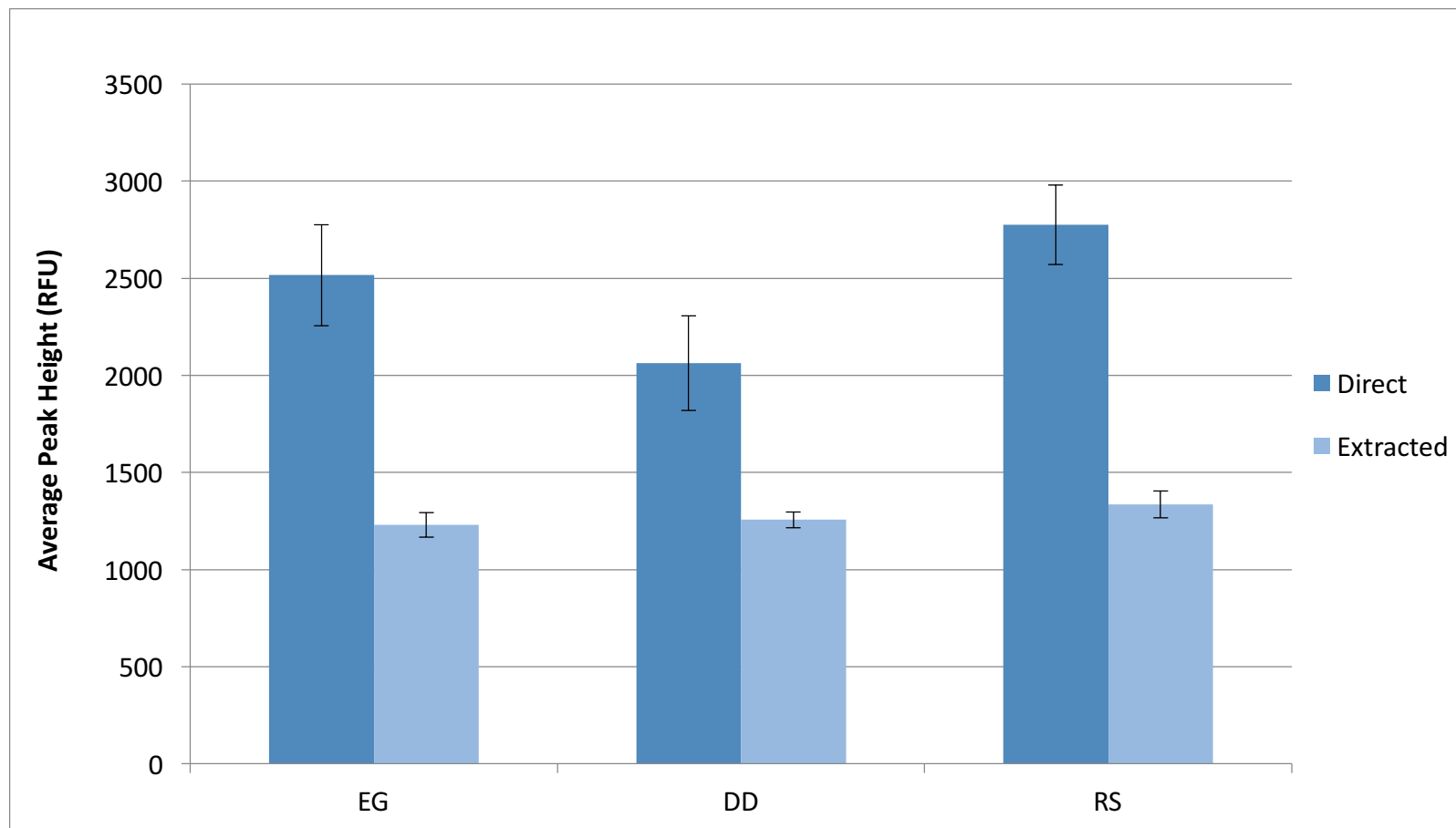


Figure 5.7: Comparison of the average peak heights obtained from plucked hairs when amplified directly or amplified after extraction. The average is based on profile replicates (4 hairs) then an overall average of 32 (alleles) for each. Error bars show 95% confidence.

As shown in the published FSI article, 60 hairs of the 150 that were screened with DD were amplified to determine the chances of obtaining a profile depending on the category into which the hair was placed. Figure 5.8-5.14 shows examples of the stained hair and the corresponding STR profile obtained after directly amplifying the stained hair. Examples of hairs and profiles from each category are shown, with Figure 5.9 showing an example of a category 1 hair and the full profile obtained after amplification.

Figures 5.13 and 5.14 show examples of hairs identified as category 3 due to the lack of visible nuclei and relatively low fluorescent signal. Figure 5.12 shows the category 3 hair that resulted in only one allele being amplified in comparison to Figure 5.13 which shows the category 3 hairs that resulted in a full STR profile.

Figure 5.15 shows the distribution of the number of hairs in each category that resulted in either full profiles or no alleles at all. There is a clear trend that category 1 hairs had a higher number of full profiles than any other category. When looking at the line of best fit for the “full profile” numbers there was a linear relationship shown by the R^2 value of 0.7723. There was also a linear trend for the “no profile” numbers with an R^2 value of 0.9339 showing that the higher the category assignment was the lower the probability of obtaining STR profiles and *vice versa*.

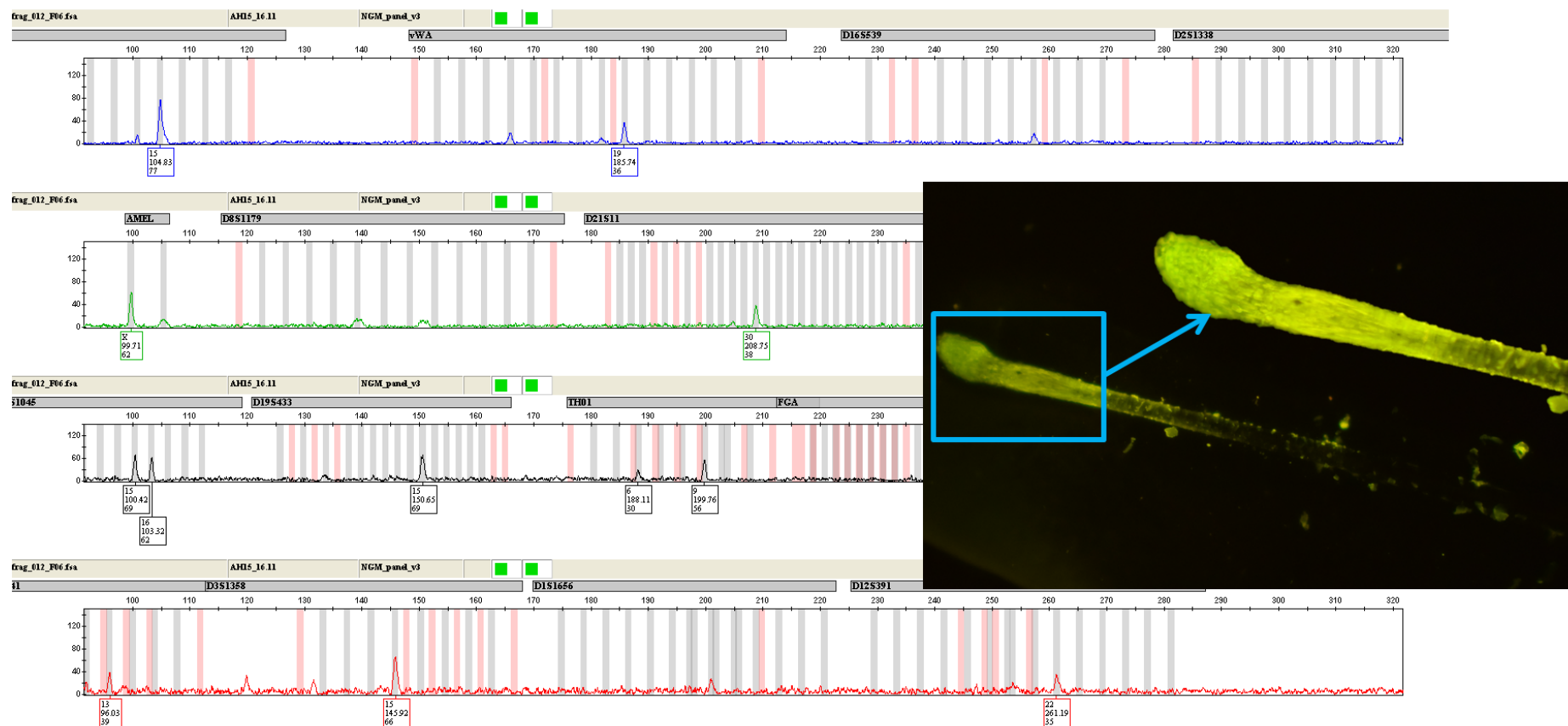


Figure 5.8: Screened hair stained with DD (20X) viewed under a fluorescent microscope at 40X magnification with an exposure time of 1 s. NGM™ Profile of directly amplified hair.

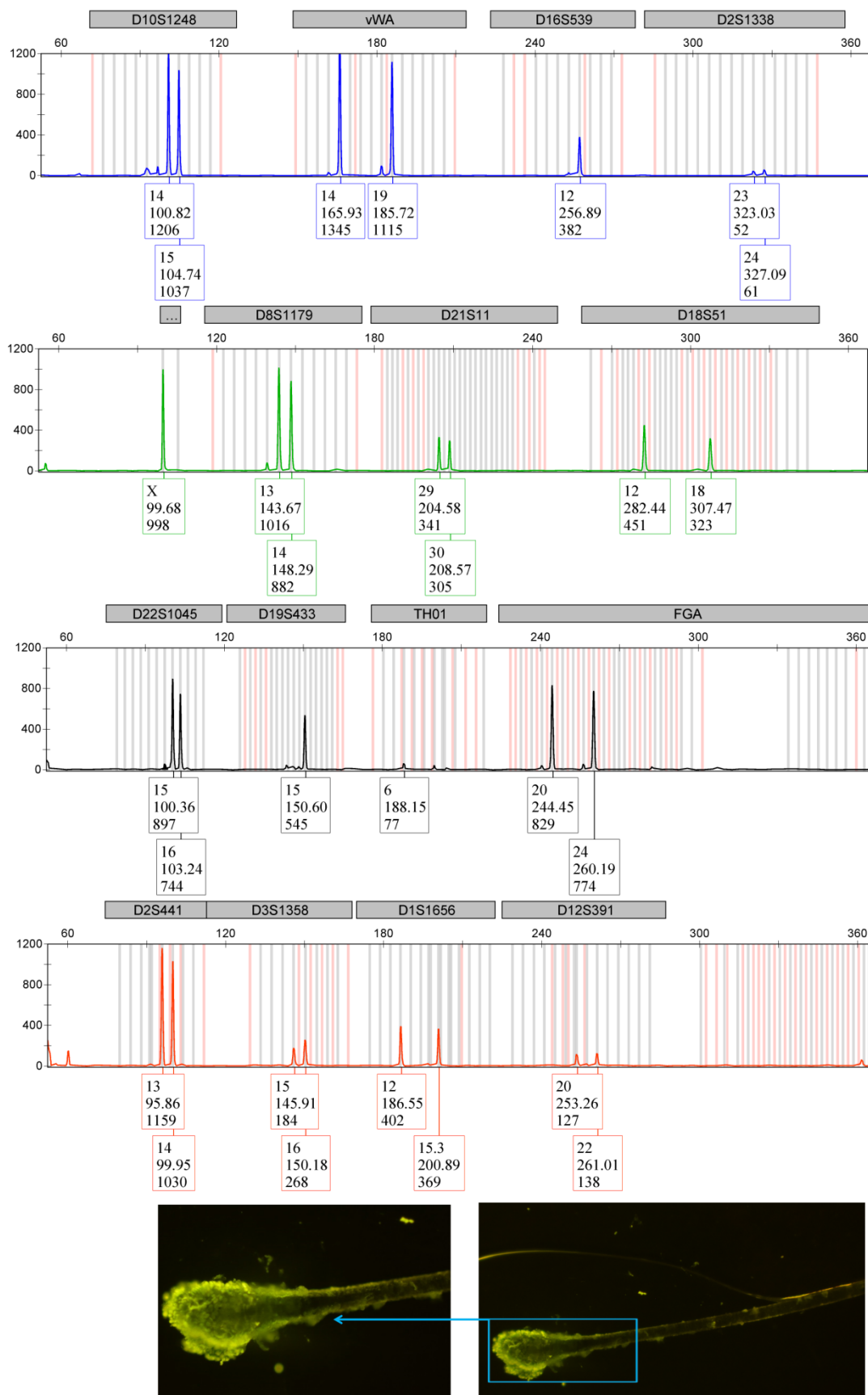


Figure 5.9: Screened hair stained with DD (20X) viewed under a fluorescent microscope at 40X magnification with an exposure time of 1 s. NGM™ Profile of directly amplified hair. Hair was placed in category 1.

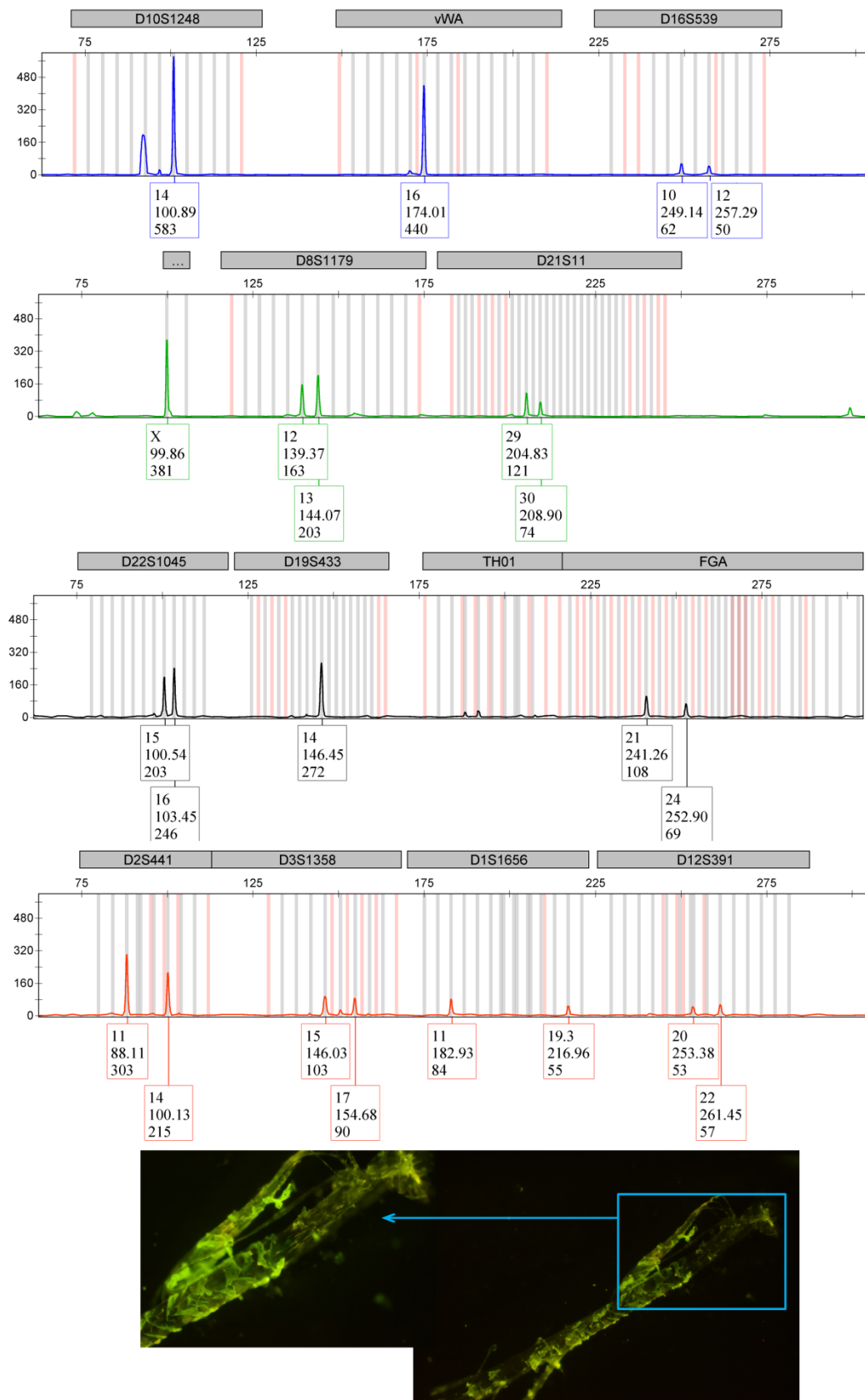


Figure 5.10: Screened hair stained with DD (20X) viewed under a fluorescent microscope at 40X magnification with an exposure time of 1 s. NGM™ Profile of directly amplified hair. Hair was placed in category 1.5.

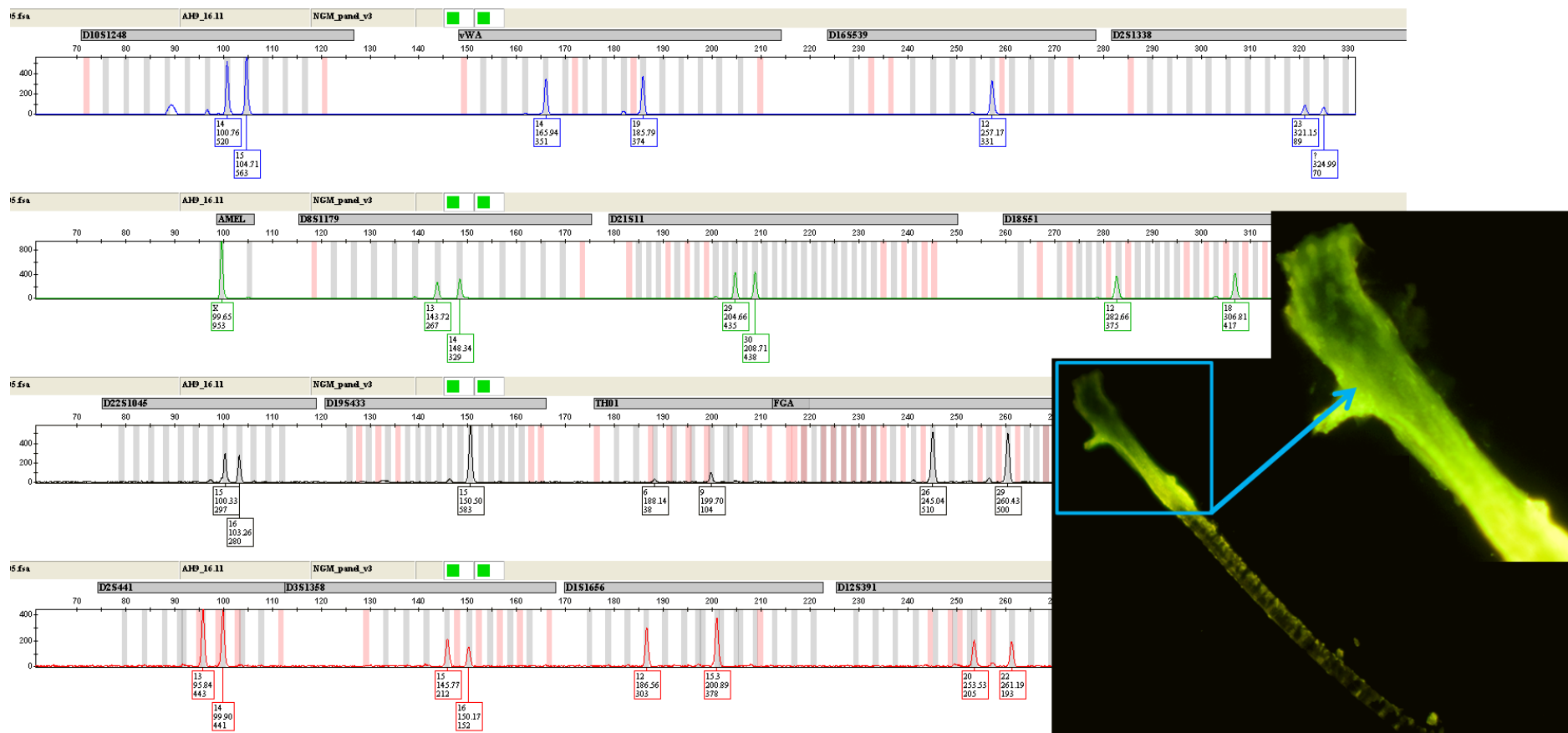


Figure 5.11: Screened hair stained with DD (20X) viewed under a fluorescent microscope at 40X magnification with an exposure time of 1 s. NGM™ Profile of directly amplified hair. Hair was placed in category 2.

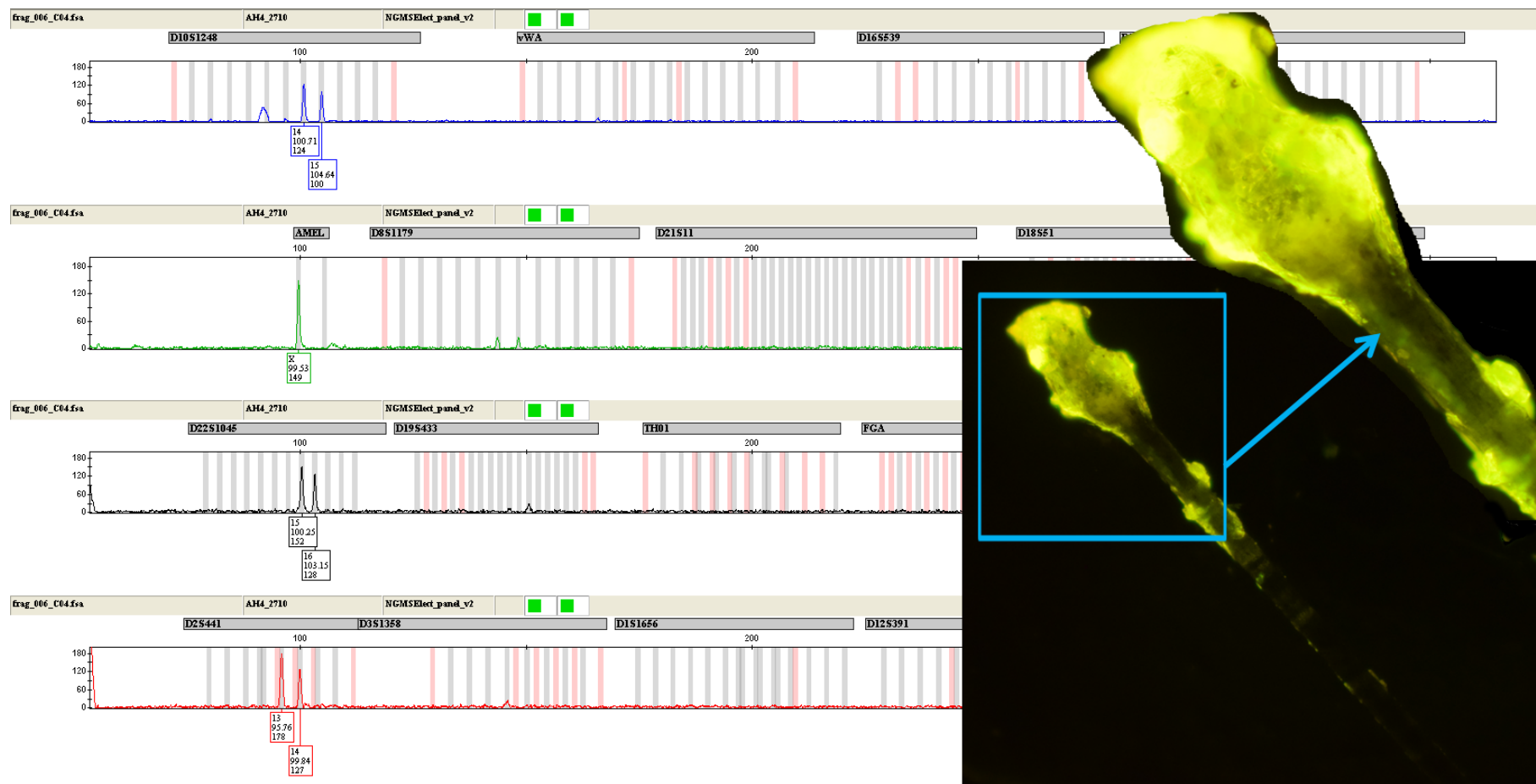


Figure 5.12: Screened hair stained with DD (20X) viewed under a fluorescent microscope at 40X magnification with an exposure time of 1 s. NGM™ Profile of directly amplified hair. Hair was placed in category 2.5.

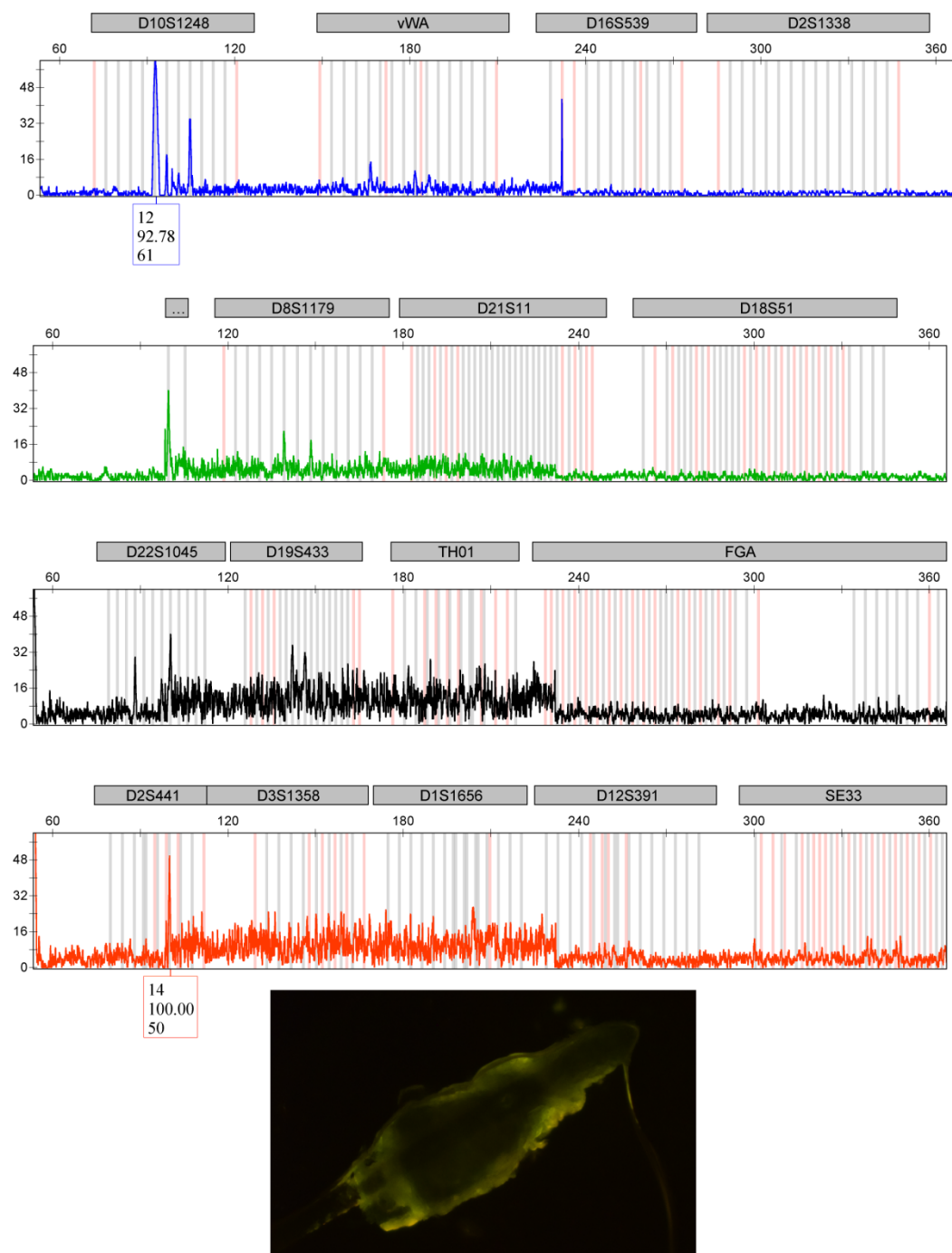


Figure 5.13: Screened hair stained with DD (20X) viewed under a fluorescent microscope at 40X magnification with an exposure time of 1 s. NGM™ Profile of directly amplified hair. Hair was placed in category 3.

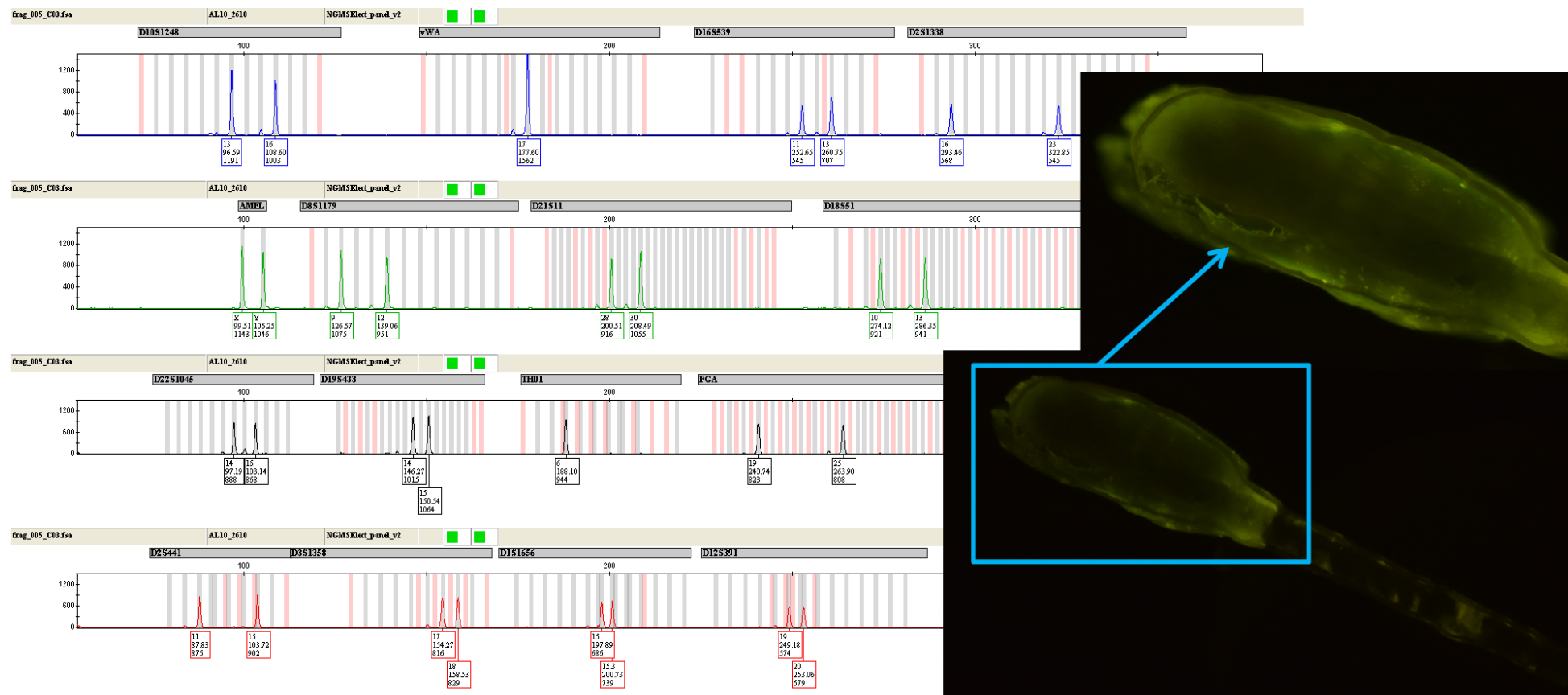


Figure 5.14: Screened hair stained with DD (20X) viewed under a fluorescent microscope at 40X magnification with an exposure time of 1 s. NGM™ Profile of directly amplified hair. Hair was placed in category 3.

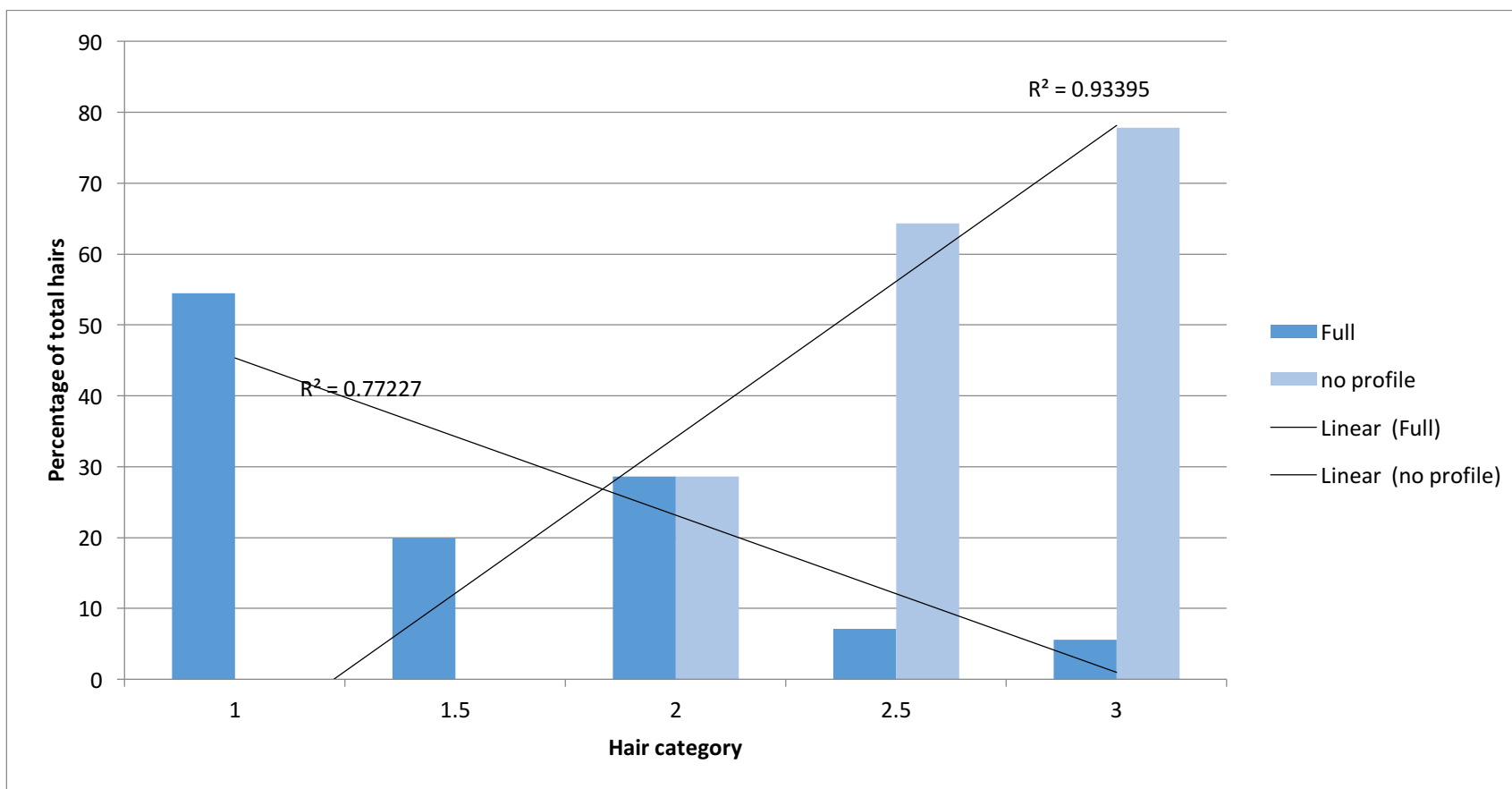


Figure 5.15: Comparison of the percentage of hairs that produce full profiles and no profiles in each of the 5 categories of the number of nuclei. The line of best fit is shown for full profile and for no profile along with R^2 values showing the linearity of the results.

5.5 OTHER PUBLICATIONS

In addition to the article submitted for publication there were two extended conference proceeding's papers published relating to the work within this Chapter. Details of the papers are listed below and the articles themselves appear on the following pages. The articles were resulting from posters presented at the *International Society of Forensic Genetics* and these appear in Appendix D.

Alicia M. Haines, Shanan S. Tobe, Hilton J. Kobus, Adrian Linacre, **Successful direct STR amplification of hair follicles after nuclear staining**, *Forensic Science International: Genetics Supplement Series*, **5** (2015), e65-e66

Resulted from the poster presentation at the International Society of Forensic Genetics (see Appendix D)

Citations: **1**

Alicia M. Haines, Shanan S. Tobe, Hilton J. Kobus, Adrian Linacre, **Duration of *in situ* fluorescent signals within hairs follicles**, *Forensic Science International: Genetics Supplement Series*, **5** (2015), e175-e176


Resulted from the poster presentation at the International Society of Forensic Genetics (see Appendix D)


Statement of Authorship

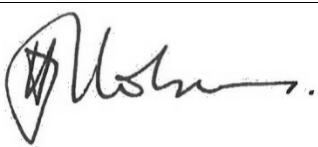
Title of Paper	Successful direct STR amplification of hair follicles after nuclear staining
Publication Status	Published 2015
Publication details	Published in <i>Forensic Science International: Genetics Supplement Series</i>


Author Contributions

By signing the Statement of Authorship, each author certified that their stated contribution to the publication is accurate and that permission is granted for the publication to be included in the candidate's thesis.

Name of Principal Author (Candidate)	Alicia M. Haines		
Contribution to the paper	Designed experimental method, performed all laboratory work and analysis, drafted the manuscript, edited manuscript and acted as corresponding author		
Signature		Date	August, 2016

Name of Co-Author	Shanan S. Tobe		
Contribution to the paper	Gave limited guidance		
Signature		Date	August, 2016

Name of Co-Author	Hilton J. Kobus		
Contribution to the paper	Edited manuscript		
Signature		Date	August, 2016

Name of Co-Author	Adrian Linacre		
Contribution to the paper	Helped design study and edited manuscript		
Signature		Date	August, 2016



Contents lists available at ScienceDirect

Forensic Science International: Genetics Supplement Series

journal homepage: www.elsevier.com/locate/FSIGSS

Successful direct STR amplification of hair follicles after nuclear staining

Alicia M. Haines^{a,*}, Shanan S. Tobe^a, Hilton Kobus^b, Adrian Linacre^a^a School of Biological Sciences, Flinders University, Adelaide, Australia^b School of Chemical and Physical Sciences, Flinders University, Adelaide, Australia

ARTICLE INFO

Article history:

Received 23 July 2015

Accepted 7 September 2015

Available online 10 September 2015

Keywords:

DiamondTM Dye

Fluorescence

Latent DNA

SYBR[®] Green I

ABSTRACT

Hairs are commonly encountered at a crime scene through natural shedding (telogen) or trauma such as during an assault (anagen). The forcible removal of anagen hairs results in retention of the root sheath and therefore the potential for DNA evidence. Telogen hairs lack a root sheath and do not provide a good source of DNA. Microscopy may be performed on all hair samples to detect whether there are cells adhering to the proximal tip to determine if there is a chance of success from subsequent DNA profiling. To aid in improving the microscopy, we report of the staining of hair roots using a range of dyes (SYBR[®] Green I, DiamondTM Nucleic Acid Dye, GelGreenTM, EvaGreenTM and RedSafeTM) and subsequent results from DNA profiling. Results showed that nuclei were visualized using all the dyes except for GelGreenTM. The hairs were then directly amplified and all samples produced an STR profile that met requirements for uploading to a DNA database. The staining procedure conducted before direct amplification had no or little effect on the PCR and electrophoresis of the STR fragments. These results show that these nucleic acid binding dyes can be used as a preliminary assessment as to the viability of the sample (number of nuclei present) for STR analysis.

© 2015 Elsevier Ireland Ltd. All rights reserved.

1. Introduction

Hairs present at crime scenes are quite common due to people shedding approximately 75–100 hairs per day [1]. The more common type of hair found at a crime scene are telogen hairs or resting hairs which are naturally shed. It has been estimated that 95% of hairs which are collected from a crime scene are identified as telogen hairs [2]. Hairs that are in the active growth stage are known as anagen hairs. These hairs can often contain skin material attached to the root of the hair as they can only be removed by a forceful action. This material is targeted for DNA profiling. Microscopy is the primary technique used for selecting hairs for DNA profiling. Other studies however have stated the usefulness of staining hairs with various dyes to visualize the hair nuclei. These dyes include haematoxylin which binds to chromatin present within DNA and histone complexes and stains the nuclei a dark violet [2,3]. DAPI a minor groove binding dye has also been used to stain hairs to visualize the number of nuclei present to determine viability for STR profiling [4,5]. DAPI is not a highly specific DNA binding dye as it has a fluorescent signal when in the presence of

detergents and other compounds. This dye only has approximately a 20 fold increase in fluorescent signal when in the presence of DNA [6,7]. This study looks at using more sensitive dyes to review their ability for staining hairs to visualize nuclei present within the root of the hairs. The dyes used in this study were SYBR[®] Green I (SG), DiamondTM Nucleic acid dye (DD), RedSafeTM (RS), GelGreenTM (GG) and EvaGreenTM (EG).

2. Methodology

2.1. Nuclear staining

The binding dyes were diluted in a buffer solution down to 20X (1 in 500 dilution) and then an aliquot (1 µL) was applied to the hair shafts (plucked) and viewed under a fluorescence microscope (Nikon Optiphot) using a B2A cube to filter the light.

2.2. STR amplification and analysis

The stained root fragment was placed into a 0.2 mL thin walled tube containing 10 µL of PCR master mix from the NGM SelectTM kit (Life Technologies, Vic., AUS) along with 5 µL of primer mix and 1 µL of AmpliTaq Gold[®] DNA polymerase. A further 9 µL of sterile water was added to make up a final volume of 25 µL. The

* Corresponding author at: Flinders University GPO Box 2100, School of Biological Sciences, Adelaide, SA, 5001, Australia.

E-mail address: alicia.haines@flinders.edu.au (A.M. Haines).

<http://dx.doi.org/10.1016/j.fsigs.2015.09.026>

1875-1768/© 2015 Elsevier Ireland Ltd. All rights reserved.

Table 1

NGM Select™ profile percentage of plucked hairs stained with DNA binding dyes and the average peak height (RFU) of profile.

	RedSafe™	Diamond™ Dye	GelGreen™	EvaGreen™	SYBR® Green
Number of alleles	30	30	30	30	21
Profile%	100	100	100	100	70
Average Peak Height (RFU)	608.8	2256	3486	2963	232.7

NGM Select™ contains 15 STR loci plus amelogenin, the number of alleles shown was not including amelogenin.

amplification was conducted using Bio-Rad thermal cycler (Bio-Rad) using the manufacturer's protocol. A standard cycle number of 29 were used throughout the study.

Capillary electrophoresis was performed on an ABI 3130 × L Genetic Analyser (Life Technologies) using POP-4 polymer (Life Technologies). An aliquot of 2 µL of the amplified samples was added to a solution containing 0.5 µL of GeneSace-600 LIZ Size Standard and 9.5 µL of Hi-Di Formamide. Samples were denatured at 95 °C for 3 min. Electrophoresis was conducted at 3 kV with a 10 s injection. The data were analyzed using GeneMapper v3.2. The detection threshold was set at 50 RFU.

3. Results and discussion

Table 1 shows the number of alleles amplified from the plucked hair samples that were stained prior to STR amplification. Full profiles were obtained for all stained hairs except for SG where there was allele drop out. The average peak height shows that there was inhibition when using the SG dye as it was substantially lower when compared to the average peak heights from the other stained hairs. When stained with GG the nuclei could not be visualized due to the dye not being cell permeable. Even though a profile was obtained this dye is not suitable for nuclear staining. The other dyes should nuclei staining and therefore could be used as a presumptive test for determining the viability of the sample for DNA analysis.

4. Concluding remarks

Full DNA profiles were obtained after nuclear staining with RS, DD, GG and EG. There was allele drop out when staining with SG resulting in only a 70% profile. This would likely be due to the

inhibiting nature of SG in the amplification step. This study has shown the ability to stain hair follicles with DNA binding dyes with successful direct amplification of STR loci and the ability for these dyes to be used as a screening methodology prior to STR analysis.

Role of funding

Funding was provided by the Attorney General's Office, South Australia.

Conflict of interest

None.

References


- [1] L. Bourguignon, B. Hoste, T. Boonen, K. Vits, F. Hubrecht, A fluorescent microscopy-screening test for efficient STR-typing of telogen hair roots, *Forensic Sci. Int. Genet.* 3 (2008) 27–31.
- [2] J. Edson, E.M. Brooks, C. McLaren, J. Robertson, D. McNevin, A. Cooper, J.J. Austin, A quantitative assessment of a reliable screening technique for the STR analysis of telogen hair roots, *Forensic Sci. Int. Genet.* 7 (2013) 180–188.
- [3] A.H. Fischer, K.A. Jacobson, J. Rose, R. Zeller, Haematoxylin and eosin staining of tissue and cell sections, *CSH Protoc.* 3 (2008) 1–2.
- [4] T. Lopez, M. Vandewoestyne, D. Van Hoofstat, D. Deforce, Fast nuclear staining of head hair roots as a screening method for successful STR analysis in forensics, *Forensic Sci. Int. Genet.* 13 (2014) 191–194.
- [5] E.M. Brooks, M. Cullen, T. Szttydna, S.J. Walsh, Nuclear staining of telogen hair roots contributes to successful forensic nDNA analysis, *Aust. J. Forensic Sci.* 42 (2010) 115–122.
- [6] M.L. Barcellona, G. Cardiel, E. Gratton, Time-resolved fluorescence of DAPI in solution and bound to polydeoxynucleotides, *Biochem. Biophys. Res. Commun.* 170 (1990) 270–280.
- [7] D. Banerjee, S.K. Pal, Dynamics in the DNA recognition by DAPI: exploration of the various binding modes, *J. Phys. Chem. B* 112 (2008) 1016–1021.


Statement of Authorship


Title of Paper	Duration of <i>in situ</i> fluorescent signals within hairs follicles
Publication Status	Published 2015
Publication details	Published in <i>Forensic Science International: Genetics Supplement Series</i>

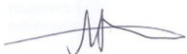
Author Contributions

By signing the Statement of Authorship, each author certified that their stated contribution to the publication is accurate and that permission is granted for the publication to be included in the candidate's thesis.

Name of Principal Author (Candidate)	Alicia M. Haines		
Contribution to the paper	Designed experimental method, performed all laboratory work and analysis, drafted the manuscript, edited manuscript and acted as corresponding author		
Signature		Date	August, 2016

Name of Co-Author	Shanan S. Tobe		
Contribution to the paper	Helped take initial image of hair		
Signature		Date	August, 2016

Name of Co-Author	Hilton J. Kobus		
Contribution to the paper	Edited manuscript		
Signature		Date	August, 2016

Name of Co-Author	Adrian Linacre		
Contribution to the paper	Helped design study and edited manuscript		
Signature		Date	August, 2016



Contents lists available at ScienceDirect

Forensic Science International: Genetics Supplement Series

journal homepage: www.elsevier.com/locate/FSIGSSDuration of *in situ* fluorescent signals within hairs folliclesAlicia M. Haines^{a,*}, Shanan S. Tobe^a, Hilton Kobus^b, Adrian Linacre^a^a School of Biological Sciences, Flinders University, Adelaide, Australia^b School of Chemical and Physical Sciences, Flinders University, Adelaide, Australia

ARTICLE INFO

Article history:

Received 17 August 2015

Accepted 16 September 2015

Available online 21 September 2015

Keywords:

DiamondTM Dye

Fluorescence

Latent DNA

SYBR[®] Green I

ABSTRACT

Nuclei within anagen hair follicles can be viewed using fluorescent microscopy after staining with a nucleic acid binding dye. Anagen hairs are still in the growth phase and generally only removed by force such as pulling, plucking or trauma and can be important evidentiary items at a crime scene. Staining of the hairs can be a fast, easy, method to determine if hair samples have DNA present making it worthwhile to attempt to obtain a DNA profile for evidentiary purposes. SYBR[®] Green I and DiamondTM Nucleic Acid Dye are two such dyes. The duration of the *in situ* fluorescent signal of both these nucleic acid dyes was studied to determine how long the samples can be kept in storage after staining yet still be capable of producing a fluorescent signal. Our results show that when stained with DiamondTM Nucleic Acid Dye the fluorescent signal could be viewed months after initial staining period. However when the hair was stained with SYBR[®] Green I there was a significant reduction in the fluorescent signal within 7 days of initial staining. Our conclusion is that DiamondTM Nucleic acid dye was a viable dye for staining hair and keeping the samples in storage for later analysis.

© 2015 Elsevier Ireland Ltd. All rights reserved.

1. Introduction

Nucleic acid binding dyes are used in gel electrophoresis, flow cytometry, real-time PCR and in DNA quantification. Conventional DNA binding dyes include: ethidium bromide which can intercalate between the base pairs of DNA [1]; DAPI which is a minor groove binding dye that is selective for AT rich regions [2]; and acridine orange that can bind to both DNA and RNA effectively [3,4]. The fluorescent enhancement upon binding to nucleic acids generally does not exceed 100-fold. There are now dyes that have a higher sensitivity and fluorescent enhancements around 1000-fold, these dyes include SYBR Green I and PicoGreen which have been used in analysis and detection methodologies [3]. Another area that DNA binding dyes are not so widely used is for staining biological samples to determine the amount of DNA that is present as a screening methodology of samples in forensic science [5]. DAPI has been used to stain hair follicles to screen and select hairs based on the number of nuclei present [5,6] leading to a presumptive test that is a quick and cheap way to determine whether or not the hair may produce an STR profile. This study shows the stability of both

DiamondTM nucleic acid dye (DD) and SYBR[®] Green I (SG) when bound to DNA present within plucked hair follicles. This aids in determining how the dyes interact with DNA within a hair follicle over time but also allows for stained hairs to be kept in storage and still view the fluorescent signal without the need to re-stain the hair follicle. Table 1 below shows the stability of the dyes stated by the manufacturer.

2. Methodology

Plucked hairs were stained with the nucleic acid binding dyes SG and DD. A dye solution of 20X (1 in 500 dilution of the stock concentration) was used to stain the hair root and shaft (1 µL). The stained hairs were then viewed under a Nikon Optiphot fluorescent microscope using a B2A filter cube. Images were taken with an exposure time of 1 s. This process from then was undertaken at varying time intervals to view the fluorescent signal.

3. Results and discussion

Fig. 1 shows the fluorescent signal produced when plucked hair follicles were stained with either DD or SG. It can be seen that for DD the signal did not decrease over time whereas the signal when using SG did substantially reduce after several days. This is in accordance with the information supplied by the manufacturer

* Corresponding author at: Flinders University GPO Box 2100, School of Biological Sciences, Adelaide, SA, 5001, Australia.

E-mail address: alicia.haines@flinders.edu.au (A.M. Haines).

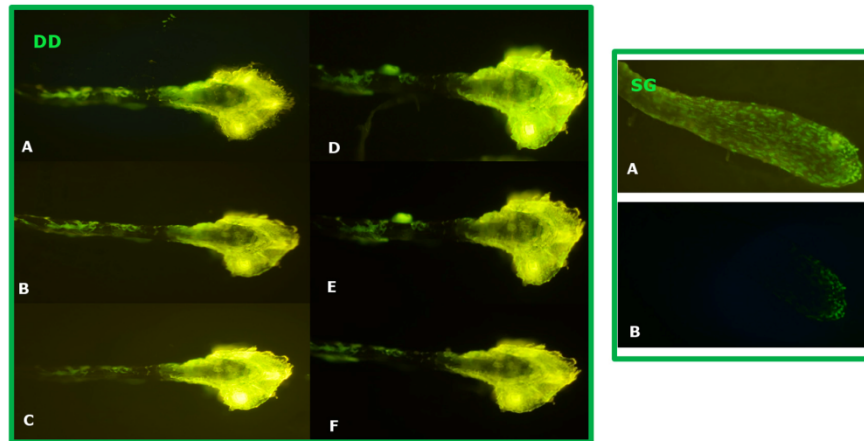
<http://dx.doi.org/10.1016/j.fsigs.2015.09.070>

1875-1768/© 2015 Elsevier Ireland Ltd. All rights reserved.

Table 1

Dye stability of SYBR® Green I and Diamond™ Dye in water, storage conditions and if unstable in the presence of light as stated by the manufacturer.

Dye	Storage	Stability	Stability in H ₂ O	Protect from light
SG (Life Technologies, Vic, AUS)	≤ −20 °C	DMSO 6 months-year	Use within 24 h	Yes
DD (Promega, NSW, AUS)	RT −20 °C	90 days 2 years	Stable	Yes

**Fig. 1.** Stability of DNA binding dyes present within plucked hair follicles over time.

that SG was only stable in water for 24 h. The signal present after 7 days was reduced due to the level of instability of SG. In comparison DD was said to be stable for around 90 days when diluted with water. This is also shown in Fig. 1 where the signal appears to not have changed over days and months.

DD shows a plucked hair stained with DD using a 20X concentration with an exposure time of 1 s (A) initial staining, (B) 7 days, (C) 14 days, (D) 30 days, (E) 2 months, (F) 6 months. SG shows a plucked hair stained with SG using a 20X concentration with an exposure time of 1 s (A) showing initial staining, (B) fluorescent signal after 7 days

4. Concluding remarks

It was found that when staining hairs with nucleic acid binding dyes, individual nuclei can be seen within the hair follicle. The fluorescent signal when using the dye DD lasted months whereas when using SG the signal only lasted for a few days and was substantially reduced after 7 days.

Conflict of interest

None.

Role of funding

Funding was provided by Forensic Science South Australia and the Attorney General's Department, South Australia.

References

- [1] C. Aaij, P. Borst, The gel electrophoresis of DNA, *Biochim. Biophys. Acta (BBA)–Nucleic Acids Protein Synth.* 269 (1972) 192–200.
- [2] D. Banerjee, S.K. Pal, Dynamics in the DNA recognition by DAPI: exploration of the various binding modes, *J. Phys. Chem. B* 112 (2008) 1016–1021.
- [3] A.I. Dragan, et al., SYBR Green I: fluorescence properties and interaction with DNA, *J. Fluoresc.* 22 (2012) 1189–1199.
- [4] M.B. Lyles, I.L. Cameron, Interactions of the DNA intercalator acridine orange, with itself, with caffeine, and with double stranded DNA, *Biophys. Chem.* 96 (2002) 53–76.
- [5] L. Bourguignon, B. Hoste, T. Boonen, K. Vits, F. Hubrecht, A fluorescent microscopy-screening test for efficient STR-typing of telogen hair roots, *Forensic Sci. Int. Genet.* 3 (2008) 27–31.
- [6] T. Lepez, M. Vandewoestyne, D. Van Hoofstat, D. Deforce, Fast nuclear staining of head hair roots as a screening method for successful STR analysis in forensics, *Forensic Sci. Int. Genet.* 13 (2014) 191–194.

5.4 Chapter Summary

This Chapter looked at the ability of using nucleic acid binding dyes for hair follicle staining to view the number of nuclei present. The DNA binding dyes GG, DD, RS, EG and SG were evaluated for their use with nuclear staining of hairs. It was found that GG was not a suitable dye for this methodology due to the dye not being able to permeate the cell membrane, thus nuclei staining was not possible. All the other dyes showed nuclei staining within hairs however SG was shown to be unstable at room temperature with the fluorescent signal reducing over time. DD was shown to be more stable at room temperature with the fluorescent signal still visible months after initial staining of hair. DD was also shown to have a lower background signal than EG. SG also inhibited the reaction as some alleles did not amplify.

After the initial evaluation of EG, SG, DD and RS for their staining ability of hairs and effects on PCR after directly amplifying the stained hairs, EG, RS and DD were selected for further evaluation. SG was not selected due to the inhibition on PCR which was also shown in previous results (Chapter 3). These three dyes were then assessed for their staining ability of shed and plucked hairs with half the hairs undergoing a DNA extraction and half being directly amplified. Due to the loss of DNA during the extraction process (see results in Chapter 3) some of the plucked hairs did not result in a DNA profile however all plucked hairs submitted for direct amplification all resulted in full profiles. The protocol had to be slightly altered with direct amplification with an increase in the extension time to reduce the number of split peaks that appeared in the profile.

DD was selected to screen a further 150 hair samples that ranged in the age of hairs, donor type (male or female) and colour. Direct amplification was chosen due to the risk of losing DNA through extraction and due to the reduction in time and consumables. Out of the 150 screened hairs 60 were amplified and the number of hairs in each category that had a full profile, high partial profile (12 alleles and above), low partial profile (1-11 alleles) and no profile were counted. It was found that there was a direct correlation with the category designation and chances of obtaining a full DNA profile.

The results from this study can be used within forensic laboratories in evidence recovery to determine whether hairs submitted for analysis would be suitable for STR profiling by using this simple, fast and cheap methodology of staining. This technique is also non-destructive to the hair hence further testing can be done if needed.

5.6 References (Supplemental to publication)

- [1] E. A. Graffy., D. R. Foran, *DNA / Hair Analysis A2 - Payne-James, Jason*, in *Encyclopedia of Forensic and Legal Medicine*. 2005, Elsevier: Oxford. p. 213-220.
- [2] L. Bourguignon., B. Hoste., T. Boonen., K. Vits., F. Hubrecht, A fluorescent microscopy-screening test for efficient STR-typing of telogen hair roots, *Forensic Science International: Genetics*. 2008, **3** 27-31.
- [3] J. R. Robertson, *Forensic examination of hair*. 2002: CRC Press.
- [4] M. M. Houck, Forensic Human Hair Examination and Comparison in the 21st Century, *Forensic Sci Rev*. 2005, **17** 51-66.
- [5] J. Edson., E. M. Brooks., C. McLaren., J. Robertson., D. McNevin., A. Cooper, et al, A quantitative assessment of a reliable screening technique for the STR analysis of telogen hair roots, *Forensic Science International: Genetics*. 2013, **7** 180-188.
- [6] E. Brooks., B. Comber., I. McNaught., J. Robertson, Digital imaging and image analysis applied to numerical applications in forensic hair examination, *Science & Justice*. 2011, **51** 28-37.
- [7] J. M. Taupin, Forensic hair morphology comparison – a dying art or junk science?, *Science & Justice*. 2004, **44** 95-100.
- [8] M. E. Taylor, Scanning Electron Microscopy in Forensic Science, *Journal of the Forensic Science Society*. 1973, **13** 269-280.
- [9] T. Lepez., M. Vandewoestyne., D. Van Hoofstat., D. Deforce, Fast nuclear staining of head hair roots as a screening method for successful STR analysis in forensics, *Forensic Science International: Genetics*. 2014, **13** 191-194.
- [10] T. Boonen., K. Vits., B. Hoste., F. Hubrecht, The visualization and quantification of cell nuclei in telogen hair roots by fluorescence microscopy, as a pre-DNA analysis assessment, *Forensic Science International: Genetics Supplement Series*. 2008, **1** 16-18.
- [11] K. P. Kirkbride., S. R. Tridico, The application of laser scanning confocal microscopy to the examination of hairs and textile fibers: An initial investigation, *Forensic Science International*. 2010, **195** 28-35.
- [12] M. Wilson., D. Polanskey., J. Butler., J. DiZinno., J. Replogle., B. Budowle, Extraction, PCR amplification and sequencing of mitochondrial DNA from human hair shafts, *Biotechniques*. 1995, **18** 662-669.
- [13] K. L. Opel., E. L. Fleishaker., J. A. Nicklas., E. Buel., B. R. McCord, Evaluation and Quantification of Nuclear DNA from Human Telogen Hairs*, *Journal of Forensic Sciences*. 2008, **53** 853-857.
- [14] K. Müller., R. Klein., E. Miltner., P. Wiegand, Improved STR typing of telogen hair root and hair shaft DNA, *ELECTROPHORESIS*. 2007, **28** 2835-2842.
- [15] R. Ottens., D. Taylor., D. Abarno., A. Linacre, Successful direct amplification of nuclear markers from a single hair follicle, *Forensic Science, Medicine, and Pathology*. 2013, **9** 238-243.

- [16] M. Hayashida., K. Iwao-Koizumi., S. Murata., K. Kinoshita, Single-Tube Genotyping from a Human Hair Root by Direct PCR, *Analytical Sciences*. 2009, **25** 1487-1489.
- [17] R. Ottens., J. Templeton., V. Paradiso., D. Taylor., D. Abarno., A. Linacre, Application of direct PCR in forensic casework, *Forensic Science International: Genetics Supplement Series*. 2013, **4** e47-e48.
- [18] A. M. Haines., S. S. Tobe., H. J. Kobus., A. Linacre, Effect of nucleic acid binding dyes on DNA extraction, amplification, and STR typing, *ELECTROPHORESIS*. 2015, **36** 2561-2568.
- [19] E. M. Brooks., M. Cullen., T. Szydla., S. J. Walsh, Nuclear staining of telogen hair roots contributes to successful forensic nDNA analysis, *Australian Journal of Forensic Sciences*. 2010, **42** 115-122.
- [20] D. McNevin., L. Wilson-Wilde., J. Robertson., J. Kyd., C. Lennard, Short tandem repeat (STR) genotyping of keratinised hair: Part 1. Review of current status and knowledge gaps, *Forensic Science International*. 2005, **153** 237-246.
- [21] S. Szabo., K. Jaeger., H. Fischer., E. Tschachler., W. Parson., L. Eckhart, In situ labeling of DNA reveals interindividual variation in nuclear DNA breakdown in hair and may be useful to predict success of forensic genotyping of hair, *International Journal of Legal Medicine*. 2012, **126** 63-70.
- [22] A. H. Fischer., K. A. Jacobson., J. Rose., R. Zeller, Hematoxylin and Eosin Staining of Tissue and Cell Sections, *Cold Spring Harbor Protocols*. 2008, **2008** pdb.prot4986.
- [23] D. Banerjee., S. K. Pal, Dynamics in the DNA Recognition by DAPI: Exploration of the Various Binding Modes, *The Journal of Physical Chemistry B*. 2008, **112** 1016-1021.
- [24] M. L. Barcellona., G. Cardiel., E. Gratton, Time-resolved fluorescence of DAPI in solution and bound to polydeoxynucleotides, *Biochem Biophys Res Commun*. 1990, **170** 270-280.
- [25] G. Cosa., K. S. Focsaneanu., J. R. McLean., J. P. McNamee., J. C. Scaiano, Photophysical properties of fluorescent DNA-dyes bound to single- and double-stranded DNA in aqueous buffered solution, *Photochem Photobiol*. 2001, **73** 585-599.
- [26] A. I. Dragan., R. Pavlovic., J. B. McGivney., J. R. Casas-Finet., E. S. Bishop., R. J. Strouse., et al, SYBR Green I: Fluorescence Properties and Interaction with DNA, *Journal of Fluorescence*. 2012, **22** 1189-1199.
- [27] F. Mao., W.-Y. Leung., X. Xin, Characterization of EvaGreen and the implication of its physicochemical properties for qPCR applications, *BMC Biotechnology*. 2007, **7** 76-76.
- [28] J. M. Butler, *Chapter 3 - DNA Quantitation*, in *Advanced Topics in Forensic DNA Typing*, Butler, J. M., Editor. 2012, Academic Press: San Diego. p. 49-67.
- [29] J.M. Butler, *Chapter 2 – DNA Extraction methods*, in *Advanced Topics in Forensic DNA Typing*, Butler, J. M., Editor. 2012, Academic Press: San Diego. p. 29-47.

- [1] A. I. Dragan., R. Pavlovic., J. B. McGivney., J. R. Casas-Finet., E. S. Bishop., R. J. Strouse, et al., SYBR Green I: Fluorescence Properties and Interaction with DNA, *Journal of Fluorescence*. 2012, **22** 1189-1199.
- [2] A. M. Haines., S. S. Tobe., H. J. Kobus.A. Linacre, Properties of nucleic acid staining dyes used in gel electrophoresis, *ELECTROPHORESIS*. 2015, **36** 941-944.
- [3] I. Kavanagh., D. Leake.G. Ball, *Dye blends*, 2013, Google Patents.

5.6 APPENDIX D

Table D-1: Peak heights for each allele from the hairs stained with EG (20X) and amplified after extraction using optimum DNA mass (1ng)

Locus	EG_P_1	EG_P_2	EG_P_3	EG_P_4	Average EG
D10S1248	3112	2000	1794	2955	2465.25
	2605	1634	1492	2504	2058.75
vWA	4092	4182.5	4178.5	4153.5	4151.625
	4092	4182.5	4178.5	4153.5	4151.625
D16S539	2402	990	472	3381	1811.25
	2033	824	432	2606	1473.75
D2S1338	1180	719	994	1720	1153.25
	599	385	635	1023	660.5
Amelogenin	3516	2203	1823	3766	2827
	7676	4850	4465	5569	5640
D8S1179	8828	7540	7892	8190	8112.5
	8262	6105	7448	7043	7214.5
D21S11	452	137	125	182	224
	455	134	127	159	218.75
D18S51	1770	583	624	728	926.25
	1479	461	557	522	754.75
D22S1045	6558	5230	4114	7095	5749.25
	7112	5340	3958	7461	5967.75
D19S433	1845	1251	528	2815	1609.75
	1620	1068	459	2446	1398.25
TH01	1267	988	475.5	2971	1425.375
	1267	988	475.5	2971	1425.375
FGA	2581	1228	1208	1079	1524
	1914	852	860	710	1084
D2S441	6737	5967	5185	7210	6274.75
	5357	2356	5391	5362	4616.5
D3S1358	1657	1409	615	2873	1638.5
	621	1047	488	2462	1154.5
D1S1656	1062	668	329	915	743.5
	1218	754	388	948	827
D12S391	851	561	392	960	691
	736	450	316	717	554.75
Average Peak Height (RFU) of profile	2967.375	2096.469	1950.594	3051.563	2516.5

Table D-2: Peak heights for each allele from the hairs stained with RS (20X) and amplified after extraction using optimum DNA mass (1ng)

Locus	RS_P_1	RS_P_2	RS_P_3	RS_P_4	Average RS
D10S1248	1998	3777	2965	803	2385.75
	1639	3329	2469	689	2031.5
vWA	4160	4034.5	4089	2557	3710.125
	4160	4034.5	4089	2557	3710.125
D16S539	636	6992	1336	2012	2744
	543	6068	1154	1740	2376.25
D2S1338	550	5993	1035	1427	2251.25
	291	4912	568	942	1678.25
Amelogenin	2026	6826	3227	1896	3493.75
	4696	7051	6895	2437	5269.75
D8S1179	7647	8602	8361	3596	7051.5
	6731	8430	7943	3302	6601.5
D21S11	134	571	183	536	356
	135	573	179	505	348
D18S51	534	4260	904	1318	1754
	434	3928	737	1088	1546.75
D22S1045	4899	6692	8410	2776	5694.25
	4908	7479	8291	2692	5842.5
D19S433	829	3632	2006	1119	1896.5
	740	3534	1714	1038	1756.5
TH01	466.5	3869.5	1684	1620	1910
	466.5	3869.5	1684	1620	1910
FGA	1355	4672	1987	795	2202.25
	943	3930	1409	617	1724.75
D2S441	5171	6586	6338	2388	5120.75
	4694	5191	2662	2323	3717.5
D3S1358	765	5756	1776	1710	2501.75
	581	4965	1310	1483	2084.75
D1S1656	453	3213	853	672	1297.75
	527	3580	962	694	1440.75
D12S391	371	3606	646	682	1326.25
	297	3097	521	567	1120.5
Average Peak Height (RFU) of profile	1993.125	4782.906	2762.094	1568.781	2776.726563

Table D-3: Peak heights for each allele from the hairs stained with DD (20X) and amplified after extraction using optimum DNA mass (1ng)

Locus	DD_P_1	DD_P_2	DD_P_3	DD_P_4	Average DD
D10S1248	1987	1916	1348	2312	1890.75
	1566	1622	1104	1865	1539.25
vWA	4153.5	4216	3777	4115.5	4065.5
	4153.5	4216	3777	4115.5	4065.5
D16S539	867	795	647	1454	940.75
	697	706	534	1257	798.5
D2S1338	390	1314	607	696	751.75
	188	759	268	360	393.75
Amelogenin	2365	2103	1866	2426	2190
	5064	4469	2949	5074	4389
D8S1179	7832	7872	5805	7363	7218
	6776	7591	4459	6696	6380.5
D21S11	134	153	89	95	117.75
	129	149	77	88	110.75
D18S51	375	717	280	395	441.75
	284	592	214	335	356.25
D22S1045	6769	4777	3678	6270	5373.5
	7230	4831	3450	6616	5531.75
D19S433	1273	646	1062	1512	1123.25
	1159	563	869	1288	969.75
TH01	921	620.5	963	1058.5	890.75
	921	620.5	936	1058.5	884
FGA	1211	1120	524	1183	1009.5
	802	825	347	803	694.25
D2S441	6046	5872	4175	6982	5768.75
	4718	3219	1013	5436	3596.5
D3S1358	1248	1051	1363	1712	1343.5
	897	825	1066	1403	1047.75
D1S1656	550	507	399	739	548.75
	653	589	436	793	617.75
D12S391	420	539	413	687	514.75
	337	446	324	576	420.75
Average Peak Height (RFU) of profile	2253.625	2070.031	1525.594	2398.875	2062.03125

Table D-4: Peak heights for each allele from the hairs stained with EG (20X) and amplified directly using NGM STR kit

Locus	EG1	2	3	4	Average
D10S1248	1616	1723	1430	1325	1523.5
	1430	1383	1005	1520	1334.5
vWA	1257.5	1531.5	1004.5	1364	1289.375
	1257.5	1531.5	1004.5	1364	1289.375
D16S539	1143	1287	805	1300	1133.75
	1124	1138	722	815	949.75
D2S1338	622	945	623	831	755.25
	703	1055	425	797	745
Amelogenin	2834	2579	2080	2271	2441
	2215	2360	2017	1891	2120.75
D8S1179	2511	2325	1804	2403	2260.75
	2101	2445	1642	1924	2028
D21S11	1996	2053	1206	1527	1695.5
	1983	1471	1095	1544	1523.25
D18S51	1096	1580	1159	1503	1334.5
	1180	1592	896	1142	1202.5
D22S1045	1945	1888	1569	1442	1711
	1823	2037	1189	1377	1606.5
D19S433	1408	1958	1114	1610	1522.5
	1249	1803	1055	1335	1360.5
TH01	1371.5	1899	864	1515.5	1412.5
	1371.5	1899	864	1515.5	1412.5
FGA	1239	1342	711	1180	1118
	1148	1185	805	998	1034
D2S441	797	814	575	715	725.25
	786	739	483	736	686
D3S1358	730	752	535	637	663.5
	569	684	395	607	563.75
D1S1656	591	541	360	484	494
	557	572	502	571	550.5
D12S391	563	599	298	489	487.25
	481	416	216	501	403.5
Average Peak Height (RFU) of profile	1303.063	1441.469	951.6563	1226.063	1230.563

Table D-5: Peak heights for each allele from the hairs stained with RS (20X) and amplified directly using NGM STR kit

Locus	RS1	2	3	4	Average
D10S1248	1462	1505	1558	1650	1543.75
	1272	1323	1607	1471	1418.25
vWA	1431.5	1337.5	1179	1686	1408.5
	1431.5	1337.5	1179	1686	1408.5
D16S539	1097	1149	769	1363	1094.5
	1093	977	631	1192	973.25
D2S1338	1053	839	384	1038	828.5
	768	817	283	808	669
Amelogenin	2523	2721	3109	2662	2753.75
	1926	2357	2795	2412	2372.5
D8S1179	2151	2273	2231	2592	2311.75
	2147	2260	2035	2544	2246.5
D21S11	2006	1823	1240	2089	1789.5
	1732	1612	1134	1646	1531
D18S51	1835	1636	846	1513	1457.5
	1159	1363	810	1559	1222.75
D22S1045	1564	1935	2396	2088	1995.75
	1379	1955	1983	2209	1881.5
D19S433	1814	1595	1703	1884	1749
	1309	1554	1940	1603	1601.5
TH01	1521	1436	1665.5	1402	1506.125
	1521	1436	1665.5	1402	1506.125
FGA	1421	1333	960	1355	1267.25
	1138	1323	746	1536	1185.75
D2S441	600	851	696	857	751
	741	701	698	1028	792
D3S1358	620	648	538	881	671.75
	647	535	575	793	637.5
D1S1656	688	640	403	751	620.5
	653	674	534	755	654
D12S391	543	561	302	586	498
	507	501	237	453	424.5
Average Peak Height (RFU) of profile	1304.781	1344	1213.5	1484.188	1336.617

Table D-6: Peak heights for each allele from the hairs stained with DD (20X) and amplified directly using NGM STR kit

Locus	DD1	2	3	4	Average
D10S1248	1382	NA	1555	NA	1468.5
	1288	NA	1174	NA	1231
vWA	1717	NA	1561	NA	1639
	1469	NA	1417	NA	1443
D16S539	1264	NA	1120.5	NA	1192.25
	1264	NA	1120.5	NA	1192.25
D2S1338	1149	NA	871	NA	1010
	942	NA	693	NA	817.5
Amelogenin	1691.5	NA	1449	NA	1570.25
	1691.5	NA	1449	NA	1570.25
D8S1179	1869	NA	1993	NA	1931
	1727	NA	2047	NA	1887
D21S11	1656	NA	1394	NA	1525
	1648	NA	1349	NA	1498.5
D18S51	1295	NA	1063	NA	1179
	1158	NA	789	NA	973.5
D22S1045	2181	NA	1877	NA	2029
	1959	NA	1608	NA	1783.5
D19S433	1238	NA	1039.5	NA	1138.75
	1238	NA	1039.5	NA	1138.75
TH01	1369	NA	844	NA	1106.5
	1456	NA	939	NA	1197.5
FGA	1304	NA	930	NA	1117
	1509	NA	758	NA	1133.5
D2S441	1459	NA	770	NA	1114.5
	1285	NA	695	NA	990
D3S1358	1377	NA	502	NA	939.5
	1474	NA	494	NA	984
D1S1656	1524	NA	425	NA	974.5
	1416	NA	440	NA	928
D12S391	1188	NA	337	NA	762.5
	1172	NA	324	NA	748
Average Peak Height (RFU) of profile	1448.75	NA	1064.594	NA	1256.672

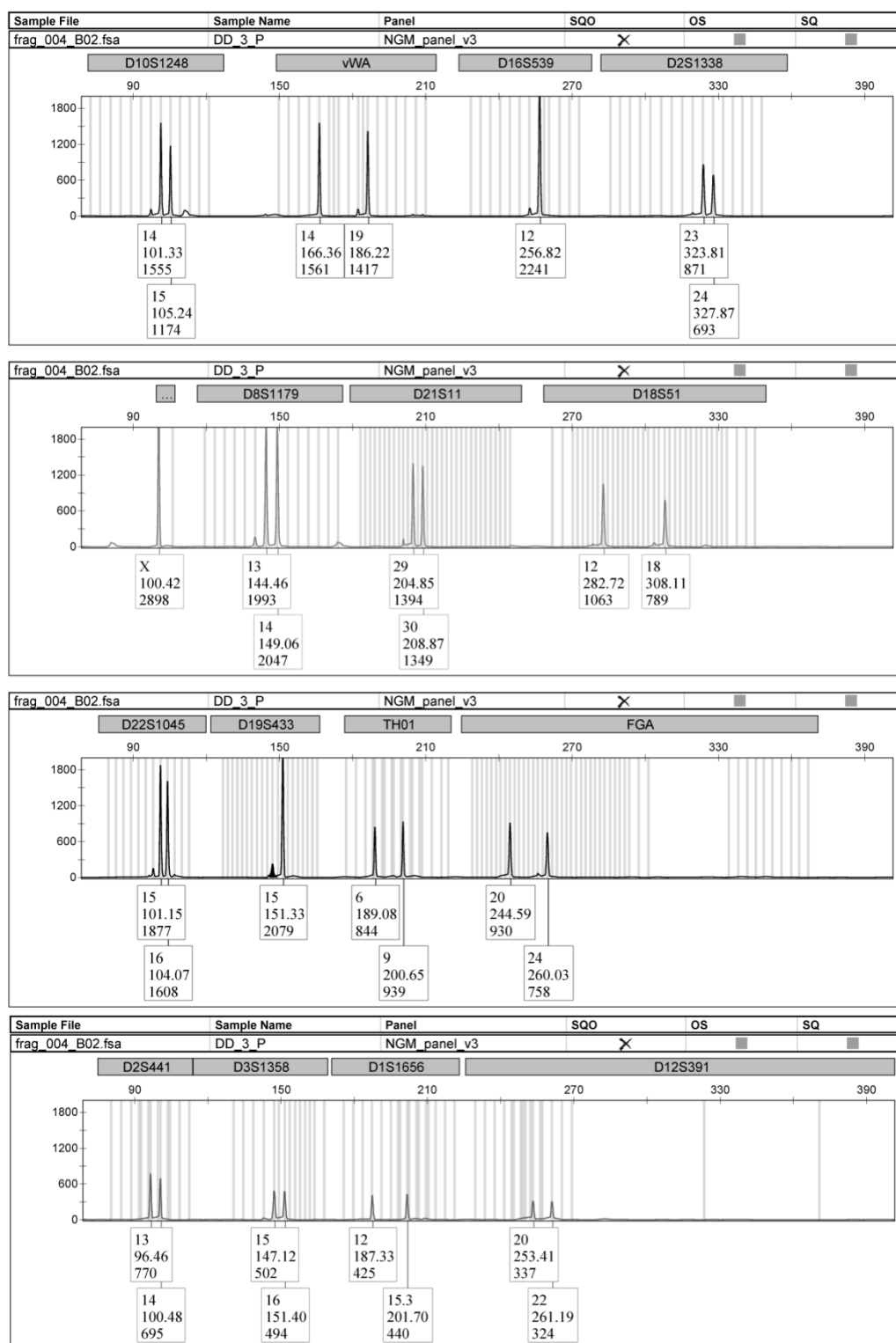


Figure D-1: Plucked hair stained with DD (20X) and amplified using NGM after extraction

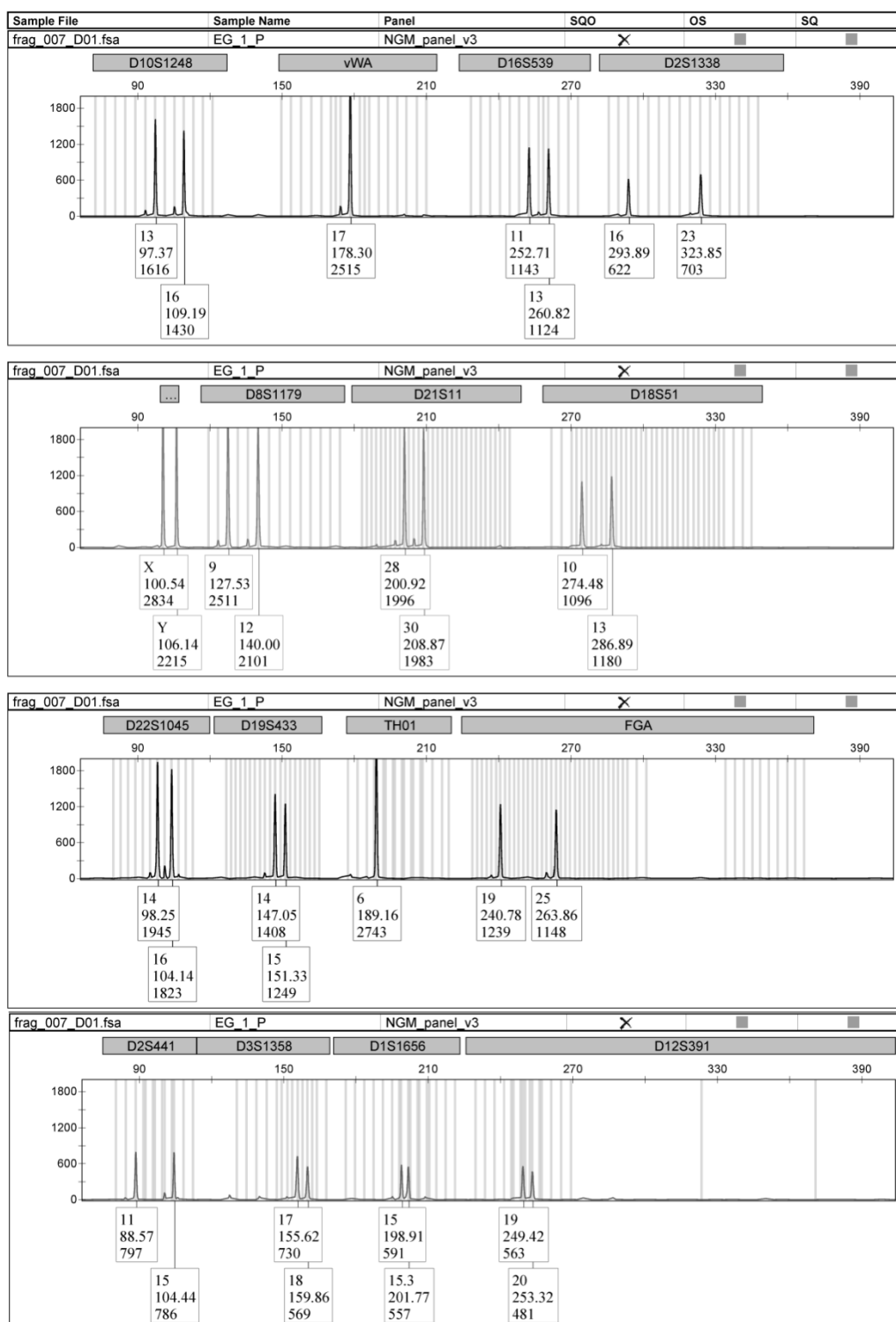


Figure D-2: Plucked hair stained with EG (20X) and amplified using NGM after extraction.

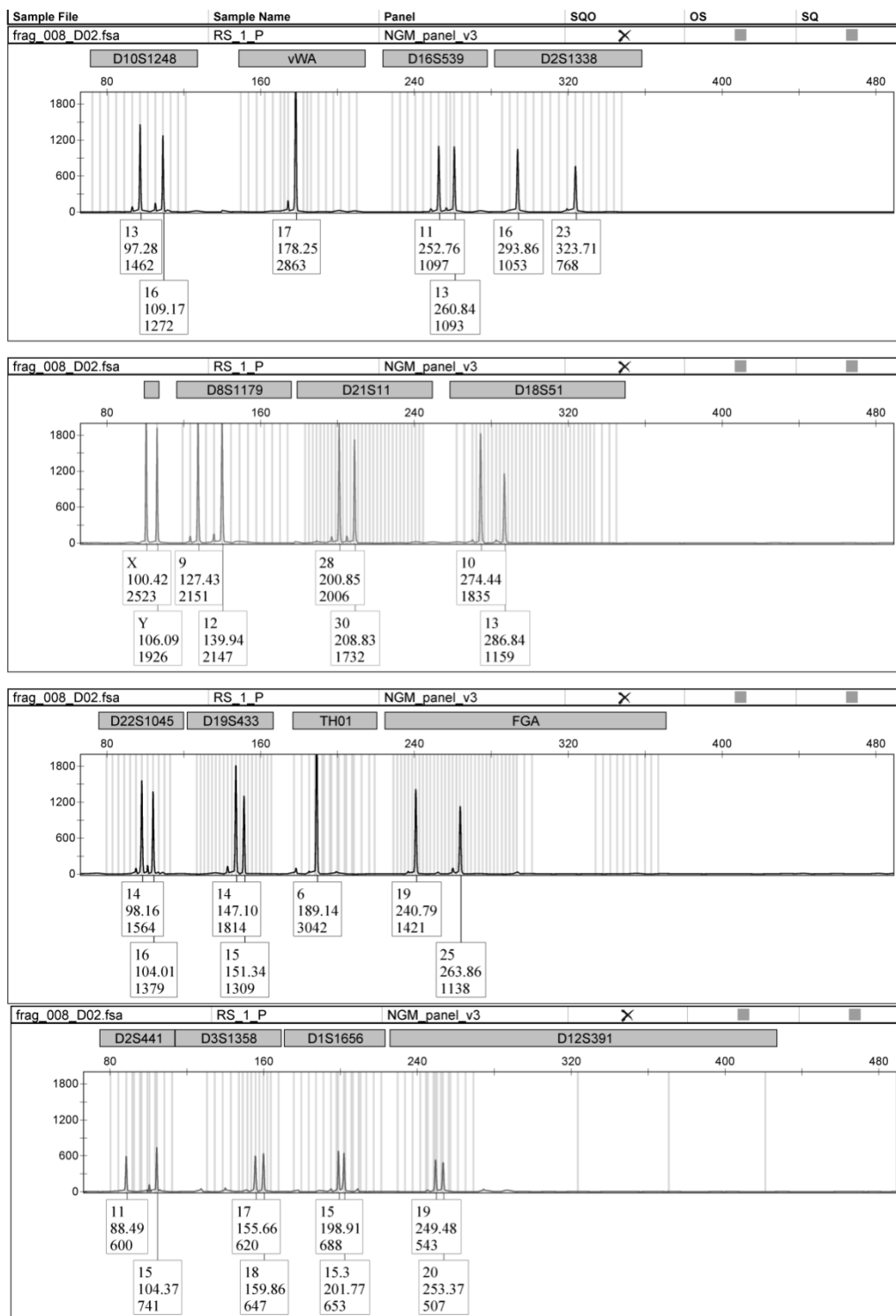


Figure D-3: Plucked hair stained with RS (20X) and amplified using NGM after extraction.

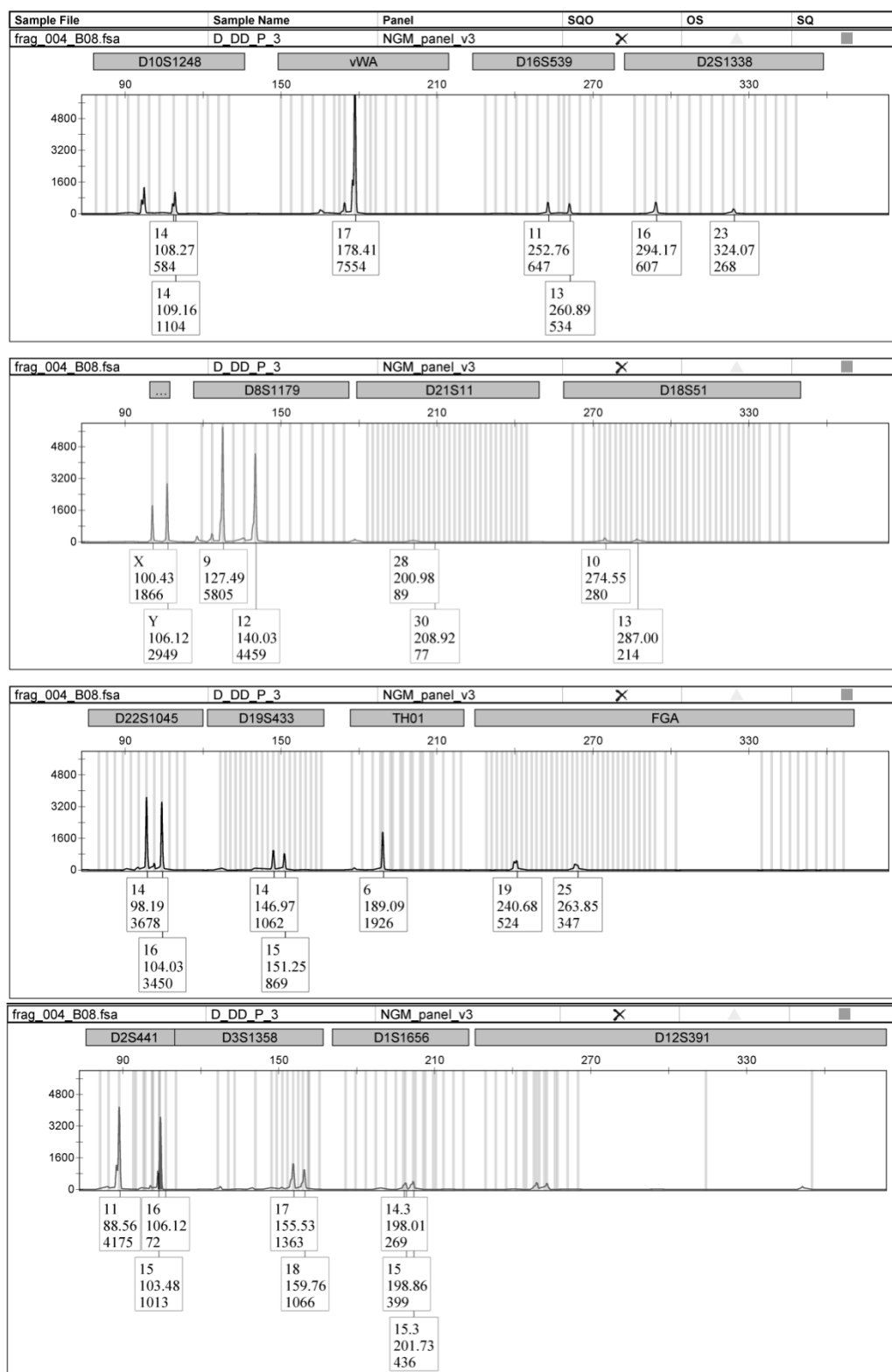


Figure D-4: Plucked hair stained with DD (20X) amplified directly with NGM.

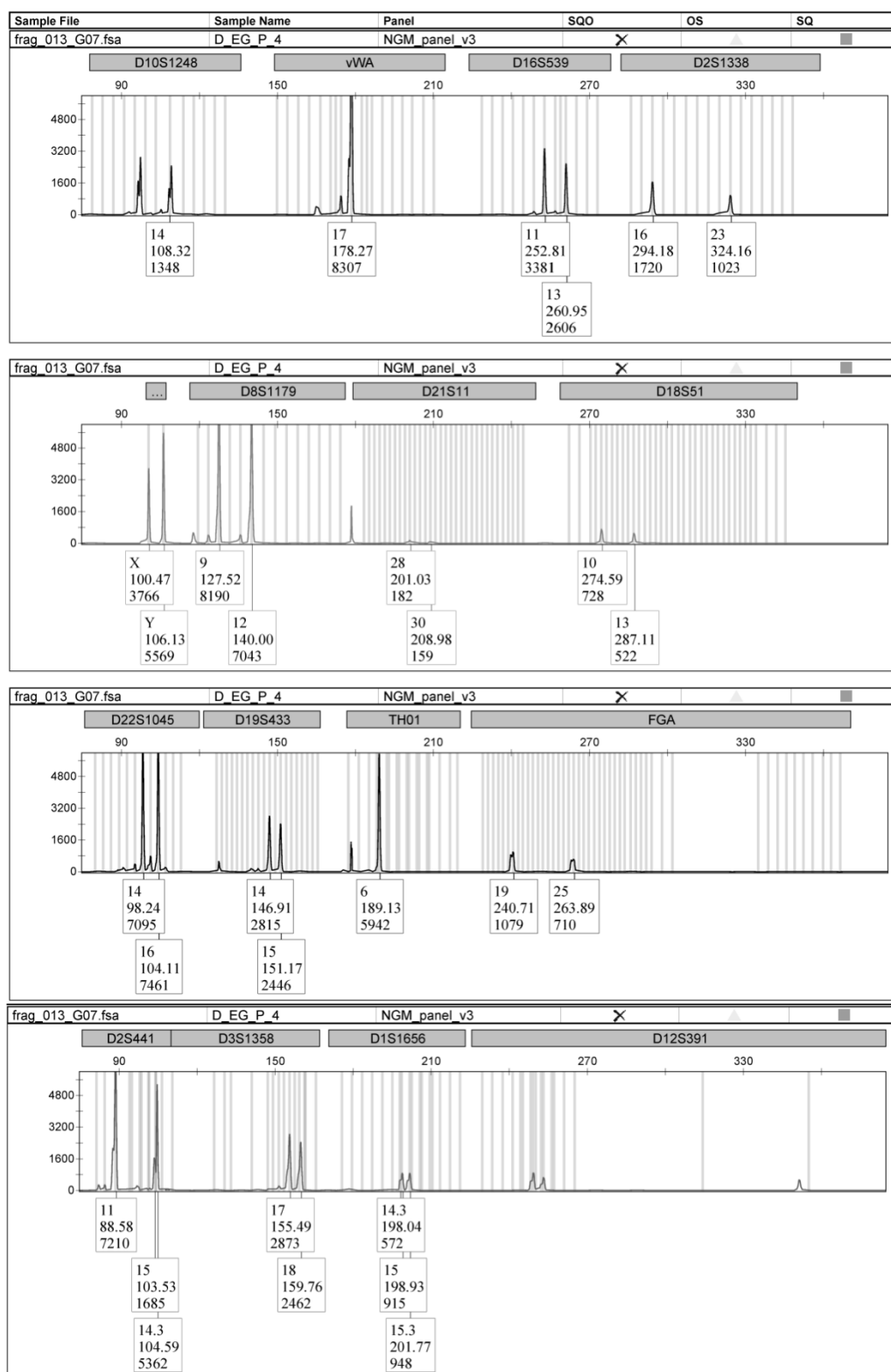


Figure D-5: Plucked hair stained with EG (20X) amplified directly with NGM.

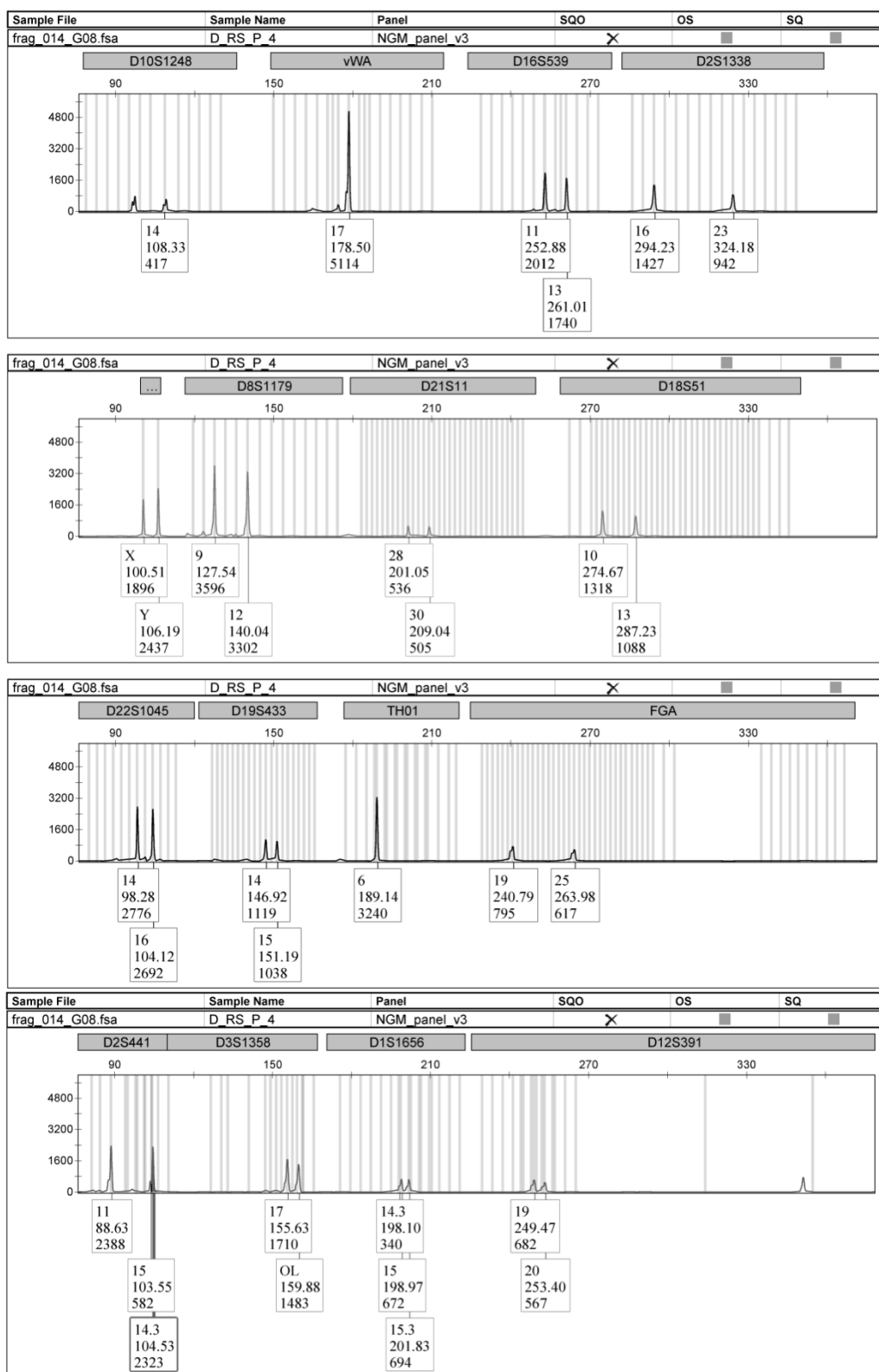


Figure D-6: Plucked hair stained with RS (20X) amplified directly with NGM.

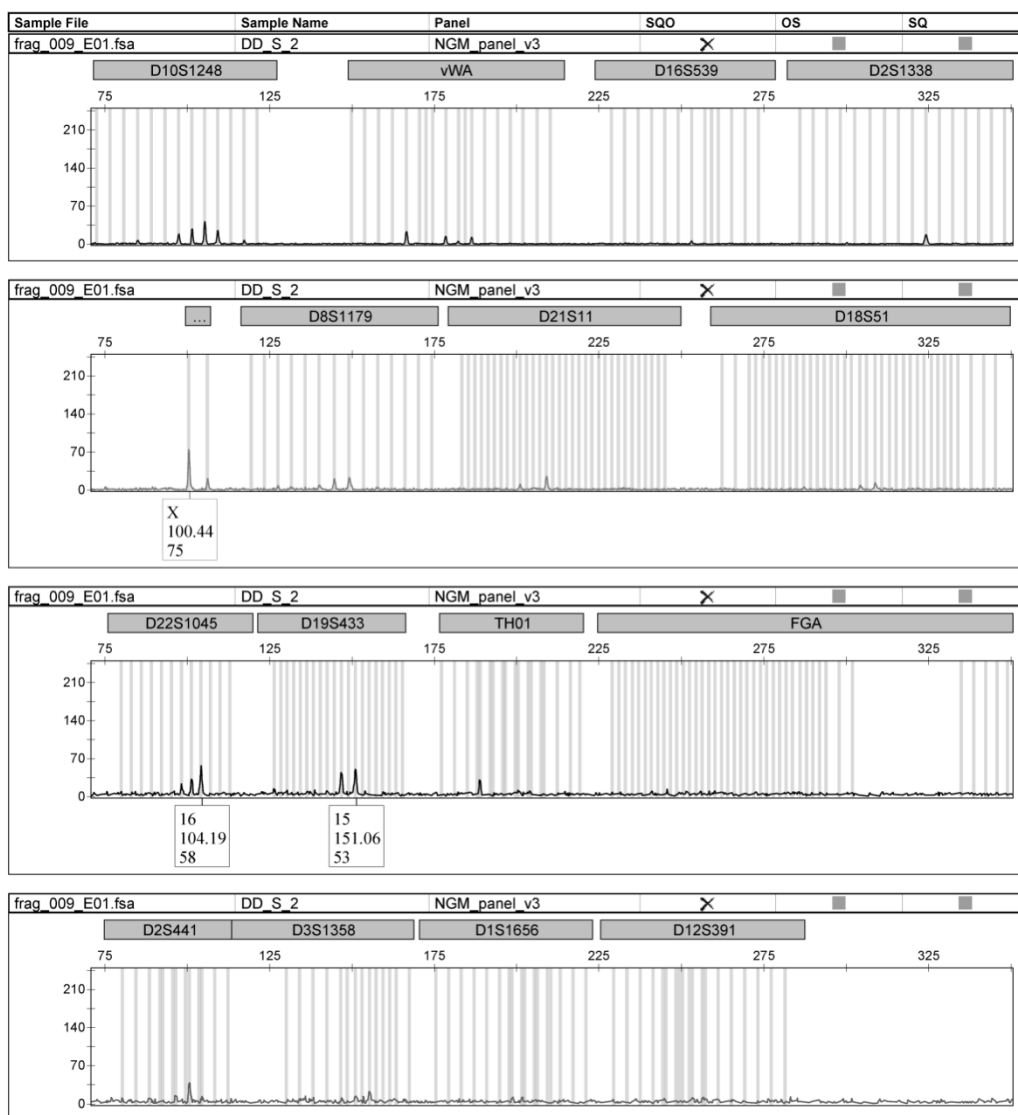


Figure D-7: Shed hair stained with DD (20X) amplified directly with NGM.

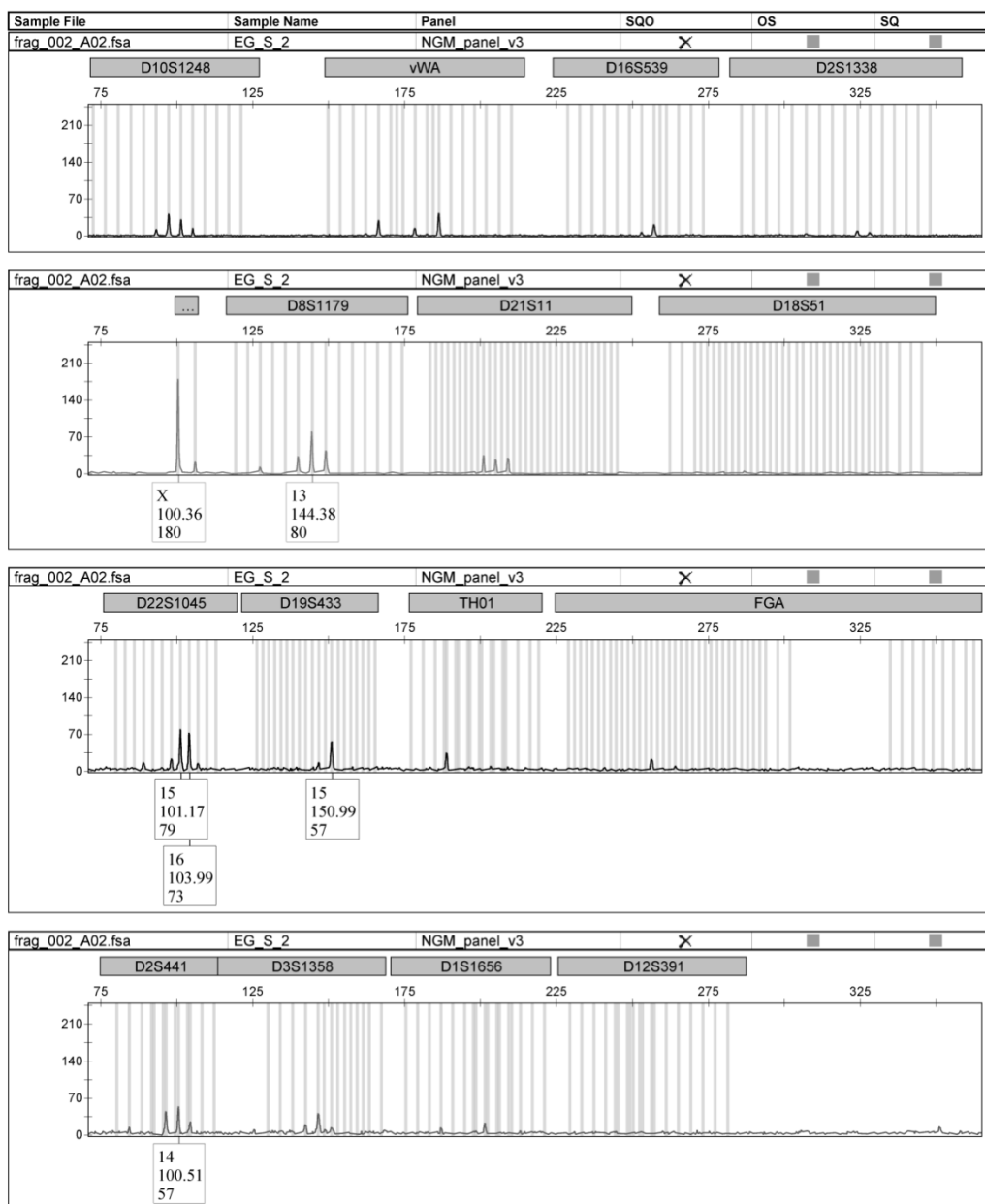


Figure D-8: Shed hair stained with EG (20X) amplified directly with NGM.

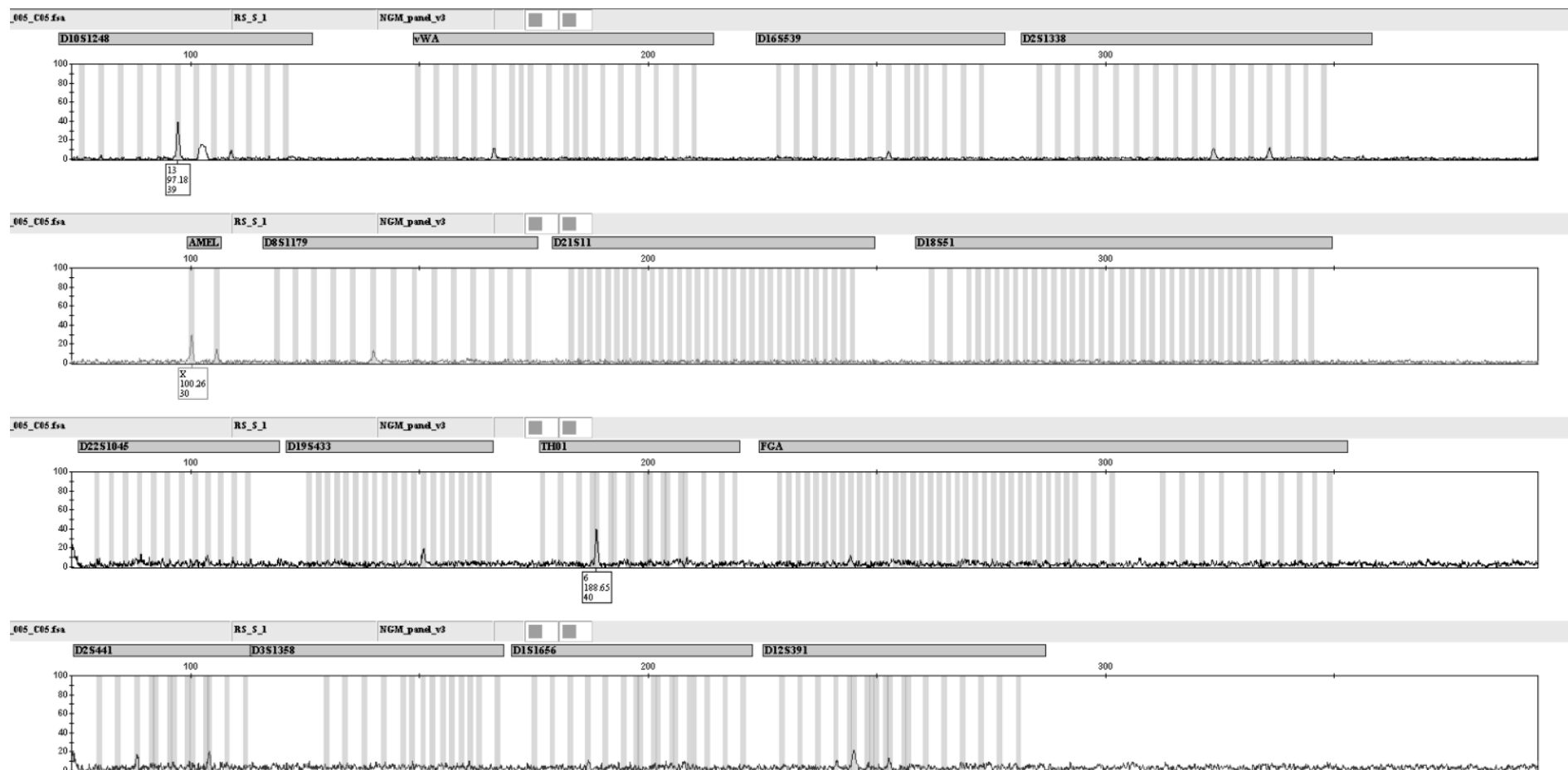


Figure D-9: Shed hair stained with RS (20X) amplified directly with NGM.

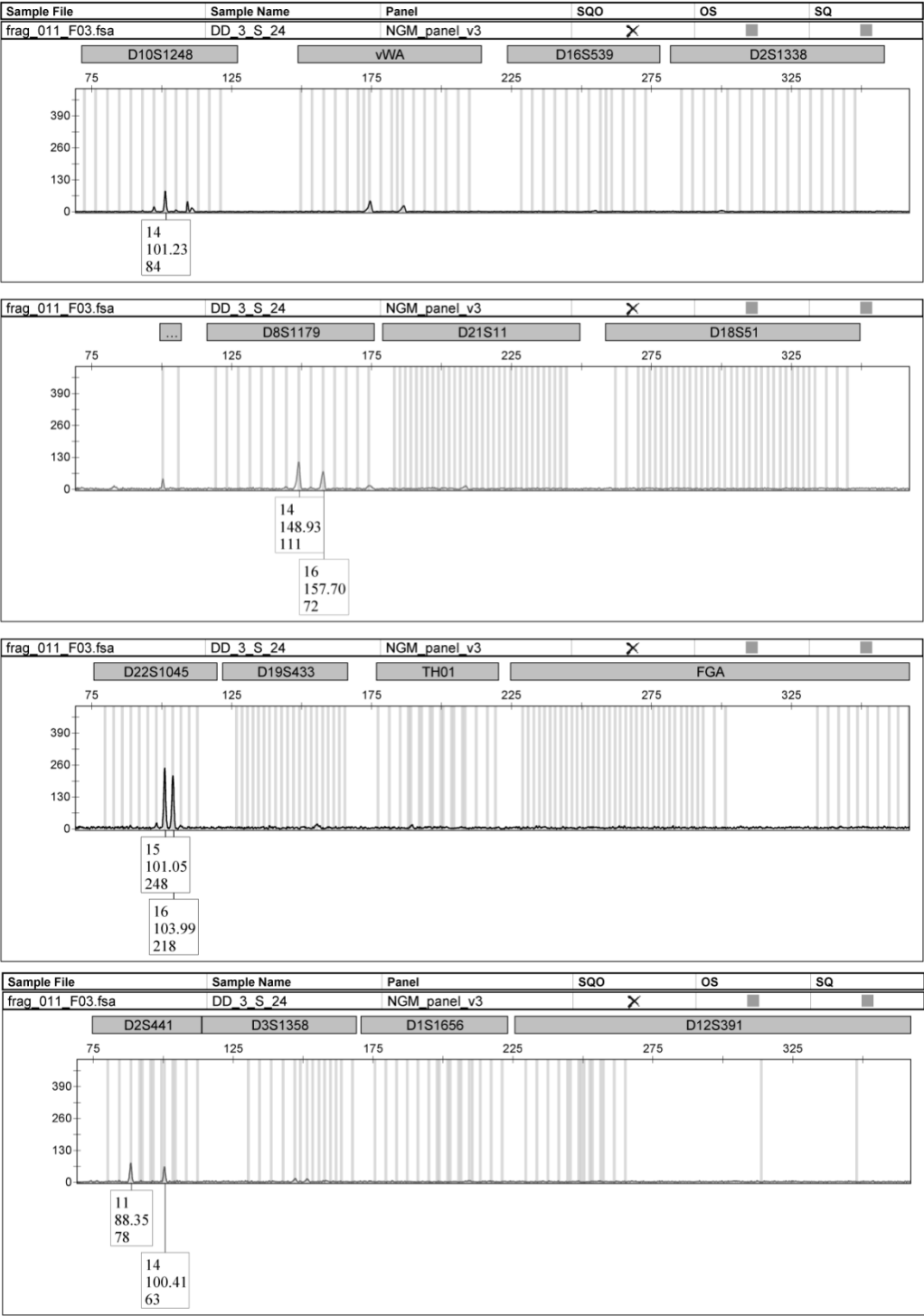


Figure D-10: Extracted shed hair stained with DD (20X) and amplified using NGM.

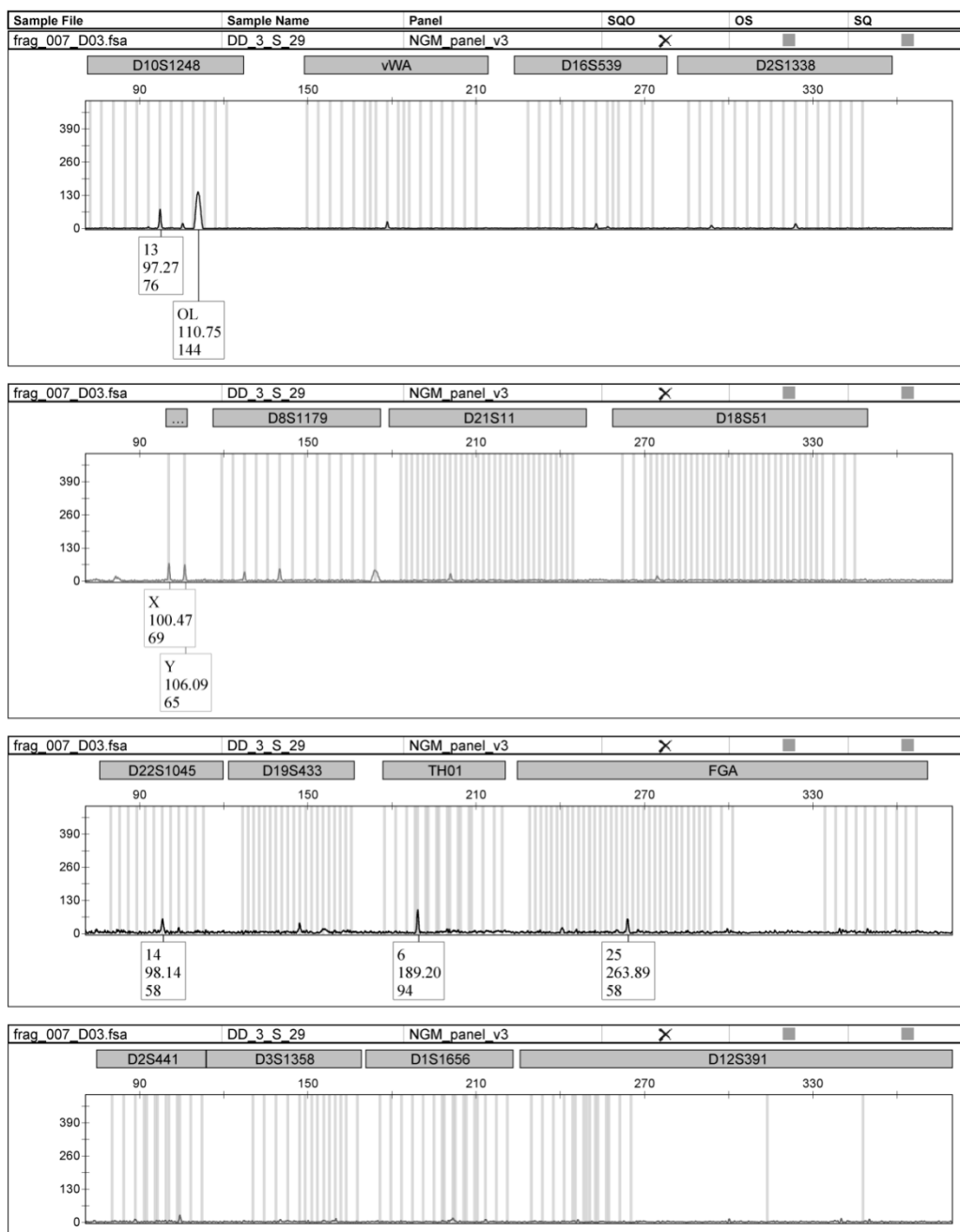


Figure D-11: Extracted shed hair stained with DD (20X) and amplified using NGM.

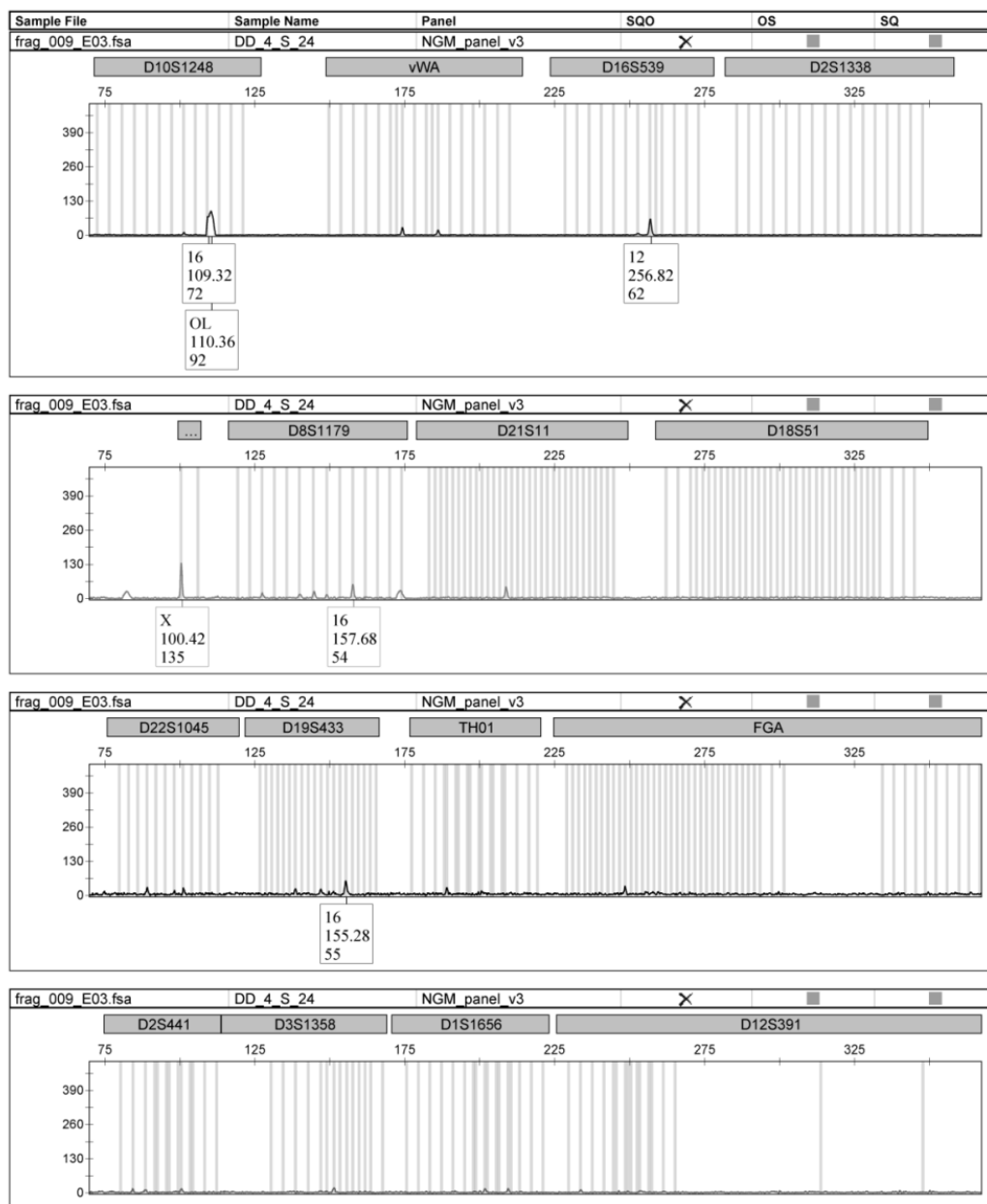


Figure D-12: Extracted shed hair stained with DD (20X) and amplified using NGM.

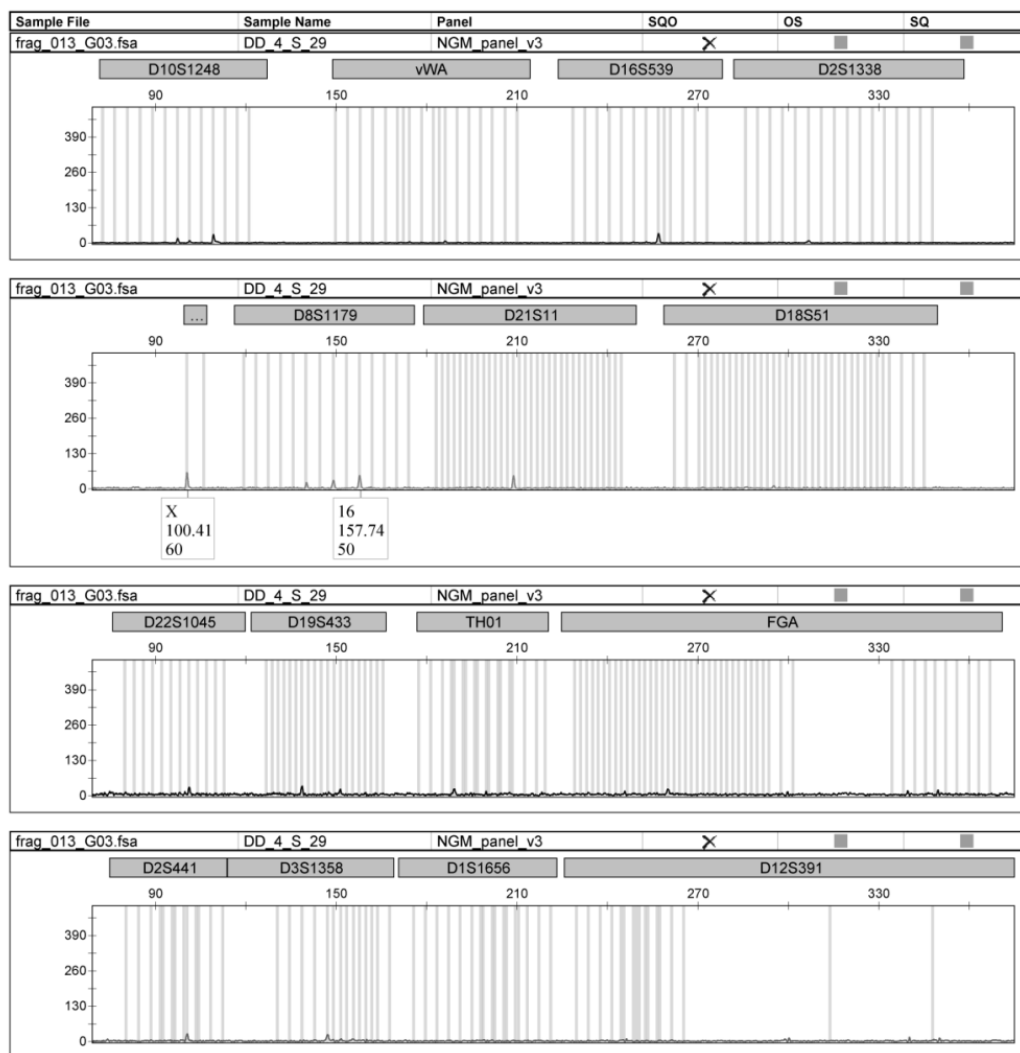


Figure D-13: Extracted shed hair stained with DD (20X) and amplified using NGM.

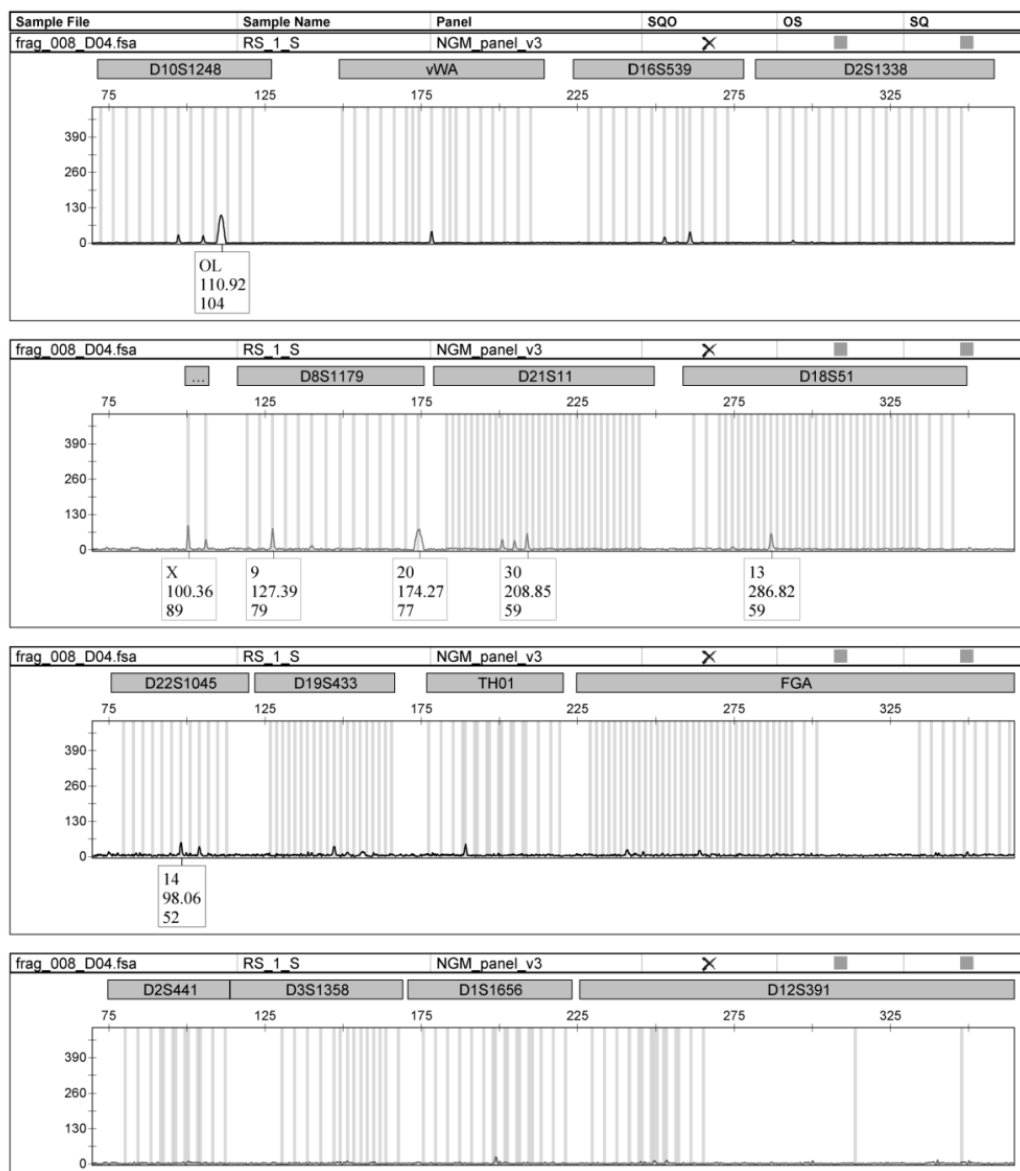


Figure D-14: Extracted shed hair stained with RS (20X) and amplified using NGM.

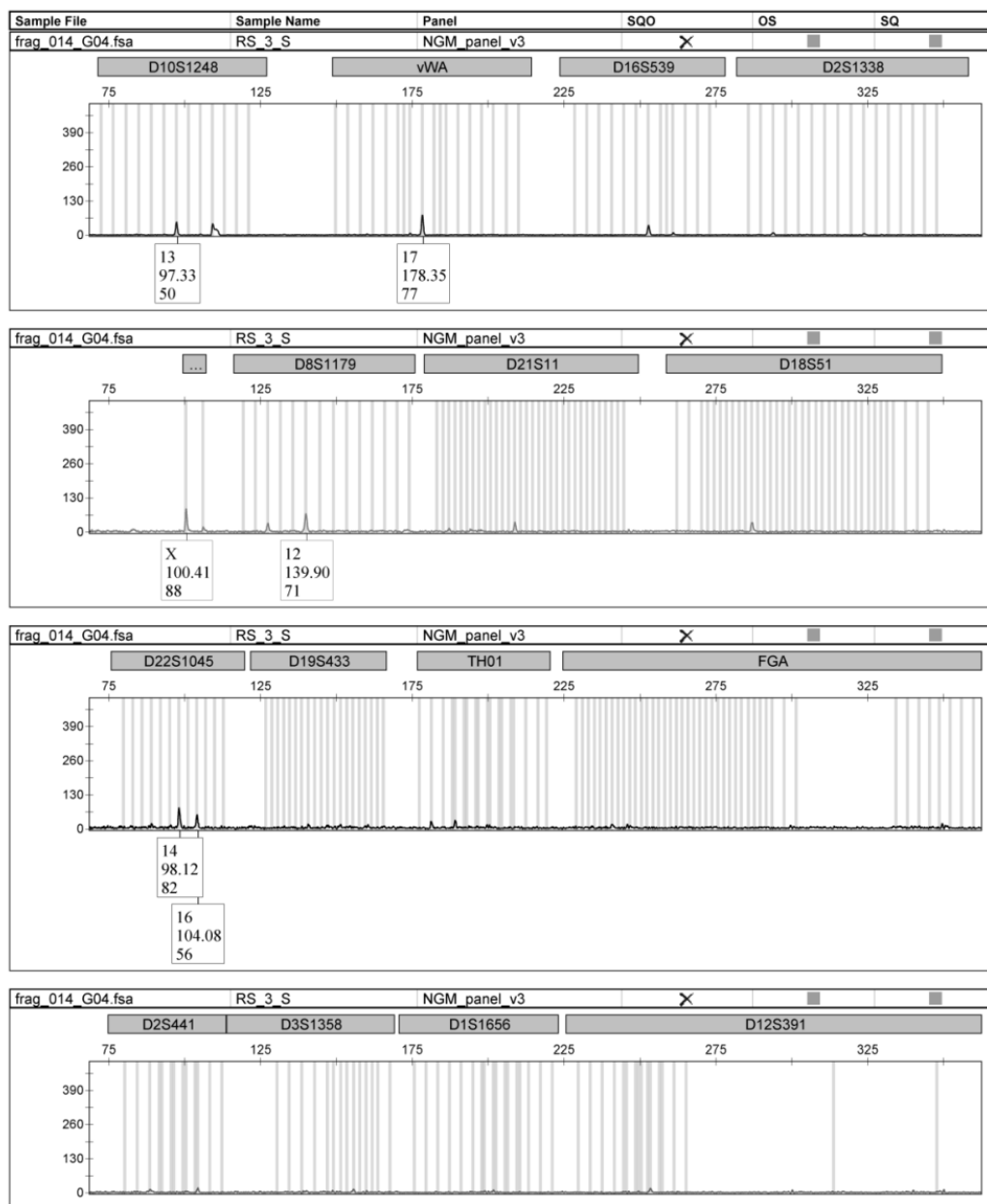


Figure D-15: Extracted shed hair stained with DD (20X) and amplified using NGM.

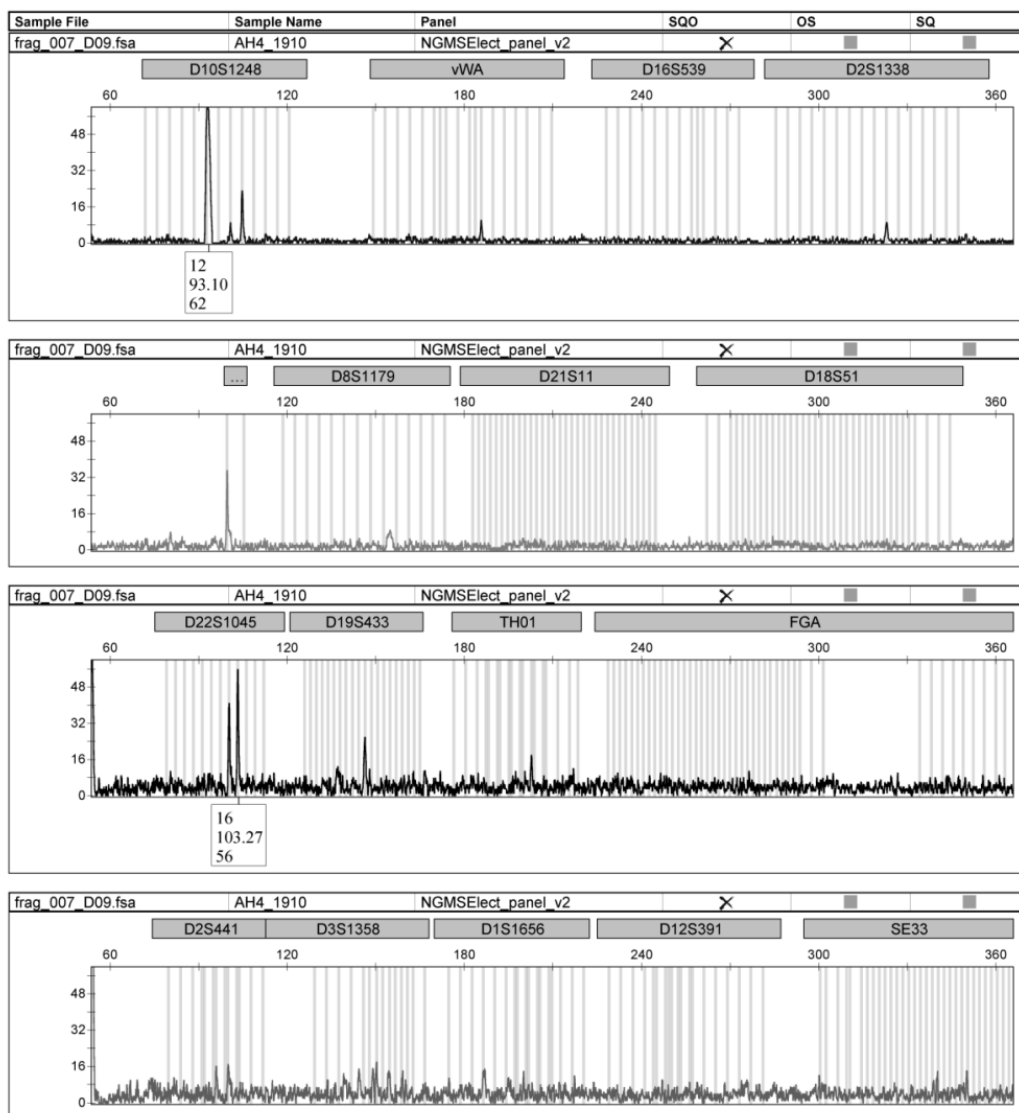


Figure D-16: Screened hair stained with DD (20X) and amplified directly using NGM.

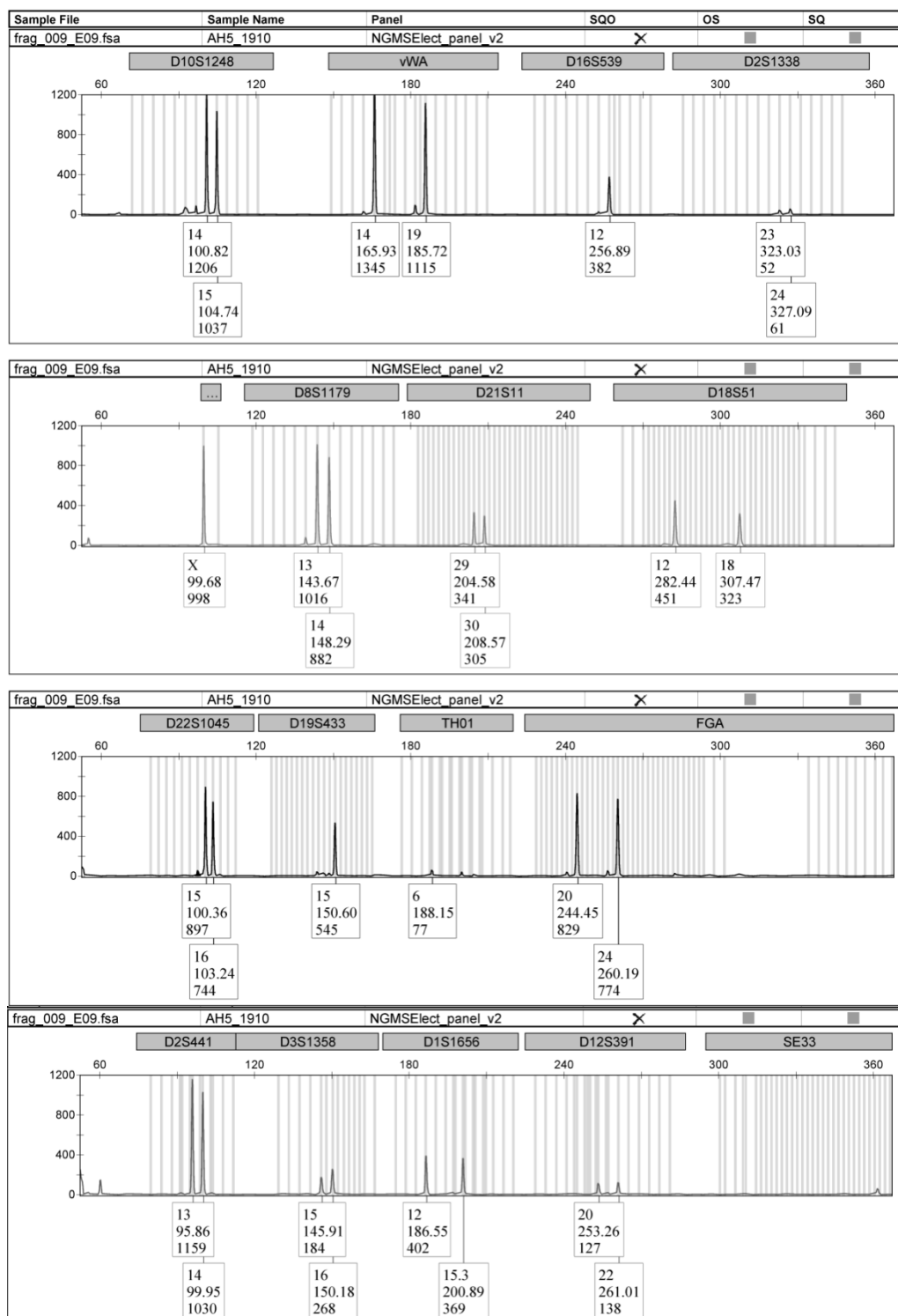


Figure D-17: Screened hair stained with DD (20X) and amplified directly using NGM.

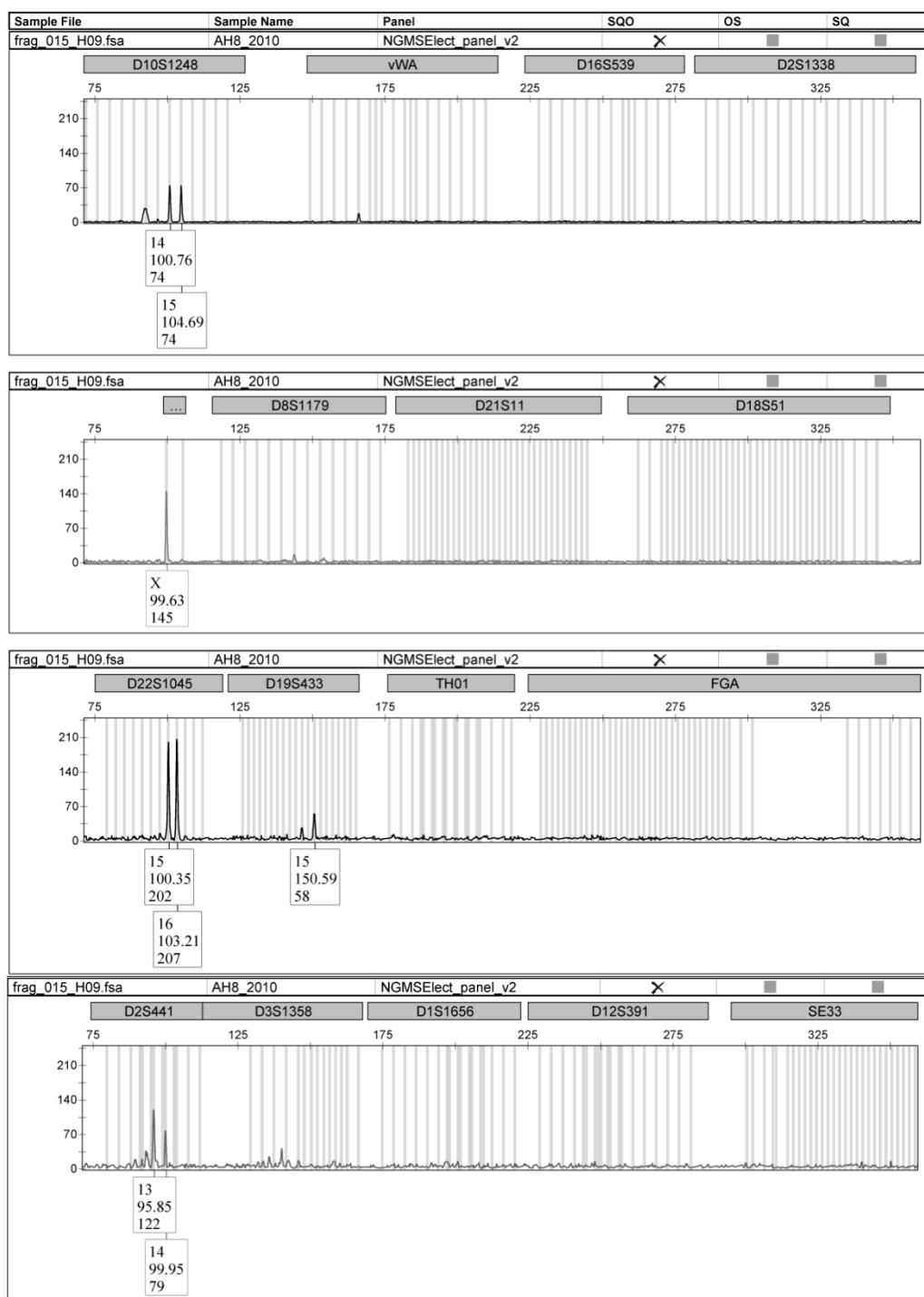


Figure D-18: Screened hair stained with DD (20X) and amplified directly using NGM.

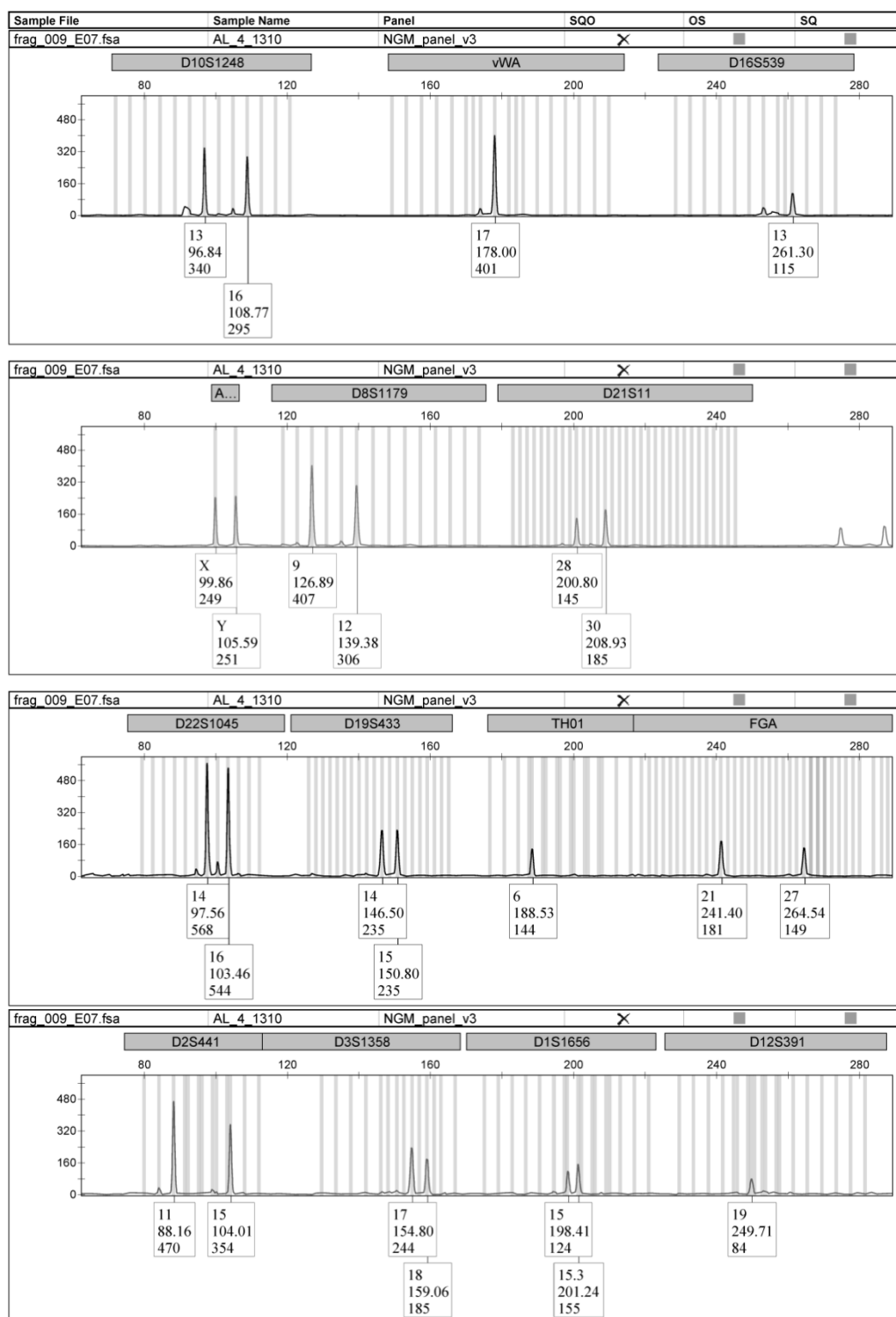


Figure D-19: Screened hair stained with DD (20X) and amplified directly using NGM.

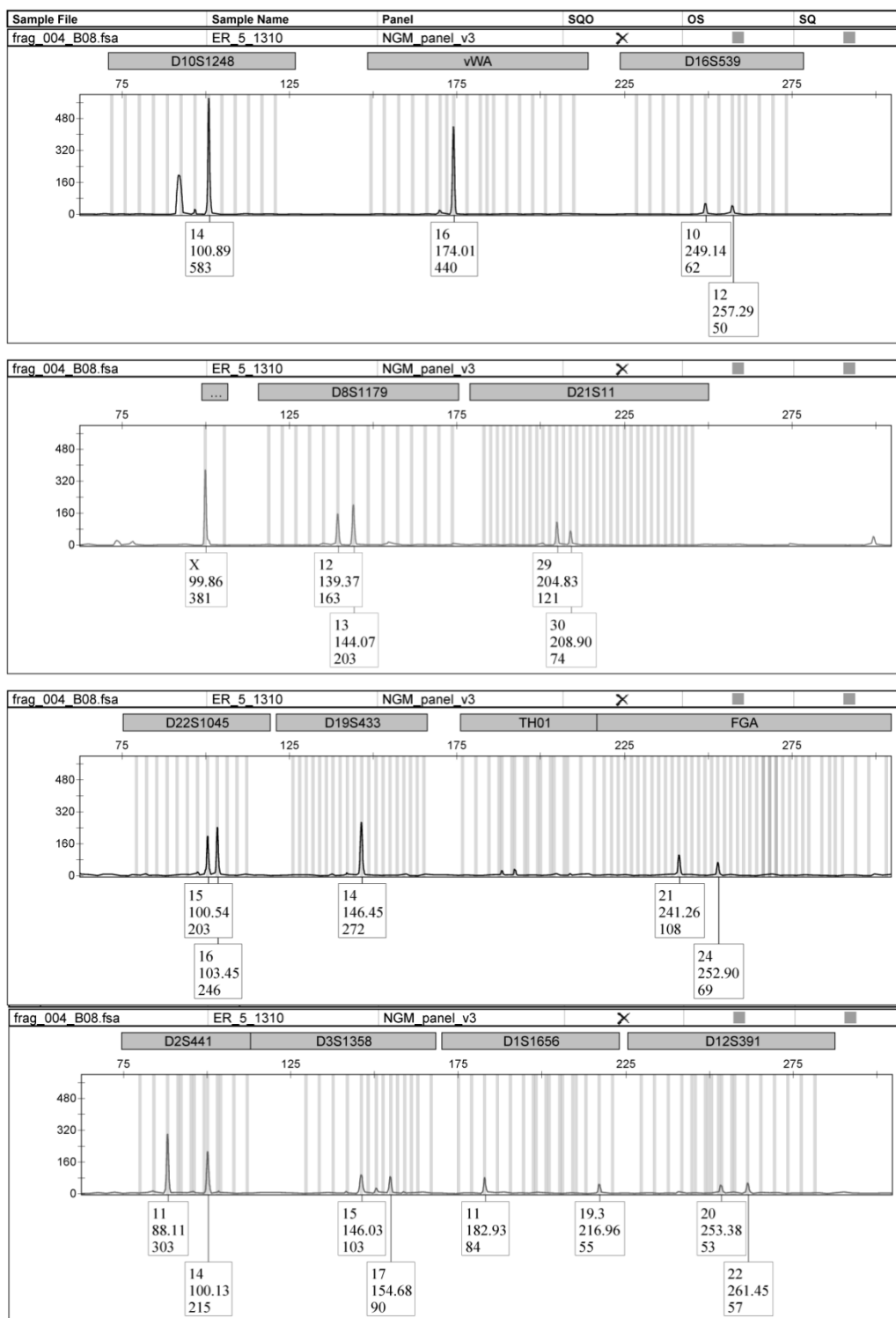


Figure D-20: Screened hair stained with DD (20X) and amplified directly using NGM.

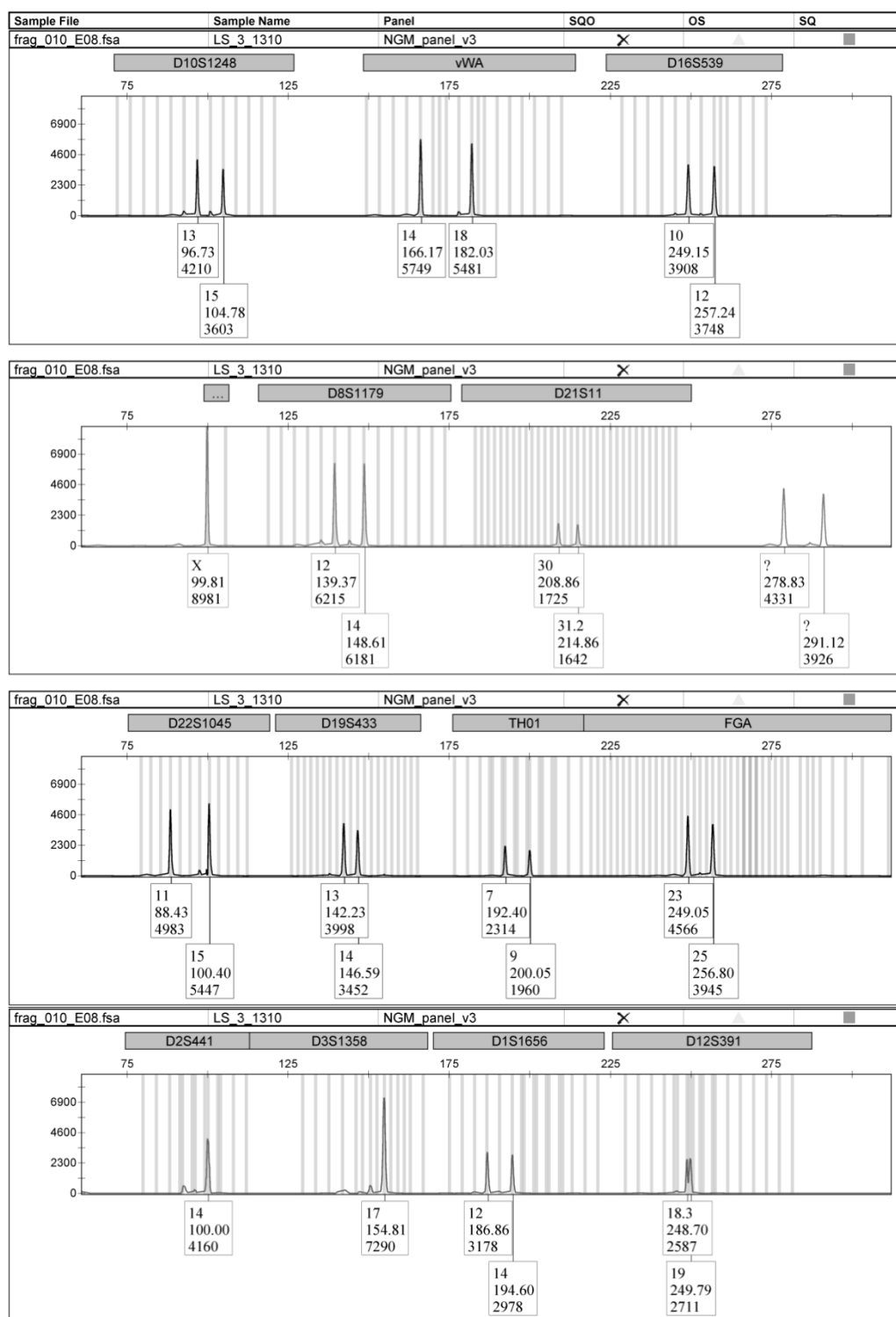


Figure D-21: Screened hair stained with DD (20X) and amplified directly using NGM.

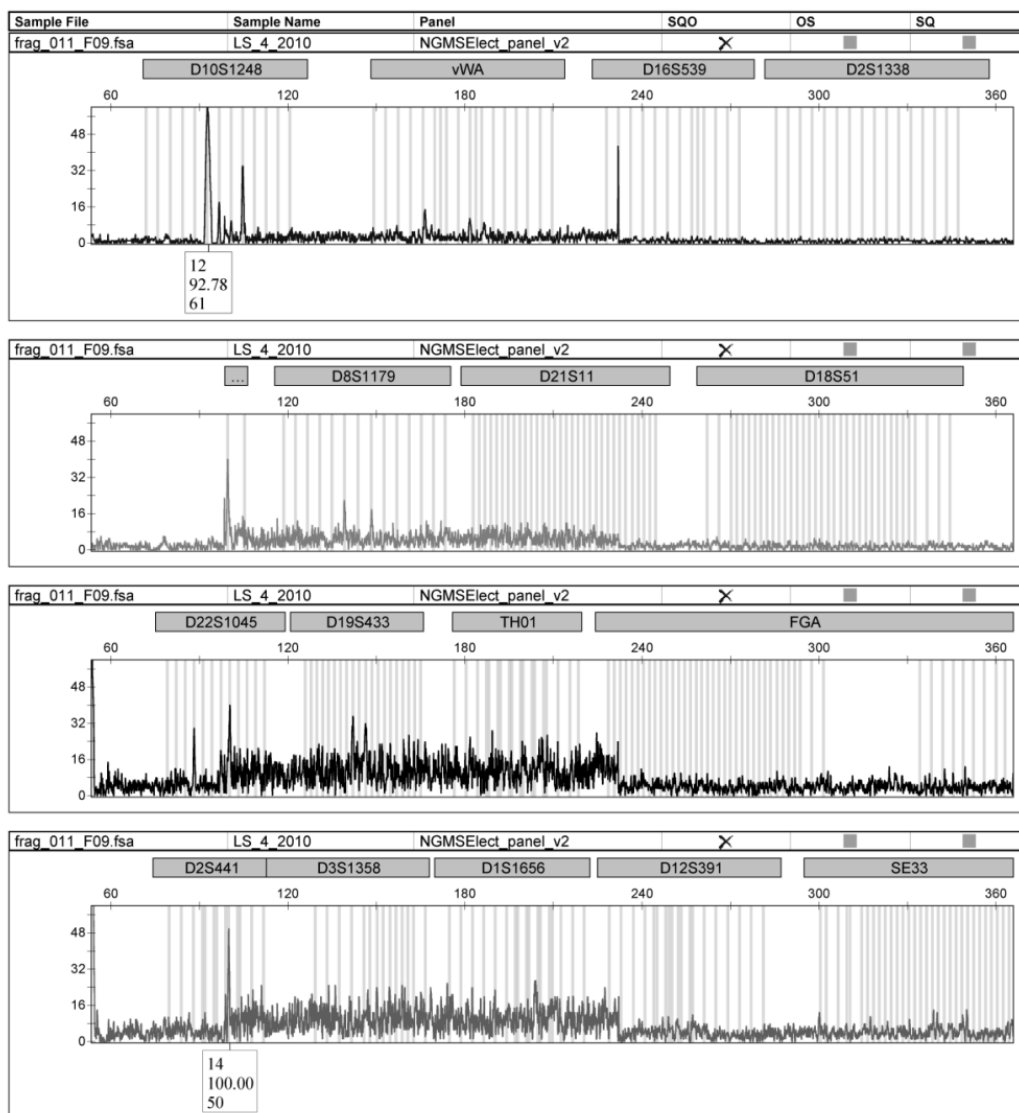


Figure D-22: Screened hair stained with DD (20X) and amplified directly using NGM.

Successful STR amplification from hair follicles after nuclear staining



Alicia M. Haines¹, Shanan S. Tobe¹, Hilton Kobus², Adrian Linacre¹

¹School of Biological Sciences, Flinders University, Adelaide, Australia

²School of Chemical and Physical Sciences, Flinders University, Adelaide, Australia



Presented at the 26th Congress of the ISFG (2015) Krakow, Poland

Funding was provided by the Attorney General's Department, South Australia

Introduction

Hairs present at crime scenes are quite common due to people shedding approximately 75-100 hairs per day [1]. The more common type of hair found at a crime scene are telogen hairs or resting hairs which are naturally shed. It has been estimated that 95% of hairs which are collected from a crime scene are identified as telogen hairs [2]. Hairs that are in the active growth stage are known as anagen hairs. These hairs can often contain skin material attached to the root of the hair as they can only be removed by a forceful action. Microscopy is the primary technique used for evaluating hairs however other studies have stated the usefulness of staining hairs with various dyes to visualize the hair nuclei. These dyes include haematoxylin which binds to chromatin present within DNA and histone complexes and stains the nuclei a dark violet [2, 3]. DAPI a minor groove binding dye has also been used to stain hairs to visualize the number of nuclei present to determine viability for STR profiling [4, 5]. DAPI is not a highly specific DNA binding dye as it has a fluorescent signal when in the presence of detergents and other compounds. This dye only has approximately a 20 fold increase in fluorescent signal when in the presence of DNA [6, 7]. This study looks at using more sensitive dyes to review their ability for staining hairs to visualize nuclei present within the root of the hairs. The dyes used in this study were SYBR[®] Green I (SG), Diamond[™] Nucleic acid dye, RedSafe[™], GelGreen[™] and EvaGreen[™].

Method

2.1 Nuclear staining

The binding dyes were diluted in a buffer solution down to 20X (1 in 500 dilution) and then an aliquot (1 μ L) was applied to the hair shafts (plucked) and viewed under a fluorescence microscope (Nikon Optiphot) using a B2A cube to filter the light.

2.2 STR amplification and analysis

The stained root fragment was placed into a 0.2 mL thin walled tube containing 10 μ L of PCR master mix from the NGM Select[™] kit (Life Technologies, Vic, AUS) along with 5 μ L of primer mix and 1 μ L of AmpliTaq Gold[®] DNA polymerase. A further 9 μ L of sterile water was added to make up a final volume of 25 μ L. The amplification was conducted using Bio-Rad thermal cycler (Bio-Rad) using the manufacturer's protocol. A standard cycle number of 29 were used throughout the study.

Capillary electrophoresis was performed on an ABI 3130XL Genetic Analyser (Life Technologies) using POP-4 polymer (Life Technologies). An aliquot of 2 μ L of the amplified samples was added to a solution containing 0.5 μ L of Liz600 LIZ Size Standard and 9.5 μ L of Hi-Di Formamide. Samples were denatured at 95 °C for 3 min. Electrophoresis was conducted at 3 kV with a 10 s injection. The data were analyzed using GeneMapper v3.2. The detection threshold was set at 50 RFU (see images below).

Results and Discussion

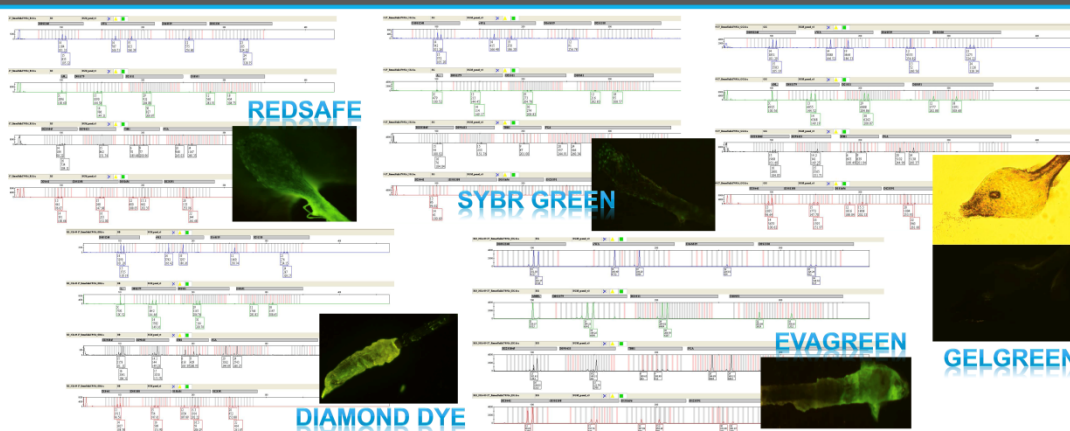


Table 1 shows the number of alleles amplified from the plucked hair samples that were stained prior to STR amplification. Full profiles were obtained for all stained hairs except for SG where there was allele drop out. The average peak height shows that there was inhibition using the SG dye as it was substantially lower when compared to the average peak heights from the other stained hairs. When stained with GG the nuclei could not be visualized due to the dye not being cell permeable. Even though a profile was obtained this dye is not suitable for nuclear staining. The other dyes should nuclei staining and therefore could be used as a presumptive test for determining the viability of the sample for DNA analysis.

Table 1- NGM Select[™] profile percentage of plucked hairs stained with DNA binding dyes and the average peak height (RFU) of profile

	RedSafe [™]	Diamond [™] Dye	GelGreen [™]	EvaGreen [™]	SYBR [®] Green
Number of alleles	30	30	30	30	21
Profile %	100	100	100	100	70
Average Peak Height (RFU)	608.8	2256	3486	2963	232.7

NGM Select[™] contains 15 STR loci plus amelogenin, the number of alleles shown was not including amelogenin

Concluding Remarks

Full DNA profiles were obtained after nuclear staining with RS, DD, GG and EG. There was allele drop out when staining with SG resulting in only a 70% profile. This would likely be due to the inhibiting nature of SG in the amplification step. This study has shown the ability to stain hair follicles with DNA binding dyes with successful direct amplification of STR loci and the ability for these dyes to be used as a screening methodology prior to STR analysis.

Correspondence: Alicia M. Haines, Flinders University, South Australia, Ph. (08) 8201 5003, alicia.haines@flinders.edu.au

References

- [1] L. Bourguignon, B. Hoste, T. Boonen, K. Vits, F. Hubrecht, A fluorescent microscopy-screening test for efficient STR-typing of telogen hair roots, *Forensic Sci Int Genet* 3 (2008) 27-31.
- [2] J. Edson, E.M. Brooks, C. McLaren, J. Robertson, D. McNevin, A. Cooper, J.J. Austin, A quantitative assessment of a reliable screening technique for the STR analysis of telogen hair roots, *Forensic Sci Int Genet* 7 (2013) 180-8.
- [3] A.H. Fischer, K.A. Jacobson, J. Rose, R. Zeller, Haematoxylin and eosin staining of tissue and cell sections, *CSH Protoc* 3 (2008) 1-2.
- [4] T. Lopez, M. Vandewoestyne, D. Van Hooftstat, D. Deforce, Fast nuclear staining of head hair roots as a screening method for successful STR analysis in forensics, *Forensic Sci Int Genet* 13 (2014) 191-4.
- [5] E.M. Brooks, M. Cullen, T. Sztayna, S.J. Walsh, Nuclear staining of telogen hair roots contributes to successful forensic rDNA analysis, *Aust J Forensic Sci* 42 (2010) 115-22.
- [6] M.L. Barcellona, G. Cardelli, E. Gratton, Time-resolved fluorescence of DAPI in solution and bound to polydeoxynucleotides, *Biochem. Biophys. Res. Commun.* 170 (1990) 270-280.
- [7] D. Banerjee, S.K. Pal, Dynamics in the DNA Recognition by DAPI: Exploration of the Various Binding Modes, *J. Phys. Chem. B* 112 (2008) 1016-1021.

Figure D-23: Poster presented at the 26th congress of the ISFG in Krakow, Poland, 2015.

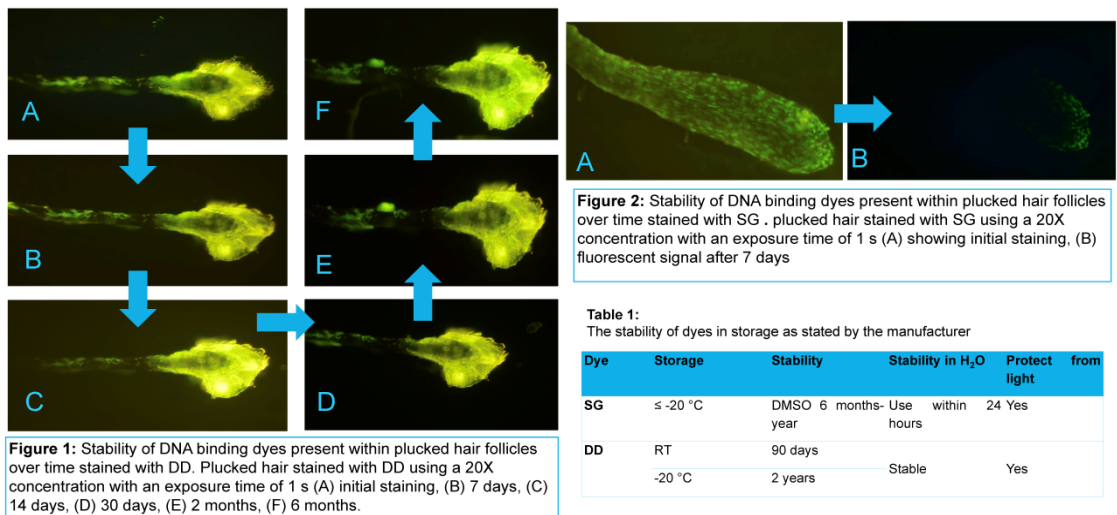
Introduction

Nucleic acid binding dyes are used in gel electrophoresis, flow cytometry, real-time PCR and in DNA quantification. Conventional DNA binding dyes include: ethidium bromide which intercalates between the base pairs of DNA [1]; DAPI is a minor groove binding dye that is selective for AT rich regions [2]; and acridine orange binds to both DNA and RNA [3, 4]. SYBR® Green I and PicoGreen are dyes that have an order of magnitude higher sensitivity and fluorescent enhancements [3]. These two dyes can also be used to determine the amount of DNA that is present as a screening methodology of samples in forensic science [5]. DAPI has been used to screen and select hairs based on the number of nuclei present to result in STR profiles [5, 6]. Such a presumptive test is a quick and cheap way to determine whether or not the hair may produce an STR profile. This study shows 1) the stability of both Diamond™ nucleic acid stain (DD) and SYBR® Green I (SG) when bound to DNA present within plucked hair follicles; 2) determining how the dyes interact with DNA within a hair follicle over time; and 3) the storage conditions and stability of dyes such that they can still view the fluorescent signal without the need to re-stain the hair follicle.

Method

Plucked hairs were stained with SG and DD using a dye solution of 20X (1 in 500 dilution of the stock concentration) to stain the hair root and shaft (1 µL). The stained hairs were then viewed under a Nikon Optiphot fluorescent microscope using a B2A filter cube. Images were taken with an exposure time of 1 s. This process from then was undertaken at varying time intervals to view the fluorescent signal.

Results



Discussion

Figure 1 show the fluorescent signal produced when plucked hair follicles were stained with DD. Figure 2 shows the staining with SG. The DD signal did not decrease over time whereas the signal when using SG did substantially reduce after several days (in accordance with the information supplied by the manufacturer that SG is unstable in water and is only stable for 24 hours). The signal present after 7 days was reduced due to the level of instability of SG. In comparison DD, as claimed by the manufacturer to be stable for around 90 days when diluted with water, the signal did not alter over a duration of 6 months (as shown in Figure 1).

Concluding Remarks

References

The two dyes tested stained individual nuclei present within the hair follicle as expected. The duration of signal when using DD was much greater, lasting for 6 months, compared to SG where the signal only lasted for a few days and then substantially reduced after 7 days.

Correspondence: Alicia M. Haines, Flinders University, South Australia, Ph. (08) 8201 5003, alicia.haines@flinders.edu.au

[1] C. Aaij, P. Borst, The gel electrophoresis of DNA, *Bioch et Biophys Acta (BBA) - Nucleic Acids and Protein Synthesis*, 269 (1972) 192-200.

[2] D. Banerjee, S.K. Pal, Dynamics in the DNA Recognition by DAPI: Exploration of the Various Binding Modes, *J Phys Chem B*, 112 (2008) 1016-1021.

[3] A.I. Dragan, et al., SYBR Green I: Fluorescence Properties and Interaction with DNA, *Journal of Fluorescence* 22 (2012) 1189-1199.

[4] M.B. Lyles, I.L. Cameron, Interactions of the DNA intercalator acridine orange, with itself, with caffeine, and with double stranded DNA, *Biophysical Chemistry*, 96 (2002) 53-76.

[5] L. Bourguignon, B. Hoste, T. Boonen, K. Vits, F. Hubrecht, A fluorescent microscopy-screening test for efficient STR-typing of telogen hair roots, *Forensic Sci Int Genet*, 3 (2008) 27-31.

[6] T. Lepez, M. Vandewoestyne, D. Van Hoofstat, D. Deforce, Fast nuclear staining of head hair roots as a screening method for successful STR analysis in forensics, *Forensic Sci Int Genet* 13 (2014) 191-4.

Figure D-24: Poster presented at the 26th congress of the ISFG in Krakow, Poland, 2015.

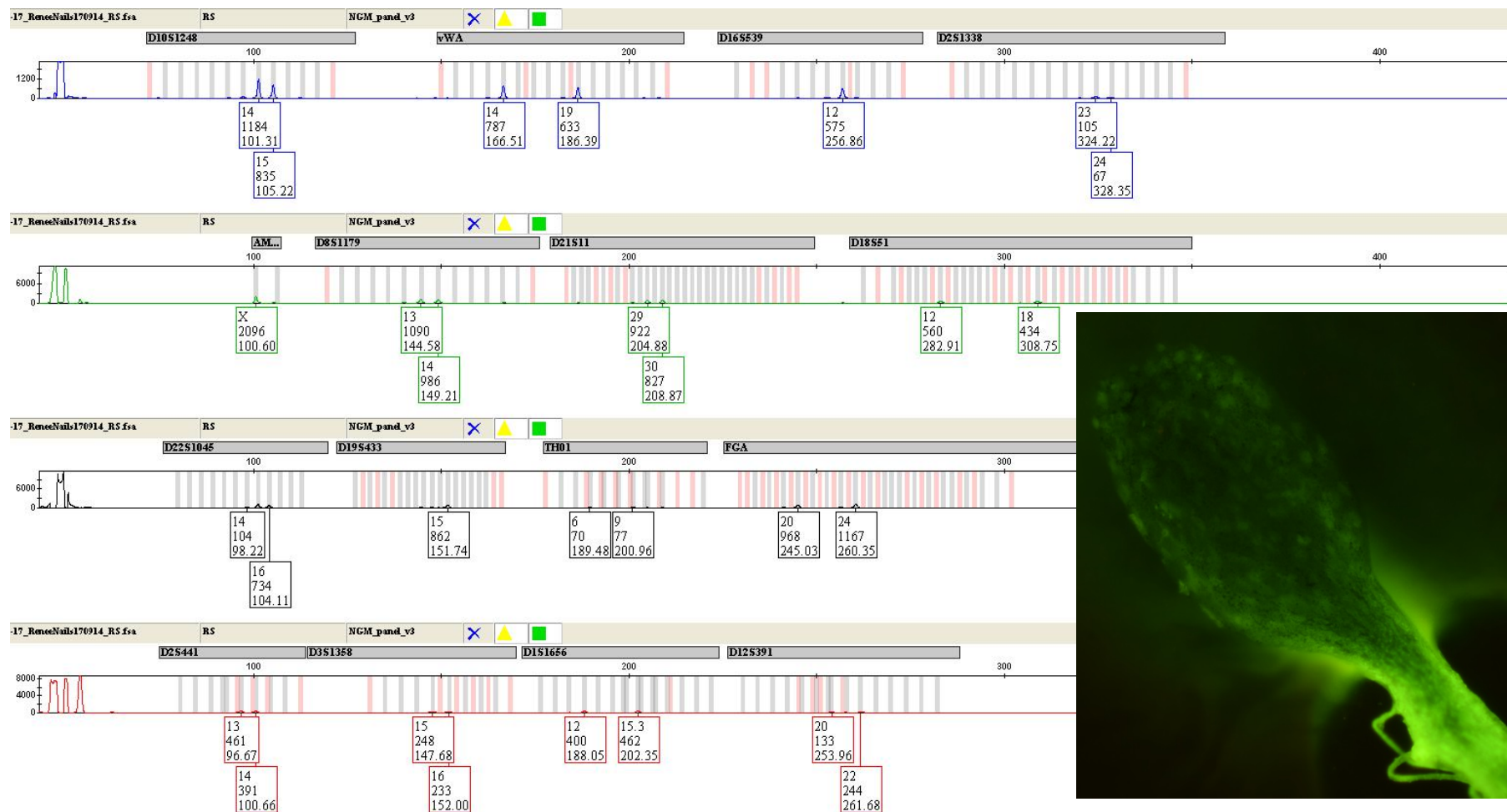


Figure D-25: Images on poster (Figure D-23), profile of stained hair follicle with RS (20X) amplified using NGM.

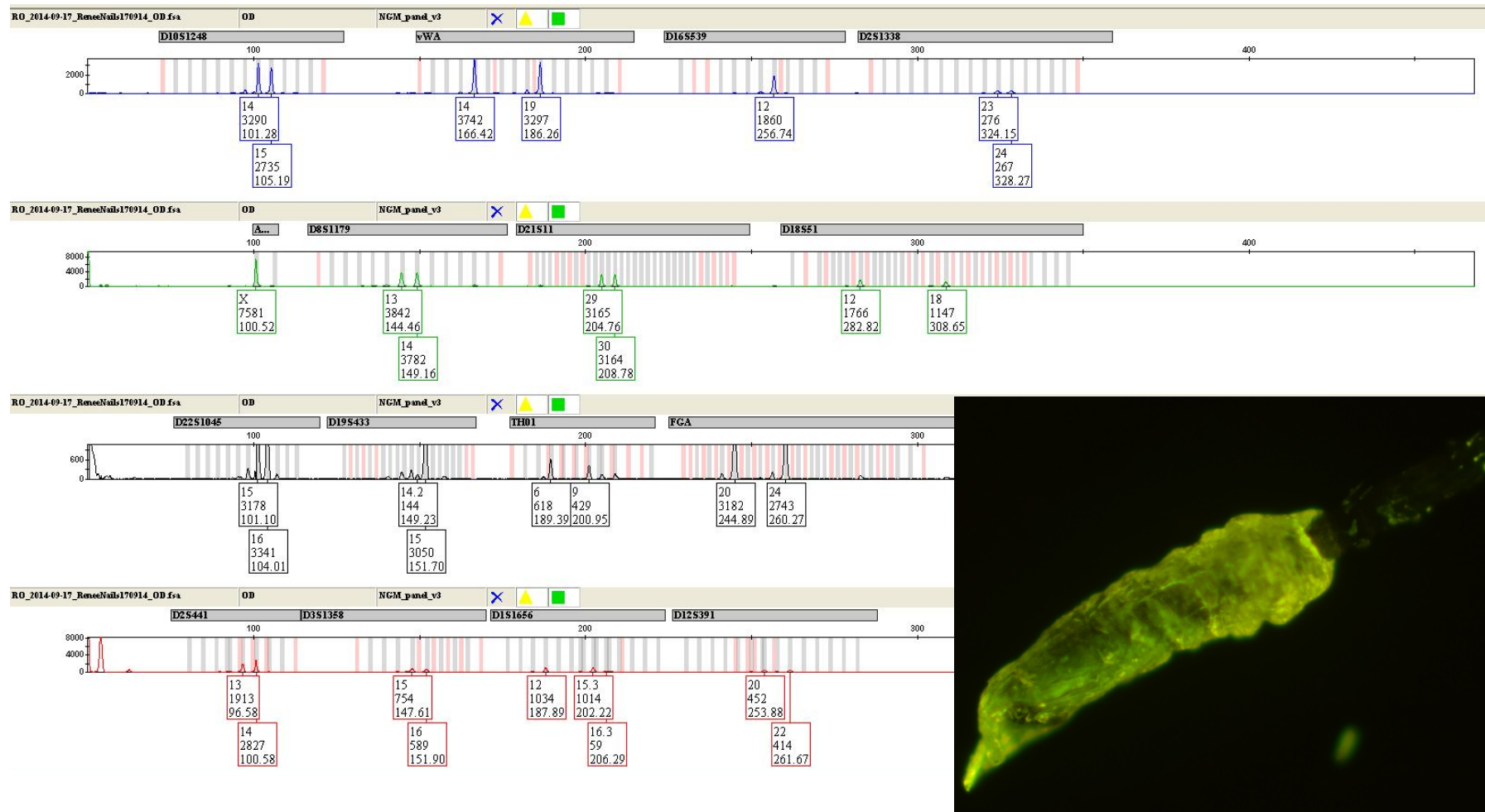


Figure D-26: Images on poster (Figure D-23), profile of stained hair follicle with DD (20X) amplified using NGM.

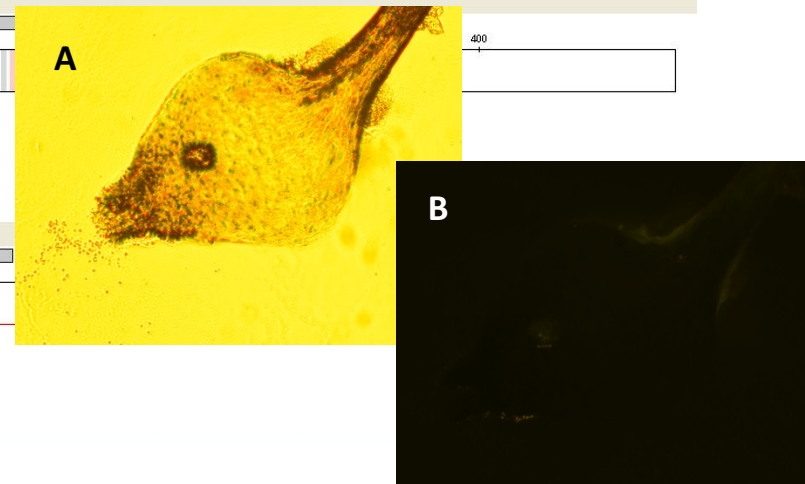
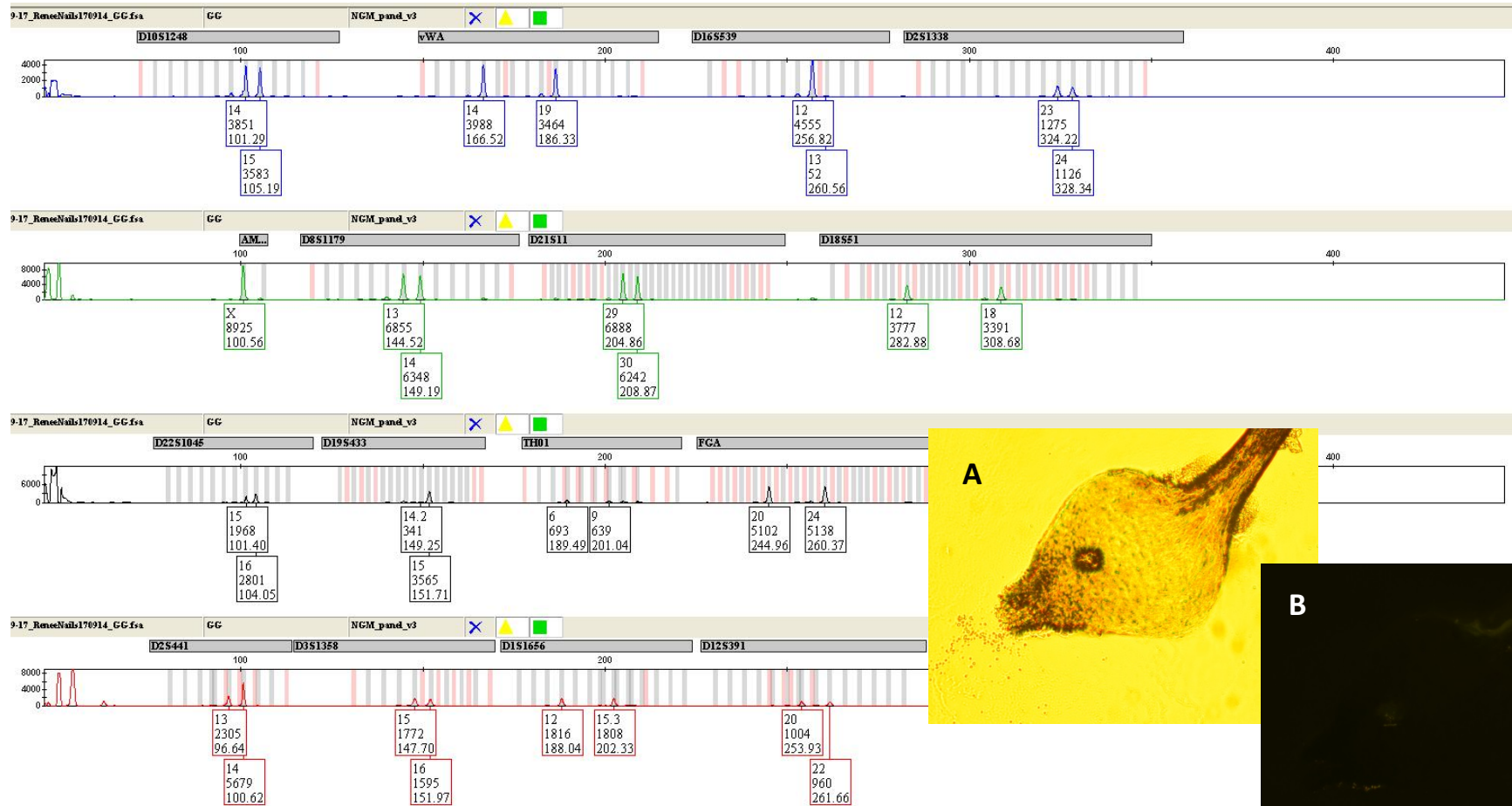


Figure D-27: Images on poster (Figure D-23), profile of stained hair follicle with GG (20X) amplified using NGM, (A) showing hair before staining under white light, (B) showing hair after staining and under blue transillumination, as the dye is impermeable to the cell membrane nuclei are not stained.

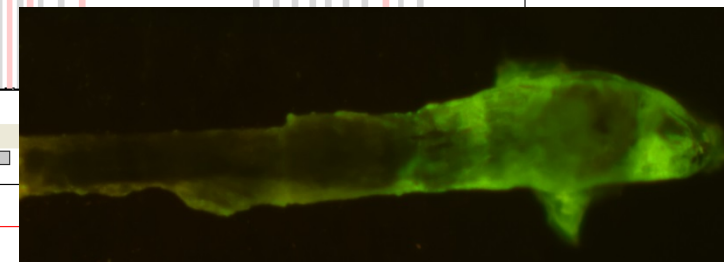
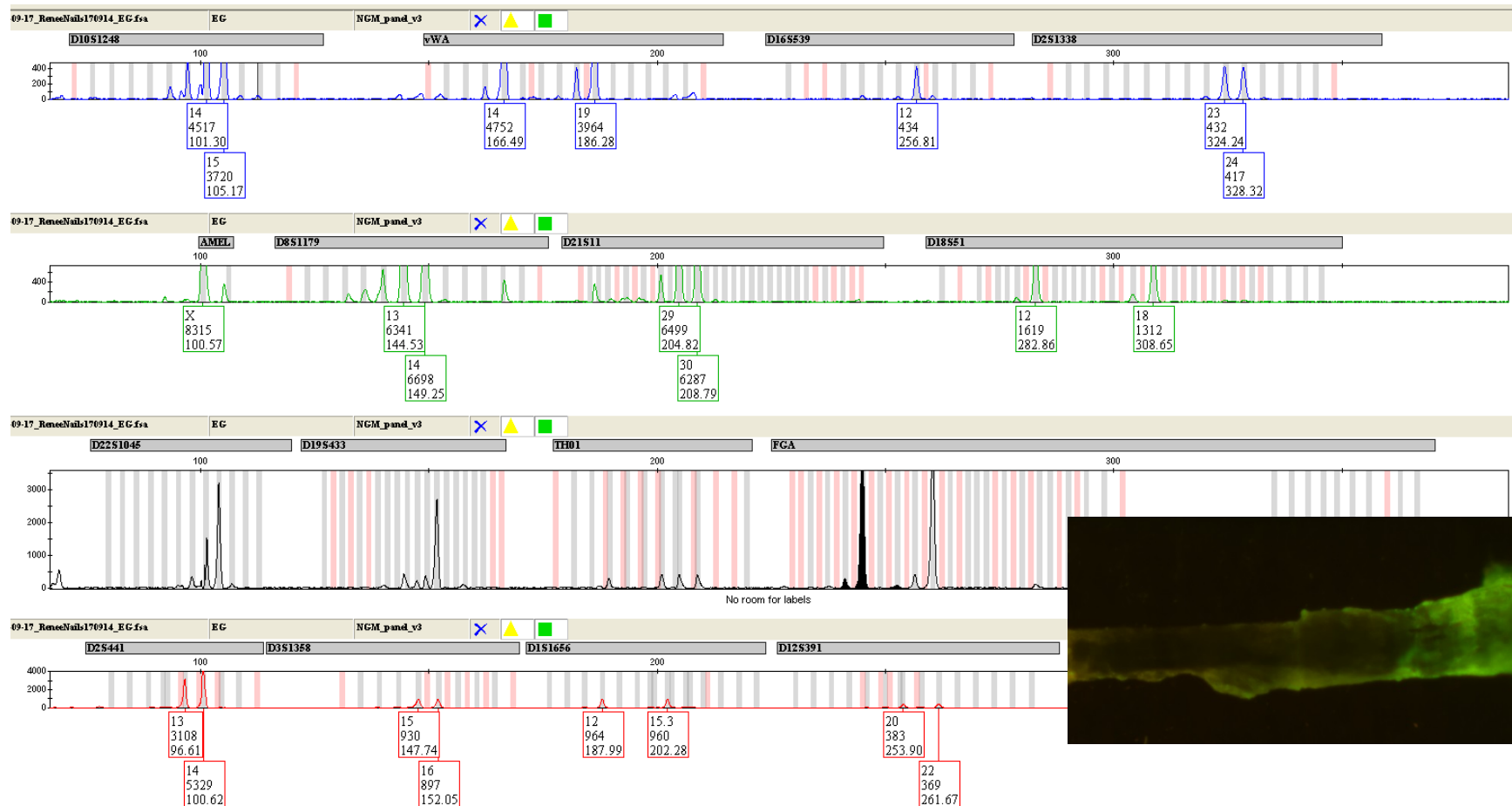


Figure D-28: Images on poster (Figure D-23), profile of stained hair follicle with EG (20X) amplified using NGM.

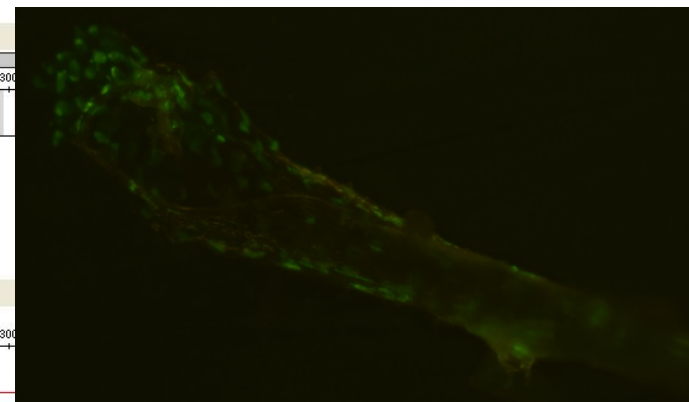
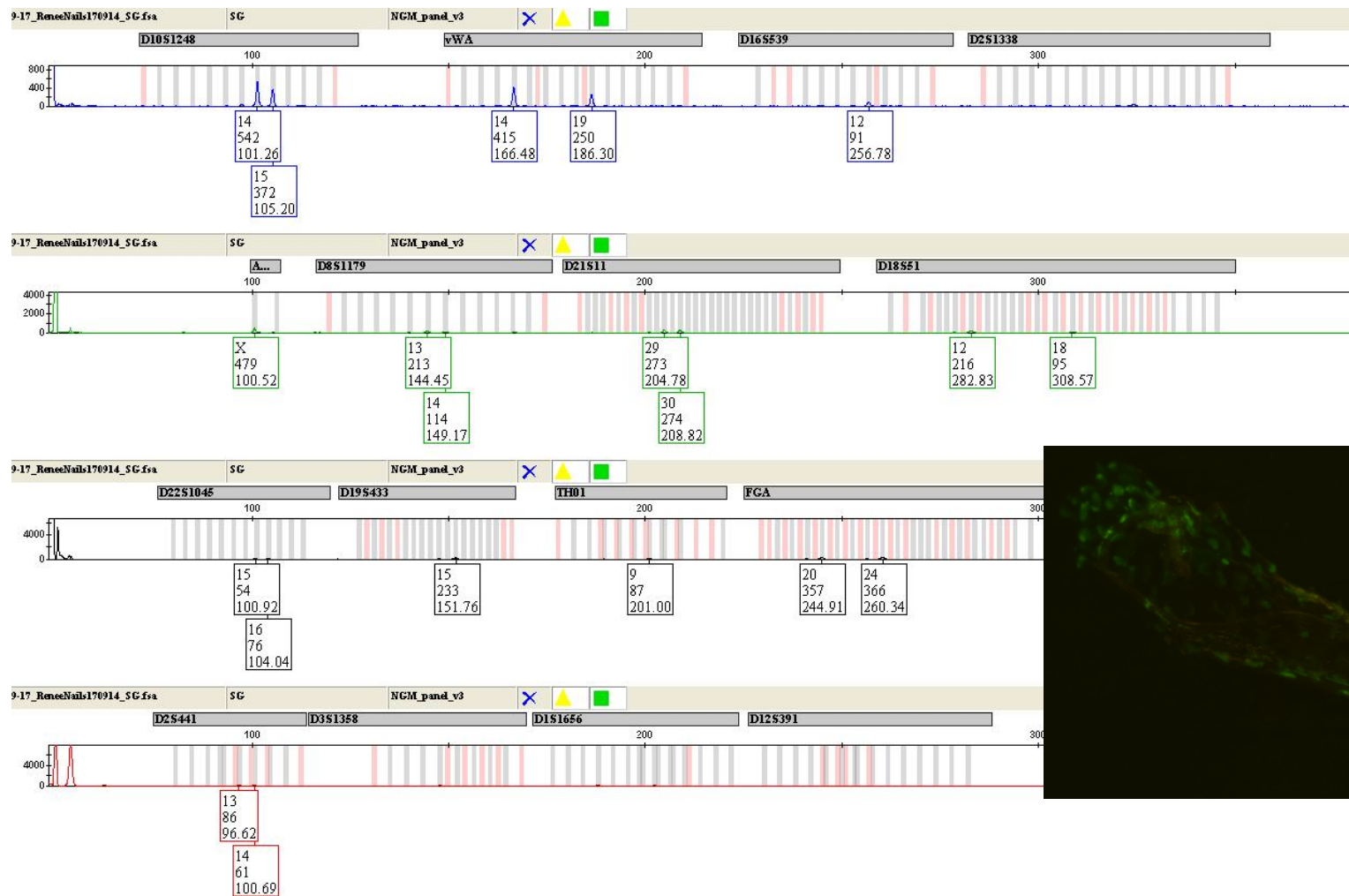


Figure D-29: Images on poster (Figure D-23), profile of stained hair follicle with SG (20X) amplified using NGM.



Flinders University
Government of South Australia
Forensic Science SA

DNA BINDING DYES FOR NUCLEAR STAINING OF HAIR FOLLICLES

Alicia M. Haines¹, Shanan S. Tobe^{1,3}, Hilton Kobus², Adrian Linacre¹

¹School of Biological Sciences, Flinders University, Adelaide, Australia
²School of Chemical and Physical Sciences, Flinders University, Adelaide, Australia
³Department of Chemistry and Physics, Arcadia University, Glenside, PA, USA

Presented at the ANZFSS 23rd International Symposium on the Forensic Sciences, Auckland, New Zealand

Funding was provided by the Attorney General's Department, South Australia



Forensic Biology Lab South Australia

Introduction

Hairs present at crime scenes are commonly encountered due to people shedding approximately 75-100 hairs per day [1]. Hairs in the telogen growth phase are the more common type of hair found as these are shed naturally with estimates of 95% of hairs collected from a crime scene are identified as telogen hairs [2]. Hairs in the active growth stage, anagen hairs, often have skin attached to the root due to a forceful action of removal.

Various dyes can be used to stain nuclei present, see Table 1. These dyes include haematoxylin, which binds to chromatin present within DNA and histone complexes, and stains the nuclei a dark violet [2, 3]. DAPI is a minor groove binding dye that has been used to stain hairs and determine viability for STR profiling [4, 5]. DAPI is not a highly specific DNA binding dye as it has a fluorescent signal when in the presence of detergents and other compounds and only a 20-fold increase in fluorescent signal when in the presence of DNA [6, 7] see Figure 1. SYBR Green (SG) has a higher enhancement (Fig. 1) but can partially inhibit the PCR so other dyes with similar properties to SG, were investigated. The dyes used in this study were Diamond™ Nucleic acid dye (DD), RedSafe™ (RS) and EvaGreen™ (EG).

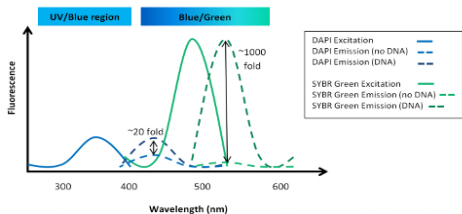


Figure 1: Schematic diagram of fluorescence spectra of DAPI compared with SG which has similar properties with EG, RS and DD, however these dyes are less inhibitory of PCR. Showing the UV/blue region and blue/green region and the comparison of the fluorescent enhancement when in the presence of DNA.

Table 1: Currently used staining methods for hair follicles

Staining method	Excitation (nm)	Emission (nm)	Cell permeable	Main Function	
Fluorescent dyes	DAPI [1, 2, 3]	358	461	Cell impermeant at low concentrations	Nuclear and chromosome counterstain
	TOTO-3 [4]	640	660	Cell impermeant	Nuclear counterstain
	Hoechst 33258 [5]	352	461	Cell permeant	Counterstain, apoptosis
Visible dyes	Haematoxylin [6, 7]				Histological staining

Method

2.1 Nuclear staining

The binding dyes were diluted in a buffer solution down to 20X (1 in 500 dilution) and then an aliquot (1 μ L) was applied to the hair shafts (plucked) and viewed under a fluorescence microscope (Nikon Optiphot) using a B2A cube to filter the light.

2.2 STR amplification and analysis

The stained root fragment was placed into a 0.2 mL thin walled tube containing 10 μ L of PCR master mix from the NGM SELECT™ kit (Life Technologies, Vic, AUS) along with 5 μ L of primer mix and 1 μ L of AmpliTaq Gold® DNA polymerase. A further 9 μ L of sterile water was added to make up a final volume of 25 μ L. The amplification was conducted using Bio-Rad thermal cycler (Bio-Rad) using the manufacturer's protocol. A standard cycle number of 29 were used throughout the study.

Capillary electrophoresis was performed on an ABI 3130XL Genetic Analyser (Life Technologies) using POP-4 polymer (Life Technologies). An aliquot of 2 μ L of the amplified samples was added to a solution containing 0.5 μ L of Liz600 LIZ Size Standard and 9.5 μ L of Hi-Di Formamide. Samples were denatured at 95 °C for 3 min. Electrophoresis was conducted at 3 kV with a 10 s injection. The data were analyzed using GeneMapper v3.2. The detection threshold was set at 50 RFU (see images below).

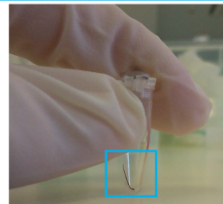


Figure 2: Stained hair for direct amplification.

Results and Discussion




Figure 3: Hair follicles (A) before staining and (B) after staining with DNA binding dyes, 1 μ L at 20X concentration.

- EG had a high background signal, see Fig. 4
- DD had a low background signal and showed better staining of the hair follicles.
- RS staining did not appear to be as sensitive as EG and DD.

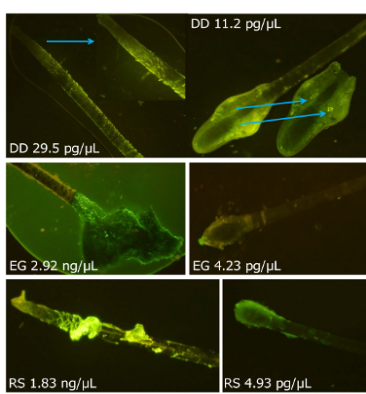


Figure 4: Comparison of hairs with their corresponding DNA concentration for RS, DD and EG.

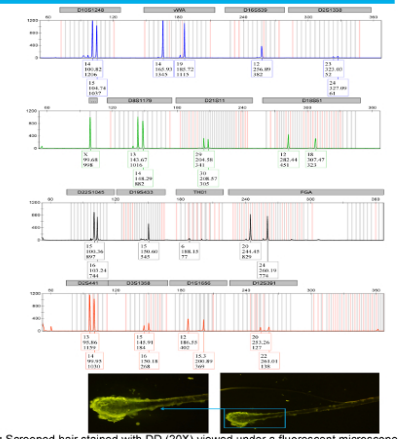


Figure 5: Screened hair stained with DD (20X) viewed under a fluorescent microscope at 40X magnification with an exposure time of 1 s. NGM™ Profile of directly amplified hair.

Concluding Remarks

The DNA binding dyes DD, RS and EG were evaluated for their use with nuclear staining of hairs.

- EG, RS and DD all showed staining of nuclei within the hair follicles
- EG and RS had higher background signals compared with DD.
- All dyes for plucked hairs showed full DNA profiles
- DD was shown to be the most suitable dye for staining hair follicles with a low background signal.

References

- [1] L. Bourguignon, B. Hoste, T. Boonen, K. VissF. Hubrecht, A fluorescent microscopy-screening test for efficient STR-typing of telogen hair roots, *Forensic Science International: Genetics*, 2008, 3 27-31.
- [2] T. Lepez, M. Vandepoel, D. Van Hoofstad, Deforce Fast nuclear staining of head hair roots as a screening method for successful STR analysis in forensics, *Forensic Science International: Genetics*, 2014, 13 191-194.
- [3] E.M. Brooks, M. Cullen, T. Sztybel, J. Walsh, Nuclear staining of telogen hair roots contributes to successful forensic DNA analysis, *Australian Journal of Forensic Sciences*, 2010, 42 115-122.
- [4] D. McNevin, L. Wilson-Wilde, J. Robertson, J. Kyd, Lennard, Short tandem repeat (STR) genotyping of keratinised hair: Part 1. Review of current status and knowledge gaps, *Forensic Science International*, 2005, 153 237-245.
- [5] S. Szabo, K. Jaeger, H. Fischer, E. Tschachler, W. Parson, Ecolant in situ labeling of DNA reveals interindividual variation in nuclear DNA breakdown in hair and may be useful to predict success of forensic genotyping of hair, *International Journal of Legal Medicine*, 2012, 126 53-70.
- [6] J. Edson, E.M. Brooks, C. McLaren, J. Robertson, D. McNevin, A. Cooper, J. J. Austin, A quantitative assessment of a reliable screening technique for the STR analysis of telogen hair roots, *Forensic Science International: Genetics*, 2013, 7 190-198.
- [7] A.H. Fischer, K.A. Jacobson, J. Rose, Zeller, Hematoxylin and Eosin Staining of Tissue and Cell Sections, *Cold Spring Harbor Protocols*, 2008.

Figure D-30: Poster presented at the ANZFSS 23rd International Symposium on the Forensic Sciences, Auckland, 2016.

308

Chapter 6

DNA binding dyes for quantitative PCR

6.1 Introduction

An important step in forensic DNA analysis is quantifying the DNA before undergoing STR typing as the STR kits are optimized to work with DNA concentrations between 0.5-1.0 ng of total DNA [1, 2]. Having too much DNA can result in split peaks and off scale peaks, having too little DNA can result in allele-drop out or no amplification product at all. There are many methods that have been used over the last decade for DNA quantification not just within forensic science but in many other scientific areas. The earlier modes of DNA quantification include: UV spectrometry, yield gels and slot blots [3]. More recently fluorometry (using intercalating dyes) and qPCR have become methods of choice. These methods will be discussed in more detail below.

Quantification methods;

- Slot blot [4]
- Intercalating dyes
 - PicoGreen[®] [5]
 - SYBR[®] Green I [6]
- Yield gels
- Hybridization probes
 - End point PCR
 - RT-PCR
- UV Spectrometry [5]

6.1.2 UV Spectrometry

Ultra-violet (UV) absorbance can be used to determine DNA concentration using a wavelength of 260 nm [5, 7]. Instruments that use this methodology of DNA quantification include the NanoDrop™ (ThermoFisher), which can also give protein concentrations as well to determine purity of the sample. This method is based on Beer-Lambert's law $A = \epsilon bC$ (where A = Absorbance, ϵ = molar absorptivity coefficient, b = path length (cm) and C = concentration) to be able to calculate the concentration of DNA based on the absorbance and the extinction coefficient. This method is not overly sensitive so other methods of DNA quantification are used in preference to UV spectrometry [8, 9].

6.1.3 Fluorometry

Intercalating dyes that are also used for gel staining can also be used in fluorescence spectrometry for DNA quantification. Dyes such as SG [9] and PG [10] are two commonly used dyes in fluorescent quantification [7]. The quantification is based on the linear relationship between the fluorescent signal and the concentration of DNA [5]. Instruments that are available for the specific use of fluorescent DNA quantification include the Qubit® Fluorometer (ThermoFisher) [11], AccuLite™ Mini Fluorometer (Biotium), or any instrument that measures fluorescence could be used for DNA quantification.

6.1.4 Slot Blots

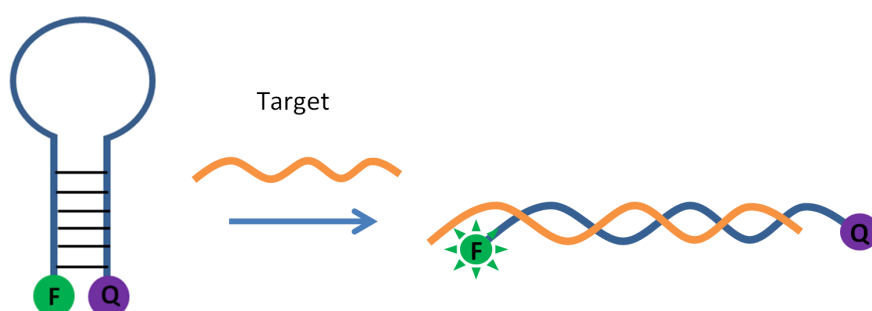
Slot blots are based on the specific hybridization of a probe that binds to the human alpha satellite by visual comparison of a sample's band intensity to known controls and standards [3]. This methodology has a high degree of species specificity and can detect as little as 150 pg of DNA. This method however doesn't give any indication on the size of the product in comparison to gels in electrophoresis [4]. There are kits that are specific for human DNA analysis such as the Quantiblot® Human DNA kit [4, 12, 13] (now phased out and no longer available).

6.1.5 Hybridization probes for nucleic acid detection

Fluorescent hybridization probes are used to detect nucleic acids *in vivo* and *in vitro* in a range of areas such as biomedical research, chemistry and more due to their high sensitivity and selectivity [14]. These probes are designed to fluoresce when in the presence of the target sequence which is complementary to the oligonucleotide sequence attached to the probe. There are two main hybridization probes, molecular beacon and binary probes [15, 16].

Molecular Beacon Probes

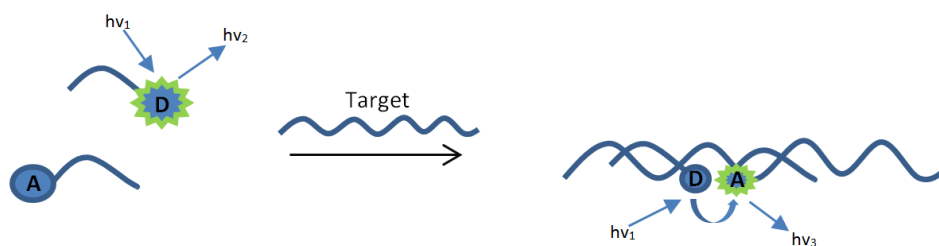
Molecular beacon probes are hairpin oligonucleotide structures that produce distinctive fluorescence signals in the presence and absence of their target molecule [15, 16]. Below Scheme 6.1 shows the general structure of a molecular beacon probe. The “Loop” contains the complementary sequence to the specific target sequence. There is a fluorophore (F) and quencher (Q) attached at opposite ends of the stem. The stem consists of five or six base pairs attached that force the fluorophore and the quencher to be in close proximity when in the absence of the target resulting in no emission of fluorescence. When in the presence of the target sequence the molecular beacon hybridizes to this sequence resulting in the open conformation of the beacon. With this open conformation the fluorophore and the quencher are spatially separated and upon excitation of the fluorophore a strong signal is produced [15, 16]. The interaction of a typical molecular beacon probe with a target sequence is shown in Scheme 6.1.



Scheme 6.1: Schematic representation of the interaction of a molecular beacon with a target sequence adapted from [16].

Binary probes

Binary probes are made up of two fluorescently labelled oligonucleotide strands that can hybridize to regions adjacent to the target and produce distinctive fluorescence signals. Standard binary probes consist of an acceptor and donor fluorophores which are attached to the ends of single-stranded oligonucleotides that are complementary to adjacent regions of the target [16]. The interaction of a binary probe and a target sequence is shown below scheme 6.2. One advantage using a binary probe over a molecular beacon is that false-positive signals can be avoided as molecular beacons can have nonspecific binding to other cellular constituents [14].



Scheme 6.2: Schematic diagram of a binary probe before and after the addition of the target adapted from [16].

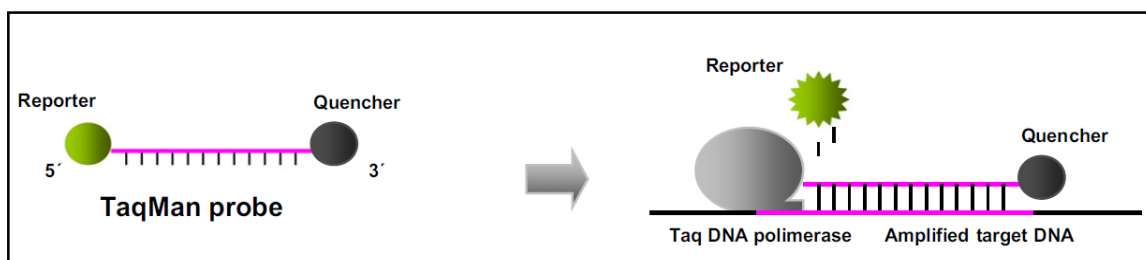
6.1.6 Quantitative PCR

Quantitative PCR (qPCR) is used within forensic laboratories for the quantification of DNA present after an extraction process. QPCR is the more sensitive mode of quantification in comparison to other techniques mentioned above: UV absorbance, yield gels, Slot blot, end point PCR and intercalating dyes (PG). Instrumentation that is available for qPCR includes ABI 7000, Qiagen Rotogene Q, iCycler and Roche LightCycler.

qPCR is the continuous collection of fluorescent signals from one or more PCRs in a range of cycles. Quantitative real-time PCR is the conversion of the fluorescent signals from each reaction into a numerical value for each sample. There are two main methods of qPCR these are using the TaqMan[®] probe assay or using a SYBR[®] Green I assay [3, 17].

5' Nuclease Assay (TaqMan[®])

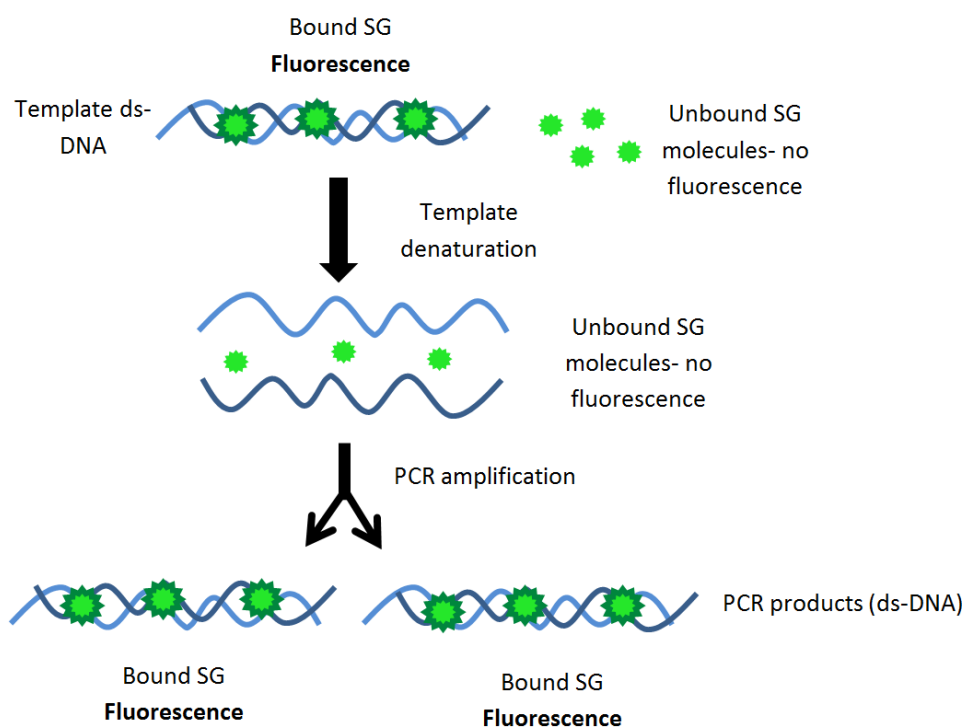
TaqMan[®] probes are labeled with two fluorescent dyes, a quencher and a reporter that emit fluorescence at different wavelengths. The sequence of the probe is designed to hybridize specifically in the DNA target region between the two PCR primers. The reporter dye is attached to the 5' end of the probe while the quencher is attached on the 3' end. When the probe is intact there is no fluorescent signal due to the fluorescent energy transfer between the two dyes suppressing the signal. The probe will be displaced from strand synthesis within the polymerization stage. The Taq DNA polymerase will chew away at any sequence in its path and when the reporter dye is released from the probe, and is no longer in close proximity to the quencher, then fluorescence can then be detected [3, 18]. Scheme 6.3 shows the binding mechanism of the TaqMan[®] probe assay [18].



Scheme 6.3: Structure and mechanism of action of hydrolysis probes of TaqMan probe assay taken from Navarro, E et al [18].

Intercalating dyes

Intercalating dyes can be used in RT-PCR because the dye molecules can attach to the PCR amplicons and as the number of PCR products increases then the number of molecules that can attach to the DNA fragments also increase and thus an increase in the fluorescent signal indicates an increase in the amount of DNA present. Dyes that are currently used for the quantification of DNA include EG [19] and SG [17, 20].



Scheme 6.4: Schematic representation of how SG molecules bind during qPCR and fluoresce when bound to ds-DNA, adapted from [21].

Human DNA Quantification Kits

- Quantifiler® (Thermo Fisher Scientific)
 - This kit is designed for the quantification of total amplifiable human DNA and human-male DNA. The use of this kit aids in determining if sufficient DNA is present to proceed with STR analysis as well as how much of the sample to use in the STR amplification.
- HY Plexor (Promega)
 - Human specific and human-male DNA in same sample reaction.
- Investigator® Quantiplex Kit (QIAGEN) [22]
 - Human specific
 - <1 pg/μL DNA
 - 48 min run time.

6.1.6 Summary

This Chapter looks at the use of new DNA binding dyes (such as GG, DD and RS) for RT-PCR and compare to dyes already used commercially for the quantification of DNA (SG, BRYT green® (BG) and EG). As these dyes mainly used for gel staining also work by either intercalating between the DNA strands or binding to the groove of DNA, then they have the potential to work in the process of qPCR and may show to be more efficient or more sensitive to SG and EG. These dyes also offer a more cost effective alternative to SG.

6.2 PUBLICATION

The results pertaining to this study on dyes used in quantitative PCR were accepted for publication in *BioTechniques*; see article below.


Alicia M. Haines, Adrian Linacre, Shanan S. Tobe, **Optimization of Diamond™ nucleic acid dye for quantitative PCR**, *BioTechniques, Report, accepted July, 2016 (see Appendix F, Figure E-4, for acceptance email)*.

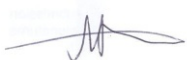
Statement of Authorship


Title of Paper	Optimization of Diamond™ nucleic acid dye for quantitative PCR		
Publication Status	Accepted July, 2016		
Publication details	<i>BioTechniques</i>		

AUTHOR CONTRIBUTIONS

By signing the Statement of Authorship, each author certified that their stated contribution to the publication is accurate and that permission is granted for the publication to be included in the candidate's thesis.

Name of Principal Author (Candidate)	Alicia M. Haines		
Contribution to the paper	Designed experimental method, performed all laboratory work and analysis, drafted the manuscript, edited manuscript and acted as corresponding author		
Signature		Date	August, 2016

Name of Co-Author	Adrian Linacre		
Contribution to the paper	Edited manuscript, supplied dye for experiment		
Signature		Date	August, 2016

Name of Co-Author	Shanan S. Tobe		
Contribution to the paper	Helped design study, edited manuscript, supplied RT-PCR reagents		
Signature		Date	August, 2016

Optimization of Diamond™ Nucleic Acid Dye for quantitative PCR

Alicia M. Haines^{a*}, Adrian Linacre^a, Shanan S. Tobe^{ab}

^a*School of Biological Sciences, Flinders University, Adelaide, Australia;* ^b*Department of Chemistry and Physics, Arcadia University, Glenside, PA, USA*

Abstract.

This study evaluates Diamond™ nucleic acid dye for its application to quantitative PCR (qPCR). Diamond™ Dye is commercially available as a stain for detection of DNA separated by gel electrophoresis but has yet to be described as a dye in qPCR. Inhibitory effects of Diamond™ Dye on qPCR were investigated between 0.1-2.5X concentration. Standard serial dilution of DNA was performed to determine the linearity of the data, efficiency and sensitivity in comparison to other commonly used fluorescent dyes such as SYBR® Green, EvaGreen™ and BRYT Green®. Diamond™ Dye applied to qPCR was determined to be comparable to the other dyes with an R^2 value above 0.9 and an efficiency of 0.83. A signal was successfully produced by Diamond™ Dye over a range of DNA dilutions from approximately 28 ng – 0.28 pg showing that the sensitivity was comparable with the other dyes investigated; this study used a mitochondrial DNA target. The Cq values of Diamond™ Dye were much lower than EvaGreen™ by almost 7 cycles, thus higher initial copy numbers of the target product are produced using Diamond™ Dye. Diamond™ Dye is a cheaper alternative that laboratories may already use for gel electrophoresis and the implementation of Diamond™ Dye into qPCR would be less expensive than SYBR® Green and also less toxic than other binding dyes such as ethidium bromide.

Method summary:

We describe the novel application of Diamond™ nucleic acid staining dye for the quantification of DNA using real-time PCR and a mitochondrial target. Comparison is made to well-known fluorescent dyes and the benefits of using Diamond Dye as a replacement for commonly used dyes is described.

Keywords: Diamond™ Nucleic Acid Dye; quantitative PCR (qPCR); Real-Time PCR; SYBR® Green

* Corresponding author. Tel: +61 8201 5003

E-mail address: alicia.haines@flinders.edu.au. Postal address; Flinders University GPO Box 2100, School of Biological Sciences, Adelaide, SA, 5001, Australia (A. M. Haines)

1. Introduction

Fluorescent dyes have been used in quantitative PCR (qPCR) for many years⁽¹⁾ where the most commonly used dye is the cyanine intercalating dye SYBR[®] Green I (SG)⁽²⁾. SG is known for its DNA binding sensitivity and was reported to have around 1,000 fold increase in fluorescent signal when in the presence of DNA^(3, 4). Other fluorescent dyes have also been established for use in qPCR such as EvaGreen[™] (EG)⁽⁵⁾, LCGreen[®]⁽⁶⁾, SYTO[®] dyes⁽⁷⁾, ResoLight[®]⁽⁸⁾ and BRYT Green[®] (BG)⁽⁹⁾ among others. A well-known issue of using SG within the laboratory is the mutagenic and toxic nature of the dye as it can permeate the cell membrane⁽¹⁰⁾. The level of mutagenicity of SG is stated to be at 33.3 µg but this is much lower than the toxicity of another commonly used dye, ethidium bromide (EtBr), at 250-500 µg⁽¹¹⁾.

Diamond[™] nucleic acid dye (DD) is an external groove binding dye that has been shown to have similar sensitivity as SG, with a limit of detection of 0.5 ng when detecting DNA within agarose gels⁽¹⁰⁾. DD can permeate the cell membrane leading to interactions with genomic DNA⁽¹⁰⁾ however studies have shown that DD is less mutagenic and genotoxic compared to EtBr⁽¹¹⁾. This may be due to the different binding mechanism DD has with DNA compared to other intercalating dyes as it does not bind between the base pairs of DNA but binds externally⁽¹⁰⁾. DD currently has not been evaluated for its use for qPCR.

EG has been established for its use within qPCR and with high resolution melt (HRM) curve analysis as it has been shown to be stable in the PCR⁽⁵⁾. SG is known for its inhibition of PCR at high concentrations and with 25 ng of DNA was shown to inhibit the reaction above 1X concentration. In comparison EG still shows amplification at 2.5X concentration, indicating that EG has a lower inhibition than SG in the PCR⁽¹²⁾.

This study investigated the use of DD for use in qPCR with comparison to the fluorescent dyes already used: SG, EG and BG. The optimal concentration of DD within the reaction was determined, the level of amplification inhibition assessed and the sensitivity and efficiency of the reaction measured. A variety of primers were chosen that had different product lengths to show if DD was a robust dye. As DD is a much cheaper dye than SG (~5 folds cheaper), and stated to be less toxic and mutagenic than EtBr (<http://www.promega.com.au/resources/pubhub/diamond-nucleic-acid-dye-is-a-safe-and-economical-alternative-to-ethidium-bromide/>), an outcome would be that DD is a suitable alternative for qPCR if the sensitivity and efficiency are comparable to dyes used currently.

2. Materials and methods

2.1 Optimization of fluorescent dye concentration for qPCR

Diamond™ nucleic acid dye (DD; Promega, AUS) at 20X was prepared in a buffer solution of 1X tris-acetate (TA), 1 in 500 dilution of stock concentration (10,000X). The primer sequences and amplicon properties used within this study are summarized in Table 1. Universal 1 and Fragment 1 primers were used to determine the inhibition effect of DD on PCR amplification. Five different reactions were prepared in quadruplicate; the quantity of DNA remained constant at 20 ng in each reaction but the final dye concentration varied at 0.1X, 0.5X, 1X, 1.5X, 2X and 2.5X in a total reaction volume of 20 µL. Amplifications were performed on a 72 Rotor-Disc on a Rotor-Gene Q (Qiagen, AUS). The channels selected for fluorescence detection were green (excitation 470 ± 10 nm, emission 510 ± 5 nm) and a modified channel labelled diamond (excitation 470 ± 10 nm, emission 557 ± 5 nm) to account for the differences in the excitation (494 nm) and emission (558 nm) of DD compared with the excitation (495 nm) and emission (520 nm) of SG. The PCR cycle proceeded with an initial hold at 95 °C for 2 min then 50 cycles at 95 °C for 10 s, 60 °C for 15 s and 72 °C for 20 s. This was followed by a melt from 72 °C-95 °C in 1 °C increments.

The median Cq value was calculated for each dye concentration and the slope of the trendline generated by plotting the median Cq value against dye concentration was used as an indicator of the degree of amplification inhibition.

Table 1: Primer sequences and amplicon properties used in qPCR, sets 1 and 2 primer design published in Tobe, S.S and Linacre A.M.T⁽¹³⁾

Primer Sets	5'—Sequence—3'	Amplicon length (bp)	T _m (°C)
1 Fragment 1	F-GACCAATGATATGAAAAACCATCGTTGT R-CAAGCATACTCTAGTAAGGATCCG	170	68.8 64.67
2 Fragment 2	F-TGAGGACAAATATCATTYTGAGGRGC R-ATCGGAATGGGAGGTGATTCTAGG	246	67.6 71.3
Primer sets 1 and 2 targeted the end of the tRNA-Glu gene and Cytochrome b gene of the mitochondrial genome. These primer sets used to test for the suitability of DD relative to other qPCR dyes, were selected based on the product size and also to ensure that there was a minimal (nil) chance of point contamination between the different dyes tested. This was accomplished by using non-human (primer set 1) and human specific primers (primer set 2).			

2.2 Determination of DD efficiency and sensitivity compared with SG, EG and BG

A series of dilutions were prepared to determine the efficiency of DD, EG and BG in qPCR and compare these to SG. Amplifications were performed using Fragment 2 primers which would result in an amplicon size of 246 bp (Table 1). Five tenfold serial dilutions were prepared from neat DNA (whole genomic DNA from a buccal swab prepared by a solid phase extraction) quantified by Qubit® dsDNA assay at 28.4 ng/μL (Thermo Fisher Scientific, NSW, AUS) to a final dilution of 1/10⁵. A no template control was prepared for quality control to determine if any contamination was present in any of the reagents.

Based on the results of part 1 of this study, 0.5X final concentration of DD was used for all reactions. The DD reactions consisted of 10 μL of KAPA Taq ReadyMix 2X (Kapa Biosystems, AUS), 0.5 μL of each primer pair (10 μM/μL), 0.5 μL of DD at 20X, 1 μL of DNA solution and 8 μL of TA buffer, in a total reaction volume of 20 μL. The SG reactions consisted of 10 μL of KAPA SYBR FAST qPCR Master Mix 2X (Kapa Biosystems, AUS), 0.5 μL of primer pair, 1 μL of DNA solution and 8.5 μL of TA buffer, in a total reaction volume of 20 μL. The BG reaction consisted of 10 μL of GoTaq® qPCR Master Mix 2X (Promega, NSW, AUS), 0.5 μL of primer pair, 1 μL of DNA solutions and 8.5 μL of TA buffer, in a total reaction volume of 20 μL. The EG reaction consisted of 10 μL of KAPA Taq ReadyMix 2X, 0.5 μL of primer pair, 1 μL of EG at 20X, 1X concentration as suggested by the manufacturer's protocol (Jomar Diagnostics P/L, SA, AUS), 1 μL of DNA solution and 7.5 μL of TA buffer, in a total reaction volume of 20 μL. A negative control (NTC) was prepared for each of the dyes tested to determine if any contamination was present, the reactions were prepared as above with an extra 1 μL of 1X TA buffer instead of DNA.

All reactions were performed in quadruplicate. Amplifications were performed on a 72 Rotor-Disc on a Rotor-Gene Q (Qiagen, AUS). The channels selected for fluorescence detection were green and diamond. The PCR cycle proceeded with an initial hold at 95 °C for 2 min then 50 cycles at 95 °C for 10 s, 60 °C for 15 s and 72 °C for 20 s. This was followed by a melt 72 °C-95 °C in 1 °C increments.

The lower limit of sensitivity of the reaction was determined by preparing a $1/10^6$ dilution as above to determine if a signal from any of the dyes could be detected. This was performed in quadruplicate.

3. Results and discussion

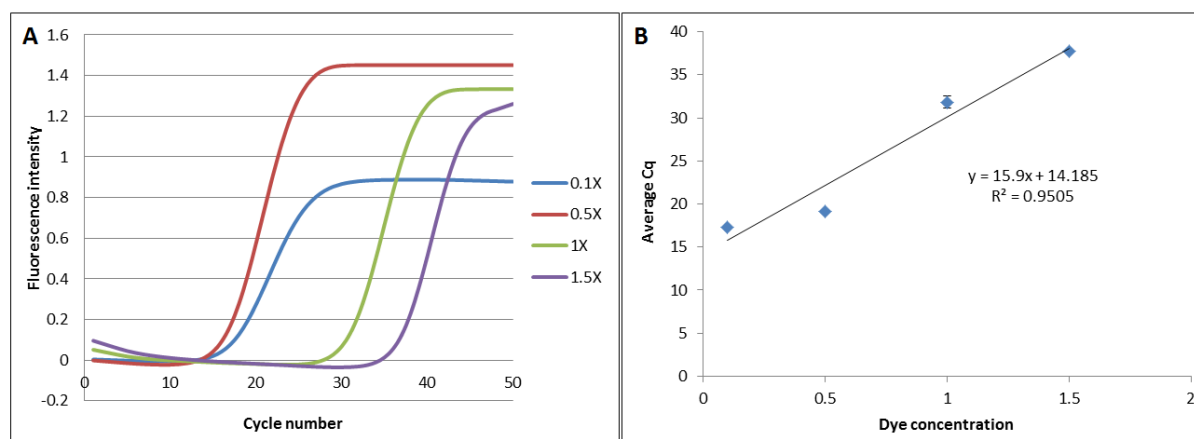


Figure 1. Effect of dye concentrations on cycle number and level of inhibition of DD on the reaction (A) Average cycling curve of normalized fluorescence intensity against cycle number with varying DD concentration (0.1X-1.5X). (B) The line of best fit for DD dye concentration against average Cq values with the threshold set at 0.12, error bars show 95% confidence. Above 1.5X concentration complete inhibition was observed.

The effect of DD concentration on the amplification process showed that the optimal concentration of DD for qPCR was 0.5X (Figure 1). The slope of the trendline (Figure 1B) indicates the degree of amplification inhibition (15.9) as the concentration of the DD increases. Complete inhibition occurred at concentrations above 1.5X, with partial inhibition at 1.5X (2 out of 4 replicates had an amplification product).

In comparison, a previous study⁽¹²⁾ has shown that at lower DNA quantities (25 ng) SG can inhibit the reaction at concentrations above 0.5X in contrast to DD that showed inhibition above 1.5X. In this same study, EG was shown to have no inhibition of the reaction above 2X, with DNA amounts ranging from 25-100 ng⁽¹²⁾, indicating that EG has a less inhibiting effect when compared to DD.

Average quantitation values (Cq) of DD ranged from 0.04 – 1.49 cycles higher when compared to SG (Table 2), higher Cq value indicates lower initial copy number of the target amplification product. DD was compared to the SG kit (KAPA SYBR FAST qPCR), which has engineered the Taq enzyme to be more resistant to the inhibitory effects of SG within the

reaction, as stated by the manufacturer. With a similar manufacturing process, it would be expected that DD would likely show improved Cq values than those determined in this study. DD in comparison to EG has lower Cq values, ranging from 3.63-7.47 cycles lower. When comparing DD to BG, on average the Cq values for DD run between 0.20-2.51 cycles lower than BG.

Total human genomic DNA was quantified using Qubit[®] dsDNA HS Assay at 28.4 ng/μL and was used as an approximation of the total amount of DNA present in the sample. The manufacturer states the assay is able to accurately detect between 0.2 pg/μL and 100 ng/μL. As the primers used in these reactions are for the mitochondrial genome, the detection limit would be expected to be lower than for primers used to target nuclear DNA. Due to the multi-copy nature of mtDNA within a single mitochondrion, and the variation in the number of mitochondria per cell, it is very difficult to determine an exact number of mitochondrial genomes per cell, however an average of 500 has been suggested ⁽¹⁴⁾. Based on this average value per cell, the neat sample (28.4 ng/μL) contains approximately 2.1 million copies of mtDNA/μL and the lowest dilution (1/10⁶) contains approximately 2 copies of mtDNA/μL. This is comparable to the sensitivity claimed by SG.

DD exhibited a curve morphology that is seen with other commonly used dyes for qPCR: such as SG, EG and BG (Figure 2), demonstrating its suitability for use in qPCR that can be easily incorporated into standard workflow.

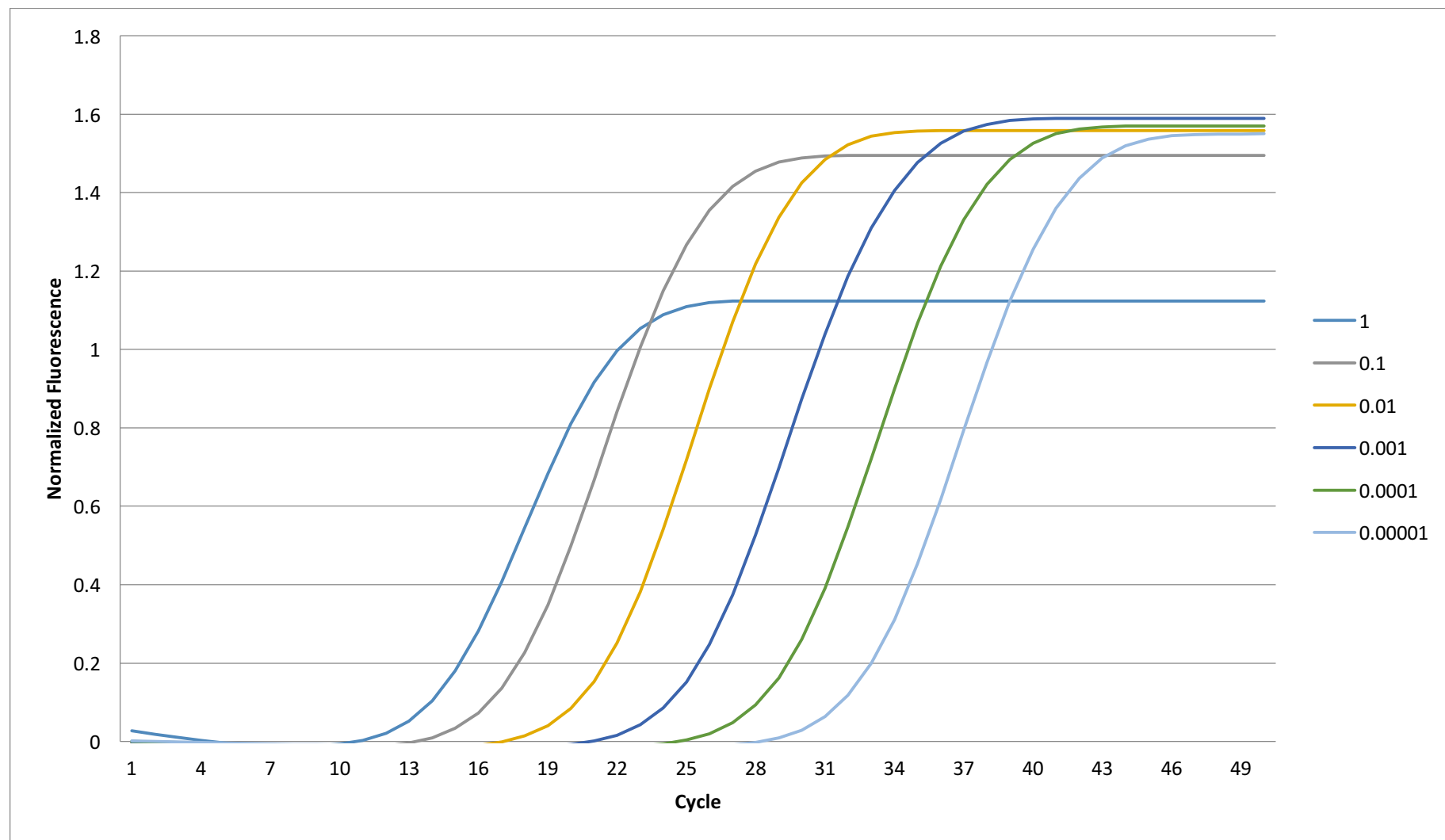


Figure 2. Average qPCR cycling with five dilution series over 50 cycles using DD at 0.5X concentration done in quadruplicate. Detection used the DD channel with 1 being the neat DNA concentration at 28.4 ng/ μ L, followed by 1/10 serial dilutions.

Table 2: Dilution series with fluorescent dyes showing average C_q values

Dilution	DD	SG	EG	BG
1	13.82 (0.02)	12.33 (0.03)	17.45 (0.03)	14.02 (0.03)
1/10	15.53 (0.02)	15.26 (0.05)	20.97 (0.07)	17.40 (0.07)
1/100	19.37 (0.20)	19.33 (0.12)	25.48 (0.11)	21.72 (0.08)
1/10³	23.17 (0.08)	22.99 (0.08)	29.84 (0.17)	25.68 (0.05)
1/10⁴	27.03 (0.71)	26.28 (0.20)	34.50 (0.42)	29.24 (0.12)
1/10⁵	32.93 (1.47)	31.93 (0.26)	39.92 (0.41)	34.51 (0.48)
Dilution series starts with an initial DNA concentration of 28.4 ng per reaction with the C _q threshold set at 0.09 with the standard deviation shown in brackets. 1/10 ⁶ dilution results were not reproducible.				

The linearity of the reaction (R^2) of the standard curves was above 0.97 for all dyes (Figure 3). Based on these data, BG had the highest R^2 value (0.996) and DD had the lowest value (0.970). The efficiency of the reaction, based on the values generated from the standard curve in relation to the slope⁽¹⁵⁾, showed DD had the highest efficiency of 0.83 and EG had the lowest value at 0.67 (Figure 3). Combining all the aspects of qPCR⁽¹⁵⁾ it can be seen that DD is comparable with other dyes that are currently commercially available.

At concentrations below 1/10⁵ dilution, the dyes were not capable of generating a reproducible signal and at 1/10⁶ samples failed to amplify. Some of the replicates that did not produce an amplification signal produced a broad melt peak around 75-77 °C (Figure 4). One of the four replicates for SG's 1/10⁶ sample (Figure 4.A) produced the target melt peak. The other three replicates had a broad peak ranging around 75-77 °C and these peaks were 5-fold smaller than the peak seen for DD (Figure 4.C). Equally, BG (Figure 4.D) had 1 of 4 replicates produced the target melt product in the 1/10⁶ dilution; all other replicates of 1/10⁶ and the no template control (NTC) had no products. The 1/10⁶ dilution for EG had 1 of 4 replicates produced the target melt peak along with a broad peak at 77 °C, 1 of 4 produced only a broad peak at 77 °C with the remaining replicates and the NTC producing no result (Figure 4.B).

DD (showed no amplification product in the 1/10⁶ and NTC samples (Figure 4C). The observed broad minor melt peaks are around 77°C which would likely correspond to the melting point of expected primer-dimer. All the other DNA dilutions for DD had peaks

around 85°C. These results from $1/10^6$ dilution may be due to the type of binding mechanism of DD in comparison to other dyes used typically. DD is an external groove binding dye meaning the DNA does not need to be double-stranded for the dye to bind. The molecular structure of DD is proprietary, which limits any further comment in this regard. In comparison SG, which intercalates between the base pairs of DNA and has electrostatic interactions, needs the DNA to be double-stranded for the dye to bind ⁽³⁾. This would be a plausible explanation as to why the DD has a signal in the NTC and in dilutions that are too low for detectable amplification.

A further study was conducted to determine if DD binds to ssDNA, there was no ssDNA amplification products (data not shown), and therefore was not the cause of the slightly higher variability in DD at the lowest dilutions (Figure 3). Furthermore, the disassociation of DD from ssDNA occurs at a low temperature, dropping off at around 73 °C (data not shown), which is about 4 degrees lower than the primer dimer observed in the reactions (Figure 4), which dropped off at 77 °C. The binding of DD to ssDNA is therefore not a foreseeable issue with normal qPCR reactions.

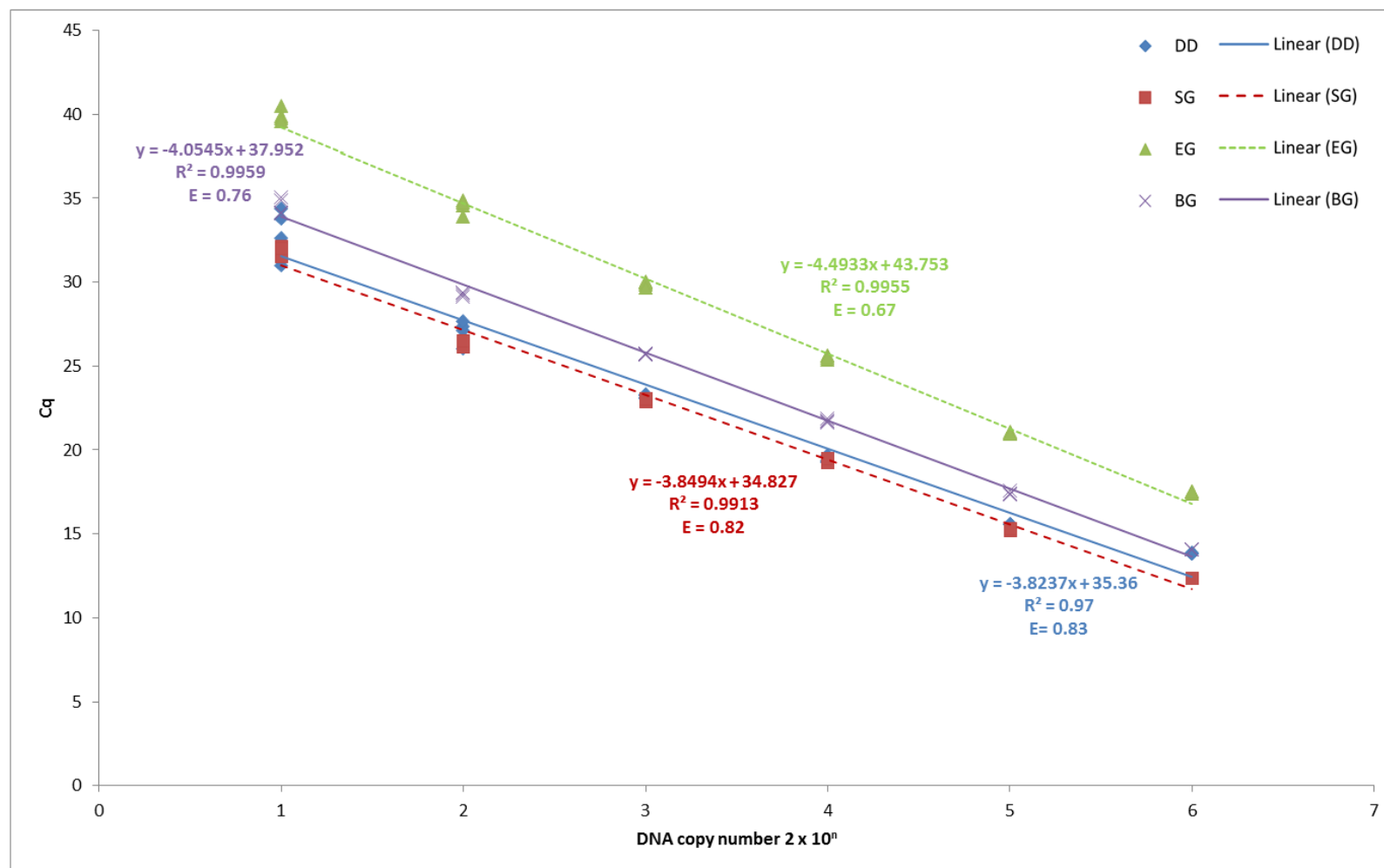


Figure 3. Standard curves of DNA concentration against Cq values; SG, BG and EG analysis through the green channel and DD channel for DD. Efficiency of the reaction and the R^2 values showing the linearity of the dyes fluorescent signals are also shown.

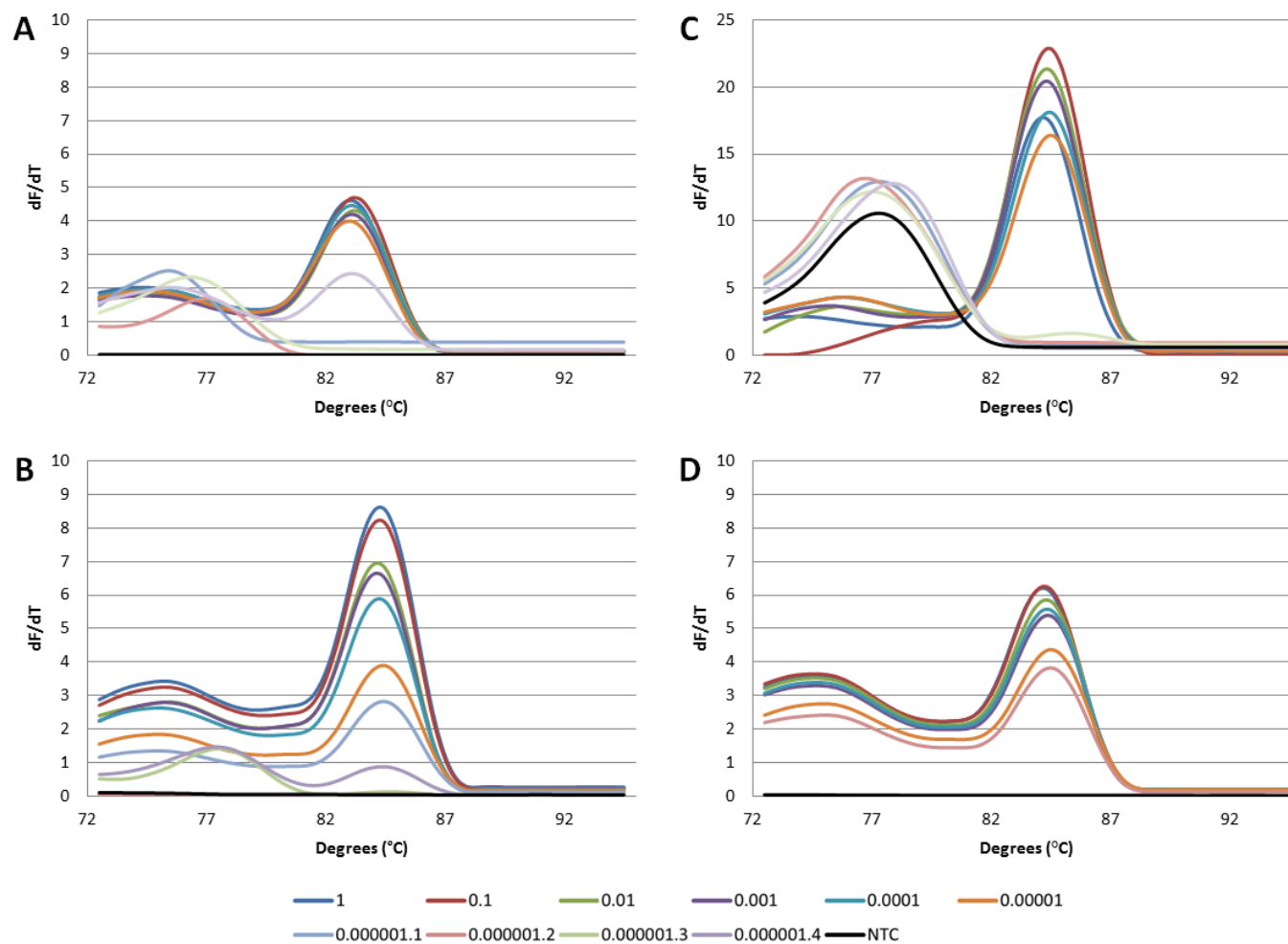


Figure 4. Average melt curve of serial dilutions of DNA (1 being the neat DNA at 28.4 ng/μL, followed by 1/10 serial dilutions) NTC = no template control, showing all replicates for 1/10⁶ dilution, (A) SG, (B) EG, (C) DD and (D) BG. Analysis through green channel for A, B and D and DD channel for C.

This is the first study to examine the use of DD for qPCR, as to date it has only been used in staining agarose gels. The inhibitory effect DD has on the PCR was investigated and was found to completely inhibit the reaction above a concentration of 1.5X. The efficiency, linearity and sensitivity of the reaction were also investigated by using serial dilutions of DNA. DD was shown to be able to detect down to 0.28 pg of DNA (approximately 20 copies of mtDNA target). This sensitivity is comparable to SG, EG and BG currently used for qPCR indicating that DD is a suitable and cheaper (by approximately 5 fold) alternative to any of the more expensive dyes used currently when performing qPCR.

Author contributions

A.M.H., S.S.T., and A.L. conceived the idea for the study. A.M.H. performed all laboratory work. A.M.H., S.S.T., and A.L. analyzed the data and drafted the manuscript. All authors approved of the final manuscript prior to submission.

Acknowledgements

Funding was provided by Forensic Science South Australia

Competing interests

The authors declare no competing interests

4. References

- 1.) **Klein, D.** 2002. Quantification using real-time PCR technology: applications and limitations. *Trends in Molecular Medicine* 8:257-260.
- 2.) **Monis, P.T., S. Giglio, and C.P. Saint.** 2005. Comparison of SYTO9 and SYBR Green I for real-time polymerase chain reaction and investigation of the effect of dye concentration on amplification and DNA melting curve analysis. *Analytical Biochemistry* 340:24-34.
- 3.) **Dragan, A.I., R. Pavlovic, J.B. McGivney, J.R. Casas-Finet, E.S. Bishop, R.J. Strouse, M.A. Schenerman, and C.D. Geddes.** 2012. SYBR Green I: Fluorescence Properties and Interaction with DNA. *Journal of Fluorescence* 22:1189-1199.
- 4.) **Cosa, G., K.S. Focsaneanu, J.R.N. McLean, J.P. McNamee, and J.C. Scaiano.** 2001. Photophysical Properties of Fluorescent DNA-dyes Bound to Single- and Double-stranded DNA in Aqueous Buffered Solution. *Photochemistry and Photobiology* 73:585-599.
- 5.) **Mao, F., W.-Y. Leung, and X. Xin.** 2007. Characterization of EvaGreen and the implication of its physicochemical properties for qPCR applications. *BMC Biotechnology* 7:76-76.
- 6.) **Wittwer, C.T., G.H. Reed, C.N. Gundry, J.G. Vandersteen, and R.J. Pryor.** 2003. High-Resolution Genotyping by Amplicon Melting Analysis Using LCGreen. *Clinical chemistry* 49:853-860.
- 7.) **Eischeid, A.C.** 2011. SYTO dyes and EvaGreen outperform SYBR Green in real-time PCR. *BMC Research Notes* 4:1-5.
- 8.) **Rouleau, E., C. Lefol, V. Bourdon, F. Coulet, T. Noguchi, F. Soubrier, I. Bièche, S. Olschwang, et al.** 2009. Quantitative PCR high-resolution melting (qPCR-HRM) curve analysis, a new approach to simultaneously screen point mutations and large rearrangements: application to MLH1 germline mutations in Lynch syndrome. *Human Mutation* 30:867-875.
- 9.) **Imperiali, C., P. Alía-Ramos, and A. Padró-Miquel.** 2015. Rapid detection of HLA-B*51 by real-time polymerase chain reaction and high-resolution melting analysis. *Tissue Antigens* 86:139-142.
- 10.) **Haines, A.M., S.S. Tobe, H.J. Kobus, and A. Linacre.** 2015. Properties of nucleic acid staining dyes used in gel electrophoresis. *Electrophoresis* 36:941-944.
- 11.) **Singer, V.L., T.E. Lawlor, and S. Yue.** 1999. Comparison of SYBR® Green I nucleic acid gel stain mutagenicity and ethidium bromide mutagenicity in the *Salmonella*/mammalian

microsome reverse mutation assay (Ames test). *Mutation Research/Genetic Toxicology and Environmental Mutagenesis* 439:37-47.

12.) **Radvanszky, J., M. Surovy, E. Nagyova, G. Minarik, and L. Kadasi.** 2015. Comparison of different DNA binding fluorescent dyes for applications of high-resolution melting analysis. *Clinical Biochemistry* 48:609-616.

13.) **Tobe, S.S, and A.M.T. Linacre.** 2008. A multiplex assay to identify 18 European mammal species from mixtures using the mitochondrial cytochrome b gene. *Electrophoresis* 29:340-347.

14.) **Satoh, M., T. Kuroiwa.** 1991. Organization of multiple nucleoids and DNA molecules in mitochondria of a human cell. *Experimental Cell Research* 196: 137–140.

15.) **Bustin, S.A., V. Benes, J.A. Garson, J. Hellemans, J. Huggett, M. Kubista, R. Mueller, T. Nolan, et al.** 2009. The MIQE Guidelines: Minimum Information for Publication of Quantitative Real-Time PCR Experiments. *Clinical chemistry* 55:611-622.

6.3 Further methodology

6.3.1 Intercalating dyes for qPCR

RS, DD, GG, GR along with the standard dyes for qPCR (SG and EG) were trialed for qPCR. The reaction consisted of 10 µL of KAPA Taq ReadyMix 2X (KAPA Biosystems, AUS), 0.5 µL of primer pair, 1 µL of DYE (20X), 1 µL of DNA solution and 7.5 µL of TA buffer, in a total reaction volume of 20 µL. The channels selected for fluorescence detection were green, RS (source at 530 nm and detector at 555 nm) and diamond. The PCR cycle proceeded with an initial hold at 95°C for 2 min then 50 cycles at 95°C for 10 s, 60°C for 15 s and 72°C for 20 s. This was followed by a melt 72°C-95°C in 1°C increments.

6.3.2 Dye combinations for qPCR

0.5 µL of DD (20 X) was added to the SG reaction mix: 10 µL of KAPA SYBR FAST qPCR Master Mix 2X (Kapa Biosystems, AUS), 0.5 µL of primer pair, 1 µL of DNA solution and 8 µL of TA buffer, in a total reaction volume of 20 µL. All reactions were performed in quadruplicate. Amplifications were performed on a 72 Rotor-Disc on a Rotor-Gene Q (Qiagen, AUS). The channels selected for fluorescence detection were green and diamond. The PCR cycle proceeded with an initial hold at 95°C for 2 min then 50 cycles at 95°C for 10 s, 60°C for 15 s and 72°C for 20 s. This was followed by a melt 72°C-95°C in 1°C increments.

Table 6.1: Primer sequences and amplicon properties used in RT-PCR [23] Alu sequences [24].

Primer	Position	5'-----Sequence-----3'	Amplicon length (bp)	T _m (°C)
Universal 1	-50	GACCAATGATATGAAAAACCATCGTTGT		68.72
Universal 2	400	TGAGGACAAATATCATTYTGAGGRGC		67.52
Human 1	624	ATCGGAATGGGAGGTGATTCCTAGG	246	71.23
Human 2	208	TTCAGCCATAATTTACGTCTCGAGT	277	65.49
ALU (forward)		GTCAGGAGATCGAGACCATCCC		
Alu (reverse)		TCCTGCCTCAGCCTCCCAAG		

6.3.3 DD interaction with ssDNA study

Each of the primers (SNPH16130 and SNPH00417) was suspended in TE buffer at a stock concentration of 100 μ M. From this stock, a tenfold dilution series of each primer was carried out to a final concentration of 10 nM. This corresponds to a copy value ranging from 6.02×10^{11} to 6.02×10^7 copies per μ L.

SNPH16130: TTTTTTTTTTTTTTTTTTTTTTTTTTTTTTTTTTTGTACTACAGGTGGTCAAGT (59 bases)

SNPH00147: TTTTTTTTTTTTTTTTAATATTGAACGTAGGTGCGATAAATAATRRRATG (51 bases)

Each dilution of each primer (1 μ L) was combined with buffer and dye, to a final concentration of 0.5X. This was performed in quadruplicate. These were then analysed on the RotorGene Q with the following changes;

1. No amplification was taking place so after 5 cycles of PCR, the instrument was paused, and the next highest dilution was substituted.
2. This was repeated until all dilutions, starting from the lowest to the highest, had been analysed.
3. A melt curve was carried out after the highest dilution was analysed.

Due to the initial reading of the RotorGene, which takes a 'background' signal that is then subtracted from each sample; it was needed to manually increase the concentration of primers in the reactions to determine if there was any increase in the fluorescent signal as the template increased.

6.4 Further results and discussion

DNA binding dyes were investigated for their use in qPCR due to having similar properties to both SG and EG, as these two dyes are currently used within qPCR for DNA quantification [20, 25, 26] and high resolution melt (HRM) curve analysis for EG only [19]. Figure 6.1 shows the initial results of amplifying DNA at 1X concentrations of the dyes, the only dye that showed amplification was DD, both RS, GG and GR showed no product amplification. Table 6.1 shows DD having a much lower average quantitation cycle (Cq) value than EG and when analyzing using the diamond channel has a lower Cq than SG. From the raw fluorescent results (see appendix F, Figure F-2) it showed that RS was a naturally fluorescing dye with a signal at a constant 100, throughout the analysis.

Table 6.2: Average Cq and standard deviation values of the dyes that amplified product analyzed using the Green and Diamond channel.

Dye	Green Channel		Diamond Channel	
	Average Cq	Standard deviation	Average Cq	Standard deviation
SG	27.60	0.09	27.95	0.13
DD	21.63	0.19	19.55	0.09
SG fast	20.07	0.12	19.78	0.05
EG	24.37	0.10	24.02	0.36
Threshold of the reaction was set at 0.05, Diamond channel excitation at 470 ± 10 nm and excitation at 557 ± 5 nm, Green channel excitation at 470 ± 10 nm and emission at 510 ± 5 nm. Primers were human 2 and universal primer 1. Neat DNA (1) was quantified by Qubit at 28.4 ng/ μ L. Reactions were done in quadruplicate.				

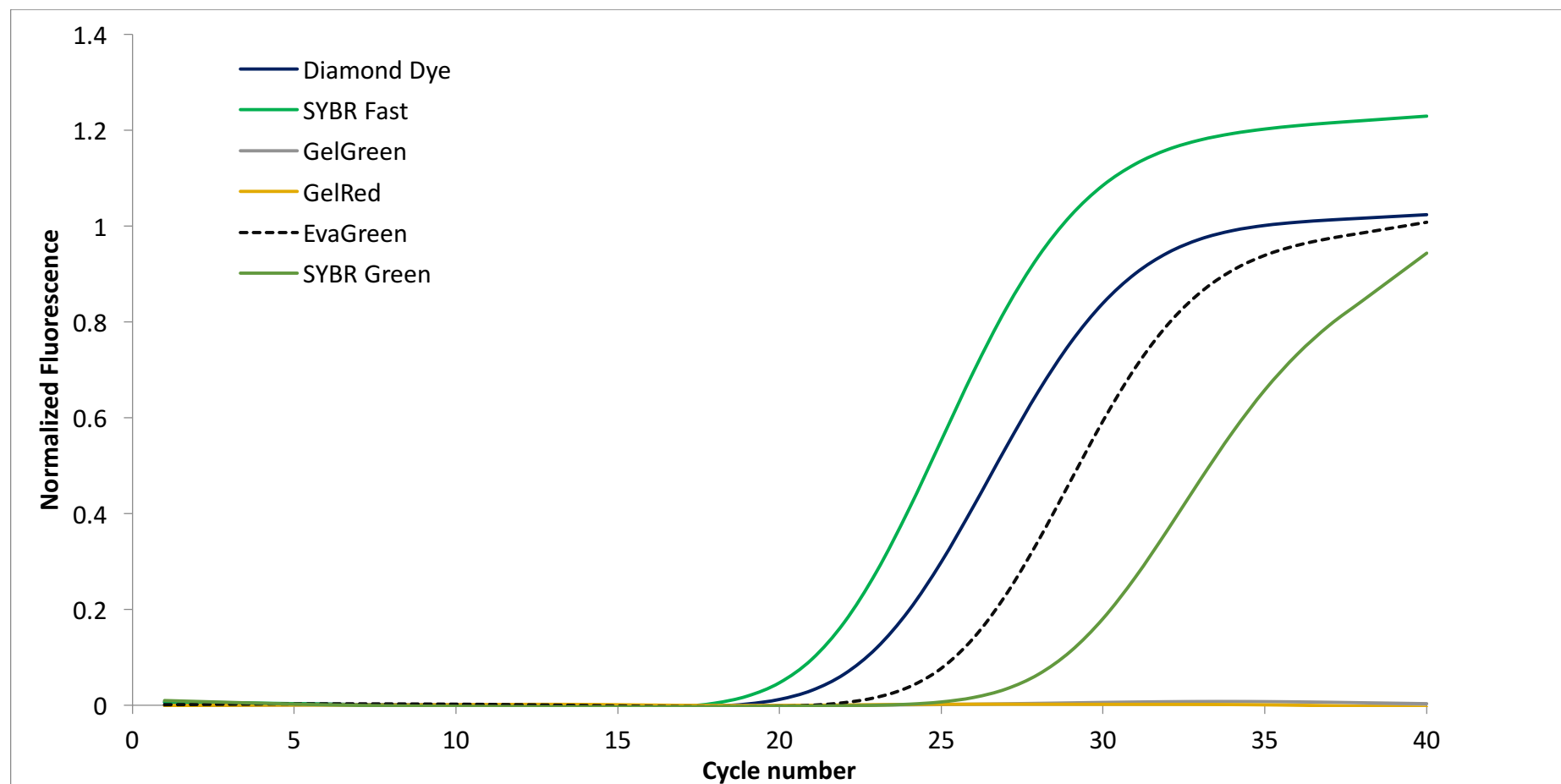


Figure 6.1: DNA binding dyes screened for potential use in qPCR, analysis was undertaken with the Green Channel with DNA at a concentration of 28.4 ng/ μ L, reactions were done in quadruplicate.

All six nucleic acid binding dyes were analyzed for their ability to be used in qPCR. SG and EG have already been established as suitable for qPCR but RS, GG, GR and DD have not been used previously. From the preliminary results (see Appendix F) it was shown that DD was the only dye out of the four that showed potential for use within qPCR. RS only showed a signal in the melt curve analysis but no signal in the cycling window.

Table 6.3: Average Cq and standard deviation values of the combination of dyes that amplified product analyzed using the Green and Diamond channel.

Dye	Green Channel		Diamond Channel	
	Average Cq	Standard deviation	Average Cq	Standard deviation
SG.K	27.32	0.04	25.18	0.16
SG.DD	27.15	0.06	23.40	0.08
SG.GG	27.17	0.18	25.20	0.20
EG	31.60	0.20	30.19	0.31
GG	-	-	37.94	0.88
Threshold of the reaction was set at 0.05, Diamond channel excitation at 470 ± 10 nm and excitation at 557 ± 5 nm, Green channel excitation at 470 ± 10 nm and emission at 510 ± 5 nm. Primers were human 2 and universal primer 1. Neat DNA (1) was quantified by Qubit at 28.4 ng/ μ L. Reactions were done in quadruplicate. SG.DD (SYBR fast with 0.5X DD present in reaction), SG.GG (SYBR fast with 1X GG present in the reaction).				

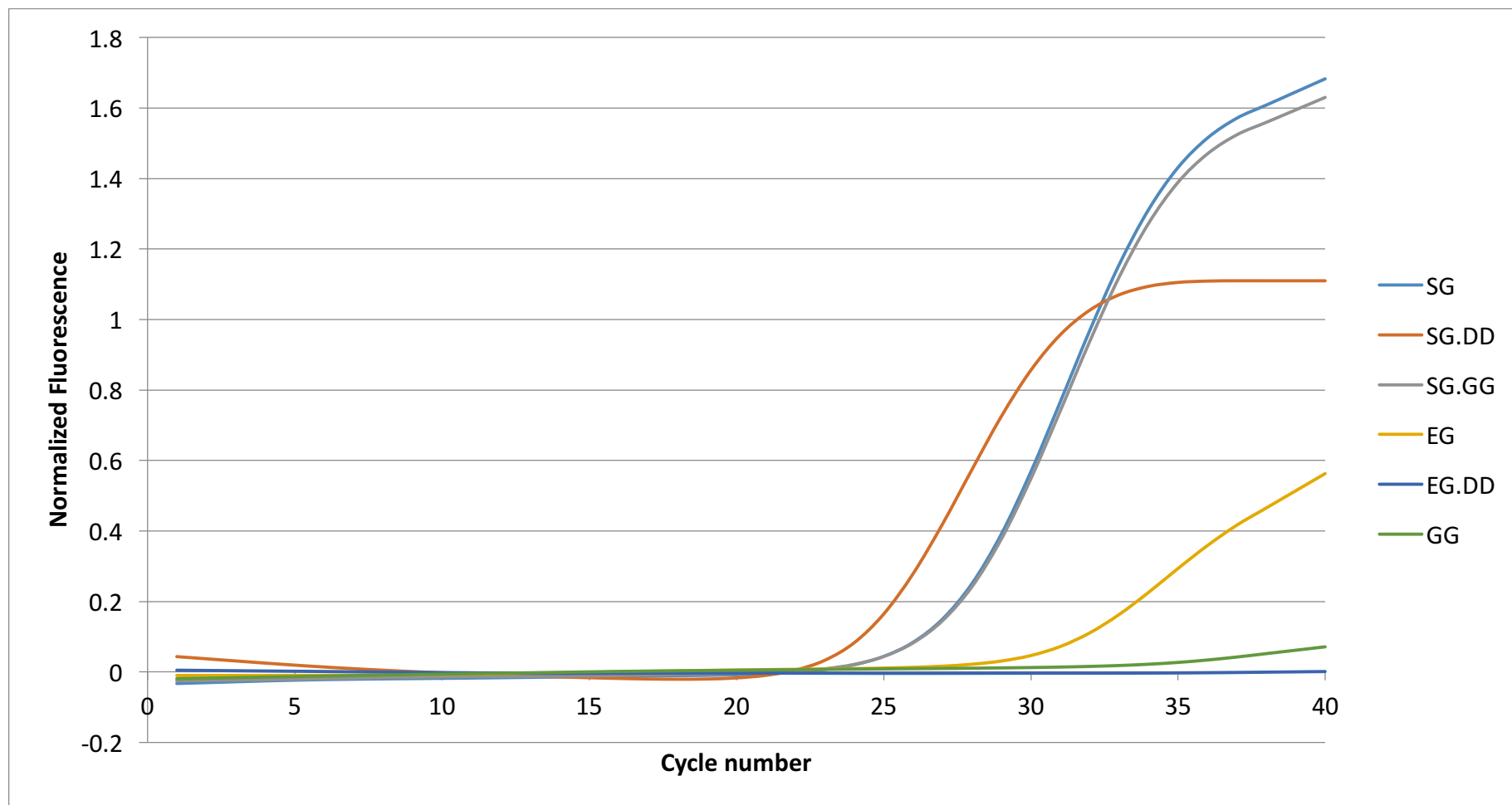


Figure 6.2: Average neat DNA analysis using DNA dye combinations, DNA concentration at 28.4 ng/ μ L, all reactions were done in quadruplicate.

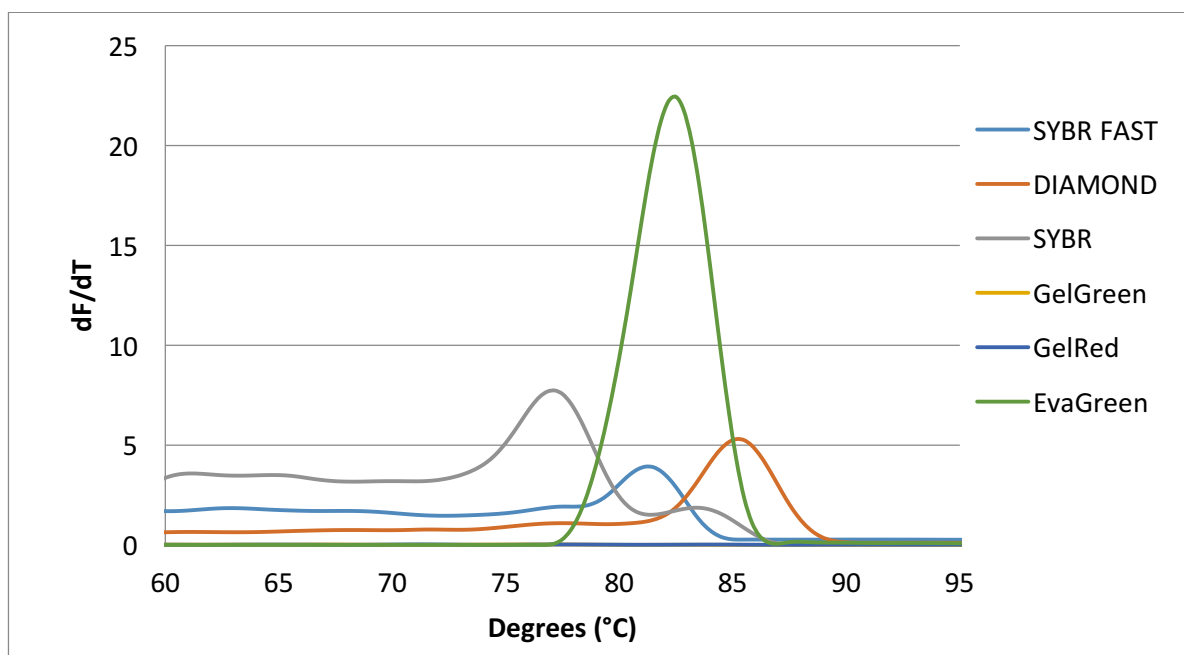


Figure 6.3: Average melt curve of screened dyes analysis was undertaken using the Green channel, reactions were done in quadruplicate.

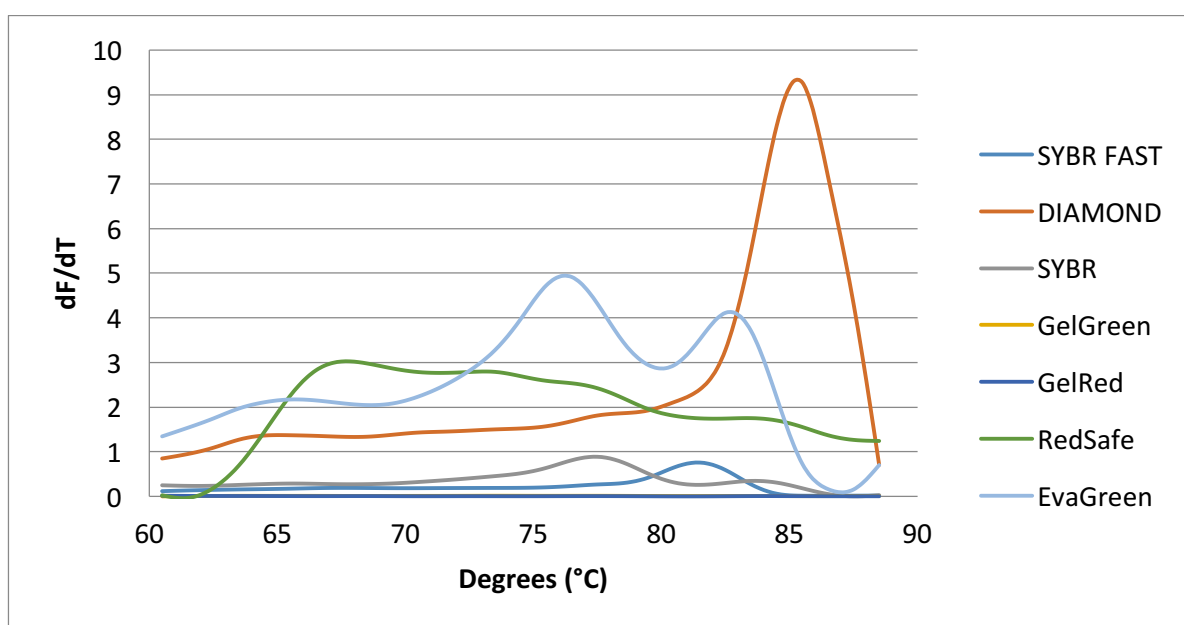


Figure 6.4: Average melt curve of screened dyes analysis was undertaken using the Diamond channel, reactions were done in quadruplicate.

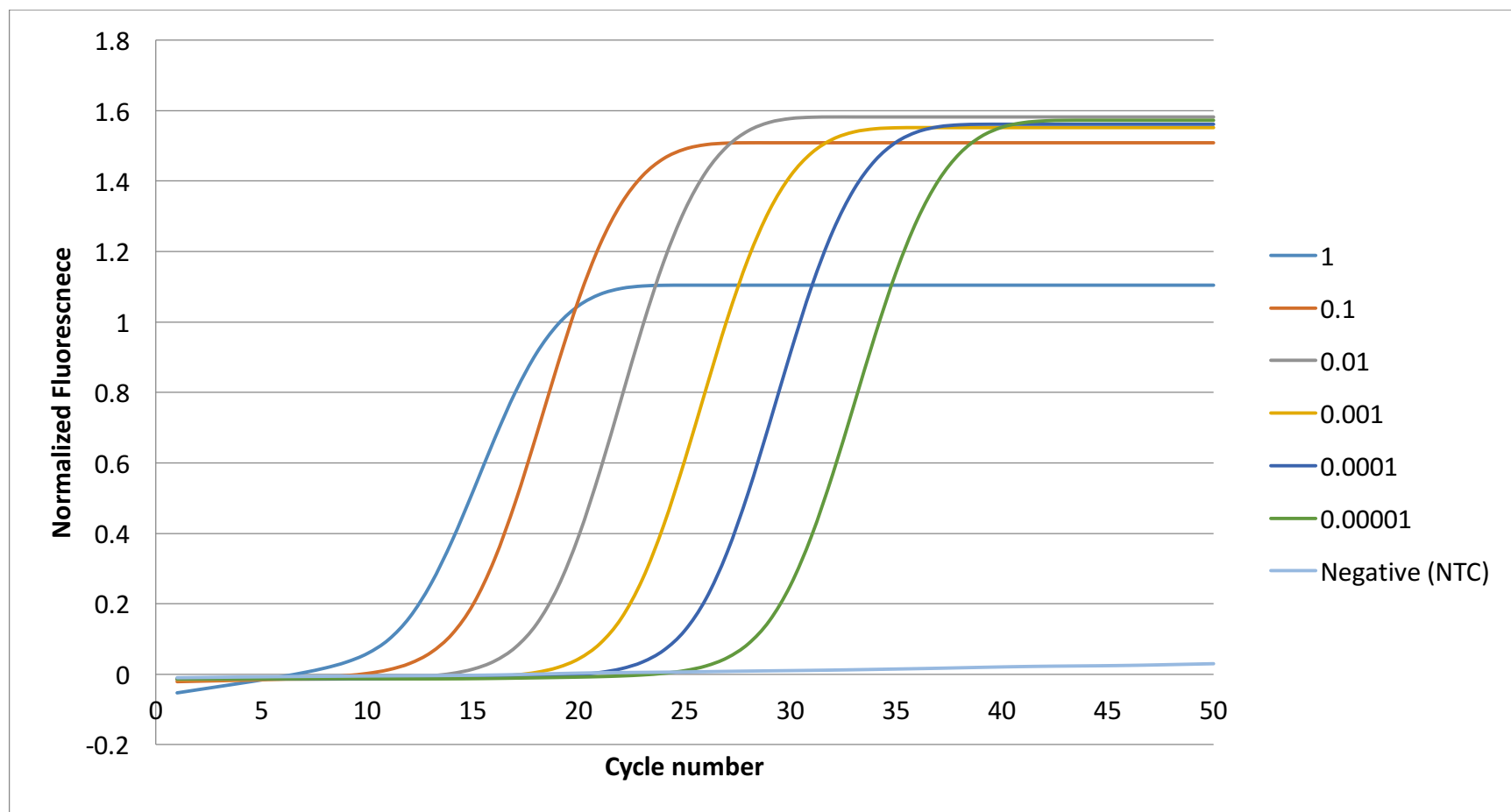


Figure 6.5: SG.DD dilution series using human fragment 2 analysis using diamond channel. All reactions were done in quadruplicate.

Table 6.3: Dilution series using dye combination of SG.DD (DD at 0.5X concentration).

Dilution	Diamond Channel		Green Channel	
	Average Cq	Standard deviation	Average Cq	Standard deviation
1	9.69	0.06	13.3	0.05
1/10	12.7	0.03	16.6	0.05
1/100	16.4	0.01	20.3	0.08
1/1000	19.4	1.68	23.2	1.61
1/10,000	23.6	0.45	27.4	0.41
1/100,000	27.3	0.80	31.3	0.86
Threshold of the reaction was set at 0.05, Diamond channel excitation at 470 ± 10 nm and excitation at 557 ± 5 nm, Green channel excitation at 470 ± 10 nm and emission at 510 ± 5 nm. Primers were human 2 and universal primer 1. Neat DNA (1) was quantified by Qubit at 28.4 ng/μL. Reactions were done in quadruplicate.				

Table 6.3 above shows the average Cq values from the SG.DD dilution series using both the Diamond channel and the Green channel. Using the Diamond channel resulted in lower average Cq values by around 4 cycles. Efficiency of the reaction can be calculated using the slope from the line of best fit (Figure 6.6), the equation is shown below [27].

$$Efficiency = 10^{\left(\frac{1}{-slope}\right)} - 1$$

The calculated efficiency for the SG.DD dilution series using the Diamond channel was 0.912 and for the Green channel was 0.897. Using the Diamond channel shows a higher efficiency of the reaction as well as lower average Cq values (3.6-4 cycles lower).

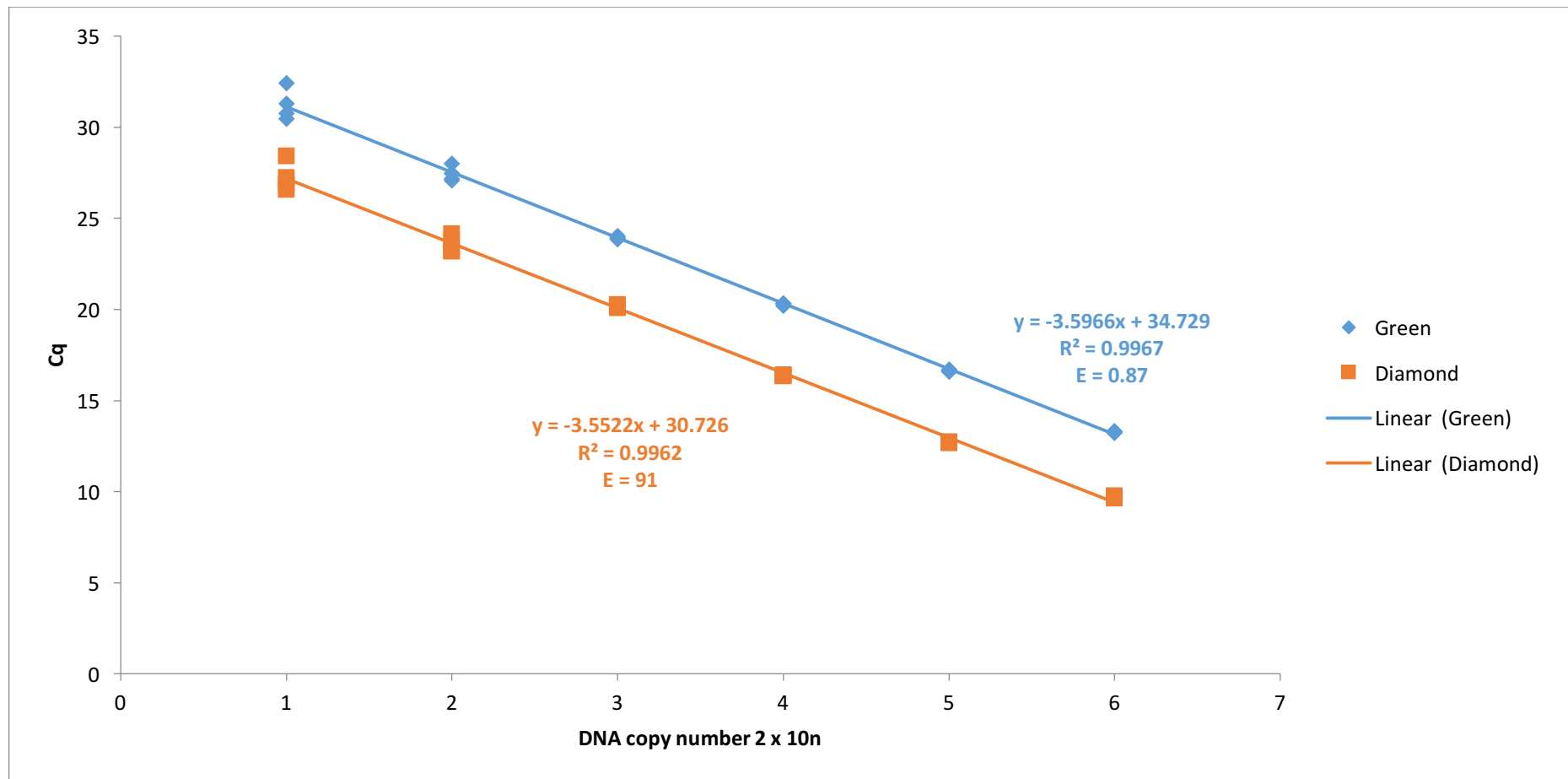


Figure 6.6: Standard curve of SG.DD showing analysis using the Diamond channel and the Green channel, reactions were done in quadruplicate.

Table 6.4: SG Kapa dilution series using human fragment 2 primers.

Dilution	Diamond Channel		Green Channel	
	Average Cq	Standard deviation	Average Cq	Standard deviation
1	9.490	0.14	11.26	0.03
1/10	12.27	0.03	14.29	0.05
1/100	16.43	0.19	18.35	0.13
1/1000	19.82	0.05	22.00	0.07
1/10,000	23.12	0.31	25.25	0.19
1/100,000	28.56	0.20	30.90	0.28
Threshold of the reaction was set at 0.05, Diamond channel excitation at 470 ± 10 nm and excitation at 557 ± 5 nm, Green channel excitation at 470 ± 10 nm and emission at 510 ± 5 nm. Primers were human 2 and universal primer 1. Neat DNA (1) was quantified by Qubit at 28.4 ng/ μ L. Reactions were done in quadruplicate.				

The comparison of the SG dilution series using both the Green channel and Diamond channel results in on average 2.06 cycles slower when using the Green channel (Table 6.4). The calculated efficiency for the SG dilution series using the Diamond channel was 0.848 and for the Green channel was 0.819 (Figure 6.7). Table 6.5 shows the comparison of the R^2 and efficiency of the SG dilution series to SG.DD dilution series. The SG.DD dilution series shows a high R^2 value and efficiency using both channels compared with the SG dilution series.

Table 6.5: Comparison of R^2 and efficiency values of SG and SG.DD dilution series using both the green and diamond channel.

	R^2 (Green)	R^2 (Diamond)	Efficiency (Green)	Efficiency (Diamond)
SG	0.992	0.991	0.819	0.848
SG.DD	0.997	0.996	0.897	0.912

Table 6.6: Difference in average Cq values for the SG.DD and SG dilution series using both Diamond and Green channels.

Dilution	Difference in Cq _(SG.DD-SG) using Diamond channel	Difference in Cq _(SG.DD-SG) using Green channel
1	0.2	2.04
1/10	0.43	2.31
1/100	-0.03	1.95
1/1000	-0.42	1.2
1/10,000	0.48	2.15
1/100,000	-1.26	0.4
Overall average difference	-0.1	1.7

Table 6.6 above shows that there were only slight differences in the average Cq when comparing the SG dilution series with SG.DD (addition of 0.5X DD) dilution series using both the Green channel and the Diamond channel. For the Diamond channel there was an overall average of -0.1 cycle of a difference between the two reactions. Using the Green channel there was an overall average of 1.7 cycle's difference between the reactions.

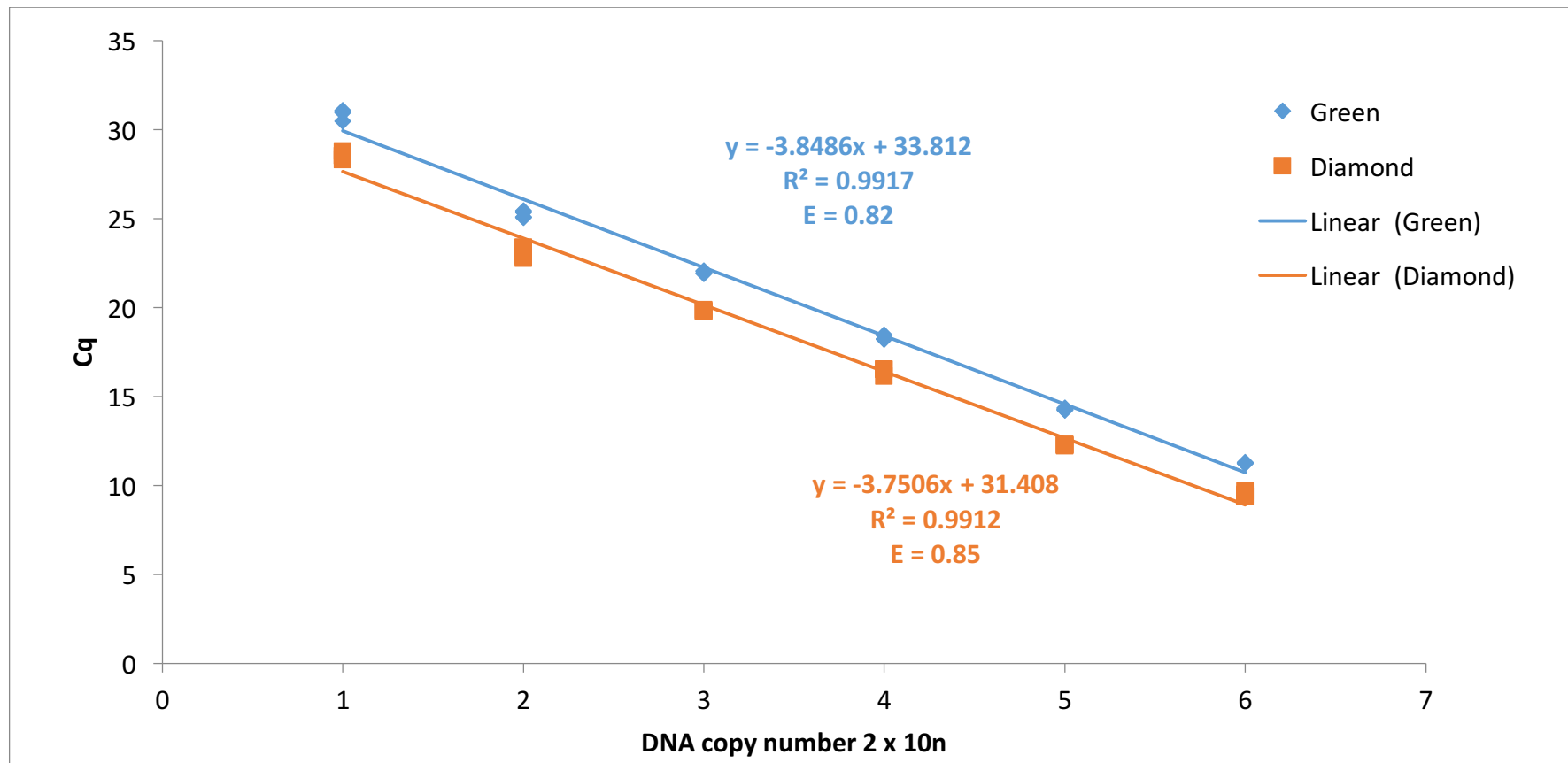


Figure 6.7: Standard curve of SG Diamond channel of SG dilution series and Green Channel of SG dilution series, and reactions done in quadruplicate.

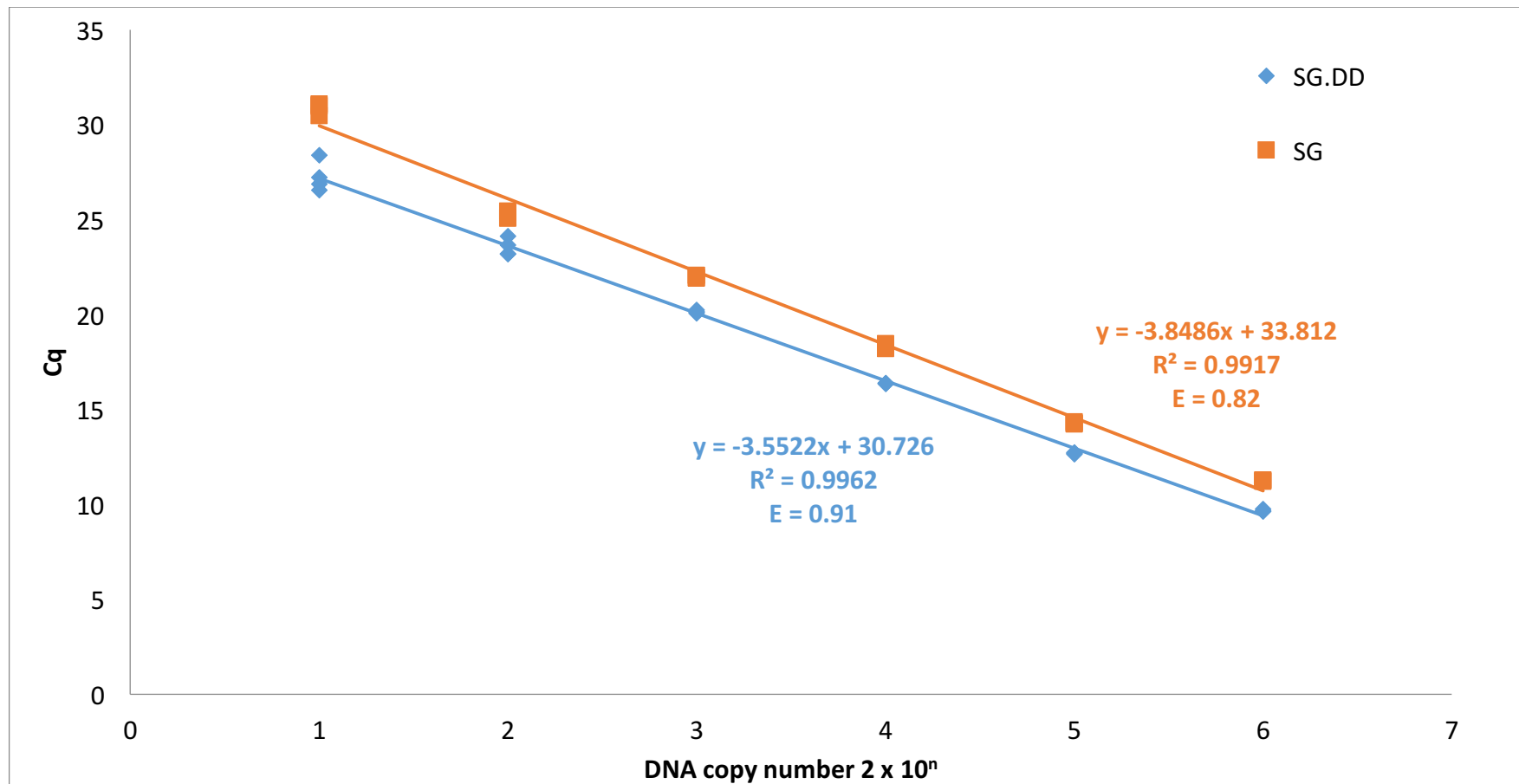


Figure 6.8: Standard curve of SG and SG.DD Diamond channel analysis was used for SG.DD and Green Channel was used for the analysis of the SG dilution series, and reactions done in quadruplicate.

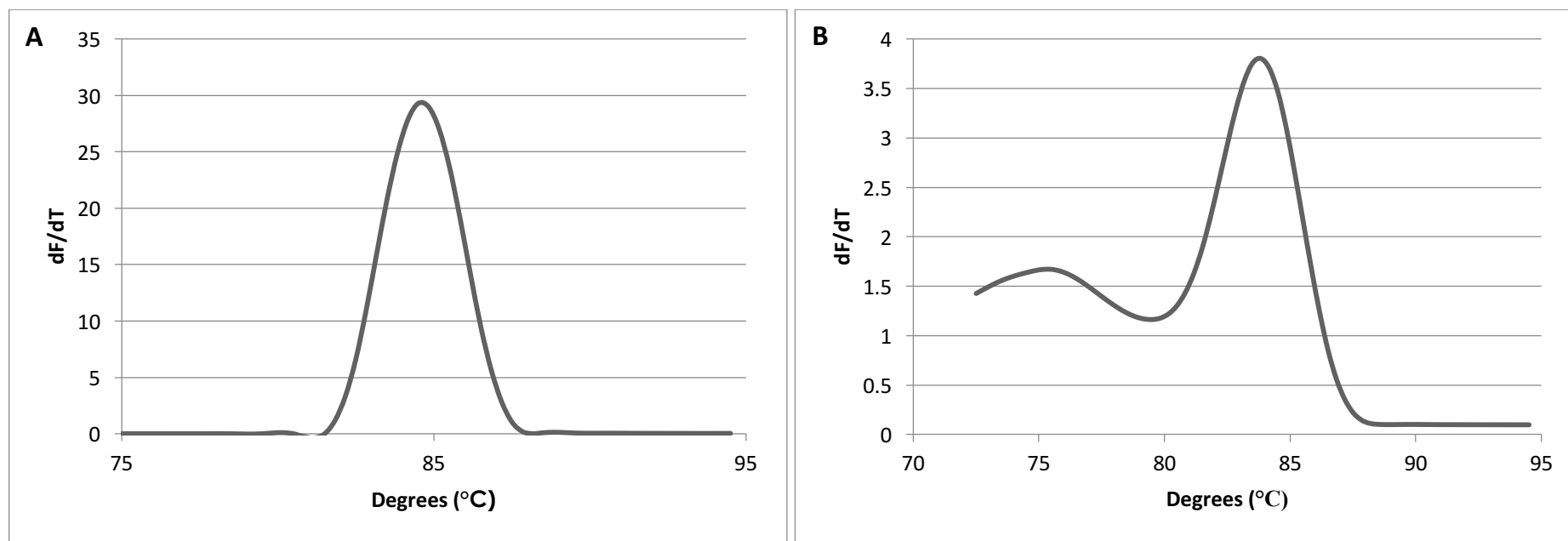


Figure 6.9: Average melt curve of SG.DD (A) Diamond channel, (B) Green channel, reactions done in quadruplicate.

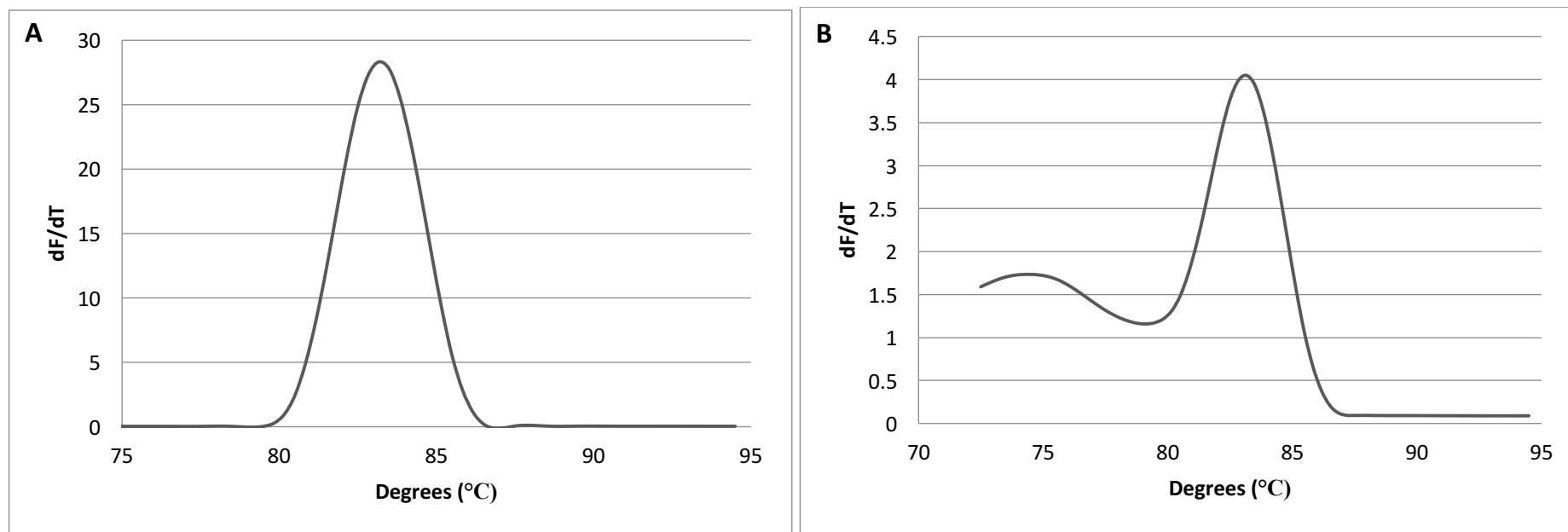


Figure 6.10: Average melt curve of SG (A) Diamond channel, (B) Green channel both reactions done in quadruplicate.

The melting curves for the SG dilution series shows an average peak at 83.5 °C using the Diamond channel and a main peak at 83.2 °C and a shoulder peak at 74.5 °C for the Green channel (see Figure 6.10). The melting curves for SG.DD shows an average peak at 84.8 °C using the Diamond channel and a main peak at 83.8 °C and a shoulder peak at 75.0 °C using the Green channel (see Figure 6.9). It should be noted that both melt curves using the Green channel show the shoulder peak; most likely representing the melting of the primers. This was not observed for the melt curves using the Diamond channel.

Figure 6.11 shows the comparison between SG reaction and when DD was added to the reaction done in quadruplicate. This shows that SG.DD had a lower C_q value compared with SG indicating that with the addition of DD to the SG reaction there was a decrease in the average C_q value for neat DNA (28.4 ng/μL).

Figure 6.12 shows the cycling curve and standard curve of DD using a human nuclear target, showing that DD can be used with both mitochondrial primers and nuclear primers. The efficiency of the reaction was high at 1.03 as well as the R² at 0.992. Both the efficiency and the R² values were higher using the nuclear target compared with the mitochondrial target with the efficiency at 0.83 and R² value at 0.97 (see Figure 4 of publication, section 6.2).

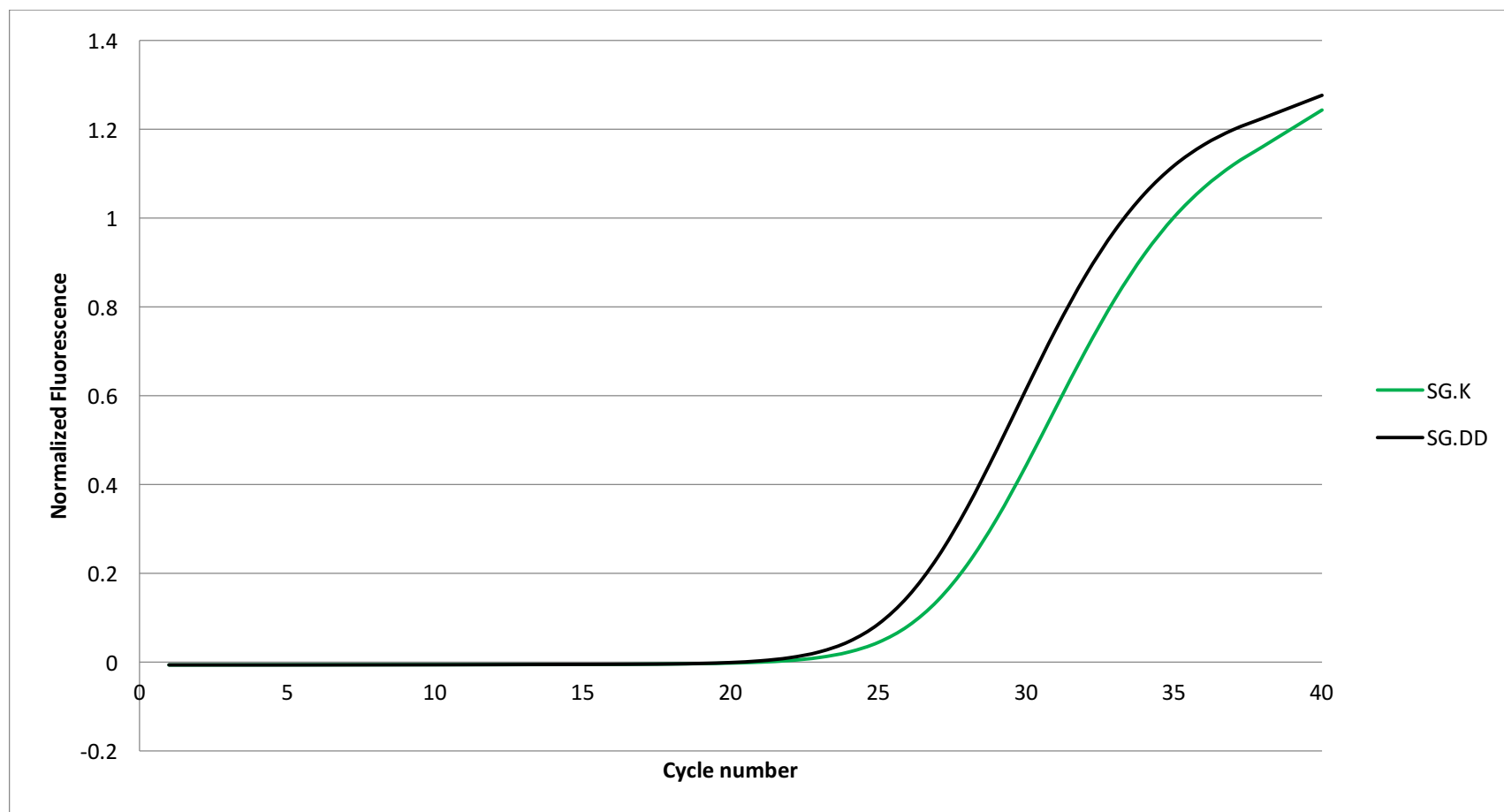


Figure 6.11: Comparison of neat DNA using SG and SG.DD reactions were done in duplicate using the green channel.

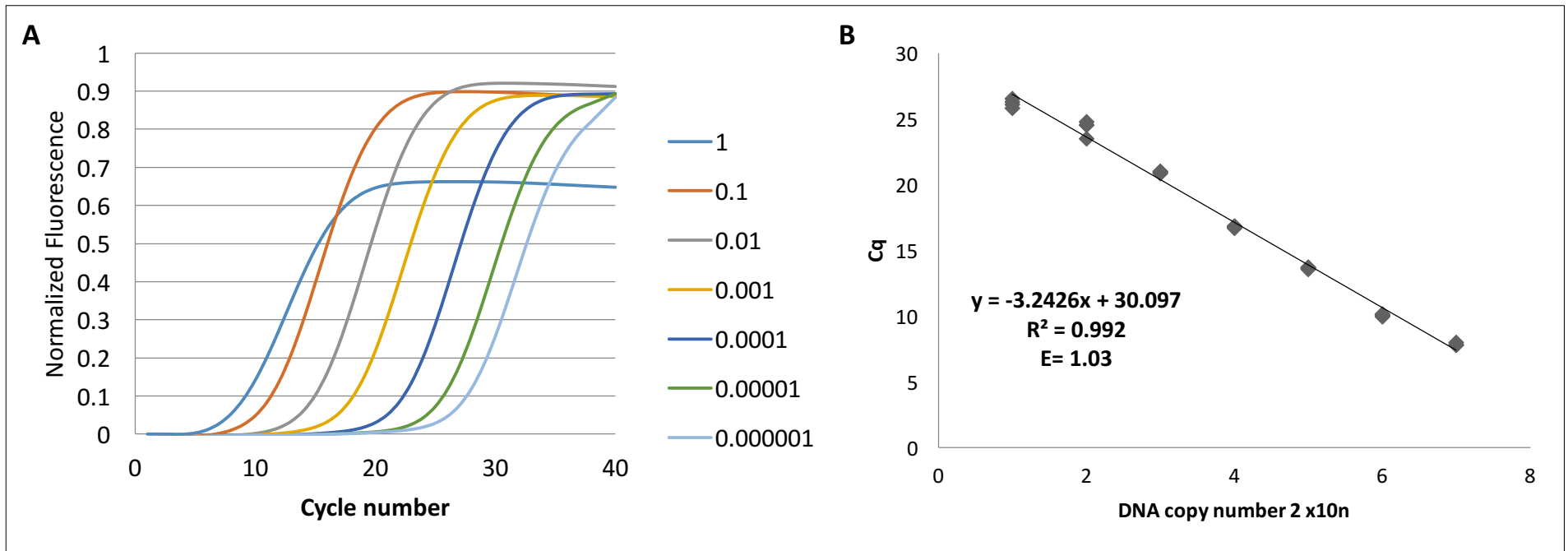


Figure 6.12: (A) Average Cycling curve using ALU nuclear DNA target, (B) Standard curve of ALU nuclear DNA target, using DD at 1X concentration with 1 being neat DNA at 28.4 ng/μL concentration.

6.4.3 Analysis of DD ssDNA binding

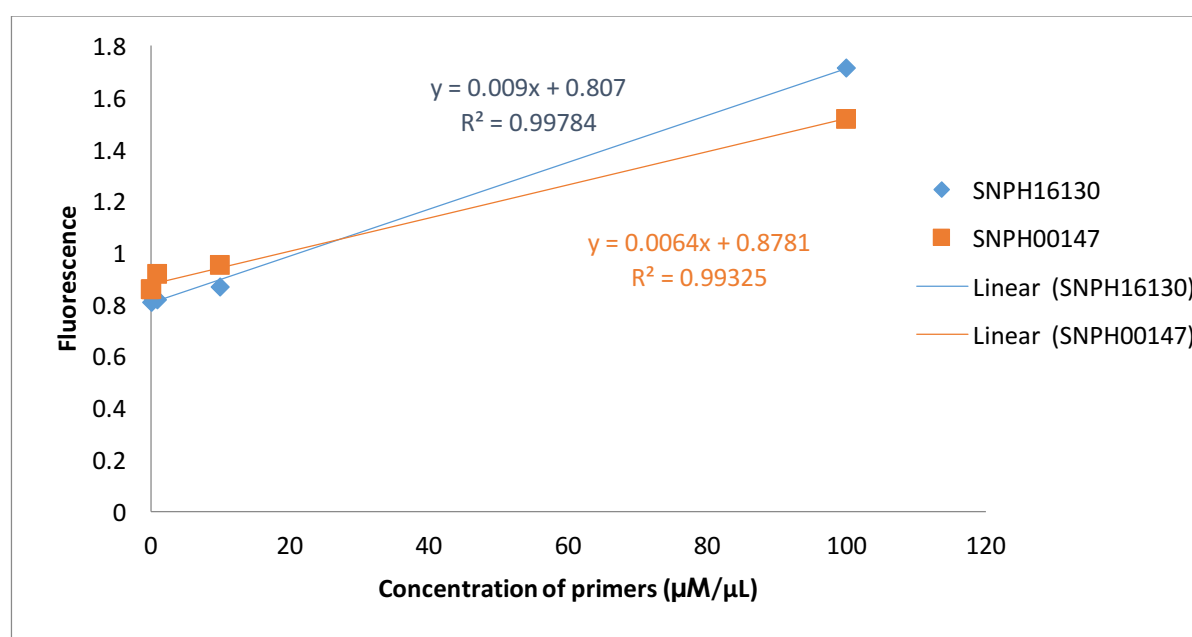


Figure 6.13: Average fluorescent signal of DD (0.5X) binding to ssDNA primers at varying concentrations and length, down in quadruplicate.

It was found that there was an increase in fluorescent signal with an increase in template as seen in Figure 6.13. This indicates that some ssDNA binding was occurring. When looking at the raw fluorescent signal when ds-DNA was present the signals produced up to 100 in fluorescence (see Appendix Figure E-2). Having ss-DNA binding at a maximum of 1.8 in fluorescence, it can be seen that this would have very minimal effect on the reaction when ds-DNA is present.

DD in Figure 6.13 has a higher fluorescent signal when binding with SNPH00147 (51 bases) compared with SNPH16130 a larger fragment (59 bases) at lower concentrations (0-10 μM/μL). At the highest concentration (100 μM/μL) there was a shift and the larger fragment now has a higher fluorescent signal than the smaller fragment. This would be as expected as the larger the fragment is the more potential binding sites DD has.

The melt curve however (Figure 6.14), indicates that this ssDNA binding was not as strong as that of dsDNA and the signal largely dies off early in the melt analysis. This was further supported by the expected melt curve morphology when a fragment was present. The DD

melt curve is the same shape and at a higher intensity than the other tested dyes (see Figure 4 in Section 6.3).

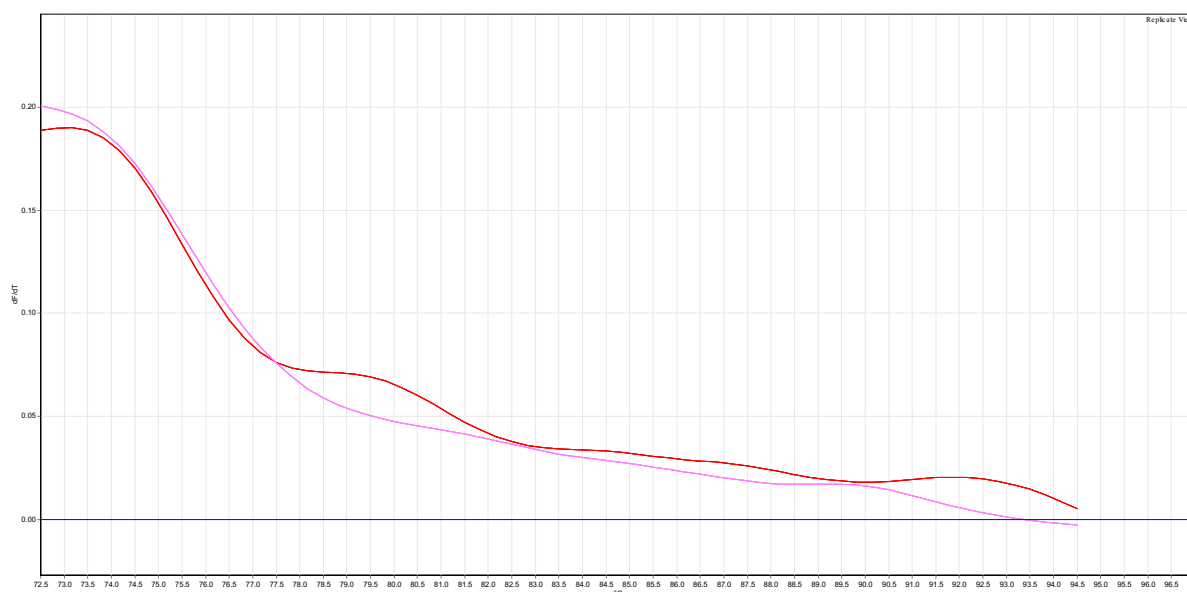


Figure 6.14: Average melt curve analysis of DD with ss-DNA primers (red indicates primer SNPH16130 59 bases and pink indicates primer SNPH00147 51 bases).

DD does bind to ssDNA as shown in the figures provided. The intensity of fluorescence can reach the same level as the plateau of an actual amplification reaction, however the initial background reading should account for this. Since there is no ssDNA amplification, the level should remain consistent throughout any reaction which was the pattern observed. Furthermore, the disassociation of DD from ssDNA occurs at a low temperature, dropping off at around 73 °C, which is about 4 degrees lower than the primer dimer observed in the reactions (Figure 6.14), which dropped off at 77 °C. The unincorporated primers do not register in the melt profiles of any of the DD samples, indicating that the background reading accounts for any ssDNA binding. The binding of DD to ssDNA is therefore not a foreseeable issue with normal qPCR reactions.

6.5 Chapter Summary

Six dyes were assessed for their use in qPCR; two of those dyes are already routinely used within laboratories and were used as a control to compare the other four nucleic acid binding dyes that have previously not been used in this application. RS, GG, GR and DD were assessed to see if any of the four dyes showed potential for use within this area. DD was the only dye that showed amplification of the samples. Further analysis of this dye was then conducted to determine the level of inhibition and the optimal concentration of DD in the reaction (0.5X).

From the results obtained from this Chapter it has been shown that DD works as efficiently and has comparable sensitivity to other fluorescent dyes used within qPCR such as SG, EG and BG. The implementation of DD within routine qPCR lab work would save money as the dye is inexpensive, approximately 5-folds cheaper than SG. The overall comparison of DD compared with the commercial qPCR dyes is shown in Figure 6.15, SG was the only dye to have a lower C_q value, this would be due to the Taq in the SG reaction that has been engineered to be more resilient and overcome PCR inhibition due to the dye.

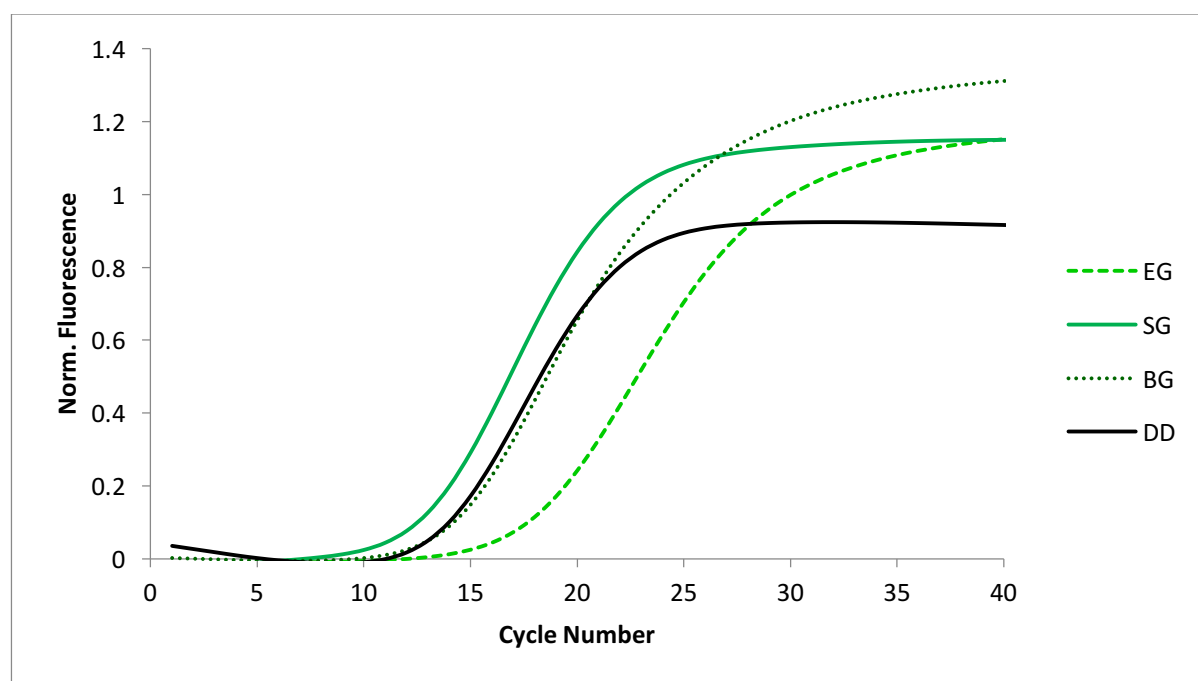


Figure 6.15: Cycling curve of fluorescence intensity against cycle number for SG, BG, EG and DD at 28.4 ng/μL. Reactions were done in quadruplicate.

6.6 References (*Supplemental to publication*)

- [1] J.M. Butler, *Chapter 5 - Short Tandem Repeat (STR) Loci and Kits*, in *Advanced Topics in Forensic DNA Typing*, Butler, J. M., Editor. 2012, Academic Press: San Diego. p. 99-139.
- [2] M.G. Ensenberger., J. Thompson., B. Hill., K. Homick., V. Kearney., K.A. Mayntz-Press., et al, Developmental validation of the PowerPlex® 16 HS System: An improved 16-locus fluorescent STR multiplex, *Forensic Science International: Genetics*. 2010, **4** 257-264.
- [3] J.M. Butler, *Chapter 3 - DNA Quantitation*, in *Advanced Topics in Forensic DNA Typing*, Butler, J. M., Editor. 2012, Academic Press: San Diego. p. 49-67.
- [4] M.C. Kline., D.L. Duewer., J.W. Redman., J.M. Butler, Results from the NIST 2004 DNA quantitation study, *J. Forensic Sci.* 2005, **50** 571-578.
- [5] J.A. Nicklas., E. Buel, Quantification of DNA in forensic samples, *Analytical and Bioanalytical Chemistry*. 2003, **376** 1160-1167.
- [6] A.I. Dragan., R. Pavlovic., J.B. McGivney., J.R. Casas-Finet., E.S. Bishop., R.J. Strouse., et al, SYBR Green I: Fluorescence Properties and Interaction with DNA, *Journal of Fluorescence*. 2012, **22** 1189-1199.
- [7] H. Goldshtein., M.J. Hausmann., A. Douvdevani, A rapid direct fluorescent assay for cell-free DNA quantification in biological fluids, *Annals of Clinical Biochemistry*. 2009, **46** 488-494.
- [8] C. Hussing., M.L. Kampmann., H.S. Mogensen., C. Børsting., N. Morling, Comparison of techniques for quantification of next-generation sequencing libraries, *Forensic Science International: Genetics Supplement Series*. 2015, **5** e276-e278.
- [9] K. Nielsen., H.S. Mogensen., J. Hedman., H. Niederstätter., W. Parson., N. Morling, Comparison of five DNA quantification methods, *Forensic Science International: Genetics*. 2008, **2** 226-230.
- [10] Y. Chen., M. Sonnaert., S.J. Roberts., F.P. Luyten., J. Schrooten, Validation of a PicoGreen-Based DNA Quantification Integrated in an RNA Extraction Method for Two-Dimensional and Three-Dimensional Cell Cultures, *Tissue Engineering Part C: Methods*. 2011, **18** 444-452.
- [11] M.O. Neill., J. McPartlin., K. Arthure., S. Riedel., N. McMillan, Comparison of the TLDA with the Nanodrop and the reference Qubit system, *Journal of Physics: Conference Series*. 2011, **307** 012047.
- [12] M. Tanaka., T. Yoshimoto., H. Nozawa., H. Ohtaki., Y. Kato., K. Sato., et al, Usefulness of a toothbrush as a source of evidential DNA for typing, *Journal of Forensic Sciences*. 2000, **45** 674-676.
- [13] S. Hayn., M.M. Wallace., M. Prinz., R.C. Shaler, Evaluation of an automated liquid hybridization method for DNA quantitation, *Journal of Forensic Sciences*. 2004, **49** 87-91.

- [14] J. Guo., J.Y. Ju., N.J. Turro, Fluorescent hybridization probes for nucleic acid detection, *Analytical and Bioanalytical Chemistry*. 2012, **402** 3115-3125.
- [15] J.R. Lakowicz, *Principles of Fluorescence Spectroscopy*. Third ed. 2006, New York, USA: Springer US.
- [16] J. Guo, J. Ju, N.J. Turro, Fluorescent hybridization probes for nucleic acid detection, *Analytical and Bioanalytical Chemistry*. 2012, **402** 3115-3125.
- [17] F. Ponchel., C. Toomes., K. Bransfield., F. T. Leong., S.H. Douglas., S.L. Field., et al, Real-time PCR based on SYBR-Green I fluorescence: an alternative to the TaqMan assay for a relative quantification of gene rearrangements, gene amplifications and micro gene deletions, *BMC Biotechnology*. 2003, **3** 18.
- [18] E. Navarro., G. Serrano-Heras., M.J. Castaño., J. Solera, Real-time PCR detection chemistry, *Clinica Chimica Acta*. 2015, **439** 231-250.
- [19] F. Mao., W.-Y. Leung., X. Xin, Characterization of EvaGreen and the implication of its physicochemical properties for qPCR applications, *BMC Biotechnology*. 2007, **7** 76-76.
- [20] S. Giglio., P.T. Monis., C.P. Saint, Demonstration of preferential binding of SYBR Green I to specific DNA fragments in real-time multiplex PCR, *Nucleic Acids Research*. 2003, **31** e136-e136.
- [21] C.J. Smith., A.M. Osborn, Advantages and limitations of quantitative PCR (Q-PCR)-based approaches in microbial ecology, *FEMS Microbiology Ecology*. 2009, **67** 6-20.
- [22] F. Di Pasquale., S. Cornelius., M. König., M. Scherer., C. Schmid., C. Dienemann., et al, Investigator® Quantiplex Kit: For reliable quantification of human DNA in forensic samples, *Forensic Science International: Genetics Supplement Series*. 2011, **3** e413-e414.
- [23] S.S. Tobe., A.M.T. Linacre, A multiplex assay to identify 18 European mammal species from mixtures using the mitochondrial cytochrome b gene, *ELECTROPHORESIS*. 2008, **29** 340-347.
- [24] J.A. Nicklas., E. Buel, Development of an Alu-based, real-time PCR method for quantitation of human DNA in forensic samples, *Journal of Forensic Sciences*. 2003, **48** 936-944.
- [25] P.T. Monis., S. Giglio., C.P. Saint, Comparison of SYTO9 and SYBR Green I for real-time polymerase chain reaction and investigation of the effect of dye concentration on amplification and DNA melting curve analysis, *Analytical Biochemistry*. 2005, **340** 24-34.
- [26] M. Buh Gašparič., T. Tengs., J.L. Paz., A. Holst-Jensen., M. Pla., T. Esteve., et al, Comparison of nine different real-time PCR chemistries for qualitative and quantitative applications in GMO detection, *Analytical and Bioanalytical Chemistry*. 2010, **396** 2023-2029.
- [27] S.A. Bustin., V. Benes., J.A. Garson., J. Helleman., J. Huggett., M. Kubista., et al, The MIQE Guidelines: Minimum Information for Publication of Quantitative Real-Time PCR Experiments, *Clinical chemistry*. 2009, **55** 611-622.

6.7 APPENDIX E (Supporting information)

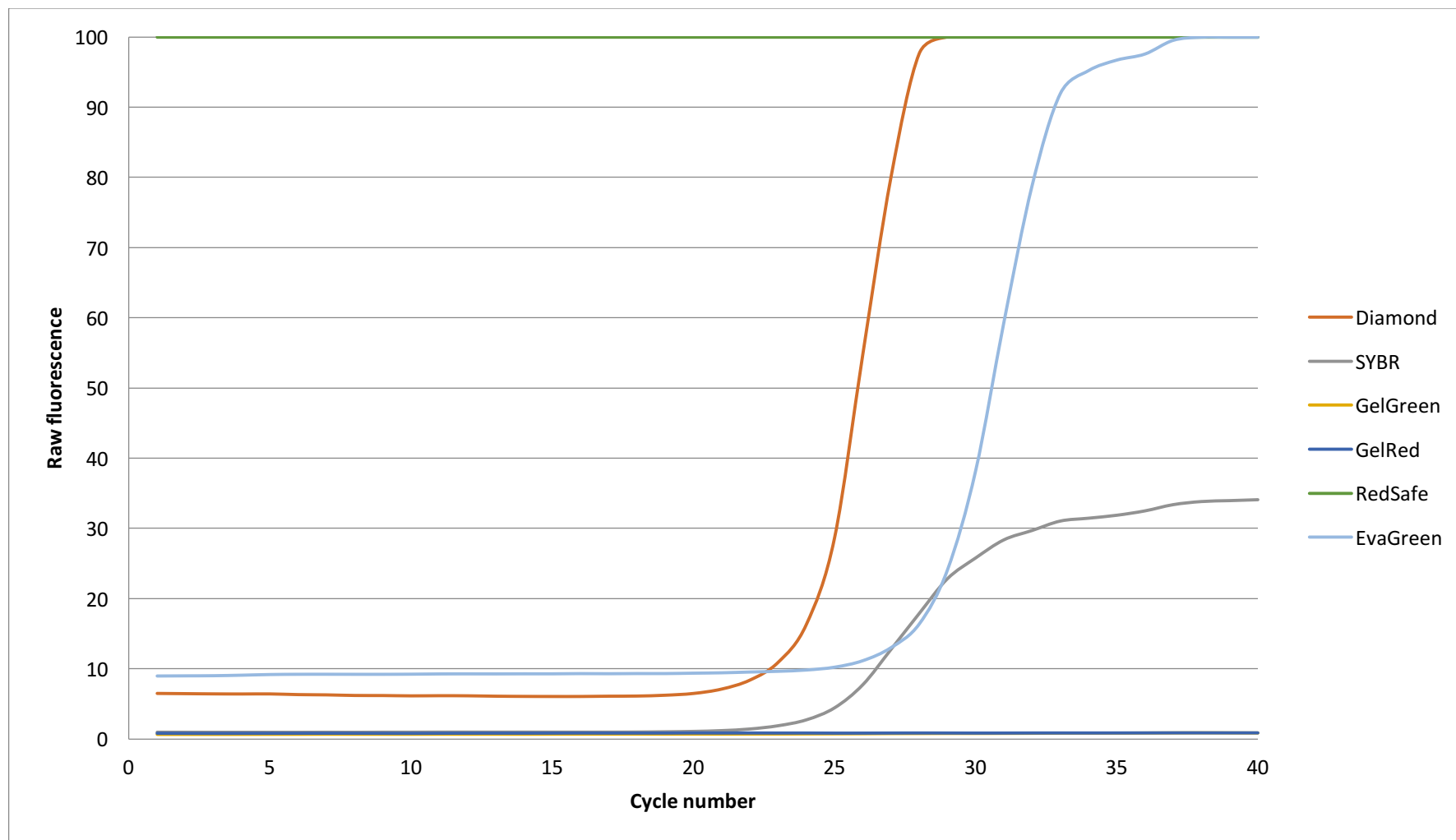


Figure E-1: Average raw fluorescent signals from the DNA binding dyes using 28.4 ng/ μ L concentration, four replicates.

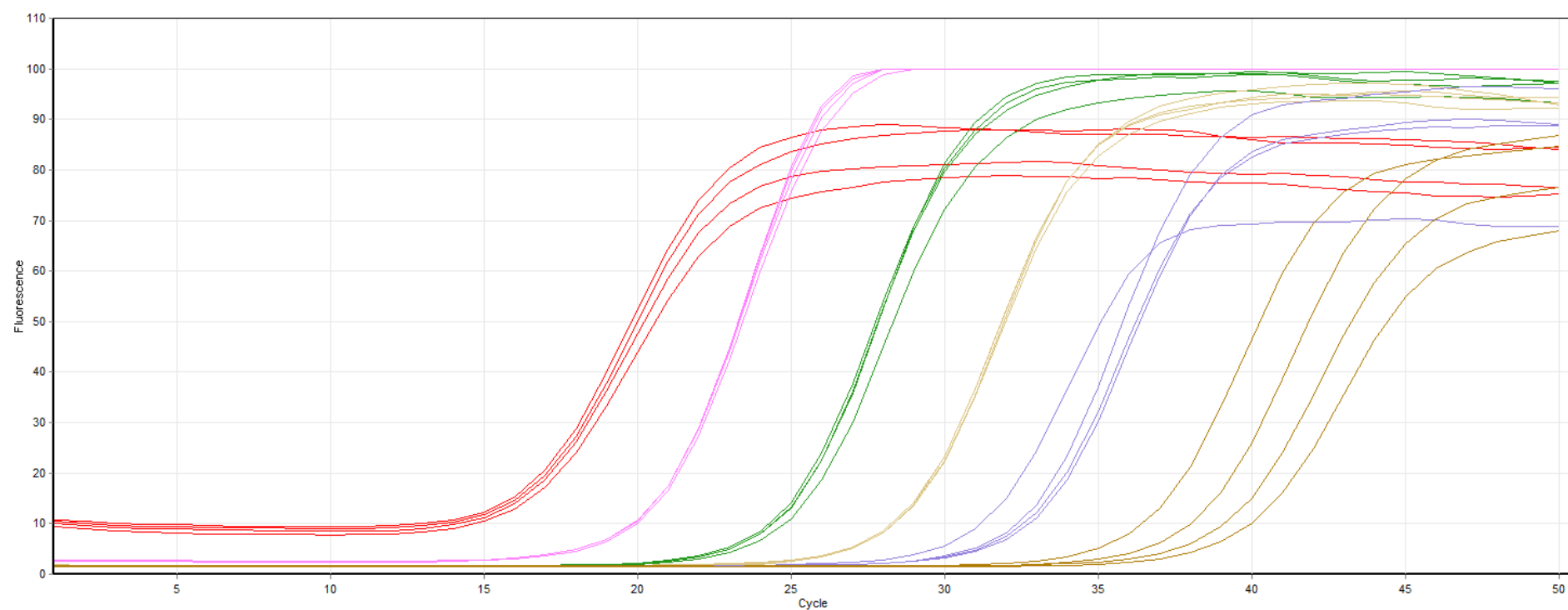


Figure E-2: Raw fluorescent signal from DD dilution series starting with 28.4 ng/μL concentration, results done in quadruplicate.

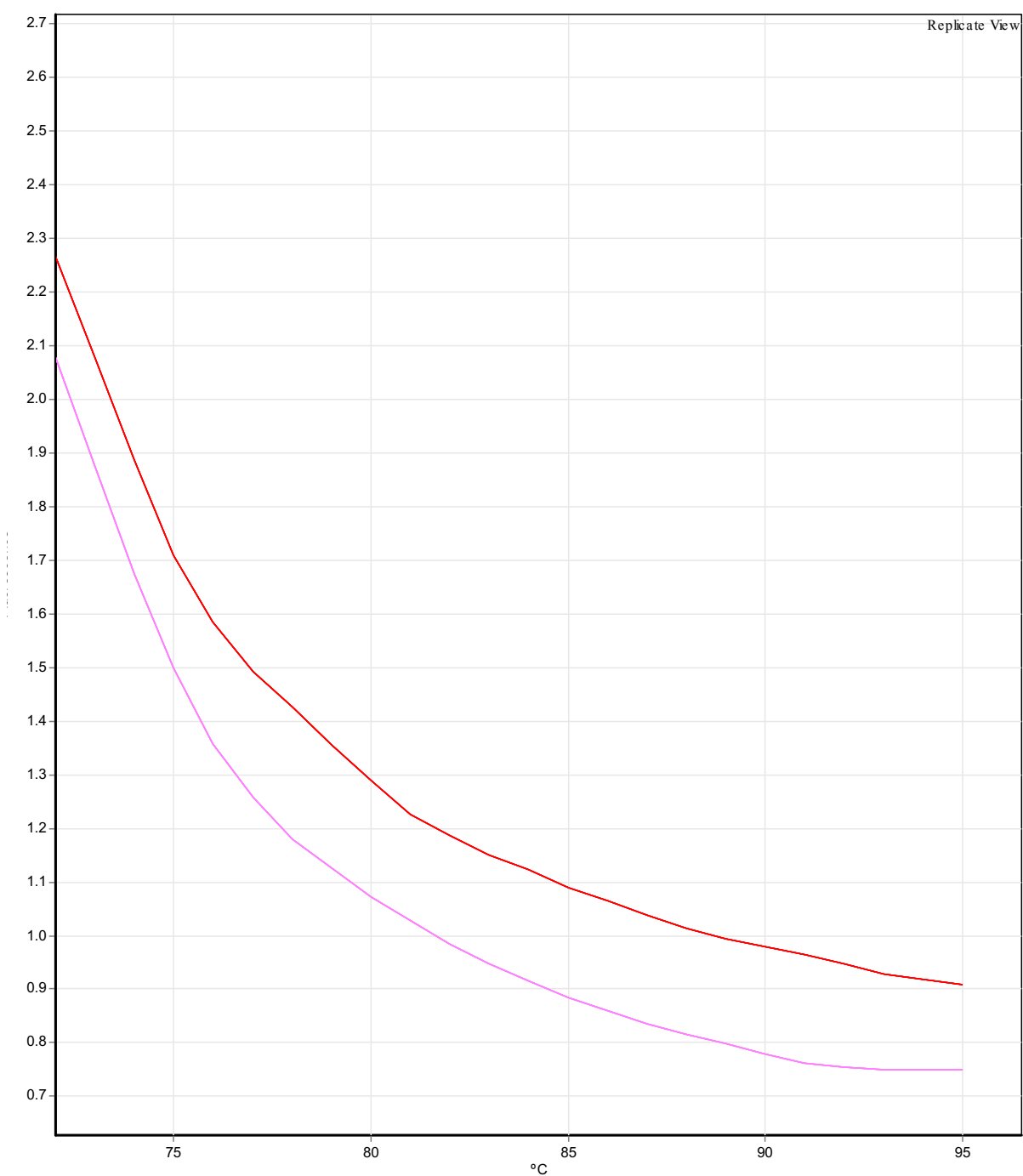


Figure E-3: Average raw fluorescent signals of DD's interaction with ss-DNA at varying temperatures using two different length primers (red indicates primer SNPH16130 59 bases and pink indicates primer SNPH00147 51 bases).

ALTERNATIVE DNA BINDING DYES FOR REAL-TIME PCR



Alicia M. Haines¹, Shanan S. Tobe^{1,3}, Hilton Kobus², Adrian Linacre¹

¹School of Biological Sciences, Flinders University, Adelaide, Australia

²School of Chemical and Physical Sciences, Flinders University, Adelaide, Australia

³Department of Chemistry and Physics, Arcadia University, Glenside, PA, USA

Forensic
Biology
Lab South
Australia

Presented at the ANZFSS 23rd International Symposium on the Forensic Sciences, Auckland, New Zealand

Funding was provided by the Attorney General's Department, South Australia

Introduction

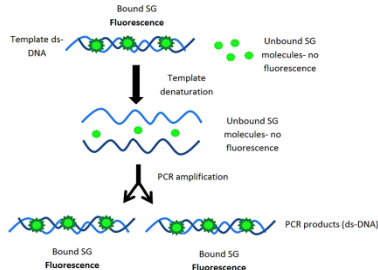


Figure 1: Schematic representation of how SYBR Green (SG) molecules bind during RT-PCR and fluorescence when bound to ds-DNA, adapted from [1]

One important aspect in forensic DNA analysis is quantifying the DNA before undergoing STR typing as the STR kits are optimized to work with DNA concentrations between 0.5-1.0 ng of total DNA [1]. There are many methods that have been used over the last decade for DNA quantification not just within forensic science but in many other scientific areas.

Intercalating dyes can be used in RT-PCR because the dye molecules can attach to the PCR amplicons and as the number of PCR products increases then the number of molecules that can attach to the DNA fragments also increase and thus an increase in the fluorescent signal indicates an increase in the amount of DNA present (Figure 1). Dyes that are currently used for the quantification of DNA include EvaGreen™ [2] and SYBR® Green I [3]. This study looks at other DNA binding dyes currently used for gel staining to see if they're applicable to real-time and quantitative PCR analysis.

Method

1. Intercalating dyes for RT-PCR

RS, DD, GG, GR along with the standard dyes for RT-PCR (SG and EG) were trialed for RT-PCR. The reaction consisted of 10 µL of KAPA Taq ReadyMix 2X (Kapa Biosystems, AUS), 0.5 µL of primer pair (Table 1), 1 µL of DYE (20X), 1 µL of DNA solution and 7.5 µL of TA buffer, in a total reaction volume of 20 µL. The channels selected for fluorescence detection were green, RS (source at 530 nm and detector at 555 nm) and diamond (excitation 470 ± 10 nm, emission 557 ± 5 nm). The PCR cycle proceeded as described in Figure 2.

2. Dye combinations for RT-PCR

0.5 µL of DD (20 X) was added to the SG reaction mix: 10 µL of KAPA SYBR FAST qPCR Master Mix 2X (Kapa Biosystems, AUS), 0.5 µL of primer pair, 1 µL of DNA solution and 8 µL of TA buffer, in a total reaction volume of 20 µL. All reactions were performed in quadruplicate. Amplifications were performed on a Rotor-Gene Q (Qiagen, AUS). The channels selected for fluorescence detection were green and diamond. The PCR cycle proceeded as described in Figure 2.

Table 1: Primer sets used in RT-PCR, fragment 1, 2 [4]

	5'—Sequence—3'	Amplicon length (bp)	T _m (°C)
Fragment 1	F- GACCAATGATATGAAAAACCATCGTTGT	246	68.72
	R- ATCGGAATGGGAGGTGATTCCTAGG		
Fragment 2	F- TGAGGACAAATATCATTYTGAGGRGC	277	72.23
	R- TTCAGCCATAATTACGTCTCGAGT		

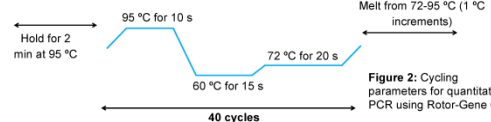


Figure 2: Cycling parameters for quantitative PCR using Rotor-Gene Q

Results and Discussion

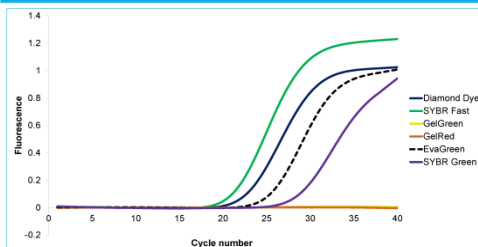


Figure 3: DNA binding dyes screened for potential use in RT-PCR, reactions were done in quadruplicate.

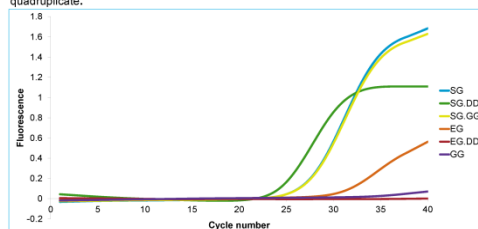


Figure 4: Neat DNA analysis using DNA dye combinations, DNA concentration at 28.4 ng/µL. All reactions were done in quadruplicate.

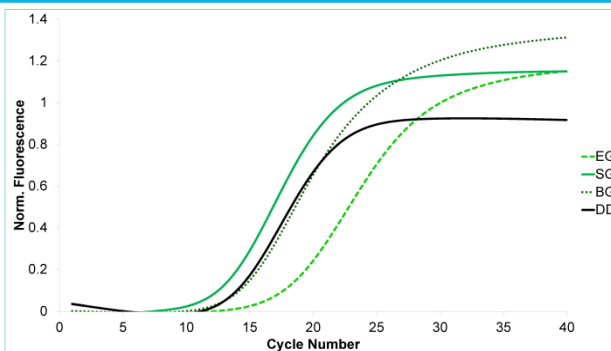


Figure 5: Average cycling curve of fluorescence intensity against cycle number for SYBR® Green (SG), BRYT® Green (BG), EvaGreen® (EG) and Diamond™ nucleic acid dye (DD) at 28.4 ng/µL. Reactions were done in quadruplicate.

- Figure 3 shows that DD was the only dye that showed an amplification product of the new dyes tested.
- Figure 2 shows that the combination of SG and DD showed a lower C_q value compared with SG alone.
- Average C_q of the different DNA binding dyes were: DD 13.82 (0.02); SG 12.33 (0.03); EG 17.45 (0.03) and BG 14.02 (0.03) for neat DNA at 28.4 ng/µL, see Figure 5 for the cycling curve of the fluorescent intensity.

Concluding Remarks

1. Diamond™ Dye is a suitable alternative to commonly used real-time reagents (SYBR®Green, EvaGreen™)
2. Other nucleic acid binding dyes such as GelGreen, GelRed and RedSafe were not suitable alternatives for real-time PCR
3. Dye combination of SYBR Green and Diamond dye shows potential with a lower C_q when compared with SYBR Green alone.

References

- [1] C. J. Smith, A. M. Osborn, Advantages and limitations of quantitative PCR (Q-PCR)-based approaches in microbial ecology, *FEMS Microbiology Ecology*, 2009, 67 6-20.
- [2] F. Mao, W.-Y. Leung, X. Xin, Characterization of EvaGreen and the implication of its physicochemical properties for qPCR applications, *BMC Biotechnology*, 2007, 7 76-76.
- [3] F. Ponchel, C. Toomes, K. Bransfield, F. T. Leong, S. H. Douglas, S. L. Field, et al. Real-time PCR based on SYBR-Green I fluorescence: an alternative to the TaqMan assay for a relative quantification of gene rearrangements, gene amplifications and micro gene deletions, *BMC Biotechnology*, 2003, 3 18.
- [4] S. S. Tobe, A. M. T. Linacre, A multiplex assay to identify 18 European mammal species from mixtures using the mitochondrial cytochrome b gene, *ELECTROPHORESIS*, 2008, 29 340-347.

Correspondence: Alicia M. Haines, Flinders University, South Australia, Ph. (08) 8201 5003, alicia.haines@flinders.edu.au

Figure E-4: Poster presentation at the ANZFSS 23rd international symposium on the forensic sciences, New Zealand.

Alicia Haines

From: em.bt.0.4c9e8b.4ea41472@editorialmanager.com on behalf of BioTechniques
<em@editorialmanager.com>
Sent: Tuesday, 19 July 2016 11:43 PM
To: Alicia Haines
Subject: BioTechniques MS#BT6199R1 ACCEPTED

Follow Up Flag: Follow up
Flag Status: Flagged

Dear Ms. Haines:

I am pleased to inform you that your manuscript "Optimization of Diamond™ Nucleic Acid Dye for quantitative PCR" has been accepted for publication.

Page proofs will be prepared and sent by email as a PDF. Please let us know of any upcoming changes in your mailing address, FAX number, or email address.

If you would like to order reprints, instructions will be provided in the page proofs email that will be sent to you in the future.

Thank you for contributing your manuscript to BioTechniques.

Best regards,
Patrick C.H. Lo, Ph.D.
Senior Editor

Figure E-5: Publication acceptance email as proofs of paper are yet to be received. Publication is slated for the October issue.

Chapter 7

Conclusion & future impact

7.1 Preface

The final Chapter of this thesis discusses the body of knowledge now available and the impact that this research has had on the forensic community, as well as new directions for this work using intercalating dyes for detecting latent DNA moving into the future. Specifically, section 7.3 discusses in detail the future directions of this work including work that is applicable within the laboratory and in the field of evidence recovery.

Laboratory-based applications include staining tape-lifts for the detection of DNA and targeted direct sampling showing preliminary results; along with common evidentiary items found at crime scenes or submitted items where touch DNA is the focus of sampling. These items could include; bullet casings, cartridge casings, firearms and wires used in explosive devices.

Field based applications require further work for the implementation of the dye as a spray to view touch-DNA at crime scenes. This would involve work on the type of spray device to get at even application of dye as well as modifications in the buffer suitable for crime scene application; quick drying, even spray with no small droplets, low dye concentration to reduce toxicity and protect crime scene investigators.

7.2 Concluding remarks

The research contained within this thesis has unquestionably had an impact on the forensic community and has highlighted the potential advantages of using intercalating dyes within forensic analyses. This has been demonstrated by: 8 publications; a total of 12 conference presentations nationally and internationally (7 posters, 5 oral presentations) with the highlight being the Best Poster Award (out of over 400 posters) at the ISFG in Krakow; as well as 6 other seminars and presentations given locally and 7 awards and scholarships to attend conferences.

The work outlined in this thesis began with little to no published knowledge on the use of intercalating dyes for the detection of latent DNA, except for a very few publications on staining hairs using DAPI [1-4], TOTO-3 [5] and Hoechst 33258 [6]. No papers had been published or even presented at conferences about the application of these dyes to detect latent DNA as a surface-based application. That is where the story and the idea started for this PhD thesis. Not only does this thesis provide the body of knowledge to undertake further research in this area but has also resulted in projects that are now applicable within a forensic laboratory. This includes the use of Diamond Dye as tool for determining the viability of a hair for STR analysis, as well as the use of the dye in quantitative PCR, as it is a much cheaper alternative to SYBR Green I.

The dyes were also evaluated for their downstream effects on extraction, quantification, amplification and STR typing; which has formed part of the body of knowledge in order to take further research steps in establishing a method for the detection of latent DNA on evidentiary items commonly found at a crime scene.

Table 7.1 shows the overall ranking of all the different properties that were investigated throughout the duration of this thesis. EG appears the most in the top three for most categories with DD not far behind. The main reason to use DD over EG is due to the background signal of EG, but also due to the fluorescent enhancement which is stated by the literature to be around 70-fold [7], although the enhancement of DD is not stated within the literature, in Chapter 4 the dyes were compared and was ~1.5 folds higher than EG in

the presence of DNA. The other reason DD appears to be superior to EG is the detection limit which is lower for DD than EG.

Table 7.1: Overall ranking of the dyes for each characteristic investigated within this thesis.

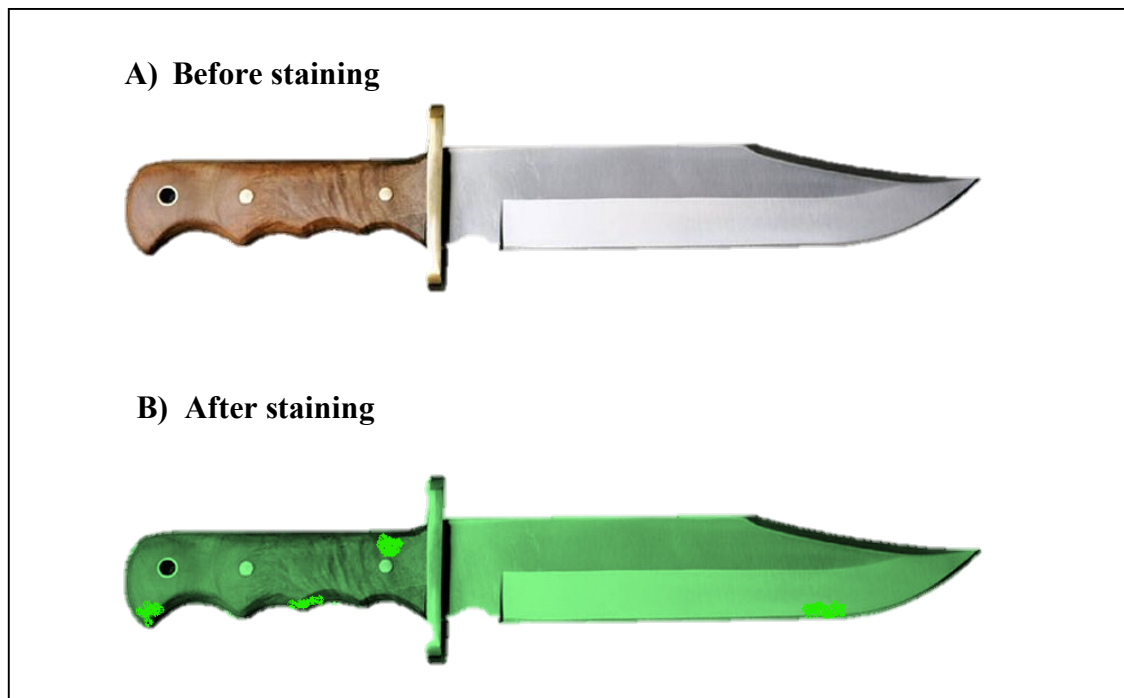
Ranking	Effect on DNA Extraction (DNA loss)	% of dye removed after extraction	Effect on DNA quantification	Effect on direct STR Typing	Enhancement with DNA	Lowest enhancement with protein	Lowest LOD (gel)	Lowest LOD (surface)
1	DD	RS	DD	GG	SG	EG	SG	DD
2	GG	EG	GG	EG	DD	GG	DD	SG
3	EG	SG	EG	RS	EG	GR	GG	EG
4	SG	DD	SG	DD	GG	DD	GR	GG
5	GR	GR	RS	SG	GR	RS	RS	GR
6	RS	-	GR	GR	RS	SG	-	RS

*LOD = Limit of detection, down to 0.5 ng

7.3 Future impact

The research conducted throughout this PhD involved staining of samples and touch-DNA on glass and plastic substrates. The next part of research would involve looking at other substrates such as wood and metal. This would then lend itself to the staining of evidentiary items submitted for DNA testing. This would lead to a DNA-targeted approach of detection and then swabbing those items to remove the touch-DNA off the surface. Scheme 7.1 shows how the staining procedure would work practically with a basic representation. This shows an item submitted for forensic testing where no apparent material can be seen visually (no blood e.g. a cleaned weapon) and how the dyes could be used to detect the DNA present and target those areas for DNA collection.

A limitation that has been found is in the application of the dye to an object as currently the samples being analyzed require minute amounts of dye easier applied with a micropipette. When moving towards larger items for DNA detection there needs to be a device able to spray the dye evenly across the object's surface and that dries quickly. The spray device used with luminol is a high pressured system adapted from spraying paint onto cars. This same application could potentially be used with this dye solution to apply the dye over much wider areas allowing for a holistic approach in DNA detection of items and at crime scenes.



Scheme 7.1: Schematic representation of how the dyes would work to find touch-DNA on evidentiary items within a forensic investigation (A) showing the item before staining where no evidentiary material can be seen (B) showing the item after staining and exciting with blue light which shows deposits of higher fluorescence indication DNA material.

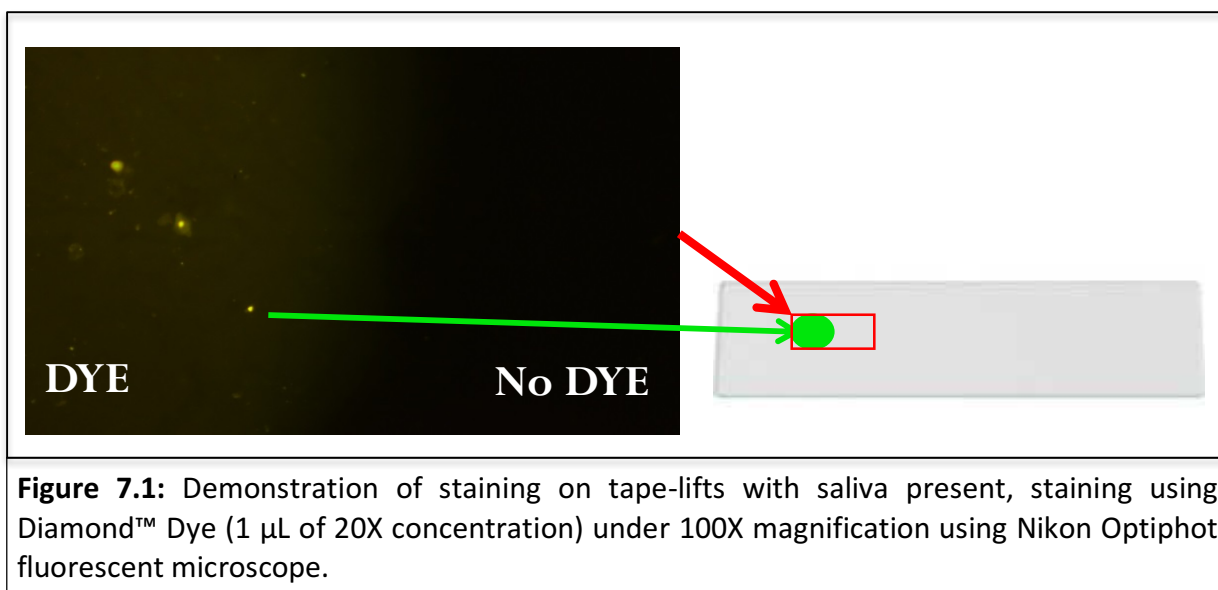
7.3.2 Staining of tape-lifts

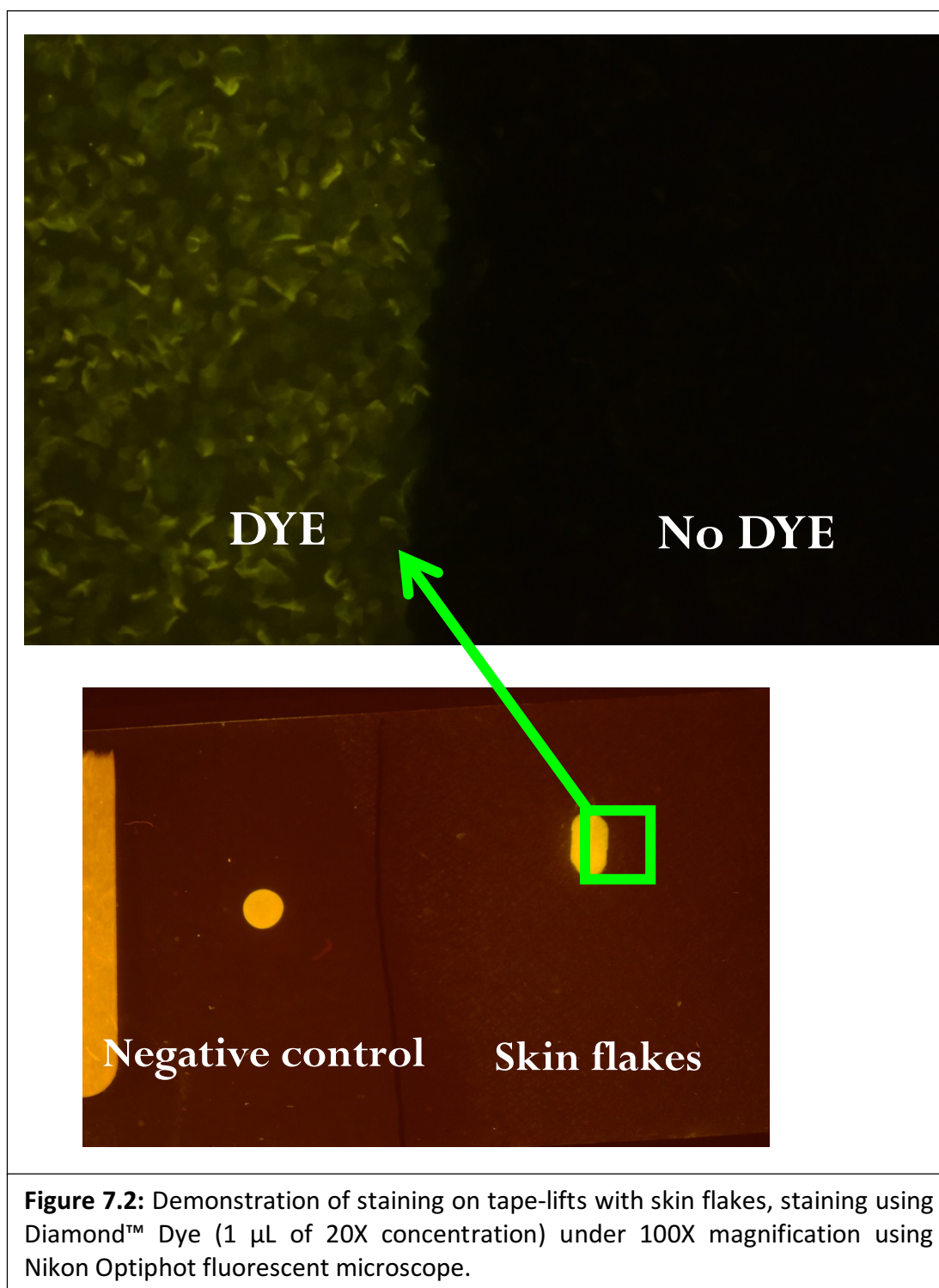
Tape-lifts are used routinely during evidence recovery but can be problematic to search and collect DNA. The goal of this future research would be to improve the practice of searching for biological material on tape-lifts using a DNA-targeted approach which has not been undertaken previously. This area of future research would advance the current knowledge detecting latent DNA on tape-lifts along with improving the current practice of analyzing tape-lifts in forensic investigations, which is often time consuming and not always producing a useful result. This future research would develop upon the current body of knowledge produced throughout this thesis; involving DNA binding dyes as a screening tool of DNA viable hair shafts as well as staining of fingerprints to aid in the detection of DNA using a fluorescent based approach.

In forensic investigations it can be common to search for biological traces on textile and porous substrates; this could involve clothing that had been present during an assault or break-in. Items of clothing and headgear, such as balaclavas, can be difficult to find the presence of traces of saliva or transferred DNA to identify the wearer [8]. This has led to the development and implementation of tape-lift procedures that can remove trace evidence while leaving the evidence intact [9]. Other methodology involves cutting the fabric and putting that through downstream forensic procedures (DNA extraction, amplification and detection), which can be time consuming and costly and often producing no result due to a lack of DNA being present. Tape-lifts provide a viable way of collecting material without damaging the artefact however due to a large surface area it can also be time consuming searching for biological traces as there is no targeted approach for the DNA detection[10-12].

From this body of knowledge the conceptualization of the use of these binding dyes to aid in the search of biological material on tape-lifts is a transfer of the same successful technology to a specific but highly relevant aspect of forensic science. A preliminary test to see whether the detection would work on an adhesive surface has been undertaken. This initial datum is shown in Figure 7.1 a tape-lift where saliva was present and dye applied. Epithelial cells are visible under a microscope on the tape-lift, with nothing visible in the region where no dye

was present. Figure 7.2 shows a tape-lift that has skin flakes present, the difference in what can be seen with dye present and without shows the potential of tape-lift staining. This preliminary study shows both the feasibility of this study but also the potential application of this research to improve current methodology by using a simple, rapid, non-destructive and cheap technique that could be easily implemented within forensic laboratories.





Although there is now a body of knowledge available from the use of these dyes on surface-based applications of the detection of latent DNA, further work needs to be undertaken to develop a methodology and reagent specifically for the detection of DNA on tape-lifts. This technique which has been preliminarily shown to work and detect saliva needs to be tested further and validated before the implementation is possible within forensic laboratories.

This would involve different staining techniques of the tape-lift; submerging the tape-lift in dye solution or spraying the dye onto the tape-lift surface. The dye buffer would also need modification in order to get the optimal working conditions and reduce background signal for detection of DNA. The filters for signal detection may need to be altered due to the background signal of the tape-lift from the adhesive residue which often fluoresces under UV and blue light. The use of the optimal detection system would then need to be tested on mock crime scene tapes to validate the method.

7.3.3 Staining of other items



Within forensic laboratories many items that are processed often result with insufficient genetic data, either no DNA present or not enough DNA present to result in an uploaded profile (above 12 alleles, CRIMTRAC). FSSA conducted an in house study on how many samples produced insufficient results and it was found that from all the items sampled there was a range of 9-100% of the samples producing no result (see Appendix G, Figure F-1, F-2). The samples that have a higher percentage of insufficient results can be targeted with this dye technique to potentially improve current results.

Some items that have a high rate of insufficient DNA results tend to be items of metal origin such as: ammunition (100 % insufficient); tools (56 %); weapons (39 %); parts of firearms (69 %); as well as tapes (70 %) that are often wrapped about seized material. These examples are shown in Figure 7.3. The ability to detect the DNA via this fluorescent approach would result in a DNA-targeted swabbing to collect the DNA.

Another aspect that has also improved the recovery of DNA from contact evidentiary items is the use of direct PCR. This process bypasses the standardized method of DNA extraction and submits the sample straight into an amplification reaction. This has been successfully shown to amplify DNA from fingerprints, hair follicles and fibres. The ability to tie both of these applications together can revolutionize the ability to obtain results that before could

not have been achieved. Further investigation is required for preliminary tests on metal to see if detection is possible, however the foundation of this research has been laid by this thesis making it possible for these future endeavours.

The first example of generating a profile from a fingerprint was in 1997 [13], cell-free nucleic acids have been found to be present in other biological samples, including saliva, blood and semen, it has been suggested by both Kita et al. and Linacre et al [14, 15] that they also exist in perspiration and touch-DNA. Cell-free DNA may be present on surfaces from the breakdown of nucleated cells from sources rich in DNA and the hands act as a vector to transfer the DNA to various substrate surfaces. Successful profiling of DNA present on fibres and hair follicles using a direct PCR method has been conducted without the use of DNA extraction. It was proposed that due to using the direct method which doesn't use DNA extraction methods that lyse the cell membrane, the profiles being generated was due to the free DNA present [14-16].

Further work needs to be conducted in the investigation of DNA within fingermarks which was mentioned briefly in Chapter 4. Examination of the level of fluorescence from the DNA gave an initial indication of the amount of DNA present, this would then need to be confirmed by amplification of the DNA present to determine whether the fluorescent signal was in accordance with the amount of DNA that could be recovered from a fingermark.

Other aspects that also need to be investigated further include the following:

- It was assumed from the outset that the presence of naturally occurring bacteria would affect the staining of any dye and therefore applying a dye solution would create much background fluorescence. While this study shows that the presence of human DNA on top of bacterial DNA can be detected effectively, a wider study may give greater confidence to the scientific community that this is indeed the case.
- A range of different adhesive tapes are used routinely for the collection of fibres, hairs, glass and cellular material. The tapes used in this study were tested for any inhibitory effects but as the forensic community use a wide

range of tapes, all with varying degrees of adhesiveness, these different brands will need to be tested as well to ensure that the DNA removed from the substrate can act effectively as a template for PCR, specifically direct PCR.

- A spray system was not perfected during this study and was outside the remit of this thesis but it was clear that a simple process to create a fine spray over a substrate needs to be developed. It is necessary that the application of the dye/solution does not have an adverse effect on the material and that marks are not left due to the drying of the solution.
- Lastly if the dye solution is applied to a substrate that already has dyes present (such as dyed fabrics) it will need to be determined whether the fluorescence from the DNA can still be visualized.

Training of crime scene technicians and the amendment to training manuals is outside the scope of this thesis, but it is noted that these are all fundamental requirements prior to the implementation of detecting latent DNA in the manner outlined in the thesis.

7.4 Final Statement

The research enclosed within the body of this thesis has certainly highlighted the advantage of being able to detect latent DNA using a fluorescent *in situ* technique and the potential impact this would have on the forensic science community. There are also aspects of this thesis that have outlined the potential of new dyes for real-time PCR showing the impact of this research outside of the forensic field.

The end goal of this research is to improve current methodologies to gain more meaningful results during forensic investigations. This has been shown with the study on staining hairs and providing a more sensitive technique in determining whether a hair sample was suitable for STR typing. This allows for a more efficient and effective way of analyzing hairs which can reduce waste of expensive reagents by only choosing hair samples that would likely obtain results.

As stated I believe the future of this research lies in the ability of detecting latent DNA on commonly submitted evidentiary items. This would improve the collection of the DNA thus improving the efficiency by obtaining more meaningful results; more DNA present more information can be obtained (number of alleles). The research conducted has now paved the way for this future research to take place and improve DNA collection, providing a DNA-targeted method, currently not available. With further research outlined within this Chapter this application of DNA detection both within the laboratory and field application is closer to the end goal of detecting DNA at crime scenes.

7.5 References

- [1] L. Bourguignon., B. Hoste., T. Boonen., K. Vits., F. Hubrecht, A fluorescent microscopy-screening test for efficient STR-typing of telogen hair roots, *Forensic Science International: Genetics*. 2008, **3** 27-31.
- [2] T. Lepez., M. Vandewoestyne., D. Van Hoofstat., D. Deforce, Fast nuclear staining of head hair roots as a screening method for successful STR analysis in forensics, *Forensic Science International: Genetics*. 2014, **13** 191-194.
- [3] T. Boonen., K. Vits., B. Hoste., F. Hubrecht, The visualization and quantification of cell nuclei in telogen hair roots by fluorescence microscopy, as a pre-DNA analysis assessment, *Forensic Science International: Genetics Supplement Series*. 2008, **1** 16-18.
- [4] E.M. Brooks., M. Cullen., T. Szytdna., S.J. Walsh, Nuclear staining of telogen hair roots contributes to successful forensic nDNA analysis, *Australian Journal of Forensic Sciences*. 2010, **42** 115-122.
- [5] D. McNevin., L. Wilson-Wilde., J. Robertson., J. Kyd., C. Lennard, Short tandem repeat (STR) genotyping of keratinised hair: Part 1. Review of current status and knowledge gaps, *Forensic Science International*. 2005, **153** 237-246.
- [6] S. Szabo., K. Jaeger., H. Fischer., E. Tschachler., W. Parson., L. Eckhart, In situ labeling of DNA reveals interindividual variation in nuclear DNA breakdown in hair and may be useful to predict success of forensic genotyping of hair, *International Journal of Legal Medicine*. 2012, **126** 63-70.
- [7] F. Mao., W.-Y. Leung., X. Xin, Characterization of EvaGreen and the implication of its physicochemical properties for qPCR applications, *BMC Biotechnology*. 2007, **7** 76-76.
- [8] B. Bhoelai., F. Beemster., T. Sijen, Revision of the tape used in a tape-lift protocol for DNA recovery, *Forensic Science International: Genetics Supplement Series*. 2013, **4** e270-e271.
- [9] T.J. Verdon., R. J. Mitchell., R.A.H. Van Oorschot, Evaluation of tapelifting as a collection method for touch DNA, *Forensic Science International: Genetics*. 2014, **8** 179-186.
- [10] S.A. Steadman., S.R. Hooper., S.C. Geering., S. King., M.A. Bennett, Recovery of DNA from Latent Fingerprint Tape Lifts Archived Against Matte Acetate, *Journal of Forensic Sciences*. 2015, **60** 777-782.
- [11] J. Joël., B. Glanzmann., U. Germann., C. Cossu, DNA extraction of forensic adhesive tapes—A comparison of two different methods, *Forensic Science International: Genetics Supplement Series*.
- [12] R. May., J. Thomson, Optimisation of cellular DNA recovery from tape-lifts, *Forensic Science International: Genetics Supplement Series*. 2009, **2** 191-192.
- [13] R. A. Van Oorschot., M. K. Jones, DNA fingerprints from fingerprints. *Nature*. 1997, **387** p.767.

- [14] T. Kita., H. Yamaguchi., M. Yokoyama., T. Tanaka., N. Tanaka, Morphological study of fragmented DNA on touched objects, *Forensic Science International: Genetics*. 2008, **3** 32-36.
- [15] A. Linacre., V. Pekarek., Y.C. Swaran., S.S. Tobe, Generation of DNA profiles from fabrics without DNA extraction, *Forensic Science International: Genetics*. 2010, **4** 137-141.
- [16] M. Vandewoestyne., D. Van Hoofstat., A. Franssen., F. Van Nieuwerburgh., D. Deforce, Presence and potential of cell free DNA in different types of forensic samples, *Forensic Science International: Genetics*. 2013, **7** 316-320.

7.6 APPENDIX F

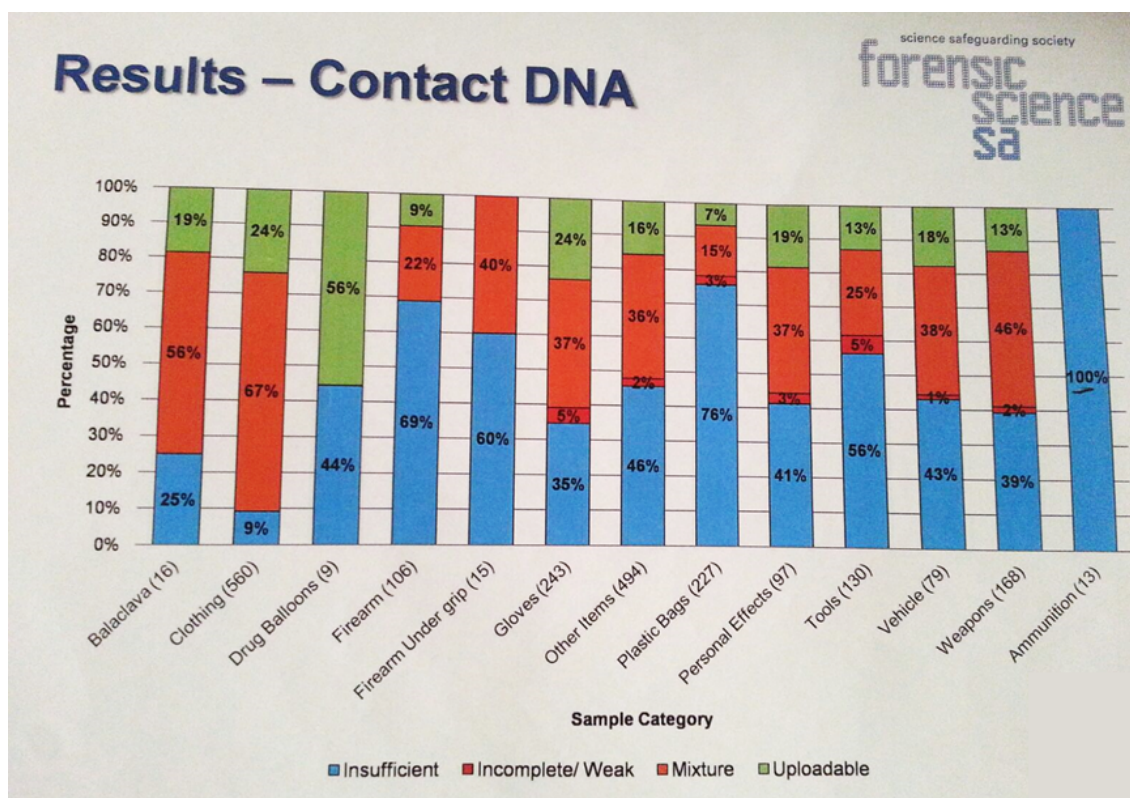


Figure F-1: Results of contact DNA analysis of different categories of items from FSSA.

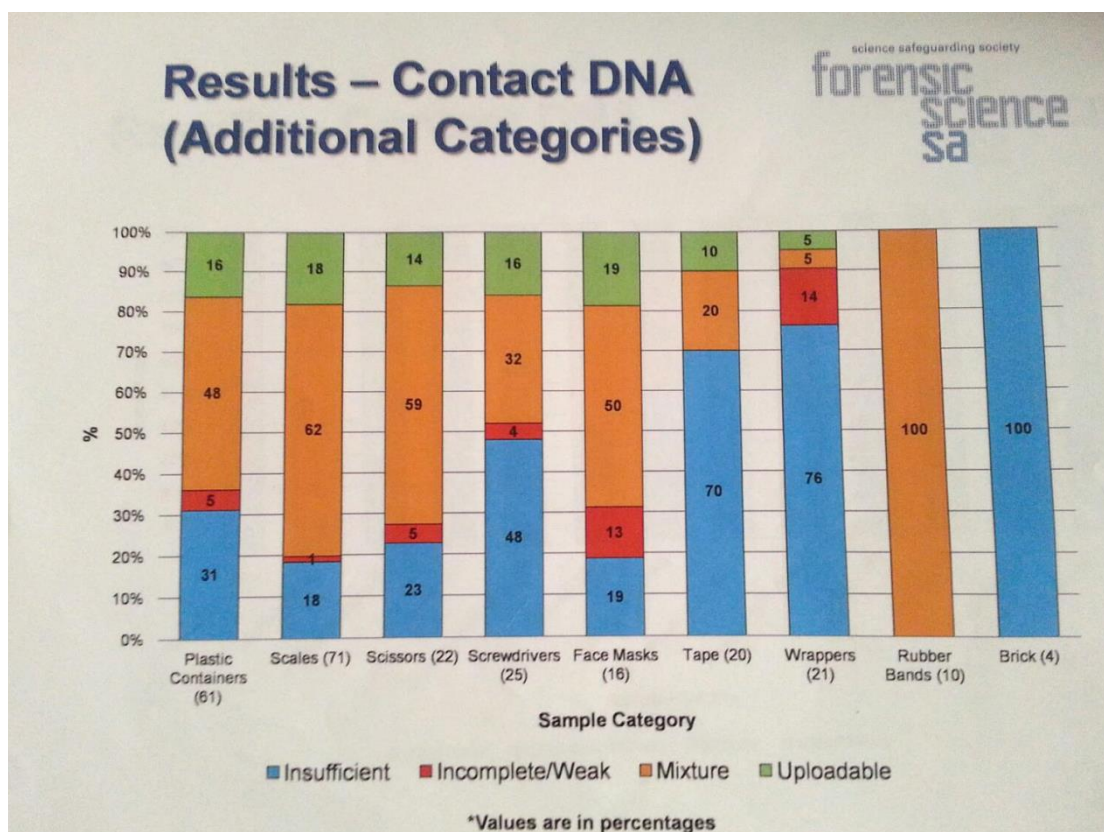


Figure F-2: Results of contact DNA analysis of different categories (additional to that in Figure F-1) of items from FSSA.